



TECHNICAL REPORT

97-10

**On the flow of groundwater
in closed tunnels**

**Generic hydrogeological modelling
of nuclear waste repository, SFL 3-5**

Johan G Holmén

Uppsala University/Golder Associates AB

June 1997

SVENSK KÄRNBRÄNSLEHANTERING AB
SWEDISH NUCLEAR FUEL AND WASTE MANAGEMENT CO

P.O.BOX 5864 S-102 40 STOCKHOLM SWEDEN
PHONE +46 8 665 28 00
FAX +46 8 661 57 19

ON THE FLOW OF GROUNDWATER IN CLOSED TUNNELS

GENERIC HYDROGEOLOGICAL MODELLING OF NUCLEAR WASTE REPOSITORY, SFL 3-5

Johan G Holmén

Uppsala University/Golder Associates AB

June 1997

This report concerns a study which was conducted for SKB. The conclusions and viewpoints presented in the report are those of the author(s) and do not necessarily coincide with those of the client.

Information on SKB technical reports from 1977-1978 (TR 121), 1979 (TR 79-28), 1980 (TR 80-26), 1981 (TR 81-17), 1982 (TR 82-28), 1983 (TR 83-77), 1984 (TR 85-01), 1985 (TR 85-20), 1986 (TR 86-31), 1987 (TR 87-33), 1988 (TR 88-32), 1989 (TR 89-40), 1990 (TR 90-46), 1991 (TR 91-64), 1992 (TR 92-46), 1993 (TR 93-34), 1994 (TR 94-33), 1995 (TR 95-37) and 1996 (TR 96-25) is available through SKB.

On the Flow of Groundwater in Closed Tunnels

*Generic Hydrogeological Modelling of
Nuclear Waste Repository, SFL 3-5*

Johan G. Holmén

Uppsala University
Golder Associates AB

June 1997

This report is a reprint of a Doctoral dissertation from Uppsala University:

Holmén, J., 1997: "On the flow of groundwater in closed tunnels. Generic hydrogeological modelling of nuclear waste repository, SFL 3-5", *Doctoral dissertation, Uppsala University, Institute of Earth Sciences, 286 pp, ISBN 91-506-1231-X.*

ABSTRACT

The purpose is to study the flow of groundwater in closed tunnels by use of mathematical models. Tunnels that form a separate isolated structure are called "closed" tunnels. Closed tunnels can be used for storage of hazardous waste. The calculations were based on three dimensional models, presuming steady state conditions. The stochastic continuum approach was used for representation of a heterogeneous rock mass. The size of the calculated flow is given as a multiple of an unknown regional groundwater flow.

The size of the flow in a tunnel has been studied, as regards:

- Direction of the regional groundwater flow. • Tunnel length, width and conductivity.
- Heterogeneity of the surrounding rock mass. • Flow barriers and encapsulations inside a tunnel.

The study includes a model of the planned repository for nuclear waste (SFL 3-5). The flow through the tunnels is estimated for different scenarios.

The stochastic continuum approach has been investigated, as regards the representation of a scale dependent heterogeneous conductivity. An analytical method is proposed for the scaling of measured conductivity values, the method is consistent with the stochastic continuum approach.

Below follow general conclusions as regards flow in closed tunnels. The regional groundwater flow is of the same size for all scenarios discussed.

- The expected flow of a tunnel in a heterogeneous rock mass will be larger than that of a similar tunnel in a homogeneous rock mass. The larger the amount of heterogeneity, the larger the expected flow. • The effects of the heterogeneity will decrease with increased tunnel length.
- If the conductivity of a tunnel is smaller than a threshold conductivity, the tunnel conductivity is the most important parameter. • If the tunnel conductivity is large and the tunnel is long, the most important parameter is the direction of the regional flow. • Consider a heterogeneous rock mass, like the rock at Äspö HRL, if the tunnel length is shorter than about 500 m, the heterogeneity will be an important parameter; for tunnels shorter than about 250 m, the heterogeneity is probably the most important parameter. • The flow through an encapsulation surrounded by a flow barrier is mainly dependent on the conductivity of the barrier.

Keywords: groundwater, flow, tunnel, heterogeneity, scale, stochastic, continuum, repository, modelling, fractured rock

ABSTRACT (in swedish)

Syftet är att studera grundvattenflöde genom stängda tunnlar med hjälp av matematiska modeller. Tunnlar som utgör en avskild isolerad enhet kallas "stängda" tunnlar. Stängda tunnlar kan användas för förvaring av miljöfarligt avfall. Beräkningarna baseras på tre-dimensionella modeller och stationärt tillstånd. En stokastisk kontinuum beskrivning har använts för att representera en heterogen bergmassa. Storleken på de beräknade flödena är angivna som multiplar av ett okänt regionalt grundvattenflöde.

Med avseende på flödet genom stängda tunnlar, har vi studerat:

- Det regionala grundvattenflödets riktning.
- Tunnlars längd, bredd och konduktivitet.
- Omgivande bergmassas heterogenitet.
- Flödes barriärer och inneslutningar i tunnlar.

Studien omfattar en modell av det planerade förvaret för långlivat lågt och medelaktivt radioaktivt avfall, kallat SFL 3-5. Flödet genom dess tunnlar har beräknats för olika scenarier.

Den stokastiska kontinuum beskrivningen har undersökts med avseende på representation av en skalberoende hydraulisk konduktivitet. I avhandlingen föreslås en analytisk metod för skalning av mätta värden på hydraulisk konduktivitet, metoden är förenlig med den stokastiska kontinuum beskrivningen.

Nedan följer allmänna slutsatser med avseende på grundvattenflöde i stängda tunnlar. Det regionala grundvattenflödet är av samma storlek i alla de diskuterade scenarierna.

- Det förväntade flödet genom en tunnel placerad i en heterogen bergmassa är större än flödet genom en likadan tunnel placerad i en homogen bergmassa. Desto större heterogenitet, desto större förväntat flöde.
- Effekterna av en heterogen bergmassa avtar med ökad längd på tunneln.
- Om en tunnels konduktivitet är mindre än en tröskelkonduktivitet, är tunnelkonduktiviteten den mest betydelsefulla parametern.
- Om tunnelkonduktiviteten är stor och tunneln lång är den mest betydelsefulla parametern riktningen på det regionala grundvattenflödet.
- Beakta en heterogen bergmassa med egenskaper som vid Äspö Berglaboratorium, om en tunnel är kortare än c:a 500m blir heterogeniteten en betydelsefull parameter; för tunnlar kortare än c:a 250m är sannolikt heterogeniteten den mest betydelsefulla parametern.
- Flödet genom en inneslutning omgiven av en flödesbarriär beror huvudsakligen av flödesbarriärens konduktivitet.

I. Table of contents

I	TABLE OF CONTENTS	v - vii
II	LIST OF FIGURES AND TABLES	viii - x
III	NOMENCLATURE AND ABBREVIATIONS	xi
IV	WHAT TO READ	xii - xiii
V	ACKNOWLEDGEMENTS	xiv
1.	INTRODUCTION AND PURPOSE OF STUDY.	1
1.1	Introduction	1
1.2	Purpose of study	1
1.3	Description of SFL 3-5	2
2.	METHODOLOGY	3
2.1	The system analysis approach	3
2.2	Mathematical approach to the studied medium	3
2.3	Definition of computer codes	5
2.4	Time dependency	5
2.5	Size of model and boundary effects	6
2.6	Simulation of regional groundwater flow	6
2.7	Size and direction of regional groundwater flow	7
2.8	The concept of flow in a tunnel	7
2.9	Hydraulic conductivity	8
2.10	Advection and diffusion	8
	Figures 2.1 and 2.2	9 - 10
3.	GENERAL ASPECTS OF FLOW IN TUNNELS, ANALYTICAL METHOD	11
3.1	Introduction	11
3.2	Analytical method	11
3.3	Definition of terms	11
3.4	General aspects of flow in a tunnel	12
3.5	General aspects of flow in an ellipsoid	13
3.6	Comparison between the analytical and the numerical method	14
3.7	Flow in an ellipsoid tunnel, regional flow along the short axis	15
3.8	Flow in an ellipsoid tunnel, regional flow along the main axis	16
3.9	Specific flow in an ellipsoid tunnel, sensitivity to direction of regional flow	16
3.10	Size of maximum flow in an ellipsoid tunnel	17
3.11	Threshold conductivity of an ellipsoid tunnel	18
3.12	Influence radius of an ellipsoid-tunnel	18
3.13	Flow in an ellipsoid-tunnel, balance as regards direction of regional flow	19
3.14	Examples of flow and conductivity of an ellipsoid-tunnel	20
	Figures 3.1 through 3.18	23 - 41
4.	METHOD FOR ESTIMATION OF BOUNDARY EFFECTS	43
4.1	Introduction	43
4.2	Cause for boundary effects	43
4.3	Number of nodes	44
4.4	Analytical method for estimation of boundary effects	44
4.5	Numerical method for estimation of boundary effects	45
4.6	Example	46
4.7	Conclusions	47
	Figures 4.1 through 4.5	48 - 52
	Table 4.1	53

5. THE STOCHASTIC CONTINUUM APPROACH AND THE HETEROGENEOUS ROCK MASS AT ÄSPÖ	55
5.1 Introduction	55
5.2 Mathematical approach	55
5.3 Definition of terms	56
5.4 Variation in hydraulic conductivity, probability distribution and scale dependency	56
5.5 Analytical method for estimation of the effective conductivity	58
5.6 Results of field investigations at the Äspö Hard Rock Laboratory	60
5.7 Representation of the measured scale dependency in a stochastic continuum model, an analytical method for scaling of measured hydraulic conductivity	61
5.8 Numerical considerations	65
5.9 Numerical simulations of scale dependency	70
5.10 What to think about when using the stochastic continuum approach	77
Table 5.1	81
Figures 5.1 through 5.17	81 - 97
6. EFFECTS OF THE HETEROGENEITY OF THE ROCK MASS AS REGARDS FLOW IN TUNNELS	99
6.1 Introduction	99
6.2 Estimation of boundary effects, stochastic continuum	99
6.3 Introduction to sensitivity analysis	100
6.4 Flow in a tunnel, heterogeneous rock, sensitivity to tunnel conductivity	103
6.5 Flow in a tunnel, heterogeneous rock, sensitivity to amount of heterogeneity	104
6.6 Flow in a tunnel, heterogeneous rock, sensitivity to tunnel length	105
6.7 Variation of specific flow inside a tunnel	106
6.8 Conclusions	108
Table 6.1	110
Figures 6.1 through 6.20	111 - 130
7. EFFECTS OF FLOW BARRIERS	131
7.1 Introduction	131
7.2 Methodology	131
7.3 Function of flow barrier	132
7.4 Flow in encapsulation and flow barrier, sensitivity to conductivity of barrier	133
7.5 Flow in the encapsulation, sensitivity to conductivity of the encapsulation	134
7.6 Flow in the encapsulation, sensitivity to extension of the flow barrier	135
7.7 Flow in the encapsulation, sensitivity to length of encapsulation and barrier	135
7.8 Flow in encapsulation and flow barrier, sensitivity to heterogeneity of rock	136
7.9 Conclusions	138
Figures 7.1 through 7.14	140 - 153
8. ESTABLISHMENT OF THE MODEL OF REPOSITORY SFL 3-5	155
8.1 Introduction	155
8.2 Conceptual model	155
8.3 Mathematical-numerical model	156
8.4 System of angles defining the direction of the regional flow	158
8.5 Estimation of boundary effects	159
8.6 The mesh selected for predictive simulations	160
8.7 Alternative lay-out of repository	160
Tables 8.1 and 8.2	161 - 162
Figures 8.1 through 8.7	163 - 169

9. RESULTS OF MODELLING OF REPOSITORY SFL 3-5	171
9.1 Introduction	171
9.2 Sensitivity to direction of regional flow	172
9.3 Sensitivity to the conductivity of the flow barriers in SFL 3 and SFL 5	174
9.4 Sensitivity to conductivity of back filling in SFL 4	175
9.5 Variation of specific flow inside the SFL 4 tunnel	177
9.6 Sensitivity to plugs in tunnels	179
9.7 Sensitivity to heterogeneity of the rock mass	180
9.8 Conclusions - Summary	182
Tables 9.1 and 9.2	184
Figures 9.1 through 9.17	185 - 201
10. GENERAL CONCLUSIONS	203
10.1 Introduction	203
10.2 Application of the results on a site specific scenario	203
10.3 Results of study	203
10.4 Order of precedence, as regards the parameters controlling the flow through a closed tunnel	204
11. REFERENCES	207 - 210

APPENDIX

A. THE FINITE DIFFERENCE METHOD	A.1
B. ANALYTICAL METHOD FOR CALCULATION OF STEADY FLOW IN CLOSED TUNNELS	B.1
C. METHOD FOR GENERATION OF REGIONAL FLOW IN A NUMERICAL MODEL	C.1
D. DISTRIBUTION OF SPECIFIC FLOW IN REPOSITORY SFL 3-5	D.1
E. PRELIMINARY LAY-OUT OF REPOSITORY SFL 3-5	E.1

II. List of figures and tables

Chapter 1. INTRODUCTION AND PURPOSE OF STUDY

Chapter 2. METHODOLOGY

Figure 2.1 Modelling approach and flow pattern	9
Figure 2.2 Different directions of the regional flow	10

Chapter 3. GENERAL ASPECTS OF FLOW IN TUNNELS, ANALYTICAL METHOD

Figure 3.1 Different directions of the regional flow in relation to an ellipsoid	23
Figure 3.2 Analytical solution, Head contours, K-contrast: 100	24
Figure 3.3 Analytical solution, Head contours, K-contrast: 10000	25
Figure 3.4 Specific and total flow in an ellipsoid-tunnel (Q.1)	26
Figure 3.5 Specific and total flow in an ellipsoid-tunnel (Q.2)	27
Figure 3.6 Specific and total flow in an ellipsoid-tunnel (A.1)	28
Figure 3.7 Specific and total flow in an ellipsoid-tunnel (A.2)	29
Figure 3.8 Specific flow in an ellipsoid-tunnel, sensitivity to direction of regional flow	30
Figure 3.9 Specific flow in an ellipsoid-tunnel, sensitivity to direction of regional flow	31
Figure 3.10 Maximum specific flow in an ellipsoid-tunnel	32
Figure 3.11 Maximum total flow in an ellipsoid-tunnel	33
Figure 3.12 Threshold conductivity of an ellipsoid-tunnel (Q)	34
Figure 3.13 Threshold conductivity of an ellipsoid-tunnel (A)	35
Figure 3.14 Flow balance as regards direction of regional flow, in an ellipsoid-tunnel	36
Figure 3.15 Analytical solution, change in head K-contrast: 100	37
Figure 3.16 Analytical solution, change in head K-contrast: 10000	38
Figure 3.17 Influence radius of ellipsoid-tunnel (1)	39
Figure 3.18 Influence radius of ellipsoid-tunnel (2)	40
Figure 3.19 Influence radius of ellipsoid-tunnel (3)	41

Chapter 4. METHOD FOR ESTIMATION OF BOUNDARY EFFECTS

Figure 4.1 Method of multiple meshes	48
Figure 4.2 Boundary effects, method of multiple meshes, B1	49
Figure 4.3 Boundary effects, method of multiple meshes, B2	50
Figure 4.4 Boundary effects, method of multiple meshes, B1	51
Figure 4.5 Boundary effects, comparison of methods for estimation	52
Table 4.1 Estimation of boundary effects	53

Chapter 5. THE STOCHASTIC CONTINUUM APPROACH AND THE HETEROGENEOUS ROCK MASS AT ÄSPÖ

Table 5.1 Results of hydraulic tests of fractured rock at äspö	81
Figure 5.1 Statistical distribution of measured conductivity	81
Figure 5.2 Deviation in analytical estimation of effective conductivity	82
Figure 5.3 Measured scale dependency, results of packer tests	83
Figure 5.4 Scale dependency, measured and interpolated	84
Figure 5.5 Discretization of the flow medium	85
Figure 5.6 Block-, equivalent- and effective conductivity as well as scale dependency	86
Figure 5.7 Models having different number of dimensions	87
Figure 5.8 Stochastic continuum, number of nodes per block	88
Figure 5.9 Stochastic continuum, homogenized K and heterogeneity	89
Figure 5.10 Stochastic continuum 2D, scale dependency, homogenization	90

Figure 5.11 Stochastic continuum 3D, scale dependency, homogenization	91
Figure 5.12 Stochastic continuum, effective K and homogenization method	92
Figure 5.13 Stochastic continuum, calibration factor for FID model	93
Figure 5.14 Stochastic continuum, equivalent K vs. scale ($\sigma_{10Lg Kblock} = 1.0$)	94
Figure 5.15 Stochastic continuum, equivalent K vs. scale ($\sigma_{10Lg Kblock} = 1.498$)	95
Figure 5.16 Stochastic continuum, equivalent K vs. scale ($\sigma_{10Lg Kblock} = 2.0$)	96
Figure 5.17 Stochastic continuum, scale effects, 3-dimensional models	97

Chapter 6. EFFECTS OF THE HETEROGENEITY OF THE ROCK MASS AS REGARDS FLOW IN TUNNELS

Table 6.1 Estimation of boundary effects, stochastic continuum	110
Figure 6.1 Model of tunnel and rockmass	111
Figure 6.2 Flow pattern in rockmass and tunnel, uniform continuum	112
Figure 6.3 Flow pattern in rockmass and tunnel, stochastic continuum	113
Figure 6.4 Flow pattern in rockmass and tunnel, uniform continuum	114
Figure 6.5 Flow pattern in rockmass and tunnel, stochastic continuum	115
Figure 6.6 Boundary effects, method of multiple meshes, stochastic continuum	116
Figure 6.7 Boundary effects, method of multiple meshes, stochastic continuum	117
Figure 6.8 Boundary effects, method of multiple meshes, stochastic continuum	118
Figure 6.9 Flow in a tunnel, sensitivity to tunnel conductivity (Y10a)	119
Figure 6.10 Flow in a tunnel, sensitivity to tunnel conductivity (Y10q)	120
Figure 6.11 Flow in a tunnel, sensitivity to tunnel conductivity (X10q)	121
Figure 6.12 Flow in a tunnel, sensitivity to tunnel conductivity, flow factor	122
Figure 6.13 Flow in a tunnel, rock mass heterogeneity, flow factor	123
Figure 6.14 Flow in a tunnel, sensitivity to rock mass heterogeneity (q)	124
Figure 6.15 Flow in a tunnel, sensitivity to rock mass heterogeneity (a)	125
Figure 6.16 Flow in a tunnel, sensitivity to tunnel length, flow (a)	126
Figure 6.17 Flow in a tunnel, sensitivity to tunnel length, flow factor (a)	127
Figure 6.18 Flow in a tunnel, sensitivity to tunnel length, flow (q)	128
Figure 6.19 Flow in a tunnel, sensitivity to tunnel length, flow factor (q)	129
Figure 6.20 Variation of specific flow inside a tunnel	130

Chapter 7. EFFECTS OF FLOW BARRIERS

Figure 7.1 Effects of a flow barrier, flow pattern	140
Figure 7.2 Model of a tunnel with a flow barrier and an encapsulation	141
Figure 7.3 Flow in a flow barrier, sensitivity to barrier conductivity	142
Figure 7.4 Flow in an encapsulation, sensitivity to barrier conductivity	143
Figure 7.5 Flow in an encapsulation, sensitivity to encapsulation conductivity	144
Figure 7.6 Model of a tunnel with an encapsulation and an uncomplete flow barrier	145
Figure 7.7 Flow in encapsulation, sensitivity to barrier extension	146
Figure 7.8 Flow in encapsulation, sensitivity to tunnel length	147
Figure 7.9 Flow in a flow barrier, sensitivity to barrier conductivity (SC)	148
Figure 7.10 Flow in an encapsulation, sensitivity to barrier conductivity (SC)	149
Figure 7.11 Flow in a barrier and an encapsulation, flow factor	150
Figure 7.12 Flow in a flow barrier, sensitivity to barrier conductivity (SC)	151
Figure 7.13 Flow in an encapsulation, sensitivity to barrier conductivity (SC)	152
Figure 7.14 Flow in a barrier and an encapsulation, flow factor	153

Chapter 8. ESTABLISHMENT OF THE MODEL OF REPOSITORY SFL 3-5	
Table 8.1 Size of repository, preliminary and generalized.	161
Table 8.2 Repository model of SFL 3-5, Hydraulic conductivity	162
Figure 8.1 Repository model, RC5, horizontal cross-section	163
Figure 8.2 Repository model, RC5, vertical cross-sections	164
Figure 8.3 Repository model, system of angles	165
Figure 8.4 Repository model, ME6	166
Figure 8.5 Repository model, UC, boundary effects, multiple meshes B1	167
Figure 8.6 Repository model, estimation of error in predicted flow	168
Figure 8.7 Alternative lay-out of repository	169

Chapter 9. RESULTS OF MODELLING OF REPOSITORY SFL 3-5	
Table 9.1 Sensitivity to alternative lay-outs, effects of plugs, Scenario 2	184
Table 9.2 Sensitivity to alternative lay-outs, effects of plugs, Scenario 3	184
Figure 9.1 Flow in the SFL 4 tunnel, homogeneous rock mass, sensitivity to direction of the regional flow	185
Figure 9.2 Flow in the SFL 3 barrier, homogeneous rock mass, sensitivity to direction of the regional flow	186
Figure 9.3 Flow in the SFL 3 encapsulation, homogeneous rock mass, sensitivity to direction of the regional flow	187
Figure 9.4 Flow in the SFL 5 barrier, homogeneous rock mass, sensitivity to direction of the regional flow	188
Figure 9.5 Flow in the SFL 5 encapsulation, homogeneous rock mass, sensitivity to direction of the regional flow	189
Figure 9.6 Flow in SFL 3 flow barrier, sensitivity to barrier conductivity	190
Figure 9.7 Flow in SFL 3 encapsulation, sensitivity to barrier conductivity	191
Figure 9.8 Flow in SFL 5 flow barrier, sensitivity to barrier conductivity	192
Figure 9.9 Flow in SFL 5 encapsulation, sensitivity to barrier conductivity	193
Figure 9.10 Flow in SFL 4, sensitivity to conductivity of SFL 4	194
Figure 9.11 Flow in SFL 3, sensitivity to conductivity of SFL 4	195
Figure 9.12 Distribution of specific flow in the SFL 4 tunnel, uniform cont. models ..	196
Figure 9.13 Distribution of specific flow in the SFL 4 tunnel, uniform continuum models and stochastic continuum models	197
Figure 9.14 Correction factors for heterogeneous rock mass, sensitivity to direction of the regional flow	198
Figure 9.15 Expected total flow in SFL 4, heterogeneous rock mass, sensitivity to direction of the regional flow	199
Figure 9.16 Expected total flow in SFL 3, heterogeneous rock mass, sensitivity to direction of the regional flow	200
Figure 9.17 Expected total flow in SFL 5, heterogeneous rock mass, sensitivity to direction of the regional flow	201

10. GENERAL CONCLUSIONS

11. REFERENCES

III. Nomenclature and abbreviations

A	Area [L ²]
D	Number of dimensions.
2D	Two dimensions
3D	Three dimensions
eLog K	The natural logarithm of a conductivity value [L / T]
10Log K	The logarithm of a conductivity value, logarithms of base 10 [L / T]
I	Gradient [-]
K	Hydraulic conductivity [L / T]
K _{BG}	Geometric mean of conductivities of rock blocks [L / T]
K _{block}	Conductivity of a rock block [L / T]
K dist	Probability distribution of conductivity values
K _E	Effective conductivity [L / T]
K _{equ}	Equivalent conductivity [L / T]
K _H	Homogenized conductivity, conductivity between two nodes [L / T]
K _{section}	Conductivity of a section of a bore hole [L / T]
K _t	Threshold conductivity [L / T]
K _x , K _y , K _z	Hydraulic conductivity along axes [L / T]
L	Spatial dimension, length
q	Specific flow [L ³ / (L ² T) = L / T]
Q	Total flow [L ³ / T]
REV	Representative elementary volume
SC	Stochastic continuum
SQ	Specific flow [L ³ / (L ² T) = L / T]
Ss	Specific storage of medium [L ⁻¹]
STD	Standard deviation
t	Time [T]
T	Dimension time
TF	Total flow [L ³ / T]
UC	Uniform continuum
VF	Volumetric flow (flow per unit volume) [1 / T]
φ	Piezometric head (potentiometric head, groundwater head) [L]
σ	Standard deviation of a set of values [L / T]
σ _K	Standard deviation of a set of K values [L / T]
σ _{eLg} , σ _{eLog}	Standard deviation of the natural logarithms of a set of values [L / T]
σ _{10Lg} , σ _{10Log}	Standard deviation of the logarithms (base 10) of a set of values [L / T]
σ _{eLg K}	Standard deviation of the natural logarithms of a set of K values [L / T]
σ _{10Lg K}	Standard deviation of the logarithms (base 10) of a set of K values [L / T]

IV. What to read

Scope of work

The study is divided into eleven chapters and five appendices. A brief description of the contents of the chapters and the appendices is given below.

- **Chapter 1.** gives the purpose of the study, defines a closed tunnel, and gives a short description of the planned repository for nuclear waste.
- **Chapter 2.** discusses the methodology, e.g. the system analysis approach, the mathematical approach to different flow media, the concept of flow in a tunnel, etc.
- **Chapter 3.** discusses general aspects of flow in a tunnel. The chapter could be looked upon as a sensitivity analysis of different parameters controlling the flow of a tunnel. The results presented are based on an analytical method, presuming an infinitely large, homogeneous rock mass.
- **Chapter 4.** discusses boundary effects that occur in numerical models and presents two methods for estimation of these effects.
- **Chapter 5.** discusses the stochastic continuum approach as regards representation of a heterogeneous flow medium with a scale dependent hydraulic conductivity. In the chapter we propose an analytical method for scaling of measured conductivity values, a method that is consistent with the stochastic continuum approach. We also present some numerical considerations. At the end of the chapter we discuss general aspects of how to use the stochastic continuum method.
- **Chapter 6.** discusses the effects of the heterogeneity of the rock mass as regards the flow of a tunnel. The results presented are based on numerical models. The effects of a homogeneous and a heterogeneous rock mass are studied.
- **Chapter 7.** discusses the effects of flow barriers and encapsulations installed inside a tunnel. Flow barriers limit the flow through an encapsulation. The results presented are based on numerical models. The effects of a homogeneous and a heterogeneous rock mass are studied.
- **Chapter 8.** discusses the model of the repository SFL 3-5. This chapter presents the establishment of the model, the generalized lay-out, the conductivity of different parts, the boundary effects, etc.
- **Chapter 9.** discusses the model of the repository SFL 3-5. This chapter presents the results of the modelling. The flow through different parts of the repository for different scenarios, the interaction between different parts of the repository, etc.
- **Chapter 10.** gives general conclusions as regards the flow in closed tunnels, gives an order of precedence as regards the parameters controlling the flow through a closed tunnel.
- **Chapter 11.** gives the references.

- **Appendix A.** discusses the continuum approach, presents the finite difference method, as applied to the differential equation defining the flow of groundwater. The appendix also gives a brief presentation of the GEOAN model.
- **Appendix B.** presents an analytical method for calculation of steady flow in tunnels.
- **Appendix C.** presents a method for generation of regional flow in a numerical model.
- **Appendix D.** gives figures demonstrating the variation of flow in repository SFL 3-5.
- **Appendix E.** gives figures demonstrating the preliminary lay-out of repository SFL 3-5

Hints on what to read

As much as possible, without making the study too heavy with repetitions, the chapters and the appendices are written in a way that each one of them can be read separately. At the end of each chapter a section is given in which conclusions are presented. Below we will give some hints about what sections to read for different fields of interests.

- If the reader wants a **summary** of the results of this study, - read the following:
Chapter 1: Sec.1.1 and 1.2,
Chapter 2: Sec.2.7 and 2.8
Chapter 3: Sec.3.4 and 3.14
Chapter 4: Sec.4.7
Chapter 5: Sec.5.10
Chapter 6: Sec.6.8
Chapter 7: Sec.7.9
Chapter 9: Sec.9.8
Chapter 10: Sec.10.3
- If the reader is interested in the flow of groundwater in closed tunnels and if the reader is also interested in the methodology of how to estimate it,
- read all chapters and all appendices.
- If the reader is interested in the flow of groundwater in closed tunnels, but not interested in the methodology, - read the following:
Chapter 1,
Chapter 2: Sec.2.7 and 2.8
Chapters 3, 6, 7, 8, 9, 10
Appendix D.
- If the reader is only interested in the effects of flow barriers,
- read Chapters 7, 9 and 10.
- If the reader is only interested in the flow through the repository SFL 3-5,
- read Chapters 1, 8, 9 and 10, as well as Appendix D.
- If the reader is only interested in the methodology of how to estimate the flow in closed tunnels and of the methodology of the stochastic continuum method,
- read Chapters 1, 2, 4 and 5 as well as Appendix A , B and C.
- If the reader is interested in the stochastic continuum approach for representation of a heterogeneous flow medium, the scale dependency of the hydraulic conductivity, numerical considerations of the stochastic continuum method, an analytical method for scaling of measured conductivity values, as well as general aspects on how to use the stochastic continuum method,
- read Chapter 5.
- If the reader is only interested in the effects of a heterogeneous flow medium,
- read Chapters 5, 6 and 7, as well as Sec.9.7 and Sec.10.3.
- If the reader is only interested in the finite difference method,
- read Appendix A.

V. Acknowledgements

This study has been conducted as a part of the research work at the program for Quaternary Geology II at the Institute of Earth Sciences, Uppsala University.

The author would like to express his gratitude to the many friends and colleagues that have supported his work; special thanks to:

Dr. Ulf Qvarfort, my PhD advisor, for encouragement and trust in my ability.

My friends and colleagues at Golder Associates AB, Dr. Sven Follin, for helping me with the problems of scale dependency and stochastic continuum modelling, Mr. Karl-Lennart Axelsson and Mr. Anders Ekstav, for our discussions.

My friends and colleagues at SKB (Swedish nuclear fuel and waste management Co.), Dr. Lars O. Ericsson and Dr. Fred Karlsson, for providing me with an interesting topic and for their interest in my work.

The author would like to thank Mr. Roger Lagerquist, for checking my english. For the design of the cover and for editorial help, the author would like to thank the Editorial office at Uppsala University, Mr. Göran Engemar and Mr. Rolf Wetterlöf.

This work is dedicated to my beloved wife Anna.

Brussels, June 1997

Johan Georg Holmén

Chapter 1.

Introduction and purpose of study

1.1 Introduction

This study relates to the flow of groundwater in closed tunnels. By "closed tunnel" we mean a tunnel, or a system of tunnels, that forms an isolated unit, separated from other tunnels and shafts by the use of plugs, such as concrete and/or bentonite plugs. We presume that the groundwater flows through the tunnel and that the flow of groundwater through the tunnel is at equilibrium with the groundwater system, i.e. a closed tunnel is not kept dry, no pumping of groundwater takes place in the tunnel. A system of closed tunnels (a repository) could be used for the final storage of hazardous waste, such as radioactive and/or toxic waste.

The groundwater flow through closed tunnels is of interest when estimating the performance of a repository. That is, the performance as regards leakage of the stored waste, leakage to the surrounding environment. The flow of groundwater through the tunnels is of interest as components of the stored waste will dissolve in the groundwater and be transported by the regional groundwater flow to the surrounding environment.

1.2 Purpose of study

The purpose of this study is to gain knowledge of how closed tunnels will hydraulically interact with a surrounding rock mass. For that purpose, theoretical calculations have been performed with the use of mathematical models.

Parameters that control the size of the regional groundwater flow are not included in this study. Such parameters are: the topography, the groundwater recharge, the absolute value of the conductivity of the rock mass, etc. This is a generic study, therefore such parameters are not included, only parameters that influence the flow through tunnels at the scale of the tunnels are included in the study. The size of the calculated flow in a tunnel will be given as a multiple of an unknown regional groundwater flow.

As regards the flow in closed tunnels, we will study the following.

- The size of the flow in a tunnel as regards the direction of the regional flow of groundwater. The size of the flow in a tunnel as regards the conductivity, the length and the width of a tunnel. The size of the maximum theoretical flow in a tunnel.
- Effects of the heterogeneity of the surrounding rock mass, as regards the flow of a tunnel. Consideration of the amount of heterogeneity and the direction of the regional flow, as well as the size and the conductivity of the tunnel.
- Effects of flow barriers in a tunnel, as regards the flow in a tunnel. Consideration of the size and the conductivity of the flow barriers, as well as the size and the conductivity of the tunnel; we will also consider a heterogeneous rock mass and different directions of the regional flow.
- As an example of a system of closed tunnels, we will study the flow through the tunnels of the planned repository for long-lived, low and middle active nuclear waste, called SFL 3-5. We will estimate the flow through this repository, considering different properties of the tunnel system.

A fractured rock has heterogeneous hydraulic properties, which are scale dependent. In this study, heterogeneous properties have been represented by using the stochastic continuum approach.

- It is a purpose of this study to investigate the stochastic continuum approach, as regards the representation of a scale dependent heterogeneous conductivity.
- It is a purpose of this study to propose a method for the scaling of measured conductivity values, a method that is consistent with the stochastic continuum approach. We will also propose a method for calculation of the node-to-node conductivity (homogenized conductivity) in finite difference models which uses the stochastic continuum method.

As a conclusion of the study, we will compare the effects of the different parameters controlling the flow of a closed tunnel or a system of closed tunnels (a repository). We will establish an order of precedence, as regards the parameters of importance.

1.3 Description of SFL 3-5

It has been proposed that the final repository for spent nuclear fuel (SFL 2) and the repository for long-lived nuclear waste (SFL 3-5) should be located at great depth (approximately 500 m below surface) in a fractured crystalline rock, a few kilometers from each other.

The repository SFL 3-5 consists of a system of tunnels, containing the nuclear waste. The preliminary lay-out of the repository is given in Forsgren *et al.*, (1996), this lay-out is briefly presented in Appendix E. The type of waste stored in the repository is discussed in Lindgren, *et al.*, (1994).

The nuclear waste will be contained and transported to the repository in different types of packages and boxes - containers. The containers will be stored in the repository. In the repository, the containers will be surrounded by different barriers. The most active waste will be surrounded by a concrete encapsulation. Between the encapsulation and the rock mass, the tunnels will be refilled with sand and/or bentonite. The repository is divided into three different parts.

- SFL 3: The most active nuclear waste will be stored in this part of the repository. The waste containers will be encapsulated in concrete. The concrete encapsulation will be surrounded by a flow barrier of sand and/or bentonite.
- SFL 4: The least active nuclear waste will be stored in this part of the repository. The waste containers will not be encapsulated in concrete. As the tunnels will be refilled with sand, the containers will be surrounded by sand.
- SFL 5: The waste containers will be encapsulated in concrete. The concrete encapsulation will be surrounded by a flow barrier of sand and/or bentonite.

For the design and for the safety analysis of the repository, it is necessary to have knowledge of how the surrounding rock mass and the repository will interact and form a hydraulic system. The site and the final design of the repository have not been decided and consequently no site-specific data are available. A generic hydraulic modelling has been performed based on a preliminarily design of the repository (Chapter 8 and 9).

Chapter 2.

Methodology

2.1 The system analysis approach

In this study the limited part of the reality that we are investigating is called *the system*. *The model* is a generalized description of the studied system.

The study is based on "the system analysis approach". The system analysis approach is a method for solving complicated problems by: (i) establishing a model of the studied system, (ii) using the model for simulations which imitate the behavior of the studied system and (iii) based on the results of the simulations, determine a solution to the investigated problem.

In this study, the method is carried out as follows. The first step is to formulate the objective of the modeling exercise. Our objective is to establish a model capable of predicting groundwater flow through a tunnel or a system of tunnels (the repository). Based on the objectives, and on available information of the system studied, a conceptual model is established. *The conceptual model* includes information of the studied media (repository and rock mass) and the physical processes governing the groundwater flow, but it includes only information relevant as regards the objectives of the study. Based on the conceptual model a formal model is established. *The formal model* is a mathematical description of the conceptual model, it is established by the use of a computer code. The formal model is used for simulations.

2.2 Mathematical approach to the studied media

A model will be established of the domain studied. The model will consist of the tunnels and the surrounding rock mass. The formal model used for simulation of the groundwater flow is a three-dimensional mathematical description of the studied hydraulic system.

The groundwater flow is controlled by the hydraulic properties of the medium in which it occurs, and of the hydraulic gradient. The gradient is created by the hydraulic properties of the medium, the local and regional topography as well as the groundwater recharge.

The repository will be located at great depth in a fractured crystalline rock mass. Groundwater flow in such a rock occurs in fractures and in fracture zones of different size and significance. These fractures and fracture zones determine the heterogeneous and anisotropic hydraulic properties of the rock mass. There are different ways of making a mathematical description of a fractured medium.

- One approach is to define the hydraulic and geometrical properties of each individual fracture larger than a certain size. By using a large number of fractures a model representing the studied medium (the rock mass) is established. This can be done in a deterministic way, if the detailed information is available, i.e. *a deterministic discrete fracture model*, or in a stochastic way if detailed information is not available, i.e. *a stochastic discrete fracture model*.
- Another approach is the continuum approach, this is the traditional and most common technique. The continuum approach replaces the fractured medium by a representative continuum in which spatially defined values of hydraulic properties can be assigned to blocks of a certain size (see Appendix A). A large number of blocks

represents the studied medium (the rock mass). Properties may be assigned to the blocks in a deterministic way, if the detailed information is available i.e. *a deterministic continuum model*. If we replace a heterogeneous property (e.g. the conductivity) with an average value and assign that value to the blocks of a model, we will get a model that we will call *a uniform continuum model*. If detailed information of the hydraulic properties are unknown, or if the medium studied is heterogeneous and the size of the blocks that we want to use is smaller than a representative elementary volume (see Appendix A), and we want to include the heterogeneity into the model, we can use *a stochastic continuum model*. In a stochastic continuum model the hydraulic properties of the blocks are described by stochastic distributions selected to fit the size of the studied blocks (see Chapter 5).

The different methods should be regarded as different ways of generalizing the system studied, when establishing a mathematical model representing the system. Each of the methods has its advantages and disadvantages. The different methods of modelling are illustrated in figure 2.1.

A tunnel may contain a flow barrier or a back filling, made of sand and bentonite; these materials are porous media, the best way to represent them is by the use of the continuum approach. Concrete barriers, such as the encapsulation of SFL 3, is probably best described as a mixture of a porous and a fractured medium, a mathematical description could be based on both, or a combination of the two approaches. A fractured rock mass is a medium with heterogeneous properties. If the studied scale is small, the medium is best described with a discrete fracture approach. If the scale is larger, a continuum approach can be used.

A mathematical model that tries to represent the physical processes as closely as possible, should use the following mathematical descriptions for the different media: a discrete fracture approach for the rock mass, a continuum approach for the sand and the bentonite, and a combined approach for the concrete encapsulation. However, when we generalize the system studied and establish a model representing it, we also have to consider the purpose of the study and the available data. Therefore, it is not always necessary to use the method that most closely imitates the physical reality to achieve the objectives.

The approach is to carry out a generic study of how a closed tunnel, or a system of closed tunnels, will hydraulically interact with a surrounding rock mass, considering different design alternatives and different properties of the rock mass. It will be a generic study, as the purpose of the study is to obtain generic information. As regards the studied repository (SFL 3-5), no specific site is selected and the final design is not yet decided. Hence, as no site specific data are available, no site specific modeling could be performed.

To meet the objectives of the study, it is concluded that the modelling will be based on the continuum approach. The continuum approach is implemented by the use of both an analytical method and a numerical method. The numerical model will represent the rock mass that surrounds a tunnel, both by the use of uniform continuum models and by the use of stochastic continuum models. An advantage of the continuum approach is that a homogeneous medium can be easily changed to a heterogeneous medium, just by changing the properties of the blocks of the model (changing from uniform continuum to stochastic continuum). Hence, a comparison between a model representing a homogeneous medium and a model representing a heterogeneous medium is simple, if we use the continuum approach.

The formal model is a three-dimensional mathematical description of the studied hydraulic system. Groundwater flow will be calculated with the use of Darcy's law (Darcy, 1856). Darcy's law assumes a non-deformable flow medium and that the inertial effects and the internal friction inside the fluid are negligible; these generalizations are applicable, considering the flow system studied. Hence, the governing equation for flow in a porous medium is the following differential equation (constant fluid density, the X direction and the Y direction lie in the horizontal plane, the Z direction in the vertical plane).

$$\frac{\partial}{\partial x} \left(K_x \frac{\partial \phi}{\partial x} \right) + \frac{\partial}{\partial y} \left(K_y \frac{\partial \phi}{\partial y} \right) + \frac{\partial}{\partial z} \left(K_z \frac{\partial \phi}{\partial z} \right) - VF = Ss \frac{\partial \phi}{\partial t} \quad (2.1)$$

$K_x, K_y, K_z =$ Hydraulic conductivity along axes $[L t^{-1}]$

$\phi =$ Piezometric head (groundwater head) $[L]$

$VF =$ Volumetric flow (flow per unit volume, inflow and outflow of water) $[T^{-1}]$

$Ss =$ Specific storage of medium $[L^{-1}]$

$t =$ Time $[T]$

The development of Equation 2.1 from Darcy's law is well known, see for example Bear and Verruit (1987), Bear and Bachmat (1990), Strack (1989) or Appendix A. As the modelled scenario is not time-dependent (See Section 2.4), Equation 2.1 will be reduced to the following equation.

$$\frac{\partial}{\partial x} \left(K_x \frac{\partial \phi}{\partial x} \right) + \frac{\partial}{\partial y} \left(K_y \frac{\partial \phi}{\partial y} \right) + \frac{\partial}{\partial z} \left(K_z \frac{\partial \phi}{\partial z} \right) - VF = 0 \quad (2.2)$$

Equation 2.2, constitutes together with initial conditions and boundary conditions, a mathematical representation of a flow system. Analytical solutions to the equation normally exist only for very generalized cases. Consequently, models representing tunnels with complicated properties, or models representing a heterogeneous flow medium, have to be models based on numerical methods - in this study the finite difference method.

2.3 Definition of computer codes

The formal model is a three-dimensional mathematical description of the studied hydraulic system. The analysis will be based on the continuum approach.

We will use an analytical model, based on a method proposed by Carslaw and Jaeger (1959), the analytical model will be implemented by simple algorithms programmed in the Fortran and in the Basic programming languages.

We will also use a numerical model, the GEOAN model, this is a finite difference model. The finite difference method and the GEOAN model are briefly presented in Appendix A, the model was first presented by Holmén (1992). The GEOAN model is programmed in the Fortran programming language.

2.4 Time dependency

During and after construction of tunnels there will be a groundwater drainage and a lowering of the groundwater head within a volume of the rock mass, larger than the volume of the tunnels. When the tunnels are abandoned and no longer kept dry, the groundwater head will rise in the tunnels and after some time reach a new equilibrium.

The tunnels will change the groundwater flow pattern, compared to the situation without the tunnels.

The models will simulate the flow through closed tunnels, i.e. the models simulate a situation when all tunnels are filled with groundwater and the groundwater situation has reached an equilibrium. Thus, the modelling is carried out under steady state conditions and is not time dependent.

2.5 Size of model and boundary effects

The analytical models presume that the tunnel studied is located in an infinitely large flow medium (rock mass). There are no outer boundaries in the analytical models. Hence, there are no boundary effects caused by such boundaries.

A numerical model defines a three-dimensional body in space, divided into a number of smaller volumes, called blocks or cells. Every cell represents a part of the studied system. The arrangement of cells is called the mesh (see Figure A.1). A numerical model represents only a limited part of the flow medium (rock mass) in which the tunnel is located. At the outer boundary of the model, boundary conditions define how the model simulates the hydraulic interaction with the flow medium not included in the model. To make a good model of the studied system, it is necessary that the model be three-dimensional, i.e. the mesh should contain cells in three dimensions and have a size larger than the studied tunnels. Three-dimensional models place great demands on computer capacity. To minimize the computation time, the number of cells in the mesh has to be limited, but still many enough to represent the flow system well. The limited size of the numerical model will influence the simulations. Such effects are called boundary effects. In this study the boundary effects have been estimated and their effect on the predicted flow quantified.

2.6 Simulation of regional groundwater flow

In nature, the groundwater flow is created on a regional scale as the result of phenomena such as: groundwater recharge, ground surface topography, hydraulic conductivity, etc. In this study we have not established a regional model, as the results of this study should be generic and not site-specific.

The regional flow in a fractured rock is a difficult concept, as it depends not only on the properties given above, but also on the heterogeneity of the rock mass. However, in this study we assume that such a flow exists and can be averaged for a rock volume of approximately the same size as the volume represented by the model. If no regional flow exists for such a rock volume, then, when equilibrium has been reached after closure of a tunnel, there will be no flow through the tunnel.

In the model, the regional groundwater flow is created at the boundary of the model according to prescribed conditions. By the use of this method, different directions and gradients of the regional groundwater flow could be generated, and the effects of different directions and gradients could be compared. The method for generation of the regional groundwater flow is given in Appendix C. Examples of different directions of the regional flow in relation to a studied structure (a tunnel), are shown in Figure 2.2.

2.7 Size and direction of regional groundwater flow

The purpose of the study is to predict the flow in closed tunnels. This flow is dependent on the regional groundwater flow and the hydraulic conductivity of the rock mass, as well as on the properties of the tunnels. As it is a generic modelling, the direction and size of the regional groundwater flow and the hydraulic conductivity of the rock mass is unknown. To overcome this problem, the regional specific flow was set to 1 [$L^3/(L^2 T)$], and the specific flow and the total flow in the tunnels were calculated as multiples of the prescribed regional specific flow. With the use of this method, the results of the study are applicable to any regional groundwater flow, as the calculated flow can be regarded as a multiple of an unknown flow. To overcome the problem of the unknown direction of the regional flow, the flow in the tunnels was calculated for different directions of the regional flow. Examples of different directions of the regional flow in relation to a studied structure (a tunnel), are shown in Figure 2.2.

2.8 The concept of flow in a tunnel

This study investigates the flow in closed tunnels, we assume that the tunnels are abandoned, no longer kept dry and that the groundwater system is in equilibrium (steady state). Under such conditions a tunnel receives water from the rock mass at different sections along the tunnel, and gives water to the rock mass at other sections along the tunnel. Thus, the flow and velocity of water inside the tunnel varies along the tunnel. We note that the tunnel is not a tube that receives water at one end and gives it away at the other end, it receives water along an upstream part and gives it away along a downstream part. What is upstream and downstream depends on the direction of the tunnel and the direction of the regional groundwater flow. The flow of water in a tunnel can be studied based on two different concepts: "specific flow" and "total flow". Both concepts are used in this study.

Specific flow is defined as a flow per unit area [$L^3 / (L^2 T) = L / T$]. It could also be looked upon as a velocity, as a flow per unit area could mathematically be reduced to a velocity [L / T]. But, when looking upon the specific flow as a velocity, one has to understand that it is not the actual velocity of the water. To calculate the actual velocity one also has to regard the effective porosity of the studied medium. The specific flow gives information about the flow at a local point. Average specific flow in a tunnel is the average of the specific flow in all cells representing the tunnel, it gives information of average flow and average velocity inside the tunnel.

Total flow is defined as the flow that enters a tunnel [L^3 / T]. The simulations occur under steady state conditions, consequently the same amount of water will leave the tunnel. The calculations of total flow are based on a mass balance taken over the envelope surface of the studied structure. The total flow gives information about the amount of water that "visits" the tunnel. The total flow could be divided by the volume of the tunnel [$(L^3 / T) / L^3 = T^{-1}$], it then provides information about the amount of water that on the average visits one unit volume of the tunnel (volumetric flow). If the tunnel system is complex, it is possible that water, which previously has been inside the tunnel system, reenters the tunnel system at some other point downstream. Such water will be added to the total flow every time it enters the tunnel system.

The flow in a tunnel depends, among other parameters, on the direction and size of the regional groundwater flow. The average specific flow and the total flow provide information of different aspects of the flow in a tunnel. Extreme values of average specific flow and total flow, do not always occur for the same direction of the regional

groundwater flow. For example: the maximum average specific flow inside a tunnel may occur when the regional flow of groundwater is directed along the length of the tunnel - a small amount of water is transported a long distance inside the tunnel with a large velocity. For the same system, maximum total flow may occur when the regional flow is approximately directed at right angles to the length of the tunnel - a large amount of water is transported with a low velocity a short distance inside the tunnel. If the permeability of the tunnel is much larger than that of the rock mass, maximum total flow and maximum average specific flow may occur for the same direction of regional flow. For such a scenario, more water is transported using a high velocity and a small area than with a low velocity and a large area.

2.9 Hydraulic conductivity

The hydraulic conductivity is a property of the flow medium; it is a measure of the ease with which the groundwater is transported through the medium. For the hydraulic conductivity we will use the letter K.

2.10 Advection and diffusion

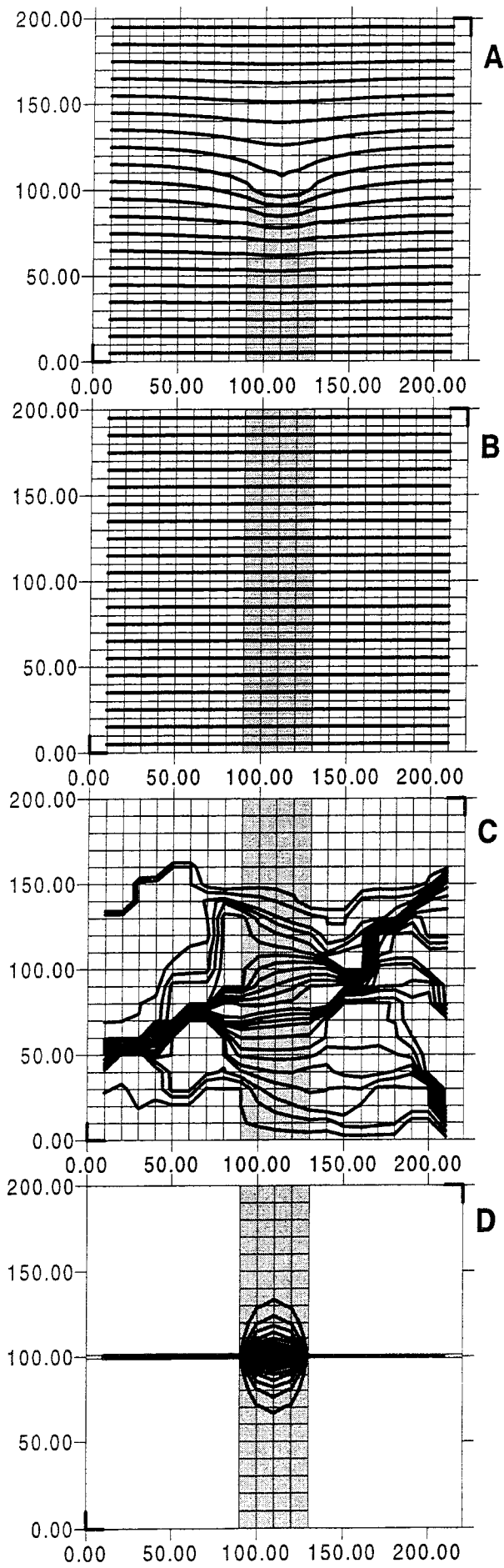
A solute is carried along with the flowing groundwater. This process is called advective transport or "advection". The amount of solute that is being transported is a function of its concentration in the groundwater and the size of the groundwater flow. A solute in water will move from a domain of greater concentration toward a domain where it is less concentrated. This process is called "diffusion". Diffusion will occur as long as a concentration gradient exists, even in the fluid is not moving.

In this study we estimate the size of the groundwater flow. Hence, for a solute in the groundwater with a known concentration, we estimate the advection. This study is a generic study of groundwater flow in tunnels, we have not studied diffusion.

The importance of diffusion as a transport process for solutes, depends on the size of the groundwater flow. "Diffusion is a relatively slow process. In zones of active groundwater flow its effects are usually masked by the effects of the bulk water movement. In low-permeability deposits such as clay or shale, in which the groundwater velocities are small, diffusion over periods of geologic time can, however, have a strong influence on the spatial distribution of dissolved constituents." Freeze and Cherry (1979).

In a highly permeable tunnel, the flow of groundwater is much larger than the regional groundwater flow in the surrounding rock mass. Hence, unless the size of the regional groundwater flow is very small, the diffusion is not the most important transport process in such tunnels. However, in a tunnel encapsulation surrounded by an effective flow barrier (see Chapter 7) or in a tunnel with a very low permeability (see Chapters 3 and 6), the flow of groundwater can be much smaller than the regional groundwater flow in the surrounding rock mass. For such systems the diffusion can be the most important transport process. Presuming that the regional groundwater flow is not to large.

This study relates to the flow of groundwater in closed tunnels; the results of this study can be used for estimation of the transport of solutes from closed tunnels. However, when estimating the transport of solutes from closed tunnels diffusion could be an important parameter, the importance of diffusion should be checked, and if necessary the effects of diffusion should be included in the estimation of the solute transport.

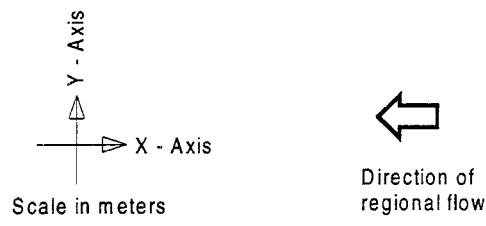


A: UNIFORM CONTINUUM MODEL
 Rock mass modeled as a uniform continuum
 Tunnel modeled as a uniform continuum
 Conductivity of rock mass = 1
 Conductivity of tunnel = 100

B: UNIFORM CONTINUUM MODEL
 Rock mass modeled as a uniform continuum
 Tunnel modeled as a uniform continuum
 Conductivity of rock mass = 1
 Conductivity of tunnel = 1

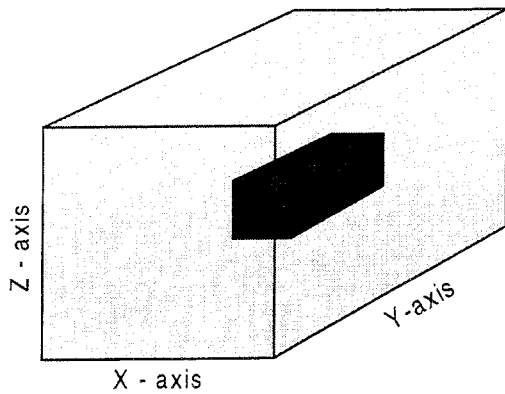
C: STOCHASTIC CONTINUUM MODEL
 Rock mass modeled as a stochastic continuum
 Tunnel modeled as a uniform continuum
 Conductivity of rock mass: Log normal distribution.
 Cell conductivity: Geo. mean = 1
 Cell conductivity: standard dev. of Log K = 2
 Conductivity of tunnel = 1
 Figure (C) demonstrates a possible flow pattern in a heterogeneous rock mass. The figure is based on one realization of the conductivity field.

D: DISCRETE FRACTURE AND CONTINUUM MODEL
 Rock mass modeled as discrete fractures in non permeable rock.
 Tunnel modeled as a uniform continuum.
 Conductivity of rock mass = 1 (in direction of X-axis)
 (Conductivity of fracture= 100, width= 2 m)
 (Conductivity of rock= 0)
 Conductivity of tunnel = 1



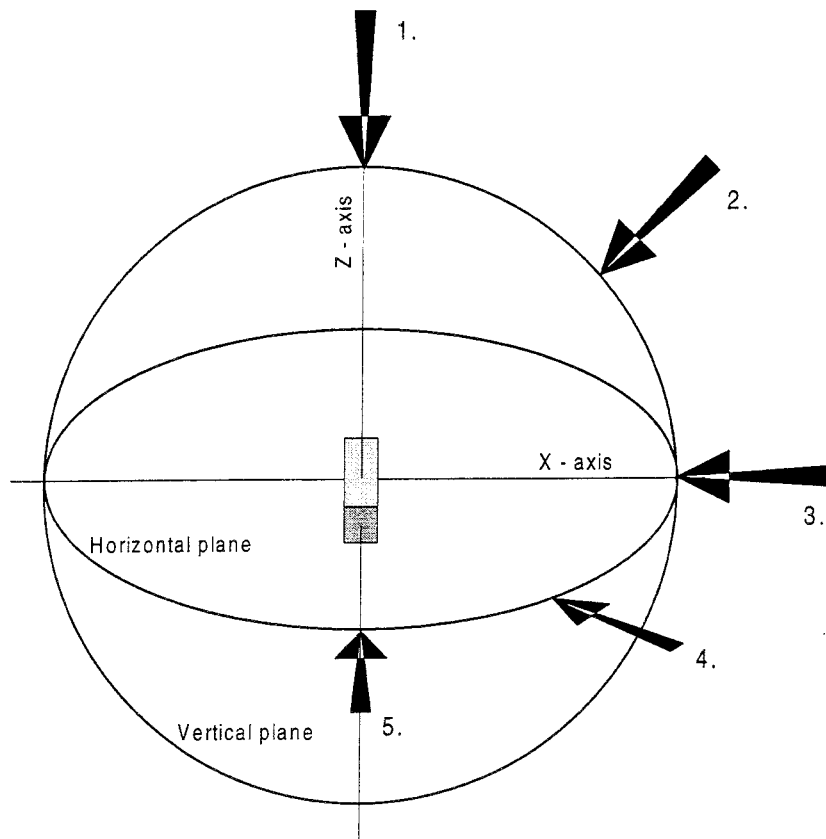
- Cells representing the tunnel.
- Cells representing the rock mass.
- Flow path, the larger the number of flowpaths in a cell, the larger the flow.

FIGURE 2.1
MODELLING APPROACH AND FLOW PATTERN
 Different modelling approaches to the studied media.
 Flow pattern of the groundwater, as given by the different methods of representation.



Three dimensional view of a model representing a studied structure and surrounding rock mass.

- Volume representing rock mass.
- Volume representing a studied structure (a tunnel, a repository etc).



Different directions of the regional flow.

1. Vertical flow. Flow at right angle to the structure, along the short axis of the structure and along the Z-axis of the coordinate system.
2. Flow at a right angle to the structure and at 45 deg. from the horizontal plane of the coord. system.
3. Flow at a right angle to the structure, along the short axis of the structure and in the horizontal plane along the X-axis of the coord. system.
4. Flow in the horizontal plane 45 deg. from the X-axis and the Y-axis of the coordinate system and 45 deg. from the direction of the structure.
5. Flow along the structure, along the main axis of the structure and along the Y-axis of the coord. system.

- Object representing the studied structure (a tunnel, an ellipsoid, etc).
The main axes of the object is in the horizontal plane.

FIGURE 2.2 DIFFERENT DIRECTIONS OF THE REGIONAL GROUNDWATER FLOW.

Chapter 3.

General aspects of flow in tunnels, analytical method

3.1 Introduction

In the following chapter, some general aspects of flow in a closed tunnel are discussed. The calculations are based on an analytical approach assuming steady state conditions, a homogeneous isotropic rock mass and a tunnel with an homogeneous isotropic conductivity. The discussion below is applicable to a situation for which the studied structure (a tunnel) has been closed and sealed. No pumping takes place in the tunnel and the groundwater situation has reached an equilibrium. The analytical method is briefly presented in Appendix B, which also includes a comparison between results obtained with an analytical and a numerical method.

3.2 Analytical method

Mathematical methods derived for calculation of conduction of heat or electric current are applicable for calculation of groundwater flow, if confined conditions could be assumed for the flow medium or the position of the phreatic surface is known. Before efficient computers became available, analytical methods were derived for a large number of problems. The problem of steady flow of heat or fluid in a medium containing an object having a different conductivity than the surrounding medium, is of technical importance and analytical methods have been derived. "Mathematically, it is precisely the same (problem) as that of induced magnetization in a body of the same shape placed in a uniform external field, and solutions will be found in text books on electricity and magnetism" (Carslaw and Jaeger, 1959).

In Appendix B analytical formulas are given, formulas that define the head inside a sphere, a cylinder and a spheroid (an ellipsoid). The formulas are taken from Carslaw and Jaeger (1959). They were originally derived for calculations of heat in solids and have been rewritten and developed to be applicable for flow of groundwater.

The formulas presume steady state conditions. The rock mass is represented by an infinitely large homogeneous isotropic medium. The basic formulas give the head inside and outside of a sphere, and an ellipsoid, for any direction of the regional flow; and the head inside a cylinder, if the regional flow is directed at right angles to the main axis of the cylinder.

We should note that the analytical method presumes that the tunnel is surrounded by a homogeneous medium. A fractured rock is a heterogeneous medium. The effects of the heterogeneity is studied in Chapter 6.

3.3 Definition of terms

In the following sections we will use terms that correspond to the geometry of an ellipsoid, terms like: main axis, short axis, cross-section at right angles to the main axis, cross-section at right angles to the short axis, etc. These terms are defined in Figure 3.1 and Figure B.1. When we discuss the direction of the regional flow, the direction will be given in relation to the shape of an ellipsoid, e.g. flow along main axes, flow along short axis, such directions are demonstrated in Figure 3.1.

3.4 General aspects of flow in a tunnel

The flow in a tunnel will vary along the tunnel. The size of the flow in a tunnel depends on: (i) lay-out, length and size of the tunnel, (ii) properties of filling and barriers inside the tunnel and (iii) direction and size of the regional groundwater flow as well as (iv) the heterogeneity of the surrounding rock mass.

From a general point of view, as regards direction of the regional flow, the flow of a tunnel (ellipsoid) will vary in the following way.

- *Specific flow.* The largest average specific flow inside a tunnel will occur when the regional flow is along the tunnel (along the main axis) or in an angle close to the direction of the tunnel. The smallest average specific flow inside a tunnel occurs when the regional flow is directed at right angles to the tunnel (along the short axis).
- *Total flow.* It is more difficult to predict the total flow than the specific flow as the total flow depends on the exposed area in the direction of regional flow, as well as on the tunnel conductivity.
 - If the conductivity of the tunnel is small compared to the conductivity of the rock mass, or slightly larger than that of the rock mass, maximum total flow will occur when a large area of the studied tunnel is exposed to the regional flow (regional flow along short axis) and minimum total flow will occur when a small area is exposed (regional flow along main axis).
 - If the conductivity of the tunnel is large compared to the conductivity of the rock mass, maximum total flow will occur when the regional flow is directed along the tunnel (along the main axis) and minimum total flow will occur when the regional flow is directed at right angles to the tunnel (regional flow along short axis).

It should be noted that extreme values (maximum or minimum) of the average specific flow and the total flow do not always occur for the same direction of the regional groundwater flow, even if the structure studied is homogeneous.

If the tunnel has a small conductivity, the flow in the tunnel will be small, if the conductivity is large the flow in the tunnel will be large. However, an increase of the conductivity of the tunnel will only have a large effect on the flow in the tunnel, if the tunnel conductivity is small. If the conductivity of a tunnel is large a much more conductive tunnel will not have a much larger flow, as the flow in such a tunnel is mainly dependent on the conductivity of the surrounding rock mass.

Above we have discussed the average specific flow of a tunnel and the total flow of a tunnel, these properties correspond to the whole of the tunnel. We will now discuss the variation (distribution) of flow inside the tunnel. For a large tunnel, the variation of the flow inside the tunnel is mainly dependent on the direction of the regional flow, in relation to the tunnel lay-out. Consider a tunnel more conductive than its surroundings; in the upstream part of the tunnel, groundwater will flow towards the tunnel from the surrounding rock mass and into the tunnel. The flow inside the tunnel will increase and reach its maximum somewhere in the middle of the tunnel. In the downstream part of the tunnel, the flow inside the tunnel will decrease, and water will flow out from the tunnel. For all directions of regional flow, there will be an upstream and a downstream part. If the regional flow is directed at right angles to the tunnel, the upstream and downstream parts are opposite and parallel along the tunnel. The variation of specific flow inside a tunnel is discussed in Sec.6.8 and Sec.9.5.

3.5 General aspects of the flow in an ellipsoid

Using the analytical method presented in Appendix B, head contours for an ellipsoid and the surrounding media have been calculated (equ.B.16 and equ.B.17). Calculations have been carried out for different directions of regional flow and different values of conductivity of the studied ellipsoid. The results are given in Figures 3.2 and 3.3.

As regards flow through a sphere or an ellipsoid (a spheroid), we can see from equations B.2, B.7 and B.16, that the head inside the spheroid varies in a linear way. Consequently, for a studied spheroid and a studied direction of regional flow, the specific flow (flow per unit area) inside the spheroid is constant, it does not change from point to point (see equation B.33). This is a special property of these bodies and it is not similar to the way the specific flow varies inside a body with a rectangular or semi-rectangular cross-section (a tunnel). In a tunnel more conductive than its surroundings and with a rectangular cross-section, the specific flow increases from the upstream end towards the middle of the tunnel and then decreases towards the downstream end (assuming a homogeneous tunnel). The reason why the specific flow is constant inside a spheroid, is the change in cross-section area along the direction of the flow. - The change in cross-section area prevents a change in specific flow.

The total flow at a cross-section inside a spheroid (flow in: length³/time) is not constant, it changes inside the spheroid, as the cross-section area changes. The total flow inside a spheroid increases, from the upstream end of the spheroid to the middle of the spheroid, as the cross-section area increases. From the middle of the spheroid and towards the downstream end the cross-section area decreases, and so does the total flow.

The total flow for a studied body can be calculated as all the water that enters or leaves the body studied, assuming mass conservation. Depending on the direction of the regional flow, somewhere inside the body a cross-section occurs - a *delimiting cross-section*, at this cross-section the flow will be in balance; upstream of it water is flowing into the body and downstream of it water is flowing out of the body. If the regional flow is directed along one of the axes of a spheroid, the above discussed delimiting cross-section occurs at the middle of the spheroid, at right angles to the direction of the regional flow. Hence, for a spheroid, if the regional flow is directed along one of the axes, all water that enters the studied body will pass through a delimiting cross-section located at the center of the spheroid. This makes it possible to calculate the total flow for a spheroid as: (i) the specific flow times, (ii) the area of the cross-section at the center of the spheroid at right angles to the direction of the regional flow.

It should be noted that for a tunnel with a rectangular (or semi-rectangular) cross-section, a rectangular parallel-piped, the product of: (i) the average specific flow inside it, times, (ii) the area of the rectangular cross-section; will not produce the total flow of the studied structure. This is because the specific flow is not constant inside such a structure and the average specific flow inside the structure is not the specific flow at the delimiting cross-section. For a tunnel with a rectangular cross-section the specific flow at the delimiting cross-section is larger or smaller than the average specific flow, depending on the tunnel conductivity. The numerical model used in this study calculates the total flow, based on a mass balance taken over the envelope of the studied structure.

Based on the discussion above it is obvious that if we use an ellipsoid as a representation of a tunnel with a rectangular or semi-rectangular cross-section, we have to select the properties of the studied ellipsoid with some care to get a good result.

3.6 Comparison between the analytical and the numerical method

The analytical method can be used for prediction of flow in tunnels. The tunnels that are studied very rarely have the shape of an ellipsoid. Therefore, if we use the ellipsoid of the analytical method for the representation of a tunnel, we have to be aware of that the results that we obtain are an approximation of the flow in the tunnel. It is of interest to select an ellipsoid that produces flow values that are as close as possible to the actual values of the studied tunnel. In Appendix B we compare flow values predicted by the analytical method to flow values predicted by a numerical method. The numerical method is a finite difference method, for the numerical method the studied body is a rectangular parallel-epiped. The analytical method is presented in Appendix B, the studied body is an ellipsoid.

Hence, we will compare the flow in a rectangular parallel-epiped to the flow in an ellipsoid. We will study different ellipsoids that give flow values which are in line with the values predicted by the numerical model.

We will select an ellipsoid which has the same length and conductivity as the studied tunnel. This is perhaps not always the best choice, but we want to have only one parameter to vary, and therefore we have decided that the studied ellipsoid should have the same length and conductivity as the studied parallel-epiped. The parameter to vary becomes the length of the short axis of the ellipsoid (the width of the ellipsoid). Two different alternatives seem natural.

- Case A. We select the length of the short axis (the width) in such a way that the cross-section at the center of the ellipsoid, at right angles to the main axis, will have an area equal to the area of the cross-section of the studied parallel-epiped (the cross-section at right angles to the length of the parallelepiped). Selecting the length of the short axis in this way will produce an ellipsoid which has a volume that is $2/3$ of the volume of the parallel-epiped, and which has an average area of cross-sections at right angles to the main axis that is $2/3$ of the cross-section of the parallel-epiped.
- Case B. We select the length of the short axis (the width) in such a way that the average area of the cross-sections, at right angles to the main axis of the ellipsoid (see Appendix B.3), will be equal to the area of the cross-section of the studied parallel-epiped (the cross-section at right angles to the length of the parallel-epiped). Selecting the length of the short axis in this way will produce a maximum area at the center of the ellipsoid (area at right angles to the main axis) which is 50% larger than the average area of the parallel-epiped, but a volume of the ellipsoid that is equal to the volume of the parallel-epiped.

Calculations have been carried out for both cases, and for different scenarios. The different scenarios represent: two different directions of regional flow (along the main axis or along the short axis) as well as different conductivity values and lengths of the studied structures. The results are given in Tables B.1 and B.2 as well as in Figures B.3 and B.4, both specific flow and total flow are given.

Regional flow directed along the short axis of the studied structures.

- For specific flow, the differences between the two methods (numerical and analytic) are approximately 30 to 40 percent for all studied scenarios and for both cases.
- For total flow, the differences vary from approximately 10 to 40 percent. Case A gives a better estimate of the total flow in the parallel-epiped if the conductivity of the studied structure is larger than that of the rock mass, differences are about 20 percent. Case B gives a better estimate of the total flow in the parallel-epiped if the

conductivity of the studied structure is smaller than that of the rock mass, differences are about 25 percent

- If one uses the analytical method for estimation of the total flow of a tunnel with a conductivity that is much larger than that of the rock mass (an empty tunnel or a tunnel filled with a highly conductive backfilling), the best results are produced by Case A. If one studies the total flow of a structure with a conductivity that is less than that of the rock mass, the best results are produced by Case B. When studying the specific flow, Case A is slightly better than Case B.

Regional flow directed along the main axis of the studied structures.

- For most scenarios, Case B produces flow values that are more in line with the flow values predicted by the numerical model than the values produced by Case A, the differences are smaller for Case B than for Case A.
- For specific flow, Case B is always better than Case A.
- For total flow, Case B is best, except if the conductivity of the structure is equal or larger than that of the rock mass, but approximately smaller than 100 times that of the rock mass. If one uses the analytical method to estimate the total flow of a tunnel with a conductivity that is much larger than that of the rock mass (an empty tunnel or a tunnel filled with a highly conductive backfilling), the best results are produced by Case B. If one studies the total flow of a structure with a conductivity that is smaller than that of the rock mass, use Case B. When studying the specific flow, use Case B.
- If the conductivity of the studied structure is larger than that of the rock mass and considering both specific flow and total flow, the differences between the two methods (analytical and numerical) are, for most scenarios, less than 15 percent.
- If the conductivity of the studied structure is smaller than that of the rock mass, the differences in total flow predicted between the two methods are, for all studied scenarios, larger than 40 percent, and for Case A the difference in total flow is about 70 percent, which is a significant difference.

The numerical models are influenced by boundary effects. Estimation of these effects have been carried out (see Chapter 4). It is estimated that the maximum error in flow that will take place in the above discussed numerical simulations, is an overestimation of the flow of about 2 percent when the conductivity contrast is 10 000 times. If the conductivity contrast is smaller, the overestimation is smaller. As the error is small, no correction has been carried out.

3.7 Flow in an ellipsoid-tunnel, for a regional flow at right angles to the ellipsoid-tunnel (flow along the short axis of an ellipsoid)

To calculate the flow in a tunnel, when the regional flow is directed at a right angles to the tunnel, we can use equations B.10 and B.11. These equations are valid for a cylinder of infinite length. The equations will provide us with a good estimate of the flow in a tunnel, if the length of the tunnel is much larger than the diameter of the tunnel. Another alternative is to represent the tunnel by an ellipsoid and use equation B.28 or B.33. This might be a better approximation if the tunnel is short compared to the tunnel diameter. However, the differences between the flow predicted by the different equations are, for most cases, minimal. But, to get a good prediction out of these equations, it is important that the tunnel is approximately straight in relation to its length, the equations do not work well for a bent tunnel. In the following examples we have used the approximation of an ellipsoid, the ellipsoid is defined according to Case B (Sec.3.6).

Equation B.28 or B.33 will give us a specific flow. The specific flow times the area of a cross-section, at right angles to the regional flow, gives the total flow. The cross-section

studied is at the center of the ellipsoid and at right angles to the short axis, which is at right angles to the direction of the regional flow. The cross-section studied is the cross-section with the largest area at right angles to the regional flow.

The specific flow and the total flow obtained is given in Figures 3.4 and 3.5, for ellipsoids of different size. The figures show the flow for (i) different conductivity values of the ellipsoid as well as (ii) different lengths of the ellipsoid (50m to 300m) and (iii) different average areas of the ellipsoid cross-section at right angles to the main axis of the ellipsoid (50m^2 or 160m^2 .)

The regional flow is at right angles to the main axis of the ellipsoid, therefore the specific flow in the ellipsoid depends on the conductivity only. For this direction of regional flow, the specific flow in the ellipsoid is not dependent on the length of the main axis (the length of the ellipsoid) or the average cross-section area in the direction of the main axis.

The value of the specific flow is twice the regional flow. This is also the maximum specific flow predicted for a cylinder (see equation B.11). The total flow is directly proportional to the specific flow and the cross-section area of the ellipsoid at right angles to the regional flow (average area).

3.8 Flow in an ellipsoid-tunnel, for a regional flow along the ellipsoid-tunnel (flow along main axis of an ellipsoid)

To calculate the flow in a tunnel, when the regional flow is directed along the tunnel, we can use equation B.27 or B.33. By the use of these equations, we represent the tunnel by an ellipsoid. The equations will provide us with a good estimate of the flow if the tunnel is straight and not bent. Calculations were carried out for an ellipsoid representing a tunnel, defined according to Case B (Sec.3.6)

Equation B.27 or B.33 will give us a specific flow. The specific flow times the area of a cross-section at right angles to the regional flow, gives the total flow. The cross-section studied is at the center of the ellipsoid and at right angles to the main axis, which is at right angles to the direction of the regional flow. The cross-section studied is the cross-section with the largest area at right angles to the regional flow.

The specific flow and the total flow obtained are given in Figures 3.6 and 3.7, for ellipsoids of different size. The figures show the flow for (i) different conductivity values of the ellipsoid as well as (ii) different lengths of the ellipsoid (50m to 300m) and (iii) different average areas of the ellipsoid cross-section at right angles to the main axis of the ellipsoid (50m^2 or 160m^2).

The regional flow is along the main axis of the ellipsoid; therefore the specific flow in the ellipsoid depend on both the conductivity and the length of the ellipsoid, as well as on the average cross-section area at right angles to the main axis of the ellipsoid. The total flow is directly proportional to the specific flow and the cross-section area of the ellipsoid at right angles to the regional flow (average area).

3.9 Specific flow in an ellipsoid-tunnel, sensitivity to direction of regional flow

To calculate the specific flow in a tunnel for any direction of the regional flow, we use equation B.33 or B.34. By the use of these equations, we represent the tunnel by an ellipsoid. The equations will provide us with a good estimate of the flow, if the tunnel is

straight and not bent. Calculations were carried out for an ellipsoid representing a tunnel defined according to Case B (Sec. 3.4). The conductivity of the ellipsoid was defined as larger or smaller than that of the surroundings. Four different conductivity contrasts were studied, contrast as regards the surroundings: (i) the ellipsoid is 100 times more conductive, (ii) the ellipsoid has an infinitely large conductivity, (iii) the ellipsoid is 0.01 times less conductive and (iv) the ellipsoid is 0.0001 times less conductive. The resulting specific flow is given in Figures 3.8 and 3.9.

The figures show contour lines representing the specific flow. The size of the flow should be regarded as a multiple of the size of an unknown regional groundwater flow. The X-axis and the Y-axis of the figures represent different angles defining the direction of the regional flow. The figures demonstrate the size of the specific flow; how it varies as the direction of the regional flow varies. The total flow of an ellipsoid will vary in a similar way.

For an ellipsoid much more conductive than its surroundings, minimum flow takes place when the regional flow is along the short axis, and maximum flow when the regional flow is along the main axis. For an ellipsoid less conductive than its surroundings, minimum flow takes place when the regional flow is along the main axis, and maximum flow when the regional flow is along the short axis of the ellipsoid. The relation between maximum and minimum flow depends on the length and conductivity of the ellipsoid (see next section).

3.10 Size of maximum flow in an ellipsoid-tunnel

From Figures 3.4 through 3.7, we see that the specific flow in the ellipsoid-tunnel increases as the conductivity increases; if the conductivity of the ellipsoid-tunnel is larger than that of the rock mass, the specific flow increases in an asymptotic way towards a maximum value. Based on an analysis of the equations giving the flow in an ellipsoid, it is possible to calculate that maximum value (see Appendix B). If the regional flow is directed along the main axis of the ellipsoid-tunnel the maximum flow is given by equation B.27 or B.34. If the regional flow is directed along the short axis of the ellipsoid-tunnel, the maximum flow is given by equation B.28 or B.34. The ellipsoid is defined according to Case B (Sec.3.6).

The maximum specific flow and the maximum total flow in an ellipsoid which has an infinitely large conductivity are given in Figures 3.10 and 3.11. The figures show the flow for, (i) different lengths of the ellipsoid (50m to 500m), (ii) different average areas of the ellipsoid cross-section at right angles to the main axis (10m^2 to 160m^2) and (iii) two different directions of regional flow, along the short axis and along the main axis.

Considering all directions of regional flow and a large conductivity, the largest value of flow in an ellipsoid-tunnel will take place for a regional flow along the main axis of the ellipsoid-tunnel. Minimum flow will take place for a regional flow along the short axis.

Figure 3.10 gives the maximum specific flow in an ellipsoid. For a regional flow along the short axis, the maximum specific flow is twice the regional flow, regardless of the size of the ellipsoid (Fig.3.10(i)). For a regional flow along the main axis, the specific flow increases with the length of the ellipsoid and decreases with the size of the cross-section area (Fig.3.10(ii)). Hence, for two ellipsoids of equal length, the largest specific flow occurs in the ellipsoid with the smallest width (smallest short axis).

Figure 3.11 gives the maximum total flow in an ellipsoid. The maximum total flow

increases with the length of the ellipsoid and the size of the cross-section area. If the regional flow is directed along the main axis, the total flow increases with the ellipsoid length in an exponential way (Fig.3.11(ii)), and if the regional flow is directed along the short axis, the total flow increases with the ellipsoid length in a linear way (Fig.3.11(i)).

If we compare the flow of the ellipsoid-tunnel, calculated for the two directions of regional flow studied, we see that the difference in flow increases with increased length of the ellipsoid-tunnel. Hence, as regards the flow of an ellipsoid-tunnel, the effect of the direction of the regional flow is larger for a long tunnel than for a short tunnel.

Considering a structure which has the shape of a sphere, the direction of regional flow becomes unimportant. The maximum specific flow for an infinitely permeable sphere is 3 times the regional flow (equation B.3) and the total flow is the cross-section area times the specific flow.

3.11 Threshold conductivity

Figures 3.4 through 3.7 demonstrate that an increase of the conductivity of the tunnel will only have a large effect on the flow in the tunnel, if the tunnel conductivity is small. If the conductivity of a tunnel is large, a much more conductive tunnel will not have a much larger flow, as the flow of such a scenario is mainly dependent on the conductivity of the surrounding rock mass. We can define a threshold conductivity as the conductivity when the derivative of the flow as regards the conductivity of the tunnel (ellipsoid) is set to a certain value. For the specific flow we set the derivative to 0.01 and for the total flow to 1:

$$\frac{dq_t}{dK_t} = 0.01 \quad ; \quad \frac{dQ_t}{dK_t} = 1 \quad (3.1)$$

q_t = specific flow, Q_t = total flow, K_t = conductivity

By approximating a tunnel with an ellipsoid and by using the analytical method, it is possible to calculate the threshold conductivity. This is done by calculating the conductivity values that produce a flow giving the derivatives as defined above. The calculations are based on equation B.33 and on numerical methods. The conductivity values (threshold conductivity) for these derivatives are given in Figures 3.12 and 3.13, they are also marked with crosses in Figures 3.4 through 3.7. The calculations were carried out for an ellipsoid representing a tunnel defined according to Case B (Sec.3.6)

The threshold conductivity is of interest when we discuss a tunnel filling. A tunnel filling has to have a conductivity which is smaller than the threshold conductivity to significantly reduce the flow in the tunnel. It is also of interest when we establish a numerical model representing a tunnel system. To get a fast and accurate numerical procedure, it is advantageous to simulate a system which has a limited difference in conductivity between the tunnel and the rock mass. When simulating a tunnel with a very large conductivity (an empty tunnel) the threshold conductivity is the smallest conductivity value that could represent such a tunnel (with a certain accuracy).

3.12 Influence radius of an ellipsoid-tunnel

An ellipsoid-tunnel more conductive than the surrounding rock will lower the head in the rock upstream of the ellipsoid-tunnel and increase the head downstream of it. The opposite will take place if the ellipsoid-tunnel is less conductive than the surroundings. Hence, the ellipsoid-tunnel will change the head in the rock compared to the undisturbed

situation. The undisturbed situation is the situation with no ellipsoid-tunnel and a uniform regional flow of groundwater. The volume of rock that will become influenced depends on the properties of the ellipsoid-tunnel and the rock, as well as on the direction of the regional flow. The analytical method, based on the uniform continuum approach, predicts that the change in head will be infinitely small at an infinitely large distance from the studied structure. The change will not be uniformly distributed around the ellipsoid, the largest change in head will occur close to the direction of the main axis.

The change in head has been calculated for different ellipsoids and different directions of the regional flow; the results are given in Figures 3.15 and 3.16. From the figures we conclude that the largest change in head will take place if the flow is directed along the main axis of the ellipsoid (tunnel), if the flow is directed along the short axis, the change is small. The larger the contrast in conductivity, the larger the change in head. However, if the conductivity is larger than the threshold conductivity, the change in head will be about the same. The figures were calculated for a regional flow of 1 m/s. Thus, the change in head could be looked upon as a multiple of an unknown regional flow, another regional flow will give the same contour line distribution, but different values of the change in head.

For all possible directions of regional flow, the largest change in head will take place if the flow is directed along the main axis of the ellipsoid-tunnel. For this situation, the largest change in head, outside of the ellipsoid-tunnel, will be in the direction of the regional flow. The change in head along this direction could be calculated in percent of the head of the undisturbed situation. Such a percentage will be the same, regardless of the size of the regional flow. The change in head in percent, along the direction of flow, for different ellipsoids, are given in Figures 3.17 through 3.19. The calculations were carried out for an ellipsoid representing a tunnel defined according to Case B (Sec.3.6)

Assume a certain change in head as a studied criterion (Y-axis of figures); for that criterion the figures show the maximum radius on which the ellipsoid will influence its surroundings (X-axis of figures). For example, study an ellipsoid with a length of 100m, an average cross-section area equal to 100m², and a conductivity contrast of 100 times (Figure 3.18(i)). For a change in head of 0.1% , the influence radius is approximately 210m. These figures will be of interest when we estimate boundary effects that will occur in numerical models (see Chapter 4).

3.13 Flow in an ellipsoid-tunnel, balance as regards direction of regional flow

The maximum flow in an ellipsoid-tunnel depends on the direction of the regional flow and the conductivity of the ellipsoid-tunnel. As regards specific flow and an empty ellipsoid-tunnel (very conductive), the largest specific flow inside the ellipsoid-tunnel will take place when the regional flow is directed along the ellipsoid-tunnel, and the smallest specific flow when the regional flow is directed along the short axis of the ellipsoid-tunnel. The total flow is dependent on the exposed area in the direction of the regional flow, as well as on the conductivity of the ellipsoid-tunnel. If the conductivity is smaller than, or slightly larger than, the conductivity of the rock mass, maximum total flow will occur when a large area of the ellipsoid-tunnel is exposed to the regional flow, and minimum total flow when a small area is exposed. The opposite will take place if the ellipsoid-tunnel is much more conductive than the rock mass.

It is possible to estimate at what ellipsoid-tunnel conductivity the total flow in the ellipsoid-tunnel is the same for: (i) regional flow along the ellipsoid-tunnel and (ii) regional flow at a right angles to the ellipsoid-tunnel. The conductivity value is estimated

by representing the tunnel with an ellipsoid, and combining equations B.27 and B.28, and include terms for the areas in the direction of the regional flow. The obtained equation is given as equation B.38. Solving this equation for ellipsoid conductivity, gives the above discussed conductivity value. The calculations were carried out for an ellipsoid representing a tunnel defined according to Case B (Sec.3.6)

The conductivity values obtained are given in Figure 3.14, the figure also gives the flow through the studied ellipsoid-tunnel at this conductivity value.

- If the conductivity of the ellipsoid is smaller than the calculated conductivity at balance, maximum total flow will occur when the regional flow is directed along, or close to along, the short axis of the ellipsoid-tunnel.
- If the conductivity of the ellipsoid is larger than the calculated conductivity at balance, maximum total flow will occur when the regional flow is directed along, or close to along, the main axis of the ellipsoid-tunnel.

3.14 Examples of flow and conductivity of an ellipsoid-tunnel

This chapter (Chapter 3) can be looked upon as a sensitivity analysis of different parameters controlling the flow of a tunnel. The basic assumptions are: (i) the tunnel can be represented by an ellipsoid, (ii) the tunnel is homogeneous, (iii) the rock mass can be represented by an infinitely large homogeneous continuum.

- Flow in a tunnel, sensitivity to tunnel conductivity, see Sec.3.7 and 3.8 as well as Fig.3.4 through 3.7
- Flow in a tunnel, sensitivity to direction of regional flow, see Sec.3.9 as well as Fig.3.8 and 3.9.
- Maximum flow in a tunnel, sensitivity to size of tunnel and direction of regional flow, see Sec.3.10 as well as Fig.3.10 and 3.11.
- Threshold conductivity, sensitivity to size of tunnel and direction of regional flow, see Sec.3.11 as well as Fig.3.12 and 3.13.
- Comparison between an analytical method (tunnel is an ellipsoid) and numerical method (tunnel is a parallel-epiped), see Sec.3.6.

The results presented in Figures 3.1 through 3.19 are given as (i) multiples of the regional specific flow, or as (ii) multiples of the conductivity of the rock mass. Thus, to obtain the flow or the conductivity of a tunnel studied, for a certain site-specific scenario, we multiply the results given in the figures by (i) the assumed size of the regional specific flow or by (ii) the assumed conductivity of the rock mass.

As a conclusion of this chapter, we will give an example of how to use Figures 3.1 through 3.19 for the estimation of flow and conductivity of a tunnel in a homogeneous rock mass. We will study a straight tunnel with a length of 100m and a cross-section area of 160 m² at right angles to the main axis of the tunnel. The tunnel could represent a cavern for storage of waste. We will assume that the size of the regional specific flow is 1x10⁻⁴ m³/(m² year) and that the conductivity of the rock mass is 1x10⁻⁹ m/s.

Figures 3.2 and 3.3 as well as Figures 3.15 and 3.16, demonstrate how the tunnel will change the head distribution in the surroundings of the tunnel.

- *Sensitivity to tunnel conductivity.* Figures 3.4 through 3.7 give the specific flow and the total flow of the tunnels, as regards different values of the tunnel conductivity. Tunnels of different sizes are studied, as well as two different directions of the regional flow.

- For a regional flow along the short axis of the tunnel studied, and if the tunnel has a filling with a conductivity equal to 1×10^{-10} m/s (bentonite), the specific flow of the tunnel will be 2×10^{-5} m³/(m² year) and the total flow of the tunnel will be 0.024 m³/year.
- For a regional flow along the main axis of the tunnel studied, and if the tunnel has a filling with a conductivity equal to 1×10^{-10} m/s (bentonite), the specific flow of the tunnel will be 1×10^{-5} m³/(m² year) and the total flow of the tunnel will be 0.0025 m³/year.

- *Sensitivity to direction of regional flow.* Figures 3.8 and 3.9 demonstrate how the flow in the tunnel will vary, depending on the direction of the regional flow, for different values of tunnel conductivity. For a tunnel with a small conductivity (e.g. bentonite filling), maximum total flow will take place when the regional flow is at right angles to the tunnel. For a tunnel with a large conductivity (e.g. an empty tunnel), maximum flow will take place when the regional flow is along the tunnel.

- *Maximum flow in a tunnel, sensitivity to tunnel size and direction of regional flow.*

Figures 3.10 and 3.11 give the maximum specific flow and the maximum total flow that will take place in a tunnel. Maximum flow will occur for an empty tunnel or for a tunnel with a very conductive filling.

- For a regional flow along the short axis of the tunnel studied, and if the tunnel is empty, the specific flow of the tunnel will be 2×10^{-4} m³/(m² year) and the total flow of the tunnel will be 0.3 m³/year.
- For a regional flow along the main axis of the tunnel studied, and if the tunnel is empty, the specific flow of the tunnel will be 1×10^{-3} m³/(m² year) and the total flow of the tunnel will be 0.6 m³/year. This is the maximum flow considering all directions of regional flow and an infinitely large conductivity.

- *Threshold conductivity, sensitivity to tunnel size and direction of regional flow.*

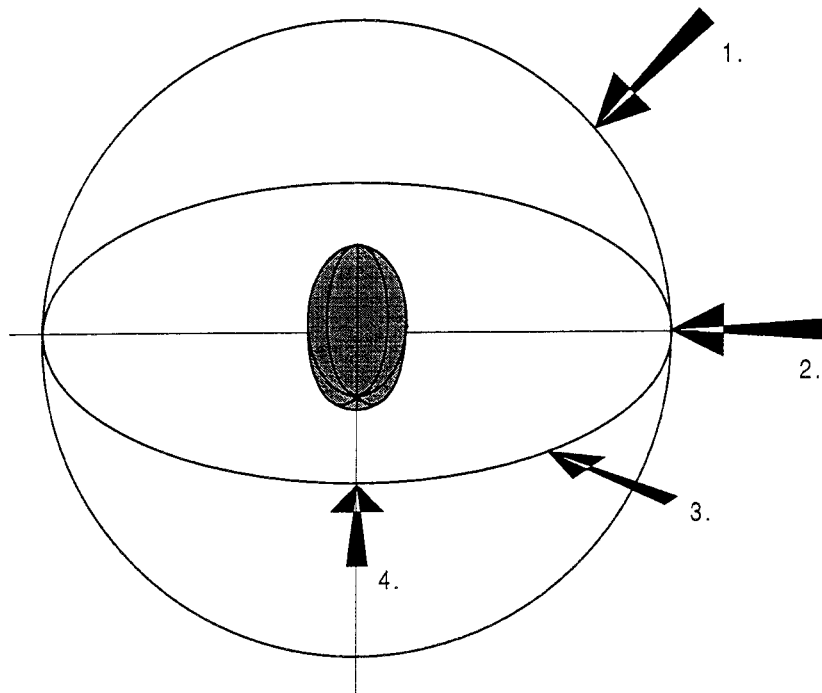
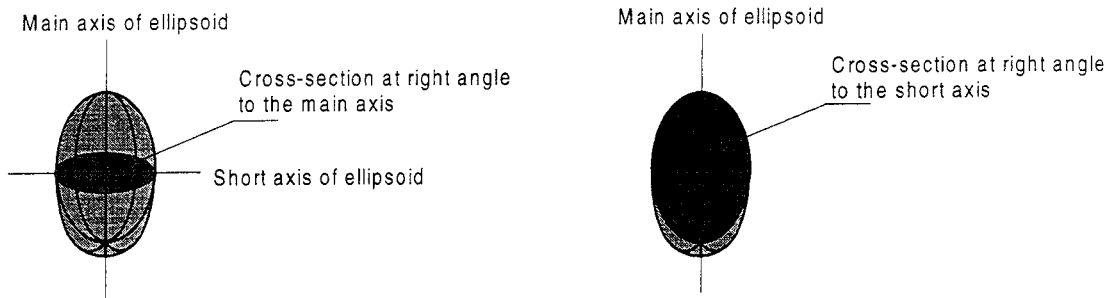
The threshold conductivity tells us how small the conductivity of the tunnel needs to be to noticeably reduce the flow in the tunnel. Figures 3.12 and 3.13 give values of the threshold conductivity for different tunnels.

- For a regional flow along the short axis of the tunnel studied, the conductivity of the tunnel needs to be smaller than 5.8×10^{-8} m/s to reduce the total flow.
- For a regional flow along the main axis of the tunnel studied, the conductivity of the tunnel needs to be smaller than 4×10^{-7} m/s to reduce the total flow.

- *Influence radius.* The tunnel will change the head distribution in the rock mass. The influence radius provides information on the size of the change in head, for different distances from the tunnel. Figures 3.17 through 3.19 give the influence radius for different tunnels, Figure 3.19 corresponds to the tunnel studied. The change in head is given in percent of the undisturbed head. For the tunnel studied, the change in head will be less than 1 percent at a distance larger than 100 m from the tunnel, assuming that the tunnel is empty or has a large conductive.


- *Flow balance as regards direction of regional flow.* Figure 3.14 tells us at which tunnel conductivity the total flow of the tunnel is the same for: (i) a regional flow along the main axis of the tunnel and (ii) a regional flow along the short axis of the tunnel. For the tunnel studied, that situation occurs for a tunnel conductivity equal to 2.2×10^{-8} m/s. If the tunnel conductivity is larger than 2.2×10^{-8} m/s, maximum total flow will take place at a direction of the regional flow which is close to the direction of the main axis. If the tunnel conductivity is smaller than 2.2×10^{-8} m/s, maximum total flow will take place at a direction of the regional flow which is close to the direction of the short axis.

The analytical solutions will provide us with good estimates if the basic assumptions are valid (see above). However, if different parts of the tunnel studied have different hydraulic properties, or if the tunnel is not straight, or if we like to study a system of tunnels with different hydraulic properties, or if we like to study the effects caused by a heterogeneous rock mass surrounding the tunnels; for such and similar scenarios we need to use numerical methods instead of the analytical method. In the following chapters we will estimate the flow in a system of tunnels and barriers, as well as estimate the effects of a heterogeneous rock mass; this will be done by the use of numerical methods.

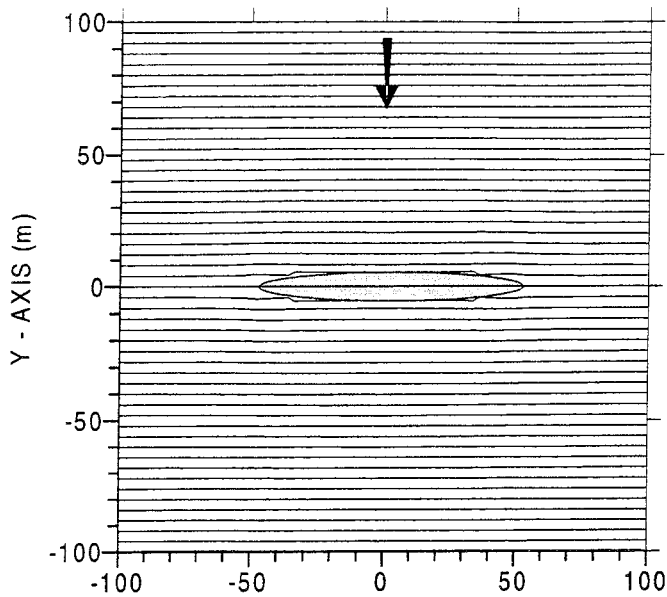


Different directions of the regional flow,
in relation to an ellipsoid.

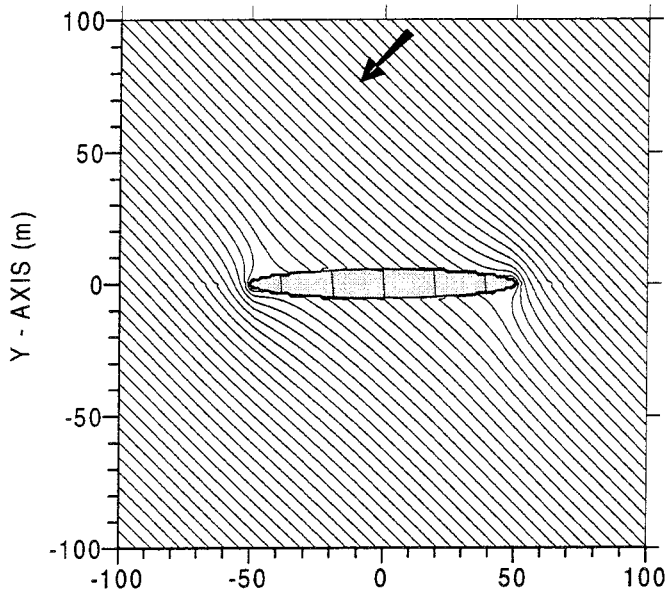
1. Along the short axis.
2. Along the short axis.
3. 45 deg. from the short axis, 45 deg from the main axis.
4. Along the main axis.

 Object representing the studied structure,
an ellipsoid, a tunnel etc.

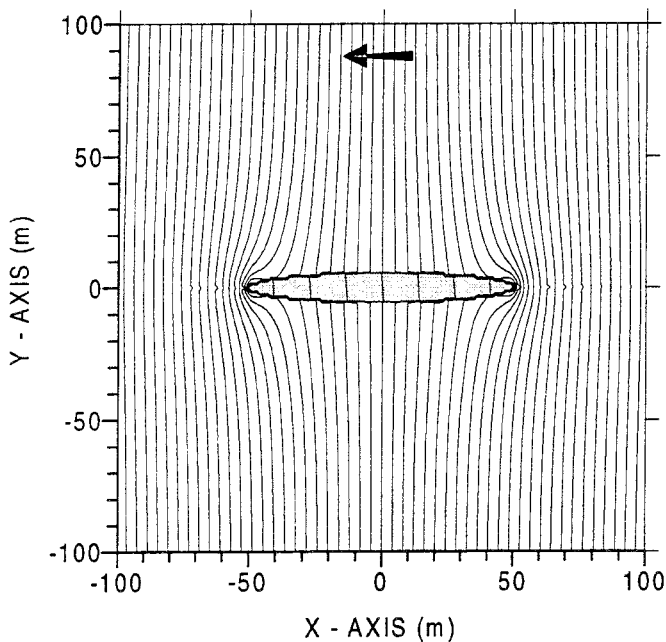
*FIGURE 3.1 DIFFERENT DIRECTIONS OF THE
REGIONAL GROUNDWATER FLOW,
IN RELATION TO AN ELLIPSOID.
DEFINITION OF CROSS-SECTIONS.*



Scenario A.
The regional flow is directed along the Y-axis,
along the short axis of the ellipsoid.



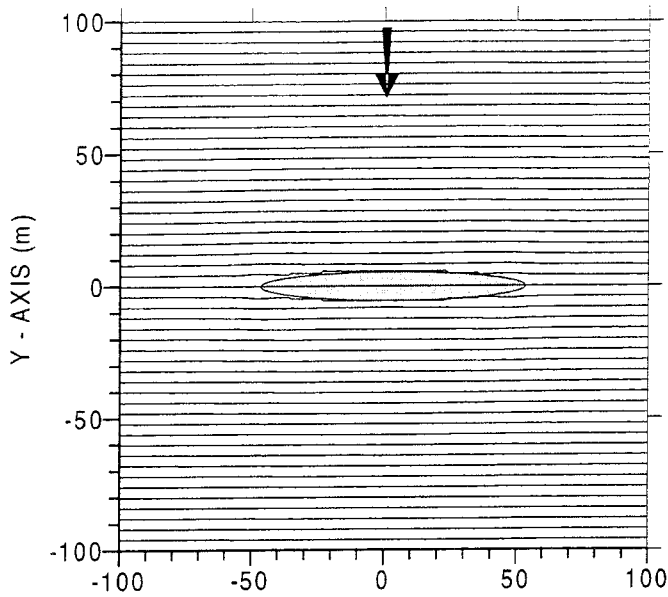
Scenario B.
The regional flow is directed at 45 degrees from
the Y-axis and the X-axis, respectively.



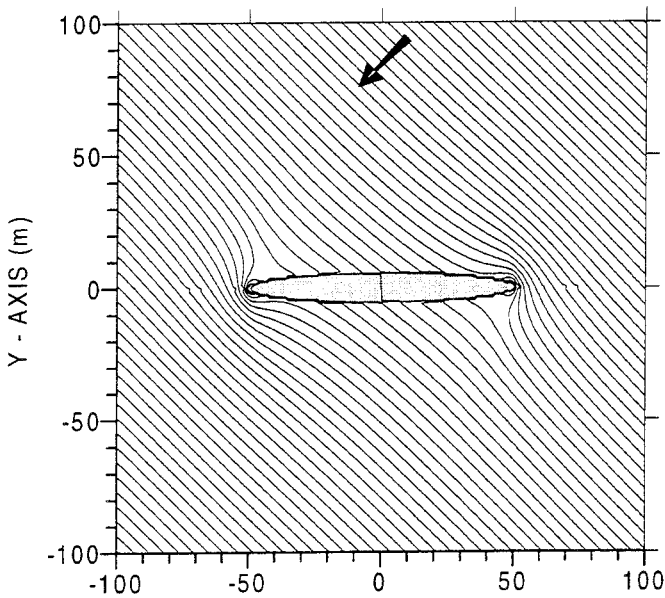
Scenario C.
The regional flow is directed along the X-axis,
along the main axis of the ellipsoid.

**FIGURE 3.2 ANALYTIC SOLUTION
HEAD CONTOURS
K-CONTRAST: 100**

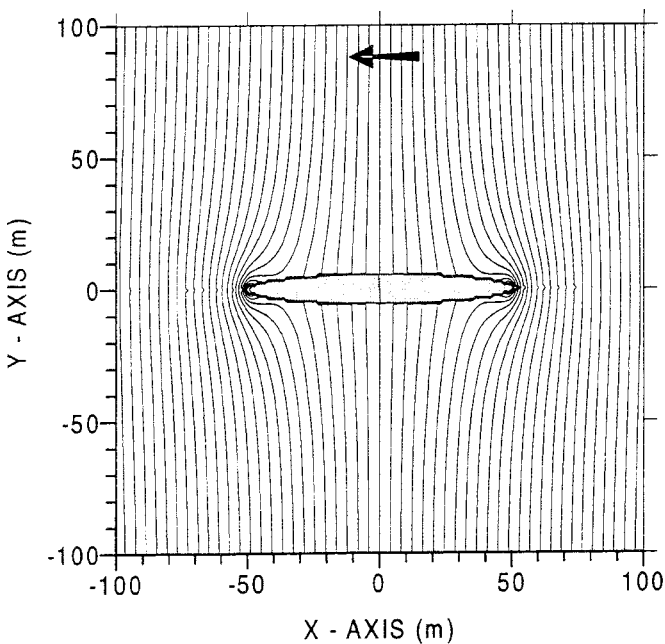
*Head contours inside and outside of an
ellipsoid. The ellipsoid is placed in an
infinitely large three-dimensional flow field.
The cross-sections are taken through the
center of the ellipsoid in the plane of the
X-axis and the Y-axes.
The ellipsoid is 100 times more permeable
than the surrounding.
Size of the regional specific flow: 1 m/s
Interval between contour lines: 4 m
Length of ellipsoid: 100 m
Length of short semi-axis: 5.6 m*



Scenario A.
The regional flow is directed along the Y-axis,
along the short axis of the ellipsoid.



Scenario B.
The regional flow is directed 45 degrees from
the Y-axis and the X-axis, respectively.



Scenario C.
The regional flow is directed along the X-axis,
along the main axis of the ellipsoid.

**FIGURE 3.3 ANALYTIC SOLUTION
HEAD CONTOURS
K-CONTRAST: 10 000**

*Head contours inside and outside of an
ellipsoid. The ellipsoid is placed in an
infinitely large three dimensional flow field.
The cross-sections are taken through the
center of the ellipsoid in the plane of the
X-axis and the Y-axis.
The ellipsoid is 10 000 times more permeable
than the surrounding.
Size of the regional specific flow: 1 m/s
Interval between contour lines: 4 m
Length of ellipsoid: 100 m
Length of short semi-axis: 5.6 m*

Fig.(i)
Specific
flow.

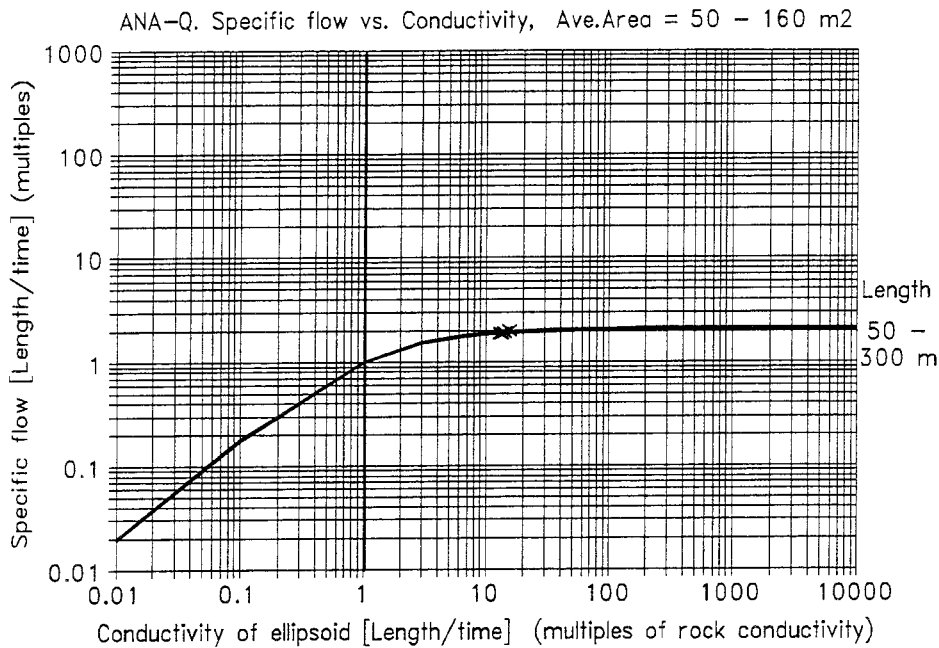


Fig.(ii)
Total
flow

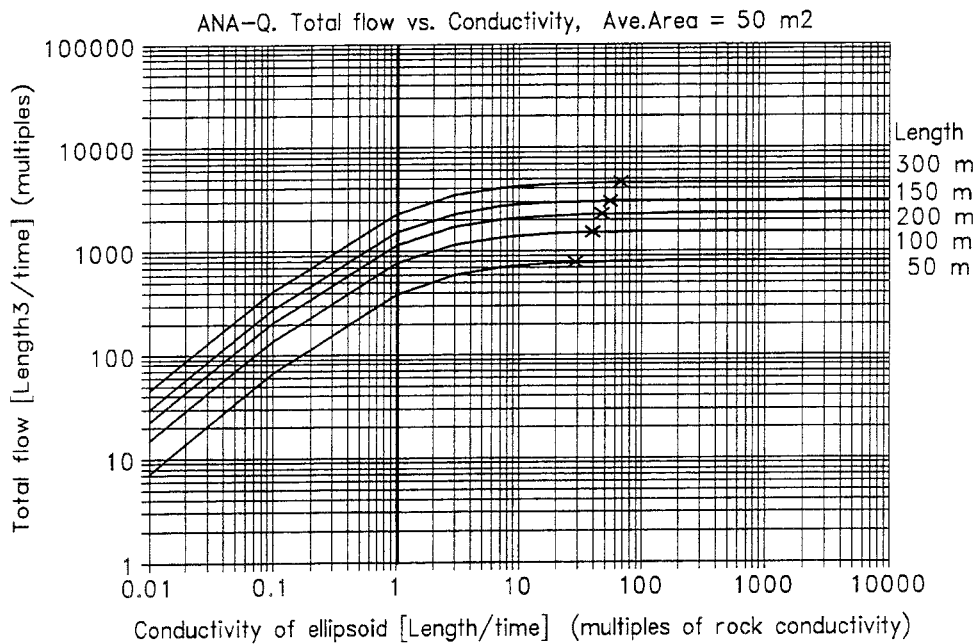


Figure 3.4

SPECIFIC AND TOTAL FLOW IN AN ELLIPSOID-TUNNEL (Q.1)

The regional flow is directed along the short axis of the ellipsoid-tunnel.

The flow in the ellipsoid-tunnel is given as a multiple of the regional groundwater flow. The conductivity of the ellipsoid-tunnel is given as a multiple of the conductivity of the surrounding rock. The average area of a cross-section at right angles to the main axis is 50 m². The total flow is the product of: the specific flow and the area of the largest cross-section in the direction of the regional flow. The crosses denote threshold conductivity. Uniform continuum approach.

Fig.(i) The specific flow for different ellipsoids (the values are close).

Fig.(ii) The total flow for ellipsoids of different lengths.

Fig (i)
Specific
flow

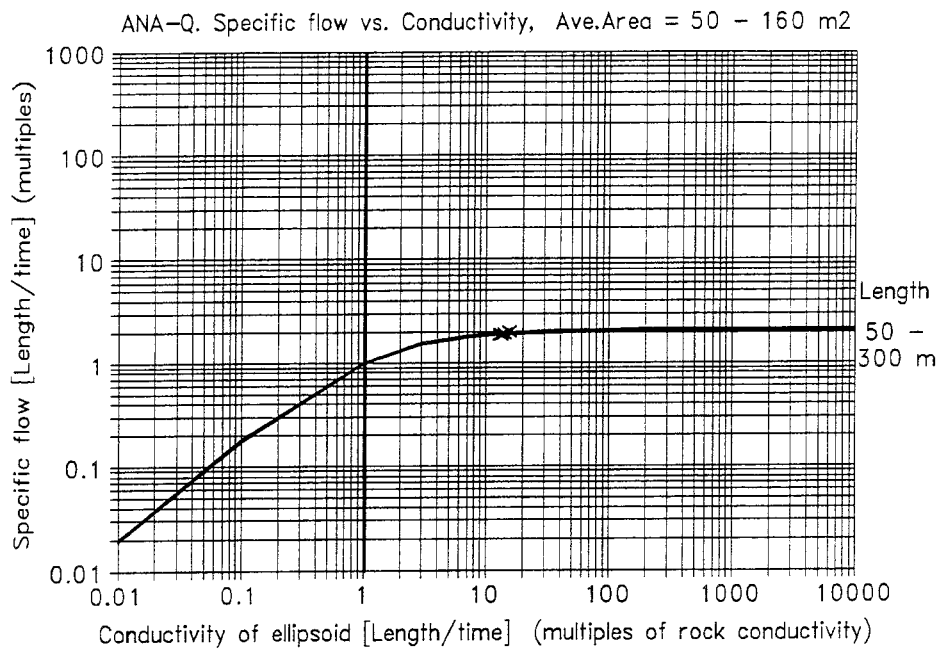


Fig.(ii)
Total
flow

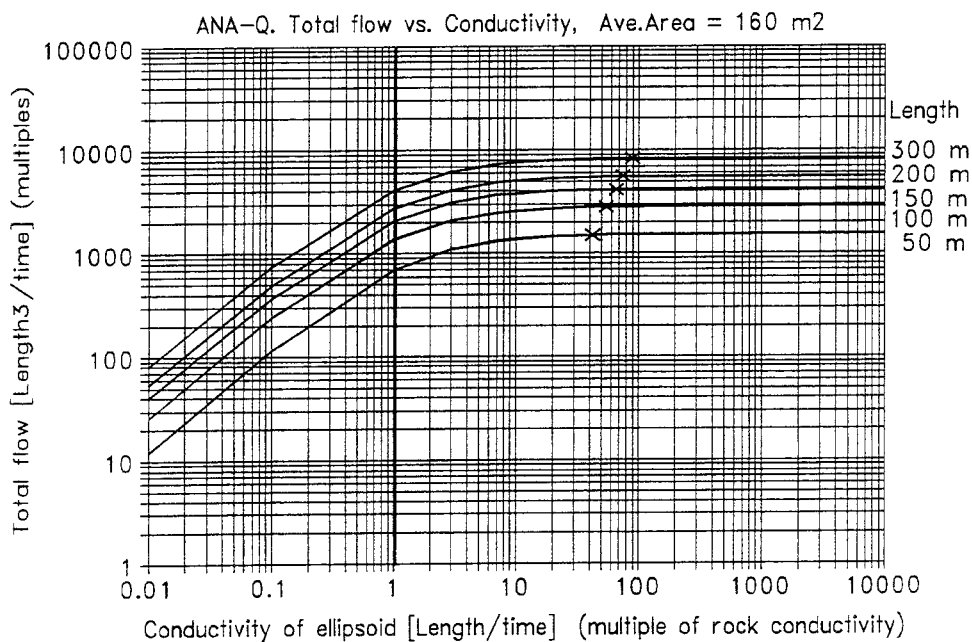


Figure 3.5

SPECIFIC AND TOTAL FLOW IN AN ELLIPSOID-TUNNEL (Q.2).

The regional flow is directed along the short axis of the ellipsoid-tunnel.

The flow in the ellipsoid-tunnel is given as a multiple of the regional groundwater flow. The conductivity of the ellipsoid-tunnel is given as a multiple of the conductivity of the surrounding rock. The average area of a cross-section at right angles to main axis is 160 m². The total flow is the product of: the specific flow and the area of the largest cross-section in direction of the regional flow. The crosses denotes threshold conductivity. Uniform continuum approach.
Fig.(i) The specific flow for different ellipsoids (the values are close).
Fig.(ii) The total flow for ellipsoids of different length.

Fig.(i)
Specific
flow

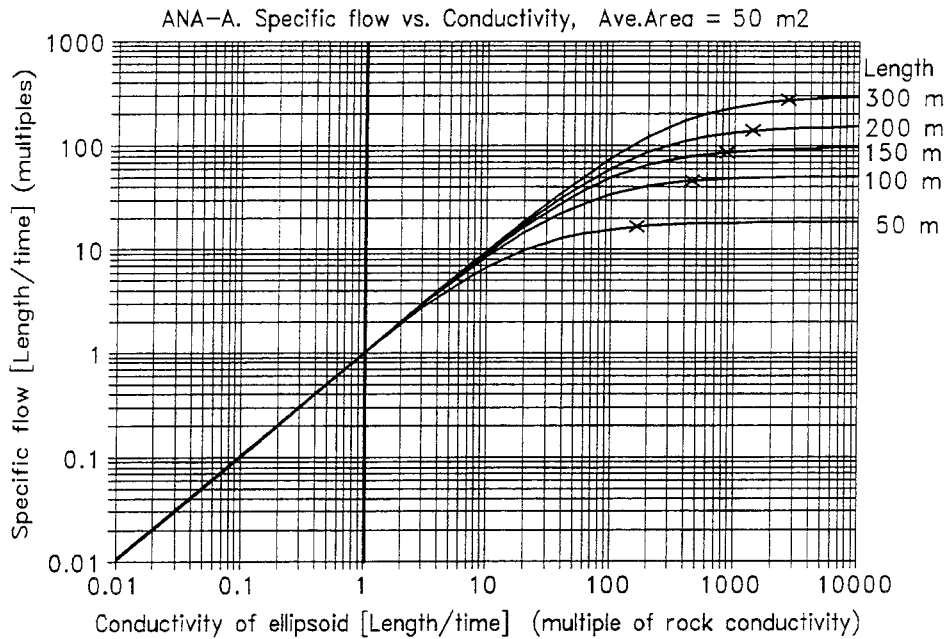


Fig.(ii)
Total
flow

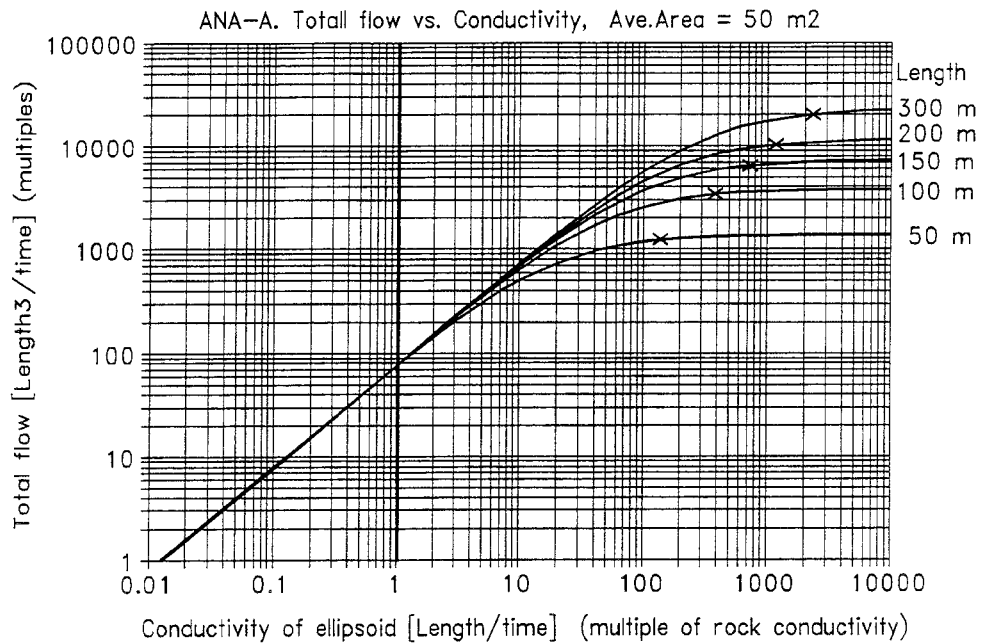


Figure 3.6

SPECIFIC AND TOTAL FLOW IN AN ELLIPSOID-TUNNEL (A.1).

The regional flow is directed along the main axis of the ellipsoid-tunnel.

The flow in the ellipsoid-tunnel is given as a multiple of the regional groundwater flow. The conductivity of the ellipsoid-tunnel is given as a multiple of the conductivity of the surrounding rock. The average area of a cross-section at right angles to main axis is 50 m². The total flow is the product of: the specific flow and the area of the largest cross-section in direction of the regional flow. The crosses denotes threshold conductivity. Uniform continuum approach.

Fig.(i) The specific flow for ellipsoids of different length.

Fig.(ii) The total flow for ellipsoids of different length.

Fig.(i)
Specific
flow

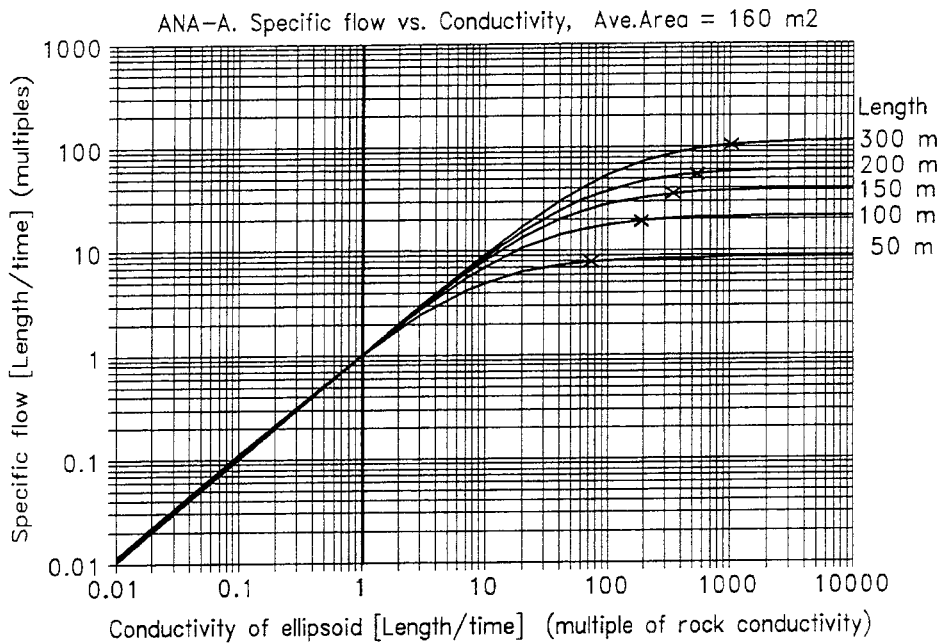


Fig.(ii)
Total
flow

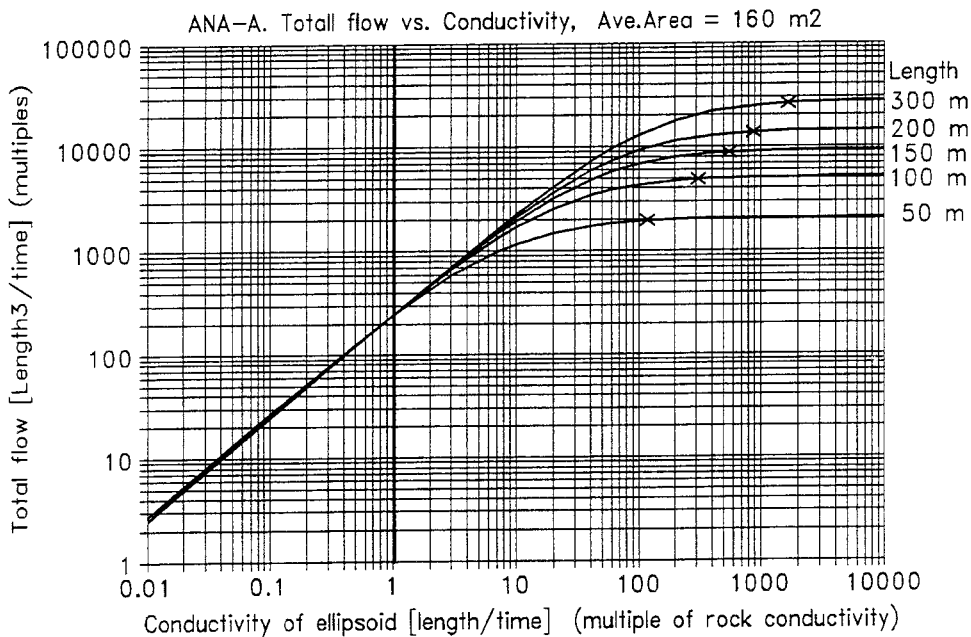


Figure 3.7

SPECIFIC AND TOTAL FLOW IN AN ELLIPSOID-TUNNEL (A.2).

The regional flow is directed along the main axis of the ellipsoid-tunnel.

The flow in the ellipsoid-tunnel is given as a multiple of the regional groundwater flow. The conductivity of the ellipsoid-tunnel is given as a multiple of the conductivity of the surrounding rock. The average area of a cross-section at right angles to main axis is 50 m². The total flow is the product of: the specific flow and the area of the largest cross-section in direction of the regional flow. The crosses denotes threshold conductivity. Uniform continuum approach.

Fig.(i) The specific flow for ellipsoids of different length.

Fig.(ii) The total flow for ellipsoids of different length.

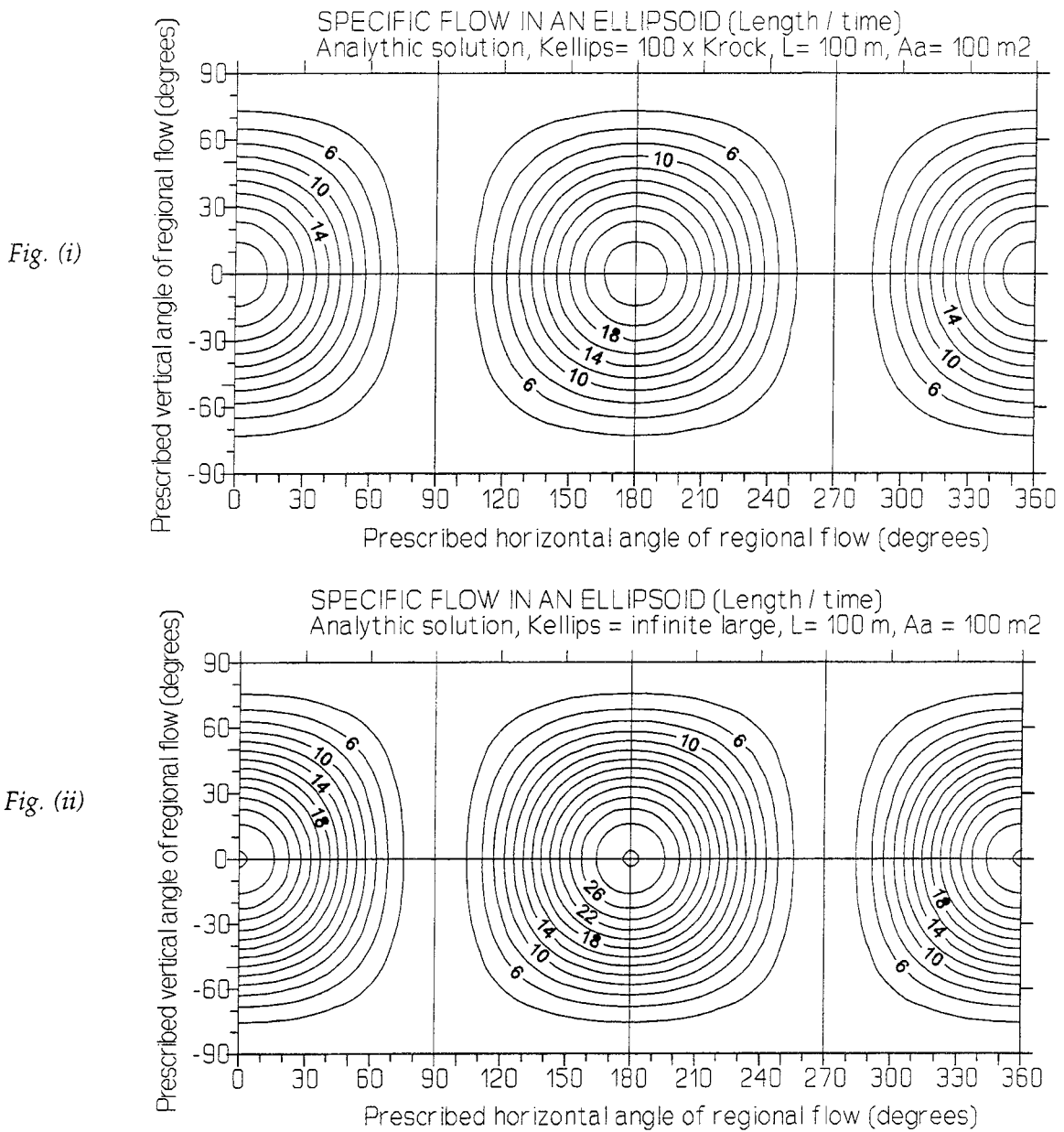


Figure 3.8

SPECIFIC FLOW IN AN ELLIPSOID-TUNNEL, SENSITIVITY TO DIRECTION OF REGIONAL FLOW.

The ellipsoid-tunnel is placed in an infinite large three dimensional flow field. The main axis of the ellipsoid-tunnel is in the horizontal plane. The calculated flow is a multiple of an unknown regional groundwater flow. Uniform continuum approach.

- Ellipsoid: Length=100 m, average area at right angles to main axis: 100 m²
- The ellipsoid is **more** conductive than the surroundings (K_{ellipsoid} > K_{rock}):

Fig.(i) K_{ellipsoid} = 100 x K_{rock}, Fig.(ii) K_{ellipsoid} is infinite large.

The X-axis and the Y-axis of the figure represent all possible directions of regional flow in the horizontal and vertical plane. The horizontal angles are given clockwise from the positive direction of the main axis of the ellipsoid. The vertical angles are given upwards (positive) or downwards (negative) from the horizontal plane. The figures are based on 648 calculated values representing the whole sphere of possible directions of the regional flow. Interpolation between the values was based on a kriging method.

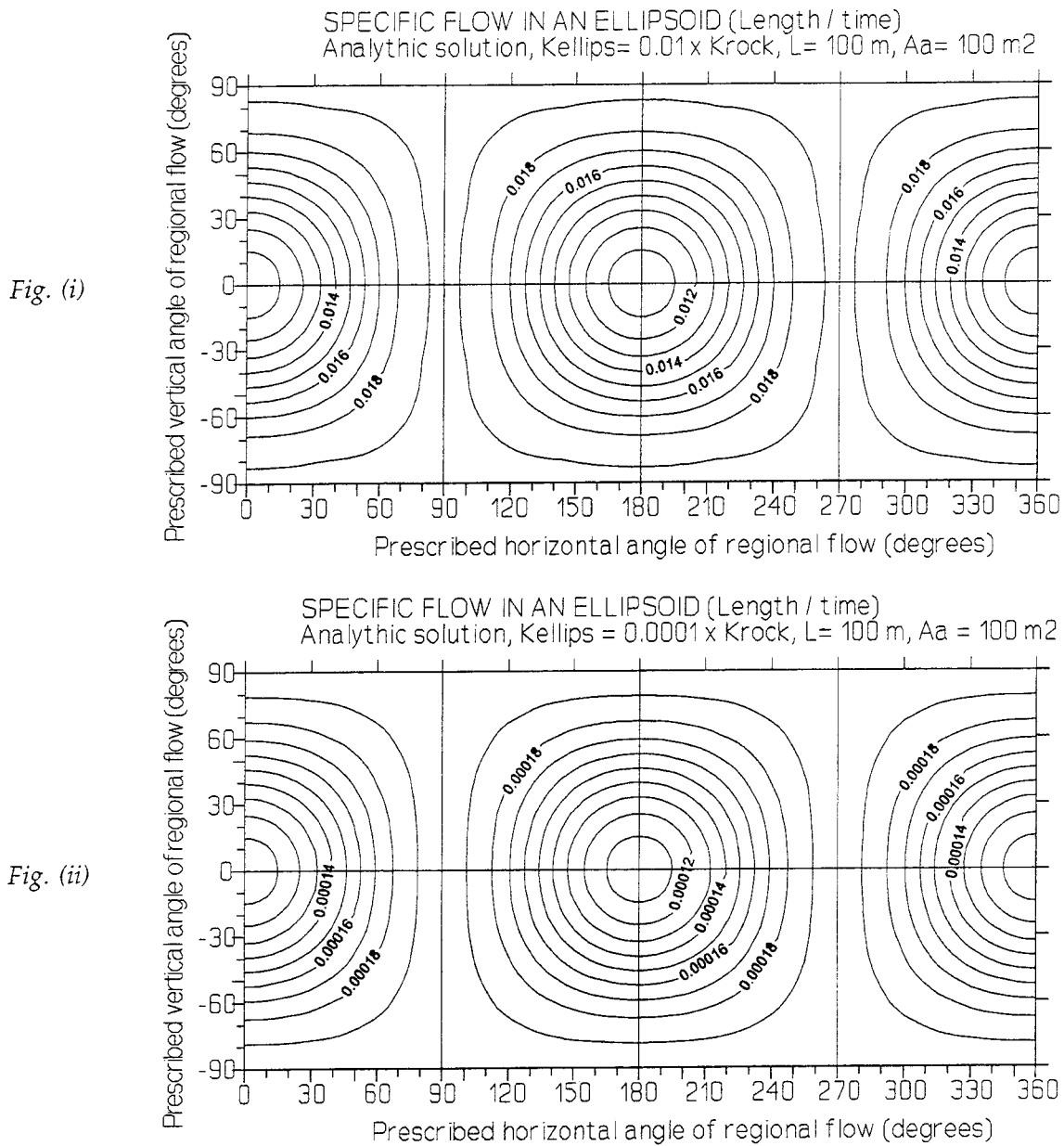


Figure 3.9

SPECIFIC FLOW IN AN ELLIPSOID-TUNNEL, SENSITIVITY TO DIRECTION OF REGIONAL FLOW.

The ellipsoid-tunnel is placed in an infinite large three dimensional flow field. The main axis of the ellipsoid-tunnel is in the horizontal plane. The calculated flow is a multiple of an unknown regional groundwater flow. Uniform continuum approach.

- Ellipsoid: Length=100 m, average area perpendicular to main axis: 100 m²
- The ellipsoid is less conductive than the surroundings ($K_{\text{ellipsoid}} < K_{\text{rock}}$):

Fig.(i) $K_{\text{ellipsoid}} = 0.01 \times K_{\text{rock}}$, Fig.(ii) $K_{\text{ellipsoid}} = 0.0001 \times K_{\text{rock}}$.

The X-axis and the Y-axis of the figure represent all possible directions of regional flow in the horizontal and vertical plane. The horizontal angles are given clockwise from the positive direction of the main axis of the ellipsoid. The vertical angles are given upwards (positive) or downwards (negative) from the horizontal plane. The figures are based on 648 calculated values representing the whole sphere of possible directions of the regional flow. Interpolation between the values was based on a kriging method.

Fig.(i)

Regional flow along short axis.

Specific flow from: 2.0 - 2.2

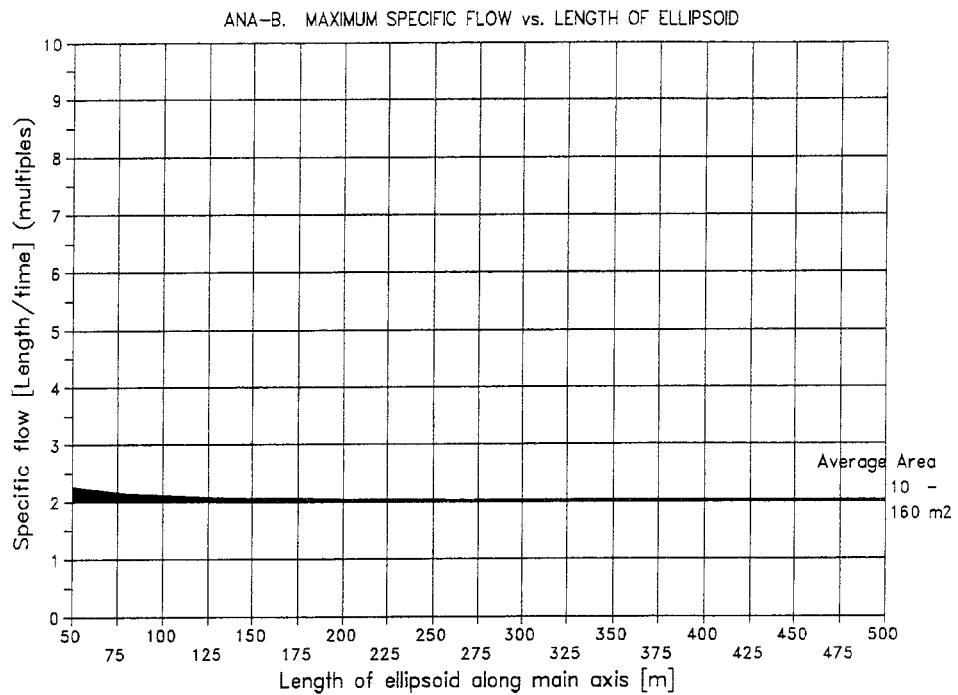


Fig.(ii)

Regional flow along main axis.

Specific flow from: 9.0 - 2950

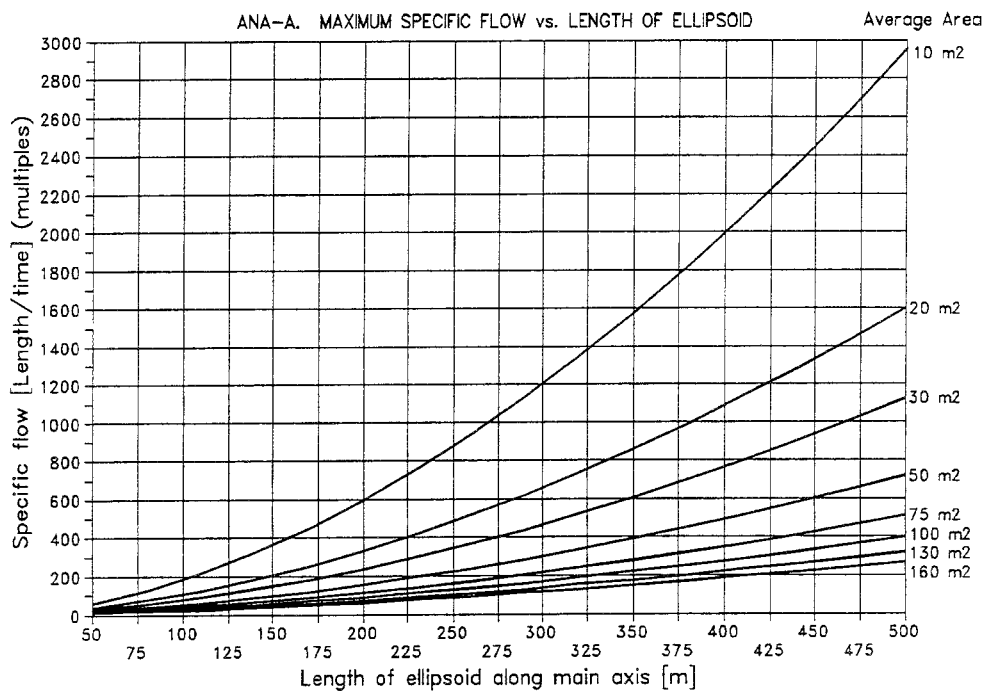


Figure 3.10

MAXIMUM SPECIFIC FLOW IN AN ELLIPSOID-TUNNEL.

The conductivity of the ellipsoid-tunnel is infinite large. The flow of the ellipsoid-tunnel is given as a multiple of the regional groundwater flow. The curves in the figure correspond to different ellipsoids having different average cross-section areas at right angles to the main axis (width of ellipsoid).

Fig.(i) The regional flow is along the short axis of the ellipsoid-tunnel.

Fig.(ii) The regional flow is along the main axis of the ellipsoid-tunnel.

Fig.(i)

Regional flow along short axis.

Total flow from: 400- 13800

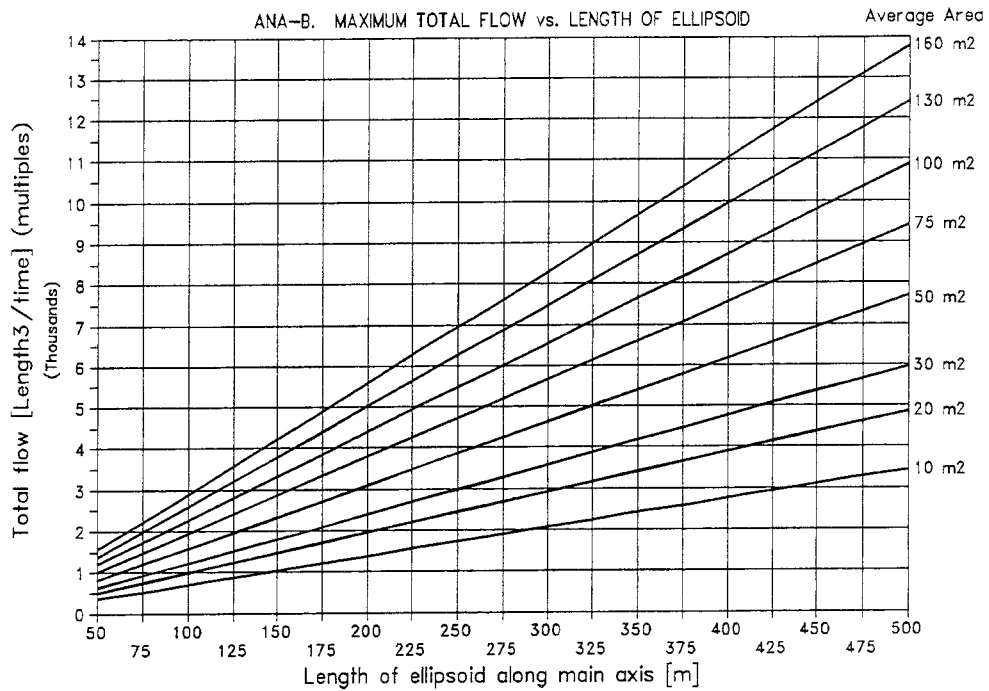


Fig.(ii)

Regional flow along main axis.

Total flow from: 900- 64000

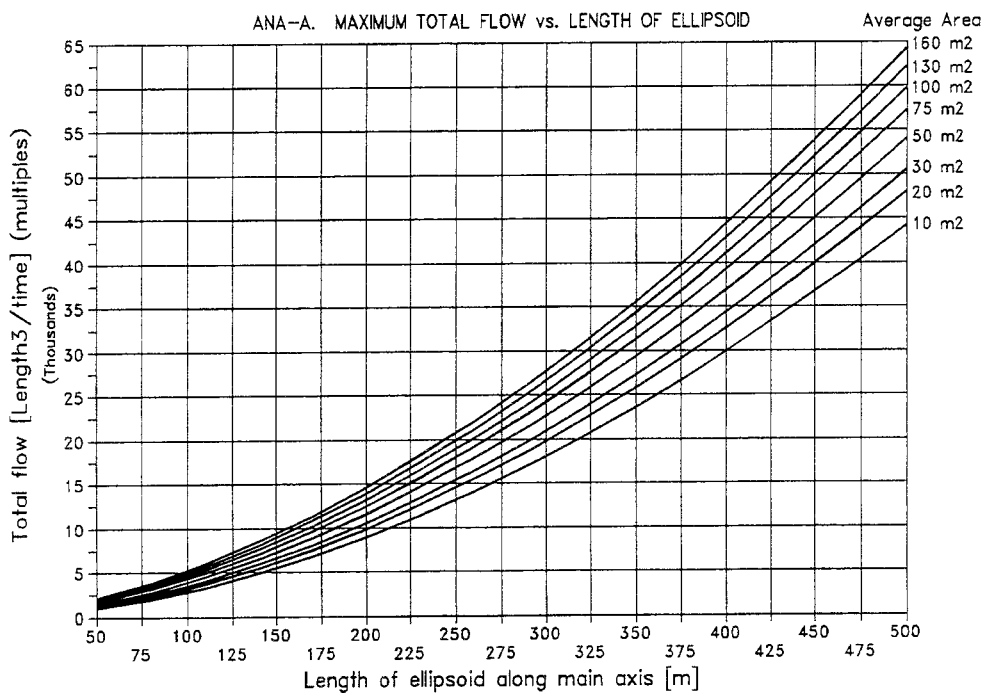


Figure 3.11

MAXIMUM TOTAL FLOW IN AN ELLIPSOID-TUNNEL.

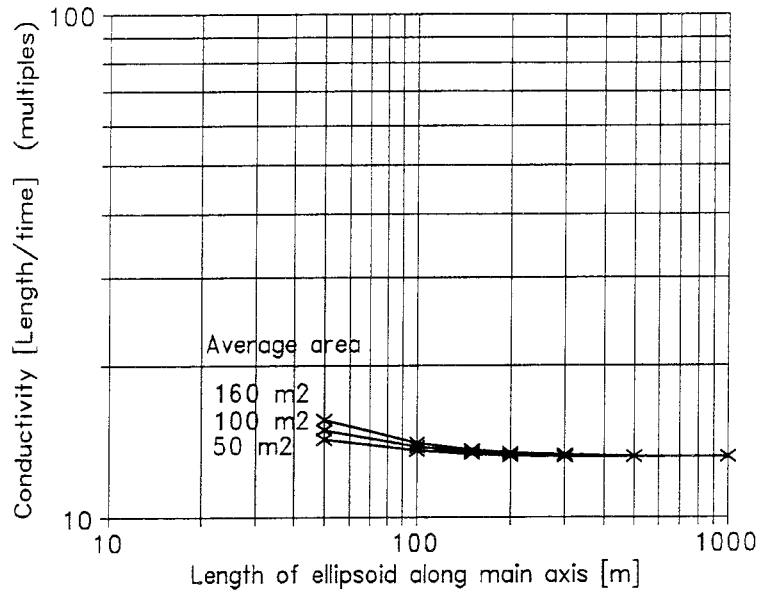
The conductivity of the ellipsoid-tunnel is infinite large. The flow of the ellipsoid-tunnel is given as a multiple of the regional groundwater flow. The curves in the figure correspond to different ellipsoids having different average cross-section areas at right angles to the main axis. The total flow of the ellipsoid is the product of the specific flow and the largest cross-section area in the direction of regional flow.

Fig.(i) The regional flow is along the short axis of the ellipsoid-tunnel.

Fig.(ii) The regional flow is along the main axis of the ellipsoid-tunnel.

ANA-A. Treshold Conductivity vs. Length of ellipsoid, Flow along short axis
 Threshold K. as regards Specific flow, $dq / dK = 0.01$

Fig.(i)
 Threshold conductivity as regards Specific flow



ANA-A. Treshold Conductivity vs. Length of ellipsoid, Flow along short axis
 Threshold K. as regards Total flow, $dTF / dK = 1$

Fig.(ii)
 Threshold conductivity as regards Total flow

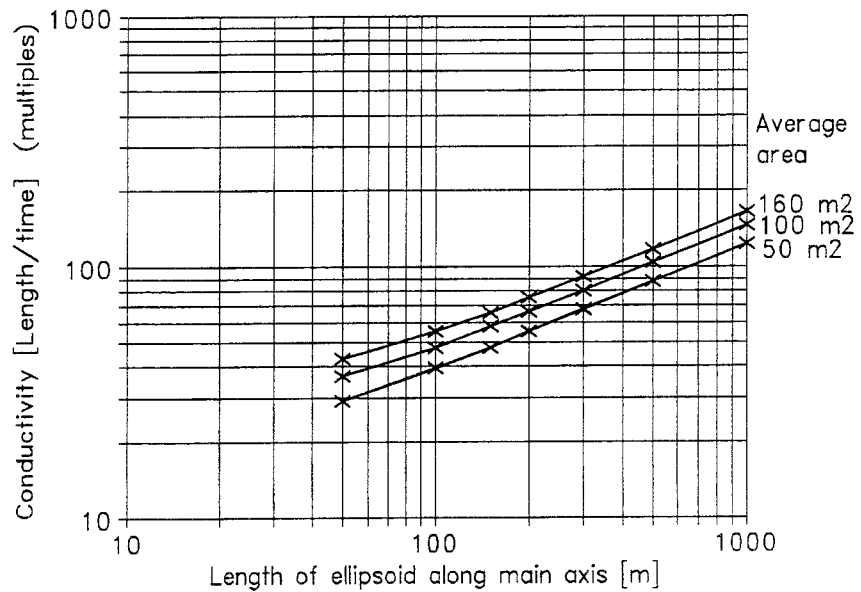


Figure 3.12

THRESHOLD CONDUCTIVITY OF AN ELLIPSOID-TUNNEL (Q).

Regional flow is directed along the short axis of the ellipsoid-tunnel.

The curves in the figure correspond to different ellipsoids having different average cross-section areas at right angles to their main axis (different widths).

The threshold conductivity is defined in Sec.3.11. The conductivity value of an ellipsoid has to be less than the threshold conductivity to noticeable reduce the flow in the ellipsoid. The models studied are based on the uniform continuum approach. The threshold cond. is given as a multiple of the cond. of the surrounding rock.

Fig.(i) Threshold cond. as regards specific flow. Regional flow along short axis.

Fig.(ii) Threshold cond. as regards total flow. Regional flow along short axis.

Fig.(i)
Threshold
conductivity
as regards
Specific flow

ANA-A. Treshold Conductivity vs. Length of ellipsoid, Flow along main axis
Threshold K. as regards Specific flow, $dq / dK = 0.01$

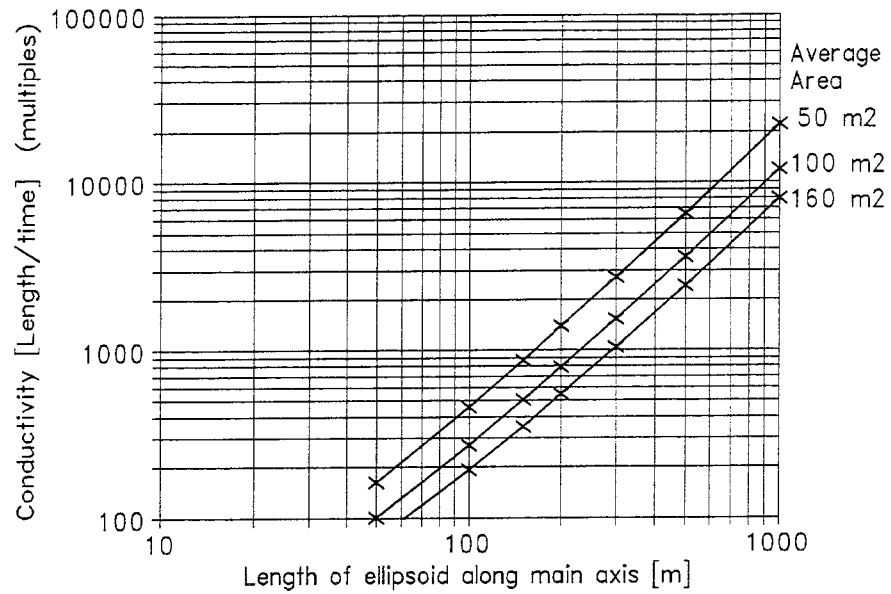


Fig.(ii)
Threshold
conductivity
as regards
Total flow

ANA-A. Treshold Conductivity vs. Length of ellipsoid, Flow along main axis
Threshold K. as regards Total flow, $dTF / dK = 1$

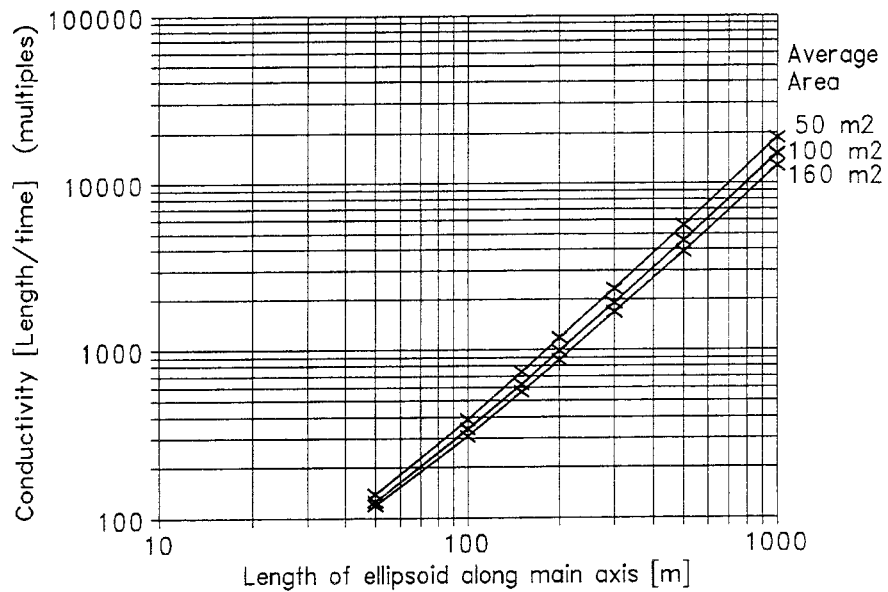


Figure 3.13

THRESHOLD CONDUCTIVITY OF AN ELLIPSOID-TUNNEL (A).

Regional flow is directed along the main axis of the ellipsoid-tunnel.

The curves in the figure corresponds to different ellipsoids having different average cross-section areas, at right angles to their main axis (different widths).

The threshold conductivity is defined in Sec.3.11. The conductivity value of an ellipsoid has to be less than the threshold conductivity to noticeable reduce the flow in the ellipsoid. The models studied are based on the uniform continuum approach. The threshold cond. is given as a multiple of the cond. of the surrounding rock.

Fig.(i) Threshold cond. as regards specific flow. Regional flow along main axis.

Fig.(ii) Threshold cond. as regards total flow. Regional flow along main axis.

Fig.(i)
Conductivity of
ellipsoid-tunnel at
balance in total flow

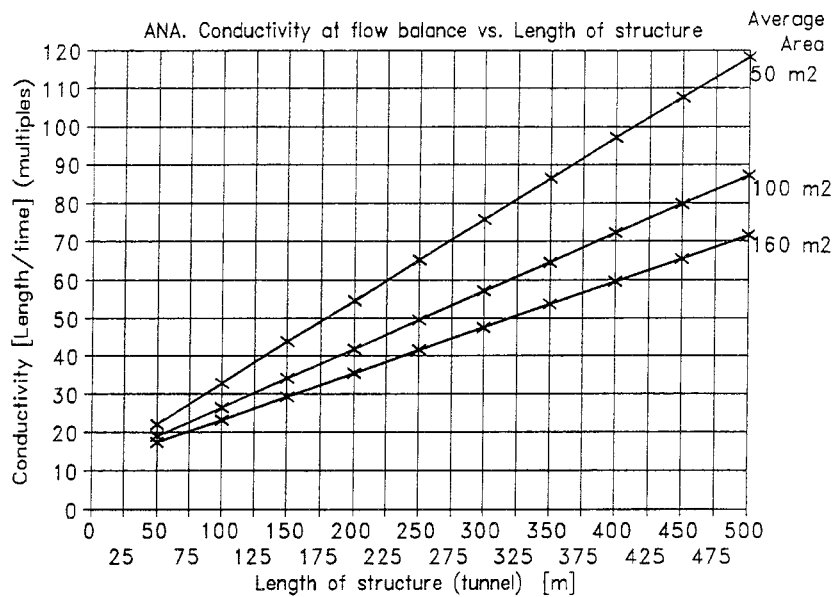


Fig.(ii)
Total flow of ellipsoid-
tunnel at balance in
total flow

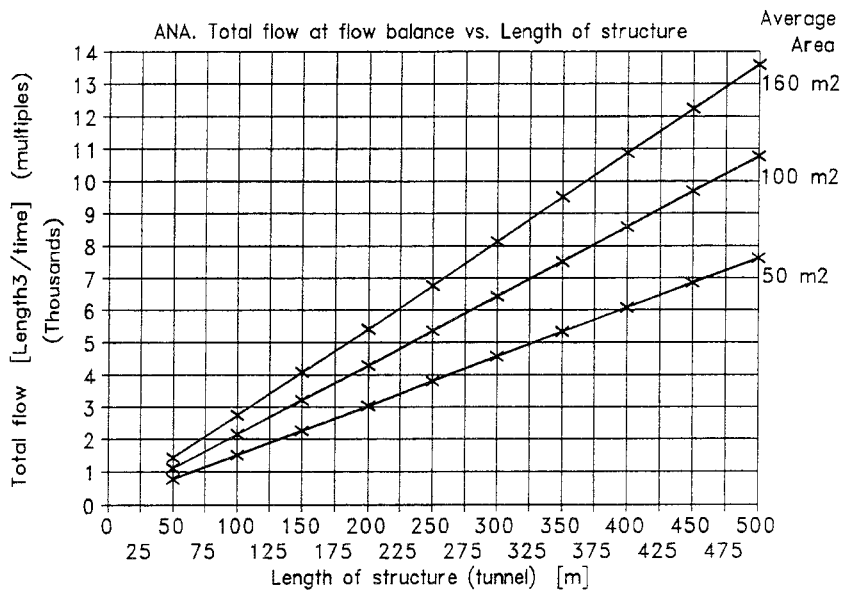


Figure 3.14

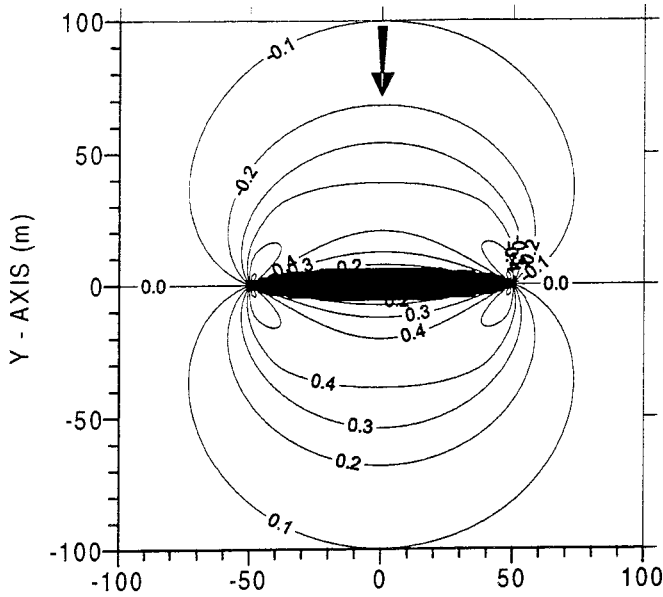
FLOW BALANCE AS REGARDS DIRECTION OF REGIONAL FLOW, IN AN ELLIPSOID-TUNNEL.

The conductivity, and the total flow, refer to that of an ellipsoid when the total flow in the ellipsoid is the same for both regional flow directed along the main axis of the ellipsoid and regional flow directed along the short axis of the ellipsoid. The conductivity of the ellipsoid is given as a multiple of the conductivity of the surrounding rock. The curves in the figure correspond to different ellipsoids having different average cross-section areas at right angles to the main axis.

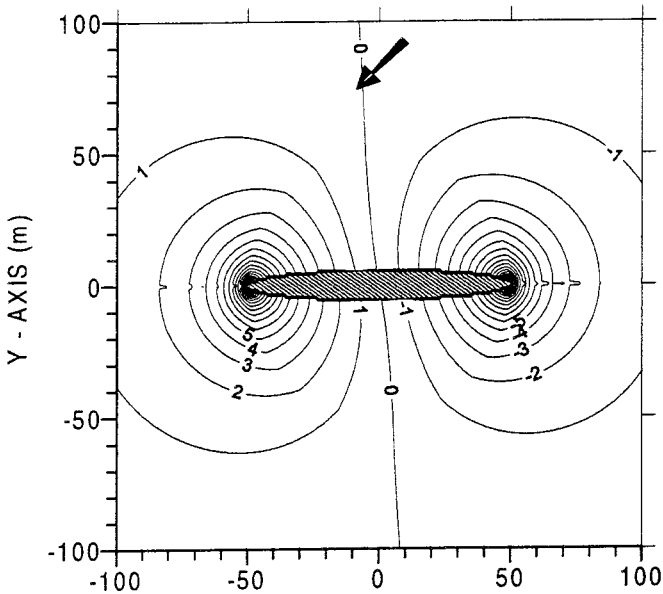
The total flow is calculated as the product of the specific flow in the ellipsoid and the largest cross-section area in the direction of the regional flow. The models are based on the uniform continuum approach.

Fig.(i) Conductivity of an ellipsoid at flow balance.

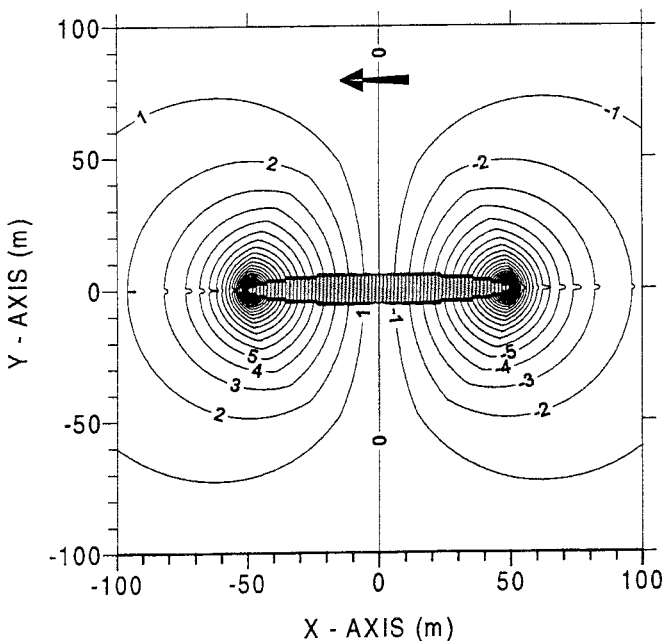
Fig.(ii) Total flow through an ellipsoid at flow balance.



Scenario A.
The regional flow is directed along the Y-axis,
along the short axis of the ellipsoid.
Interval between lines: 0.1 m.



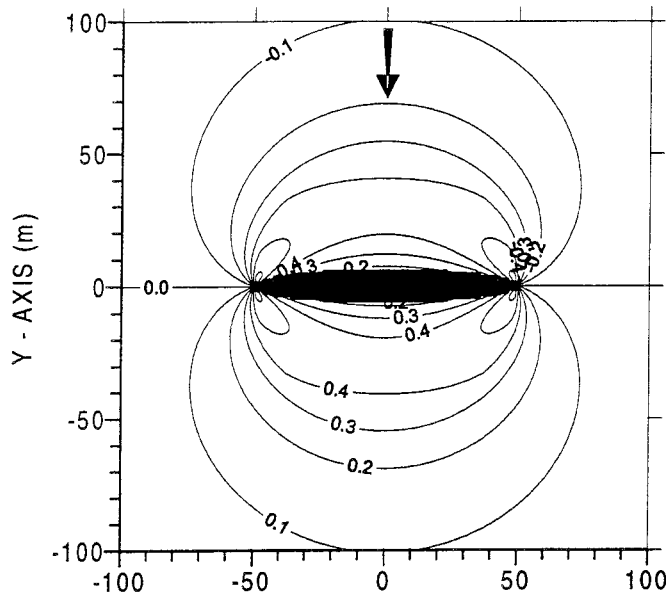
Scenario B.
The regional flow is directed 45 degrees from
the Y-axis and the X-axis, respectively.
Interval between lines: 1 m.



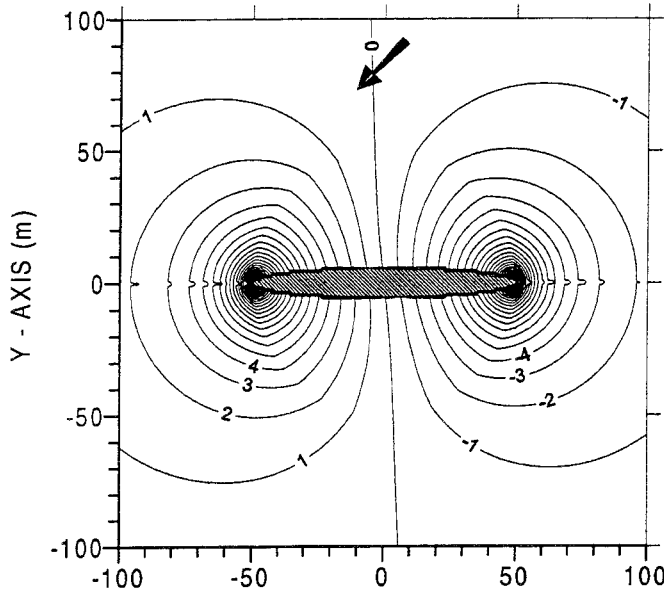
Scenario C.
The regional flow is directed along the X-axis,
along the main axis of the ellipsoid.
Interval between lines: 1 m.

**FIGURE 3.15 ANALYTIC SOLUTION
CHANGE IN HEAD
K-CONTRAST: 100**

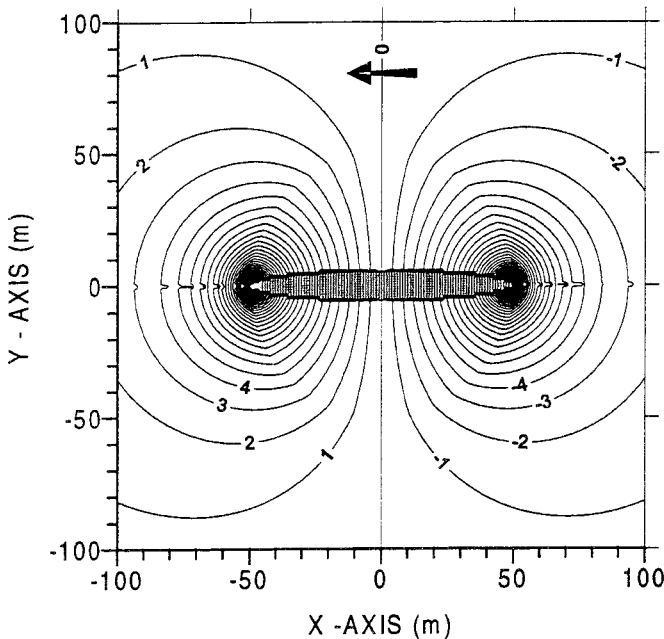
*Change in head inside and outside of an ellipsoid.
The change is given in meters, compared to the
head of the undisturbed regional flow
(without an ellipsoid). The ellipsoid is placed in
an infinitely large three-dimensional flow field.
The cross-sections are taken through the center
of the ellipsoid in the plane of the X-axis and
the Y-axis. The ellipsoid is 100 times more
permeable than the surroundings.
The regional specific flow is 1 m/s.
Length of ellipsoid: 100 m
Length of short semi-axis: 5.6 m*



Scenario A.
The regional flow is directed along the Y-axis,
along the short axis of the ellipsoid.
Interval between lines: 0.1 m.



Scenario B.
The regional flow is directed 45 degrees from
the Y-axis and the X-axis, respectively.
Interval between lines: 1 m.



Scenario C.
The regional flow is directed along the X-axis,
along the main axis of the ellipsoid.
Interval between lines: 1 m.

FIGURE 3.16 ANALYTIC SOLUTION
CHANGE IN HEAD
K-CONTRAST: 10 000

Change in head inside and outside of an ellipsoid. The change is given in meters, compared to the head of the undisturbed regional flow (without an ellipsoid). The ellipsoid is placed in an infinitely large three-dimensional flow field. The cross-sections are taken through the center of the ellipsoid in the plane of the X-axis and the Y-axis. The ellipsoid is 10 000 times more permeable than the surroundings. The regional specific flow is 1 m/s. Length of ellipsoid: 100 m. Length of short semi-axis: 5.6 m

Fig.(i)
 Ellipsoid data:
 Conductivity
 contrast=100
 Ac.area=50m²
 Length=...

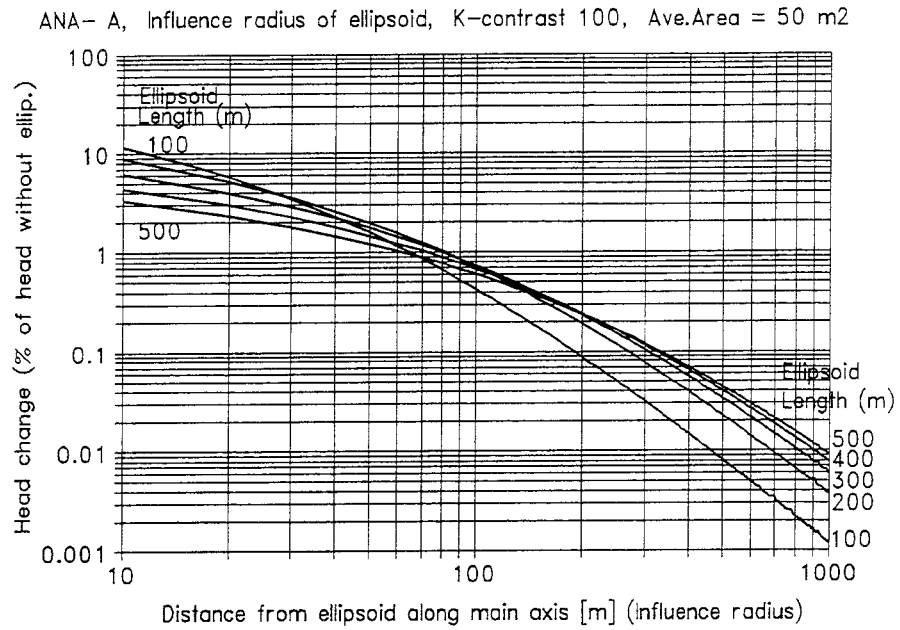


Fig.(ii)
 Ellipsoid data:
 Conductivity
 contrast=10000
 Ac.area=50m²
 Length=...

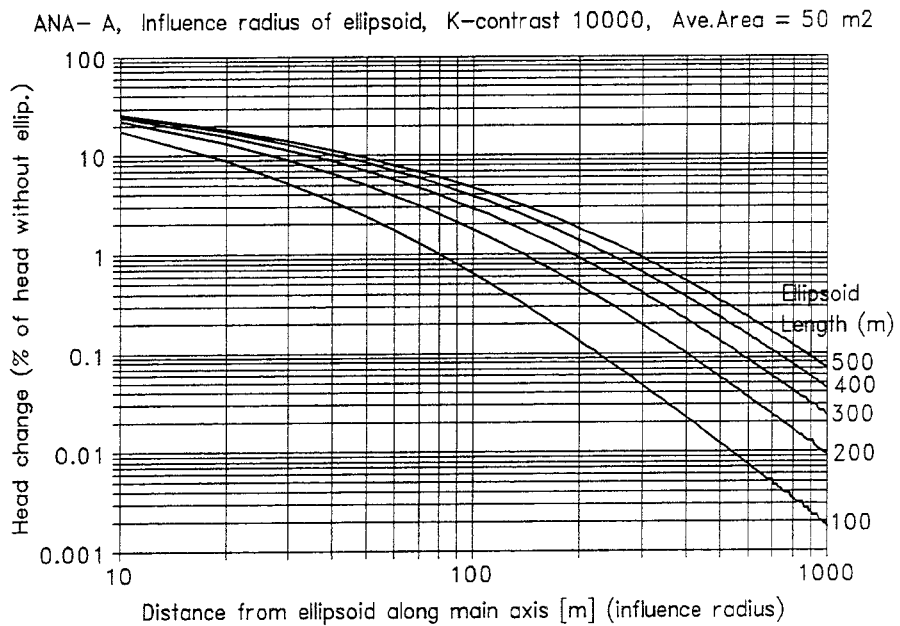


Figure 3.17

INFLUENCE RADIUS OF ELLIPSOID-TUNNEL (1).

The regional flow is directed along the main axis of the ellipsoid.

An ellipsoid-tunnel will change the head in the surrounding rock mass, compared to a situation without an ellipsoid-tunnel. For ellipsoid-tunnels of different properties, the figure gives the influence radius and the corresponding change in head. The change in head is given in percent of the head without the ellipsoid. Hence, the values are the same, regardless of the size of the regional flow. The models are based on the uniform continuum approach.

The average cross-section at right angles to the main axis of the ellipsoid is 50 m²

Fig.(i) Conductivity of the ellipsoid is 100 times that of the rock mass.

Fig.(ii) Conductivity of the ellipsoid is 10000 times that of the rock mass.

Fig.(i)
 Ellipsoid data:
 Conductivity
 contrast=100
 Ac.area=100m²
 Length=...

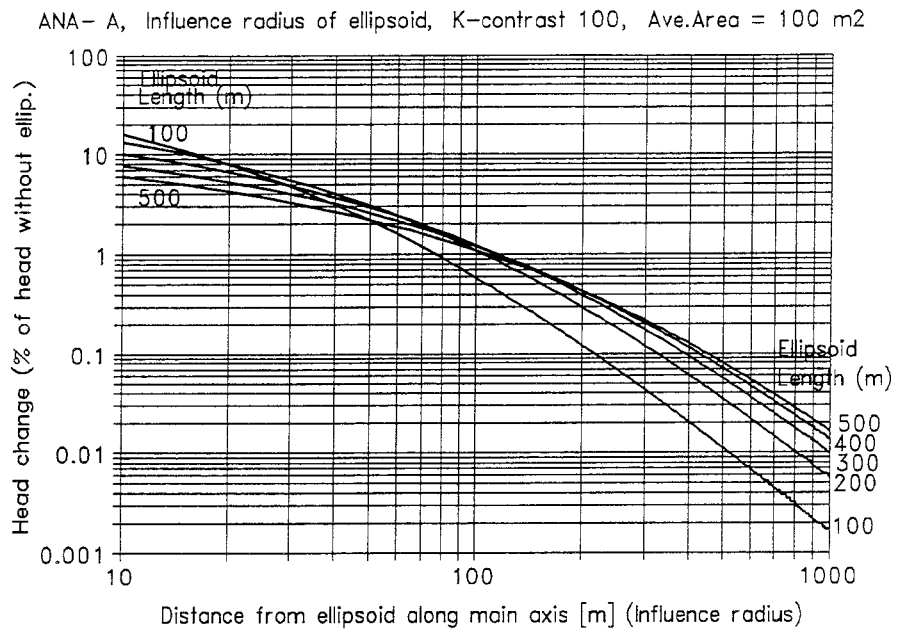


Fig.(ii)
 Ellipsoid data:
 Conductivity
 contrast=10000
 Ac.area=100m²
 Length=...

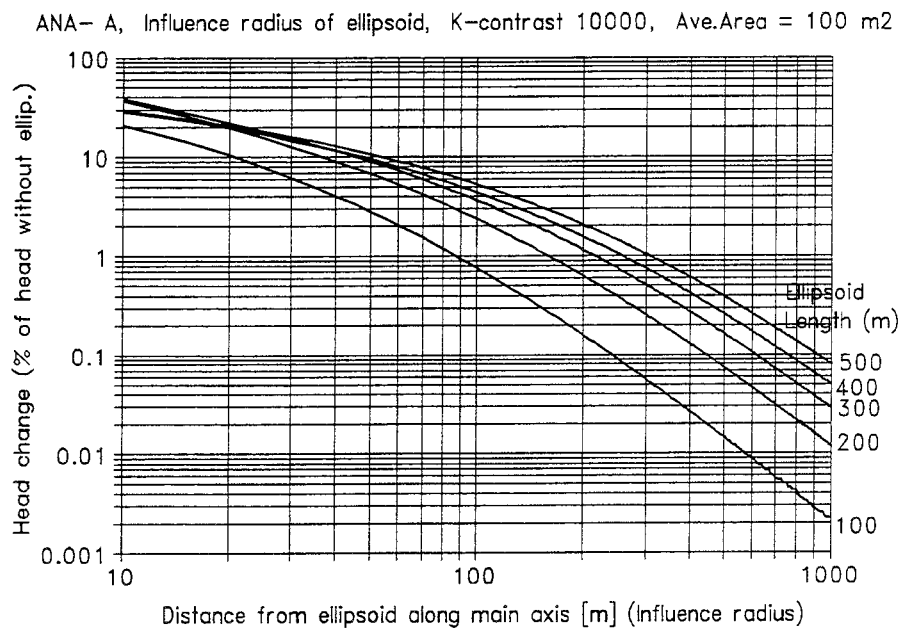


Figure 3.18

INFLUENCE RADIUS OF ELLIPSOID-TUNNEL (2).

The regional flow is directed along the main axis of the ellipsoid.

An ellipsoid-tunnel will change the head in the surrounding rock mass, compared to a situation without an ellipsoid-tunnel. For ellipsoid-tunnels of different properties, the figure gives the influence radius and the corresponding change in head. The change in head is given in percent of the head without the ellipsoid.

Hence, the values are the same, regardless of the size of the regional flow. The models are based on the uniform continuum approach.

The average cross-section at right angles to the main axis of the ellipsoid is 100 m²

Fig.(i) Conductivity of the ellipsoid is 100 times that of the rock mass.

Fig.(ii) Conductivity of the ellipsoid is 10000 times that of the rock mass.

Fig.(i)
 Ellipsoid data:
 Conductivity
 contrast=100
 Ac.area=160m²
 Length=...

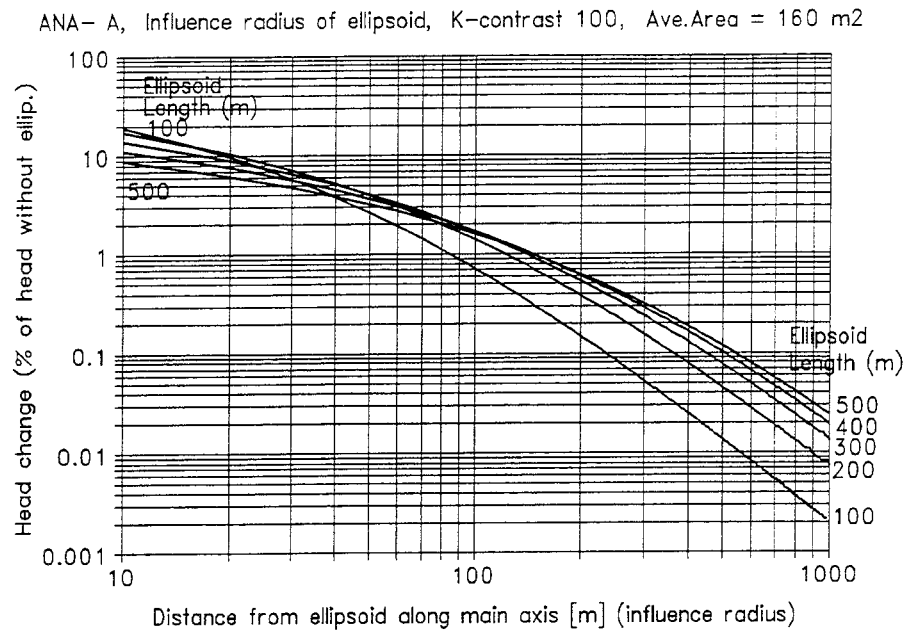


Fig.(ii)
 Ellipsoid data:
 Conductivity
 contrast=10000
 Ac.area=160m²
 Length=...

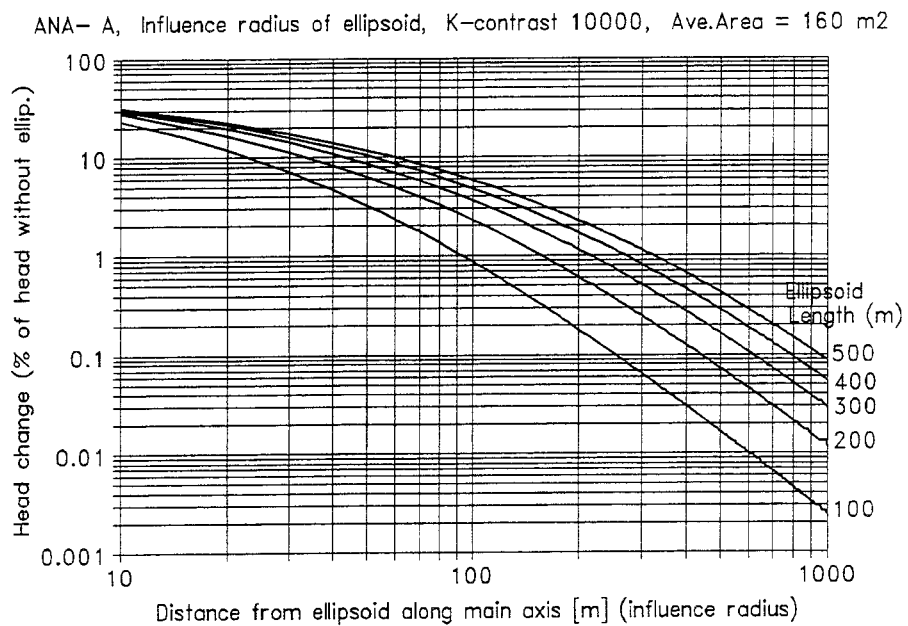


Figure 3.19

INFLUENCE RADIUS OF ELLIPSOID-TUNNEL (3).

The regional flow is directed along the main axis of the ellipsoid.

An ellipsoid-tunnel will change the head in the surrounding rock mass, compared to a situation without an ellipsoid-tunnel. For ellipsoid-tunnels of different properties, the figure gives the influence radius and the corresponding change in head. The change in head is given in percent of the head without the ellipsoid. Hence, the values are the same, regardless of the size of the regional flow. The models are based on the uniform continuum approach.

The average cross-section at right angles to the main axis of the ellipsoid is 160 m²

Fig.(i) Conductivity of the ellipsoid is 100 times that of the rock mass.

Fig.(ii) Conductivity of the ellipsoid is 10000 times that of the rock mass.

Chapter 4.

Method for estimation of boundary effects

4.1 Introduction

A numerical model solves the governing differential equation at a limited number of points, called nodes. A node and surrounding medium is called a cell. The nodes (cells) are arranged in what is called a mesh, representing the studied domain. To minimize the computation time the number of nodes in the mesh has to be limited, but still large enough to adequately represent the studied domain (flow system). The limited size of the model will influence the results. Such effects are called boundary constraints or boundary effects, below follows an estimation of these effects.

4.2 Cause for boundary effects

A tunnel or a repository will change the groundwater flow pattern in the rock mass. If the tunnel is more conductive than the surrounding rock mass, groundwater will flow towards the tunnel at the upstream part and away from the tunnel at the downstream part of it, the opposite will occur if the tunnel is less conductive than the surroundings. The tunnel will change the head in the rock mass surrounding the tunnel. The volume of rock mass affected by the tunnel could be larger than the volume of rock represented in the model.

The boundary of the model could be defined with either a prescribed head boundary condition (specified head boundary) or a no-flow boundary condition. The prescribed head at the boundary is estimated before the model starts the simulation and corresponds to a situation without the tunnel, the head at the boundary is the head of a uniform regional flow without the tunnel. The no-flow boundary condition will have a head calculated by the model during the simulation, based upon the condition that no flow will pass the boundary.

It follows from this that the head at the boundary of the model will be wrong, it will be either too large or too small, compared to the actual head distribution surrounding a tunnel in a regional groundwater flow. Consequently, the flow through the tunnel will be overestimated or underestimated by the model. It will be an overestimation if the difference in head between the boundaries of the model is larger than the actual head difference. If the difference in head between the boundaries of the model is smaller than the actual head difference the model will underestimate the flow.

The flow in the tunnels depend on the direction of the regional groundwater flow and the conductivity of the tunnel. The largest error in flow estimation will occur when the regional flow is directed along the tunnel and the conductivity contrast between the tunnel and the surroundings is large (maximum change compared to undisturbed conditions). The smallest error in flow estimation will occur at the opposite conditions (minimum change compared to undisturbed conditions).

In the numerical model the head at the boundary is the head of an undisturbed regional flow (theoretical head without a tunnel structure inside the mesh). The difference in head between: (i) the head of the undisturbed flow (without tunnel) and (ii) the head of the disturbed flow (with tunnel); could be expressed in percent of the head of the undisturbed flow. We will call this, the head change.

4.3 Number of nodes

The actual head distribution in the surroundings of a tunnel varies in a non linear way, the head change decreases as the distance from the studied structure increases. To represent this non linear head distribution in a model, at a limited number of nodes, we need many nodes, the more nodes the better. Hence, the flow predicted by a model will partly be dependent on the number of nodes representing the non-linear variation of head. The influence of the studied structure decreases with distance (e.g. Figure: 3.2, 3.3, 3.15, 3.16), it is important to have a short distance between the nodes close to the studied structure. Far away from the studied structure we can have a large distance between the nodes.

4.4 Analytical method for estimation of boundary effects

If a prescribed head condition is assigned to all cells at the boundaries of the model, and the prescribed head at the boundaries is the head of an uniform undisturbed flow; these head values will produce a larger gradient between the boundaries than the actual gradient. Hence, the boundary condition will cause an increase in gradient, compared to the actual conditions. The increase in gradient can be compared to the head change, if both entities are expressed in percent. If the shape of the boundaries of the model coincide exactly with the shape of the contours of head change (e.g. Figure 3.16), the increase in gradient (in percent) is equal to the head change (in percent). For a flow system represented by a model with boundaries that do not exactly coincide with the contours of head change, the increase in gradient is approximately equal to the head change.

Equation B.32 in Appendix B demonstrates that the flow in an ellipsoid is directly proportional to the regional flow in the surrounding medium. The regional flow in the surrounding medium is directly proportional to the head gradient of the regional flow. Hence, for the studied structure (the tunnel) the increase in flow (in percent), caused by boundary effects, is approximately equal to the head change (in percent) at the boundary.

Based on the analytical method presented in Appendix B it is possible to calculate the head change in the rock surrounding an ellipsoid-shaped tunnel. At some distance from the ellipsoid, the head change caused by an ellipsoid is probably very similar to the head change caused by a tunnel of approximately the same size. If the boundary of the numerical model is placed at a certain distance from the studied structure, we can calculate the head change at this distance by approximating the studied structure by an ellipsoid and use the analytical method.

The head change, at different distances from an ellipsoid, is calculated analytically for different ellipsoids, the results are given in Figures 3.17 through 3.19. For a model with prescribed head conditions at all boundaries, the head change values (in percent) could be looked upon as an approximation of the overestimation of flow in a studied structure (a tunnel), caused by boundary effects. For example, if we model a tunnel with a rectangular cross-section of 100 m², a length of 100 m and a conductivity which is 100 times larger than that of the surroundings, by using a model in which we have defined a prescribed head boundary at a distance of 100 m from the tunnel; the boundary effects will cause an overestimation of flow in the tunnel which is approximately 0.6 percent (see Figure 3.18), presuming that the mesh contains a sufficient number of nodes.

The analytical method presumes that the studied structure could be represented by a homogeneous ellipsoid. For a straight tunnel this is a fair representation, but for a bent

tunnel, or a system of tunnels, or tunnels which include flow barriers, etc. it is not a good representation. The method could however be used as a part of a sensitivity analysis, if the boundary of the studied model is placed at a large distance from the tunnels.

4.5 Numerical method for estimation of boundary effects - method of multiple meshes

The larger the model, the smaller the error in predicted flow. By starting with a small mesh and increasing it, different flow values will be predicted. The mesh is increased by adding a new layer of cells at all faces of the mesh. Examples of different meshes used for estimation of boundary effects are given in Figure 4.1. As the model is increased in size, the number of cells and the distance to the model boundary grow larger and the predicted flow becomes closer to the unknown correct value. By plotting the size of mesh and the predicted flow, a non-linear relation is revealed (see Figures 4.2 and 4.4).

The boundaries of a numerical model must be assigned a boundary condition. Two alternatives are possible: method B1 which assigns the prescribed head boundary condition to all cells at the boundaries (at all faces of the mesh), or method B2 which assigns the prescribed head boundary condition to the cells of the upstream- and downstream faces of the mesh and the no flow boundary condition to the cells between the upstream and downstream faces. The first alternative (B1) is easy to apply for all directions of the regional flow and for all meshes. The second alternative (B2) could also be used for all directions of regional flow and all meshes, but the method demands that only a selected part of the cells should be assigned the prescribed head condition, which makes it a little more complicated to use, unless the direction of regional flow is at a right angles to the faces of the mesh. Both methods of assigning boundary conditions (B1 and B2) have been studied.

The method of multiple meshes is based on the difference in predicted flow, revealed when comparing the flow predicted by meshes of different size. The basic assumption is as follows:

- If the mesh is increased in size by adding a new layer of cells at all faces of the mesh, the new mesh will predict a flow in the studied structure which is different from the flow predicted by the previous mesh. If the change in predicted flow is expressed in percent of the previous predicted flow, the logarithms of these values (the logarithms of the change in percent) will decrease in an approximately linear way, if plotted against the logarithms of the distance to the boundary of the new mesh (see Figure 4.2[ii] and Figure 4.4[ii]).

Based on this approximately linear relationship, it is possible to calculate the change in predicted flow (in the studied structure) for successively larger meshes, without having to perform the actual simulations. As the change in predicted flow is estimated, it is possible to estimate the flow that these successively larger meshes would have predicted if the actual simulations had been performed.

The change in predicted flow will decrease as the distance from the studied structure to the boundary becomes larger. Accepting a certain change in predicted flow as a permitted error makes it possible to use the flow calculated for the corresponding mesh as the correct flow, assumed to be unaffected by boundary constraints. By the use of the assumed correct flow it is possible to calculate the error in predicted flow for all other smaller meshes. The error, expressed in percent, is the overestimation or underestimation caused by boundary effects, for a particular mesh and a particular distance from the studied structure to the boundary.

As it is possible to calculate an error, it is also possible to calculate a correction factor and correct the flow predicted by a mesh of a certain size. However, the error and the correction factor correspond to a certain flow scenario and are dependent not only of the size of the mesh but also on tunnel lay-out, conductivity values, direction of regional flow etc, and should not be used as a general correction factor.

An advantage of the method of multiple meshes compared to the analytical method is that the method could be used for any type of studied structure. However, the method of multiple meshes has to be used with some care. The quality of the estimate of the boundary effects, produced by the method of multiple meshes, depends on the size of the meshes used in the analysis. The larger the meshes, the better the estimate. Used in a proper way, the method of multiple meshes will give a good estimate of the correct flow.

4.6 Example

Two finite difference models were established. The models represent two different tunnels and surrounding rock mass. The tunnels have a rectangular cross-section of 100 m^2 , a length of either 100 m or 250 m, and a conductivity which is 1000 times larger than that of the surroundings. In the model, the regional flow was directed along the tunnel, as this is the direction that will cause the largest boundary effects. The cell size in the model was $10 \times 10 \times 10 \text{ m}$. The boundary effects were estimated both with the analytical and the numerical method of multiple meshes.

Numerical method - method of multiple meshes

The average flow of the tunnels was calculated for meshes of different size. The method of multiple meshes is demonstrated in Figure 4.1 through Figure 4.4 and in Table 4.1. The boundary conditions were either prescribed head at all faces (method B1) or prescribed head only at the upstream and downstream faces (method B2).

The figures and the table demonstrate that method B1 will overestimate the flow in the tunnels and approach the correct value from larger values, as the distance to the boundary increases. The figures also demonstrates that method B2 will underestimate the flow in the tunnels and approach the correct value from smaller values, as the distance to the boundary increases.

A comparison between method B1 and B2 reveals that method B2 gives a better estimate than method B1, for the same size of mesh. But, method B2 will only give a better estimate if the prescribed head conditions are assigned to the correct parts of the mesh. For a direction of regional flow that is not at right angles to the faces of the mesh, method B1 is more easy to use.

The extrapolated specific flow, used for calculation of error and correction factors, corresponds to a change in estimated specific flow smaller than 0.001 percent when the mesh is increased by adding a new layer of cells at all faces of the mesh (one spherical layer of cells).

Analytical method

The analytical method was also used to estimate the boundary effects, as described in Sec.4.4.

Comparison between the analytical and numerical methods

A comparison between the two methods was carried out and is presented in Figure 4.5. The figures gives the boundary effects as predicted by the two methods: (i) analytical

method and (ii) numerical method of multiple meshes. The boundary effects are represented by values of overestimation and underestimation. That is, the error in estimation of flow that a numerical model will produce for different distances to the boundary.

The figure demonstrates that if the distance to the boundary is small, the boundary effects will be large. As the distance to the boundary increases, the difference between values predicted by the two methods becomes smaller. The difference is caused by: (i) the analytical method using an ellipsoid as a representation of the studied tunnel, and (ii) the boundaries of the numerical models not perfectly coinciding with the contours of the head change.

As the distance from the studied structure increases, the head values caused by an ellipsoid become more or less the same as the head values caused by a rectangular tunnel, and both methods will predict about the same boundary effect.

We note that a small tunnel (Fig.4.5(i)) will cause a smaller boundary effect than a large tunnel (Fig.4.5(ii)). A tunnel with a small conductivity contrast will also cause a smaller boundary effect than a tunnel with a large conductivity contrast (Table 4.1). But, as regards the conductivity contrast, the threshold conductivity (see section 3) gives an approximate upper limit in effects caused by an increased tunnel conductivity.

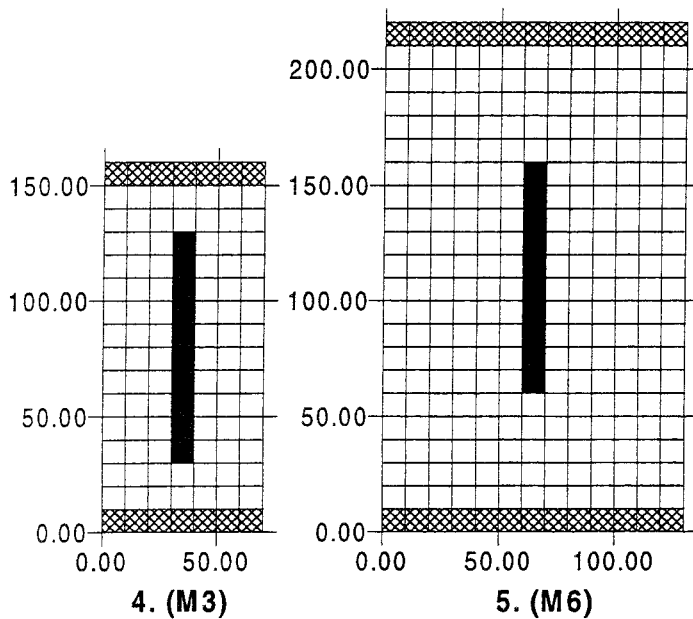
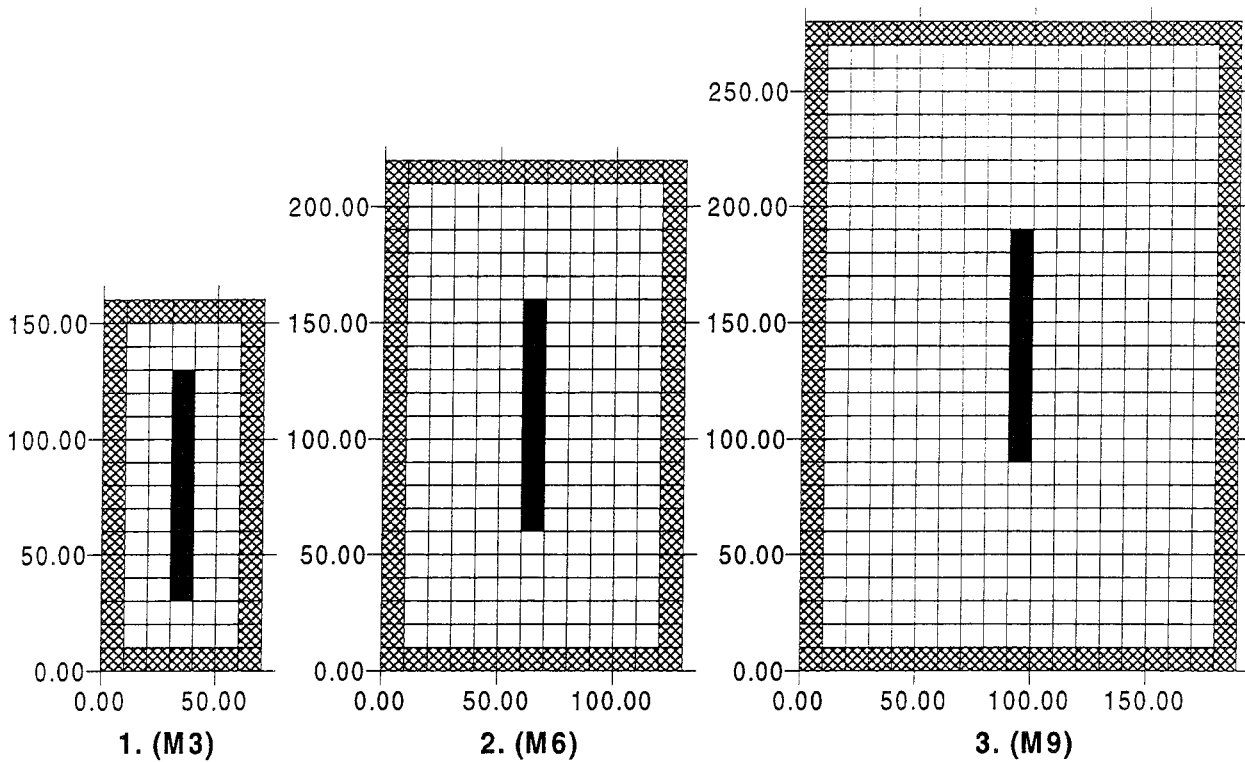
The figure also demonstrates the effect of using smaller or larger meshes in the method of multiple meshes. If we base the method of multiple meshes on small meshes, the method will predict larger boundary effects than if we use large meshes. This effect occurs as the change in flow, given in Figure 4.2(ii) through 4.4(ii), does not decrease in a perfectly linear way.

4.7 Conclusions

It is concluded that a numerical model will overestimate or underestimate the flow in a tunnel. The error in estimation is caused by boundary effects. These effects are unavoidable as the models represent a limited domain i.e is finite in size. However, it is possible, by the use of either an analytical method or the method of multiple meshes, to estimate the boundary effects.

The method of multiple meshes demonstrates, that when modeling a system of tunnels we can use several models, representing successively larger and larger domains, and by comparing the results produced by these models, estimate the boundary effects.

As an alternative to the use of a large model, which may need to be very large to limit the boundary effects, one can use several small models and reach the same result. It is from a numerical point of view, sometimes convenient to use several small models instead of one large model.



METHOD B1

Meshes used for numerical method B1. Specified head boundary condition at all cells along the boundary of the mesh.

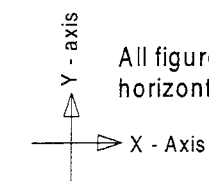
- 1. M3, minimum dist. to spec.head is 25m.
- 2. M6, minimum dist. to spec.head is 55m.
- 3. M9, minimum dist. to spec.head is 85m.

METHOD B2

Meshes used for numerical method B2. Regional flow along tunnel (in horizontal plane). Specified head boundary condition at the upstream and downstream faces of the mesh.

- 4. M3, minimum dist. to spec.head is 25m.
- 5. M6, minimum dist. to spec.head is 55m.

- Cells representing rock mass.
- Cells representing a tunnel, length 100 m.
- Cells representing the rock mass, these cells are assigned the specified head boundary condition.



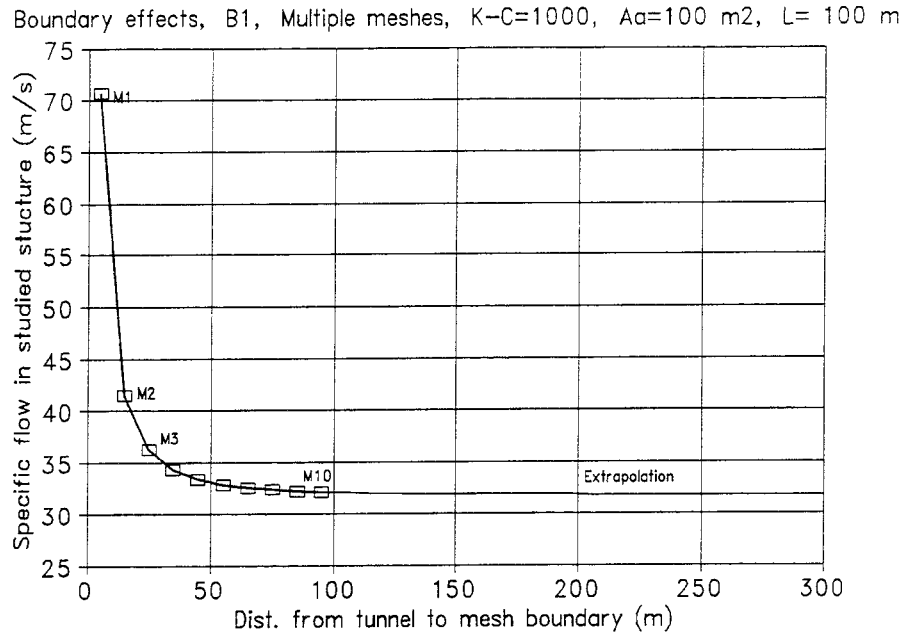
All figures are cross-sections in the horizontal plane, through the tunnel.

Scale in meters

FIGURE 4.1 METHOD OF MULTIPLE MESHES

The figure demonstrates different meshes used for estimation of the boundary effects.

(i)
Size of specific
flow in a
tunnel versus
size of mesh.



(ii)
Change in
specific flow in
a tunnel versus
size of mesh.

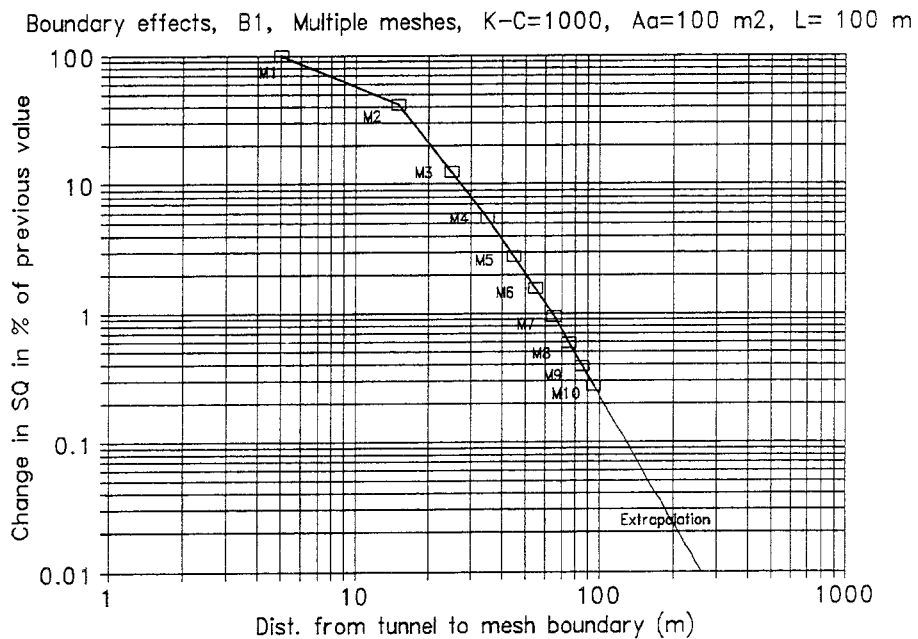
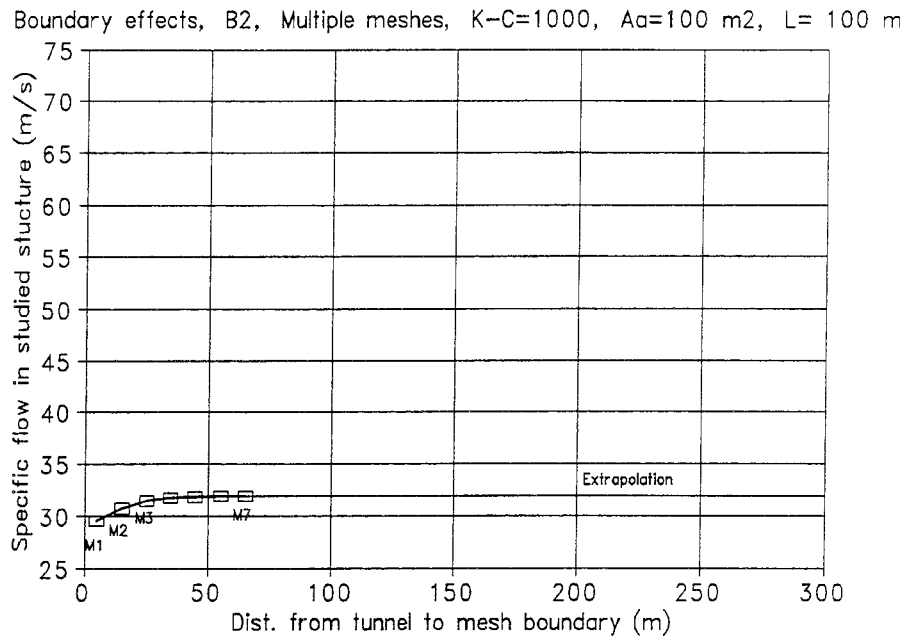


Figure 4.2

BOUNDARY EFFECTS, METHOD OF MULTIPLE MESHES, B1.

Change in calculated specific flow (SQ) in tunnels, versus size of finite difference mesh (model). The change in specific flow is expressed in percent of the specific flow predicted by the previous smaller mesh. M1 - M10 denotes different meshes. Specified head boundary condition occur at all faces of the studied mesh. The model represents a tunnel with a rectangular cross-section of 100 m^2 , tunnel length 100 m . Conductivity of the tunnel is 1000 times that of the rock mass. Cell size in the model is $10 \times 10 \times 10 \text{ m}$. Regional flow directed along the tunnel size 1 m/s

(i)
Size of specific
flow in a
tunnel versus
size of mesh.



(ii)
Change in
specific flow in
a tunnel versus
size of mesh.

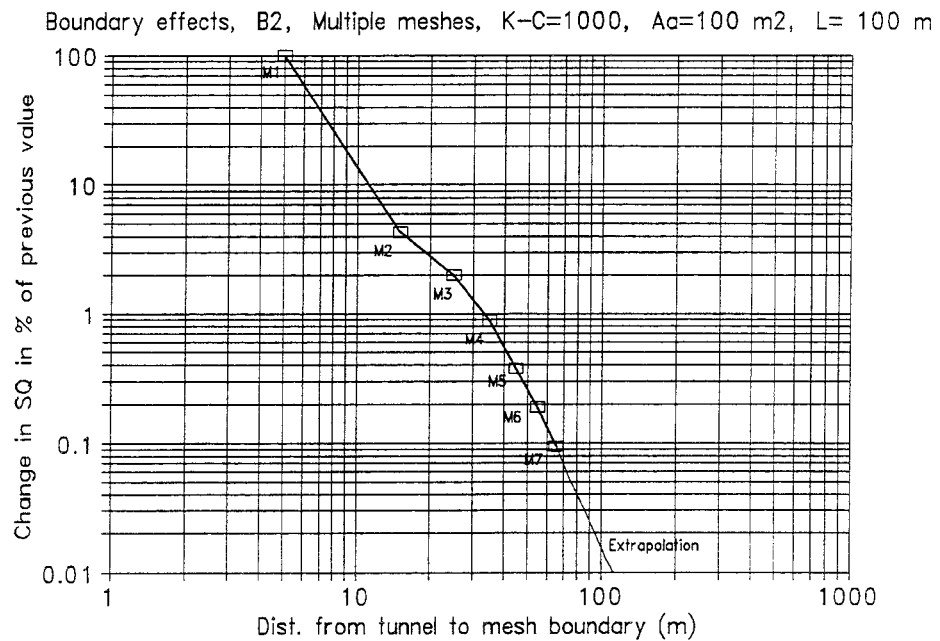
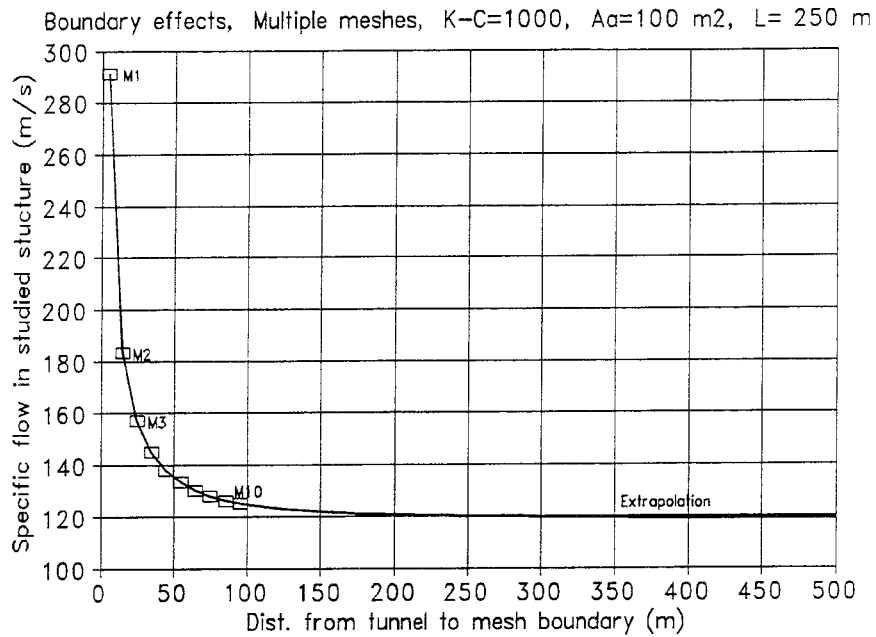


Figure 4.3

BOUNDARY EFFECTS, METHOD OF MULTIPLE MESHES, B2.

Change in calculated specific flow (SQ) in tunnels, versus size of finite difference mesh (model). The change in specific flow is expressed in percent of the specific flow predicted by the previous smaller mesh. M1 - M10 denotes different meshes. Specified head boundary conditions occur at the upstream and at the downstream faces of the studied mesh. The model represents a tunnel with a rectangular cross-section of 100 m^2 , tunnel length 100 m . Conductivity of the tunnel is 1000 times that of the rock mass. Cell size in model is $10 \times 10 \times 10 \text{ m}$. Regional flow directed along the tunnel, size 1 m/s .

(i)
Size of specific
flow in a
tunnel versus
size of mesh.



(ii)
Change in
specific flow in
a tunnel versus
size of mesh.

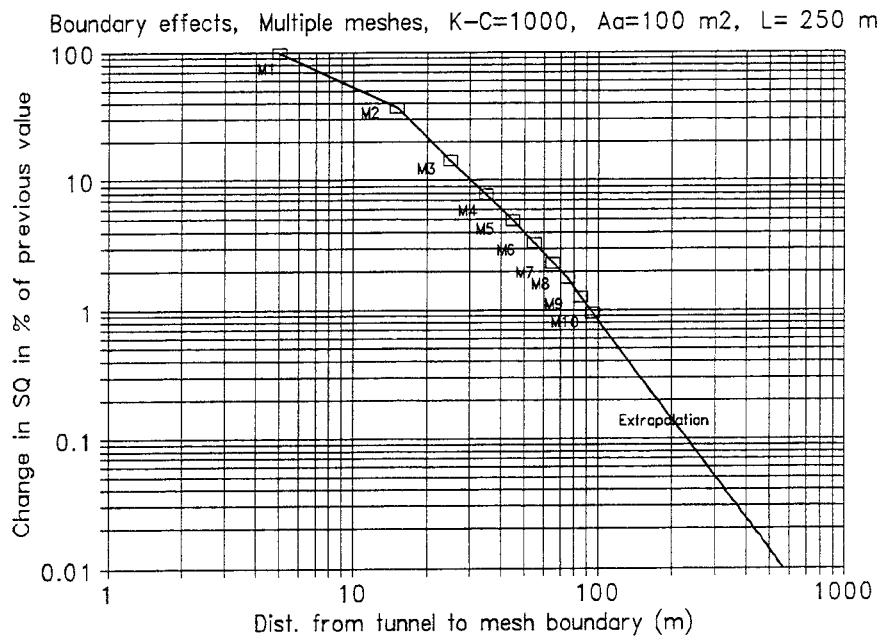
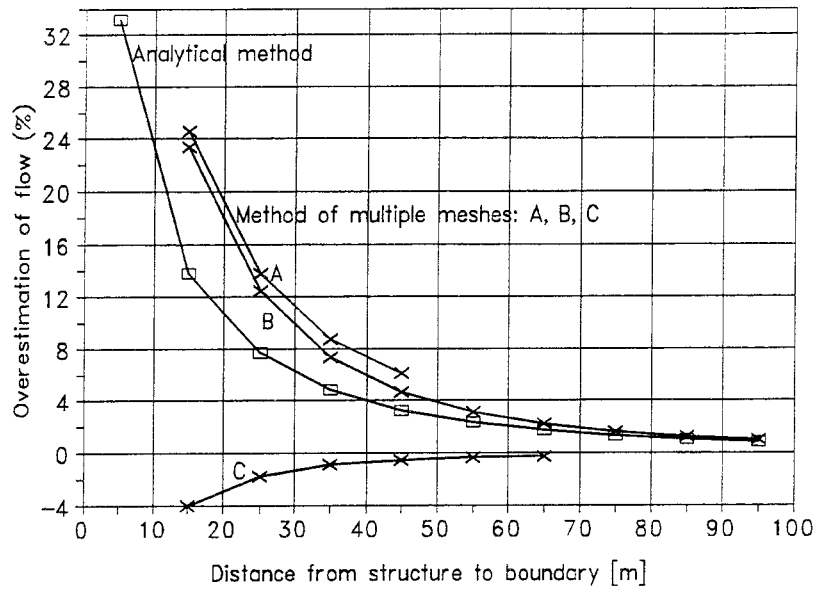


Figure 4.4 **BOUNDARY EFFECTS, METHOD OF MULTIPLE MESHES, B1.** Change in calculated specific flow (SQ) in tunnels, versus size of finite difference mesh (model). The change in specific flow is expressed in percent of the specific flow predicted by the previous smaller mesh. M1 - M10 denotes different meshes. The model represents a tunnel with a rectangular cross-section of 100 m^2 , tunnel length 250 m . Conductivity of the tunnel is 1000 times that of the rock mass. Cell size in model is $10 \times 10 \times 10 \text{ m}$. Regional flow directed along the tunnel, size 1 m/s .

(i)
Overestimation of specific flow in a tunnel vs. size of mesh. Length of tunnel 100 m.

ANA - A - N, RF:A, Boundary constraints, K-C= 1000, Aa= 100 m², L= 100 m



(ii)
Overestimation of specific flow in a tunnel vs. size of mesh. Length of tunnel 250 m.

ANA - A - N, RF:A, Boundary constraints, K-C= 1000, Aa= 100 m², L= 250 m

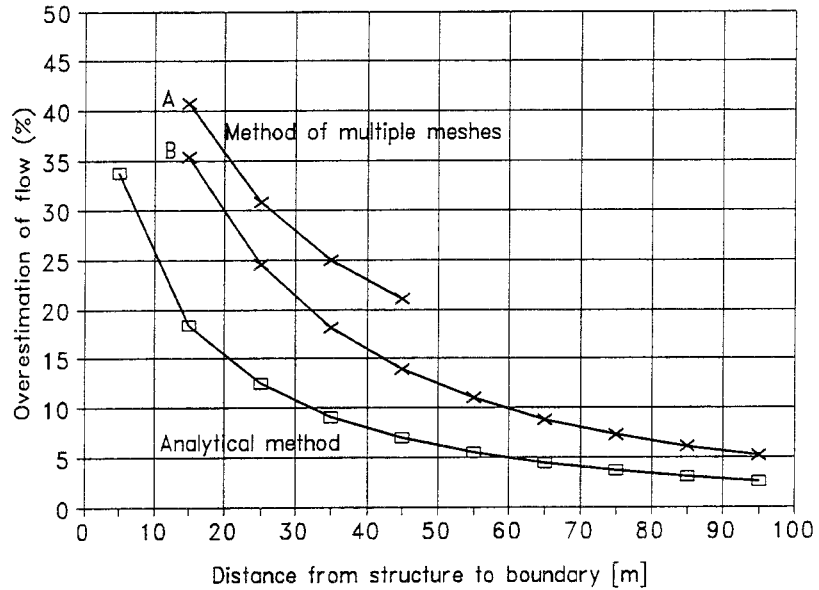


Figure 4.5

BOUNDARY EFFECTS, COMPARISON OF METHODS FOR ESTIMATION.
The analytical method is compared to the method of multiple meshes. The analysis relates to specific flow in a tunnel. The model represents a tunnel with a rectangular cross-section of 100 m², tunnel length is either 100m or 250m. Conductivity of the tunnel is 1000 times that of the rock mass. Cell size 10x10x10 m. Regional flow is directed along the tunnel, size: 1 m/s.

- Analytical method is denoted by squares.
- Method of multiple meshes is denoted by crosses.
Curve A, Method B1, three meshes used, distance to boundary: 25m, 35m, 45m.
Curve B, Method B1, three meshes used, distance to boundary: 75m, 85m, 95m.
Curve C, Method B2, three meshes used, distance to boundary: 45m, 55m, 65m.

Table 4.1 ESTIMATION OF BOUNDARY EFFECTS.
 Estimation of boundary effects as regards meshes of different size, numerical methods and different systems studied.

		Properties of system studied			
Numerical method		B1	B1	B2	B1
Direction of Regional flow		Horizontal along tunnel	Horizontal along tunnel	Horizontal along tunnel	Horizontal along tunnel
Length of tunnel		100 m	100 m	100 m	250 m
Tunnel Conductivity		100 x K rock	1000 x K rock	1000 x K rock	1000 x K rock
MESH	Distance to (1) boundary (m)	Error in predicted specific flow [%] (2)			
M2	15	17.2	23.45	4.1	35.3
M3	25	9.1	12.4	1.8	24.5
M4	35	5.3	7.3	0.92	18.2
M5	45	3.3	4.7	0.54	13.9
M6	55	2.1	3.1	0.35	11.0
M7	65	1.5	2.2	0.26	8.9
M8	75	1.0	1.6	-	7.2
M9	85	0.7	1.2	-	6.0
M10	95	0.5	1.0	-	5.1
(1) Minimum distance between tunnel and boundary of mesh. (2) The specific flow is defined as flow per unit area. The predicted specific flow is the average specific flow of all cells representing the tunnel. The error in predicted specific flow is based on the extrapolated specific flow, set as the correct flow. The error is defined as: $\text{Error} = \text{ABS}(100 - [(\text{correct.spec.flow}) / (\text{calc.spec.flow} / 100)])$					

Chapter 5.

The stochastic continuum approach and the heterogeneous rock mass at Äspö

5.1 Introduction

Groundwater flow in fractured rock occurs in fractures and in fracture zones of different size. The fractures and fracture zones determine the heterogeneous and anisotropic hydraulic properties of the rock mass. We will in this Chapter study the stochastic continuum approach, as a mathematical method of representation of a flow medium with a heterogeneous hydraulic conductivity. We will also study the scale dependency of the heterogeneous hydraulic conductivity, measured at Äspö Hard Rock Laboratory (Äspö HRL). We will propose a method of scaling of the measured hydraulic conductivity, a method that is consistent with the stochastic continuum method.

5.2 Mathematical approach

There are different ways of making a mathematical description of a fractured medium (see Section 2). One way to represent the heterogeneity of the rock mass is by the use of the *stochastic continuum approach*. The use of the stochastic continuum approach for representation of a fractured medium was proposed by Neuman (1987, 1988). The approach is based on the assumption that the actual varying hydraulic properties of the rock mass can be represented in a model by a number of smaller volumes - blocks, having a defined size and varying hydraulic properties. The varying hydraulic properties of the blocks are defined based on probability distributions defining a set of stochastic variables. The concept of blocks, cells and nodes are given in Figure 5.5. For the theoretical development of the stochastic continuum approach we refer to studies by: Matheron (1967), Gelhar (1976), Bakr *et al* (1978), Gutjhar *et al* (1978), Dagan (1979, 1982, 1984, 1986, 1987, 1988), Gelhar and Axness (1983) and Neuman *et al* (1987). A review of the theory is given in Follin (1992a).

We will use the stochastic continuum approach as a mathematical method of representing the varying hydraulic properties of a heterogeneous medium i.e. the fractured rock. It is necessary to understand that the method will only provide us with a generalized description of the actual hydraulic properties of the fractured rock. As it is a generalized method, it is not capable of reproducing all the hydraulic properties of a fractured rock.

The flow medium (the rock mass) will be divided into a number of volumes - the blocks. The blocks will be assigned an hydraulic conductivity according to defined probability distributions, every block will have a random conductivity value based on the probability distributions. Hence, the conductivity is considered to be a regionalized variable, which has a different size at different locations. Different sets of conductivity values (realizations) can be generated with equal probability. If a number of realizations are performed, they demonstrate a possible variation in conductivity distribution. The actual conductivity distribution of a studied site constitutes one possible realization.

To use the stochastic continuum approach we need information about how the studied parameter (i.e. the conductivity) varies in the studied medium (i.e. fractured rock). Based on such information, we can establish a probability distribution that describes the variation of the studied parameter.

5.3 Definition of terms

In a stochastic continuum model, it is important to distinguish between the hydraulic properties of the blocks (local properties) and the hydraulic properties of the system of blocks (regional properties).

When we use the following expressions: "conductivity of block" and "conductivity of cell", we mean the conductivity of the individual blocks or cells - the local hydraulic properties. In a stochastic continuum model, the conductivity of the blocks (the block conductivity field) is given by a block conductivity probability distribution.

When we use the following expressions: "model conductivity", "equivalent conductivity" and "effective conductivity", we mean the conductivity of the system of blocks - regional hydraulic properties. These properties represent the conductivity of the studied model, regarding a flow through the model.

The model conductivity or the equivalent conductivity is the conductivity of a model containing a certain number of blocks. For a given block conductivity probability distribution, the equivalent conductivity is a property that will not be constant, but vary for different realizations of the block conductivity field. If the number of blocks is large, the variation in equivalent conductivity will be small. If the variation in equivalent conductivity is zero, the equivalent conductivity is equal to the effective conductivity.

Hence, the effective conductivity is equal to the equivalent conductivity, if the model contains a sufficiently large number of blocks. When comparing models that contain successively larger number of blocks, we note that equivalent conductivity comes closer to the effective conductivity in an asymptotic way. The sufficient number of blocks depends on (i) the number of dimensions represented in the model and (ii) the standard deviation of the block conductivity distribution, as well as (iii) the acceptable discrepancy between the equivalent conductivity and the effective conductivity.

The concept of block conductivity, equivalent conductivity and effective conductivity is demonstrated in Figure 5.6.

5.4 Variation in hydraulic conductivity, probability distribution and scale dependency

The hydraulic conductivity of a fractured rock is given by the ease with which a studied fluid is transported through the fracture system - the transport capacity of the system. Hence, it is determined by the hydraulic properties of the fracture system. The transport capacity of a fully saturated fracture, defined by two parallel planes, is given by a relationship between the aperture (opening) between the planes and the properties of the transported fluid, see Equation 5.1. This equation, often referred to as the "cubic law", has been derived and studied by many authors, e.g. Bird *et al* (1960), Snow (1968), Whitherspoon *et al* (1980), Hässler (1991) and Bear (1993).

$$Q = W \frac{\gamma g a^3}{\mu 12} \frac{\partial \phi}{\partial l} \quad (5.1)$$

Q =flow (m^3/s), W =width of section (m), γ =density (Kg/m^3), g =gravity (m/s^2) μ =viscosity ($Pa s$), a =aperture (m), ϕ =piezometric head (m), l =length in direction of flow (m)

Studying the equation above, we note that the possible flow through a fracture is an exponential function of the fracture aperture. This indicates the following: for small

volumes of fractured rock it is likely (but not necessarily so), that a naturally occurring variation in fracture aperture (within and between different fractures) will cause a variation in conductivity of the small volumes, which is log-normal distributed (a log-normal probability distribution). On a large scale, spatial properties of the system of fractures are important, properties such as: connectivity, fracture clustering etc, which may produce another distribution of the conductivity.

The conductivity of a studied volume of fractured rock depends on the properties of the fractures inside the studied volume. The fractures have varying properties, so the conductivity will vary between different locations of the studied volume. As the conductivity of a fractured rock depends on a large number of connected fractures, having different properties, the conductivity of fractured rock becomes scale dependent, this is discussed below. The conductivity of a fractured rock is also different for different directions (anisotropic conductivity).

The scale dependency in conductivity of a fractured rock is mainly attributed to three properties of the fracture system: (i) the variation in transport capacity (conductivity) of the fractures and (ii) the variation in consistency (length) of the fractures, as well as (iii) the distribution of the fractures which gives the connectivity of the fracture system.

If we study a small volume of rock, only a few fractures will be included in the volume; the conductivity of the volume will be determined by the integrated properties of a few fractures. If we study a large volume, a large number of fractures will be included; the conductivity of the volume will be determined by the integrated properties of a large number of fractures. The probability of having very large and permeable fractures inside a small volume is less than the probability of having them inside a large volume. The integrated properties depend on: (i) the conductivity of chains of individual fractures of different length and (ii) the structure of the network of fractures, the number of connections between different chains of fractures in 1, 2 or 3 dimensions. The integrated properties of a few fractures and a large number of fractures are not the same. Thus, the conductivity becomes scale dependent. But, as the scale increases the differences in integrated properties, obtained when comparing scales of different size, becomes small. Thus, the scale dependency decreases with increased scale and for scales larger than a very large scale, no scale dependency occurs. At such large scales, the heterogeneity of the fractured rock is unimportant. At this scale the volume of fractured rock is a representative elementary volume, an REV (for a definition of an REV, see Appendix A).

If we study a large volume of fractured rock, divided into several small volumes, the conductivity of a single small volume will probably be different from that of the large volume of rock. The large volume of rock will have one conductivity and the small volumes inside it will have different conductivities. The conductivity of the large volume is given by the interaction of the small volumes. The conductivity of a studied volume of fractured rock is applicable for that specific volume only.

However, the actual flow of groundwater in a small volume of fractured rock, located inside a larger volume of fractured rock, is not only determined by the conductivity of the small volume. The fractures of the studied small volume is a part of a larger system of fractures. Hence, the flow through the studied small volume is determined by the flow through the larger system. Thus, the groundwater flow is given by the integrated properties of a large system of fractures and boundaries, and not by the conductivity of a single small volume of fractured rock. One should note the difference between the conductivity of different volumes of fractured rock and the flow of groundwater through the fractured rock.

Field investigations have shown that for a given formation, the variation in hydraulic conductivity can generally be described by a log-normal probability density distribution, e.g: Krumbein (1936), Law (1944), Walton & Neil (1963), Freeze (1975), Neuman (1982). The log-normal distribution of the conductivity and the scale dependency of the conductivity in the fractured rock at Äspö is documented in Gustafson *et al* (1989) and Wikberg *et al* (1991). In the following simulations we will base the probability distributions and scale dependency on results of field investigations at the Äspö Hard Rock Laboratory.

5.5 Analytical method for estimation of the effective conductivity of a stochastic continuum

Mathematical methods derived for calculation of conduction of heat or electric current are applicable for calculation of groundwater flow, if confined conditions could be assumed for the flow medium or the position of the phreatic surface is known. Before efficient computers became available, analytical methods were derived for a large number of problems. Such analytical solutions are given by Carslaw and Jaeger (1959), see Chapter 3 and Appendix B.

For a flow medium defined in accordance with the stochastic continuum approach, the hydraulic conductivity is a random function in space, i.e. two different blocks of the medium will have different conductivity values. For such a medium, Matheron (1967) has shown the following.

- If the flow is macroscopically uniform (parallel flow lines on the average), whatever the number of dimensions of the flow medium and whatever the distribution of the conductivity of the blocks and its spatial correlation, the average conductivity (the effective conductivity) always ranges between the harmonic mean and the arithmetic mean of the conductivity of the blocks.
- If the probability density function of the conductivity of the blocks is log-normal and unvarying by rotation, in two dimensions, the average conductivity (*effective conductivity*) is exactly equal to the geometric mean.
- It is not possible to define an average conductivity (*effective conductivity*) for steady state and radial flow.

As regards the electrodynamic analogy, Landau and Lifshitz (1960) have demonstrated similar conclusions; and so have Hashin and Shtrikman (1962).

For uniform flow in isotropic and stationary porous media, Landau and Lifshitz (1960) as well as Matheron (1967), propose to extend the results, in two dimensions, to a D number of dimensions. For the case of Log-normal block conductivity distribution, the formula is given below, it is a first order approximation of the effective conductivity.

In addition, Gelhar (1976), Bakr *et al* (1978), Gutjahr *et al* (1978), have given linearized approximations of the effective conductivity of a three-dimensional flow medium represented by a stochastic continuum, presuming that the conductivity of the blocks is log-normal distributed and that the flow is macroscopically uniform. Gutjar *et al* (1978) proposes an equation which is also a first order approximation. Dagan (1993) carries the calculations to the fourth order. Abrahamovich & Indelman (1995) carry the calculations to the sixth order.

Effective conductivity

$$\begin{aligned}
 (i) \text{ 2-dimensions: } & K_E = K_{BG} \\
 (ii) \text{ Matheron, 1967: } & K_E = K_{BG} \exp \left(\sigma_{eLg Kblock}^2 \left(\frac{1}{2} - \frac{1}{D} \right) \right) \\
 (iii) \text{ Gutjahr et al, 1978: } & K_E = K_{BG} \left(1 + \left(\frac{1}{2} - \frac{1}{D} \right) \sigma_{eLg Kblock}^2 \right) \\
 (iv) \text{ Dagan, 1993: } & K_E = K_{BG} \left(1 + \left(\frac{1}{2} - \frac{1}{D} \right) \sigma_{eLg Kblock}^2 + \frac{1}{2} \left(\frac{1}{2} - \frac{1}{D} \right)^2 \sigma_{eLg Kblock}^4 \right)
 \end{aligned} \tag{5.2}$$

K_E = Conductivity of medium, effective conductivity (Length / time).
 K_{BG} = Conductivity of blocks, geometric mean (Length / time).
 $\sigma_{eLg Kblock}$ = Conductivity of blocks, standard deviation of $eLog K_{block}$ (Length / time).
 D = Number of dimensions.

Equation 5.2(iii) and Equ.5.2(iv) can be looked upon as modifications of Equ.5.2(ii). One may look upon Equ.5.2(iii) as a Taylor's series expansion of the exponential in Equ.5.2(ii) including the first order terms; Equ.5.2(iv) is the same, but includes first and second order terms. They have therefore been used to justify Equ.5.2(ii). Equation 5.2(iii) and Equ.5.2(iv) are not applicable to large values of σ_{Kblock} . As regards the formula of Gutjahr *et al* (1978), the authors state that it is not known to what amount the formula is applicable to large values of σ_{Kblock} .

However, this is not a drawback of Equ.5.2(ii) as it is applicable to large values of σ_{Kblock} , provided that one remembers that the formula is an approximation, but still considers it as applicable. The validity of Equ.5.2(ii) has been investigated by many authors. Comparisons with numerical simulations have shown small deviations between the effective conductivity calculated with Equ.5.2(ii) and the effective conductivity calculated with numerical methods, as long as σ_{Kblock} is reasonably small. Dykaar and Kitanidis (1992) found a deviation of only 4 percent and these results are confirmed by Neuman and Orr (1993) up to values of: $\sigma_{eLg Kblock}^2 = 7$ ($\sigma_{eLg Kblock} = 2.6$, $\sigma_{10Lg Kblock} = 1.13$).

In the field it is often observed that in a given formation, samples of the conductivity are correlated in space. As regards spatial correlation, Lachassagne *et al* (1989) claim that: "It can be shown that the above results (equation 5.2) on the averaging of permeability still apply even if they are spatially correlated". De Wit (1995), has shown that for correlated isotropic media, the coefficient in $\sigma_{eLg Kblock}^2$ depends on the form of the correlation function. This is contrary to the equation proposed by Matheron (1967).

It has to be noted that the formulas given above are applicable to a flow medium large enough to fulfill the condition of macroscopically uniform flow. Consequently, for a numerical model that represents a heterogeneous flow medium by the use of a stochastic continuum, equation 5.2 is only applicable if the models includes a sufficient number of blocks with individual conductivity values. The necessary number of blocks depends on the represented number of dimensions and the conductivity distribution of the blocks, this is discussed in Section 5.8.

A comparison of values predicted by the different formulas, for estimation of the effective conductivity, is given in Figure 5.2. The figure gives the effective conductivity, presuming a block conductivity distribution with a geometric mean equal to 1. The standard

deviation of the block conductivity distribution has been varied and is represented by the X-axis. The figure also gives the quota between different estimates, as a way of demonstrating the deviation between the different formulas for estimation of the effective conductivity. Major differences between the estimates takes place if the standard deviation of $e\text{Log } K_{\text{block}}$ is larger than about 3 ($\sigma_{e\text{Log } K_{\text{block}}} > 3$, $\sigma_{10\text{Log } K_{\text{block}}} > 1.3$).

5.6 Results of field investigations at the Äspö Hard Rock Laboratory

To determine the conductivity of the fractured rock at Äspö, packer tests were carried out in a number of bore holes. A summary of the results of the tests are presented in Table 5.1. Table after Follin (1992a), based on data given by Liedholm (1991 a, b).

The interpretations of the packer tests were based on the methods given by Jacob & Lohman (1952) and Moye (1967). These are the most common methods for interpretation, but they are better fitted for a sand aquifer than for a fractured rock. The methods are based on the following assumptions: (i) the flow medium can be represented by a homogeneous and isotropic continuum, (ii) the flow regime surrounding the tested section is spherical-radial. These are not the properties of a fractured rock.

Nevertheless, the method produces conductivity values that are a measure of the actual permeability of the fractured rock. Both our model and the interpretations are based on the continuum approach. Additionally, we are not making a site specific model. We are only interested in the type of distribution and the range within which the values vary. We are not interested in the absolute conductivity of the tested rock. Therefore, we believe that the conductivity values interpreted by the method discussed above can be used in our model study.

The obtained conductivity values were found to be log-normal distributed. An example is given in Figure 5.1, which presents the distribution of the conductivity values obtained from the double packer tests in Bore hole Kas 03 with a packer spacing of 3 m (test scale 3 m). The figure demonstrates that the conductivity values obtained are log-normal distributed. The drop in values at the left part of the distribution corresponds to the minimum flow (conductivity value) possible to measure with the used test equipment.

The scale dependency of the conductivity values measured at Äspö, by the use of packer tests, is demonstrated in Figure 5.3. The figure is based on similar figures in Gustafson *et al* (1989). The tests were conducted as double packer tests, with a packer spacing of 3 m and 30 m, the entire bore hole was also tested as one section. Hence, the bore holes were tested by the use of three different scales, 3 m, 30 m, and the entire bore hole. The geometric mean, the arithmetic mean and the standard deviation of the conductivity values for each test scale were calculated (the geometric mean is equal to: the base of the logarithms, raised to the arithmetic mean of the logarithms of the observations). As the obtained conductivity values are log-normal distributed, the arithmetic mean of the values is much affected by sections giving a very large conductivity. The results obtained from these sections may be affected by limitations in the measuring equipment. The distributions are better defined by the geometric mean, "The geometric mean, which is close to the median, is far more accurate since it is dominated by the most commonly measured values", Gustafson *et al* (1989). The geometric mean values of different scales can be expressed as relative values, by dividing the values with the average bore hole conductivity, this makes a comparison between different bore holes possible. Figure 5.3 (i) demonstrates that the geometric mean conductivity, expressed as a relative conductivity, is scale dependent, it increases with increased scale and converges towards the average bore hole conductivity. The standard deviations of the logarithms of the conductivity

values (eLog K and 10Log K) obtained from different test scales are given in Figure 5.3 (ii). The figure demonstrates that the standard deviation is scale dependent and decreases with increased scale. Figures 5.3 (i) and (ii) also demonstrate another interesting aspect of scale dependency, extrapolation of the curve in (i) and the straight line in (ii) tells us that at a test scale larger than about 1000m, no scale dependency occurs, as the standard deviation becomes equal to zero. Hence, at a scale larger than about 1000m, it is possible that no scale dependency takes place, the conductivity will not vary and the heterogeneous fractured rock mass could be regarded as a uniform continuum. At such a scale the fractured rock is a representative elementary volume (REV).

Figure 5.3 presents measured data at Äspö and an interpreted scale dependency. The figure is taken from [i] ([i]= Gustafson *et al* (1989)) and it is based on data from three bore holes at Äspö. In [ii] ([ii]=Wikberg *et al* (1991)) similar figures are presented, but those figures are based on data from a larger number of bore holes at Äspö. The interpretation of the scale dependency as given in [i] (Figure 5.3) is not the same as the one given in [ii]. The large number of data in [ii] makes alternative interpretations possible. Actually, the large number of data in [ii] makes several different interpretations of the scale dependency possible. In this study we will use the interpretation of the scale dependency as given in [i]. This is because we judge the relationship between geometric mean conductivity and scale in [i] as a better interpretation than the relationship given in [ii]. The relationship given in [i] is non linear and gives the largest scale dependency at small scales and a decreasing scale dependency with increased scale. This seems to be a better interpretation than the relationship given in [ii], which is linear. A linear relationship will give a scale dependency that does not decrease with scale, which seems wrong.

5.7 Representation of the measured scale dependency in a stochastic continuum model, an analytical method for scaling of measured hydraulic conductivity

In a stochastic continuum model we will use blocks of a defined size. We will select the size of these blocks in such a way that the model gives an acceptable representation of the heterogeneity of the flow medium and the structures of the studied system, as well as a reasonable number of blocks that can efficiently be handled by the numerical procedure. Sometimes it is convenient to use blocks of different size in the same model.

The rock mass at Äspö has been tested by the use of double packer tests. The relationship is complicated between: (i) the conductivity values derived from packer tests with a certain test scale, and (ii) the best corresponding block size and block conductivity distribution, in a stochastic continuum model. The relationship has been studied by the use of stochastic continuum models (e.g. Follin, 1992a and 1992b). The above discussed relationship and other scale effects have also been studied by the use of stochastic discrete fracture flow models (e.g. Axelsson *et al* 1990, Geier & Axelsson 1991, Geier *et al* 1992, Geier & Doe 1992, La Pointe *et al* 1995).

We will select a probability distribution for the block conductivity, which gives a scale dependency of the model, that is in line with the observed scale dependency at Äspö. The packer tests at Äspö were evaluated by the use of methods that involve large generalizations. When we compare a block size and a test scale we have to remember the generalization of the evaluations methods. We also note that the tested volume of rock is not equal to the volume of a sphere or a cube having a diameter or a side equal to the packer spacing. In a packer test of a fractured rock, the actual volume of tested rock mass will vary depending on the properties of the fracture network. For example it is possible that a highly permeable rock mass will lead to a large volume of tested rock mass, and vice versa. When using conductivity values obtained for one test scale and upscaling

these values for the use in models having a larger block size than the test scale, we may have to consider an anisotropy in conductivity of the blocks of the model. This has been investigated by Follin (1992a). Such an anisotropy has not been introduced to the conductivity of the blocks of these models.

Thus, the relationship between tests scale and block size is not a simple one, a test scale (packer spacing) of 10 m does not necessarily correspond directly to a block size of 10x10x10 m. Nevertheless, it is likely that the probability distribution, representing the conductivity of blocks of size 10x10x10 m, should have a standard deviation that is in the range of the standard deviations obtained from packer tests with a test scale (packer spacing) of 3 m or 30 m, and close to an interpolated value representing a test scale of 10m.

The measured scale dependency is not directly applicable to a stochastic continuum model. The probability distributions that define the conductivity of blocks of different size, in a stochastic continuum model, has to fulfil the condition of constant effective conductivity. Hence, regardless of the selected size of blocks, the effective conductivity should be the same for a model of very large size (a very large number of blocks). The effective conductivity of a three dimensional flow medium, defined as a stochastic continuum, can be calculated by the use of equation 5.2

If we use equation 5.2 and the values given by the curves in Figure 5.3, and calculate the effective conductivity for different scales; we note that the effective conductivity will not be constant for different scales. Hence, if we presume that the scale in the figure corresponds to the block size of a stochastic continuum model, we will get a different effective conductivity for different block sizes and, as a consequence, the flow through the model will depend on the size of the blocks. This is not satisfying, the flow through the model should be the same, regardless of the selected size of the blocks. Why will not the measured scale dependency fulfil the condition of constant effective conductivity ? Probably due to the following reasons:

- i. The curve, fitted to the measured scale dependency, is not a good representation of the actual and unknown scale dependency - no good method for fitting the curve.
- ii. The stochastic continuum approach is not a perfect way to represent the heterogeneous properties of a fractured rock, especially not if the studied volumes of rock are small.
- iii. The theoretical generalizations of the methods of evaluation of the packer tests are not applicable for small volumes of fractured rock. Additionally, from a practical point of view, the packer tests have a measurement limit, corresponding to a minimum conductivity. The measurement limit influences the results of the tests, especially for small volumes of rock, for which the probability of a low permeability is large. Furthermore, the measured "scale" (packer spacing) is not directly comparable to the block size.
- iv. The analytical method for estimation of the effective conductivity of a stochastic continuum model (equation 5.2) is applicable to steady state macroscopic uniform flow in three dimensions. However, it is possible that the hydraulic properties (geometric mean conductivity and standard deviation) derived from a large number of packer tests of different small volumes of rock, assuming radial flow etc., do not represent the same thing as the hydraulic properties of the blocks of a 3-dimensional stochastic continuum model.

- v. The analytical methods for estimation of the effective conductivity of a stochastic continuum model (equation 5.2) will perhaps not produce a good estimate if the standard deviation of the conductivity distribution is large ($\sigma_{eLg \text{ block}} > 3$, $\sigma_{10Lg \text{ block}} > 1.3$).

Nevertheless, as we are using the stochastic continuum approach we need to define a scale dependency that will produce probability distributions for the conductivity of the blocks, in such a way that the model will get a constant effective conductivity, regardless of the block size. We can get such a scale dependency by fitting the right curves to the measured scale dependency. The curves should: (i) give an acceptable fit to measured values of conductivity and standard deviation (measured scale dependency), as well as (ii) fulfil the condition of constant effective conductivity, additionally (iii) we want a scale dependency that, in an acceptable way, can be reproduced by a stochastic continuum model. The concept of: block conductivity, equivalent conductivity, effective conductivity and scale dependency in block conductivity, is shown in Figure 5.6.

We will use the following method:

- Estimate an effective conductivity and at what scale the effective conductivity is applicable, a scale at which the standard deviation in equivalent conductivity is approximately equal to zero.
- Fit a function to the measured scale dependency in geometric mean conductivity.
- Based on this function, calculate values of the geometric mean of the block conductivity, for desired scales.
- Calculate the standard deviation of the block conductivity, for desired scales, based on (i) the obtained values of the geometric mean of the block conductivity, (ii) by the use of equation 5.3 and (iii) the given constant value of effective conductivity.

The function should primary be fitted to the measured geometric mean conductivity and not to the standard deviation of the logarithms of the measured values. This is because we estimate that the measured geometric mean conductivity is a more reliable property than the standard deviation of the logarithms of the measured conductivity.

The method described above will produce a function that can be looked upon as an interpolation between measured values, conditioned to represent the properties of a stochastic continuum; the properties of the stochastic continuum is estimated by the use of analytical methods. The method is a direct and analytical method for scaling of conductivity values, based on the stochastic continuum approach.

In Figure 5.4 the curves marked with an **A** are the same as the curves in the previous figure (Figure 5.3), these curves do not produce a constant effective conductivity. However, the curves marked with **B** (**B1** and **B2**) are based on the method described above, they will give an acceptable fit to measured values and will also define conductivity distributions that will give a constant effective conductivity, regardless of the size of blocks. They are also defined in such a way that the standard deviation of the block conductivity distributions is zero for a scale of 1000 m. Additionally, curve **B** gives a good fit to the simulated scale dependency, discussed in Section 5.9.

Curves **B** (**B1** and **B2**), represent the scale dependency at Äspö, they are based on the functions defined by equation 5.3. By the use of equation 5.3, curves can be produced that define a scale dependency with a constant effective conductivity. Four parameters: P_1 , P_2 , P_3 and P_4 are used to fit a function to the measured scale dependency. The first parameter defines the block size for which the standard deviation in block conductivity is set to zero (scale for which the effective conductivity is applicable). The other three parameters define the shape of the function for block sizes smaller than this value.

The difference between curve **B1** and **B2** is that they are based on different formulas for estimation of the effective conductivity, **B1** is based on Gutjahr *et al* (1978) and **B2** is based on Matheron (1967). The major differences occur at small scales, smaller than 10 m. At small scales the stochastic continuum approach is not a good representation of a fractured rock. Both curves are to be looked upon as estimates.

Considering curve **B** (**B1** and **B2**) in Figure 5.4, we note that the fit to measured values is good for the geometric mean conductivity. As regards the fit to the standard deviation of the measured values, the curves deviate from the measured values, at small scales. For curve **B1** the deviation occurs at scales smaller than about 7 m, for curve **B2** the deviation occurs at scales smaller than about 3 m. Furthermore, if the scale is small the standard deviation, predicted by curve **B1** and **B2**, changes dramatically for small variations in scale. This demonstrates that for small scales, the use of the stochastic continuum approach for representation of a fractured rock involves large uncertainties.

Functions defining scale dependency, to be used in a stochastic continuum model

$$K_{BG} = \frac{2 \operatorname{atan}(X)^{P_2} - \operatorname{atan}(P_1)^{P_2}}{\operatorname{atan}(P_1)^{P_2}} \frac{\operatorname{atan}(X P_3)}{\operatorname{atan}(P_1 P_3)} \frac{X^{P_4}}{P_1^{P_4}} K_E$$

Alternative i, Gutjahr *et al*, 1978: $\sigma_{eLgKblock} = \sqrt{\frac{6K_E}{K_{BG}} - 6}$ (5.3)

Alternative ii, Matheron, 1967: $\sigma_{eLgKblock} = \sqrt{6 e \operatorname{Log} \left(\frac{K_E}{K_{BG}} \right)}$

- K_E = Effective conductivity of the flow domain represented by a stochastic continuum.
- K_{BG} = Log-normal block conductivity distribution: Geometric mean of the distribution.
- $\sigma_{eLgKblock}$ = Log-normal block conductivity distribution: Standard deviation of the natural logarithms of the distribution (STD of $e \operatorname{Log} K_{block}$).
- X = Scale of field measurements as well as size of blocks in stochastic continuum model.

Curve fitting parameters

P_1 = Curve fitting parameter, corresponding to the block size for which the standard deviation of the block conductivity is set to zero.

P_2 = Curve fitting parameter.

P_3 = Curve fitting parameter.

P_4 = Curve fitting parameter.

Parameters defining curve: B

	P_1	P_2	P_3	P_4	K_E
Curve B	1000	2.65	0.14	0.04	1

5.8 Numerical considerations

To solve the original differential equation with its boundary conditions, we will use a numerical method. The numerical method might produce a solution that is different from a solution derived by an analytical method, even if boundary effects are considered. A not calibrated, finite difference (FID) model will underestimate the equivalent conductivity, a not calibrated, finite element (FEM) model will overestimate the equivalent conductivity; if the domain studied is represented by a stochastic continuum.

The model we will use is the GEOAN model, Holmén, (1992), briefly presented in Appendix A. This is a FID model which uses the block centered flow approach and a variable number of nodes per block. For the concept of block, cells and nodes, see Figure 5.5. For the concept of models representing different number of dimensions, see Figure 5.7

The FID model will underestimate the flow of a stochastic continuum and as a consequence it will produce an equivalent conductivity which is too small. The reason why the FID model underestimates the flow, comes from the way the model represents the conductivity (or conductance or resistance) between the nodes. Presuming that we use one node per block, the nodes represent different blocks (volumes) of the flow medium and these blocks will have different conductivity values. However, a FID model uses only one value of conductivity between two nodes, even if every node represents a block with a different conductivity value, this one value is called the homogenized conductivity. The model calculates that one value (the homogenized conductivity) based on a given method of averaging. The physically correct method, presuming that the block conductivity is constant within each block, is to calculate the homogenized conductivity between the nodes as the harmonic mean conductivity. Assuming that the volumes are of equal size, the harmonic mean conductivity is calculated as:

$$K_H = \frac{N}{\sum_{i=1}^N K_i^{-1}} \quad (5.4)$$

K_H = Harmonic mean conductivity between nodes (homogenized conductivity).

N = Number of nodes to compare (normally two nodes).

K = Conductivity of the domain represented by the node.

The problem is, as discussed above, that this method will lead to an underestimation of the equivalent conductivity, compared to analytical predictions.

In a model that uses the deterministic continuum approach, the flow medium is defined with a few domains having different conductivity values. The underestimation could be ignored in such a model, as a domain having a different conductivity value is represented by a large number of nodes and the effect discussed above will only occur at the boundary of such a domain. But, in a stochastic continuum model, the flow medium is defined with a large number of blocks, all having different conductivity values and normally only one node per block.

One way of avoiding the problem is to have a large number of nodes per block; the effect of having a different number of nodes per block is given in Figure 5.8, for a two-dimensional as well as a three-dimensional model. The figure demonstrates that the geometric mean of the equivalent conductivity of a FID model comes closer to the effective conductivity predicted by an analytical method, as the number of nodes per block is increased. However, the analytical method presumes that the flow is macroscopically uniform. For the models studied, this assumption is applicable for the model representing a two-dimensional flow medium, but not for the model representing a

three-dimensional flow medium. For the three-dimensional model, used for the calculations given in Figure 5.8, the discrepancy between the values predicted by the FID method and the analytical method is not only attributed to the underestimation of flow, as discussed above, but also to boundary effects, as the size of the model is too small to fulfil the condition of macroscopically uniform flow in three-dimensions.

An interesting effect demonstrated in Figure 5.8(ii) is, that the standard deviation of the logarithms of the equivalent conductivity is not much affected by the number of nodes per block. The model seems to get a correct heterogeneity of the flow medium when the homogenized conductivity is calculated as the harmonic mean, regardless of number of nodes per block.

Thus, an FID model will underestimate the geometric mean of the equivalent conductivity but not the standard deviation of the logarithms of the equivalent conductivity, if the homogenized conductivity is calculated as the harmonic mean. If we try to correct the underestimation in equivalent conductivity by the use of a large number of nodes per block, it will become clear that it is not a good method, due to numerical reasons. The total number of nodes in such a model will be too large to be efficiently handled by a numerical procedure.

Could another method for calculation of the homogenized conductivity produce a better estimate of the equivalent conductivity, another method than the harmonic mean? Different methods of calculating the homogenized conductivity are given below, we may call them different averaging methods.

Methods for calculation of homogenized conductivity, different averaging methods.

$$\begin{aligned}
 \text{(i) Harmonic: } K_H &= \frac{2}{K_1^{-1} + K_2^{-1}} \\
 \text{(ii) Arithmetic: } K_H &= \frac{K_1 + K_2}{2} \\
 \text{(iii) Geometric: } K_H &= \sqrt{K_1 K_2} \\
 \text{(iv) Method A: } K_H &= \frac{K_2 - K_1}{e \text{Log} (K_2 / K_1)} \\
 \text{(v) Method B: } K_H &= \frac{K_1 K_2}{K_2 - K_1} e \text{Log} \left(\frac{K_2}{K_1} \right) \\
 \text{(vi) Method C: } K_H &= \frac{2}{K_1^a + K_2^a} \\
 \text{(vii) Calibrated harmonic: } K_H &= \frac{2}{C K_1^{-1} + C K_2^{-1}}
 \end{aligned} \tag{5.5}$$

K_H = Homogenized conductivity between two nodes (blocks).

K_1 = Conductivity of block 1, represented by node 1.

K_2 = Conductivity of block 2, represented by node 2.

a = Exponent to be used in general formula for averaging (vi).

C = Calibration factor to be used in formula (vii).

We can look upon the different methods as based on possible ways of variation of the conductivity between the nodes. For example, the harmonic method assumes that the conductivity is constant within each block and that the change in conductivity occurs at the boundary of the blocks, we could instead assume that the conductivity varies in a linear way between the nodes; what method of averaging will that produce?

Larsson (1997) has mathematically derived method (i) to (v) based on different variations of the conductivity between the nodes. (i) The harmonic method presumes a discrete variation of the conductivity of the nodes (two values). (ii) The arithmetic method presumes a linear variation of the squares of the conductivity of the nodes. (iii) The geometric method presumes a linear variation of the square root of the conductivity of the nodes. (iv) Method A presumes a linear variation of the conductivity of the nodes. (v) Method B presumes a linear variation of the logarithms of the conductivity of the nodes.

(vi) Method C is based on the general formula for averaging. With the use of different exponents, a , different types of averages can be obtained. Lachassagne *et al* (1989) have proposed a value of: $a = -0.23$, to minimize the underestimation of the equivalent conductivity.

(vii) Another way of avoiding the underestimation of flow is to introduce a method of correction. The most straightforward method of correction seems to be the introduction of a calibration factor in equation 5.4. If we study Figure 5.8 we note that one way of correcting the FID model is to increase the conductivity between the nodes, by increasing the geometric mean of the specified block conductivity distribution, but not changing the standard deviation of the logarithms of the specified conductivity distribution. This can be done by the use of a calibration factor when the harmonic mean conductivity between the nodes is calculated, as in equation 5.5(vii).

The above defined methods for calculation of homogenized conductivity (Equ 5.5) have been investigated. The distributions of the homogenized conductivity produced by different methods are given in Figure 5.9. We note that the methods produce very different distributions of the homogenized conductivity, especially for large values of the standard deviation of the logarithms of the block conductivities ($\sigma_{10Lg\ Kblock}$). It is important to study the standard deviation of the logarithms of the homogenized conductivity ($\sigma_{10Lg\ KH}$) as this is a measure of the heterogeneity of the flow medium. We believe that the $\sigma_{10Lg\ KH}$ predicted by the harmonic methods (Equ.5.5 i and vii) is the most correct one, this is because the value does not change with increased number of nodes per block, it is also a conservative value as it is the largest value. Hence, a different method that will produce a much smaller $\sigma_{10Lg\ KH}$ is not recommended, even if it gives a good estimate of the equivalent conductivity, as such a method will reduce the heterogeneity of the flow medium, and the reason why we use the stochastic continuum approach is because we want to study the effects of the heterogeneity of the flow medium.

The next step, after we have studied the homogenized conductivity, is to study what equivalent conductivity and what effective conductivity the different methods produce. To do this we will have to carry out flow simulations, in models representing a two- and a three-dimensional flow medium. The equivalent conductivity was calculated on the base of Darcy's law (Darcy, 1856), as given below.

$$K_{equ} = \frac{Q}{I A} \quad (5.6)$$

K_{equ} = Equivalent conductivity of model [L / T].

Q = Groundwater flow through model [L³ / T].

I = Regional head gradient [-].

A = Cross section area of model in direction of regional flow [L²].

The regional head gradient will cause the flow. The gradient was created by application of the specified head boundary condition. Specified head will be assigned to the blocks (cells) of two opposite faces of the studied models. All other faces will have the no flow boundary condition. The blocks at the specified head faces will be of a non continuous type (specified head), all other blocks in the model will be of the continuous type. Hence, the models will have boundary conditions in the same way as model 4 and 5 in Figure 4.1, but the size of the models will be different and no tunnel will be included in the models. The length of the models will be defined by the distances between the nodes at the center of the specified head blocks of the two opposite faces.

For a stochastic continuum model many realizations have to be performed and included in the statistical analyses of each studied scenario (see Section 5.10). In this section the equivalent conductivity is studied, the number of necessary realizations depend on the acceptable uncertainty and the size of the variation in the calculated equivalent conductivity. For the models studied in this section, the number of realizations have been varied from about 400 to more than 2000 realizations, for each scenario studied.

When we do flow simulations, we need to be aware of boundary effects and select a model of such a size that we can ignore them or control them. The boundary effects (scale dependency) for two dimensional models are illustrated in Figure 5.10 and for three dimensional models in Figure 5.11. The figures gives the equivalent conductivity for different sizes of models and for different methods of homogenization.

- *Size of model. Two-dimensional flow medium.* For a two-dimensional model containing a few blocks, the geometric mean of the equivalent conductivity will not change with increased model size. Even for very small models (10 blocks), the value is the same as for large models (>1000 blocks), but different values will be produced by different methods of homogenization. The standard deviation of the logarithms of the equivalent conductivity ($\sigma_{10Lg\ Kequ}$) decreases with increased scale but will not be reduced to a small value unless the numbers of blocks are large (>1000 blocks). We also note that the methods that had the largest $\sigma_{10Lg\ KH}$ will also have the largest $\sigma_{10Lg\ Kequ}$. The exponent proposed by Lachassagne *et al* (1989) together with Method C, will produce a much smaller $\sigma_{10Lg\ Kequ}$ than the other methods. • Thus, if we want to study the effective conductivity of a two-dimensional flow medium, we could use a small model containing e.g. 100 blocks or even a smaller number of blocks. The effective conductivity is given by the geometric mean of the equivalent conductivity.
- *Size of model. Three-dimensional flow medium.* For a three-dimensional model, the geometric mean of the equivalent conductivity increases with increased model size, but the change is small for large models (>3000 blocks). Different values will be produced by different methods of homogenization. The standard deviation of the logarithms of the equivalent conductivity ($\sigma_{10Lg\ Kequ}$) decreases with increased scale but will not be reduced to a small value unless the numbers of blocks are large (>3000 blocks). We also note that the methods that had the largest $\sigma_{10Lg\ KH}$ will also have the largest $\sigma_{10Lg\ Kequ}$. • Thus, if we want to study the effective conductivity of a three-dimensional flow medium, we need a large model containing e.g. >3000 blocks, or

even a larger number of blocks if the $\sigma_{10Lg\ Kblock}$ is large. The effective conductivity is given by the geometric mean of the equivalent conductivity.

To decide which method of homogenization gives the best representation of the heterogeneous flow medium, we will compare the effective conductivity predicted by models that use different methods of homogenization, with the effective conductivity predicted by analytical methods. We will also compare the heterogeneity of the flow medium produced by different methods of homogenization, this will be done by comparing the produced values of $\sigma_{10Lg\ KH}$. A comparison of the effective conductivity predicted by models that uses different methods of homogenization; with the effective conductivity predicted by analytical methods, is given in Figure 5.12(i) for a two dimensional flow medium and in Figure 5.12(ii) for a three dimensional flow medium.

- Homogenization method. Two-dimensional flow medium.* For a two-dimensional flow medium the analytical solution is well defined. • The smallest deviations between analytical and numerical predictions of the effective conductivity, is obtained with the calibrated harmonic method. With this numerical method we can get exactly the same value of the effective conductivity, as the value predicted by the analytical method. The second smallest deviation is obtained with Method C, and then comes Method B. The geometric method overestimates, and the not calibrated harmonic method underestimates, the effective conductivity with about the same size of deviation.

• The heterogeneity of the flow medium is given by $\sigma_{10Lg\ KH}$, a comparison of the methods that produce the best estimate of the effective conductivity (see Fig.5.9 and Fig.5.12), demonstrate the following. The calibrated harmonic method produces the largest and probably the best estimate of $\sigma_{10Lg\ KH}$ (largest heterogeneity). Method C gives a $\sigma_{10Lg\ KH}$ which is much too small, that method should not be used. Method B gives about the same $\sigma_{10Lg\ KH}$ as the calibrated harmonic method. • Thus, for a two dimensional flow medium, the best method for calculation of the homogenized conductivity is the calibrated harmonic method, calibrated against a two-dimensional analytical solution. Second best is Method B, third best is the not calibrated harmonic method, and the fourth best method is the geometric method. The geometric method is not as good as the not calibrated harmonic method, as it gives a smaller $\sigma_{10Lg\ KH}$
- Homogenization method. Three-dimensional flow medium.* For a three-dimensional flow medium several different analytical solutions exist, the methods proposed by: Matheron (1967), Gutjhar *et al* (1978) and Dagan (1993) are discussed in previous sections. For small values of $\sigma_{10Lg\ Kblock}$ the deviation between predictions by the different analytical methods is small, but if $\sigma_{10Lg\ Kblock}$ is large, the deviation between predictions by the different analytical methods is large as well. • We will compare the different numerical predictions of the effective conductivity with the different analytical predictions of the effective conductivity. The smallest deviations between numerical and analytical predictions is obtained with the calibrated harmonic method, calibrated against an analytical solution for three dimensions. With this numerical method we can get exactly the same value of effective conductivity, as the value predicted by an analytical method, but we have to decide which analytical method to compare with. The second smallest deviations is obtained with the geometric method. The geometric method predicts numerical values close to the analytical prediction by Gutjhar *et al* (1978), but values smaller than the analytical predictions by Matheron (1967) and Dagan (1993). The third smallest deviations are produced by the harmonic method, calibrated for two dimensions, the fourth smallest by Method B.

• The heterogeneity of the flow medium is given by $\sigma_{10Lg\ KH}$, a comparison of the methods that produce the best estimate of the effective conductivity (see Fig.5.9 and Fig.5.12), demonstrate the following. The harmonic methods (calibrated and not calibrated) produces the largest and probably the best estimate of $\sigma_{10Lg\ KH}$ (largest

heterogeneity). The geometric method gives a $\sigma_{10Lg KH}$ which is distinctively smaller than the value predicted by the harmonic methods. Method B gives about the same $\sigma_{10Lg KH}$ as the harmonic methods. • Thus, for a three-dimensional flow medium, the best method for calculation of the homogenized conductivity is the calibrated harmonic method, calibrated against a three-dimensional analytical solution. Second best is the geometric method, if one can accept the smaller $\sigma_{10Lg KH}$. Third best is the harmonic method calibrated for two dimensions and fourth best is Method B.

As we have recommended the calibrated harmonic method, we will now discuss how to calculate the calibration factor. The calibration factor depends on the probability distributions defining the conductivity of the blocks; it depends on the defined standard deviation of those distributions. It is also dependent on how the FID method is implemented in the numerical algorithm, e.g. method of representation, number of nodes per block, position of nodes, etc.

For a given probability distribution of the block conductivity, the calibration factor is calculated as:

$$C = \frac{K_{E.a}}{K_{equ.1}} \quad (5.7)$$

C = Calibration factor [-].

$K_{E.a}$ = Effective conductivity, e.g. estimated by the analytical method [L / T].

$K_{equ.1}$ = Geometric mean of a distribution of equivalent conductivity values, produced by a not calibrated FID model of large size (C is equal to 1 in the not calibrated model) [L / T].

Therefore, the calibration factor is the quota between a known value of the effective conductivity and the equivalent conductivity of a not calibrated model. The equivalent conductivity of the model should be an estimate of the effective conductivity, so the model needs to be of such a size that the boundary effects can be ignored.

Examples of calibration functions, defining calibration factors for different values of the $\sigma_{10Lg Kblock}$ are given in Figure 5.13. The functions are applicable to an FID model, which uses the block centered flow approach and one node per block, presuming that the block conductivity is given by a log-normal probability distribution and that the flow medium is two-dimensional or three-dimensional. For a three-dimensional flow medium different calibration functions correspond to the different analytical solutions by: Matheron (1967), Gutjhar *et al* (1978) and Dagan (1993).

5.9 Numerical simulations of scale dependency

Introduction

In an uniform continuum model, with a flow medium of homogeneous hydraulic properties, the flow will be uniform between two boundaries with different head values (potential), if the flow domain between the boundaries has a constant geometric shape, such as a rectangular plane or a cube; the flow will be uniform regardless of model size or number of nodes (blocks) included in the model.

For the same system, but with the flow medium defined as a stochastic continuum, the flow will be macroscopically uniform only if the flow domain contains a sufficient number of blocks. Hence, if the number of blocks is smaller than the sufficient number, the equivalent conductivity will depend on the number of blocks in the domain studied; a stochastic continuum model is influenced by boundary effects in a way that a uniform continuum model is not.

These boundary effects are the reason why we will have a scale dependency in a stochastic continuum model. The scale dependency in a stochastic continuum model can be compared to the measured scale dependency of a fractured rock. As was demonstrated in Figure 5.3 and Figure 5.4 the conductivity of a studied volume of fractured rock varies with the studied scale. In the following section we will investigate the scale dependency of a stochastic continuum representation of a heterogeneous rock mass and compare it to the measured scale dependency at Äspö.

We will study the equivalent conductivity of different models. Models of different size (different number of blocks) and different number of dimensions; the models will contain blocks in one, two and three dimensions. We will also study the effect of different values of the standard deviation in the probability distribution defining the conductivity of the blocks ($\sigma_{10Lg Kblock}$).

In different models, the blocks will be assigned conductivity values according to three different log-normal probability distributions. All three distributions have different standard deviations, but the geometric mean is the same and equal to one.

The exercise that we will present below can be looked upon as a method for scaling of conductivity values. The base for the scaling is the known conductivity distribution of blocks of the size 10x10x10 m. Larger sizes of blocks will be represented by models made up by several blocks of size 10x10x10 m. The conductivity distribution of larger sizes is given by the distribution of the equivalent conductivity of the models containing several blocks of the size 10x10x10 m. This method for scaling, presented below, is an indirect and numerical method and it is often called the Laplacian method. The curve fitting method, presented in Section 5.7, is a direct and analytical method for scaling of conductivity values.

The models

We will establish models of different size and geometric shape. They will all consist of a number of blocks arranged in different ways. The blocks will have a cubic shape and a size of 10x10x10 m. A block represents a certain volume of the fractured rock. The blocks will be arranged in three different types of models, see Figure 5.7.

- a **column**, representing a 1-dimensional model.
- a **plane**, representing a 2-dimensional model.
- a **cube**, representing a 3-dimensional model.

The number of blocks in the models will be increased, from a small number to a large number. In that way the models will become larger and larger and the different scales will be studied.

Boundary conditions

A flow will be simulated through the models by application of the specified head boundary condition. Specified head will be assigned to the blocks (cells) of two opposite faces of the studied models. All other faces will have the no flow boundary condition. The blocks at the specified head faces will be of a non continuous type (specified head), all other blocks in the model will be of the continuous type. Hence, the models will have boundary conditions in the same way as model 4 and 5 in Figure 4.1, but the size of the models will be different and no tunnel will be included in the models. The length of the models that we will use in this section, will be defined by the distances between the nodes at the center of the specified head blocks of the two opposite faces.

Size of blocks

In our model we will use a block size which is 10x10x10 m. This is a block size which corresponds well to the size of the tunnels in SFL 3-5. A smaller block size will probably

not improve our model, because: (i) We want the model to represent the heterogeneous properties at Äspö; the hydraulic properties of the blocks will be based on measured properties at Äspö, see Figure 5.3 and 5.4. As we are using a stochastic continuum model, the blocks should have properties that are in line with the properties given by the scaling method presented in Figure 5.4. The scaling method demonstrates the following: For a stochastic continuum model, the hydraulic properties of blocks smaller than 10x10x10 m are very uncertain. Or with other words, the block conductivity distribution becomes very uncertain for blocks smaller than 10x10x10 m. This is further discussed in Section 5.10. (ii) A smaller block size would be unpractical as the number of blocks in the models will be too large to be efficiently handled by numerical algorithms and computers.

Conductivity of the blocks

A block represents a certain volume of the fractured rock. Each block will include one node located at the center of the block. The governing differential equation will be solved at these nodes. A block will represent a limited volume of the fractured rock mass. As previously discussed and as demonstrated in Figure 5.1, the conductivity of a volume of a fractured rock will vary in a way that can be represented by a log-normal probability distribution. Consequently, the blocks in our models will be assigned conductivity values according to a log-normal distribution. The probability distribution should, as much as possible, represent the heterogeneity of the fractured rock, as measured at Äspö. But, as our model is not site specific, we are interested in the variation of the conductivity values only, we are not interested in the absolute size of the conductivity. The geometric mean of the block conductivity distributions used in our models will be set to 1. In this way the results of our modelling will solely demonstrate the effects of the heterogeneity, as the equivalent conductivity of the model will be directly given as a multiple of the block conductivity.

The models will represent the measured heterogeneity at Äspö, as all models will have a standard deviation of the logarithms of the block conductivity distributions ($\sigma_{10\log K_{block}}$), selected in accordance with the measured scale dependency at Äspö.

Figure 5.3(ii) demonstrates the scale dependency at Äspö; the figure demonstrates the different conductivity distributions obtained for different test scales. In Figure 5.4 curve **B** has been added, curve **B** (**B1** and **B2**) demonstrates a conditioned interpolation between measured values, a conditioning based on a stochastic continuum representation of the measured properties (direct analytical method for scaling). Depending on the used interpolation function (**B1** or **B2**) we see that a test scale of 3 m produces a standard deviation that will be in the range of $10\log K= 1.7$ to $10\log K= 6.9$, which also can be written as $\sigma_{10\log K}= 1.7$ to 6.9 ($\sigma_{e\log K}= 3.9$ to 15.9); and a test scale of 30 m produces a $\sigma_{10\log K}= 0.8$ to 2.7 ($\sigma_{e\log K}= 1.8$ to 6.2). For a test scale of 10 m, the functions (**B1** or **B2**) given in Figure 5.4 produces a $\sigma_{10\log K}= 1.0$ to 1.5 ($\sigma_{e\log K}= 2.3$ to 3.5).

Three different standard deviations of $10\log K$ ($\sigma_{10\log K}$) have been selected: 1, 1.498 and 2. Based on these three values, three probability distributions will be created, distributions that represent the block conductivity. The distributions will be tested in the models to see which distribution produces a scale dependency that gives the best fit to the functions representing the scale dependency at Äspö.

Due to numerical reasons, it is necessary to define a maximum and a minimum conductivity that can be assigned to the blocks. In the used models the minimum possible block conductivity is 4 orders of magnitude less than the geometric mean, the maximum possible block conductivity is 4 orders of magnitude larger than the geometric mean. These boundaries gives a possible range of block conductivity which is 8 orders of magnitude.

Thus, the conductivity of all blocks will be given by probability distributions having a log-normal distribution, a geometric mean of 1 and a $\sigma_{10Lg K}$ of either: 1, 1.498 or 2.

Numerical considerations

The homogenized conductivity (node-to-node conductivity) of the two and three dimensional models, was calculated on the base of the calibrated harmonic method (see previous sections). The 1-dimensional models were not corrected by the use of a calibration factor; for these models the harmonic method was used. The calibration factors of the two-dimensional models were based on the analytical solution of a two dimensional stochastic continuum. The calibration factors of the three dimensional models were based on the analytical solution of a three-dimensional stochastic continuum, by Gutjahr *et al* (1978).

Spatial correlation of conductivity values

The results of the packer tests, at different bore holes at Äspö, demonstrate some spatial correlation between sections with extreme conductivity values, when the test scale (packer spacing) was set to 3 m. Based on the results of the 3 m tests, correlation ranges have been calculated for different boreholes (Liedholm, 1991 a,b and Follin, 1992a), these values are given in Table 5.1. The correlation ranges vary between 3 m and 27 m with an average of 12.4 m. The block size in our models is 10x10x10 m. A comparison between the calculated correlation ranges (Äspö) and the block size (model), reveals that at the used block size, a spatial correlation as regards block conductivity is small if any. As a consequence, in the models no spatial correlation was applied as regards conductivity. A block will be assigned a conductivity value without considering the conductivity values of its neighboring blocks.

Procedure of simulations

As the flow medium, the rock mass, is represented by a stochastic continuum, a large number of simulations (realizations) will be carried out for each studied size and type of model, and the results of these simulations will be statistically evaluated. The following procedure will take place.

- 1... A finite difference mesh of blocks is established, representing a geometrical body of a certain shape and size.
- 2... All blocks in the mesh are assigned conductivity values according to a probability distribution. These conductivity values represent one possible realization of the rock mass. The blocks are assigned a boundary condition.
- 3... The governing differential equation (Equation 2.2) is solved at all blocks by the use of a finite difference algorithm (the GEOAN model). Properties of the studied system are calculated, e.g. the flow through the studied model. Based on the flow and the size of the model, the conductivity of the model is calculated (the equivalent conductivity).
- 4... Moments 2 and 3 are repeated a large number of times.
- 5... A statistical analysis is carried out on the results obtained from all the studied realizations of the conductivity field, e.g. calculations are carried out of the geometric mean and the standard deviation of the obtained values of flow and conductivity.
- 6... The mesh is increased by adding one layer of blocks in all studied dimensions.
- 7... The procedure is repeated from moment 2 and onwards.

The equivalent conductivity is calculated on the base of Darcy's law (Darcy, 1856), as given in Equ.5.6. The number of realizations that we have included in the statistical analyses of each scenario is the number of times that moment 2 and 3 have been repeated. This number have been varied dependent on the acceptable uncertainty and the size of the variation in the calculated equivalent conductivity. The number have been varied from about 400 times to more than 2000 times, dependent on studied scenario.

Results: Introduction

Simulations were carried out for 1-, 2- and 3-dimensional models. The results of the simulations are the geometric mean and the standard deviation of the obtained equivalent conductivity of the studied models, the results are given in Figures 5.14, 5.15 and 5.16.

Three different probability distributions of block conductivity were used, the difference being the standard deviation. The results given in Figure 5.14 are calculated using the standard deviation of $10\text{Log } K = 1$ ($\sigma_{10\text{Log } K}=1$), the results given in Figure 5.15 are calculated using the standard deviation of $10\text{Log } K = 1.498$ ($\sigma_{10\text{Log } K}=1.498$) and the results given in Figure 5.16 are calculated using the standard deviation of $10\text{Log } K = 2$ ($\sigma_{10\text{Log } K}=2$). Based on the figures, the following conclusions are made.

Results: Geometric mean of equivalent conductivity

For a three dimensional model (a cube), the geometric mean of the equivalent conductivity increases as the number of blocks and the model scale (length) increases (block size is constant). In the model there will be some blocks with a small conductivity and some blocks with a large conductivity. Blocks with a large conductivity may provide the flowing water a way around blocks with a small conductivity. Paths consisting of blocks with a large conductivity are called efficient pathways. It follows that the model's equivalent conductivity will not be directly determined by the blocks with a small conductivity, but by the number and the conductivity of the efficient pathways. As the model scale increases, more and more efficient pathways will become available, this effect is more important than the increase in cross section area; consequently, the geometric mean of the equivalent conductivity will become larger as the scale is increased. However, the number of new efficient pathways that will become available as the scale increases, will not be as large for a large model as for a small model. For a large model the efficient pathways will be long and of complicated geometry and they will interact with each other. A model that has such a size that the efficient pathways are long and complicated, will not be as much affected by a change in scale (change in pathway length) as a small model, which has shorter efficient pathways. Hence, the size of the increase in equivalent conductivity (the derivative of the model's equivalent conductivity as regards model length) will slowly be reduced as the model scale is increased, and at some large scale no increase in equivalent conductivity will take place when the model scale is increased. For such a scale, the flow through the model can be regarded as macroscopically uniform.

The model's equivalent conductivity is proportional not only to the model scale, but also to the standard deviation of the probability distribution defining the block conductivity. If the standard deviation is zero, we will have no heterogeneity in the conductivity of the flow medium, a constant model conductivity and no scale dependency. A standard deviation of the probability distribution defining the block conductivity which is larger than zero, will produce a heterogeneous flow medium and a certain scale dependency in model conductivity. The larger the standard deviation, the larger the heterogeneity, the larger the scale dependency and the larger the equivalent conductivity.

For a two-dimensional model (a plane) the number of efficient pathways that will become available as the model scale is increased, is not as large as in a three dimensional model. A two dimensional model will behave in a way similar to a three dimensional model, but the development of new efficient pathways will be balanced by the increase in cross-section area, as the scale is increased. Hence, the equivalent conductivity will not be scale-dependent for a two-dimensional flow medium, but constant.

For a one-dimensional model (a column) the geometric mean of the model conductivity decreases as the model scale increases. In a one-dimensional model there is no efficient

pathway around a block with a small conductivity, the blocks with the smallest conductivity will determine the model conductivity. The probability that at least one block in the model has a small conductivity increases as the model scale increases and the number of blocks grows large. It follows that the model conductivity decreases as the scale increases.

Results: Standard deviation of equivalent conductivity.

The number of blocks in a small model is smaller than the number of blocks in a large model (block size is constant). The probability that a realization of the conductivity values of the blocks will be extreme, both as regards the absolute values and as regards the spatial distribution, is larger for a small model than for a large model, as a small model contains fewer blocks. An extreme realization of the block conductivity field will produce an extreme equivalent conductivity. It follows from this, that it is more likely that a small model will have an extreme equivalent conductivity than a large model. Thus, the distribution of values of equivalent conductivity obtained from the simulations, will have a larger standard deviation if the studied model is small than if the studied model is large.

Assuming that we compare models of the same scale (length), a three-dimensional model contains more blocks than a two-dimensional model, which in turn contains more blocks than a one-dimensional model. Additionally, the larger the number of dimensions the less sensitive the model will be to the spatial distribution of the block conductivity (it is more likely to find an efficient pathway in three dimensions than it is in two dimensions). It follows from this, that for models of the same scale the probability distribution of values of equivalent conductivity, obtained from the simulations, will have a larger standard deviation if the studied model is of one dimension than if it is of two dimensions, the smallest standard deviations will be obtained for a three-dimensional model.

Comparison between different representations of the scale dependency at Äspö

We will compare different representations of the scale dependency at Äspö:

- i.* The results of the field measurements at Äspö, individual measured values and a visual interpolation between measured values.
- ii.* The direct analytical method of scaling. The method is a conditioned interpolation between measured values. The interpolation is conditioned to represent the properties of a stochastic continuum, properties estimated by the use of analytical methods.
- iii.* The indirect numerical method of scaling (the Laplacian method of scaling). This is the result of numerical simulations with models of different size and number of blocks, based on the stochastic continuum approach.

The packer tests at Äspö were carried out using different scales (different distances between the packers). When comparing the measured values and the results of the modelling (the indirect numerical scaling), we note that a comparison can only be carried out at a scale larger than 10 m, as this is the block size of the models.

When comparing the geometric mean of the equivalent conductivity and the geometric mean conductivity of the packer tests, we cannot compare the absolute conductivities, as the conductivity of the packer tests are given as relative conductivities. We can only compare the size of the increase in conductivity with scale, i.e. the derivative of the conductivity as regards scale, i.e. the shape of the function.

A comparison between the scaling methods and the values measured at Äspö is given in Figure 5.17. The figure gives the geometric mean of the equivalent conductivity versus scale (size of blocks and length of models). The different methods of scaling are:

- The indirect numerical method of scaling (triangles, crosses and filled squares).
- The direct analytical method of scaling, which is a conditioned interpolation between measured values (curve **B**).
- Visual interpolation between measured values (curve **A**). The measured values are also given (empty squares).

The figure demonstrates that the best fit, between the equivalent conductivity of the indirect numerical scaling (the models) and the interpolated functions representing the measured properties (curve **A** and curve **B**), is obtained when the models of the numerical method has a block size of 10x10x10 m and a standard deviation of the block conductivity distribution which is $10\text{Log } K = 1.498$, and when the measured properties are represented by the direct analytical method of scaling (curve **B**).

It should be noted that the function **B** has been matched to the values produced by the numerical method (the models); it is the shape of the curve **B** that should be matched to the values, not the absolute size of the values. The shape of function **B** matches well to the values predicted by the indirect numerical method of scaling (the models) if the block size is 10x10x10 m and the standard deviation of the block conductivity distribution is: $10\text{Log } K = 1.498$.

The direct analytical method of scaling (curve **B**) and the visual interpolation between measured values (curve **A**) could also represent the scale dependency as regards the standard deviation of the logarithms of the equivalent conductivity ($\sigma_{10\text{Log } K_{equ}}$). A comparison between $\sigma_{10\text{Log } K_{equ}}$ of these two methods and the $\sigma_{10\text{Log } K_{equ}}$ of the indirect numerical method of scaling (the models) is given in Figure 5.14(ii), 5.15(ii) and 5.16(ii).

The comparison demonstrates that the numerical method has a tendency to produce values of $\sigma_{10\text{Log } K_{equ}}$ which are smaller than the values predicted by the other two methods. The best fit between the $\sigma_{10\text{Log } K_{equ}}$ of the numerical scaling (the models) and $\sigma_{10\text{Log } K_{equ}}$ of the other two methods takes place for the direct analytical method (curve **B**) when the numerical method uses a block size of 10x10x10 m, and the standard deviation of the block conductivity distribution is: $10\text{Log } K = 1.498$ ($\sigma_{10\text{Log } K_{block}} = 1.498$).

The tendency of the numerical method (the models) to produce values of $\sigma_{10\text{Log } K_{equ}}$ that are smaller than the measured values (curve **A** and **B**) seems to be inherent with the method. The actual flow in a fractured rock takes place in an interconnected network of fractures and the conductivity values of that network is anisotropic. However, in the models the blocks are assigned an isotropic conductivity. An anisotropic formulation is better, but the problem is that the standard evaluation of the packer tests gives no information of anisotropy and therefore it is not possible to specify anisotropic conditions for the block conductivity distribution. The underestimation of $\sigma_{10\text{Log } K_{equ}}$ could also be an effect of the fact that the packer tests do not test a constant volume of rock, even if the distance is constant between the packers. The volume of tested rock in a packer test depends on the conductivity of the rock - a large permeability gives a large volume of tested rock and vice versa. The varying size of the tested volume of rock in the packer tests may give rise to an increased range of conductivity values, compared to the range derived from simulations with the models, because in the models the studied volume is constant, regardless of permeability of the flow medium. Finally, we can argue that the indirect numerical scaling (the models) is not capable of reproducing both the geometric mean and the $\sigma_{10\text{Log}}$ of the conductivity distributions derived from packer tests. The conductivity distributions of the numerical models and those of the packer tests, could perhaps not be directly compared as they represent different volumes of rock, different flow regimes etc.

- *Conclusions*

By the use of the stochastic continuum approach, the models are, in a generalized way, capable of reproducing the scale dependency and the flow that occurs in a heterogeneous rock mass, having hydraulic properties similar to the properties measured at Äspö.

Using a block size of 10x10x10 m, the best fit to the measured hydraulic properties is obtained when the block conductivity is given by a log-normal distribution having a standard deviation of $10\text{Log } K = 1.498$.

A block size of 10x10x10 m and a standard deviation of the block conductivity distribution which is $10\text{Log } K = 1.498$ produces hydraulic properties corresponding to the Äspö rock, a larger standard deviation, e.g. $10\text{Log } K = 2$, gives properties representing a more heterogeneous rock and a smaller standard deviation, e.g. $10\text{Log } K = 1$, gives properties representing a less heterogeneous rock

5.10 What to think about when using the stochastic continuum approach

Introduction

As a finishing section we will below discuss some aspects of the stochastic continuum approach, aspects that need to be considered when using the method for studies of a heterogeneous flow medium. The aspects discussed below are also discussed in the previous sections of this chapter (5).

The representation of a rock block in the model

The stochastic continuum approach is based on the random (stochastic) conductivity of blocks of the flow medium, as defined by a probability distribution. The properties of the probability distribution depend on the size of the blocks. Hence, it is important that the representation of the blocks in the model is consistent with the stochastic continuum approach. This implies that the model, or rather the numerical method used for solving the differential equation, uses a system of nodes and blocks that is able to represent, in a consistent way, the studied blocks of the flow medium. For example, the finite difference method with the block-centered flow approach uses a representation in which conductivity values are assigned to blocks of a defined volume, the nodes are evenly distributed inside the blocks (one node per block means that the node is placed at the center of the block). This approach is consistent with the stochastic continuum approach. If one uses another numerical representation e.g. a finite difference representation that is not based on the block centered flow approach, a finite element method, or some other method, it is important that one adapts this method in such a way that it becomes consistent with the stochastic continuum approach.

The numerical method and its implication on the results

To solve the differential equation with its boundary conditions, we will use a numerical method. The numerical method might produce a solution that is different from a solution derived with an analytical method, even if boundary effects are considered. A not calibrated finite difference model (FID) will underestimate the equivalent conductivity, a not calibrated finite element model (FEM) will overestimate the equivalent conductivity, if the domain studied is represented by a stochastic continuum. This problem arises as all blocks have different conductivity values, the problem depends on the way the conductivity between the nodes (the homogenized conductivity) is calculated by the model. In FID and FEM models different methods can be used to minimize this problem. One should consider this problem and try to minimize its effects. In Sec.5.8 we propose a method that removes the underestimation of the equivalent conductivity of an FID model, and preserves the heterogeneity of the represented flow medium.

The selection of the block size of the model

The purpose of a stochastic continuum study may differ, but it will always involve the effects of the heterogeneity of the flow medium. The heterogeneity of the model comes from the block conductivity distribution assigning different conductivity values to the blocks. If we use a method of scaling of the block conductivity distribution that is consistent with field findings, we will get the following relationship; the larger the blocks, the smaller the heterogeneity. Or with other words; the larger the blocks, the smaller the standard deviation of the block conductivity distribution.

It is important that one selects a size of the blocks in the model which is reasonable considering the purpose of the study. Depending on the studied scenario and the purpose of the study, the heterogeneity of the rock mass may be of varying importance. For example, if we want to study the total flow of water in a tunnel, without considering the distribution of the flow along the tunnel, we could use a larger size of blocks than if we also want to include the distribution, and if we study the groundwater transport of solutes in a heterogeneous rock mass, we need smaller blocks than if we only study the size of the groundwater flow. It is important to remember that the different methods of scaling of the block conductivity distributions do not include all the aspects of the heterogeneity, even if the methods are consistent with the stochastic continuum approach. For example, the method presented in Section 5.7 does not include the anisotropy in the block conductivity or the effective porosity of the blocks. Additionally, there is the aspect of simple geometry, large blocks are large and they do not correspond well to small structures that we may want to include in the model. Hence, large blocks may produce results that do not include all the effects caused by the heterogeneity of the flow medium.

Therefore, it seems to be a good idea to use small blocks. However, other problems will arise with small blocks. First there is of course the problem with the number of blocks; small blocks give a large number of blocks in the model, which is heavy to handle from a numerical point of view. The second problem is the uncertainty in the properties of the block conductivity distribution. At small scales, field measurements of the rock properties and the evaluation of the measurements show a large uncertainty. The same problem occurs if one uses a method of scaling of the block conductivity distribution that is consistent with the stochastic continuum approach, such as the method presented in Section 5.7. This method demonstrates that if one uses field data from Äspö and small blocks (blocks smaller than about 10x10x10 m), the uncertainty in the properties predicted for the block conductivity distribution will be large.

Another aspect of the selected block size is the boundary effects, the special boundary effects that come with the stochastic continuum method. A flow medium defined as a stochastic continuum will be influenced by special boundary effects if the number of blocks is smaller than the number necessary to obtain macroscopically uniform flow. For example, a model which contains blocks in three dimensions, but too few blocks to get a macroscopically uniform flow; for such a model the boundary effects will give an equivalent conductivity of the model which is smaller than the equivalent conductivity produced by a model containing a larger number of blocks. If the flow is macroscopically uniform, the equivalent conductivity will not change with the number of blocks, the equivalent conductivity for such a model is equal to the effective conductivity. The number of blocks necessary to obtain macroscopically uniform flow depends on the number of studied dimensions and the standard deviation of the block conductivity distribution. Thus, if we select a large block size, boundary effects might influence the results of our simulations.

For a uniform continuum model, we could, without conceptual problems, use a mesh in which the sizes of the blocks vary, e.g. the block size is increased towards the outer

boundary of the model. For a stochastic continuum model it is more complicated. If blocks of different size represent the same heterogeneous medium, we will get different conductivity distributions that represent the same type of rock mass in the same model. This will cause effects that need to be considered. For example: (i) some blocks could have a shape that is not cubical, what scale do such blocks represent and how to compare them to the scale of other blocks with other shapes, (ii) if the number of blocks is small the equivalent conductivity of a domain with a few large blocks will not be the same as the equivalent conductivity of a domain with a large number of smaller blocks, even if the theoretical effective conductivity is the same for both domains (the special boundary effect). One can represent the same heterogeneous medium with blocks of different size in the same model, but it has to be done with care.

Thus, selecting the best size of the blocks is difficult; large blocks may produce results that do not include all the effects caused by the heterogeneity of the flow medium, small blocks will produce results that involve a large uncertainty. Additionally, a large block size, or blocks of different size in the same model, might produce special boundary effects, effects that will influence the results. These problems should be considered in relation to the purpose of the study, when one selects the block size.

The scaling of measured properties to the used block size

To get knowledge of the properties of a flow medium, field measurements are carried out. Tests of the rock are conducted at different scales. For a fractured rock the tests will show different rock properties at different scales, this is the scale dependency. The tests are uncertain as regards the exact scale of the tested volume of rock. The results of the tests are also uncertain as regards assumptions and generalizations in the methods for evaluation of the tests. These uncertainties will influence the results of the tests. Nevertheless, based on the results we have to produce the necessary input to the model, i.e. the block conductivity distribution. It is this distribution that determines the heterogeneous properties of the model. If the rock mass has been tested at different scales, we have results corresponding to different scales. However, these scales may not correspond to the size of block that we want to use in the model. For this reason and also for the understanding of the nature of the studied flow medium, we need a method of scaling the results obtained from field tests i.e the block conductivity distribution, so that the results can be applied to any scale. Methods for scaling of conductivity values have been in the interest of hydrogeologists since the 1960s. An overview of different methods is given in, Wen & Gómez-Hernández (1996). If the method of scaling should be applied to a stochastic continuum model, the method needs to be conditioned for the stochastic continuum approach. We propose the method given in Section 5.7, this method produces a block conductivity distributions for any block size; the method is conditioned in such a way that the effective conductivity of the stochastic continuum model will always be the same, regardless of the selected block size. The method of scaling is important, because at small scales different methods may come up with block conductivity distributions that are order of magnitudes apart. Hence it is important that the method is consistent with the stochastic continuum approach. Before starting a stochastic continuum modelling exercise, one should investigate the scale dependency of the studied flow medium.

Number of realizations to study

The results of a stochastic continuum model should be based on a statistical analysis of many realizations of the fields of the studied stochastic variables e.g. conductivity and/or effective porosity etc. As different realizations give different fields, one should distinguish between results based on one realization and results based on a statistical analysis of many realizations. One realization demonstrates an example of a possible outcome, many realizations demonstrate the variation in the possible outcome.

The number of realizations necessary to include in the statistical analysis depends on: (i) the purpose of the study, (ii) the tolerated uncertainty in the results and (iii) the size of the variation of the results. If the variation in the resulting properties is small, it is not necessary to perform as many realizations as if the variation is large. And the larger the tolerated uncertainty in the results, the smaller the necessary number of realizations.

To investigate the necessary number of realizations, one should perform statistical analyses for different numbers of realizations. By comparing the results of the statistical analyses for different number of realizations, one should be able to see that the uncertainty of the results decreases with increased number of realizations. One should select the number of realizations that produces an acceptable uncertainty of the results.

If the variation in the resulting properties is small, 50 realizations or less might be enough, but if the variation is large, the necessary number might be much larger than 1000. If the studied models include more than one stochastic variable, the necessary number of realizations increases with the number of stochastic variables included. If the results can be matched to a theoretical statistical distribution (such as the log-normal distribution), the necessary number of realizations might be very much reduced.

Table 5.1 RESULTS OF HYDRAULIC TESTS OF FRACTURED ROCK AT ÄSPÖ. Results of packer tests of bore holes at the Äspö Hard Rock Laboratory, Sweden. Summarized statistics of the conductivity obtained using double packer tests and a test scale of 3 m (distance between packers was 3 m). Table after Follin (1992a), based on data given by Liedholm (1991 a, b).

Bore hole	Tested interval [m]	Hydraulic conductivity (packer spacing 3 m)		
		Geometric mean [10Log(m/s)]	Standard deviation [10Log(m/s)]	Correlation range [m]
KAS 02	102-801	-10.8	1.70	< 27
KAS 03	103-547	-9.1	1.78	< 6
KAS 04	133-454	-9.1	2.30	< 3
KAS 05	157-541	-10.4	2.13	< 6
KAS 06	105-591	-9.3	2.70	< 6
KAS 07	106-592	-9.3	2.09	< 18
KAS 08	106-577	-9.8	2.78	< 21

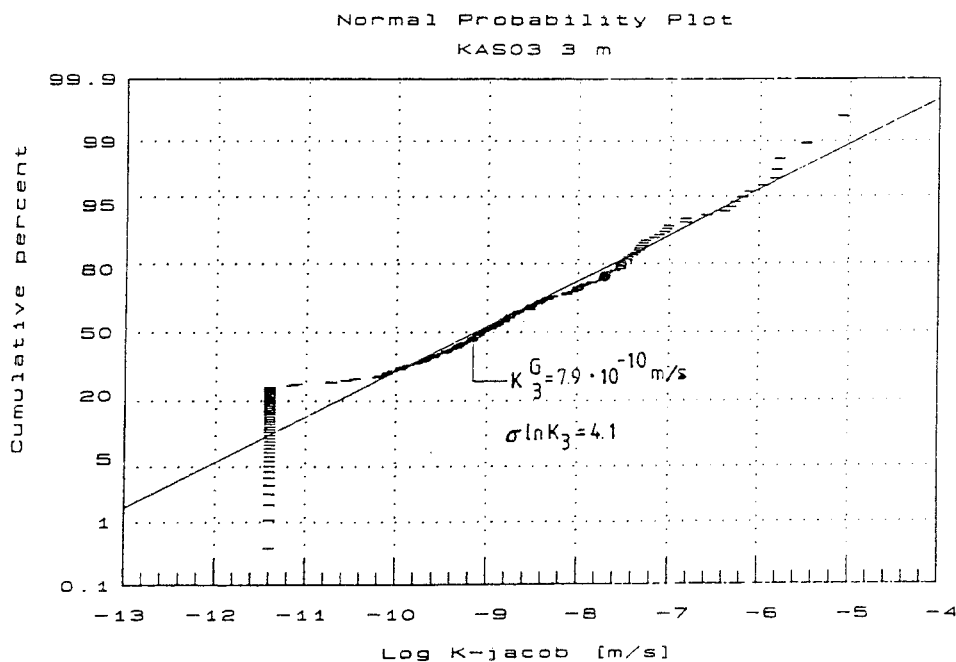
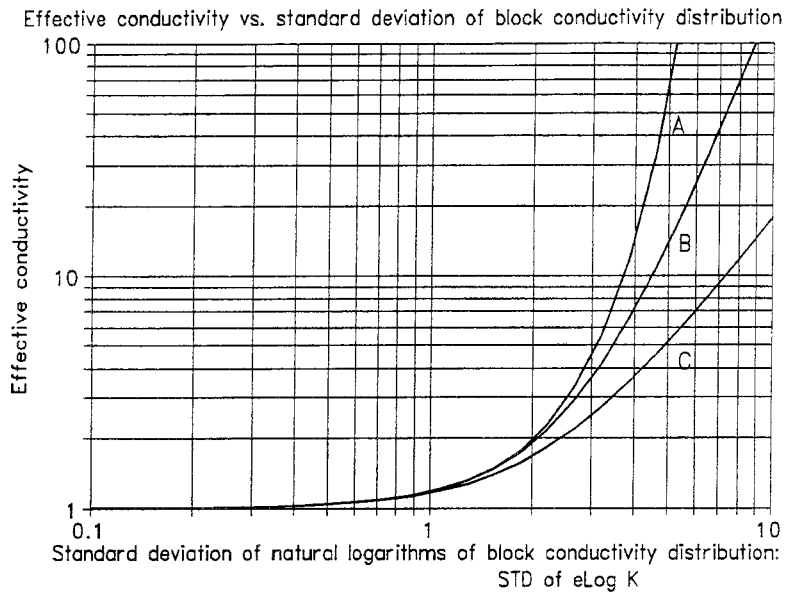


Figure 5.1 STATISTICAL DISTRIBUTION OF MEASURED CONDUCTIVITY. Statistical distribution of hydraulic conductivity values. The values were obtained by double packer tests and a test scale of 3 m (distance between packers was 3 m). The tests were conducted in bore hole KAS 03 at the Äspö Hard Rock Laboratory. The figure demonstrates that the conductivity values obtained are Log-normal distributed. The drop in values at the left part of the distribution corresponds to the minimum flow (conductivity value) possible to measure with the used test equipment. The figure is reproduced from Nilsson (1989).

- (i)
Estimated effective conductivity
 A: Matheron (1967)
 B: Dagan (1993)
 C: Gutjahr et al (1978)



- (ii)
Relation factor, a measure of the deviation between estimates.
 $F1 = PM / PM$
 $F2 = PG / PM$
 $F3 = PD / PM$
 PM = Estimate by Matheron
 PG = Estimate by Gutjahr et al
 PD = Estimate by Dagan

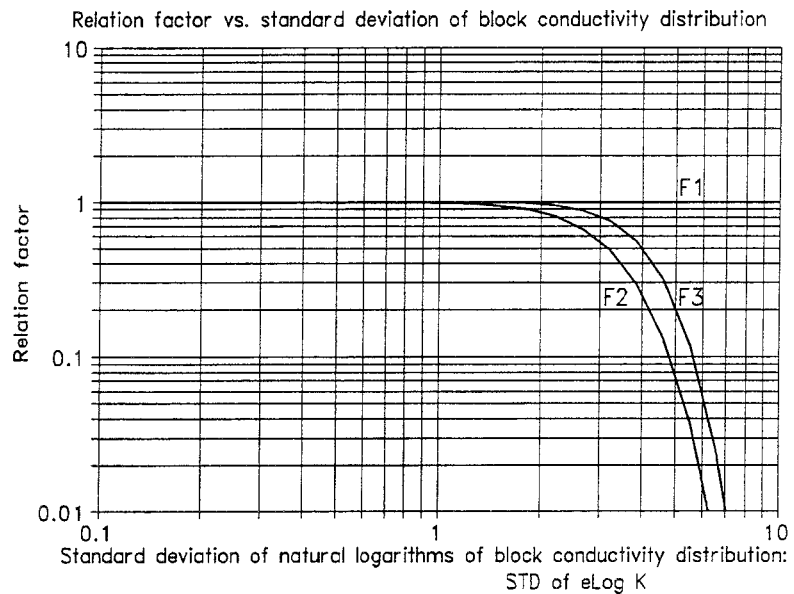
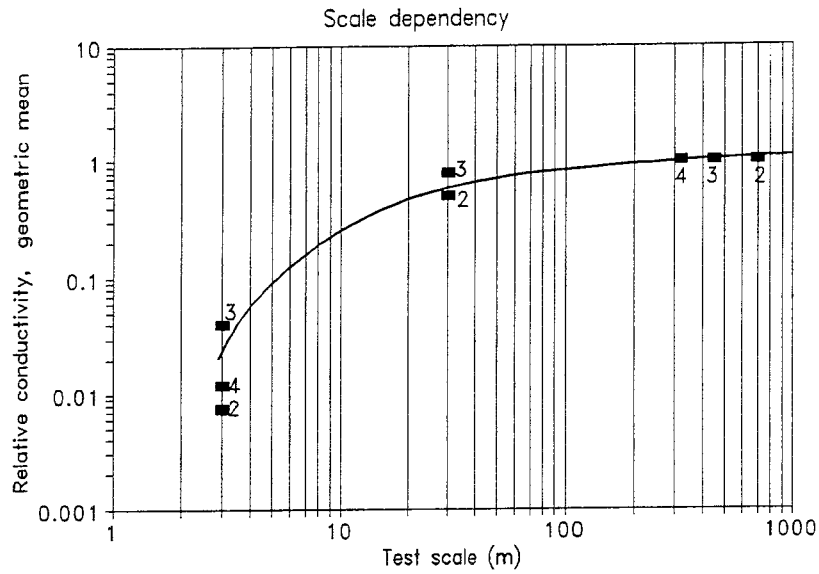


Figure 5.2 **DEVIATION IN ANALYTIC ESTIMATION OF EFFECTIVE CONDUCTIVITY**
 The effective conductivity of a fractured rock mass, represented by a stochastic continuum, can be estimated, presuming that the conductivity of the blocks is log-normal distributed and that the flow is macroscopically uniform. For the estimation, different analytical formulas have been proposed. The figure gives the effective conductivity produced by different formulas; presuming a block conductivity distribution with a geometric mean equal to 1. The standard deviation of the block conductivity distribution has been varied and is represented by the X-axis. Major differences between estimates take place if the standard deviation of $e\text{Log } K_{\text{block}}$ is larger than about 3 ($10\text{Log } K_{\text{block}}$ larger than about 1.3).
 A: Effective conductivity according to Matheron (1967) Equ.5.2(ii).
 B: Effective conductivity according to Dagan (1993) Equ.5.2(iv).
 C: Effective conductivity according to Gutjahr et al (1978) Equ.5.2(iii).

(i)
Conductivity of rock
Geometric mean
K_{rel} = relative conduct.
K_{sect} = section conduct.
K_{all} = conduct. of all sect.
K_{rel} = *K_{sect}* / *K_{all}*



(ii)
Conductivity of rock
Standard deviation

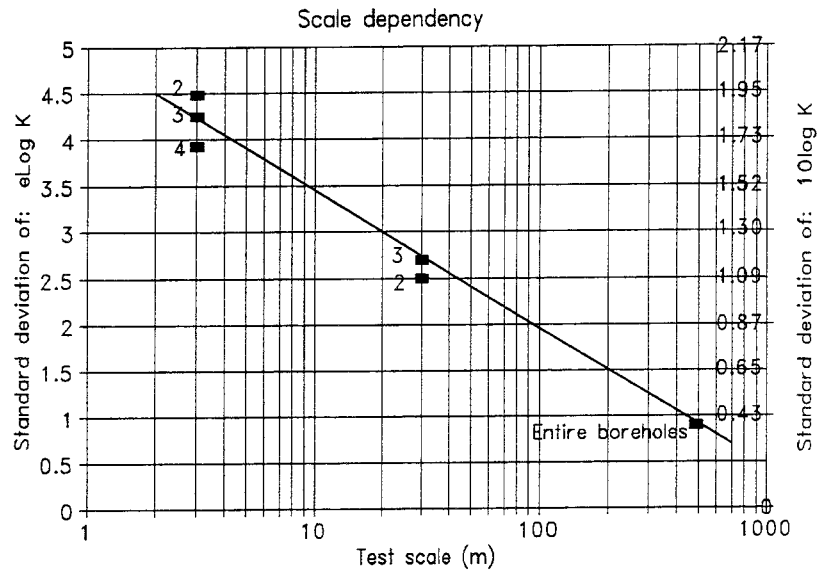
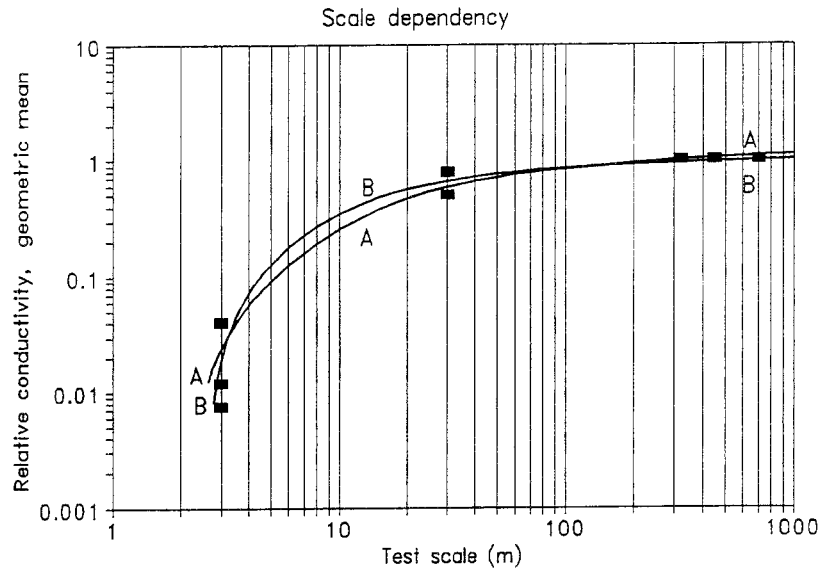


Figure 5.3 MEASURED SCALE DEPENDENCY, RESULTS OF PACKER TESTS.
 The conductivity (*K*) of a fractured rock mass varies depending on the position of studied volumes. It is also scale dependent as regards the size of studied volumes. The variation of *K* in a fractured rock can be represented by log-normal or log-normal similar distributions. The geometric mean and the standard deviation of such distributions are dependent on the size of studied rock volumes. The above given figure illustrates this, it is based on results of packer tests at the Äspö Hard Rock Laboratory. The test scale correspond to the length of the tested section of the studied bore hole. Results from the following bore holes at Äspö are used: KAS 02 (marked: 2), KAS 03 (marked: 3) and KAS 04 (marked: 4). The Figures are based on similar figures in Gustafson et al. (1989).

(i)
Conductivity of rock
Geometric mean
 K_{rel} = relative conduct.
 K_{sect} = section conduct.
 K_{all} = conduct. of all sect.
 $K_{rel} = K_{sect} / K_{all}$



(ii)
Conductivity of rock
Standard deviation

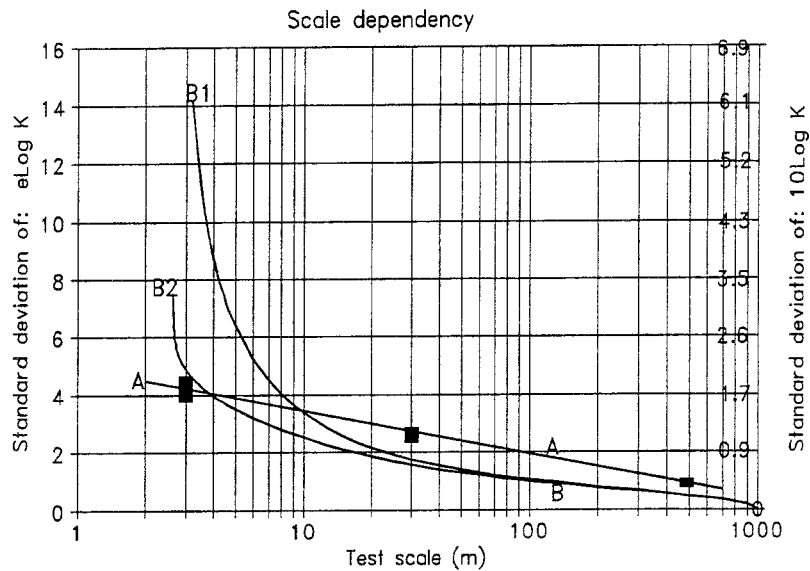


Figure 5.4

SCALE DEPENDENCY, MEASURED AND INTERPOLATED.

The measured scale dependency is not directly applicable to a stochastic continuum model. The probability distributions that define the conductivity of blocks of different size in a stochastic continuum model, has to fulfil the condition of constant effective conductivity. Hence, regardless of the selected size of blocks, the effective conductivity should be the same for a model of a very large number of blocks. The curves marked with an A define conductivity distributions that will not give a constant effective conductivity for different sizes of blocks. The curves marked with B (B1 and B2) have been selected in such a way that they will give an acceptable fit to measured values and also define conductivity distributions that will give a constant effective conductivity, regardless of size of blocks.

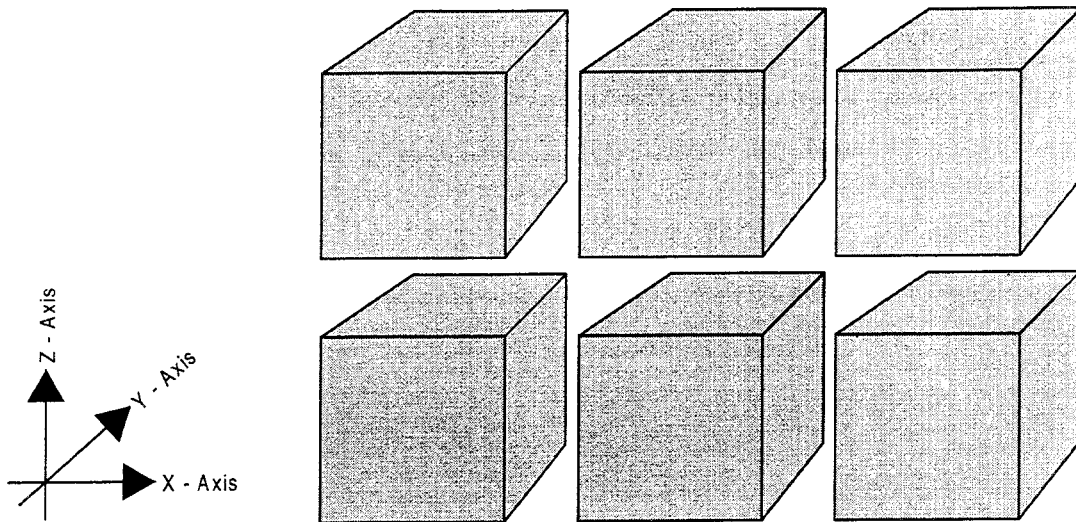
A: Acceptable fit to measured values, but effective conductivity varies.

B (B1, B2) : Acceptable fit to measured values and constant effective conductivity.

B1: Constant effective conductivity, based on Gutjahr et al (1978).

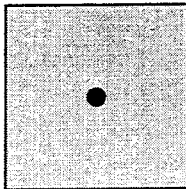
B2: Constant effective conductivity, based on Matheron (1967).

Discretisation of the flow medium into a finite number of blocks, each block representing a part of the flow medium.

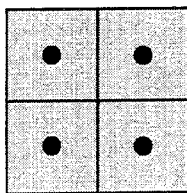


A studied volume of the flow medium is divided into a number of blocks. All blocks have the same geometric size (the same volume). One value of hydraulic conductivity is generated for each block. The conductivity value is generated based on a probability function. The probability function describes the possible variation in conductivity for a block of the studied size.

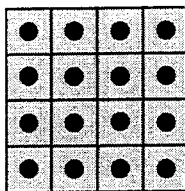
Discretisation of the blocks into a finite number of nodes/cells, each node/cell representing a part of a block.
The volume represented by a node is called a cell.



Two dimensional model: 1 node at the center of the block.
 Three dimensional model: 1 node at the center of the block.
 One conductivity value for the block.
 One node/cell representing the block



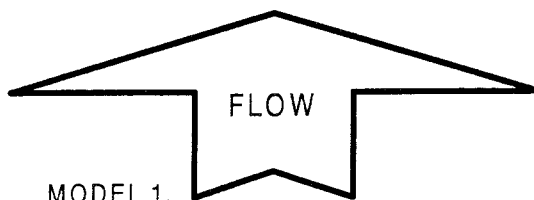
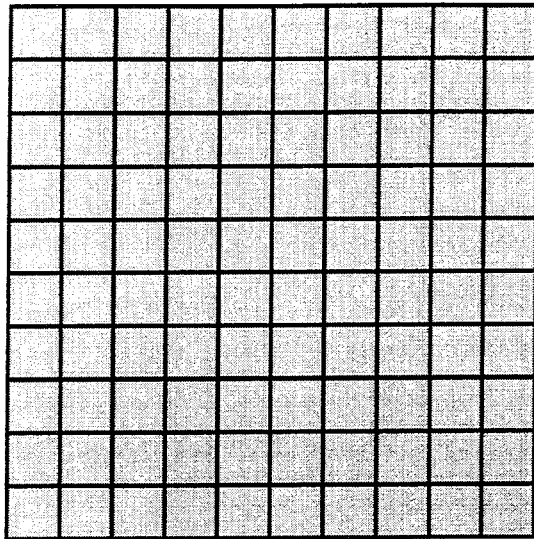
Two dimensional model: 4 nodes equally distributed in the block.
 Three dimensional model: 8 nodes equally distributed in the block.
 One conductivity value for the block.
 Several nodes/cells representing the block.



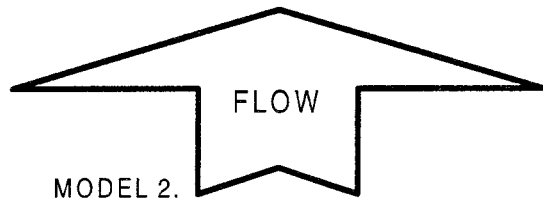
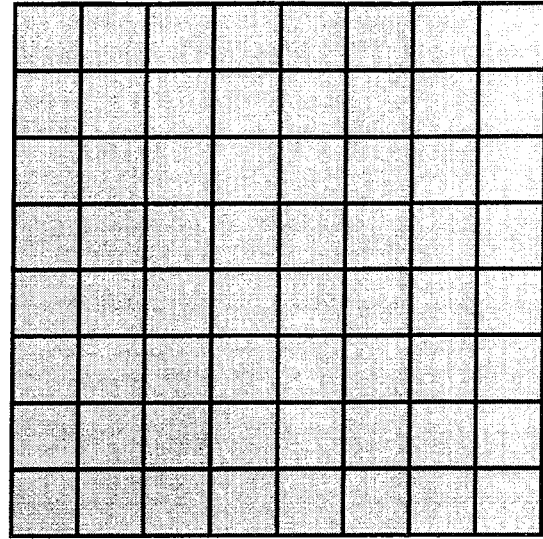
Two dimensional model: 16 nodes equally distributed in the block.
 Three dimensional model: 64 nodes equally distributed in the block.
 One conductivity value for the block.
 Several nodes/cells representing the block.

● Location of a node.

FIGURE 5.5 DISCRETISATION OF THE FLOW MEDIUM.
 The figure illustrates how the flow medium is represented in a finite difference model, using the block centered flow approach and the stochastic continuum approach.



MODEL 1.
Stochastic continuum model,
containing 100 blocks.
Block size 10 x 10 m.
Block conductivity is given by
probability distribution 1.



MODEL 2.
Stochastic continuum model,
containing 64 blocks.
Block size 12.5 x 12.5 m.
Block conductivity is given by
probability distribution 2.

BLOCK CONDUCTIVITY. All blocks have different values of hydraulic conductivity. The block conductivity is a local property. The block conductivity is generated based on a probability distribution. The probability distribution describes the possible variation in conductivity for a block of the studied size.

EQUIVALENT CONDUCTIVITY. A flow through the model gives a conductivity of the model, in the direction of the flow. This is a regional property, called, the equivalent conductivity. It varies between different realizations of the block conductivity field. The variation depends on (i) number of studied dimensions, (ii) number of blocks and (iii) standard deviation of the block conductivity distribution.

EFFECTIVE CONDUCTIVITY. The larger the number of blocks in the model, the smaller the variation in equivalent conductivity. If the variation is zero, the equivalent conductivity is equal to the effective conductivity. The effective conductivity occurs at a scale when the flow is macroscopically uniform and the model is an REV.

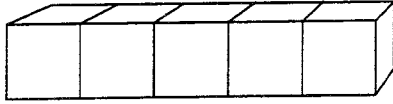
SCALE DEPENDENCY

The effective conductivity could be estimated analytically, presuming that the flow is macroscopically uniform. In a numerical model, a macroscopically uniform flow will take place if the number of blocks is large enough.

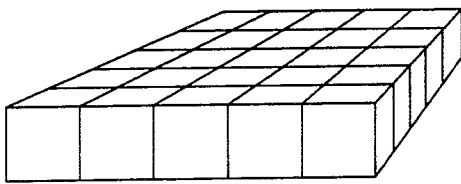
For a fractured rock represented by a stochastic continuum, the probability distribution defining the block conductivity should depend on size of blocks (scale dependency). However, the effective conductivity represents the properties of the fractured rock at a regional scale and should be constant, regardless of the selected size of the blocks. This must be considered when selecting the size and conductivity probability distribution of the blocks.

Thus, if the models above should represent the same fractured rock, the probability distributions defining the conductivity of the blocks should be selected in a way that: (i) Model 1 produces an effective conductivity which is equal to the effective conductivity produced by Model 2 and (ii) the selected probability distributions should as much as possible follow the measured scale dependency. The number of blocks should also be considered, especially if the models should include blocks in three-dimensions.

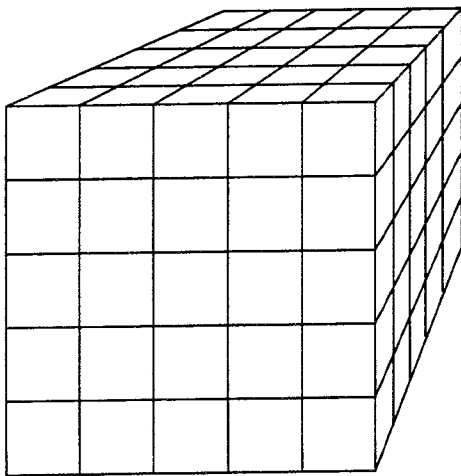
FIGURE 5.6 BLOCK , EQUIVALENT AND EFFECTIVE CONDUCTIVITY, AS WELL AS SCALE DEPENDENCY OF A STOCHASTIC CONTINUUM MODEL



A one-dimensional model, representing a column.
 The model consists of 5 cells.
 A cell size of 10x10x10 m gives a length of model equal to 50 m.
 Direction of regional flow: along the X-axis.



A two-dimensional model, representing a plane.
 The model consists of 25 cells.
 A cell size of 10x10x10 m gives a length of model equal to 50 m.
 Direction of regional flow: along the X or Y axis.



A three-dimensional model, representing a cube.
 The model consists of 125 cells.
 A cell size of 10x10x10 m gives a length of model equal to 50 m.
 Direction of regional flow: along the X, Y or Z axis.

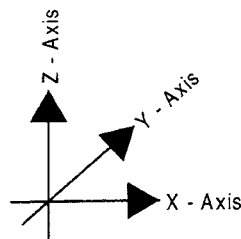
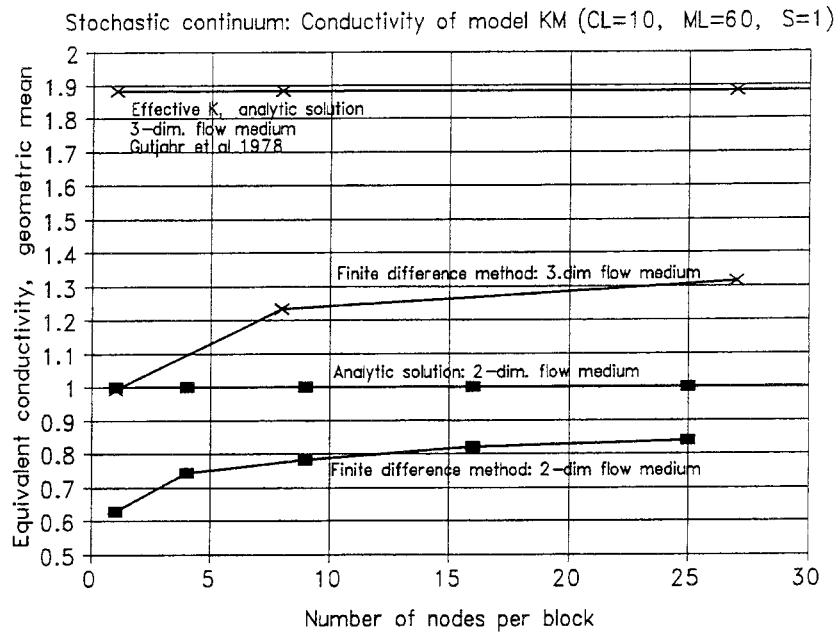


FIGURE 5.7 MODELS HAVING DIFFERENT NUMBER OF DIMENSIONS

The figure illustrates three different types of model, the difference being the number of dimensions represented in the model. These three different types of model were used in the study of scale effects in the hydraulic conductivity of a model with a stochastic continuum representation of the flow domain, indirect numerical scaling.

(i)
Equivalent K vs. number of nodes per block.
Geometric mean.
 2D plane 6x6=36 blocks
 3D cube 6x6x6=216 blocks
 Block properties
 Size: 10x10x10 m
 K distribution:
 Log-normal,
 Mean 10Lg K= 0
 STD 10Lg K= 1



(ii)
Equivalent K vs. number of nodes per block.
Standard deviat.
 2D plane 6x6=36 blocks
 3D cube 6x6x6=216 blocks
 Block properties
 Size: 10x10x10 m
 K distribution:
 Log-normal,
 Mean 10Lg K= 0
 STD 10Lg K= 1

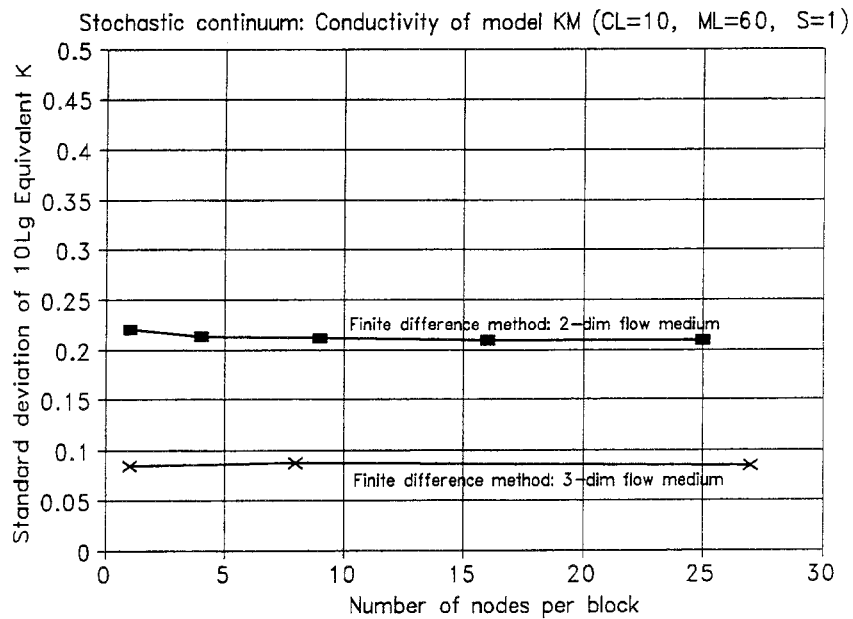
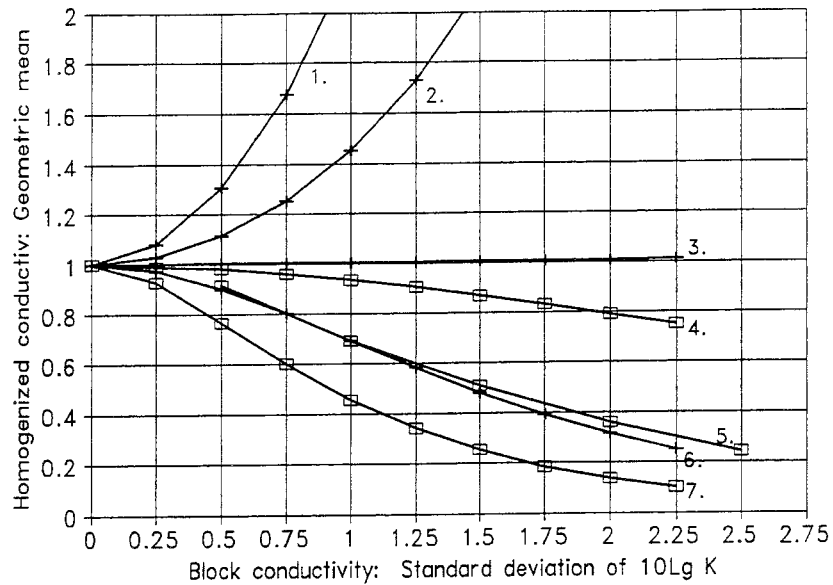


Figure 5.8

STOCHASTIC CONTINUUM, NUMBER OF NODES PER BLOCK

Models were established, representing a plane (2D) 6x6 blocks, and a cube (3D) 6x6x6 blocks. Block size was 10x10x10m and the blocks contained 1 - 27 nodes per block. The blocks had a varying conductivity according to a log-normal probability distribution. A flow was simulated through the model and the equivalent conductivity of the model was calculated. A large number of simulations were carried out for each scenario (number of nodes per block). The geometric mean and the standard deviation of the equivalent conductivity were calculated on the base of the results of these simulations. The figures demonstrate that the geometric mean of the equivalent conductivity, predicted by a not calibrated standard FID model, will deviate from analytical estimates of the effective conductivity. However, a large number of nodes per block will reduce the deviations.

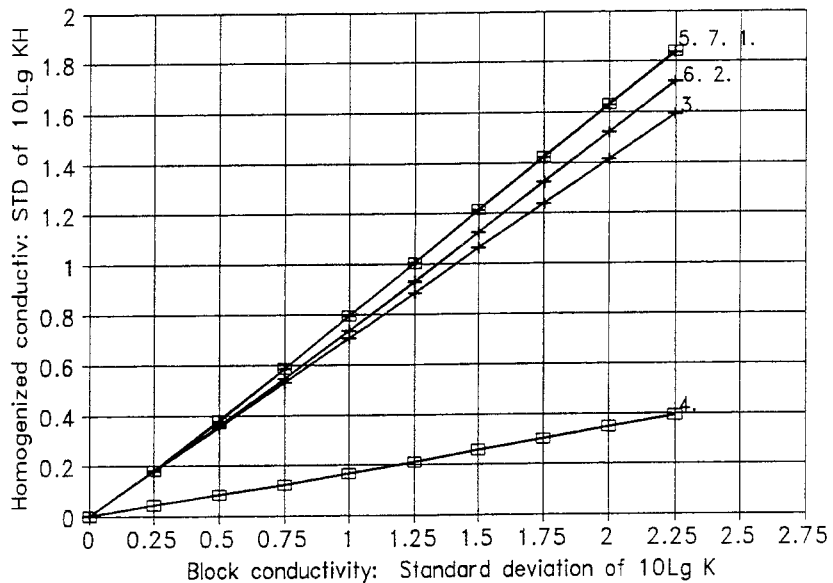
(i)
Homogenized K vs. Heterogeneity of flow medium.
Geometric mean
 Results are independent of the number of dimensions included in the models (isotropic K), models consist of blocks.
 Block properties
 Size: 10x10x10 m
 K distribution:
 Log-normal,
 Mean 10Lg K=0
 STD 10Lg K=...



Different methods of homogenization:

- | | | |
|---------------|--|-----------------------------|
| 1. Arithmetic | 4. Method C | 6. Method B |
| 2. Method A | 5. Harmonic calibrated for 2D solution | 7. Harmonic, no calibration |
| 3. Geometric | | |

(ii)
Homogenized K vs. Heterogeneity of flow medium.
Stand. deviation
 Results are independent of the number of dimensions included in the models (isotropic K), models consist of blocks.
 Block properties
 Size: 10x10x10 m
 K distribution:
 Log-normal,
 Mean 10Lg K=0
 STD 10Lg K=...

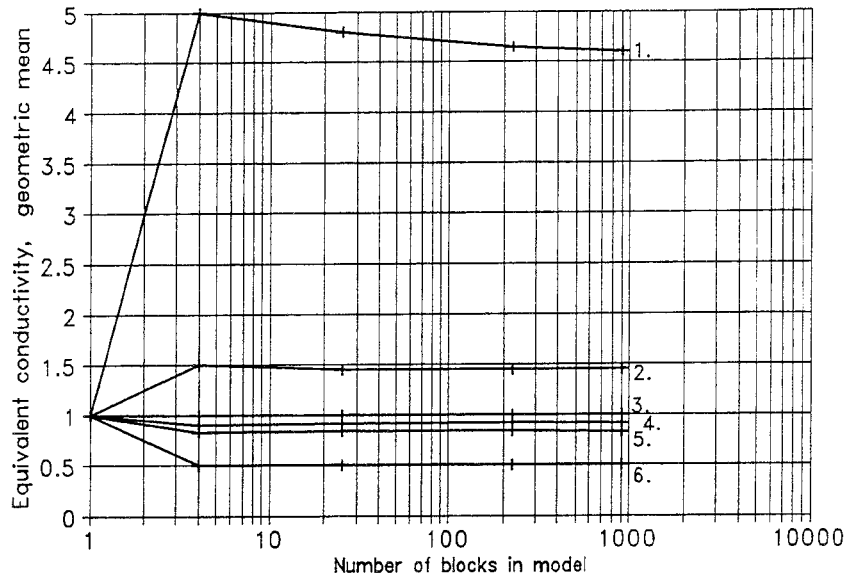


Different methods of homogenization:

- | | | |
|---------------|--|-----------------------------|
| 1. Arithmetic | 4. Method C | 6. Method B |
| 2. Method A | 5. Harmonic calibrated for 2D solution | 7. Harmonic, no calibration |
| 3. Geometric | | |

Figure 5.9 **STOCHASTIC CONTINUUM, HOMOGENIZED K AND HETEROGENEITY**
 Models were established containing about 40000 blocks, having 1 node per block. The blocks had a varying conductivity according a to log-normal probability distribution, with a geometric mean equal to 1 and different $\sigma_{10\text{Log } K_{\text{block}}}$. Inside the blocks, K is isotropic. The model uses one value of the conductivity between the nodes. This value is the homogenized conductivity and it is calculated based on the conductivity values of the blocks. The figure gives statistics of the distribution of the homogenized conductivity, for different values of the standard deviation of the block conductivity distribution and different methods of homogenization. The figure shows that different methods of homogenization produces very different distributions of the homogenized cond., the deviation between the methods grow larger with increased heterogeneity. Note, no flow simulation has been carried out.

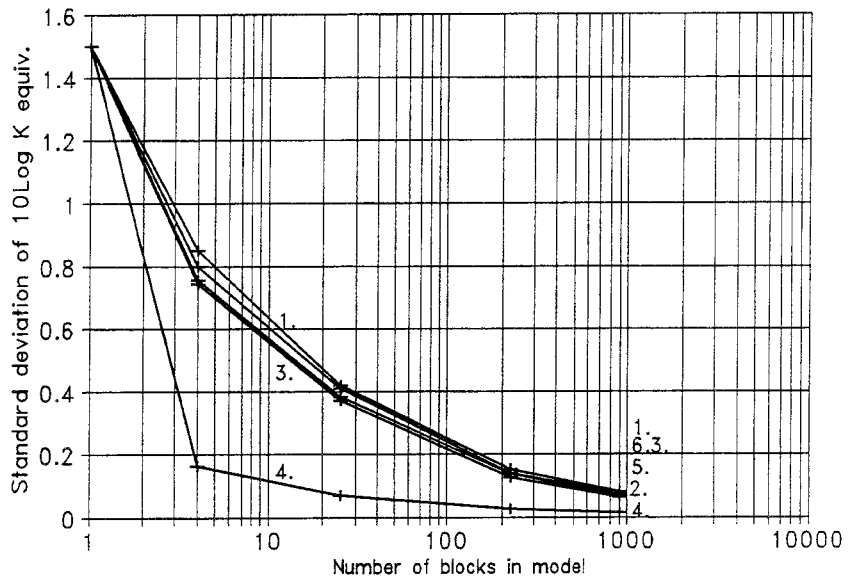
(i)
2-dim. models.
Equivalent K vs.
size of model.
Geometric mean
 2-dim. models of
 a plane consisting
 of blocks.
 Block properties
 Size: 10x10x10 m
 K distribution:
 Log-normal,
 Mean $10\text{Lg } K=0$
 STD $10\text{Lg } K=1.5$



Different methods of
 homogenization:

- | | |
|---------------------------------|----------------------------|
| 1. Arithmetic | 4. Method C |
| 2. Geometric | 5. Method B |
| 3. Harmonic, calibrated for 2D, | 6. Harmonic, no correction |

(ii)
2-dim. models.
Equivalent K vs.
size of model.
Stand. deviation
 2-dim. models of
 a plane consisting
 of blocks.
 Block properties
 Size: 10x10x10 m
 K distribution:
 Log-normal,
 Mean $10\text{Lg } K=0$
 STD $10\text{Lg } K=1.5$

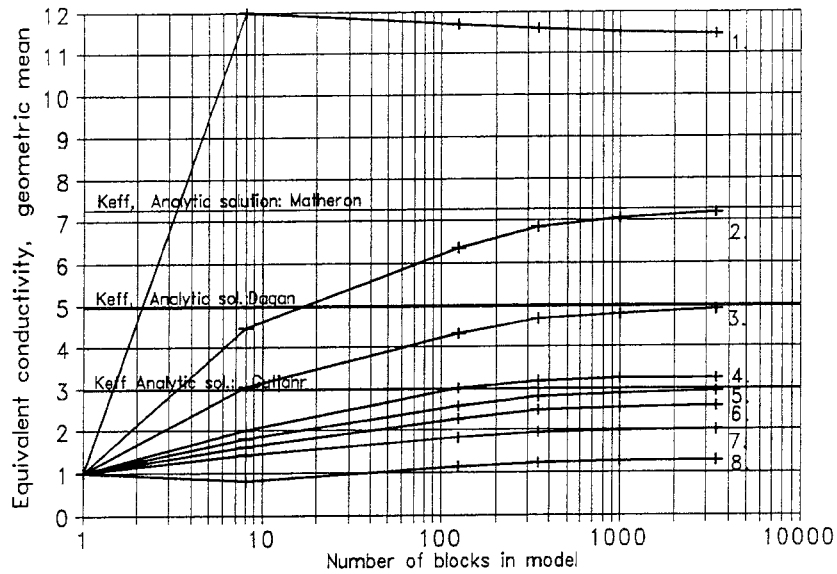


Different methods of
 homogenization:

- | | |
|---------------------------------|----------------------------|
| 1. Arithmetic | 4. Method C |
| 2. Geometric | 5. Method B |
| 3. Harmonic, calibrated for 2D, | 6. Harmonic, no correction |

Figure 5.10 **STOCHASTIC CONT. 2D, SCALE DEPENDENCY, HOMOGENIZATION**
 Different models representing a plane (2D) were established. The models contained different number of blocks, having 1 nod per block. The blocks had a varying conductivity according to a log-normal probability distribution, with geometric mean equal to 1 and $\sigma_{10\text{Log } K_{\text{block}}}=1.5$. A flow was simulated through the model and the equivalent conductivity (K_{equ}) was calculated. A large number of simulations were carried out for each size of model and the method of homogenization of block to block conductivity. According to analytical formulas, the effective conductivity (K_E) should be equal to the geometric mean of the block conductivity. Different methods of homogenization produce different K_{equ} . The obtained K_{equ} will not change much with the size of model, regardless of the method of homogenization.

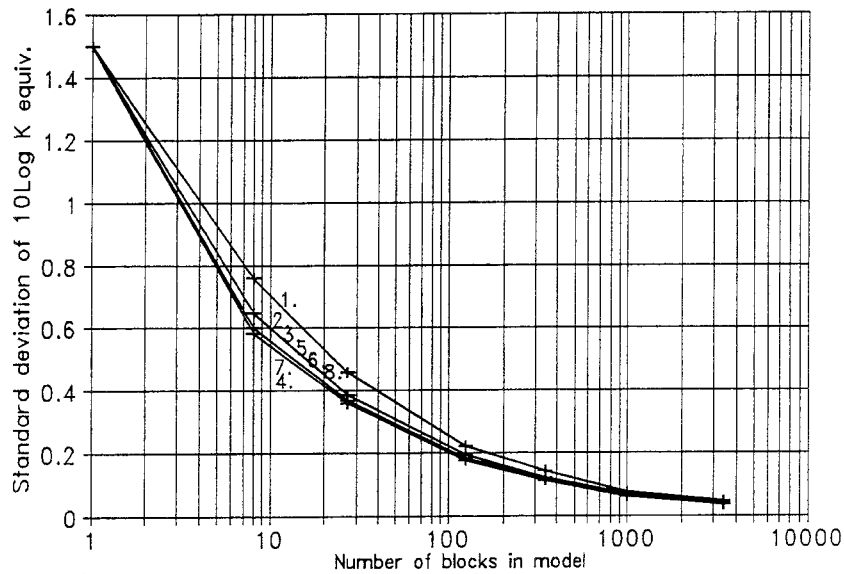
(i)
3-dim. models.
Equivalent K vs.
size of model.
Geometric mean
 3-dim. models of
 a cube, consisting
 of blocks.
 Block properties
 Size: 10x10x10 m
 K distribution:
 Log-normal,
 Mean 10Lg K=0
 STD 10Lg K=1.5



Different methods of
 homogenization:

- | | |
|--|--|
| 1. Arithmetic | 5. Harmonic, calibrated for 3D,
(Solution according to: Gujjar et al) |
| 2. Harmonic, calibrated for 3D, (Solution: Matheron) | 6. Harmonic, calibrated for 2D |
| 3. Harmonic, calibrated for 3D, (Solution: Dagan) | 7. Method B |
| 4. Geometric | 8. Harmonic, no correction |

(ii)
3-dim. models.
Equivalent K vs.
size of model.
Stand. deviation
 3-dim. models of
 a cube, consisting
 of blocks.
 Block properties
 Size: 10x10x10 m
 K distribution:
 Log-normal,
 Mean 10Lg K=0
 STD 10Lg K=1.5

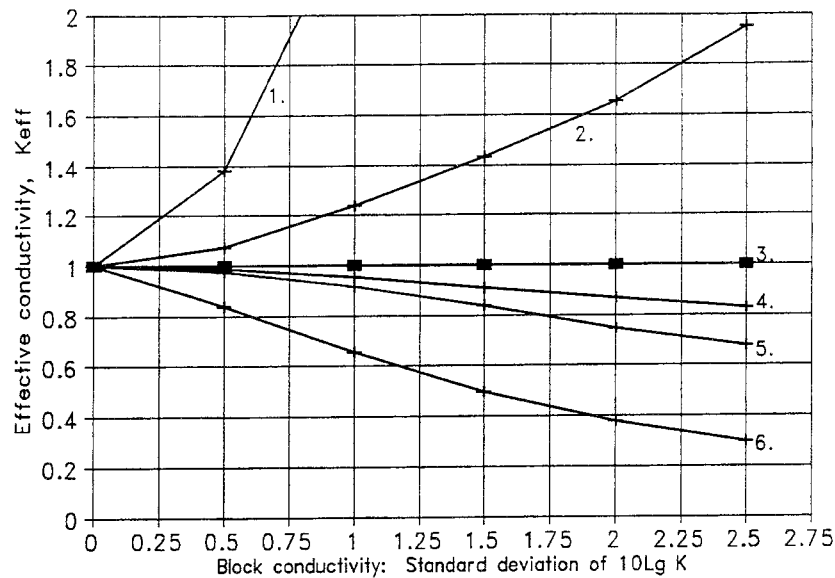


Different methods of
 homogenization:

- | | |
|--|--|
| 1. Arithmetic | 5. Harmonic, calibrated for 3D,
(Solution according to: Gujjar et al) |
| 2. Harmonic, calibrated for 3D, (Solution: Matheron) | 6. Harmonic, calibrated for 2D |
| 3. Harmonic, calibrated for 3D, (Solution: Dagan) | 7. Method B |
| 4. Geometric | 8. Harmonic, no correction |

Figure 5.11 STOCHASTIC CONT. 3D, SCALE DEPENDENCY, HOMOGENIZATION
 Different models representing a cube (3D) were established. The models contained different number of blocks, having 1 node per block. The blocks had a varying conductivity according to a log-normal probability distribution, with $K_{BG}=1$ and $\sigma_{10Lg K_{block}}=1.5$. A flow was simulated through the model and the equivalent conductivity (K_{equ}) was calculated. A large number of simulations were carried out for each size of model and each method of homogenization of block to block conductivity. The effective conductivity (K_E) according to different analytical formulas are also given. Different methods of homogenization produces different K_{equ} . For models that contain more than about 3000 blocks, the K_{equ} does not change much for further increase in model size, regardless of the method of homogenization

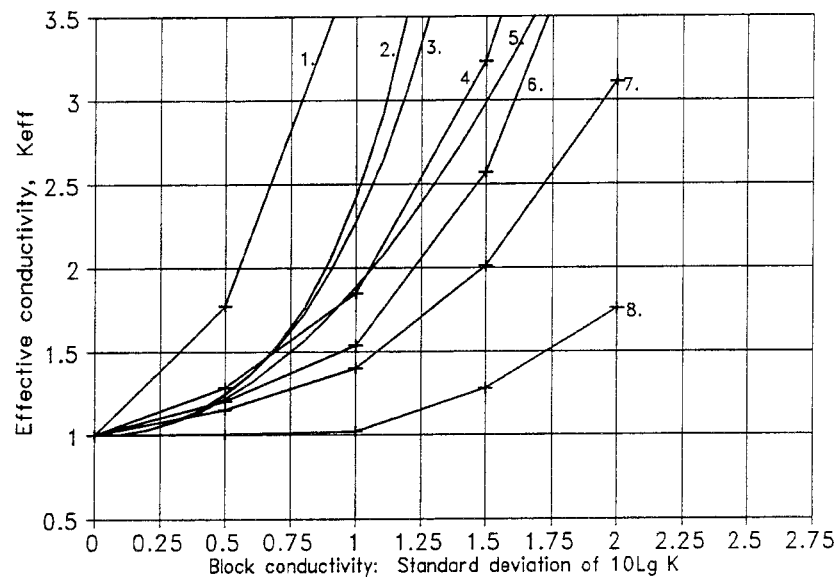
(i)
2-dim. models.
Effective K vs.
Heterogeneity of
flow medium
 2-dim. models of
 a plane consisting
 of blocks.
 Block properties
 Size: 10x10x10 m
 K distribution:
 Log-normal,
 Mean 10Lg K=0
 STD 10Lg K=...



Different methods of
 homogenization:

- | | |
|--|------------------------------------|
| 1. Arithmetic method | 4. Method C |
| 2. Geometric method | 5. Method B |
| 3. Analytical 2D solution and Harmonic method calibrated for this solution | 6. Harmonic method, no calibration |

(ii)
3-dim. models.
Effective K vs.
Heterogeneity of
flow medium
 3-dim. models of
 a cube, consisting
 of blocks.
 Block properties
 Size: 10x10x10 m
 K distribution:
 Log-normal,
 Mean 10Lg K=0
 STD 10Lg K=...



Different methods of
 homogenization:

- | | |
|---|--|
| 1. Arithmetic method | 6. Harmonic method, calibrated for 2D solution |
| 2. Analytic sol.(Matheron) and Harmonic method calibrated for this | 7. Method B |
| 3. Analytic sol.(Dagan) and Harmonic method calibrated for this | 8. Harmonic method, no calibration |
| 4. Geometric method | |
| 5. Analytic sol.(Gutjahr et al) and Harmonic method calibrated for this | |

Figure 5.12

STOCHASTIC CONT., EFFECTIVE K AND HOMOGENIZATION METHOD
 Different models representing a plane (2D) and a cube (3D) were established. The models contained such a large number of blocks (3375) that the geometric mean of the obtained equivalent K (K_{equ}) is approximately equal to the effective K (K_E). The blocks had a varying conductivity according to log-normal probability distributions with different $\sigma_{10Lg Kblock}$. A flow was simulated through the model and K_E was calculated for different values of $\sigma_{10Lg Kblock}$ and different methods of homogenization of block to block conductivities. The effective conductivity (K_E) according to different analytical formulas are also given. The best method for homogenization is to use the harmonic method and calibrate it for the analytical solution that one believes is applicable for the studied scenario.

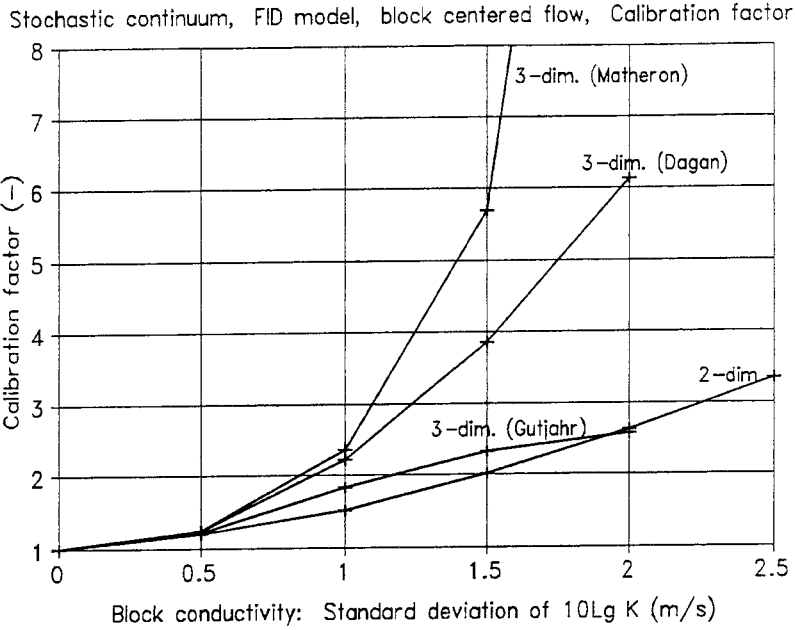


Figure 5.13

STOCHASTIC CONTINUUM, CALIBRATION FACTOR FOR FID MODEL.

A not calibrated finite difference (FID) model will underestimate the conductivity of a domain studied (the equivalent conductivity and the effective conductivity) if the domain is represented by a stochastic continuum. The FID model needs to be calibrated (corrected) as regards the probability distribution defining the conductivity of the blocks. The use of a calibration factor in the formula for calculation of the harmonic mean conductivity between two nodes will produce a good estimate of the correct geometric mean and the correct standard deviation of the equivalent and the effective conductivity. The calibration factors given above are applicable to an FID model, which uses the block-centered flow approach and one node per block, presuming that the block conductivity is given by a log-normal probability distribution. The calibration factor is calculated on the base of: (i) the effective conductivity predicted by a not calibrated model (numerical value) and (ii) the effective conductivity predicted by an analytical method (analytical value). The calibration factor is equal to the analytical value divided by the numerical value. For a three-dimensional flow medium, different analytical methods gives different calibration factors, the methods are the ones by: Matheron (1967), Gutjahr et al (1978) and Dagan (1993). For a 3-dimensional flow medium, large differences take place when the standard deviation of the block conductivity distribution is large ($\sigma_{10Lg block} > 1.3$).

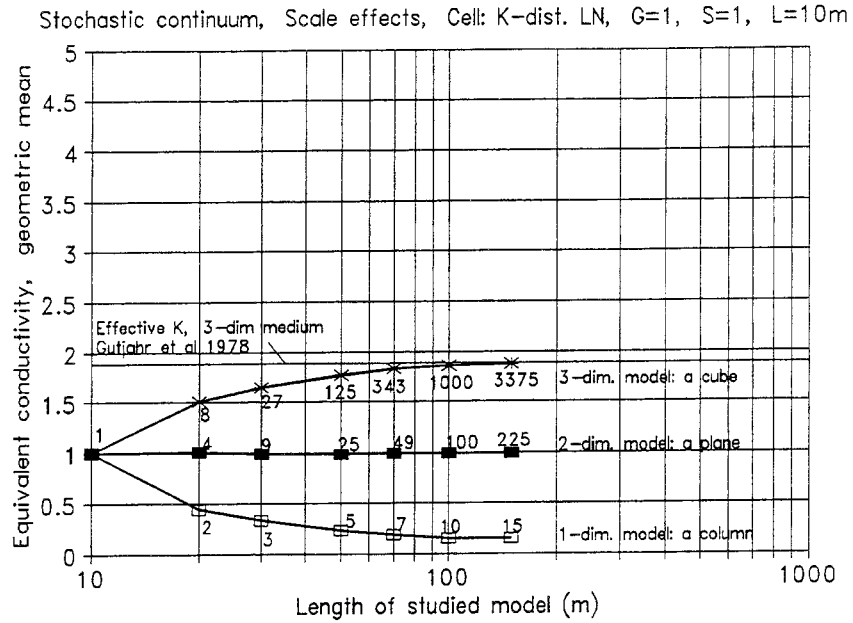
The calibration factor depends on: (i) the number of studied dimensions and on (ii) the standard deviation of the probability distribution defining the conductivity of the blocks. The factor should be used when the model calculates the homogenized conductivity between nodes, as given below.

$$K_H = \frac{2}{C K_1^{-1} + C K_2^{-1}}$$

- K_H = Homogenized conductivity between two nodes (blocks).
- K_1 = Conductivity of block 1, represented by node 1.
- K_2 = Conductivity of block 2, represented by node 2.
- C = Calibration factor.

(i)
Equivalent K vs. size of model.
Geometric mean
 Block properties
 Size: 10x10x10 m
 K distribution:
 Log-normal,
 Mean $10LgK=0$
 Std $10LgK=1.0$
 Calibration factor:
 $C_{2Dim} = 1.5$
 $C_{3Dim} = 1.8$

The numbers denote the number of blocks in that model.



(ii)
Equivalent K vs. size of model.
Stand. deviation
 Block properties
 Size: 10x10x10 m
 K distribution:
 Log-normal,
 Mean $10LgK=0$
 Std $10LgK=1.0$
 Calibration factor:
 $C_{2Dim} = 1.5$
 $C_{3Dim} = 1.8$

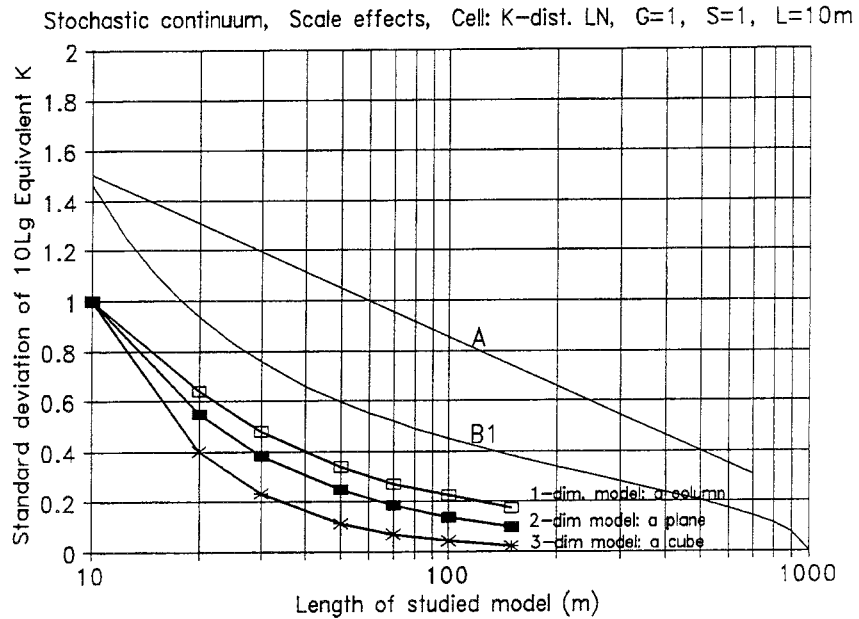
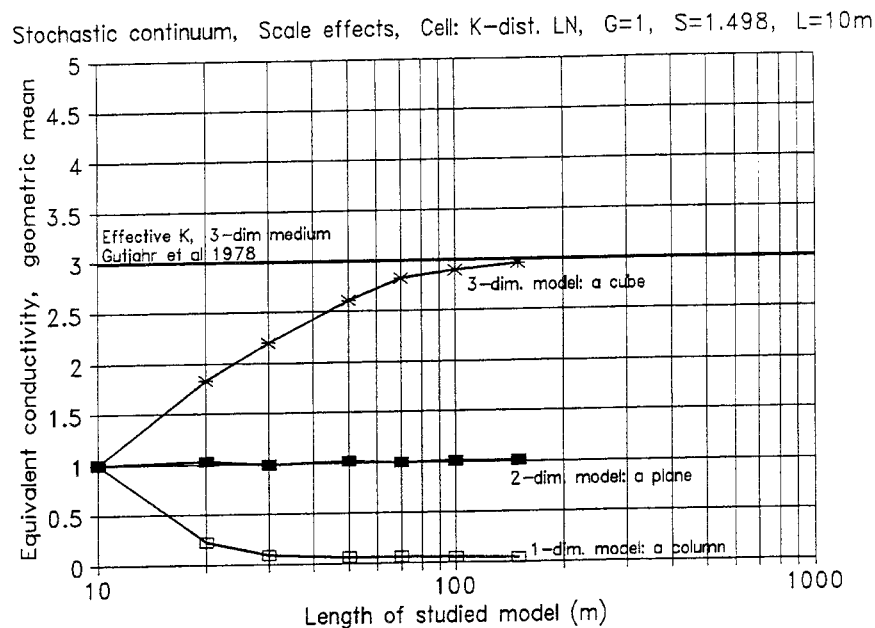


Figure 5.14 STOCHASTIC CONTINUUM, EQUIVALENT K vs. SCALE ($\sigma_{10Lg K_{block}} = 1.0$)
 Three different models were established representing a column (1-dim.), a plane (2-dim.) and a cube (3-dim.). All models contain blocks of size 10x10x10 m, with varying conductivity. The size of the models was increased by adding blocks to the models. For the column, blocks were added in one dimension, for the plane in two dimensions and for the cube in three dimensions. A flow was simulated through the models and the equivalent conductivity of the models was calculated. A large number of simulations was carried out for each size and type of model, the geometric mean and the standard deviation of the equivalent conductivity were calculated, based on the results of these simulations.

(i)
Equivalent K vs. size of model.
Geometric mean
 Block properties
 Size: 10x10x10 m
 K distribution:
 Log-normal,
 Mean $10\text{Lg}K = 0$
 Std $10\text{Lg}K = 1.498$
 Calibration factor:
 $C_{2\text{Dim}} = 2.0$
 $C_{3\text{Dim}} = 2.3$



(ii)
Equivalent K vs. size of model.
Stand. deviation
 Block properties
 Size: 10x10x10 m
 K distribution:
 Log-normal,
 Mean $10\text{Lg}K = 0$
 Std $10\text{Lg}K = 1.498$
 Calibration factor:
 $C_{2\text{Dim}} = 2.0$
 $C_{3\text{Dim}} = 2.3$

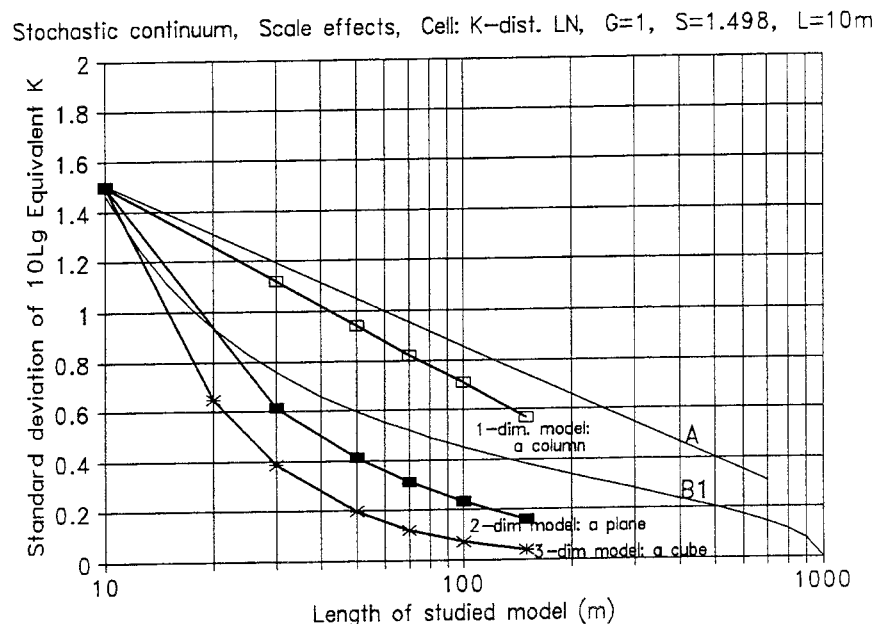
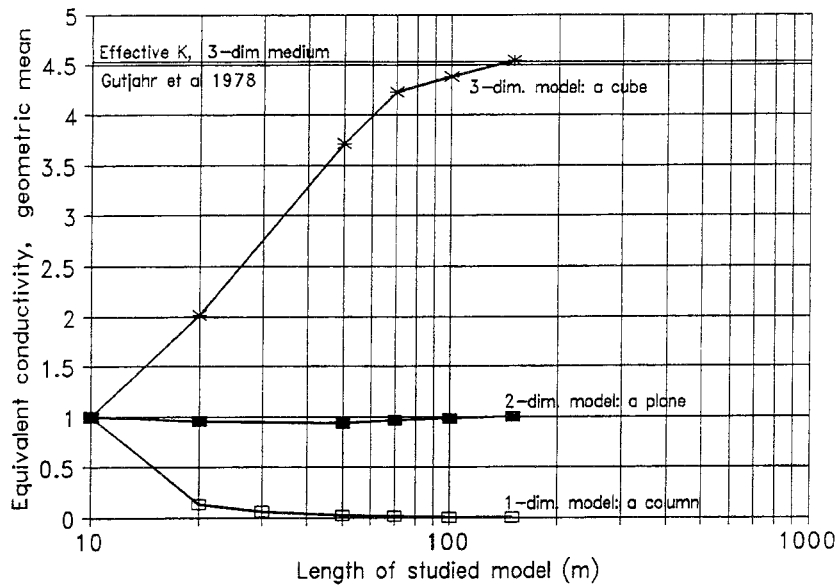


Figure 5.15 STOCHASTIC CONTINUUM, EQUIVALENT K vs. SCALE ($\sigma_{10\text{Lg}K_{\text{block}}} = 1.498$)
 Three different models were established representing a column (1-dim.), a plane (2-dim.) and a cube (3-dim.). All models contain blocks of size 10x10x10 m, with a varying conductivity. The size of the models was increased by adding blocks to the models. For the column, blocks were added in one dimension, for the plane in two dimensions and for the cube in three dimensions. A flow was simulated through the models and the equivalent conductivity of the models was calculated. A large number of simulations was carried out for each size and type of model, the geometric mean and the standard deviation of the equivalent conductivity were calculated, based on the results of these simulations.

(i)
Equivalent K vs.
size of model.
Geometric mean
 Block properties
 Size: 10x10x10 m
 K distribution:
 Log-normal,
 Mean $10LgK=0$
 Std $10LgK=2.0$
 Calibration factor:
 $C_{2Dim} = 2.60$
 $C_{3Dim} = 2.58$

Stochastic continuum, Scale effects 3D, Block: K-dist. LN, G=1, S=2, L=10m



(ii)
Equivalent K vs.
size of model.
Stand. deviation
 Block properties
 Size: 10x10x10 m
 K distribution:
 Log-normal,
 Mean $10LgK=0$
 Std $10LgK=2.0$
 Calibration factor:
 $C_{2Dim} = 2.60$
 $C_{3Dim} = 2.58$

Stochastic continuum, Scale effects, Cell: K-dist, LN, G=1, S=2, L=10m

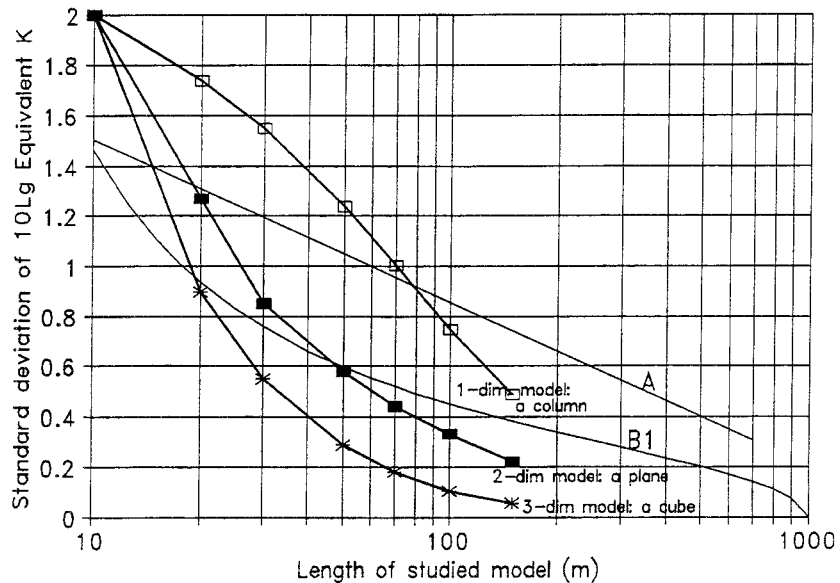


Figure 5.16 STOCHASTIC CONTINUUM, EQUIVALENT K vs. SCALE ($\sigma_{10Lg K_{block}} = 2.0$)
 Three different models were established representing a column (1-dim.), a plane (2-dim.) and a cube (3-dim.). All models contain blocks of size 10x10x10 m, with varying conductivity. The size of the models was increased by adding blocks to the models. For the column, blocks were added in one dimension, for the plane in two dimensions and for the cube in three dimensions. A flow was simulated through the models and the equivalent conductivity of the models was calculated. A large number of simulations was carried out for each size and type of model, the geometric mean and the standard deviation of the equivalent conductivity were calculated, based on the results of these simulations.

(i)

Comparison between Scaling methods

Scaling by indirect numerical method

Block properties

Size: 10x10x10 m

K distribution:

Log-normal,

Standard deviation:

• 10LogK= 1.0

(Triangles)

• 10LogK= 1.498

(Filled squares)

• 10LogK= 2.0

(Crosses)

Scaling by direct

analytical method

Conditioned analytical

interpolation between

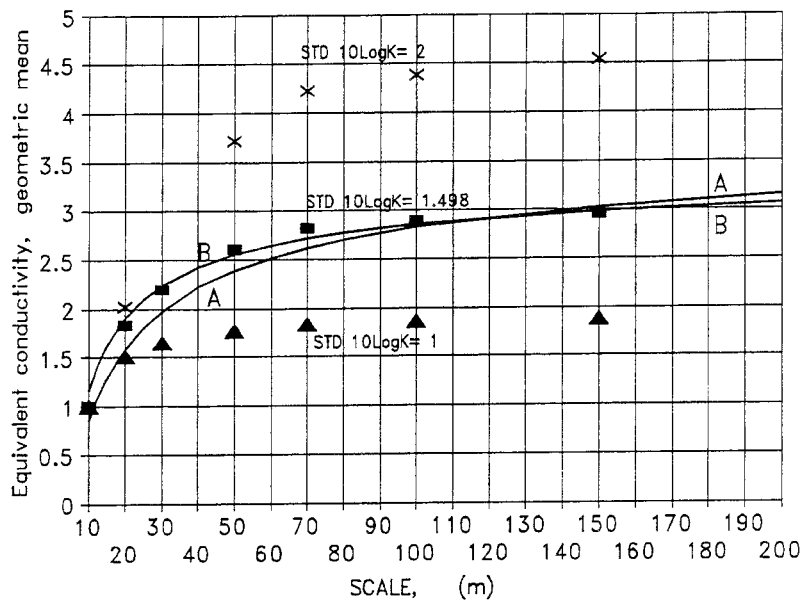
measured data

(Curve B).

Interpolation between

measured data(CurveA)

Stochastic continuum, Scale effects 3d, Cell: K-dist. LN, G=1, S=x, L=10m



(ii)

Comparison between:

• Scaling methods

• Measured data

Scaling by indirect

numerical method

Block properties

Size: 10x10x10 m

K distribution:

Log-normal,

STD 10LogK= 1.498

(Filled squares)

Scaling by direct

analytical method

Conditioned analytical

interpolation between

measured data.

(Curve B)

Measured data at Äspö

Results (Empty squares)

Stochastic continuum, Scale effects 3d, Cell: K-dist. LN, G=1, S=1.498, L=10m

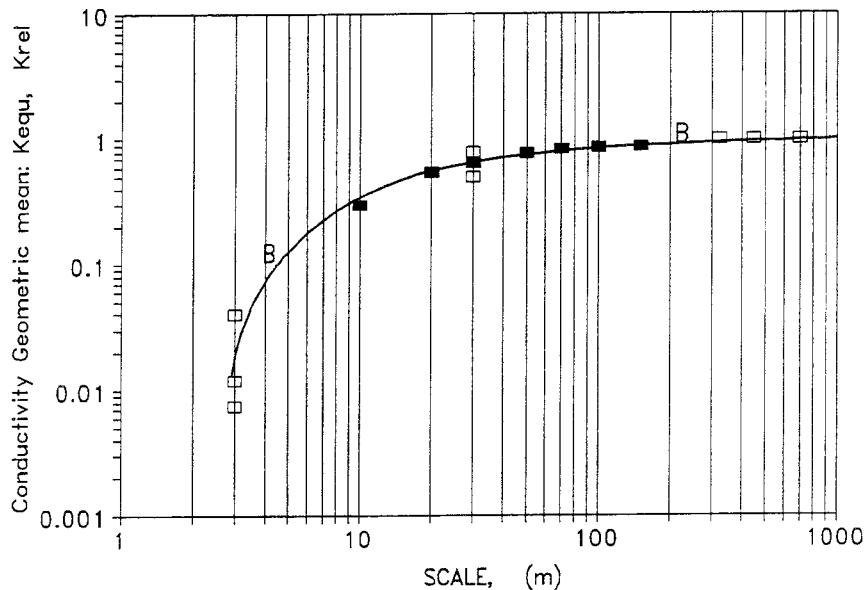


Figure 5.17 STOCHASTIC CONTINUUM, SCALE EFFECTS, 3-DIMENSIONAL MODELS

A comparison between: • simulated scale dependency, which is the same as a method for indirect numerical scaling, • direct analytical method for scaling and • measured scale dependency at Äspö. The figures show the conductivity predicted by the different methods as well as the results of the field measurements, versus length of models and scale of field measurements. It is the shape of the curves and the tendency of the plotted data that should be compared, not the absolute values. The best fit between the two scaling methods and the best fit to measured data is obtained for curve B, for models with a block size of 10x10x10 m and with a STD 10Log K equal to 1.498 ($\sigma_{10Lg K_{block}} = 1.498$).

Chapter 6.

Effects of the heterogeneity of the rock mass as regards flow in tunnels

6.1 Introduction

In the following chapter, we will simulate the flow of a closed tunnel located in either a homogeneous flow medium or in a heterogeneous flow medium. The flow medium represents the fractured rock mass at Äspö Hard Rock Laboratory. A closed tunnel is in the flow medium, it is not kept dry, but is filled with groundwater and the groundwater flow in the tunnel is at equilibrium with the groundwater system. The homogeneous flow medium will be represented by a uniform continuum, the heterogeneous flow medium will be represented by a stochastic continuum. To investigate the effects of the heterogeneity of the rock mass, we will compare the flow in a tunnel predicted by models representing a heterogeneous flow medium (stochastic continuum), to the flow predicted by models representing a homogeneous flow medium (uniform continuum).

In the following section we will use the terms: effective conductivity, equivalent conductivity and block conductivity. For a stochastic continuum model these terms are defined in Chapter 5. For a uniform continuum model the effective conductivity and the equivalent conductivity, as well as the block conductivity, will be the same and this value will not change with the size of model. We will also use the term: homogenized conductivity which is defined in Chapter 5 as well as the term: threshold conductivity, defined in Chapter 3.

6.2 Estimation of boundary effects, stochastic continuum.

Introduction

As discussed in Chapter 4, boundary effects will influence the predicted flow in the tunnel. In this section we will estimate the size of these boundary effects and, based upon the results, select an appropriate size of model.

Elimination of scale dependency in model conductivity

In the following sections we will use a stochastic continuum approach for the representation of the heterogeneous rock mass. We will use three-dimensional models of different sizes, to be able to calculate the boundary effects. The homogenized conductivity will be calculated by the use of the harmonic method (see Chapter 5).

In the models discussed in the previous section (Chapter 5), the geometric mean of the block conductivity distribution was set to 1. This will produce a geometric mean of the equivalent conductivity of the model, which is larger than 1 (scale dependency). If we want the geometric mean of the equivalent conductivity to be 1 (or close to 1), we should set the geometric mean of the block conductivity distribution to the inverse of the equivalent conductivity, obtained when the geometric mean of the block conductivity was set to 1. Ergo, we adjust the block conductivity distribution in such way that the equivalent conductivity distribution will have a geometric mean equal to 1.

Hence, if we have a model of a certain size and want this model to reproduce the heterogeneous hydraulic properties at Äspö and have a geometric mean of the equivalent conductivity distribution as close as possible to 1, we need to do as follows. Set the block size to 10x10x10 m, set the block conductivity distribution to Log-normal, the standard deviation to $10 \log K = 1.498$ and the geometric mean to 1. Perform a large number of

simulations, calculate the geometric mean of the obtained equivalent conductivity of the model (GMKE). The inverse of this value ($1/GMKE$) should be assigned as the geometric mean of the block conductivity distribution. Such a geometric mean of the block conductivity distribution will produce a geometric mean of the equivalent conductivity distribution which is 1 or close to 1.

To compensate for the scale dependency in the equivalent conductivity, we have followed the method described above. For all meshes and directions of regional flow used for estimation of the boundary effects, we have calculated the block conductivity distribution that, without a tunnel, produces an equivalent conductivity distribution with a geometric mean close to 1. Thus, the models used in the estimation of boundary effects have been assigned a block conductivity distribution in such a way that the models, without a tunnel, will have a geometric mean equivalent conductivity which is close to 1.

In this way we have eliminated the scale dependency in the equivalent conductivity. The phenomenon will not influence the estimation of boundary effects, when comparing the flow through a tunnel predicted by meshes of different size.

Method for estimation of boundary effects

We will study the flow in a tunnel when the regional flow is directed along the tunnel or at right angles to the tunnel. We will use the numerical method of multiple meshes, method B2, as described in Chapter 4.

Results

The results of the analyses are given in Figures 6.6 through 6.8 and Table 6.1. As demonstrated in the figures and the table, the error in predicted flow decreases as the size of the model increases. Using a three-dimensional model with a block size of $10 \times 10 \times 10$ m and a minimum number of 7 blocks between a studied tunnel of 100m length and the boundary of the model (model M7), we will overestimate the flow in the tunnel. The error in predicted flow will be less than or about 5 percent of the flow predicted. Such an error is considered as acceptable. Hence, for the simulations presented in this chapter, we will use models with a minimum number of 7 blocks between the tunnel and the model boundary. Such models will contain 6000 block or more, dependent on the tunnel length. For a tunnel of 100m length, the model mesh is given in Figure 6.1.

6.3 Introduction to sensitivity analysis.

Methodology

We will study the flow in a closed tunnel, the tunnel is filled with water and the flow in the tunnel is at equilibrium with the groundwater system. To investigate the effects of the heterogeneity of the rock mass, we will compare the flow in a tunnel predicted by models representing a heterogeneous flow medium (stochastic continuum) to the flow predicted by models representing a homogeneous flow medium (uniform continuum).

In order to make such a comparison, it is necessary that the effective conductivities of the models representing a heterogeneous flow medium are the same as the conductivities of the models representing a homogeneous flow medium, in the direction of the regional flow. However, the models representing a heterogeneous flow medium will be influenced by scale effects and we need to compensate for these effects. It is the effective conductivity of all models that should be the same, not the conductivities of the blocks. In the stochastic continuum models the block conductivity will vary, but for the size of models that we will use, the effective conductivity is approximately equal to the geometric mean of the equivalent conductivity. The probability distribution defining the

conductivity of the blocks in the stochastic continuum models is adjusted in such a way that the geometric mean of the equivalent conductivity, without the tunnel and in the direction of the regional flow, will be the same for the stochastic continuum models as for the uniform continuum models. This will produce the same regional flow for all models.

As discussed in Chapter 5, there are different methods of estimation of the effective conductivity of a three-dimensional stochastic continuum, different methods that predict different values. The different predictions could cause some uncertainty. We will avoid the uncertainty by selecting a block conductivity distribution that produces an effective conductivity of the stochastic continuum models, equal to the conductivity of the uniform continuum models. We can do this as we are only interested in the relations between: (i) the specified regional flow and (ii) the flow of a tunnel placed in uniform continuum model as well as (iii) the flow of a tunnel placed in a stochastic continuum model. Our modeling exercise is not a site-specific one, we do not need to know a site-specific effective conductivity or a site-specific regional flow.

The stochastic continuum model can be calibrated to match any analytical prediction of the effective conductivity. Such a calibration can be implemented when the homogenized conductivity is calculated (see Chapter 5.). However, we do not need to do that, as we use the approach with constant effective conductivity in all models (discussed above). The most important parameter of our models is the heterogeneity of the flow medium of the stochastic continuum models. It is important that the heterogeneity of the models corresponds to measured values. In our models the measured heterogeneity will be preserved in the conductivity field, as we calculate the homogenized conductivity as the harmonic mean (see Chapter 5).

Studied scenarios

In the following models we will study a straight tunnel with a length of 10m-200m and a rectangular cross-section of: $10\text{m} \times 10\text{m} = 100 \text{ m}^2$, placed in a rock mass of either heterogeneous or homogeneous hydraulic properties. All blocks in the models had the same size, which was $10 \times 10 \times 10\text{m}$. For a tunnel of 100m length, the model mesh is given in Figure 6.1. The tunnel was defined with a uniform conductivity that was varied between different scenarios, it was varied between 0.001 - 100000 times the effective conductivity of the rock mass (the effective conductivity was calculated as the geometric mean of the equivalent conductivity of the rock mass). Hence, both very impermeable tunnels and very permeable tunnels were studied.

In the models studied, the regional flow was directed either along the tunnel or at right angles to the tunnel. These two directions represent two extreme directions. Directions of the regional flow that are different from the two directions studied, will produce effects that are in size between the effects produced by the two directions studied (presuming a straight tunnel). The regional flow was created by assigning the specified head boundary condition to the blocks of two opposite faces of the model. The specified head was set in a way that a regional flow was created. All other blocks were of the continuous type.

Examples of flow pattern in rock mass and tunnel

To illustrate the flow pattern of the groundwater, different scenarios have been studied by the use of flowpaths. The flowpaths are created by simulated particles that follow the flow of the groundwater. The particles are released at a boundary of the model, the path of the particles through the model gives the flowpaths. Both a high permeable and a low permeable tunnel has been studied as well as a homogeneous and a heterogeneous rock mass. The regional flow was directed either along or at right angles to the tunnel.

The flow patterns of a homogeneous rock mass are given in Figure 6.2 and 6.4. If the

tunnel is more permeable than the rock mass (Fig.6.2), the flow will converge towards the upstream part of the tunnel and diverge from the downstream part of the tunnel. The flow strives to use the tunnel as it has a smaller resistance than the rock mass. If the tunnel has a low permeability (Fig.6.4) the opposite will occur. The largest and most visible effects of the tunnel takes place when the regional flow is along the tunnel.

To represent a heterogeneous rock mass, the stochastic continuum approach was used. The same conductivity field, representing the heterogeneous rock mass, was used in all scenarios illustrating the flow of a heterogeneous rock mass, which makes a comparison between different scenarios possible. Examples of flow patterns of a heterogeneous rock mass are given in Figure 6.3 and 6.5. In a heterogeneous medium most of the flow occurs in efficient pathways. Efficient pathways are paths through the rock mass with a small resistance. These paths are given by the conductivity distribution of the rock mass (the conductivity field). Many of the efficient pathways of the rock mass include the tunnel, if it has a high permeability (Fig.6.3), and avoids the tunnel, if it has a low permeability (Fig.6.5). These effects are clearly seen if we compare Fig.6.3 and Fig.6.5. Hence, the overall flow pattern of the heterogeneous medium is the same as for a homogeneous medium. And as for a homogeneous medium, the largest and most visible effects of the tunnel takes place when the regional flow is along the tunnel.

The concept of specific flow, total flow and flow factors

The flow in a tunnel will be given as a specific flow or as a total flow (see Chapter 2). The flow values given are to be regarded as multiples of an unknown regional flow. To calculate the multiples, the regional specific flow was set to 1 m/s in the models. This was achieved by setting the effective conductivity of the stochastic continuum models to 1 and the conductivity of the uniform continuum models to 1 as well. The regional gradient was also set to 1 in all models.

The flow in a tunnel can also be given as a flow factor. The flow factor corresponds to a tunnel placed in a heterogeneous rock (stochastic continuum) and represents the flow in such a tunnel expressed in relation to the flow of a similar tunnel placed in a homogeneous rock mass (uniform continuum), as defined below. Hence, the flow factor demonstrates the effect of the heterogeneity of the rock mass.

$$SQFAC = \frac{SQ_{stochastic\ continuum}}{SQ_{uniform\ continuum}} \tag{6.1}$$

$$TFFAC = \frac{TF_{stochastic\ continuum}}{TF_{uniform\ continuum}}$$

- SQFAC = Specific flow factor.
- $SQ_{stochastic\ continuum}$ = Specific flow in a tunnel placed in a heterogeneous medium.
- $SQ_{uniform\ continuum}$ = Specific flow in a tunnel placed in a homogeneous medium.
- TFFAC = Total flow factor.
- $TF_{stochastic\ continuum}$ = Total flow in a tunnel placed in a heterogeneous medium.
- $TF_{uniform\ continuum}$ = Total flow in a tunnel placed in a homogeneous medium.

Number of realizations

This chapter includes about 70 scenarios, representing different tunnel properties and rock block conductivity distributions as well as directions of the regional flow. For the uniform continuum models only one realization is necessary for each scenario. For the stochastic continuum models many realizations are necessary for each scenario; the number of realizations that we have included in the statistical analysis of each scenario has been varied, dependent on the acceptable uncertainty and the size of the variation in the

calculated flow, the number has been varied from about 30 to 100 realizations.

Statistical considerations as regards the results of the stochastic continuum modelling

The effects of the heterogeneity of the rock mass were studied by using the stochastic continuum approach (see Chapter 5). The results of the stochastic continuum modelling are based on statistical analyses of many realizations of the conductivity field.

Every scenario studied is represented by a number of realizations, each realization produces a value of the flow in the tunnel. For each scenario the values obtained form a statistical distribution. The different scenarios demonstrate statistical distributions which are fairly symmetrical, but slightly skewed to the right, the upper tail is somewhat longer than the lower tail. For the distributions obtained, the difference between the arithmetic mean, the median, the mode and the geometric mean is small, compared to the size of the standard deviation. The distributions obtained can be reasonably represented both by normal and log-normal statistical distributions. For all of the distributions obtained, the standardized coefficients tests for deviations from the normal distribution (standardized skewness and standardized kurtosis) are within the range -1.0 to +1.5. For most of the distributions the range are within -0.5 to +1.0.

In the following sections, when we refer to the flow of a tunnel placed in a heterogeneous rock mass, we mean the average flow of many different realizations, - the most probable outcome, the expected flow. The possible variation of the flow of a tunnel, depending on the heterogeneous properties of the rock mass, is described by the standard deviation and is given in the figures of this chapter. The general conclusions given in the following sections are valid for at least 70 percent of the realizations of a studied scenario, - the expected value plus and minus one standard deviation ($m-\sigma$ and $m+\sigma$). Hence, they are valid with a probability of at least 70 percent.

6.4 Flow in a tunnel, heterogeneous rock, sensitivity to tunnel conductivity.

The tunnel is defined as having a length of 100 m and a uniform conductivity that was varied between different scenarios. The rock mass is defined as a heterogeneous medium (stochastic continuum) with hydraulic properties representing Äspö, or as a homogeneous medium (uniform continuum). The results of the simulations are given in Figures 6.9 through 6.12. The figures demonstrate that the flow in the tunnel will not be the same for a model which includes the heterogeneity of the rock mass (stochastic continuum), compared to a model with a homogeneous rock mass (uniform continuum); even if the effective conductivity of the models representing a heterogeneous rock is the same as the conductivity of the models representing a homogeneous rock.

- **Regional flow along the tunnel** (Figures 6.9, 6.11 and 6.12). A heterogeneous rock mass will give an expected flow in the tunnel which is larger than that of a homogeneous rock mass, both as regards specific flow and total flow. Considering the total flow, we will have the largest deviations (flow factor, see Equ.6.1) when the tunnel conductivity is smaller than the effective conductivity of the rock mass. The threshold conductivity of the tunnel filling is about 10 000 times the effective conductivity of the rock mass.
- **Regional flow at a right angles to the tunnel** (Figures 6.10 and 6.12). A heterogeneous rock mass will give an expected flow in the tunnel which is larger than that of a homogeneous rock mass, if the tunnel conductivity is larger than the effective conductivity of the rock mass, or much smaller. Considering the total flow, we will have the largest deviations (flow factor) when the tunnel conductivity is much larger

than the effective conductivity of the rock mass. The threshold conductivity of the tunnel filling is about 1000 times the effective conductivity of the rock mass.

We conclude, regardless of the conductivity of the tunnel filling, the expected flow in the tunnel will be larger if the rock mass is defined as a heterogeneous medium than if it is defined as a homogeneous medium. If the tunnel is very permeable, the largest deviations in tunnel flow (flow factor) will take place if the regional flow is directed at right angles to the tunnel. If the tunnel has a low permeability the largest deviations will take place if the regional flow is directed along the tunnel. Considering the expected flow in a tunnel, the variation as regards the direction of the regional flow will be smaller if the rock mass is defined as a heterogeneous medium than if it is defined as a homogeneous medium.

6.5 Flow in a tunnel, heterogeneous rock, sensitivity to amount of heterogeneity.

The tunnel is defined as having a length of 100 m and a conductivity which is 10000 times the effective conductivity of the rock mass. The rock mass is defined as a heterogeneous medium (stochastic continuum) with hydraulic properties representing Äspö, or with properties different from those at Äspö. As a reference scenario the rock mass is defined as a homogeneous medium (uniform continuum). We want to study the effects caused by different amounts of heterogeneity of the rock mass; to be able to do so we need to define a measure of the heterogeneity of our stochastic continuum model. In a stochastic continuum model the conductivity of the blocks is given by a probability distribution (the block conductivity distribution); the standard deviation of this distribution defines the size of variation in conductivity that may take place among the blocks. Hence, the given standard deviation of the block conductivity distribution is proportional to the obtained heterogeneity of the studied medium. We will use the standard deviation of the block conductivity distributions as a measure of the heterogeneity of the rock mass.

Different amounts of heterogeneity were defined in relation to the heterogeneity of the model representing the properties at Äspö. Hence, the heterogeneity are defined in relation to the standard deviation (STD) of the probability distribution defining the conductivity of the blocks in the model representing Äspö. The properties representing Äspö (Block size 10x10x10m, Block K distribution Log-normal, STD 10Log K= 1.498) is defined as a heterogeneity of 100%. A homogeneous rock mass has a heterogeneity which is 0% of the heterogeneity at Äspö. Three different values of heterogeneity were studied: (i) 50% of Äspö (STD 10Log K= 1.197), (ii) 100% of Äspö (STD 10Log K= 1.498) and (iii) 318% of Äspö (STD 10Log K= 2). The effective conductivity of the models, without the tunnel, was the same for all models.

The results of the simulations are given in Figures 6.13 through 6.15.

- **Regional flow along the tunnel** (Figure 6.13). A heterogeneous rock mass will give an expected flow in the tunnel which is larger than that of a homogeneous rock mass, both as regards specific flow and total flow. The larger the heterogeneity, the larger the expected flow in the tunnel. As regards the flow factor for average total flow (expected total flow), a heterogeneity of 50% gives a factor of 1.63, a heterogeneity of 100% gives a factor of 1.75 and a heterogeneity of 318% gives a factor of 2.06
- **Regional flow at right angles to the tunnel** (Figure 6.14). A heterogeneous rock mass will give an expected flow in the tunnel which is larger than that of a homogeneous rock mass, both as regards specific flow and total flow. The larger the heterogeneity, the larger the expected flow in the tunnel. As regards specific flow, the flow factor

increases much faster with increased heterogeneity than the flow factor for total flow. This is an effect of the way the specific flow is calculated. The specific flow is calculated as the average specific flow of all blocks representing the tunnel. For a model with a heterogeneous flow medium and when the tunnel is at right angles to the regional flow, the specific flow in the tunnel will be very different at different sections, and the average specific flow will be strongly influenced by the blocks with the largest specific flow (see Figure 6.20). This effect illustrates that the specific flow of the tunnel (average specific flow in the tunnel) does not represent the volume of water that visits the tunnel. However, the total flow represents the volume of water that visits the tunnel. As regards the flow factor for average total flow (expected total flow), a heterogeneity of 50% gives a factor of 2.27, a heterogeneity of 100% gives a factor of 2.66 and a heterogeneity of 318% gives a factor of 4.31

We conclude, a heterogeneous rock mass will give a larger expected flow in a tunnel than a homogeneous rock mass. The expected flow in the tunnel depends on the amount of heterogeneity, it increases with increasing heterogeneity. Studying how the flow in the tunnel increases with increasing heterogeneity, we see that the largest change in flow will occur at small amounts of heterogeneity. Hence, it can be important to study the heterogeneity even if the uncertainty in amount of heterogeneity is large. Considering the direction of the regional flow, the largest change in expected flow, expressed as a flow factor, will occur when the regional flow is directed at right angles to the tunnel. As regards the expected flow in a tunnel, the flow factors for heterogeneities between 50% and 318% demonstrates a nearly linear relationship for both directions of flow studied.

The effects of different amounts of heterogeneity of the rock mass and the effects of different values of tunnel conductivity as regards the expected flow in the tunnel, are demonstrated in Figure 6.15. The figure gives the flow factor for average flow (expected flow) of a tunnel for different values of tunnel conductivity and different values of the heterogeneity of the rock mass. The regional flow was directed along the tunnel. Two different heterogeneities of rock mass were studied: 100% and 318%. The figure demonstrates that the increase in heterogeneity, from a heterogeneity of 100% to a heterogeneity of 318% does not dramatically increase the flow in the tunnel, regardless of tunnel conductivity. The flow factor as regards total flow does not change much for different values of tunnel conductivity; the flow factor is approximately constant, regardless of tunnel conductivity.

6.6 Flow in a tunnel, heterogeneous rock, sensitivity to tunnel length

The flow in tunnels of different lengths has been calculated (10m-200 m). The conductivity of the tunnels was 10000 times the effective conductivity of the rock mass. The rock mass was defined as a heterogeneous medium (stochastic continuum) with hydraulic properties representing Äspö, or as a homogeneous medium (uniform continuum). The effective conductivity of the models, without the tunnel, were the same.

The results of the simulations are given in Figures 6.16 through 6.19.

- **Regional flow along the tunnel** (Figures 6.16 and 6.17). A heterogeneous rock mass will give an expected flow in a tunnel which is larger than that of a homogeneous rock mass, both as regards specific flow and total flow, if the tunnel is shorter than about 1000 m. The largest deviations in flow factor will take place when the tunnel is short, the longer the tunnel the smaller the deviation. As regards the flow factor for average total flow (expected total flow), it decreases from 2.0 for a 50m long tunnel to 1.4 for a 200m long tunnel. An extrapolation of the curve predicts that at a tunnel

length of about 700m, both models predict about the same flow in the tunnel (the flow factor is close to one).

- **Regional flow at a right angles to the tunnel** (Figures 6.18 and 6.19). A heterogeneous rock mass will give an expected flow in a tunnel which is larger than that of a homogeneous rock mass, both as regards specific flow and total flow. As regards specific flow, the flow factor increases with tunnel length, this may look strange but it is an effect of the way the specific flow is calculated. The specific flow is calculated as the average specific flow of all blocks representing the tunnel. For a model with a heterogeneous flow medium and when the tunnel is at right angles to the regional flow, the specific flow in the tunnel will be very different at different sections, and the average specific flow will be strongly influenced by the blocks with the largest specific flow. This effect illustrates that the specific flow of the tunnel (average specific flow in the tunnel) does not represent the volume of water that visits the tunnel. However, the total flow represents the volume of water that visits the tunnel. The flow factor for total flow decreases with increasing tunnel length, as one might expect, but it decreases slowly. As regards the flow factor for average total flow (expected total flow), it decreases from 2.82 for a 50m long tunnel, to 2.79 for a 100m long tunnel and to 2.70 for a 200 m long tunnel. An non-linear extrapolation of the curve predicts that at a tunnel length of about 2000m, both models predict about the same flow in the tunnel (the flow factor is close to one).

We conclude, a heterogeneous rock mass will give a larger expected flow in a tunnel than a homogeneous rock mass, when both types of rock have the same effective conductivity. The difference in flow can be expressed as a flow factor (Equ.6.1); the flow factor decreases with increased tunnel length. For total flow, the decrease in flow factor, as the length of the tunnels is increased, is slower when the regional flow is directed at right angles to the tunnel than when it is directed along the tunnel.

At a tunnel length of about 700m-2000m, dependent on direction of the regional flow, the models predict about the same flow in a tunnel for both a homogeneous rock mass and a for a heterogeneous rock mass (the flow factor is close to one). This is in accordance with the scale dependency in conductivity, measured at Äspö and given in Figure 5.3. That figure indicates that at a scale of about 1000m-2000m, the standard deviation of the measured conductivity is zero. Thus, at such a scale, a model representing Äspö properties should predict the same flow in a tunnel, both with a heterogeneous flow medium and with a homogeneous flow medium.

6.7 Variation of specific flow inside a tunnel

In the previous sections we have discussed the expected average specific flow of a tunnel and the expected total flow of a tunnel, these properties correspond to the whole of the tunnel. In this section we will study the variation (distribution) of the flow inside a tunnel.

Inside a tunnel the flow will vary, depending on:

- The tunnel lay-out, e.g. length, size, filling etc.
- The direction of the regional flow.
- The heterogeneity of the surrounding rock mass.

For a large tunnel, the variation of the flow inside a tunnel is mainly dependent on the direction of the regional flow, in relation to the tunnel lay-out. Consider a tunnel more conductive than its surrounding, in the upstream part of the tunnel groundwater will

flow towards the tunnel from surrounding rock mass and into the tunnel. The flow inside the tunnel will increase and reach its maximum somewhere in the middle of the tunnel. In the downstream part of the tunnel the flow inside the tunnel will decrease and water will flow away from the tunnel. For all directions of regional flow, there will be an upstream and a downstream part. If the regional flow is directed at right angles to the tunnel, the upstream and downstream parts are opposite and parallel along the tunnel.

The variation of flow inside a tunnel in a homogeneous rock mass will be smooth and continuous. For a tunnel placed in a heterogeneous rock mass, the increase and decrease of flow, will be given by the total effect of all fractures that are connected to the tunnel, as well as by the nature of the tunnel. A tunnel, with or without filling, could be described as a continuous medium and if the tunnel is large, many fractures are connected to the tunnel. Therefore, the flow inside a tunnel, placed in a heterogeneous rock mass, will not be as heterogeneous as the flow of the surrounding rock mass; compared to the heterogeneous flow of the rock mass, the variation of the flow inside a tunnel is smooth and continuous.

Close to large connecting fracture zones it is likely that the flow in a tunnel is large, but not necessarily larger than at other sections of the tunnel, where few or no fractures connect to the tunnel. This follows from the condition of continuity of flow and because the tunnel, with or without filling, is a large structure that connects many fractures.

This is illustrated in Figure 6.20, the figure gives the variation of the specific flow inside tunnels of lengths 100m and 200m, for two different directions of the regional groundwater flow. In the models, the rock mass was defined as a homogeneous medium (uniform continuum) or as a heterogeneous medium (stochastic continuum). The flow inside a long curved tunnel (SFL 4), for different directions of the regional flow, is discussed in Sec.9.5 and demonstrated in Figures 9.12 and 9.13, as well as in Appendix D.

We have compared the variation of flow inside a tunnel of a homogeneous rock mass (uniform continuum), to the variation of flow obtained for possible realizations of a heterogeneous rock mass (stochastic continuum, Äspö properties); the comparison yields the following conclusions.

- The expected flow inside a tunnel is larger if the tunnel is in a heterogeneous rock mass than if the tunnel is in a homogeneous rock mass.
- Along a tunnel, the general trend of increase and decrease of flow inside the tunnel is the same for a tunnel in a homogeneous rock mass and for a tunnel in a heterogeneous rock mass. This is the variation produced by the direction of the regional flow.
- For a heterogeneous rock mass of Äspö properties and for tunnels that have a length of more than 150m (approximately), the absolute size of the flow variation inside a tunnel is mainly dependent on the direction of the regional flow and not so much dependent on the heterogeneity of the surrounding rock mass.
- The difference between the flow inside a tunnel in a homogeneous rock mass, and the flow inside a tunnel in a heterogeneous rock mass, can be expressed as a flow factor (Equ.6.1). For such relative differences, the largest effects of a heterogeneous rock mass takes place when the regional flow is directed at right angles to the tunnel. The increase in specific flow, at a section of a tunnel, can for such a scenario be large (>10 times), see Figure 6.19(i). The smallest effects occur if the regional flow is directed along the tunnel, see Figure 6.17(i)

6.8 Conclusions

In Chapter 6, we have simulated the flow of a closed tunnel, located in either a homogeneous flow medium or in a heterogeneous flow medium. The flow medium represents the fractured rock mass at Äspö Hard Rock Laboratory.

- *Methodology.* The effects of the heterogeneity of the rock mass were studied by use of the stochastic continuum approach (see Chapter 5). The results of the study are based on statistical analyses of many realizations of the conductivity field. In the following discussion, when we refer to the flow of a heterogeneous rock mass, we mean the average flow of many different realizations, - the most probable outcome, the expected flow. The general conclusions are valid for at least 70 percent of the realizations of a studied scenario. Hence, they are valid with a probability of at least 70 percent.

- *General change of size of flow in a tunnel.* Regardless of the conductivity of the tunnel filling, the expected flow in a tunnel will be larger if the tunnel is in a heterogeneous rock mass than if the tunnel is in a homogeneous rock mass, presuming that the regional flow is the same for both types of rock mass. If a tunnel is very permeable, the largest relative change in expected tunnel flow (when comparing a homogeneous rock mass to a heterogeneous rock mass) will take place if the regional flow is directed at right angles to the tunnel. If a tunnel has a low permeability, the largest relative change will take place if the regional flow is directed along the tunnel.

- *Effects of the direction of the regional flow.* Considering the flow in a tunnel, the variation in expected tunnel flow as regards the direction of the regional flow will be smaller if the rock mass is a heterogeneous medium than if it is a homogeneous medium. However, the general trends will be the same, both for a homogeneous rock mass and for a heterogeneous rock mass of Äspö type.

- *Effects of amount of heterogeneity.* By simulating different amounts of heterogeneity in the rock mass, different from the heterogeneity at Äspö, the following conclusion was obtained. The expected flow in a tunnel depends, among other parameters, on the amount of heterogeneity of the rock mass. The expected flow increases with increasing heterogeneity, presuming that the effective conductivity of the rock mass is constant. Studying how the expected flow in a tunnel increases with increasing rock mass heterogeneity, we see that the largest change in flow will occur at small amounts of heterogeneity.

- *Effects of length of tunnel.* The difference in expected flow between a tunnel in a homogeneous rock mass and that of a tunnel in a heterogeneous rock mass will decrease with increased tunnel length, assuming that the difference is expressed as a relative value (in percent of the flow of a tunnel in a homogeneous medium). The difference (percent) in expected total flow will diminish as the length of the tunnel is increased. If the regional flow is along the tunnel the difference is zero at a tunnel length of about 700m. If the regional flow is at right angles to the tunnel, the difference is zero at a tunnel length of about 2000m. Hence, for a rock mass of Äspö properties and at a tunnel length of about 700m-2000m, dependent on the direction of the regional flow, the models predict about the same total flow in the tunnels, both for a homogeneous flow medium and for a heterogeneous flow medium. This is in accordance with the scale dependency in conductivity, measured at Äspö HRL (see Chapter 5).

- *Example.* The expected total flow of a tunnel in a heterogeneous rock mass (stochastic continuum model) can be expressed in relation to the flow of a similar tunnel located in a homogeneous rock mass (uniform continuum model). For a 100m long tunnel having a cross-section of 10x10m, located in a heterogeneous rock mass with hydraulic properties similar to those at Äspö, the expected total flow in the tunnel will be:

- Case (i) 1.8 - 2.8 times larger than the flow of a tunnel in a homogeneous rock mass, dependent on direction of the regional flow, presuming that the tunnel has a large permeability.
- Case (ii) 1.2 - 5.5 times larger than the flow of a tunnel in a homogeneous rock mass, dependent on the direction of the regional flow, presuming that the tunnel has a very small permeability (the conductivity of the filling is 0.001 times the effective conductivity of the rock mass).

If the tunnel is longer, the factors will be smaller. If the tunnel is shorter, the factors will be larger. Note that the absolute size of the expected flow is about three to four orders of magnitude larger in Case (i) compared to Case (ii).

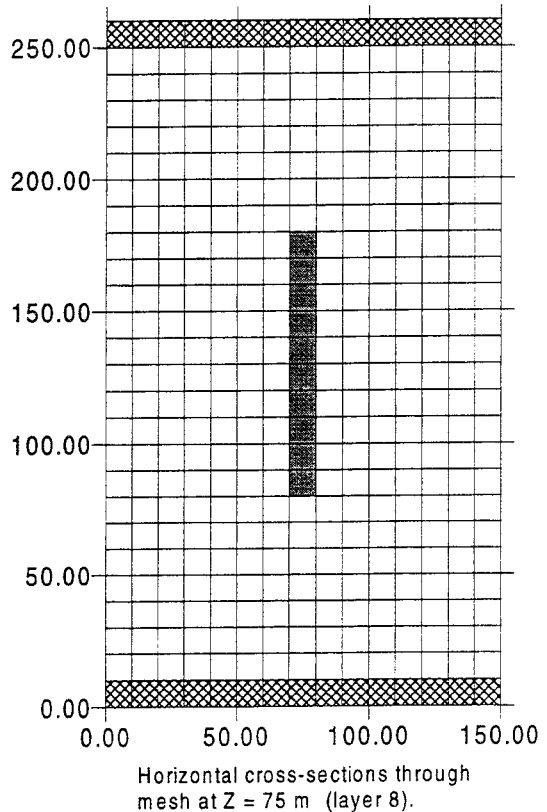
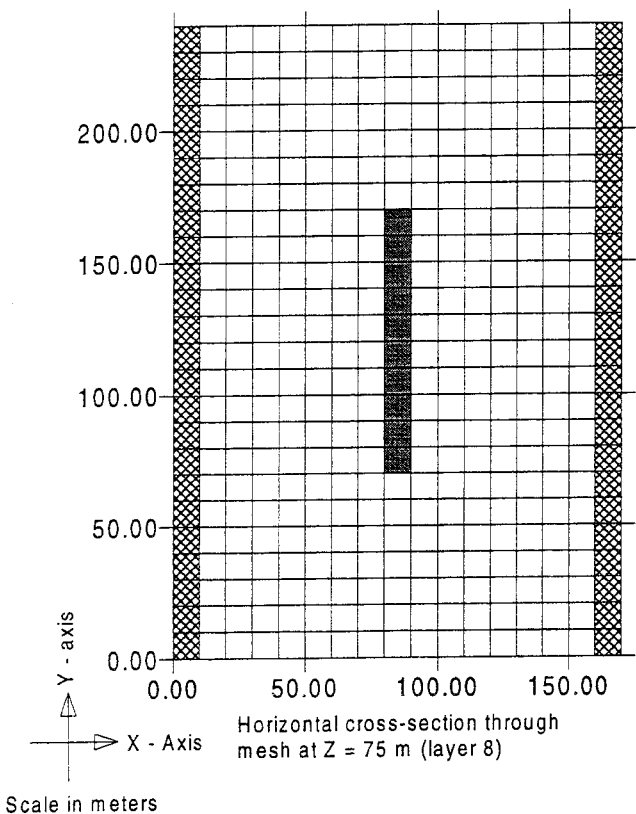
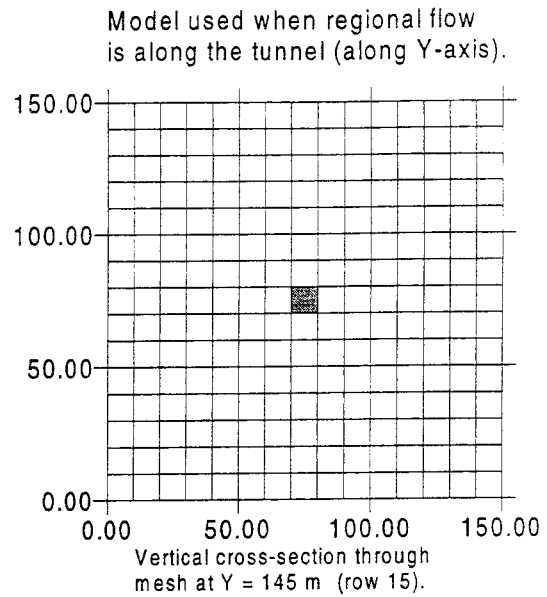
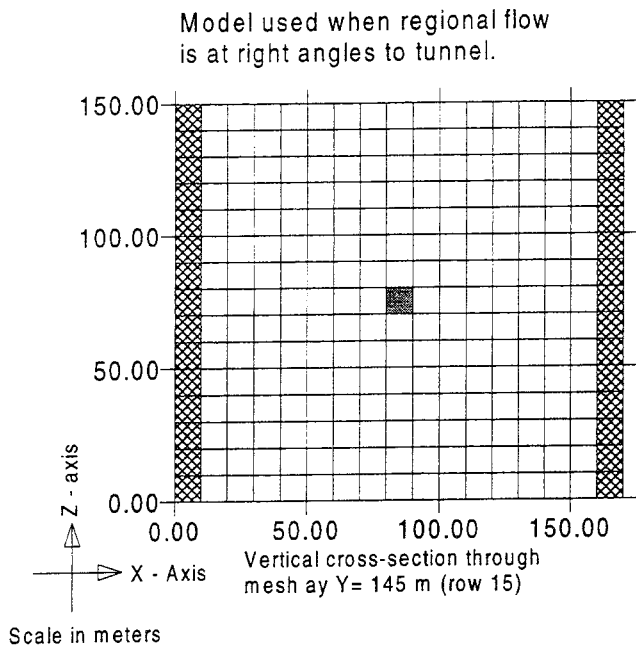
- *Case (i), a tunnel with a high permeability.* The reason why the expected tunnel flow is larger if the tunnel is in a heterogeneous rock mass than if the tunnel is in a homogeneous rock mass, is that most of the flow in a heterogeneous flow medium takes place in efficient pathways. The highly permeable tunnel will connect efficient pathways of the rock mass and increase the conductivity of the rock mass close to the tunnel. Many efficient pathways will include sections of the highly permeable tunnel.

- *Case (ii), a tunnel with a low permeability.* The reason why the expected tunnel flow is larger if the tunnel is in a heterogeneous rock mass than if the tunnel is in a homogeneous rock mass, is that most of the flow in a heterogeneous flow medium takes place in efficient pathways. If such a pathway is blocked by a tunnel of low permeability, there is no easy way around the tunnel, as the flow medium that surround the efficient pathway is also low permeable. Consequently, a large amount of the groundwater of a blocked efficient pathway will have to pass through the tunnel of low permeability, to reach an efficient pathway on the other side of the tunnel. The path through the tunnel is often the preferred path, as it has the smallest resistance, even if the tunnel has a low permeability. In a homogeneous rock mass most water avoids the tunnel and the main flow will be around the tunnel, but that is not always possible in a heterogeneous rock mass.

- *Variation of flow inside a tunnel.* The variation of flow inside a tunnel in a homogeneous rock mass will be smooth and continuous. For a tunnel placed in a heterogeneous rock mass, the increase and decrease of flow will be given by the total effect of all fractures that are connected to the tunnel, as well as by the nature of the tunnel. A tunnel, with or without filling, could be described as a continuous medium, and if the tunnel is large, many fractures are connected to the tunnel. Therefore, the flow inside a tunnel, placed in a heterogeneous rock mass, will not be as heterogeneous as the flow of the surrounding rock mass; compared to the heterogeneous flow of the rock mass, the variation of the flow inside a tunnel is smooth and continuous. Close to large connecting fracture zones it is likely that the flow in a tunnel is large, but not necessarily larger than at other sections of the tunnel, where few or no fractures connect to the tunnel. This follows from the condition of continuity of flow and because the tunnel, with or without filling, is a large structure that connects many fractures.

Table 6.1 ESTIMATION OF BOUNDARY EFFECTS, STOCHASTIC CONTINUUM.
 Estimation of boundary effects for meshes of different size and different systems studied.

		Properties of system studied		
Numerical method (1)		B2	B2	B2
Direction of Regional flow		Horizontal along tunnel	At right angles to tunnel	Horizontal along tunnel
Length of tunnel		100 m	100 m	100 m
Tunnel Conductivity		10 000 x K rock	10 000 x K rock	10 000 x K rock
Rock mass heterogeneity (2) STD of $\log K$ block		1.498	1.498	2
Block size		10x10x10 m	10x10x10 m	10x10x10 m
MESH	Distance to (3) boundary (m)	Error in predicted total flow [%] (4)		
M3	25	9.2	16.5	37.3
M4	35	4.4	8.6	14.3
M5	45	1.8	12.3	7.4
M6	55	0.7	6.9	4.3
M7	65	0.3	4.2	3.2
<p>(1) The different types of numerical methods for estimation of boundary effects are discussed in Chapter 4.</p> <p>(2) The heterogeneity of the rock mass is given by the standard deviation of the probability distribution that defines the block conductivity. The table gives the standard deviation of the logarithms of the conductivity values.</p> <p>(3) Minimum distance between tunnel and boundary of mesh.</p> <p>(4) The error in predicted total flow is based on the extrapolated total flow, set as the correct flow. The error is defined as: Error = ABS(100 - [(correct.total.flow) / (calc.total.flow / 100)])</p>				






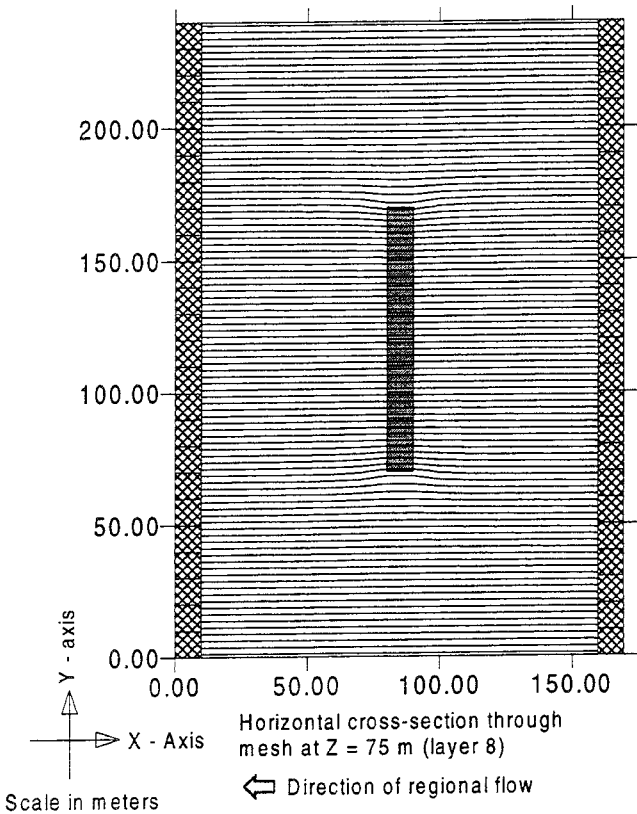
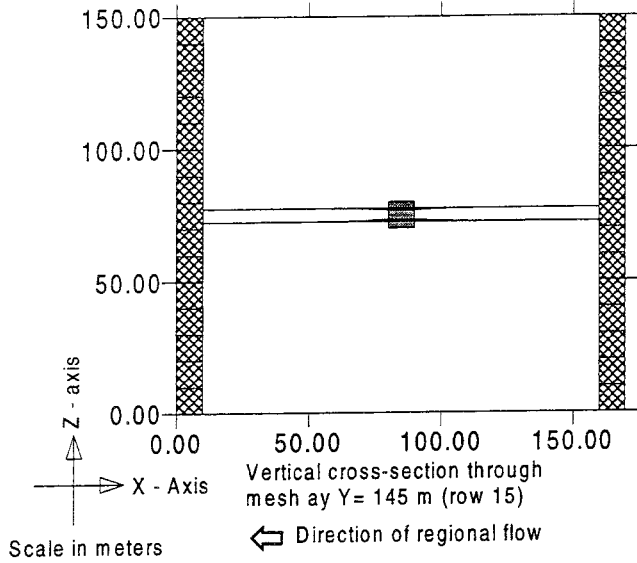
-  Cells (blocks) representing the rock mass.
-  Cells (blocks) representing the tunnel
-  Cells (blocks) representing the rock mass. These cells have a prescribed head boundary condition.

FIGURE 6.1
MODEL OF TUNNEL AND ROCK MASS.
 Example of mesh, horizontal and vertical cross-sections.
 Minimum distance between tunnel and boundary is represented by seven cells (blocks).
 Rock mass, block size: 10x10x10m.
 Tunnel block size: 10x10x10m, length: 100m.

UNIFORM CONTINUUM

Scenario (i)

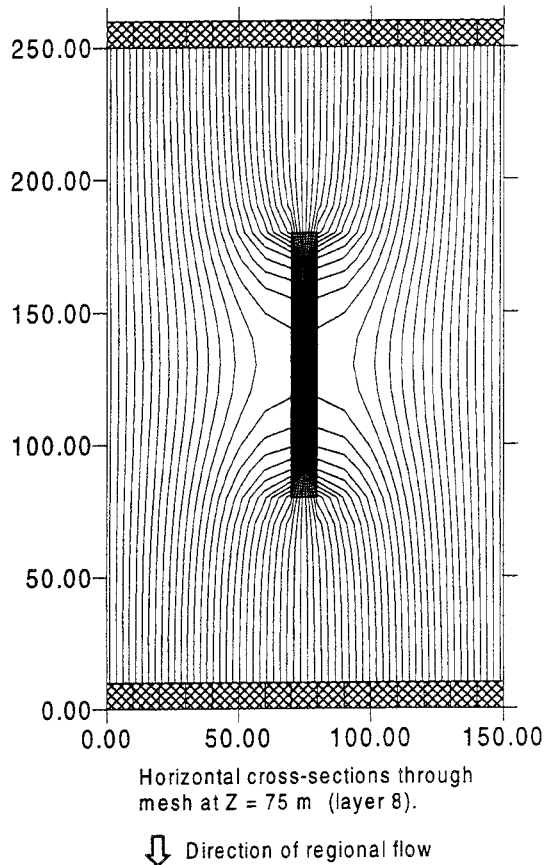
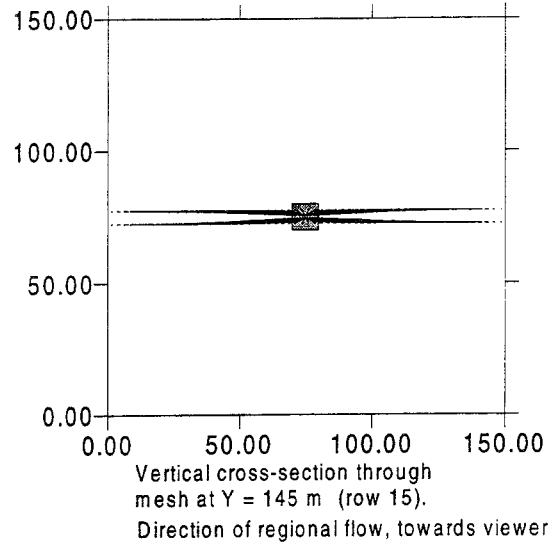
The regional flow is at right angles to the tunnel (along the X-axis).






UNIFORM CONTINUUM

Scenario (ii)

The regional flow is along the tunnel (along the Y-axis).



-  The rock mass.
-  The tunnel. Block 10x10x10m. $K_{\text{tunnel}} = 10000 \times K_{\text{rock}}$
-  Prescribed head boundary condition.

— Flowpath

FIGURE 6.2 FLOW PATTERN IN ROCK MASS AND TUNNEL, UNIFORM CONTINUUM.

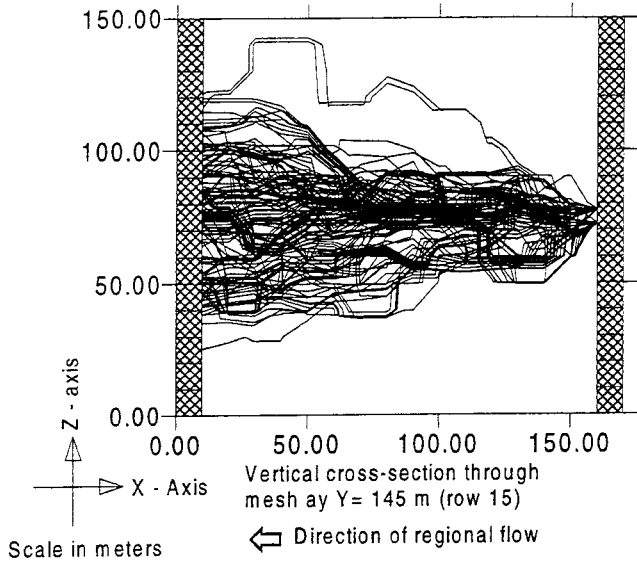
The flowpaths represent the groundwater flow, they are released along two sections at the boundary. The larger the number of flowpaths, the larger the flow. The flowpaths are plotted in their full length, they are not bound to a specific layer or section.

The conductivity of the tunnel is 10000 times the effective conductivity of the rock mass.

STOCHASTIC CONTINUUM

Scenario (i)

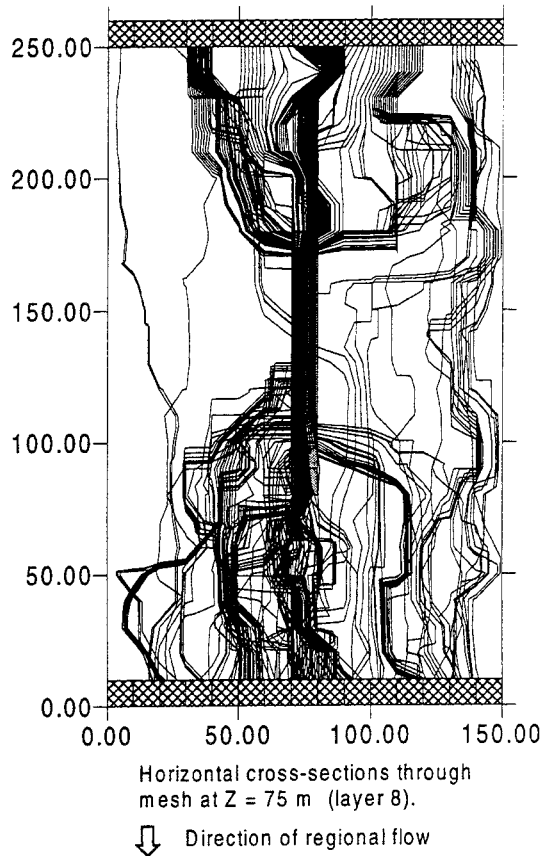
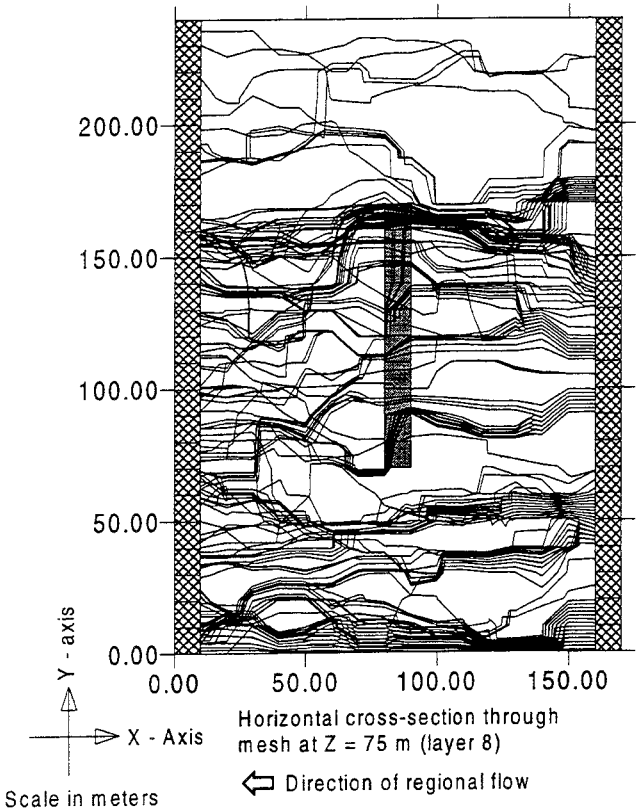
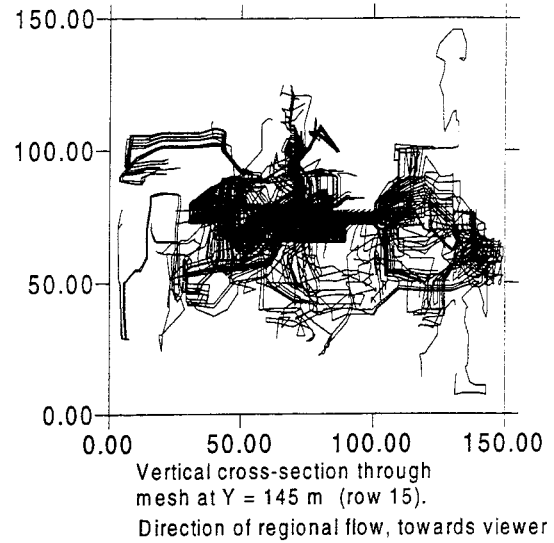
The regional flow is at right angles to the tunnel (along the X-axis).



STOCHASTIC CONTINUUM

Scenario (ii)

The regional flow is along the tunnel (along the Y-axis).







-  The rock. Block 10x10x10m
STD of 10Log Kblock = 1.5
-  The tunnel. Block 10x10x10m
Ktunnel = 10000 x Krock
-  Prescribed head boundary condition.
-  Flowpath

FIGURE 6.3 FLOW PATTERN IN ROCK MASS AND TUNNEL, STOCHASTIC CONTINUUM.

An example of a possible flow pattern in a heterogeneous rock mass surrounding a tunnel with a large permeability.

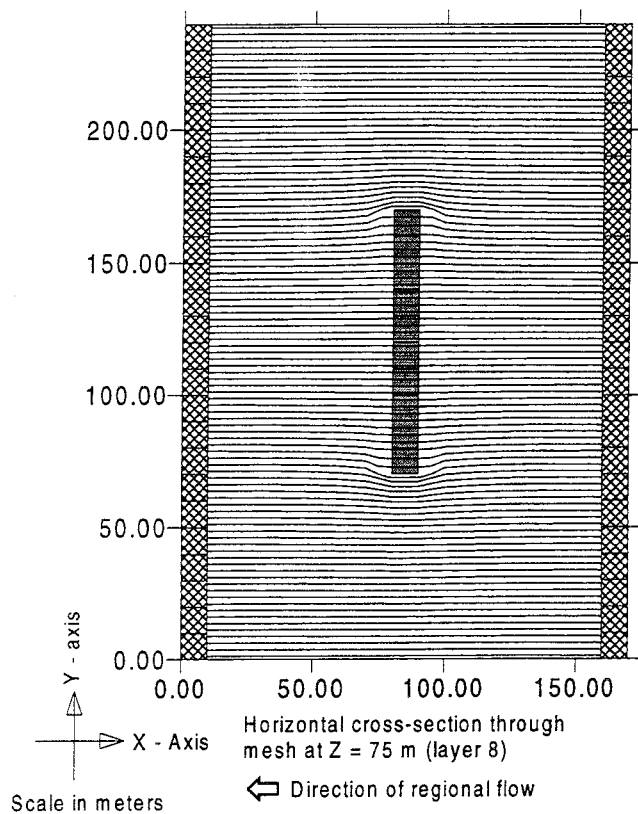
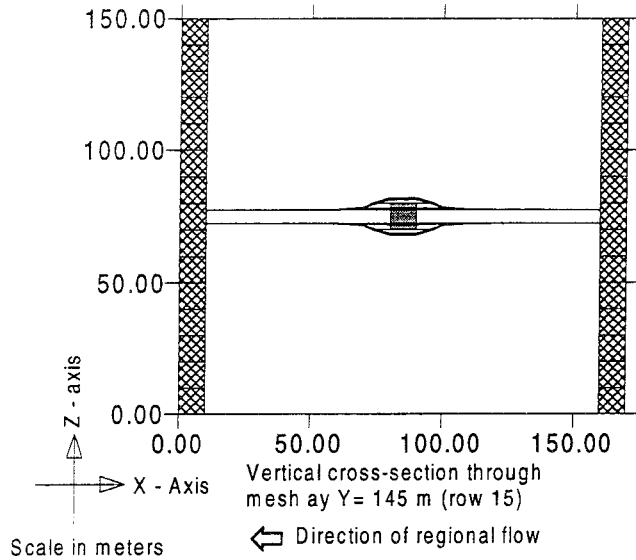
The flowpaths represent the groundwater flow, they are released along two sections at the boundary. The larger the number of flowpaths, the larger the flow. The flowpaths are plotted in their full length, they are not bound to a specific layer or section.

The conductivity of the tunnel is 10000 times the effective conductivity of the rock mass. The rock mass is defined as a heterogeneous medium. The conductivity field of the rock mass was the same in all scenarios of this figure, the same conductivity field was also used in Figure 6.5.

UNIFORM CONTINUUM

Scenario (i)

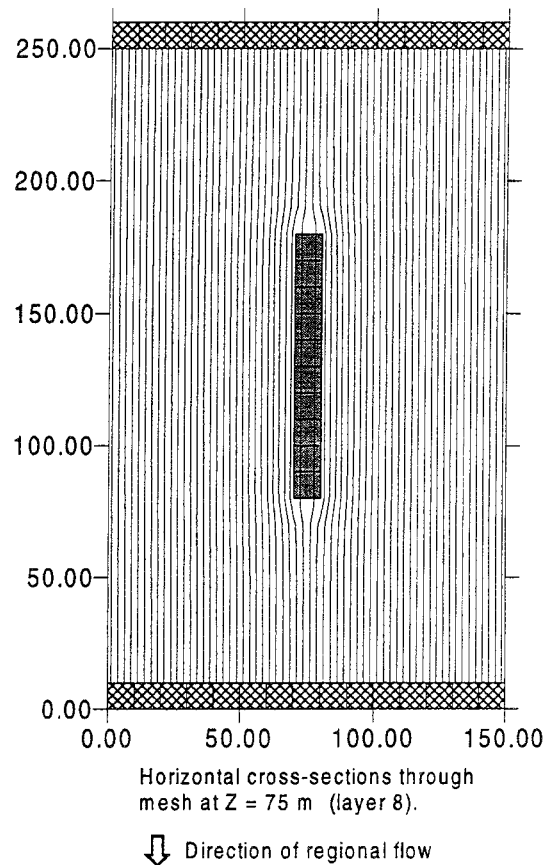
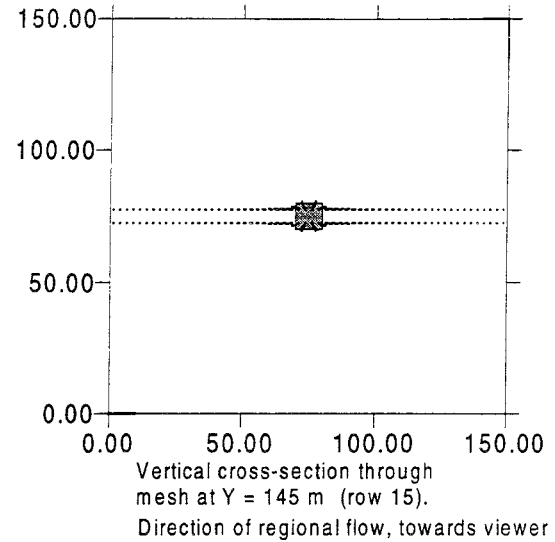
The regional flow is at right angles to the tunnel (along the X-axis)



UNIFORM CONTINUUM

Scenario (ii)

The regional flow is along the tunnel (along Y-axis).







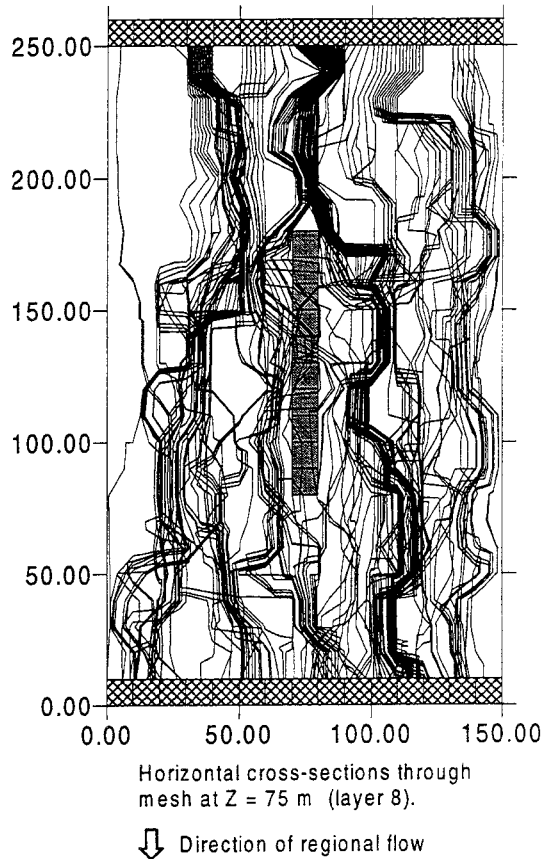
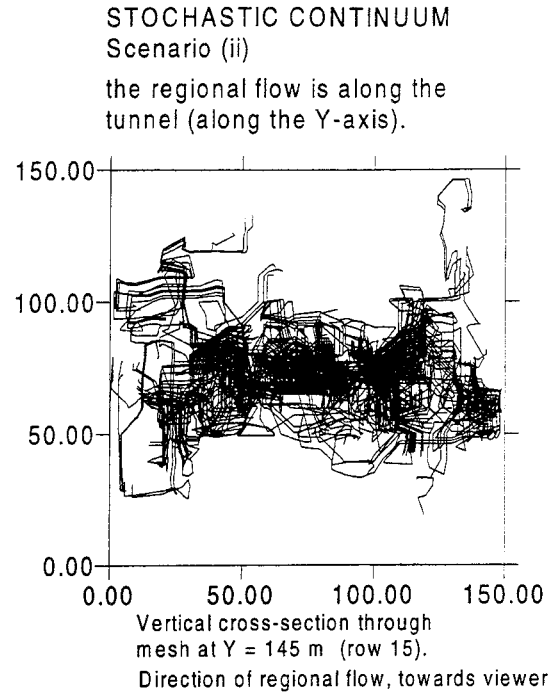
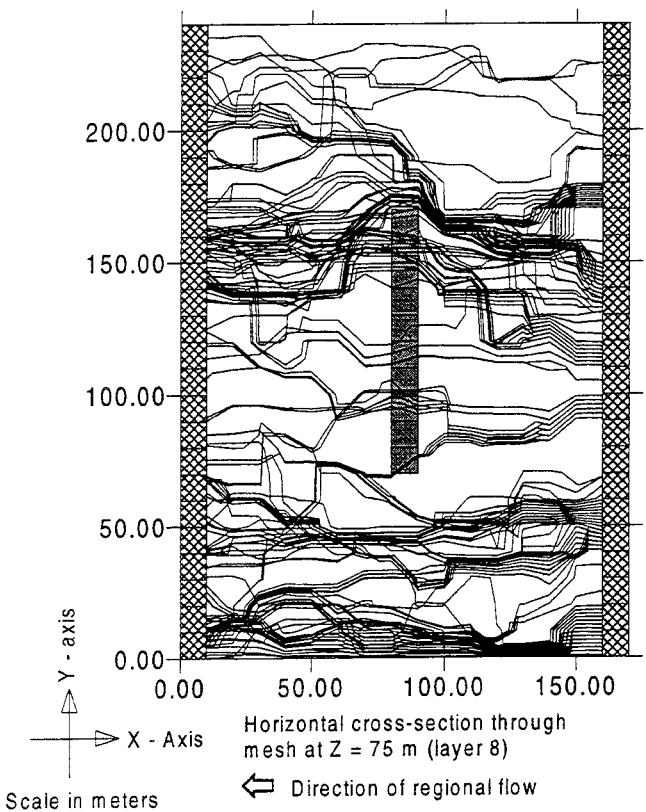
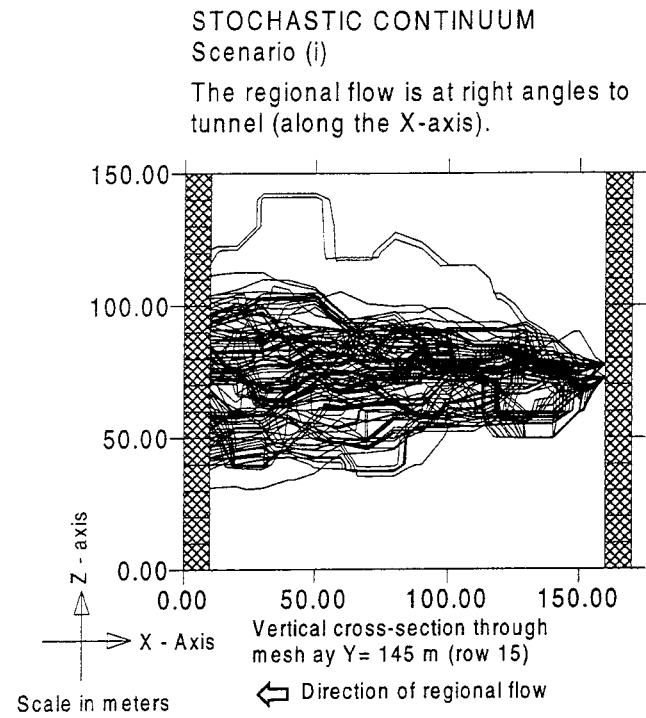
-  The rock mass.
-  The tunnel. Block 10x10x10m.
 $K_{\text{tunnel}} = 0.001 \times K_{\text{rock}}$
-  Prescribed head boundary condition.
-  Flowpath

FIGURE 6.4 FLOW PATTERN IN ROCK MASS AND TUNNEL, UNIFORM CONTINUUM.

The flowpaths represent the groundwater flow, they are released along two sections at the boundary. The larger the number of flowpaths, the larger the flow. The flowpaths are plotted in their full length, they are not bound to a specific layer or section. The conductivity of the tunnel is 0.001 times the effective conductivity of the rock mass.







-  The rock. Block 10x10x10m
STD of 10Log K_{block}= 1.5
-  The tunnel. Block 10x10x10m
K_{tunnel} = 0.001 x K_{rock}
-  Prescribed head boundary condition.
-  Flowpath

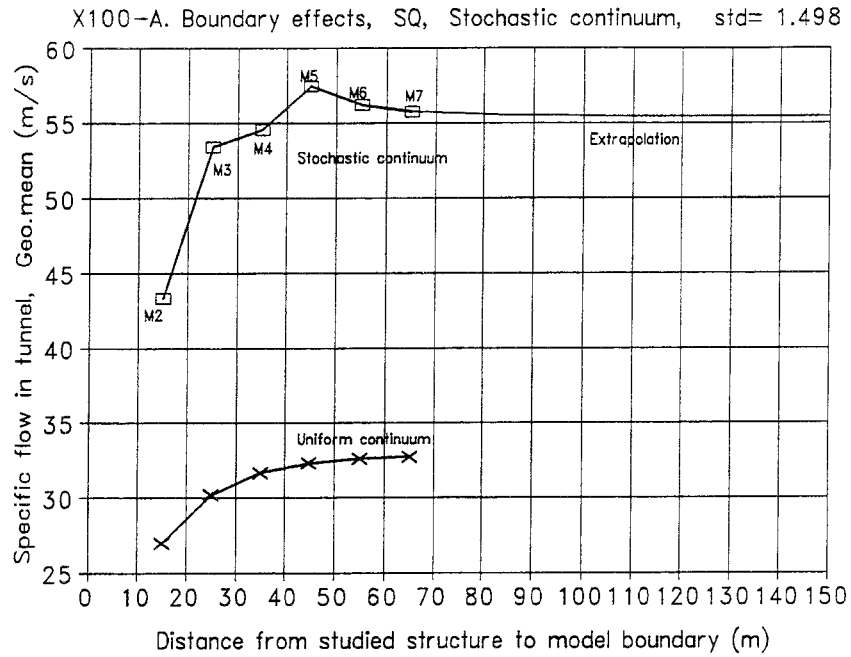
FIGURE 6.5 FLOW PATTERN IN ROCK MASS AND TUNNEL, STOCHASTIC CONTINUUM.

An example of a possible flow pattern in a heterogeneous rock mass surrounding a tunnel with a small permeability.

The flowpaths represent the groundwater flow, they are released along two sections at the boundary. The larger the number of flowpaths, the larger the flow. The flowpaths are plotted in their full length, they are not bound to a specific layer or section.

The conductivity of the tunnel is 0.001 times the effective conductivity of the rock mass. The rock mass is defined as a heterogeneous medium. The conductivity field of the rock mass was the same in all scenarios of this figure, the same conductivity field was also used in Figure 6.3.

(i)
Size of specific
flow in a
tunnel versus
size of mesh.



(ii)
Size of total
flow in a
tunnel versus
size of mesh.

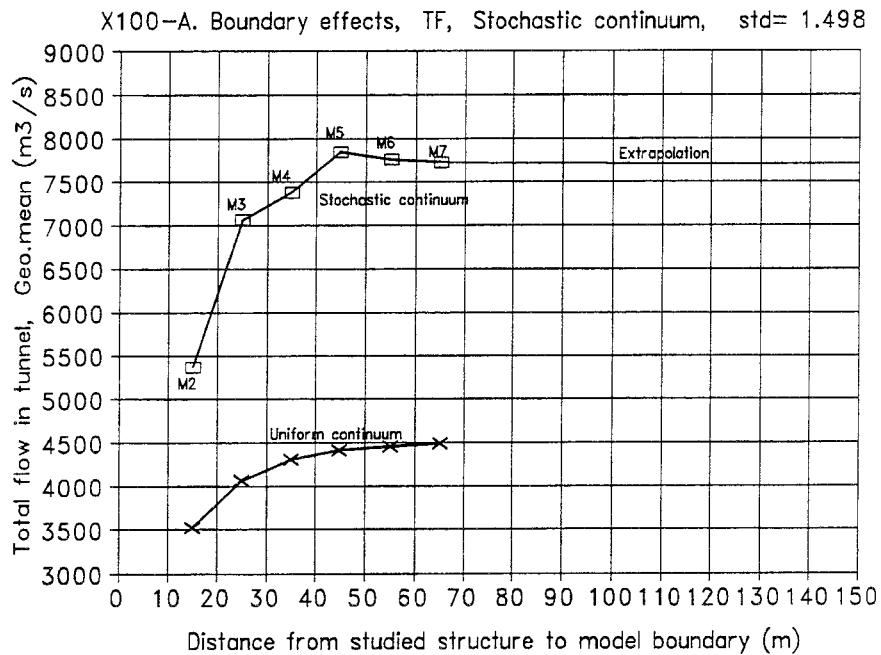
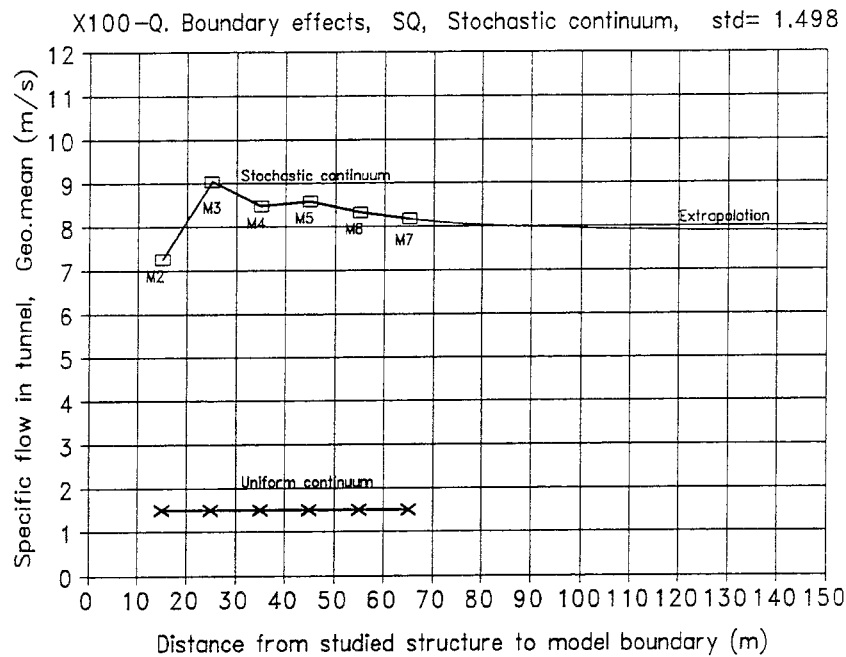


Figure 6.6 BOUNDARY EFFECTS, METHOD OF MULTIPLE MESHES, STOCH.CONT. THE REGIONAL FLOW IS ALONG THE TUNNEL. Geometric mean of calculated specific flow (i) and total flow (ii), representing the flow in a tunnel, versus size of finite difference mesh. M1 - M7 denotes different meshes. The rock mass is represented by a stochastic continuum or a uniform continuum. The tunnel has a rectangular cross-section of 100 m², length 100 m and a K value which is 10000 times the effective conductivity of the rock mass. Block size in model is 10x10x10 m. In the stochastic continuum model, block conductivity is Log-normal distributed, standard deviation of 10Log K is 1.498. Size of regional specific flow is 1 m/s.

(i)
Size of specific
flow in a
tunnel versus
size of mesh.



(ii)
Size of total
flow in a
tunnel versus
size of mesh.

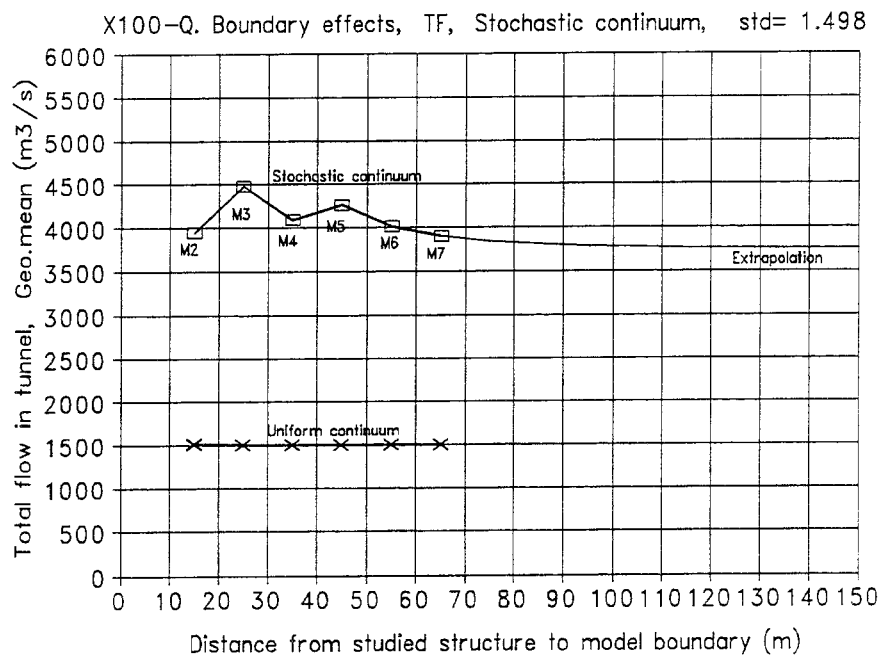
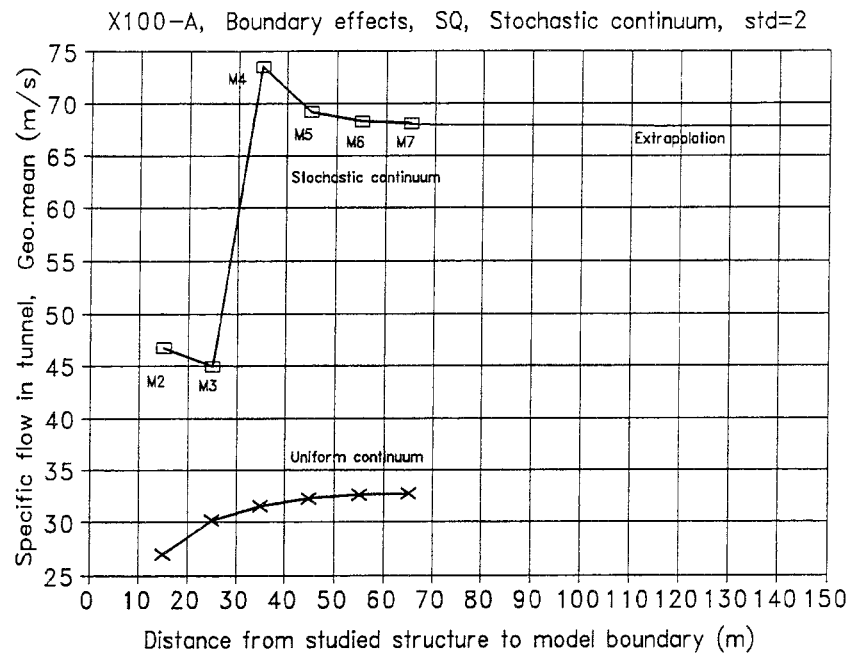


Figure 6.7 BOUNDARY EFFECTS, METHOD OF MULTIPLE MESHES, STOCH.CONT. THE REGIONAL FLOW IS AT RIGHT ANGLES TO THE TUNNEL. Geometric mean of calculated specific flow (i) and total flow (ii), representing the flow in a tunnel, versus size of finite difference mesh. M1 - M7 denotes different meshes. The rock mass is represented by a stochastic continuum or a uniform continuum. The tunnel has a rectangular cross-section of 100 m^2 , length 100 m and a K value which is 10000 times the effective conductivity of the rock mass. Block size in model is $10 \times 10 \times 10 \text{ m}$. In the stochastic continuum model, block conductivity is Log-normal distributed, standard deviation of $10 \text{Log } K$ is 1.498 . Size of regional specific flow is 1 m/s .

(i)
Size of specific
flow in a
tunnel versus
size of mesh.



(ii)
Size of total
flow in a
tunnel versus
size of mesh.

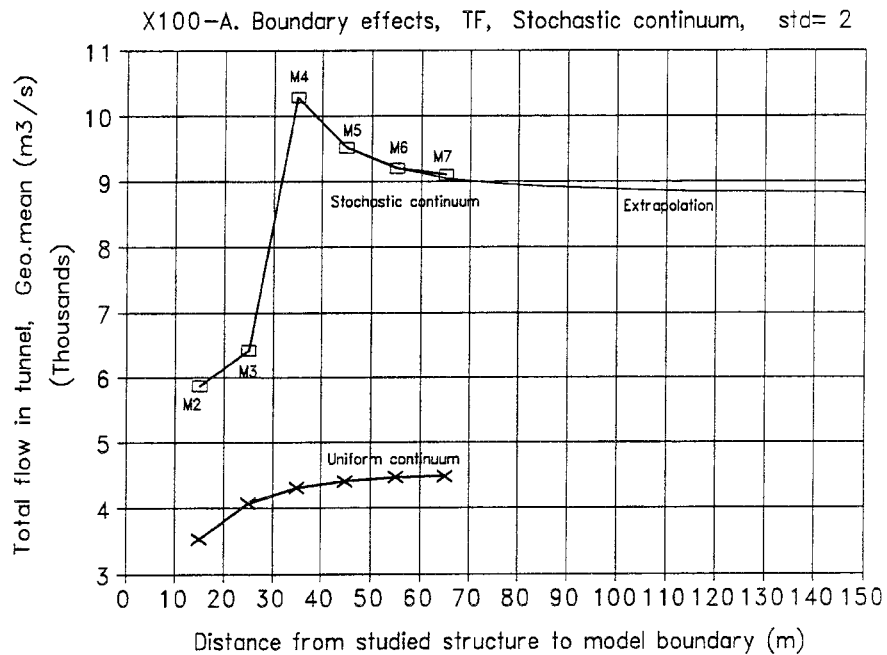
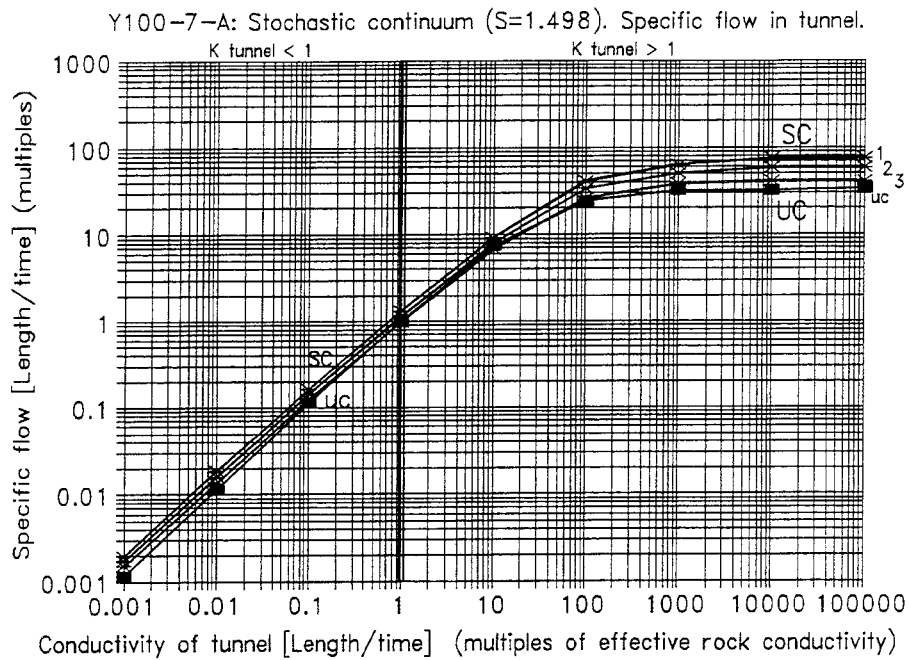


Figure 6.8 BOUNDARY EFFECTS, METHOD OF MULTIPLE MESHES, STOCH.CONT. THE REGIONAL FLOW IS ALONG THE TUNNEL. Geometric mean of calculated specific flow (i) and total flow (ii), representing the flow in a tunnel, versus size of finite difference mesh. M1 - M7 denotes different meshes. The rock mass is represented by a stochastic continuum or a uniform continuum. The tunnel has a rectangular cross-section of 100 m², length 100 m and a K value which is 10000 times the effective conductivity of the rock mass. Block size in model is 10x10x10 m. In the stochastic continuum model, block conductivity is Log-normal distributed, standard deviation of 10Log K is 2. Size of regional specific flow is 1 m/s.

(i)
 Specific flow
 in tunnel.
 Tunnel data
 Length =100m
 Cross-S=100m²



(ii)
 Total flow
 in tunnel.
 Tunnel data
 Length =100m
 Cross-S=100m²

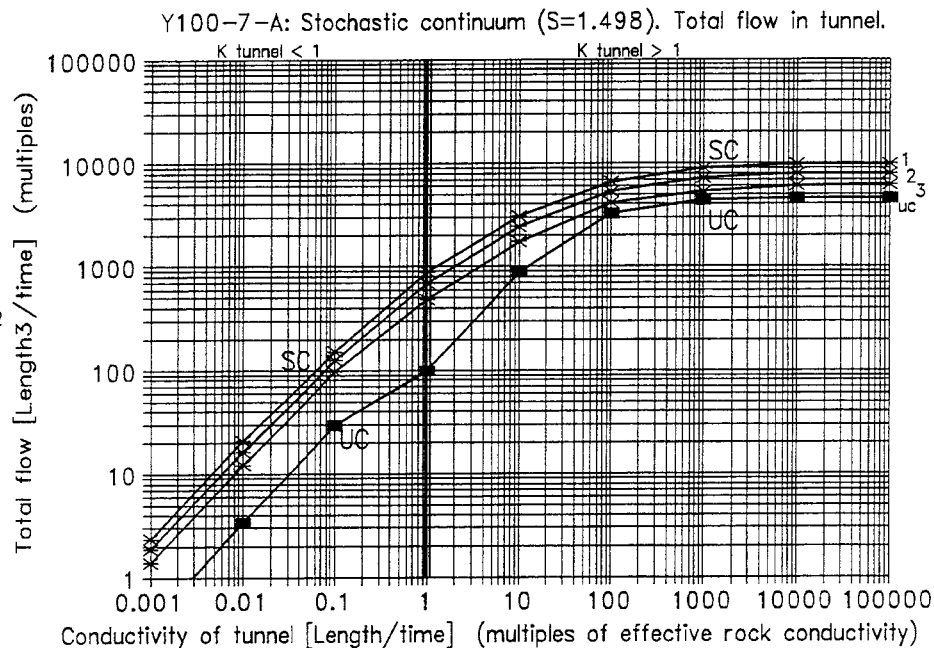


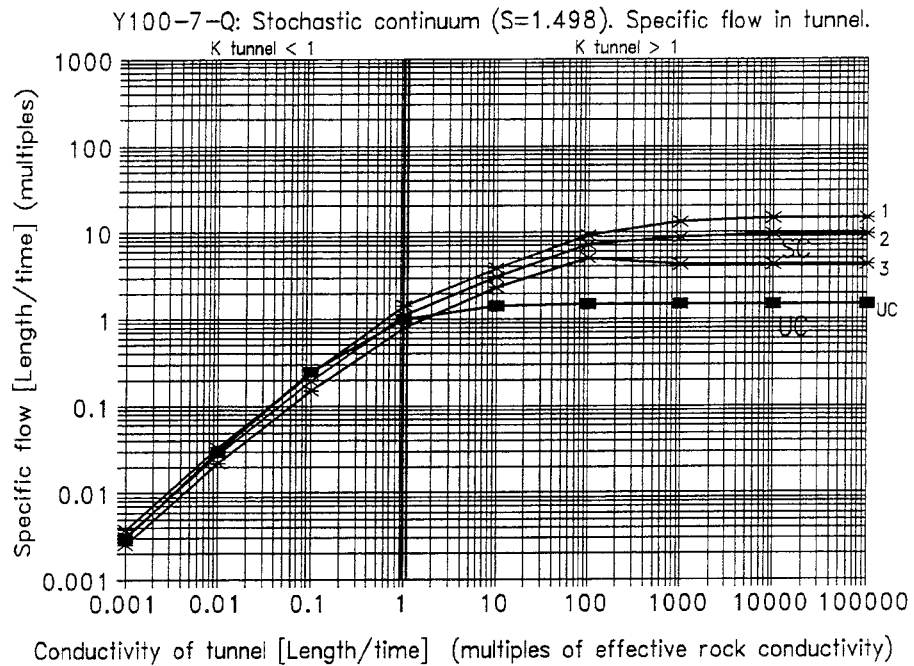
Figure 6.9

FLOW IN A TUNNEL, SENSITIVITY TO TUNNEL CONDUCTIVITY (Y10a), THE REGIONAL FLOW IS ALONG THE TUNNEL.

Specific flow (i) and Total flow (ii) in a 100 m long tunnel, versus the conductivity of the tunnel. The rock mass is defined as, homogeneous - uniform continuum model, or as heterogeneous - stochastic continuum model with properties representing Äspö (block size 10x10x10m, block K dist: STD 10Log K= 1.498). The flow in the tunnel is given as multiples of an unknown regional flow.

- Stochastic continuum SC, is denoted by stars: (1) average flow plus one standard deviation, (2) average flow and (3) average flow minus one standard deviation.
- Uniform continuum UC, is denoted by filled squares.

(i)
Specific flow
in tunnel.
Tunnel data
Length = 100m
Cross-S = 100m²



(ii)
Total flow
in tunnel.
Tunnel data
Length = 100m
Cross-S = 100m²

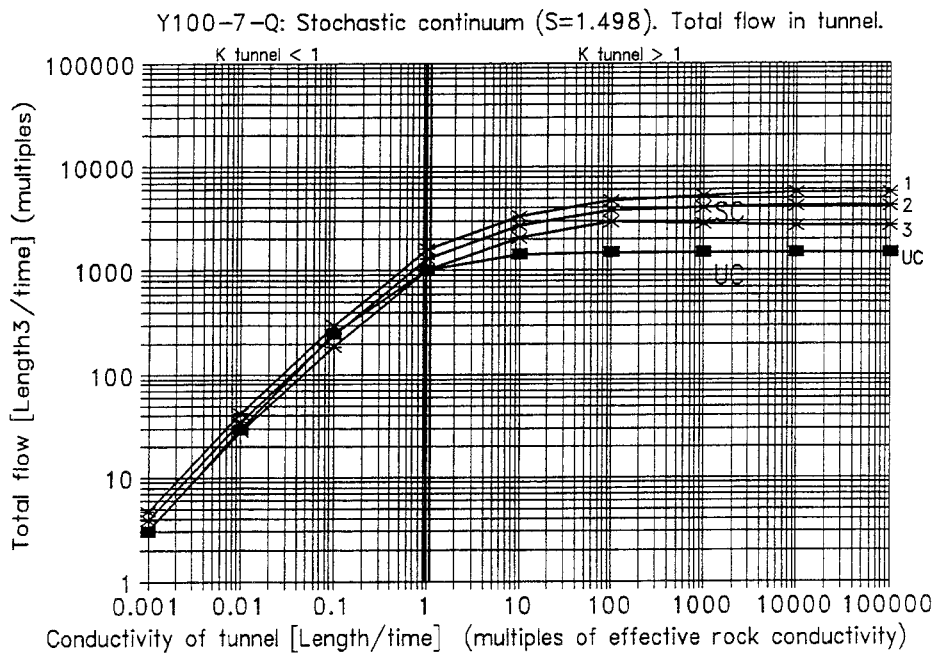


Figure 6.10

FLOW IN A TUNNEL, SENSITIVITY TO TUNNEL CONDUCTIVITY (Y10q), THE REGIONAL FLOW IS AT RIGHT ANGLES TO THE TUNNEL. Specific flow (i) and Total flow (ii) in a 100 m long tunnel, versus the conductivity of the tunnel. The rock mass is defined as, homogeneous - uniform continuum model, or as heterogeneous - stochastic continuum model with properties representing Äspö (block size 10x10x10m, block K dist: STD 10Log K= 1.498). The flow in the tunnel is given as multiples of an unknown regional flow.

- Stochastic continuum SC, is denoted by stars: (1) average flow plus one standard deviation, (2) average flow and (3) average flow minus one standard deviation.
- Uniform continuum UC, is denoted by filled squares.

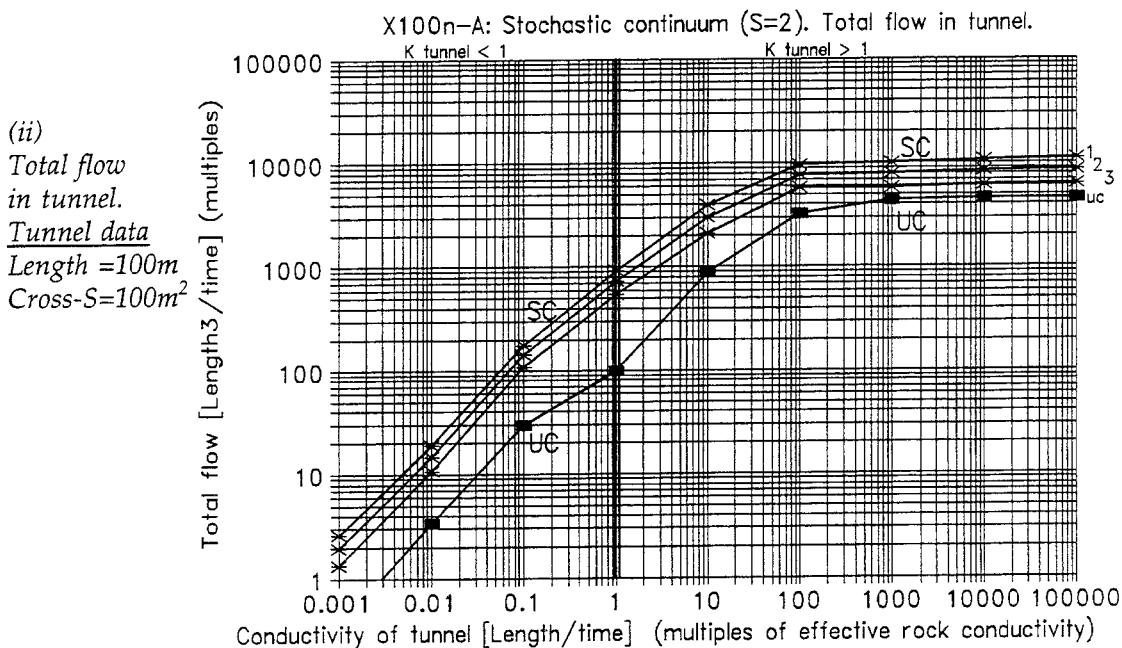
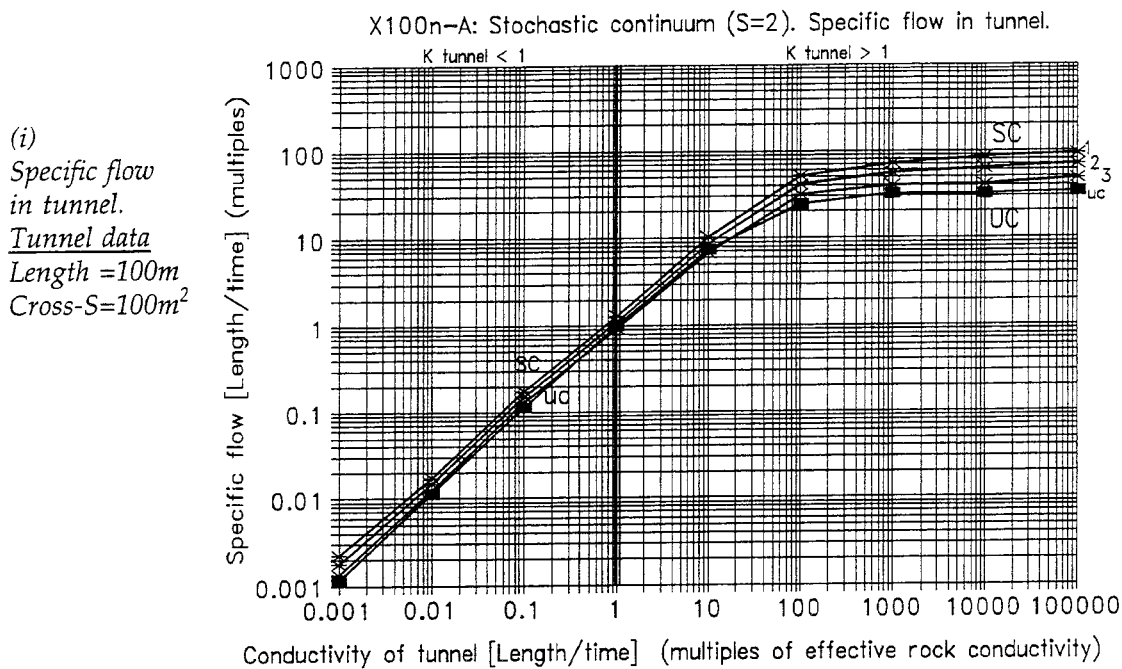
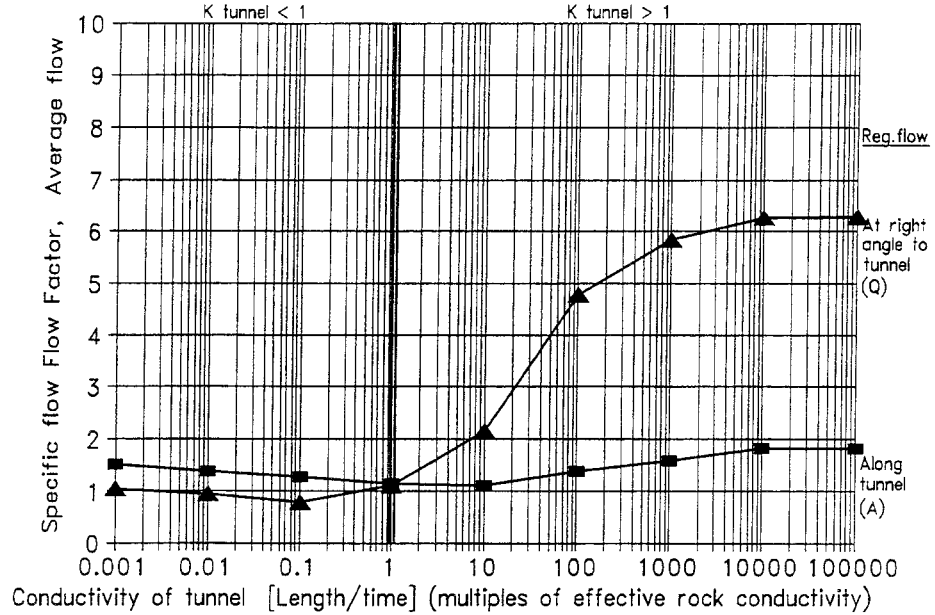


Figure 6.11 FLOW IN A TUNNEL, SENSITIVITY TO TUNNEL CONDUCTIVITY (X10a), THE REGIONAL FLOW IS ALONG THE TUNNEL.
Specific flow (i) and Total flow (ii) in a 100 m long tunnel, versus the conductivity of the tunnel. The rock mass is defined as, homogeneous - uniform continuum model, or as heterogeneous - stochastic continuum model with properties more heterogeneous than at Äspö (block: size 10x10x10m, K dist: STD 10Log K= 2). The flow in the tunnel is given as multiples of an unknown regional flow.

- Stochastic continuum SC, is denoted by stars: (1) average flow plus one standard deviation, (2) average flow and (3) average flow minus one standard deviation.
- Uniform continuum UC, is denoted by filled squares.

Y100-7-A-Q: Specific flow factor of a tunnel, (L=100m, A=100m², S=1.498)

(i)
Specific flow factor of a tunnel:
Tunnel data
Length =100m
Cross-S=100m²



Y100-7-A-Q: Total flow factor of a tunnel (L=100m, A=100m², S=1.498)

(ii)
Total flow factor of a tunnel:
Tunnel data
Length =100m
Cross-S=100m²

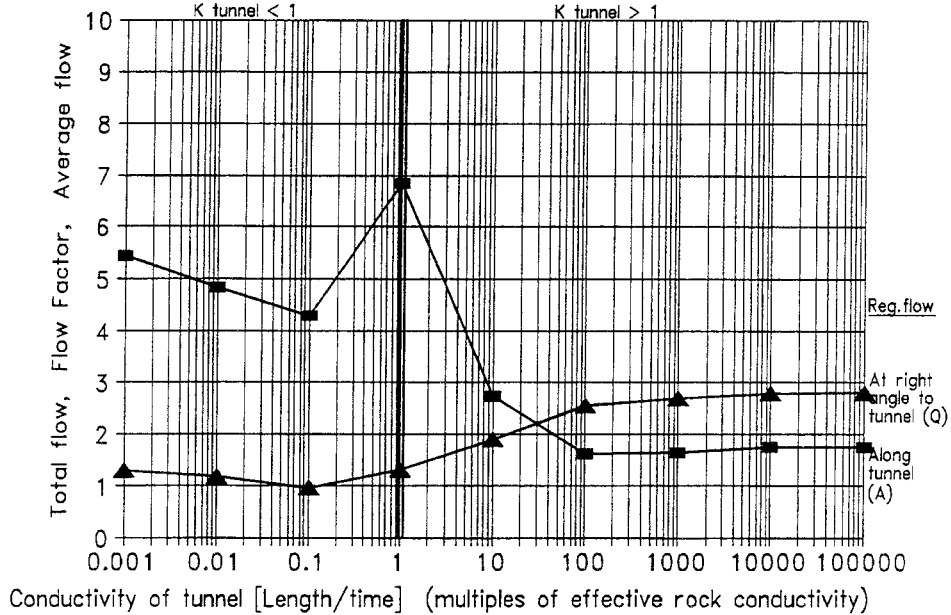
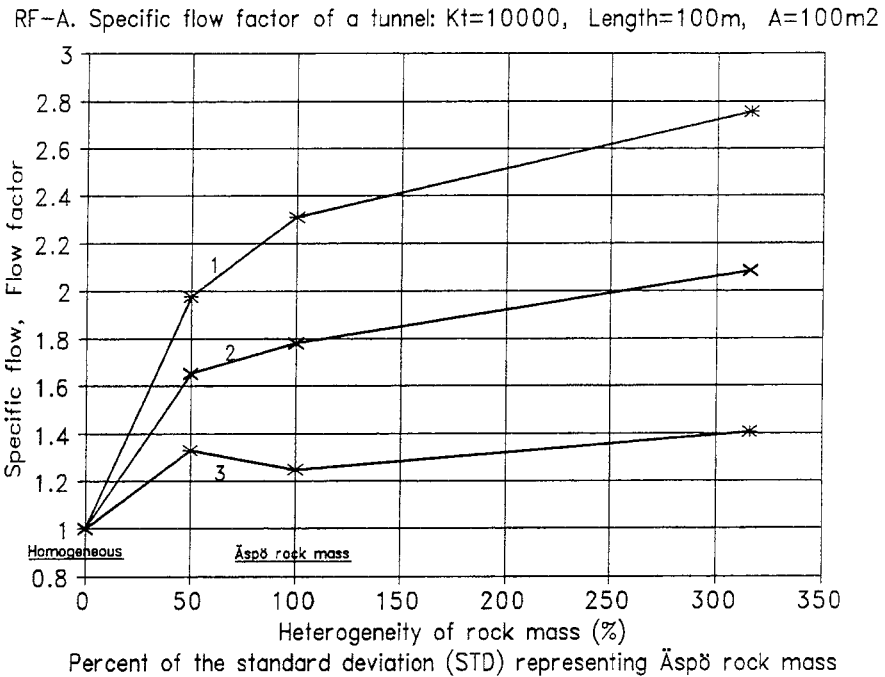


Figure 6.12 FLOW IN A TUNNEL, SENSITIVITY TO TUNNEL COND., FLOW FACTOR. Specific flow factor (i) and Total flow factor (ii) for a 100m long tunnel, versus the conductivity of the tunnel. Homogeneous flow medium - uniform continuum model. Heterogeneous flow medium - stochastic continuum model with properties representing Äspö (block: 10x10x10m, K dist STD 10Log K=1.498). The flow factor given in the figure, corresponds to average flow, average as regards the flow of different realizations. Flow factor = $Flow_{Stochastic} / Flow_{Uniform}$. Figure (i) gives the flow factor as regards specific flow, Figure(ii) the flow factor as regards total flow.

- Regional flow along tunnel is denoted by squares.
- Regional flow at right angles to tunnel is denoted by triangles

(i)
Specific flow factor of a tunnel.
Tunnel data
Length =100m
Cross-S=100m²
Conductivity:
10000 times effective rock conductivity



(ii)
Total flow factor of a tunnel.
Tunnel data
Length =100m
Cross-S=100m²
Conductivity:
10000 times effective rock conductivity

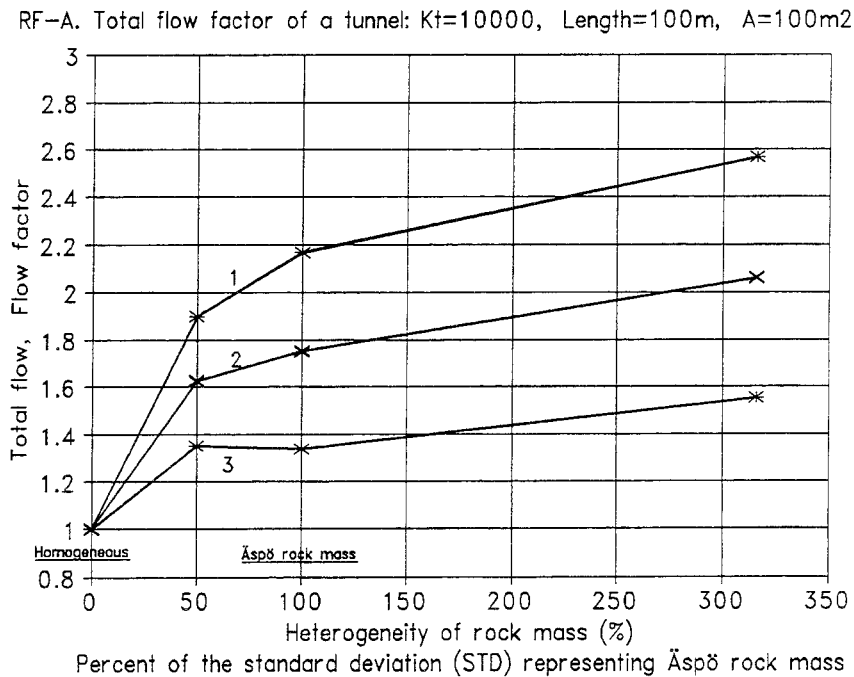


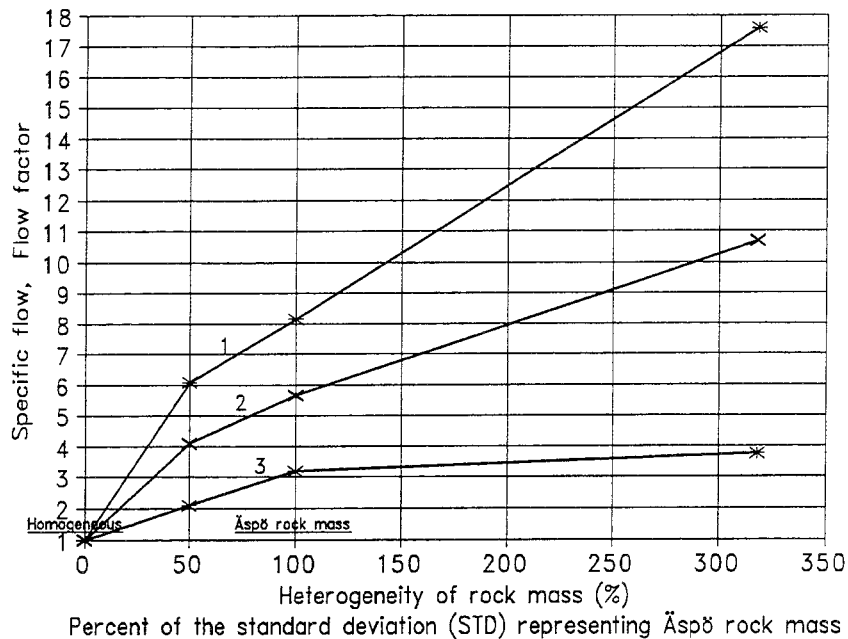
Figure 6.13 FLOW IN A TUNNEL, ROCK MASS HETEROGENEITY, FLOW FACTOR. THE REGIONAL FLOW IS ALONG THE TUNNEL.

Specific flow factor (i) and Total flow factor (ii) for a 100 m long tunnel, versus the heterogeneity of the rock mass. The heterogeneity is defined in relation to the heterogeneity at Äspö, based on the standard deviation (STD) of the block conductivity distribution. The properties representing Äspö (Block: size 10x10x10m, $STD \log K = 1.498$) are defined as a heterogeneity of 100 percent.

- (1) Flow factor representing average flow plus one standard deviation
- (2) Flow factor representing average flow, average as regards different realizations.
- (3) Flow factor representing average flow minus one standard deviation.

(i)
 Specific flow factor of a tunnel.
 Tunnel data
 Length = 100m
 Cross-S = 100m²
 Conductivity: 10000 times effective rock conductivity

RF-Q. Specific flow factor of a tunnel: $Kt=10000$, Length=100m, $A=100m^2$



(ii)
 Total flow factor of a tunnel.
 Tunnel data
 Length = 100m
 Cross-S = 100m²
 Conductivity: 10000 times effective rock conductivity

RF-Q. Total flow factor of a tunnel: $Kt=10000$, Length=100m, $A=100m^2$

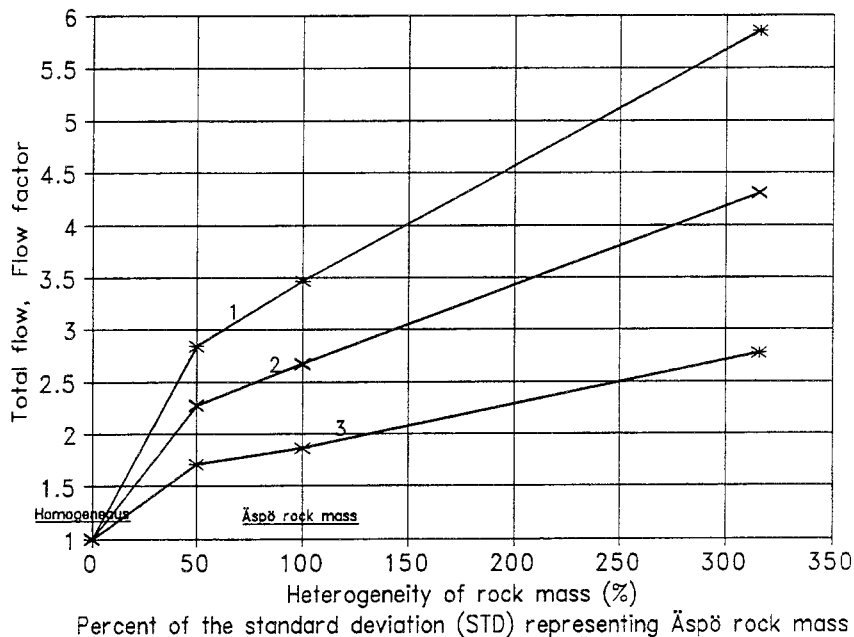


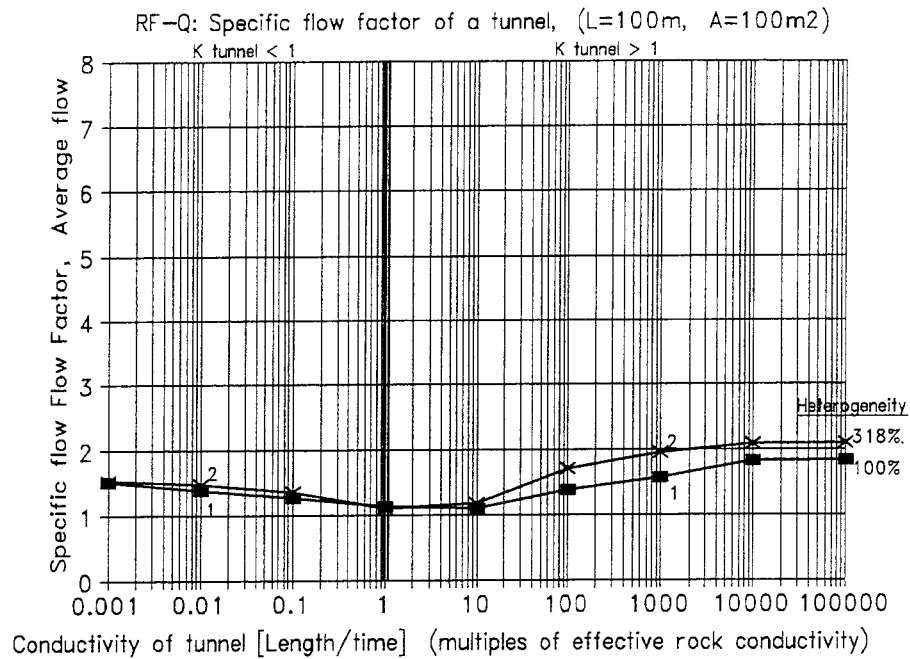
Figure 6.14

FLOW IN A TUNNEL, SENSITIVITY TO ROCK MASS HETEROGENEITY. THE REGIONAL FLOW IS AT RIGHT ANGLES TO THE TUNNEL.

Specific flow factor (i) and Total flow factor (ii) for a 100 m long tunnel, versus the heterogeneity of the rock mass. The heterogeneity is defined in relation to the heterogeneity at Äspö, based on the standard deviation (STD) of the block conductivity distribution. The properties representing Äspö (Block: size 10x10x10m, STD $10\log K = 1.498$) are defined as a heterogeneity of 100 percent.

- (1) Flow factor representing average flow plus one standard deviation
- (2) Flow factor representing average flow, average as regards different realizations.
- (3) Flow factor representing average flow minus one standard deviation.

(i)
Specific flow factor of a tunnel.
Tunnel data
Length =100m
Cross-S=100m²



(ii)
Total flow factor of a tunnel.
Tunnel data
Length =100m
Cross-S=100m²

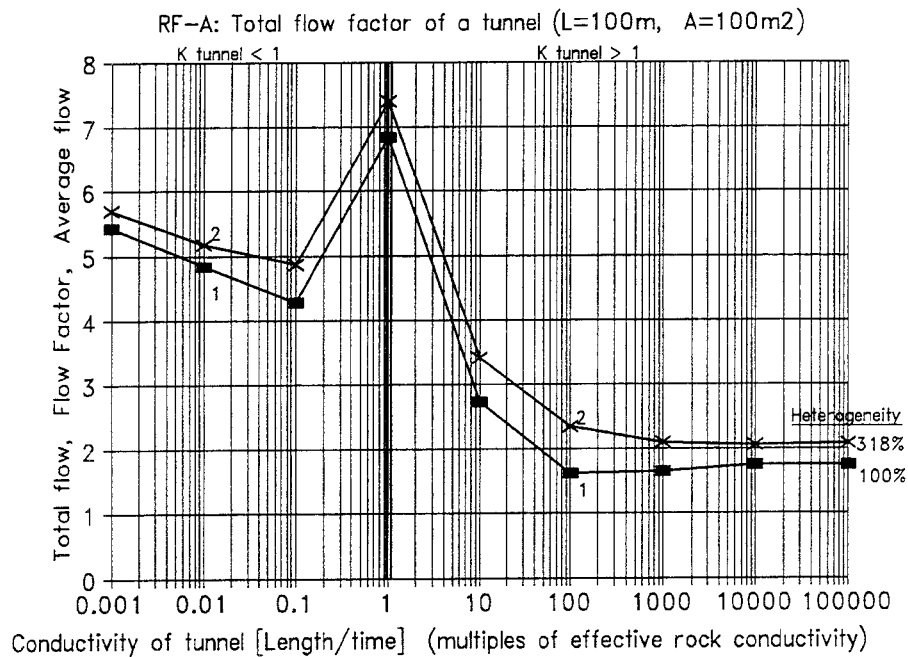


Figure 6.15 FLOW IN A TUNNEL, SENSITIVITY TO ROCK MASS HETEROGENEITY. THE REGIONAL FLOW IS DIRECTED ALONG THE TUNNEL. Specific flow factor (i) and Total flow factor (ii) in a 100 m long tunnel, versus the conductivity of the tunnel. Homogeneous flow medium - uniform continuum model. Heterogeneous flow medium - stochastic continuum model with properties representing Åspö (block: 10x10x10m, K dist STD 10Log K=1.498). The flow factor given in the figure, corresponds to average flow, average as regards the flow of different realizations. Flow factor = $\text{Flow}_{\text{Stochastic}} / \text{Flow}_{\text{Uniform}}$
(1) Flow factor representing average flow in tunnel, rock mass heterogeneity 100%
(2) Flow factor representing average flow in tunnel, rock mass heterogeneity 318%

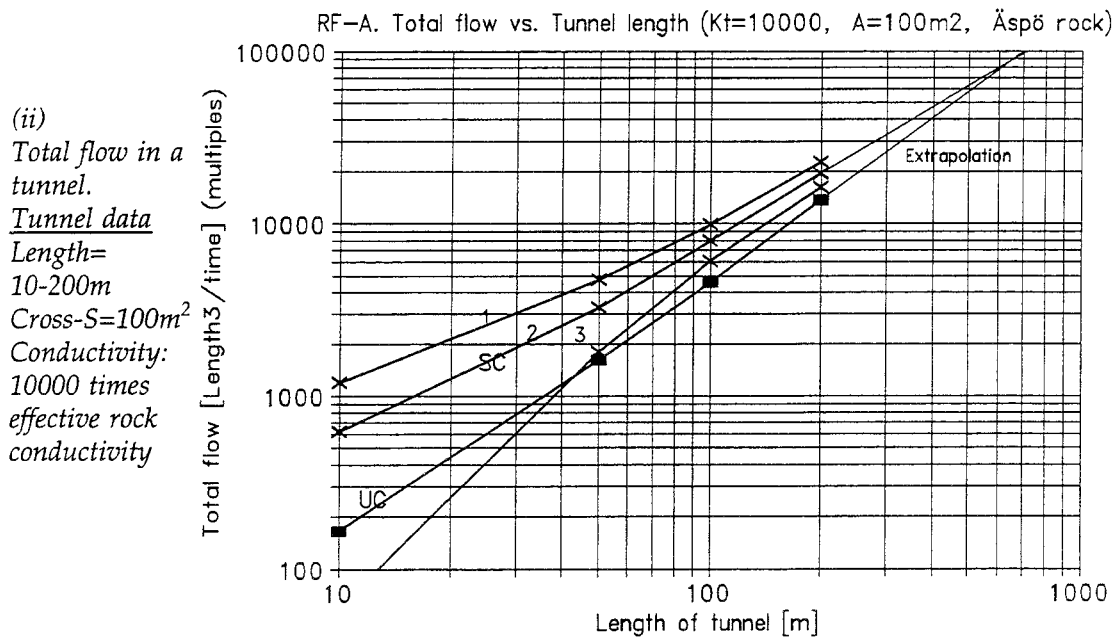
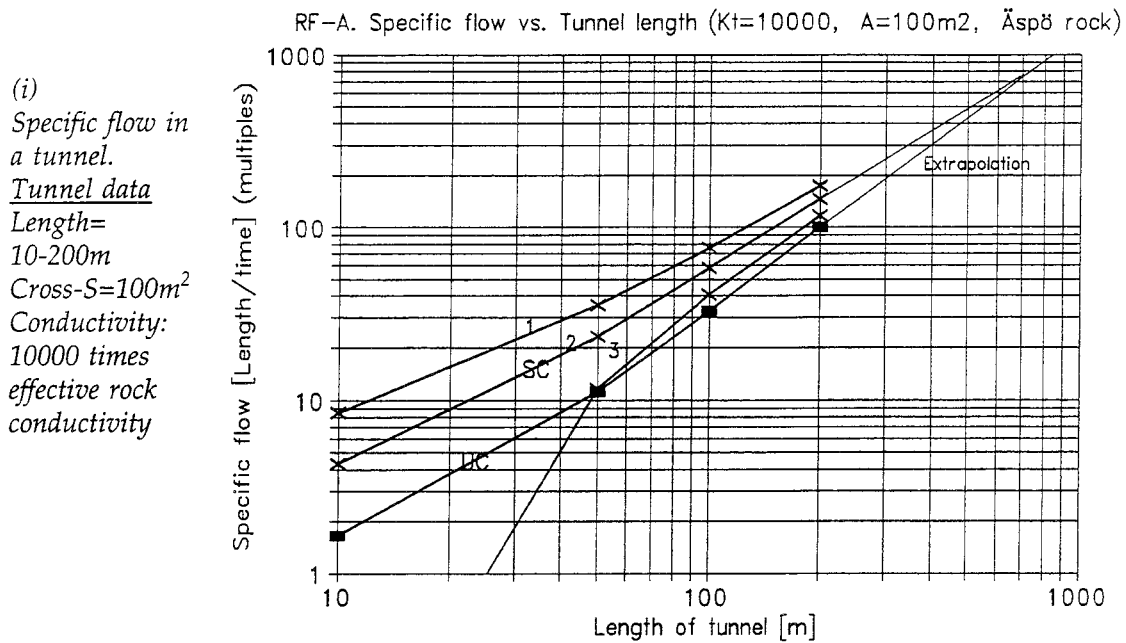
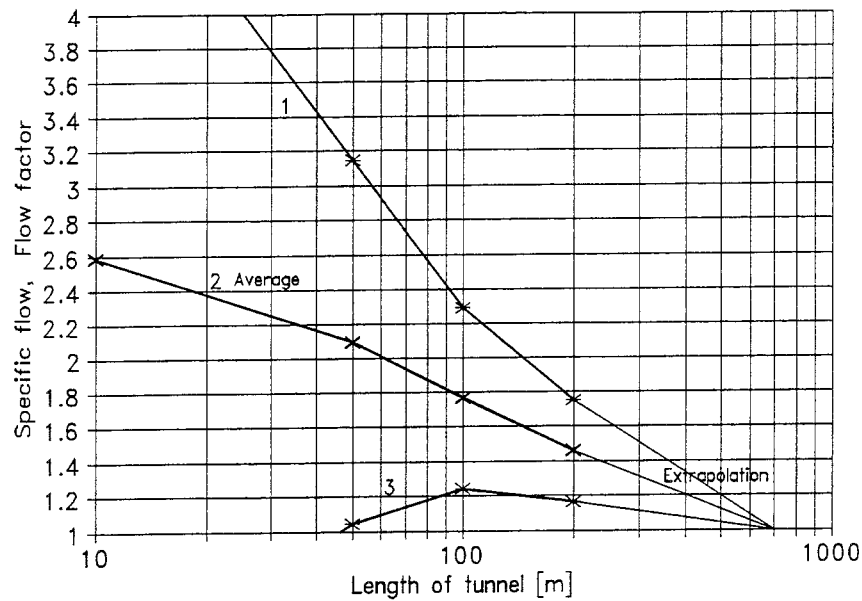


Figure 6.16 FLOW IN A TUNNEL, SENSITIVITY TO TUNNEL LENGTH.
THE REGIONAL FLOW IS ALONG THE TUNNEL.
Specific flow (i) and Total flow (ii) in a tunnel, versus the length of the tunnel.
The rock mass is defined as, homogeneous - uniform continuum model, or as heterogeneous - stochastic continuum model with properties representing Äspö (block size: 10x10x10m, block conductivity distribution: STD 10Log K= 1.498).
The flow in the tunnel is given as multiples of an unknown regional flow.

- Stochastic continuum SC, is denoted by stars: (1) average flow plus one standard deviation, (2) average flow and (3) average flow minus one standard deviation.
- Uniform continuum UC, is denoted by filled squares.

(i)
 Specific flow factor of a tunnel.
Tunnel data
 Length= 10-200m
 Cross-S=100m²
 Conductivity: 10000 times effective rock conductivity

RF-A. Specific flow factor vs. Tunnel length (Kt=10000, A=100m², Äspö rock)



(ii)
 Total flow factor of a tunnel.
Tunnel data
 Length= 10-200m
 Cross-S=100m²
 Conductivity: 10000 times effective rock conductivity

RF-A. Total flow factor vs. Tunnel length (Kt=10000, A=100m², Äspö rock)

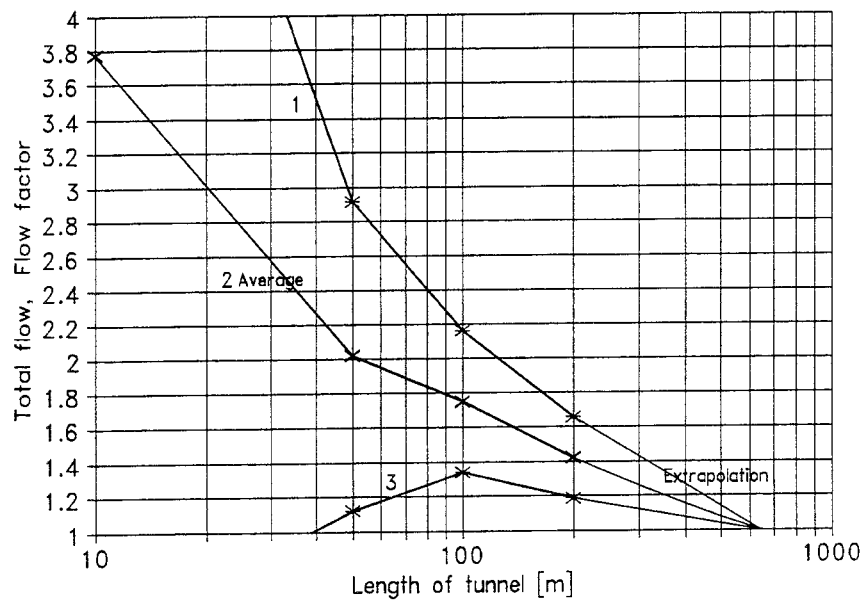


Figure 6.17

**FLOW IN A TUNNEL, SENSITIVITY TO TUNNEL LENGTH.
 THE REGIONAL FLOW IS ALONG THE TUNNEL.**

Specific flow factor (i) and Total flow factor (ii) of a tunnel, versus the length of the tunnel. The rock mass is defined as, a homogeneous medium - uniform continuum model, or as a heterogeneous medium - stochastic continuum model with hydraulic properties representing Äspö (Block: size 10x10x10m, block conductivity distribution: STD 10Log K=1.498).

- (1) Flow factor representing average flow plus one standard deviation
- (2) Flow factor representing average flow
- (3) Flow factor representing average flow minus one standard deviation.

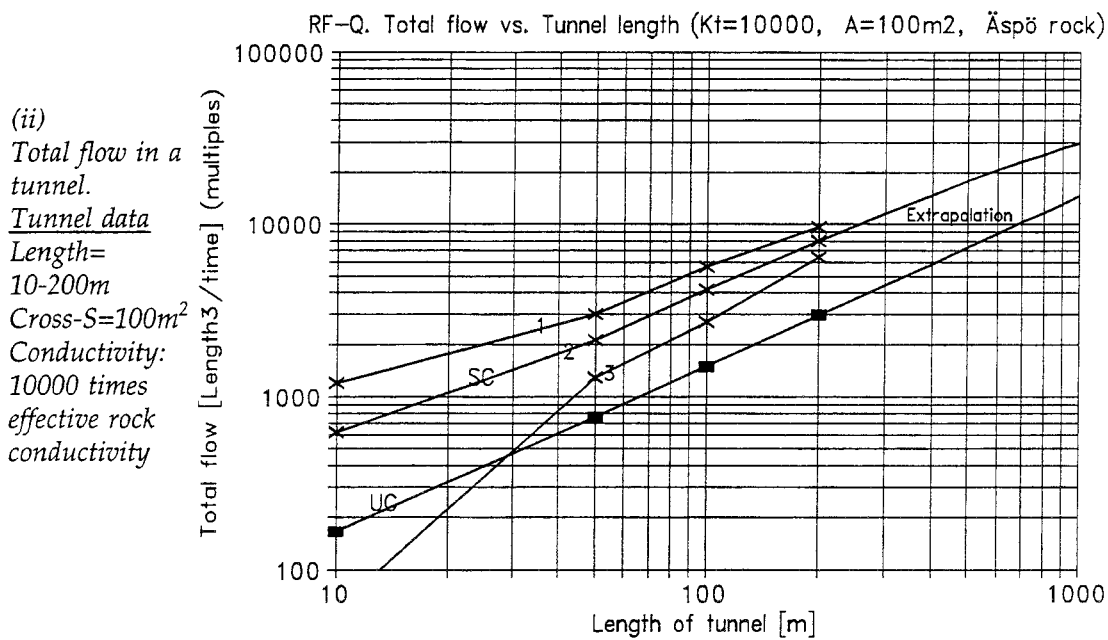
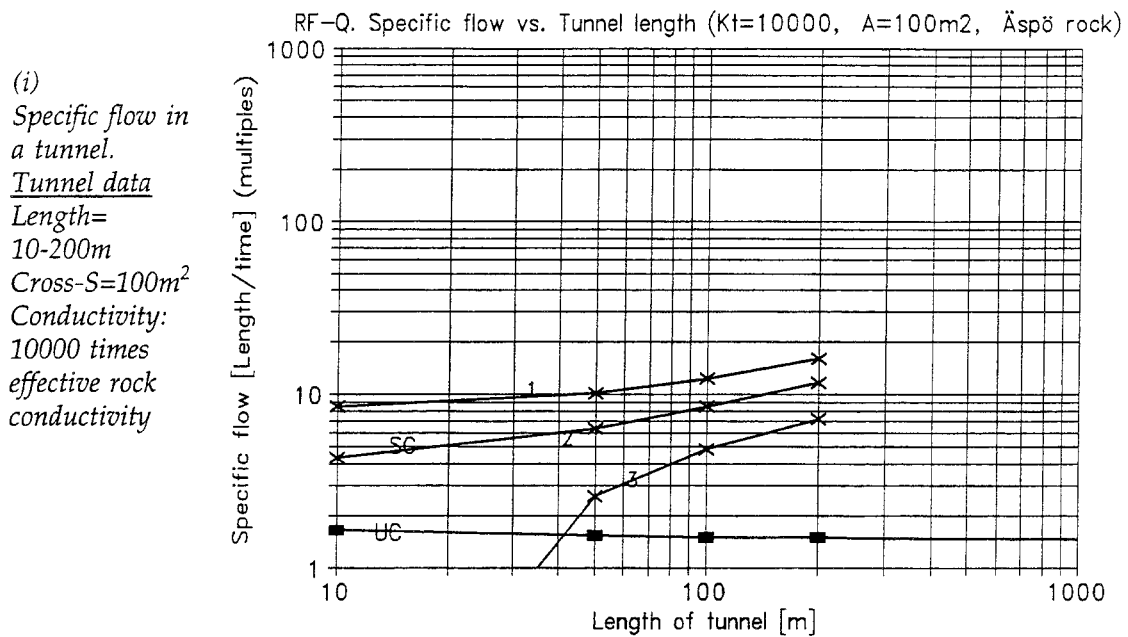
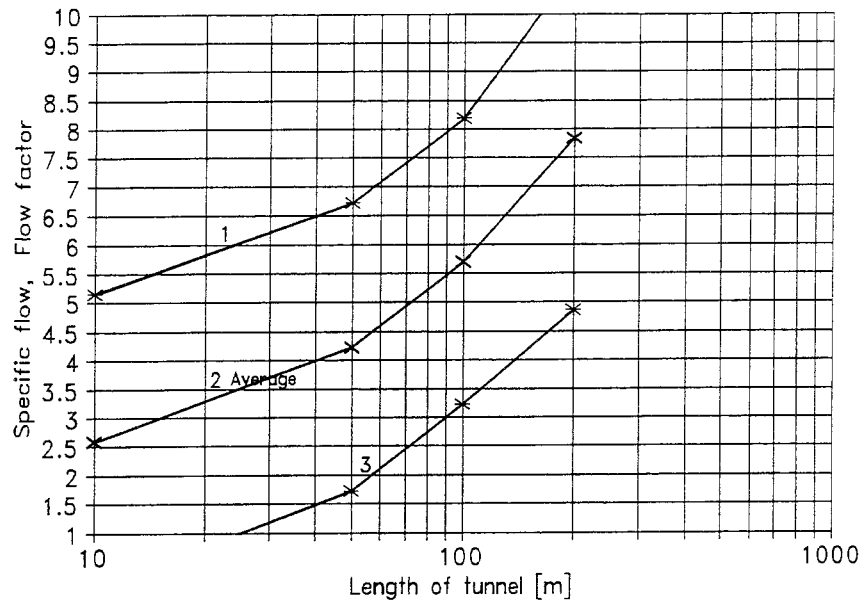


Figure 6.18 FLOW IN A TUNNEL, SENSITIVITY TO TUNNEL LENGTH.
THE REGIONAL FLOW IS AT RIGHT ANGLES TO THE TUNNEL.
Specific flow (i) and Total flow (ii) in a tunnel, versus the length of the tunnel.
The rock mass is defined as, homogeneous - uniform continuum model, or as heterogeneous - stochastic continuum model with properties representing Äspö (block size: 10x10x10m, block conductivity distribution: STD 10Log K= 1.498).
The flow in the tunnel is given as multiples of an unknown regional flow.

- Stochastic continuum SC, is denoted by stars: (1) average flow plus one standard deviation, (2) average flow and (3) average flow minus one standard deviation.
- Uniform continuum UC, is denoted by filled squares.

(i)
 Specific flow factor of a tunnel.
Tunnel data
 Length= 10-200m
 Cross-S=100m²
 Conductivity: 10000 times effective rock conductivity

RF-Q. Specific flow factor vs. Tunnel length (Kt=10000, A=100m², Äspö rock)



(ii)
 Total flow factor of a tunnel.
Tunnel data
 Length= 10-200m
 Cross-S=100m²
 Conductivity: 10000 times effective rock conductivity

RF-A. Total flow factor vs. Tunnel length (Kt=10000, A=100m², Äspö rock)

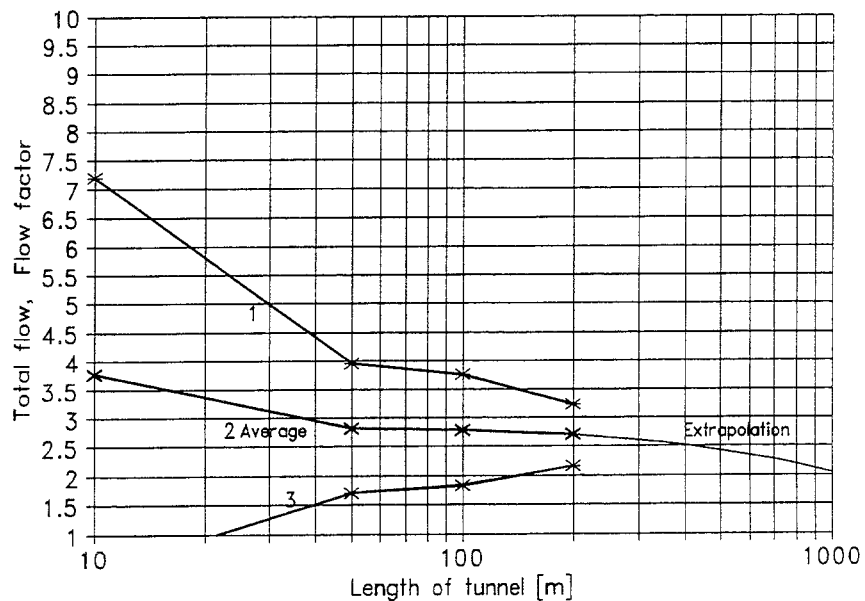
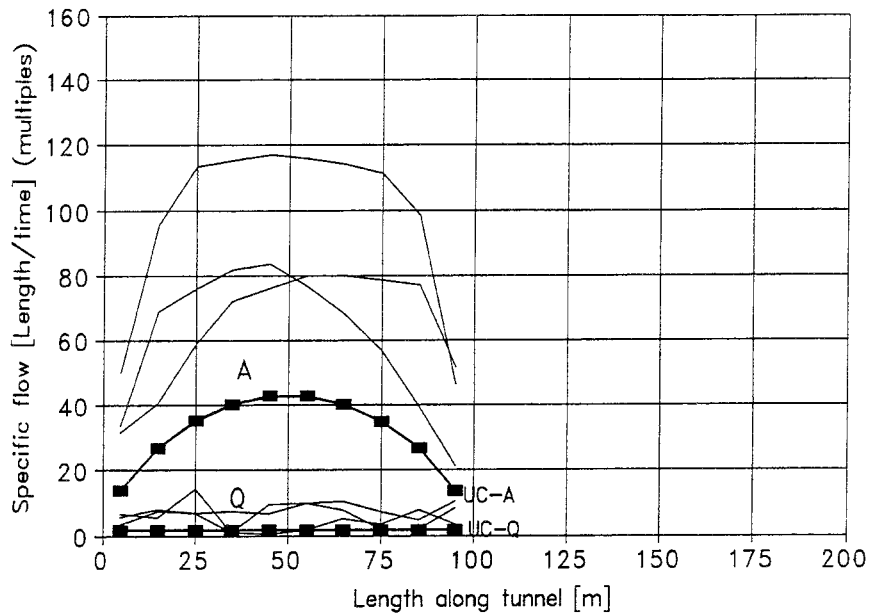


Figure 6.19

FLOW IN A TUNNEL, SENSITIVITY TO TUNNEL LENGTH.
 THE REGIONAL FLOW IS AT RIGHT ANGLES TO THE TUNNEL.
 Specific flow factor (i) and Total flow factor (ii) of a tunnel, versus the length of the tunnel. The rock mass is defined as, a homogeneous medium - uniform continuum model, or as a heterogeneous medium - stochastic continuum model with hydraulic properties representing Äspö (Block: size 10x10x10m, block conductivity distribution STD 10Log K=1.498).
 (1) Flow factor representing average flow plus one standard deviation
 (2) Flow factor representing average flow
 (3) Flow factor representing average flow minus one standard deviation.

(i)
 Specific flow,
 variation inside a
 tunnel.
Tunnel data
 Length= 100m
 Cross-S=100m²
 Conductivity:
 1000 times
 effective rock
 conductivity

RF: A, Q: Distribution of specific flow in 100 m long tunnel. UC and SC models



(ii)
 Specific flow,
 variation inside a
 tunnel.
Tunnel data
 Length= 200m
 Cross-S=100m²
 Conductivity:
 1000 times
 effective rock
 conductivity

RF: A, Q: Distribution of specific flow in 200 m long tunnel. UC and SC models

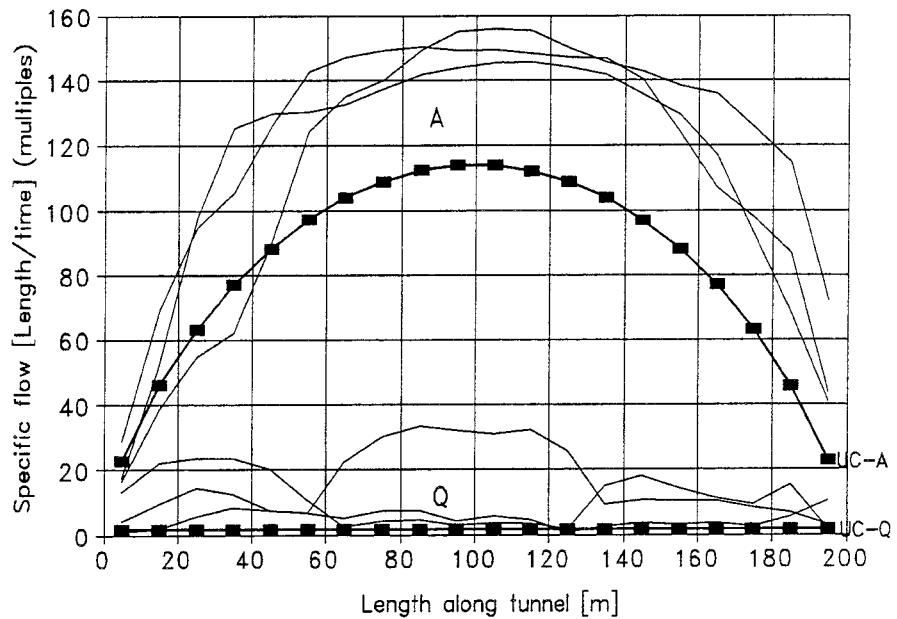


Figure 6.20

VARIATION OF SPECIFIC FLOW INSIDE A TUNNEL.

Specific flow inside: (i) a 100 m and (ii) a 200 m, long tunnel; versus the length of the tunnel. The rock mass is defined as, a homogeneous medium (uniform continuum model), or as a heterogeneous medium (stochastic continuum model) with hydraulic properties representing Äspö (Block: size 10x10x10m, block conductivity distribution STD 10Log K=1.498).

Direction of regional flow:

- | | |
|-------------------------------|--|
| A. Along the tunnel: | Homogeneous rock (UC-A): filled squares with line.
Heterogeneous rock, 3 different realizations: lines. |
| Q. At right angles to tunnel: | Homogeneous rock (UC-Q): filled squares with line
Heterogeneous rock, 3 different realizations: lines. |

Chapter 7.

Effects of flow barriers

7.1 Introduction

In the following sections we will discuss barriers that limit the groundwater flow in a tunnel. Limiting of the flow is of interest if the tunnels are to be used for storage of long-lived hazardous waste. A limited groundwater flow will give a small transport of hazardous material from the tunnel to the rock mass.

If a tunnel is used for storage of waste, the waste should be placed in an encapsulation. An encapsulation is a structure located inside the tunnel, it is the structure that contains the waste and the units in which the waste is delivered. For example, in SFL 3-5 the encapsulation is a concrete construction of cells. The waste units are stacked in the cells, after which the remaining empty space of the cells is filled with porous concrete. So, finally the encapsulation will be filled with waste units and concrete back fill, and be a more or less homogeneous concrete construction.

To limit the groundwater flow that passes through an encapsulation inside a tunnel, a flow barrier can be installed between the encapsulation and the tunnel walls. The following sections will discuss different aspects of such a barrier.

7.2 Methodology

We will study the flow in a tunnel which is closed, the tunnel is not kept dry, but is filled with groundwater, and the groundwater flow in the tunnel is at equilibrium with the groundwater system. The tunnel will contain an encapsulation and a flow barrier. We will investigate the function of the flow barrier as regards: extension of barrier, conductivity of barrier, conductivity of encapsulation, and length of tunnel. We will also investigate how the heterogeneity of the rock mass will influence the function of the flow barrier.

In the following sections we will study a straight tunnel by using of three-dimensional models. The tunnel will have a length of about 100m or 200m and a rectangular cross-section of: $10\text{m} \times 10\text{m} = 100 \text{ m}^2$. For an encapsulation of 100m length the mesh is given in Figure 7.2. The flow barrier surrounding the encapsulation will have a thickness of 2m. The tunnel will be placed in a rock mass of either heterogeneous or homogeneous hydraulic properties. A uniform continuum model will represent a homogeneous flow medium, a stochastic continuum model will represent a heterogeneous flow medium (see Chapter 5).

In the models, different directions of regional flow were studied. Extreme values of flow in the tunnels (minimum or maximum flow), will occur when the regional flow is directed either, (i) close to or along the tunnel, or (ii) at right angles to the tunnel. Directions of the regional flow that are different from these two cardinal directions, will produce a tunnel flow that in size are between the tunnel flow produced by the two cardinal directions (presuming a straight tunnel). The regional flow was created by assigning the specified head boundary condition to the blocks of two opposite faces of the model. The specified head was set in such a way that a regional flow was created. All other blocks were of the continuous type.

The models are affected by boundary constraints. The boundary effects have been estimated by the use of the methods given in Chapter 4. The error in predicted flow is small. If the conductivity contrast between the flow barrier and the rock mass is less than

1000 times, the error is less than 1 percent of the predicted flow. If the conductivity contrast between the flow barrier and the rock mass is larger, and the direction of the regional flow produces a large flow in the tunnel, the error in predicted flow may be in the range of 5 percent of the predicted flow. This is considered as an acceptable error.

The flow in a tunnel will be given as a specific flow or as a total flow (see Chapter 2). The flow values given are multiples of an unknown regional flow. To calculate the multiples, the regional specific flow was set to 1 m/s in the models. This was done by giving the rock mass a conductivity (effective conductivity) which is equal to 1 and setting the regional gradient to 1. Without the tunnel the effective conductivity of all models will be the same in the direction of the regional flow. The flow in a tunnel will also be given as a flow factor. The flow factor corresponds to a tunnel placed in a heterogeneous rock (stochastic continuum) and represents the flow in such a tunnel expressed in relation to the flow of a similar tunnel placed in an homogeneous rock mass (uniform continuum), see Section 6.3 and Equation 6.1. The flow factor is the quota between the flow of a stochastic continuum model and that of a uniform continuum model.

In the following sections we will discuss the efficiency of the flow barrier. By efficiency of the flow barrier, we mean the ability of the flow barrier to reduce the flow in the encapsulation. We will compare the efficiency of different flow barriers by comparing how much flow that remains in the encapsulation for different flow barriers. The remaining flow can be expressed in percent of the flow in the encapsulation of a reference scenario (see Equation 7.1). For example, the reference scenario may represent a situation without a flow barrier.

$$R_{flow} = \frac{F_s}{F_0} * 100 \quad (7.1)$$

R_{flow} = Remaining flow in encapsulation [percent]

F_0 = Flow in the encapsulation, for a reference scenario.

F_s = Flow in the encapsulation, for a studied scenario.

This chapter includes about 250 scenarios, representing different directions of the regional flow as well as different properties of encapsulation, barrier and rock block conductivity distributions. For the uniform continuum models only one realization is necessary for each scenario. For the stochastic continuum models, the number of realizations included in the statistical analysis of each scenario has varied depending on the acceptable uncertainty and the size of the variation in the calculated flow, the number has been varied from about 50 to 100 realizations.

7.3 Function of flow barrier

The purpose of a flow barrier is to limit the flow that passes through the encapsulation. The barrier is positioned inside the tunnel between the rock mass and the encapsulation. The barrier can be a structure less permeable than the rock mass, and divert the flow away from the encapsulation; such a barrier is called a negative barrier. The barrier can also function as a structure more permeable than the rock mass and the encapsulation, and lead the flow around the encapsulation; such a barrier is called a positive barrier. The function of a flow barrier is demonstrated in Figure 7.1. The figure demonstrates the effect of a negative barrier and a positive barrier by the use of two-dimensional models and flowpaths, both for a homogeneous rock mass (uniform continuum models) and for a heterogeneous rock mass (stochastic continuum models). Note that all predictive simulations presented in this study are based on three-dimensional models, the models in

the figure are solely for demonstration purposes. As regards a demonstration of three-dimensional flow in rock mass and tunnels, we refer to Figures 6.2 through 6.5, these figures are applicable to a system of a flow barrier and an encapsulation. A tunnel with a large permeability influences the groundwater flow of the rock mass in the same way as a positive barrier. A tunnel with a small permeability influences the groundwater flow of the rock mass in the same way as a negative barrier.

The flow through an encapsulation that is protected by a negative flow barrier, is directly proportional to the flow through the barrier. As a negative barrier is less conductive than the surrounding rock mass, the water that passes through the barrier will follow the shortest path through the barrier and the encapsulation. Hence, depending on the lay-out of the barrier and the encapsulation, a certain amount of the water entering the barrier will also pass through the encapsulation. This goes for all barriers having a conductivity which is smaller than those of both the rock mass and the encapsulation.

The flow through an encapsulation protected by a positive flow barrier is not directly proportional to the flow through the barrier. The flow of a positive barrier reaches a maximum value for large values of barrier conductivities, in an asymptotic way. For large values of barrier conductivities, the flow in the barrier will only change minimally for different values of barrier conductivities. However, even if the size of the flow in the barrier does not change much, the flow pattern of the water flowing through the barrier and the encapsulation changes with different large values of the barrier conductivity. As the conductivity of the barrier becomes larger, less and less water will leave the barrier and flow through the encapsulation and nearly all the flow takes place in the barrier. Therefore, the efficiency of a positive barrier will be increased, if the conductivity of the barrier is increased. The larger the conductivity contrast between the encapsulation and the barrier, the smaller the flow through the encapsulation. This goes for all barriers having a conductivity which is larger than that of both the rock mass and the encapsulation.

7.4 Flow in encapsulation and flow barrier, sensitivity to conductivity of flow barrier

To estimate the effect of a flow barrier, models were established containing a tunnel with a flow barrier and an encapsulation, see Figure 7.2. The rock mass was set as homogeneous (uniform continuum). The flow in the flow barrier and the encapsulation was calculated using different values of conductivity of the flow barrier and different directions of the regional groundwater flow. The flow in the encapsulation and the flow barrier was calculated as a specific flow and as a total flow. The predicted flow should be regarded as a multiple of an unknown regional flow.

In these simulations, the conductivity of the encapsulation was set equal to the conductivity of the rock mass. Hence, when the barrier was assigned a conductivity equal to that of the rock mass the whole system had the same conductivity and the model will predict a flow in the encapsulation which equal to the flow in the rock mass.

The effect of the barrier was investigated by making simulations with the conductivity of the barrier either smaller (negative barrier) or larger (positive barrier) than the conductivity of the rock mass. For each conductivity value of the barrier, simulations were carried out for the two cardinal directions of the regional groundwater flow.

The results of the simulations demonstrate that a well functioning flow barrier can reduce the flow through an encapsulation with several orders of magnitudes. The results are given in Figure 7.3 and 7.4.

- *Flow barrier.* The flow in the flow barrier will vary depending on the conductivity of the flow barrier. The flow in the barrier will be similar to the flow of a homogeneous tunnel, see Chapter 3. If the flow barrier has a small conductivity the flow will be small, if the conductivity is large the flow will be large. For a barrier, as for a homogeneous tunnel, an increase of the conductivity of the flow barrier will only have a large effect on the flow in the barrier if the barrier conductivity is small. If the conductivity of a flow barrier is large a much more conductive barrier will not have a much larger flow, as the flow of such a barrier is mainly dependent on the permeability of the surrounding rock mass. The threshold conductivity, defined in Chapter 3, is also applicable to the flow barrier.

- *Encapsulation.* The flow in the encapsulation will also vary depending on the conductivity of the flow barrier. The flow barrier will reduce the flow in the encapsulation. The larger the contrast between (i) the conductivity of the flow barrier and (ii) the conductivity of the rock mass and the encapsulation, the smaller the flow in the encapsulation. A positive barrier is approximately as effective as a negative barrier.

7.5 Flow in the encapsulation, sensitivity to conductivity of the encapsulation

In the previous section (7.4) the conductivity of the encapsulation was set equal to the conductivity of the rock mass. If the encapsulation has a conductivity which differs from the conductivity of the rock mass, it will influence the efficiency of the flow barrier.

To illustrate this, simulations were carried out with a model (Figure 7.2) in which the conductivity of the encapsulation was set as 1, 10 or 100 times smaller or larger than the effective rock conductivity. Two directions of the regional flow were studied: along or at right angles to the tunnel. The rock mass was set as homogeneous (uniform continuum). The results of the simulations are given in Figure 7.5.

The flow through the encapsulation depends, among other parameters, on the conductivity of the encapsulation. The flow through a low-conductivity encapsulation is smaller than the flow through a more conductive encapsulation. Hence, it is of interest to make the conductivity of the encapsulation as low as possible. Additionally, the conductivity of the encapsulation will also effect the ability of the barriers to reduce the flow in the encapsulation - the efficiency of the barriers.

Consider an encapsulation that is less conductive than the rock mass. The flow of such an encapsulation will be less than the flow of an encapsulation having the same conductivity as the rock mass. An encapsulation that is less conductive than the rock mass will increase the efficiency of a positive barrier and reduce the efficiency of a negative barrier, compared to an encapsulation having the same conductivity as the rock mass. A negative barrier can only be effective if it is less conductive than the rock mass and also less conductive than the encapsulation.

Consider an encapsulation that is more conductive than the rock mass. The flow of such an encapsulation will be larger than the flow of an encapsulation having the same conductivity as the rock mass. An encapsulation that is more conductive than the rock mass will increase the efficiency of a negative barrier and reduce the efficiency of a positive barrier, compared to an encapsulation having the same conductivity as the rock mass. A positive barrier can only be effective if it is more conductive than the rock mass and also more conductive than the encapsulation.

A positive or a negative barrier with a too small conductivity contrast, in relation to the rock mass and the encapsulation, will not reduce the flow of the encapsulation.

7.6 Flow in the encapsulation, sensitivity to extension of the flow barrier

The efficiency of the barrier depends on the size of the barrier. It is the thickness of the barrier, together with the barrier conductivity, that determines the transport capacity of the barrier. By using a very low-permeable or a very high-permeable barrier material, the transport capacity of the barrier can be large or small, for any reasonable thickness of barrier. Hence, from a practical point of view, it is the conductivity of the barrier that is of importance. The thickness of the barrier can be determined by aspects of design and construction of the encapsulation. However, it is very important that the flow barrier is complete. By a complete barrier we mean a barrier that exists at all sides of the encapsulation, a barrier that completely covers the encapsulation. An incomplete barrier, a barrier that does not extend over the whole of the encapsulation, will not limit the flow through an encapsulation in an effective way.

The effect of an incomplete barrier has been studied by the use of the model given in Figure 7.6. This model contains a 100m long encapsulation, with a cross section of 10x10m. The encapsulation is covered by a barrier, above and at both sides. No flow barrier exists below the encapsulation. Thus, the model is identical to the model given in Figure 7.2, except that no flow barrier exists below the encapsulation. Two different directions of the regional flow have been studied: along and at right angles to the tunnel. The rock mass was set as homogeneous (uniform continuum).

The results of the simulations of the incomplete barrier are given in Figure 7.7. The results can be compared to the results given in Figure 7.5, which represent a complete barrier. Studying the results, we see that when the flow is directed along the tunnel, the barrier is of no use, it will not reduce the flow through the tunnel, it may even lead to an increase in flow, if the barrier is a positive barrier. When the flow is at right angles to the tunnel the barrier is effective, but the efficiency is slightly reduced, compared to a complete barrier. These results are only applicable to a barrier which is incomplete in the way the simulated barrier is.

The following general conclusion can be made. A well functioning flow barrier needs to cover the whole of the encapsulation. An incomplete flow barrier may even increase the flow in the encapsulation.

7.7 Flow in the encapsulation, sensitivity to length of encapsulation and barrier

The flow in a long tunnel is larger than the flow in a short tunnel. Hence, it is of interest to make the encapsulation and the tunnel as short as possible. The length of the tunnel will also influence the efficiency of a flow barrier, the shorter the tunnel the more efficient the flow barrier. Therefore, the efficiency of the barrier depends, among other things, on the size of the encapsulation - length and cross-section area. A comparison of two different encapsulations has been carried out. The first model is the one given in Figure 7.2, the encapsulation of this model having a length of 100m and a cross sectional area of 100m². The second model looks the same, except that the encapsulation has a length of 200m. The thickness and the properties of the barriers are the same in both models, except for the length of the barrier. Two different directions of the regional flow have been studied: along and at right angles to the tunnel. The rock mass was set as homogeneous.

The effect of the barriers of the two models is given in Figure 7.8. For a regional flow at right angles to the tunnel, the flow of the encapsulation of the 200m long tunnel is twice that of the 100m long tunnel (Fig.7.8(ii)). For a regional flow along the tunnel, the flow of the encapsulation of the 200m long tunnel is approximately the same as that of the 100m

long tunnel, for small values of the conductivity contrast between the barrier and the rock mass. For large values of the conductivity contrast between the barrier and the rock mass, the flow of the encapsulation of the 200m long tunnel is larger than that of the encapsulation of the 100m long tunnel (Fig.7.8(i)).

As defined in equation 7.1, the remaining flow in the encapsulation can be expressed in percent of the flow of a reference scenario, - percentage remaining flow. For the reference scenario we use the flow of the studied encapsulation when the barrier has the same conductivity as the rock mass, that is when the barrier has no effect. The percentage of remaining flow in the encapsulation, for different values of barrier conductivity, is a measure of the efficiency of the flow barrier.

For a regional flow at right angles to the tunnel, the remaining flow of the encapsulation decreases with increased conductivity contrast between the barrier and the rock mass (Fig.7.8(ii)). Given in percent, the different values of the remaining flow will be the same for both a 100m and a 200m long tunnel. This means that if the regional flow is at right angles to the tunnel, the efficiency of the barrier is the same, regardless of the length of the tunnel.

For a regional flow along the tunnel, the remaining flow of the encapsulation decreases with increased conductivity contrast between the barrier and the rock mass (Fig.7.8(i)). Given in percent, the different values of the remaining flow will not be the same for a 100m and a 200m long tunnel, the percentage of remaining flow decreases more for a 100m long tunnel than for a 200m long tunnel. This means that if the regional flow is along the tunnel, the efficiency of the barrier will be reduced as the length of the tunnel is increased. To get the same percentage of remaining flow in the encapsulation of the two studied tunnels, we need to increase the conductivity contrast of the 200m long tunnel. For example, the percentage remaining flow in the encapsulation of the 100m long tunnel surrounded by a positive barrier having a conductivity contrast of 10000 times, is approximately the same as that of the encapsulation of the 200m long tunnel surrounded by a positive barrier having a conductivity contrast of 25000 times.

Hence, if the regional flow is at right angles to the tunnel the efficiency of a barrier is independent of the length of the tunnel. For all other directions of the regional flow, the efficiency of the barrier will be reduced as the length of the tunnel is increased. The largest reduction of efficiency takes place if the regional flow is along the tunnel. However, compared to the large reduction of flow that can be obtained with a flow barrier having a large conductivity contrast, the loss in efficiency is insignificant.

7.8 Flow in encapsulation and flow barrier, sensitivity to heterogeneity of rock mass

The effect of a heterogeneous rock mass on the flow in a barrier, and in an encapsulation, has been investigated. The heterogeneous flow medium was simulated by the use of the stochastic continuum approach. The stochastic continuum models used the same mesh as the uniform continuum models, the mesh is given in Figure 7.2. The establishment of the stochastic continuum models followed the method given in Section 6.2. The scale dependency was eliminated in the same way and the boundary effects were estimated in the same way. The error in predicted flow, due to boundary constraints, will be less than or about 5 percent of the predicted flow, which is considered as acceptable.

As the effects of the heterogeneity of the rock mass were studied by use of the stochastic continuum approach, the results of the study are based on statistical analyses of many realizations of the conductivity field. Every scenario studied is represented by a number

of realizations forming a statistical distribution, the distributions obtained are fairly symmetrical. For the distributions obtained, the differences between the arithmetic mean, the median, the mode and the geometric mean are small, compared to the size of the standard deviation. In the following discussion, when we refer to the flow of a heterogeneous rock mass, we mean the average flow of many different realizations - the most probable outcome, the expected flow. The possible variation of the flow of a tunnel, depending on the heterogeneous properties of the rock mass, is described by the standard deviation and is given in the figures of this section. The general conclusions given in the following section are valid for at least 70 percent of the realizations of a studied scenario, - the expected value plus and minus one standard deviation ($m-\sigma$ and $m+\sigma$). Hence, they are valid with a probability of at least 70 percent.

Two scenarios were studied, in the first scenario the conductivity of the encapsulation was set equal to the effective rock conductivity, in the second scenario it was set as 10 times larger than the effective rock conductivity. For both scenarios, the flow medium of the stochastic continuum models was assigned properties representing the heterogeneous properties at Äspö: block size 10x10x10m, log-normal block conductivity distribution with a standard deviation of $10\log K$ equal to 1.498. The effective rock conductivity was set equal to one. The effect of the barrier was investigated by making simulations with the conductivity of the barrier either smaller (negative barrier) or larger (positive barrier) than the conductivity of the rock mass. For each conductivity value of the barrier, simulations were carried out for the two cardinal directions of the regional groundwater flow.

The results of the modelling are given in Figures 7.9 through 7.11 for the first scenario, and in Figures 7.12 through 7.14 for the second scenario.

- *Flow barrier.* The heterogeneity of the rock mass will influence the flow in a barrier in the same way as the heterogeneity will influence the flow in a homogeneous tunnel, compare Figure 7.9 with Figures 6.9(ii) and 6.10(ii). The heterogeneity of the rock mass will increase the expected flow in the barrier, except if both the regional flow is along the tunnel and the barrier conductivity is very small. The deviation between the expected flow predicted with a homogeneous rock mass and that with a heterogeneous rock mass, is given by the flow factor (see Equation 6.1). The flow factor of a barrier, and that of a homogeneous tunnel, varies, as regards the conductivity of the tunnel, in a very similar way, compare Figures 7.11(i) and 6.12(ii). The only difference in behavior, between the expected flow in a barrier and in a homogeneous tunnel, occurs when the regional flow is along the tunnel and for small values of the barrier permeability; for such a scenario the flow factor is smaller in a barrier than in a homogeneous tunnel. The second scenario demonstrates the same type of behavior, compare Figures 7.11(i) and 7.14(i). Differences occur only when the conductivity contrast between the rock and the barrier is small; for such scenarios the conductivity of the encapsulation is more important than the conductivity of the barrier. Note that when the regional flow is at right angles to the tunnel and the conductivity of the encapsulation is 10 times that of the rock, or larger, Figure 7.12(ii), the expected flow of the barrier decreases somewhat as the conductivity of the barrier increases beyond the conductivity of the encapsulation. This is because the flow is given as a total flow and the total flow is the amount of water that visits the barrier; the total flow makes no difference between water that has previously been in the barrier and water that has not. When the encapsulation is as conductive as the barrier, water will flow through the barrier and further on through the encapsulation, and then again through the barrier. Water of such a flowpath will be added twice to the total flow. As the barrier becomes more permeable than the encapsulation, the flow pattern of the barrier changes towards a pattern in which nearly no water passes through the encapsulation, nearly all the water stays in the barrier and less and less water will be counted twice. - The total flow of the barrier decreases.

- *Encapsulation.* For a heterogeneous rock mass, like for a homogeneous rock mass, the flow in the encapsulation will be very much reduced if the encapsulation is protected by a flow barrier with a conductivity that is either much smaller or much larger than the conductivity of the rock mass (see Figure 7.10 and 7.13). However, the heterogeneity of the rock mass will influence the flow of the encapsulation, although the encapsulation is protected by a flow barrier. A heterogeneous rock mass will produce a larger expected flow in the barrier than a homogeneous rock mass. A larger flow in the barrier will give a larger flow in the encapsulation. The deviation between the flow predicted with a homogeneous rock mass and that with a heterogeneous rock mass, is given by the flow factor (see Equation 6.1). The size of the flow factor varies for different values of barrier conductivity. However, the flow factor of the barrier and that of the encapsulation is of about the same size (compare Figure 7.11(i) with 7.11(ii) and compare 7.14(i) with 7.14(ii)). So, the heterogeneity of the rock mass will influence the flow in an encapsulation in the same way as the heterogeneity will influence the flow in a homogeneous tunnel. The heterogeneity of the rock mass will increase the expected flow in the encapsulation, except if both the regional flow is along the tunnel and the barrier conductivity is very small.

Thus, the flow in the barrier is influenced by the heterogeneity of the rock mass in the same way as the flow in a homogeneous tunnel. The analysis of the effects of the heterogeneity, given in Chapter 6, is also applicable to a flow barrier. The flow of the encapsulation is also influenced by the heterogeneity of the rock mass, although the encapsulation is protected by a flow barrier. The heterogeneity of the rock mass will increase the expected flow in the barrier and in the encapsulation, except if both the regional flow is along the tunnel and the barrier conductivity is very small.

A heterogeneous rock mass produces a larger expected flow in a flow barrier than a homogeneous rock mass. A larger flow in the flow barrier gives a larger flow in the encapsulation. Hence, we can say that the heterogeneity of the rock mass will reduce the efficiency of a flow barrier. However, the same reduction of flow that is obtained with a barrier in a homogeneous rock mass, can be obtained for a barrier in a heterogeneous rock mass if the conductivity contrast is increased. For an encapsulation in a heterogeneous rock mass of Äspö properties, the same reduction of flow is achieved with a barrier having a conductivity contrast that is about half an order of magnitude larger than that of a barrier in a homogeneous rock mass.

7.9 Conclusions

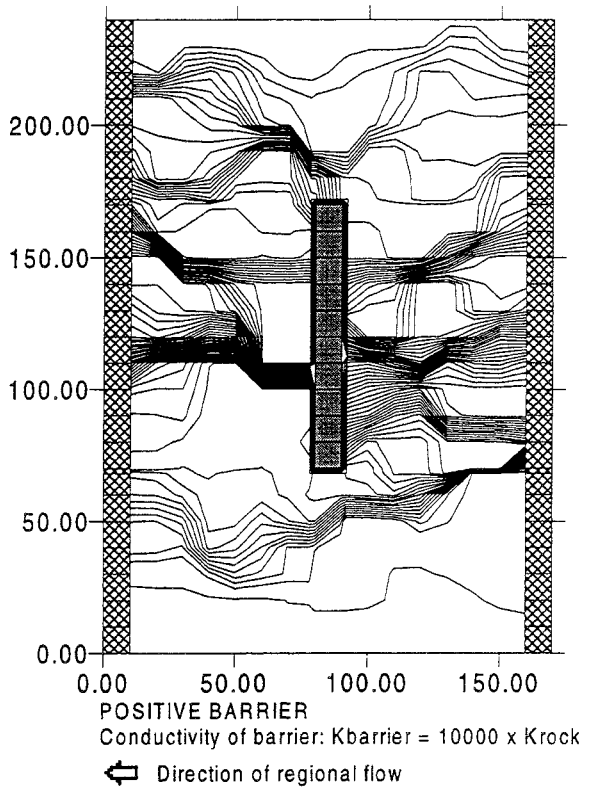
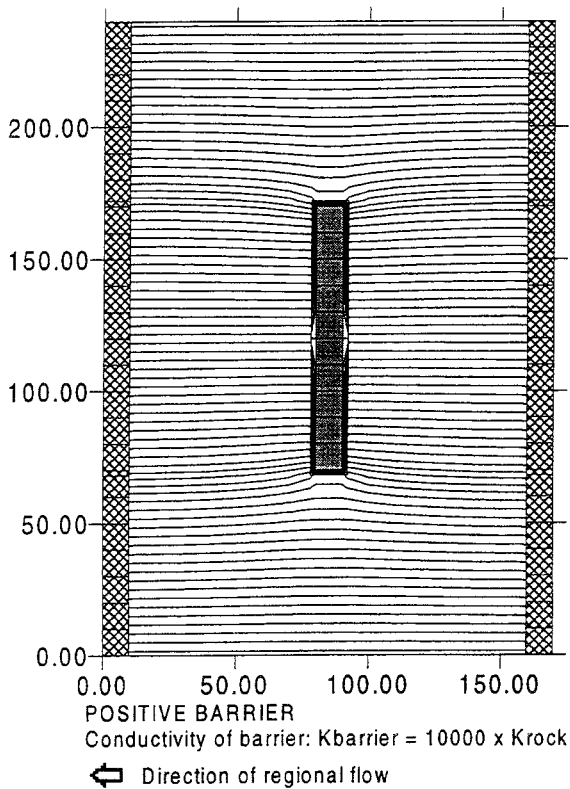
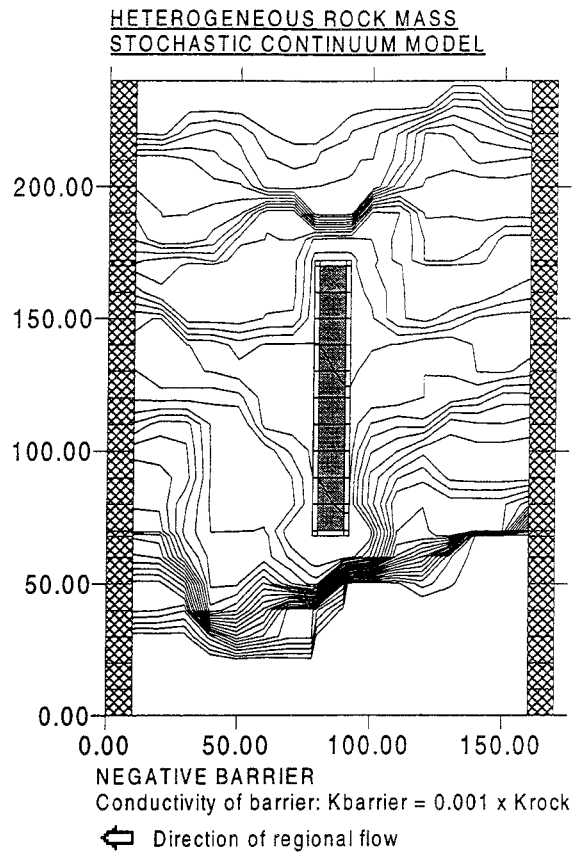
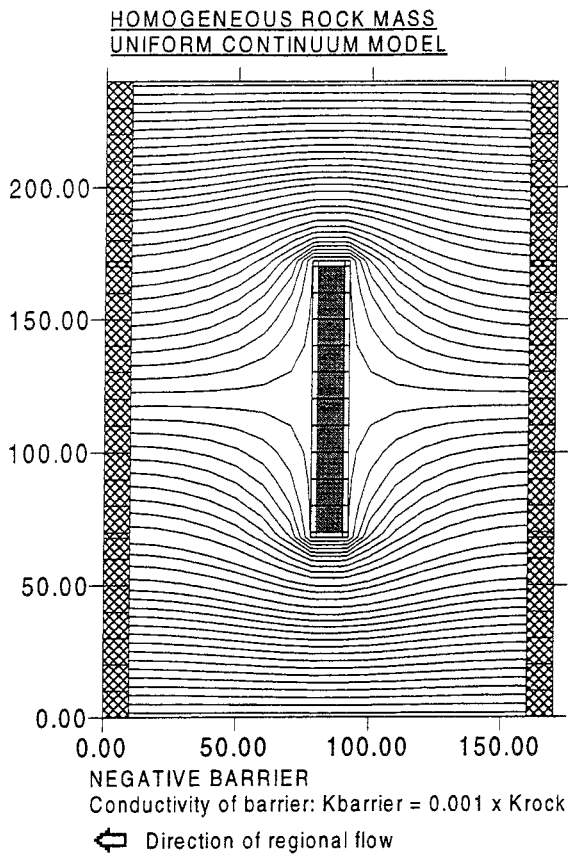
- *Function of a flow barrier.* The purpose is to limit the flow that passes through an encapsulation. The barrier is positioned inside the tunnel between the rock mass and the encapsulation. The barrier can be less permeable than the rock mass, and divert the flow away from the encapsulation; such a barrier is called a negative barrier. The barrier can be more permeable than the rock mass and the encapsulation, and lead the flow around the encapsulation; such a barrier is called a positive barrier. A well functioning flow barrier can reduce the flow through an encapsulation with several orders of magnitudes.





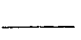
- *Flow in a flow barrier.* The flow in the flow barrier will vary depending on the conductivity of the barrier. The flow in the barrier will be similar to the flow of a homogeneous tunnel. If the flow barrier has a small conductivity the flow will be small, if the conductivity is large the flow will be large. For a barrier, as for a homogeneous tunnel, an increase of the conductivity of the barrier will only have a large effect on the flow in the barrier if the barrier conductivity is small. If the conductivity of a flow barrier is large a much more conductive barrier will not have a much larger flow, as the flow of such a barrier is mainly dependent on the permeability of the surrounding rock mass. The

threshold conductivity, defined in Chapter 3, is also applicable to the flow barrier.

- *Flow in an encapsulation.* The flow in the encapsulation will vary depending on the conductivity of the flow barrier and the conductivity of the encapsulation. A well functioning flow barrier will reduce the flow in the encapsulation.
- *Conductivity of a flow barrier and an encapsulation.* The larger the contrast between (i) the conductivity of the flow barrier and (ii) the conductivity of the rock mass and the encapsulation, the smaller the flow in the encapsulation. A positive barrier is approximately as effective as a negative barrier. The smaller the conductivity of the encapsulation, the smaller the flow of the encapsulation. However, the encapsulation conductivity will also influence the efficiency of a flow barrier.
- An encapsulation that is less conductive than the rock mass will increase the efficiency of a positive barrier and reduce the efficiency of a negative barrier. A negative barrier can only be effective if it is less conductive than the rock mass and also less conductive than the encapsulation.
- An encapsulation that is more conductive than the rock mass will increase the efficiency of a negative barrier and reduce the efficiency of a positive barrier. A positive barrier can only be effective if it is more conductive than the rock mass and also more conductive than the encapsulation.
- *Extension of a flow barrier.* A well functioning flow barrier needs to cover the whole of the encapsulation. An incomplete flow barrier could, instead of reducing the flow in the encapsulation, increase the flow in the encapsulation.
- *Length of tunnel-encapsulation.* As regards a regional flow at right angles to a tunnel, the efficiency of a barrier is independent of the length of the tunnel. For all other directions of the regional flow, the efficiency of the barrier will be reduced as the length of the tunnel is increased. The largest reduction of efficiency takes place if the regional flow is along the tunnel. However, compared to the large reduction of flow that can be obtained with a flow barrier having a large conductivity contrast, the loss in efficiency is insignificant.
- *Heterogeneity of rock mass.* The flow in a flow barrier is influenced by the heterogeneity of the rock mass in the same way as the flow in a tunnel without barriers and encapsulations (see Chapter 6). The flow of the encapsulation is also influenced by the heterogeneity of the rock mass, although the encapsulation is protected by a flow barrier. A heterogeneous rock mass produces a larger expected flow in a flow barrier than a homogeneous rock mass. A larger flow in the flow barrier gives a larger flow in the encapsulation. Hence, we can say that the heterogeneity of the rock mass will reduce the efficiency of a flow barrier. However, the same reduction of flow that is obtained with a barrier in a homogeneous rock mass, can be obtained for a barrier in a heterogeneous rock mass, if the conductivity contrast is increased. For an encapsulation in a heterogeneous rock mass of Äspö properties, the same reduction of flow is achieved with a barrier having a conductivity contrast that is about half an order of magnitude larger than that of a barrier in a homogeneous rock mass.

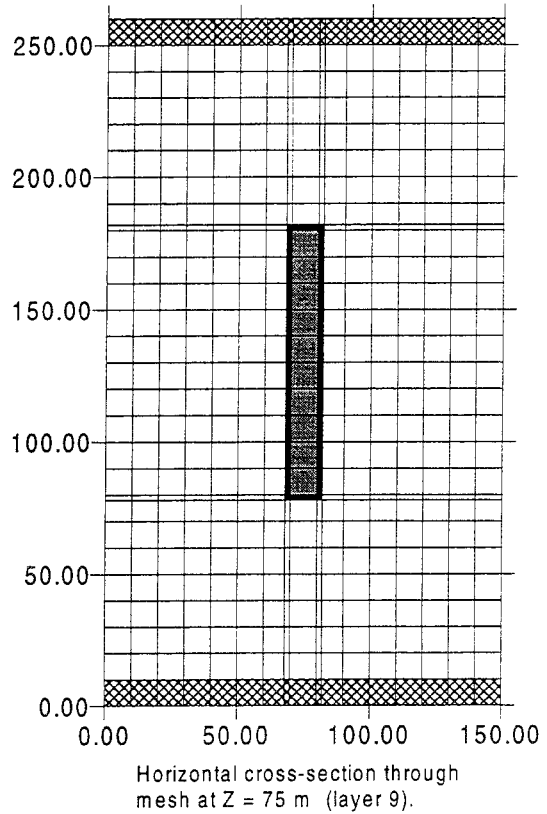
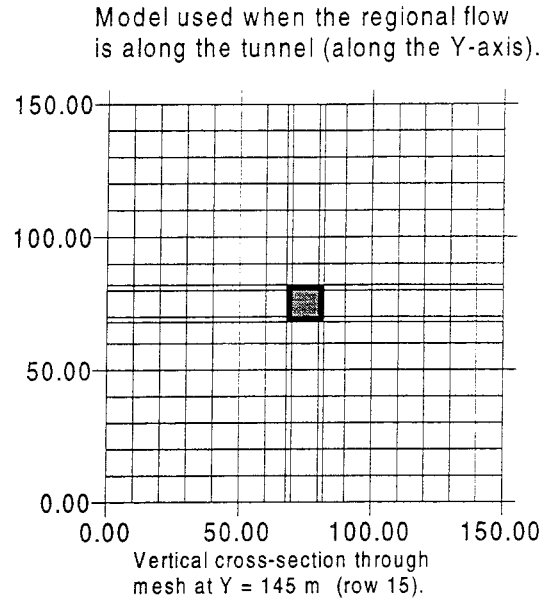
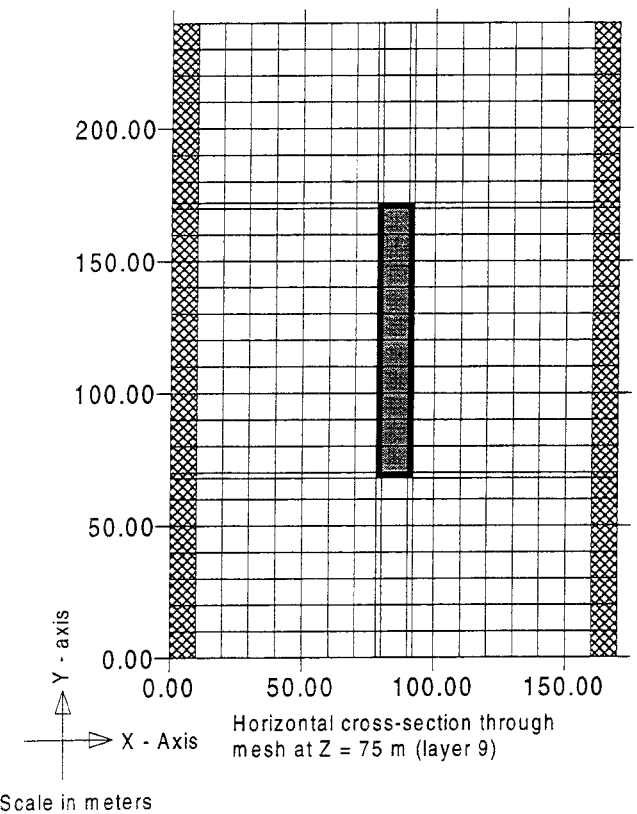
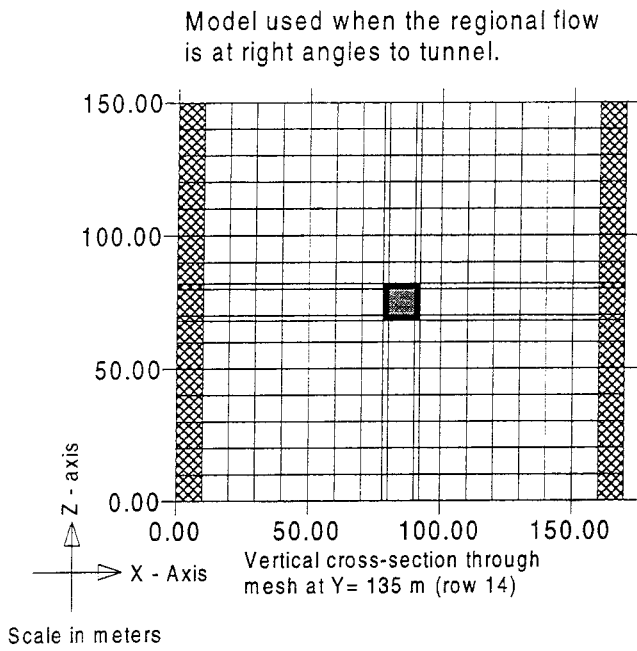
Studying the results of this chapter, and remembering that the effective conductivity of the rock mass is small, it is concluded that a large reduction of the flow of an encapsulation is more easily obtained if the flow barrier is a positive barrier than if it is a negative barrier. This follows from the fact that it is difficult to make a flow barrier which is much less permeable than the effective conductivity of the rock mass (bentonite barrier), but it is very easy to make a flow barrier which is much more permeable than the effective conductivity of the rock mass (sand or gravel barrier, etc).



-  The rock mass.
-  The flow barrier.
-  The encapsulation.
-  Prescribed head boundary condition.
-  Flowpath

Y - axis
X - Axis
Scale in meters

FIGURE 7.1 EFFECTS OF A FLOW BARRIER, FLOW PATTERN
Two dimensional models illustrating the effects of a negative and a positive flow barrier, both for a homogeneous and a heterogeneous rock mass. The flowpaths represent the groundwater flow. The larger the number of flowpaths, the larger the flow.







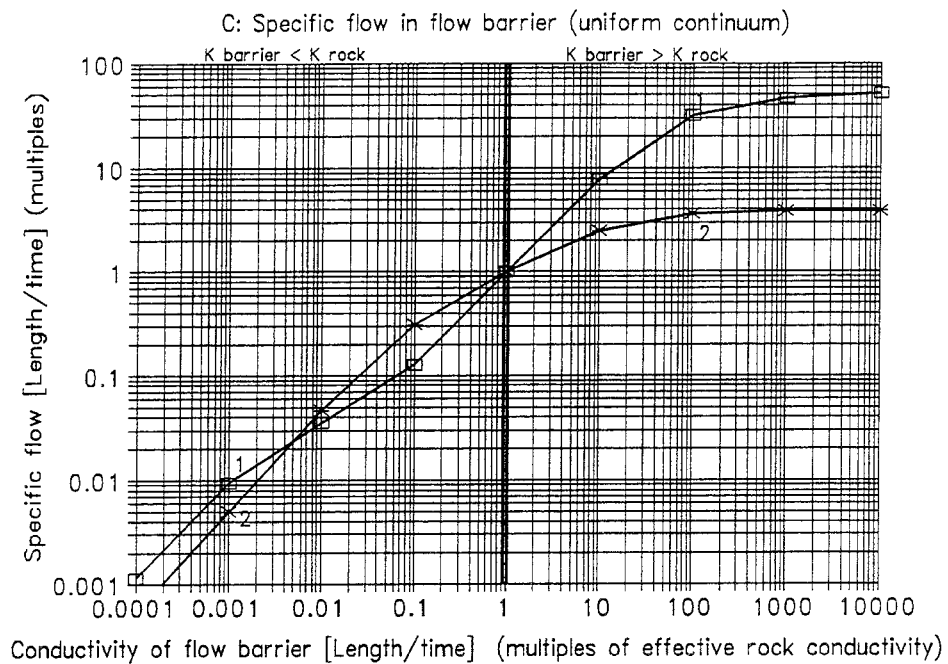
-  Cells (blocks) representing the rock mass.
-  Cells (blocks) representing the flow barrier.
-  Cells (blocks) representing the encapsulation.
-  Cells (blocks) representing the rock mass. These cells have a prescribed head boundary condition.

FIGURE 7.2
MODEL OF A TUNNEL WITH A FLOW BARRIER AND AN ENCAPSULATION.
 Example of mesh, horizontal and vertical cross-sections. Minimum distance between flow barrier and boundary is represented by seven cells (blocks). Rock mass, block size: 10x10x10m. Encapsulation block size: 10x10x10m, length: 100m. Flow barrier, thickness: 2m, at all sides of the encapsulation.

(i)
 Specific flow
 in flow barrier.
Encapsulation
 Length =100m
 Cross-S=100m²
 Conductivity=1
Flow barrier
 At all sides
 Thickness= 2m
 Conductivity=..



(ii)
 Total flow
 in flow barrier.
Encapsulation
 Length =100m
 Cross-S=100m²
 Conductivity=1
Flow barrier
 At all sides
 Thickness= 2m
 Conductivity=..

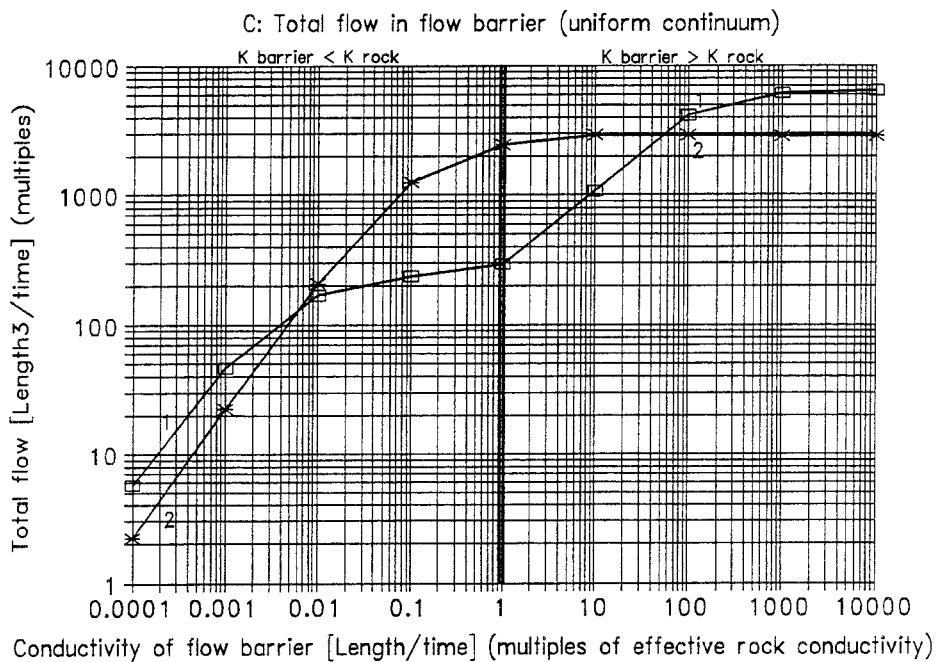
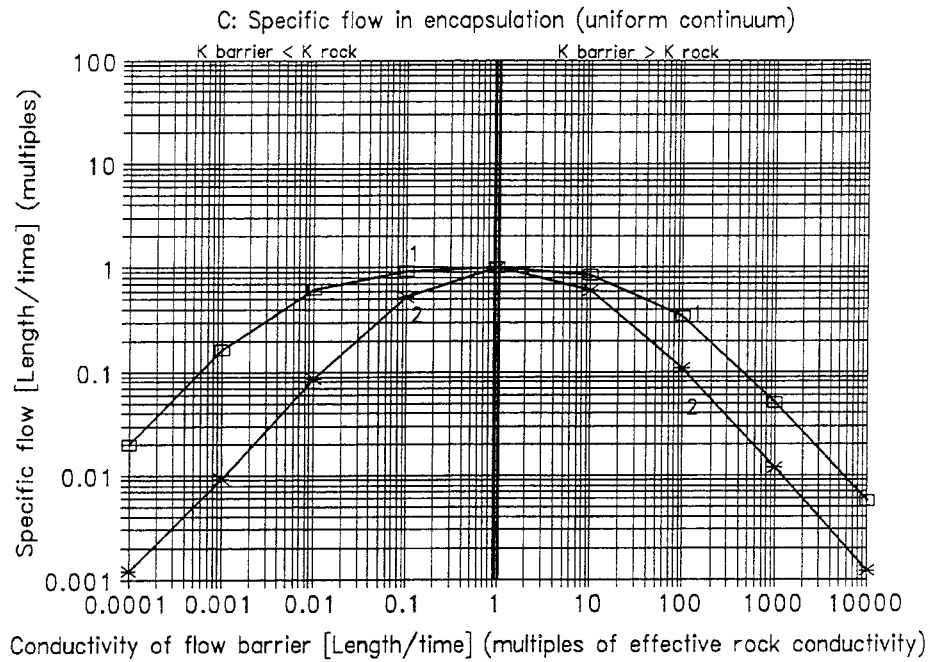


Figure 7.3 FLOW IN A FLOW BARRIER, SENSITIVITY TO BARRIER CONDUCTIVITY
 Specific flow (i) and Total flow (ii) in a flow barrier surrounding an encapsulation,
 versus the conductivity of the flow barrier. The conductivity of the encapsulation is
 equal to the effective conductivity of the rock mass. The rock mass is defined as
 homogeneous - uniform continuum model.
 The flow is given as multiples of an unknown regional flow.

The regional flow is directed:

- 1: Along the tunnel, denoted by squares.
- 2: At right angles to tunnel, denoted by crosses.

(i)
 Specific flow in
 encapsulation.
Encapsulation
 Length =100m
 Cross-S=100m²
 Conductivity=1
Flow barrier
 At all sides
 Thickness= 2m
 Conductivity=..



(i)
 Total flow in
 encapsulation.
Encapsulation
 Length =100m
 Cross-S=100m²
 Conductivity=1
Flow barrier
 At all sides
 Thickness= 2m
 Conductivity=..

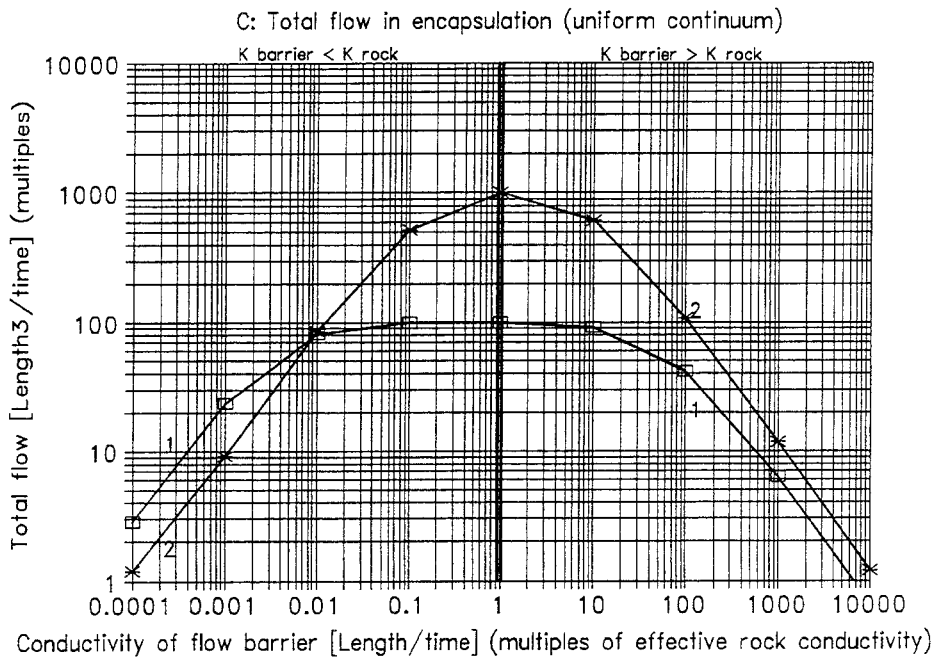
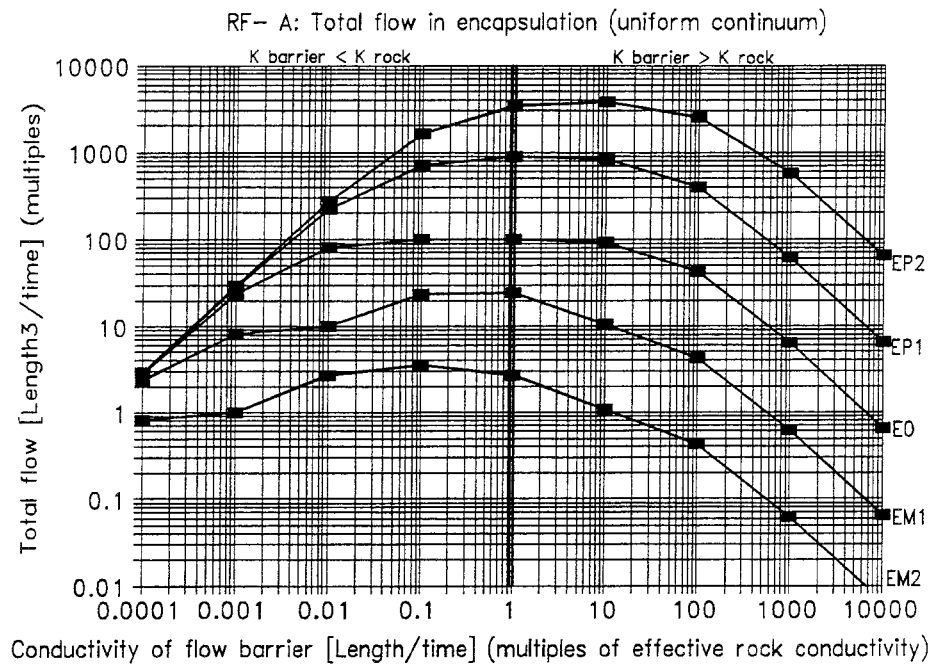


Figure 7.4 FLOW IN ENCAPSULATION, SENSITIVITY TO BARRIER CONDUCTIVITY
 Specific flow (i) and Total flow (ii) in an encapsulation, surrounded by a flow barrier, versus the conductivity of the flow barrier. The conductivity of the encapsulation is equal to the effective conductivity of the rock mass. The rock mass is defined as homogeneous - uniform continuum model. The flow is given as multiples of an unknown regional flow.

The regional flow is directed:
 1: Along the tunnel, denoted by squares.
 2: At right angles to tunnel, denoted by crosses.

(i)
Regional flow
along tunnel

Encapsulation
 Length = 100m
 Cross-S = 100m²
 Conductivity = ..
Flow barrier
 At all sides
 Thickness = 2m
 Conductivity = ..



(ii)
Regional flow
at right angles
to tunnel

Encapsulation
 Length = 100m
 Cross-S = 100m²
 Conductivity = ..
Flow barrier
 At all sides
 Thickness = 2m
 Conductivity = ..

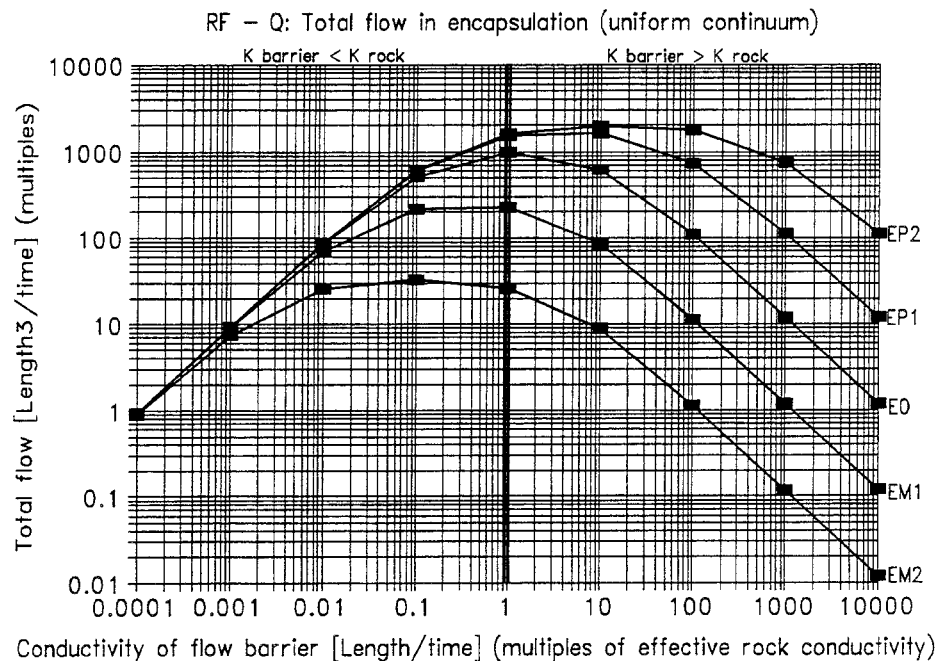
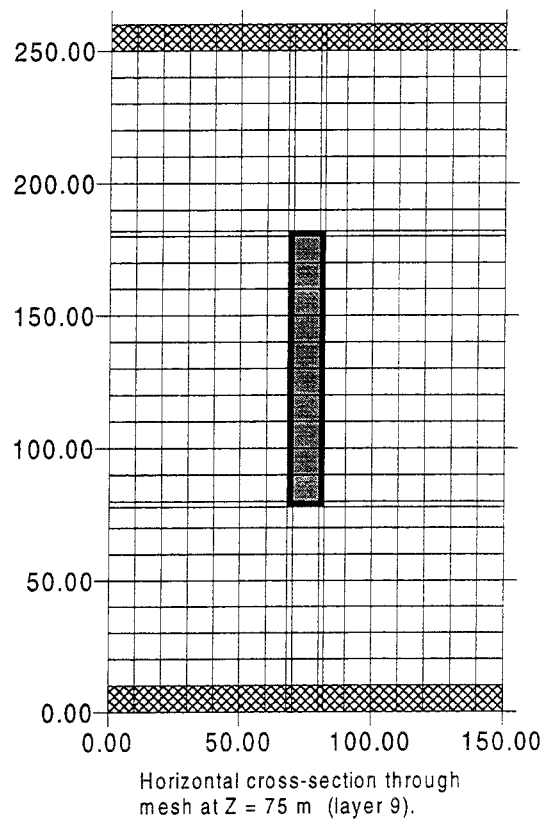
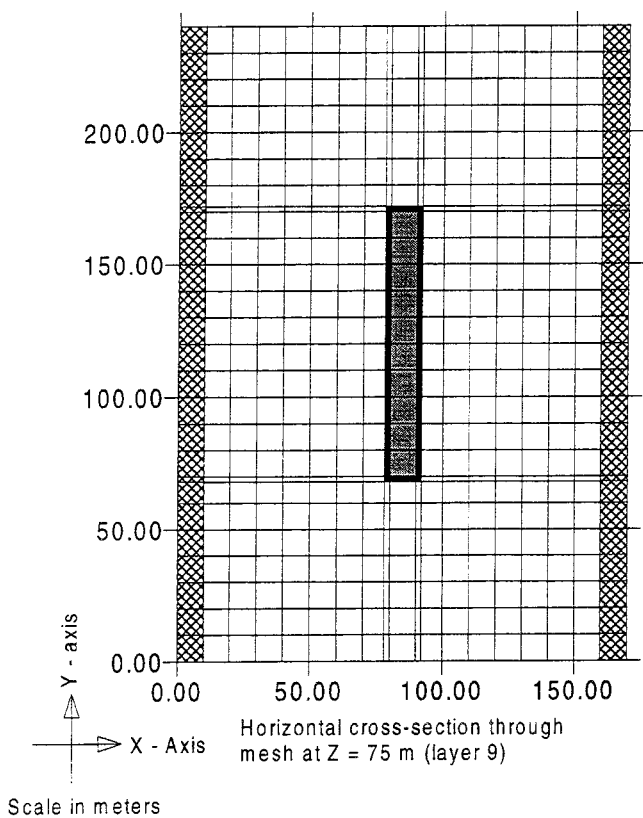
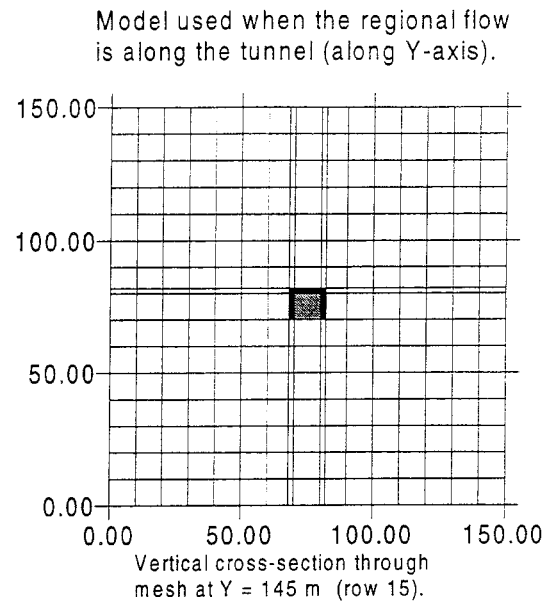
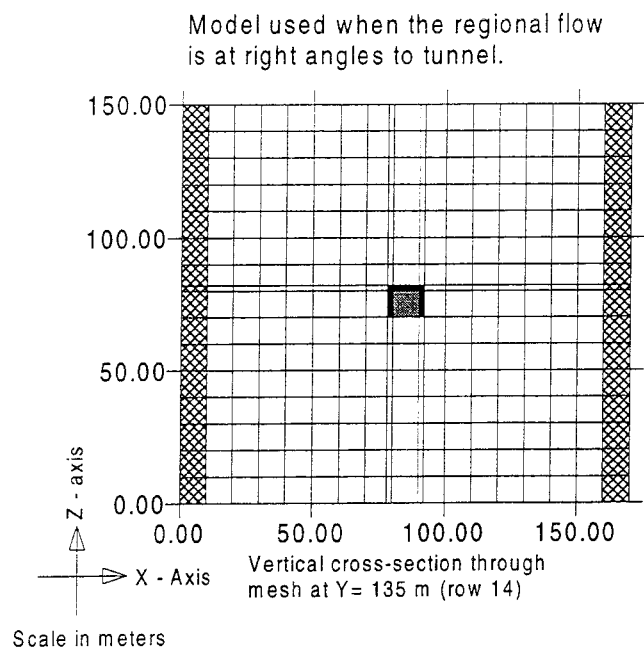


Figure 7.5 *FLOW IN ENCAPSULATION, SENSITIVITY TO ENCAPS. CONDUCTIVITY.*
 Total flow in an encapsulation, surrounded by a flow barrier, versus the conductivity of the flow barrier and the encapsulation. Uniform continuum model. The regional flow is directed along or at right angles to the tunnel. The flow is given as multiples of an unknown regional flow.

EP2 = The encapsulation conductivity is 100 times the effective rock conductivity.
 EP1 = The encapsulation conductivity is 10 times the effective rock conductivity.
 E0 = The encapsulation conductivity is equal to the effective rock conductivity.
 EM1 = The encapsulation conductivity is 0.1 times the effective rock conductivity.
 EM2 = The encapsulation conductivity is 0.001 times the effective rock conductivity.







-  Cells (blocks) representing the rock mass.
-  Cells (blocks) representing the flow barrier.
-  Cells (blocks) representing the encapsulation.
-  Cells (blocks) representing the rock mass. These cells have a prescribed head boundary condition.

FIGURE 7.6
MODEL OF A TUNNEL WITH AN ENCAPSULATION AND AN UNCOMPLETE FLOW BARRIER.
 Example of mesh, horizontal and vertical cross-sections. Minimum distance between flow barrier and boundary is represented by seven cells (blocks). Rock mass, block size: 10x10x10m. Encapsulation, block size: 10x10x10m, length: 100m. Flow barrier, thickness: 2m, above and at sides of encapsulation. No barrier below encapsulation.

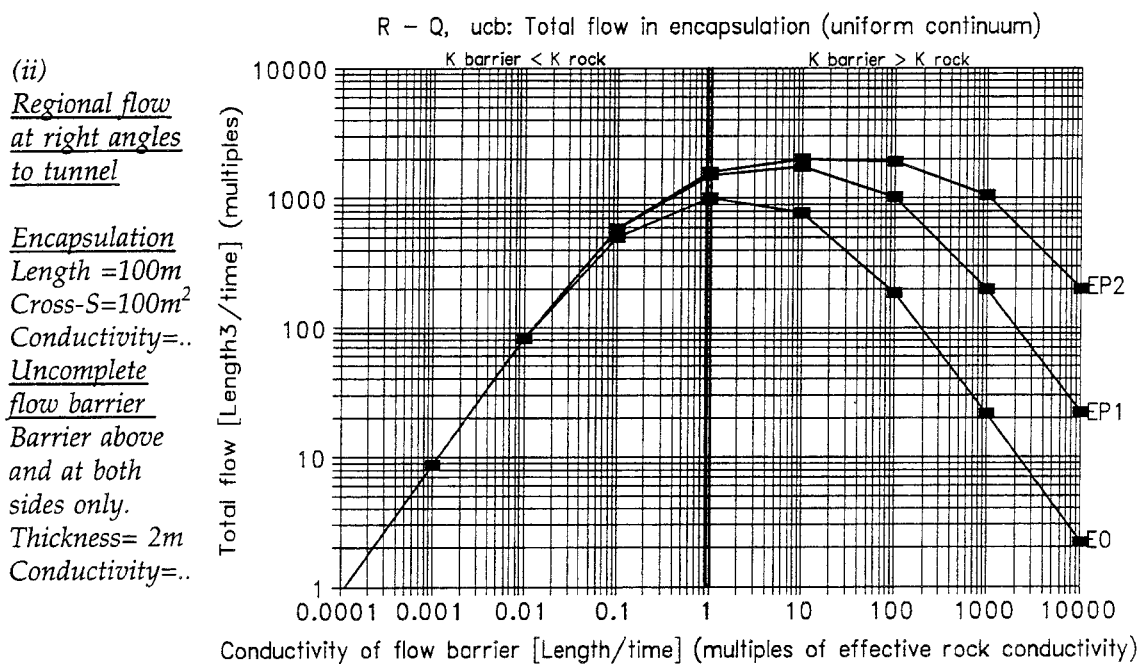
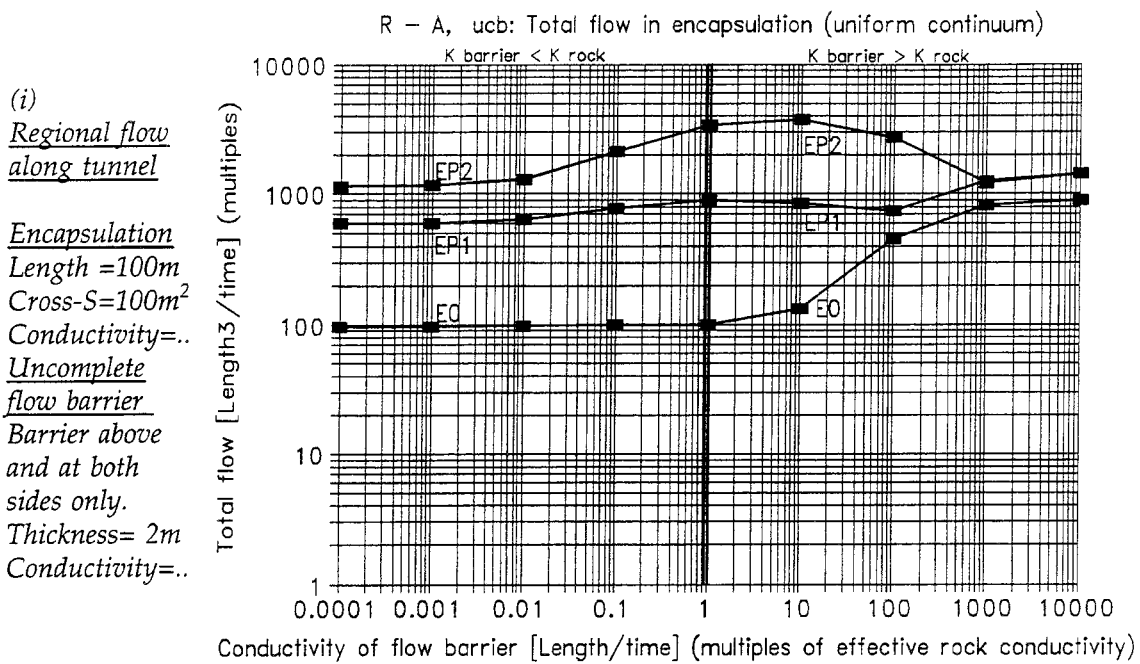
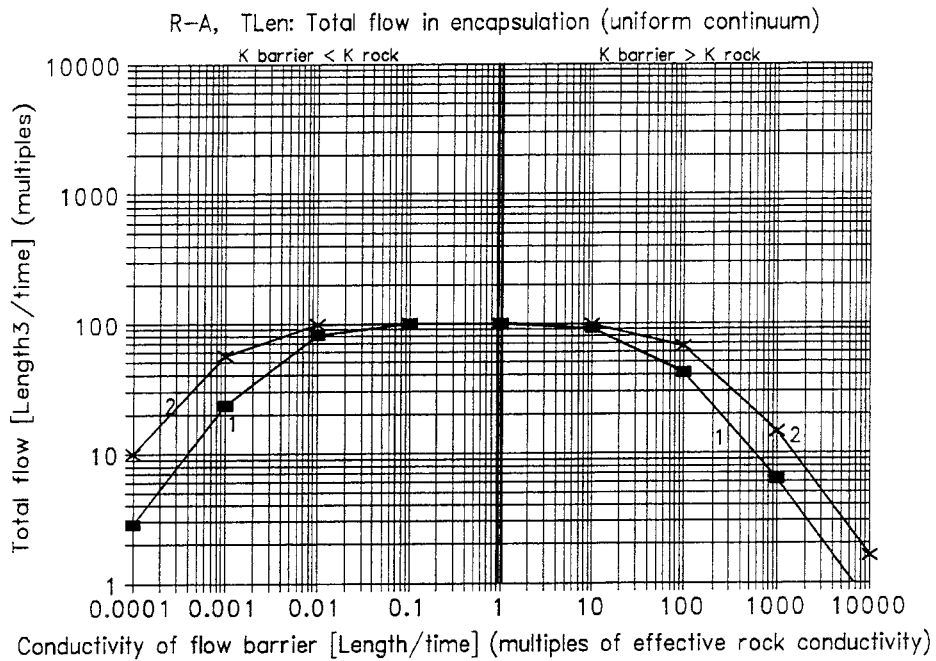


Figure 7.7 FLOW IN ENCAPSULATION, SENSITIVITY TO BARRIER EXTENSION. Total flow in an encapsulation, surrounded by an uncomplete flow barrier, versus the conductivity of the flow barrier and the encapsulation. The barrier exists above and at both sides of the encapsulation, no barrier at the bottom of the encapsulation. Uniform continuum model. The regional flow is directed along, or at right angles to the tunnel. The flow is given as multiples of an unknown regional flow.

EP2 = The encapsulation conductivity is 100 times the effective rock conductivity.
 EP1 = The encapsulation conductivity is 10 times the effective rock conductivity.
 E0 = The encapsulation conductivity is equal to the effective rock conductivity.

(i)
Regional flow along tunnel
Encapsulation
 Length =..
 Cross-S=100m²
 Conductivity=..
Flow barrier
 At all sides:
 Thickness= 2m
 Conductivity=..



(ii)
Regional flow at right angles to tunnel
Encapsulation
 Length =..
 Cross-S=100m²
 Conductivity=..
Flow barrier
 At all sides:
 Thickness= 2m
 Conductivity=..

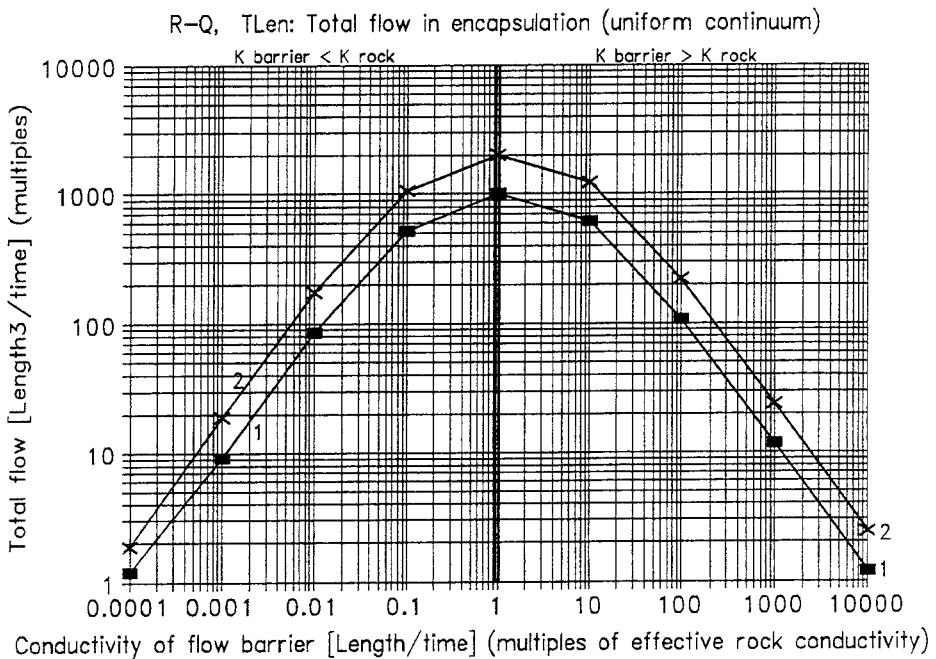


Figure 7.8 **FLOW IN ENCAPSULATION, SENSITIVITY TO TUNNEL LENGTH.**
 Total flow in an encapsulation, surrounded by a flow barrier, versus the conductivity of the flow barrier, as well as the length of the encapsulation (length of the tunnel). Uniform continuum model. The regional flow is directed along or at right angles to tunnel. The flow is given as multiples of an unknown regional flow.
 1 = The encapsulation length is 100m (filled squares).
 2 = The encapsulation length is 200m (crosses).

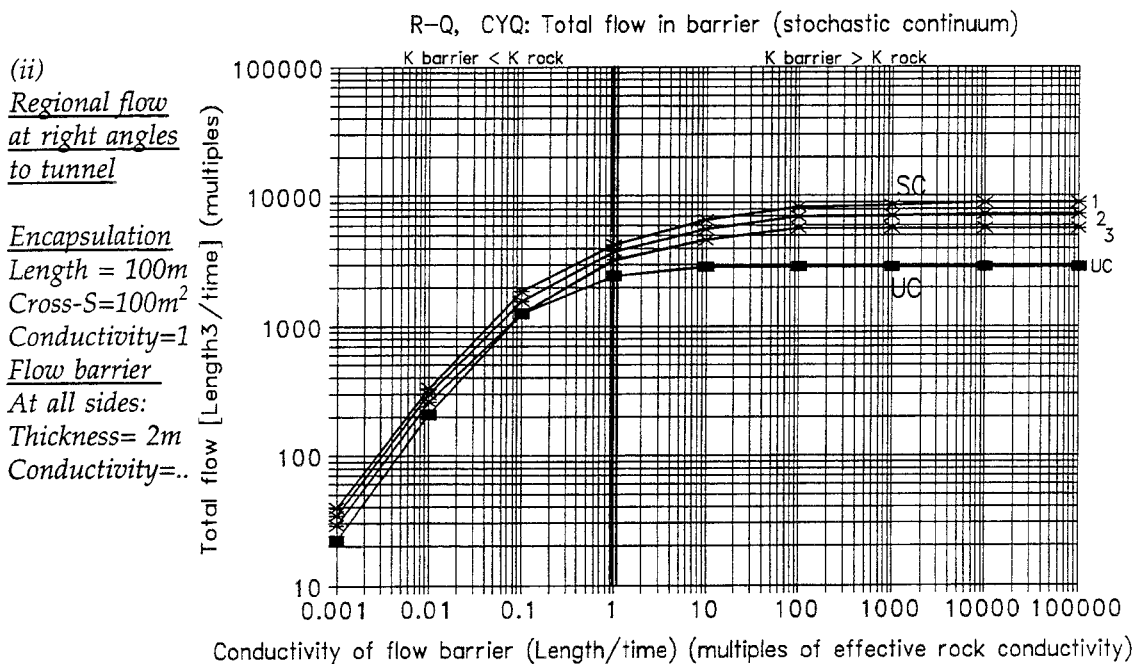
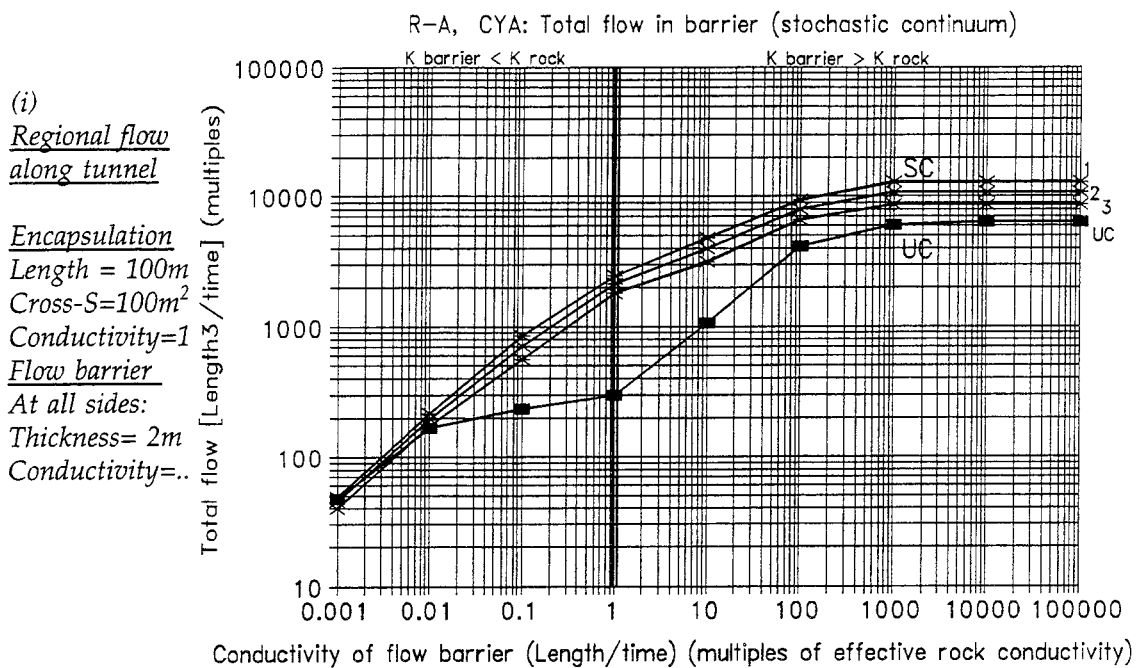
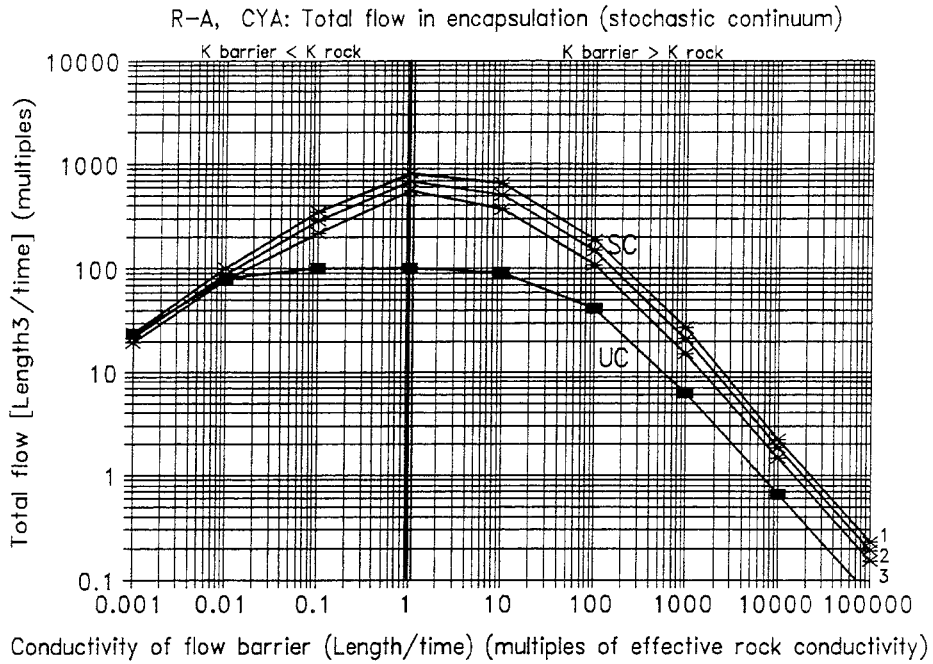


Figure 7.9 FLOW IN A FLOW BARRIER, SENSITIVITY TO BARRIER CONDUCTIVITY
 Total flow in a barrier, surrounding an encapsulation, versus the conductivity of the flow barrier. Homogeneous flow medium - uniform continuum model.
 Heterogeneous flow medium - stochastic continuum model with properties representing Äspö (block: size 10x10x10m, K dist: STD 10Log K= 1.498).
 Conductivity of encapsulation is equal to the effective rock conductivity.
 The flow is given as multiples of an unknown regional flow.

- Stochastic continuum SC, is denoted by stars: (1) average flow plus one standard deviation, (2) average flow and (3) average flow minus one standard deviation.
- Uniform continuum UC, is denoted by filled squares.

(i)
Regional flow
along tunnel

Encapsulation
 Length = 100m
 Cross-S=100m²
 Conductivity=1
Flow barrier
 At all sides:
 Thickness= 2m
 Conductivity=..



(ii)
Regional flow
at right angles
to tunnel

Encapsulation
 Length = 100m
 Cross-S=100m²
 Conductivity=1
Flow barrier
 At all sides:
 Thickness= 2m
 Conductivity=..

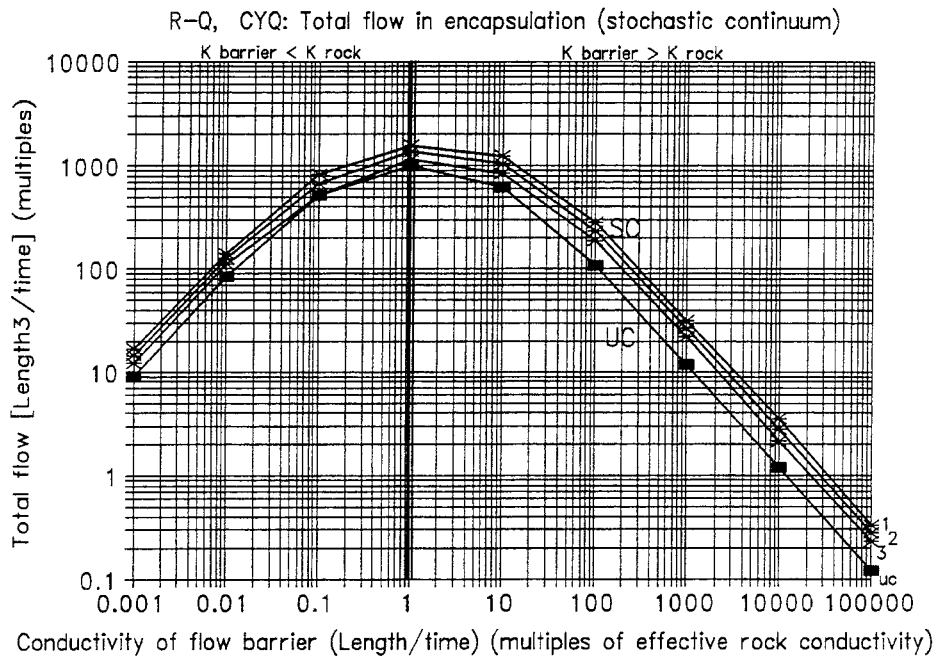


Figure 7.10 FLOW IN ENCAPSULATION, SENSITIVITY TO BARRIER CONDUCTIVITY

Total flow in an encapsulation, surrounded by a flow barrier, versus the conductivity of the flow barrier. Homogeneous flow medium - uniform continuum model. Heterogeneous flow medium - stochastic continuum model with properties representing Äspö (block: size 10x10x10m, K dist: STD 10Log K= 1.498). Conductivity of encapsulation is equal to the effective rock conductivity. The flow is given as multiples of an unknown regional flow.

- Stochastic continuum SC, is denoted by stars: (1) average flow plus one standard deviation, (2) average flow and (3) average flow minus one standard deviation.
- Uniform continuum UC, is denoted by filled squares.

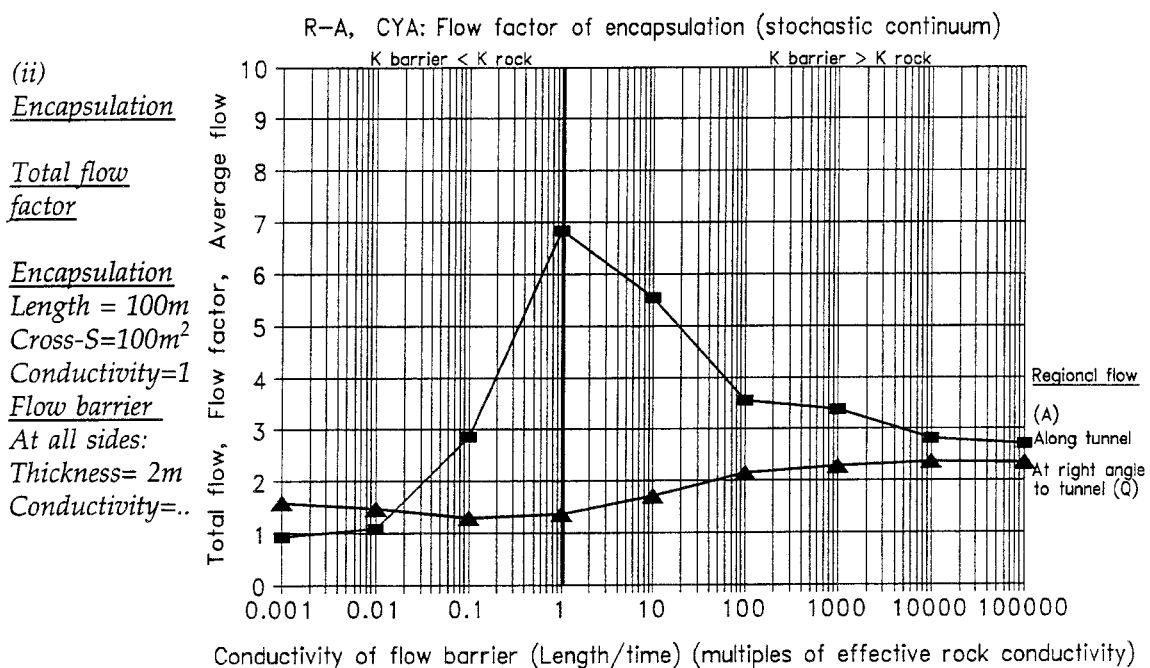
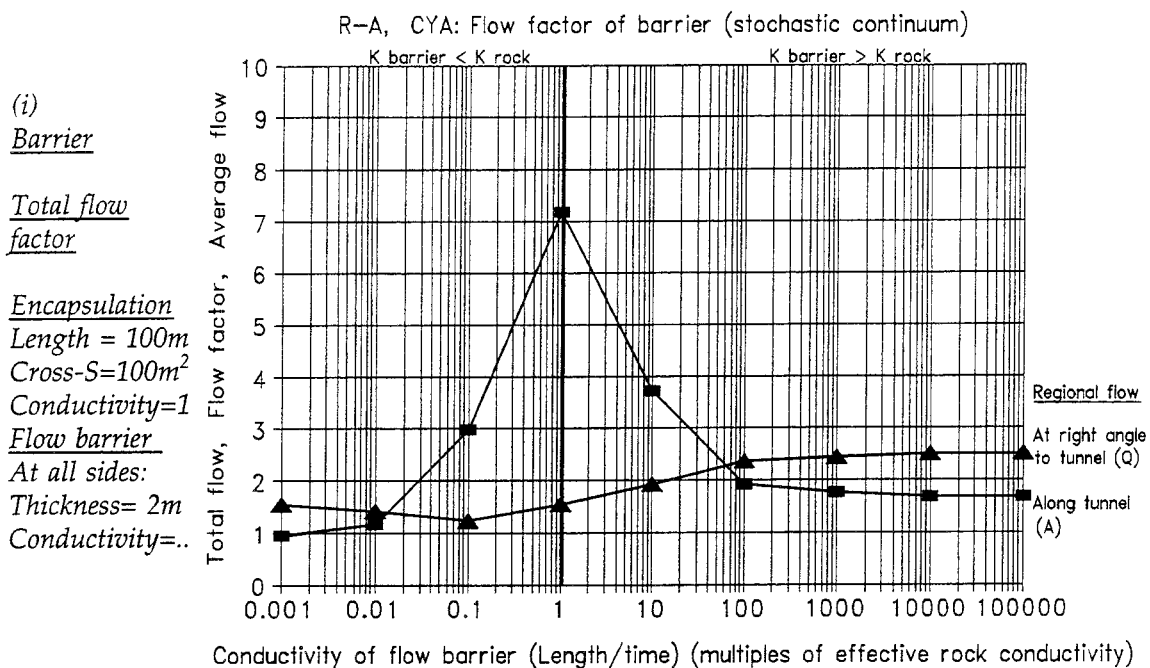
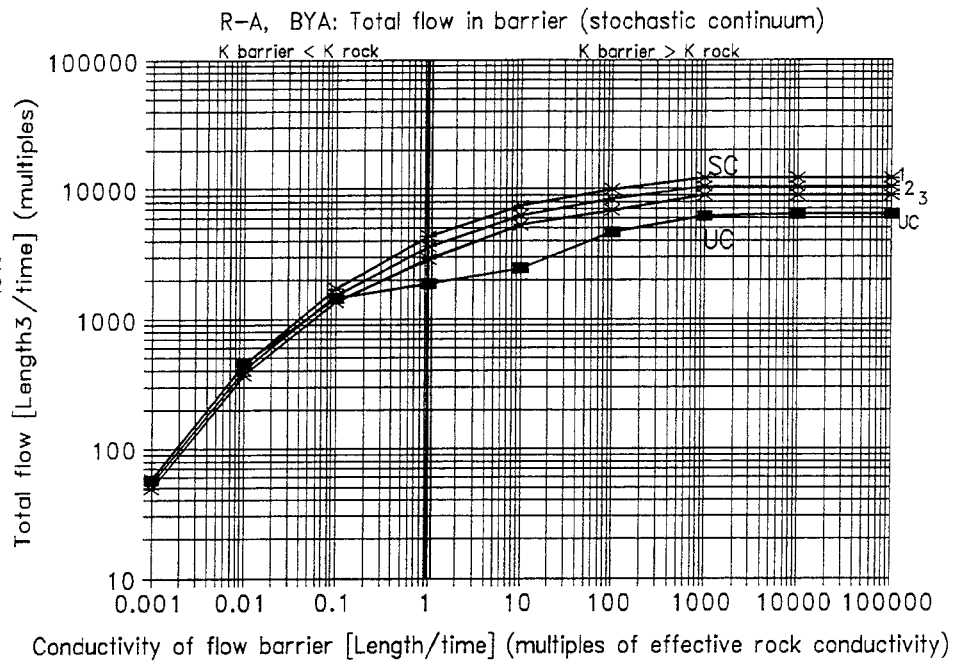


Figure 7.11 FLOW IN A BARRIER AND AN ENCAPSULATION, FLOW FACTOR
 Total flow factor of a barrier and of an encapsulation, versus the conductivity of the flow barrier. Homogeneous flow medium - uniform continuum model. Heterogeneous flow medium - stochastic continuum model with properties representing Åspö (block: size 10x10x10m, K dist: STD 10Log K= 1.498). The conductivity of the encapsulation is equal to the effective rock conductivity. The flow factor corresponds to average flow, average as regards the flow of different realisations. $Total\ flow\ factor = \frac{Total\ flow_{Stochastic}}{Total\ flow_{Uniform}}$

- Regional flow along the tunnel is denoted by squares.
- Regional flow at right angles to tunnel is denoted by triangles

(i)
Regional flow
along tunnel

Encapsulation
 Length = 100m
 Cross-S=100m²
 Conductiv.=10
Flow barrier
 At all sides:
 Thickness= 2m
 Conductiv.=..



(ii)
Regional flow
at right angles
to tunnel

Encapsulation
 Length = 100m
 Cross-S=100m²
 Conductiv.=10
Flow barrier
 At all sides:
 Thickness= 2m
 Conductiv.=..

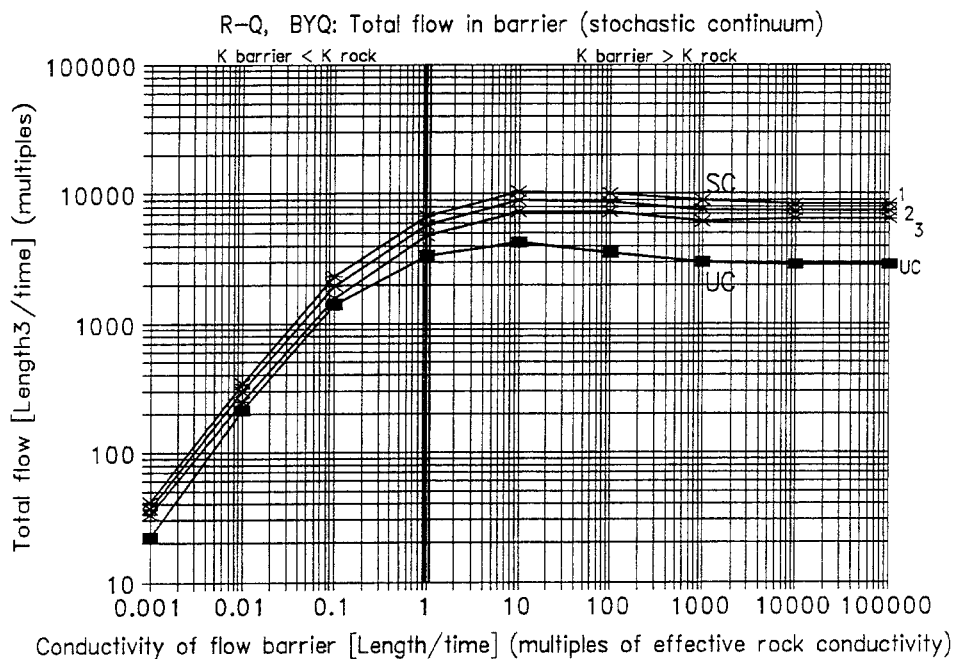
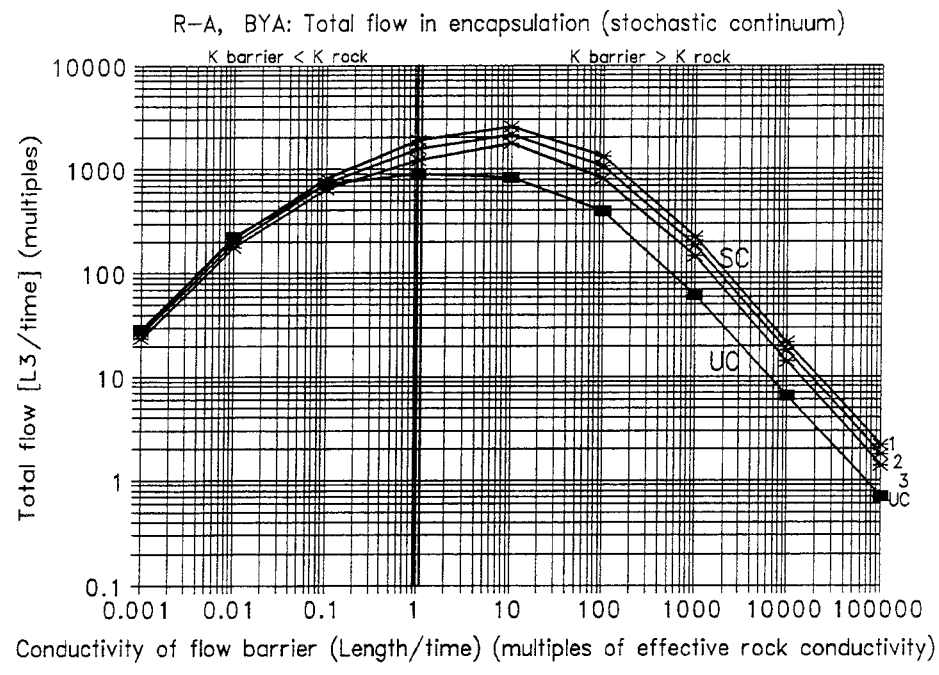


Figure 7.12 FLOW IN A FLOW BARRIER, SENSITIVITY TO BARRIER CONDUCTIVITY
 Total flow in a barrier, surrounding an encapsulation, versus the conductivity of the flow barrier. Homogeneous flow medium - uniform continuum model.
 Heterogeneous flow medium - stochastic continuum model with properties representing Äspö (block: size 10x10x10m, K dist: STD 10Log K= 1.498). The conductivity of the encapsulation is 10 times the effective rock conductivity.
 The flow is given as multiples of an unknown regional flow.

- Stochastic continuum SC, is denoted by stars: (1) average flow plus one standard deviation, (2) average flow and (3) average flow minus one standard deviation.
- Uniform continuum UC, is denoted by filled squares.

(i)
Regional flow
along tunnel

Encapsulation
 Length = 100m
 Cross-S=100m²
 Conductiv.=10
Flow barrier
 At all sides:
 Thickness= 2m
 Conductiv.=..



(ii)
Regional flow
at right angles
to tunnel

Encapsulation
 Length = 100m
 Cross-S=100m²
 Conductiv.=10
Flow barrier
 At all sides:
 Thickness= 2m
 Conductiv.=..

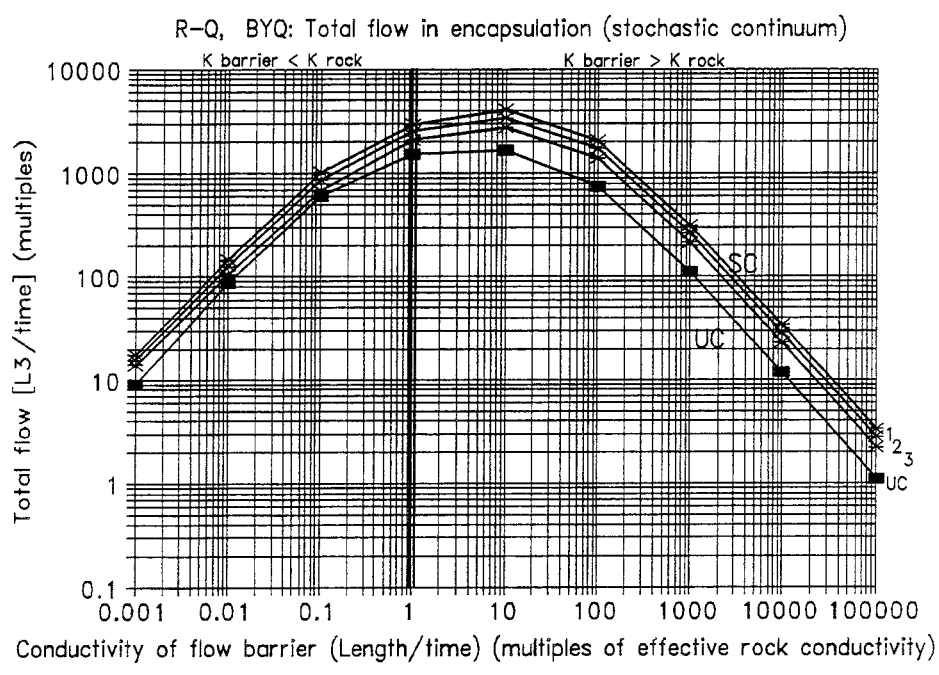


Figure 7.13 **FLOW IN ENCAPSULATION, SENSITIVITY TO BARRIER CONDUCTIVITY**
 Total flow in an encapsulation, surrounded by a flow barrier, versus the conductivity of the flow barrier. Homogeneous flow medium - uniform continuum model. Heterogeneous flow medium - stochastic continuum model with properties representing Aspö (block: size 10x10x10m, K dist: STD 10Log K= 1.498). The conductivity of the encapsulation is 10 times the effective rock conductivity. The flow is given as multiples of an unknown regional flow.

- Stochastic continuum SC, is denoted by stars: (1) average flow plus one standard deviation, (2) average flow and (3) average flow minus one standard deviation.
- Uniform continuum UC, is denoted by filled squares.

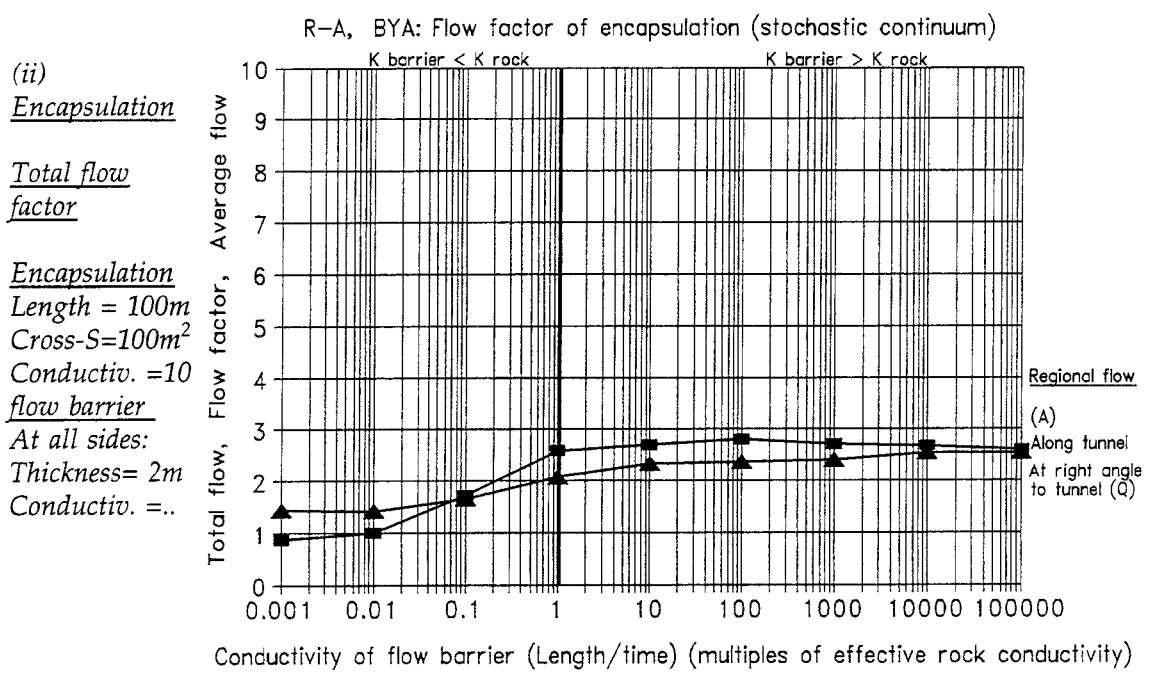
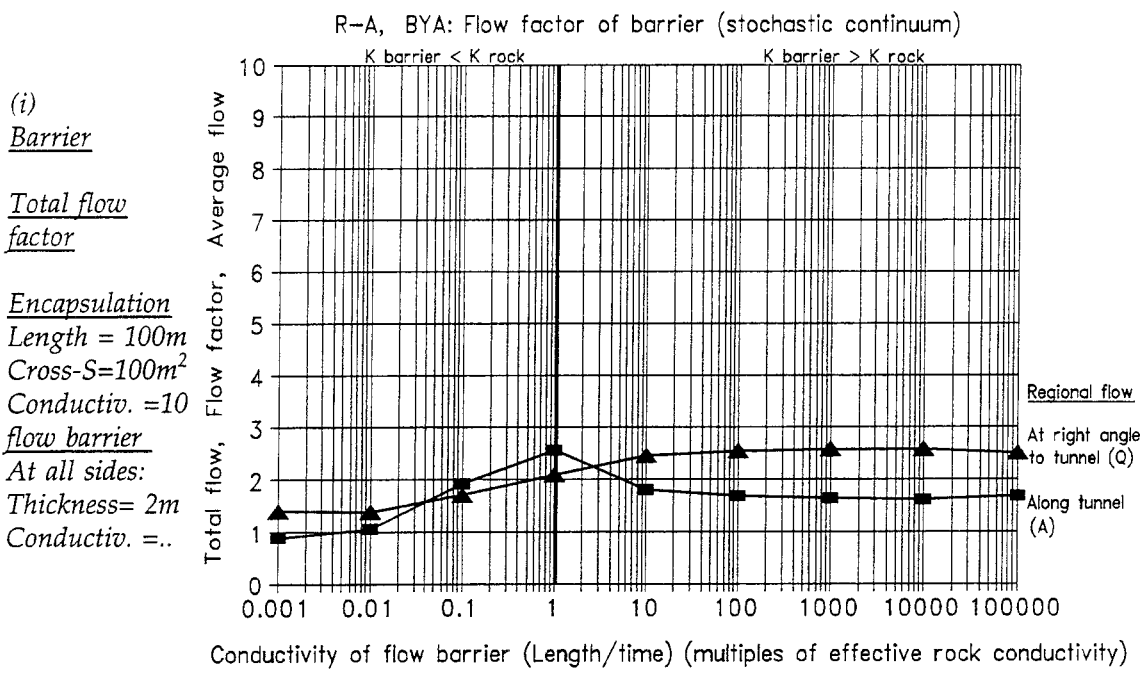


Figure 7.14 FLOW IN A BARRIER AND AN ENCAPSULATION, FLOW FACTOR
Total flow factor of a barrier and of an encapsulation, versus the conductivity of the flow barrier. Homogeneous flow medium - uniform continuum model. Heterogeneous flow medium - stochastic continuum model with properties representing Åspö (block: size 10x10x10m, K dist: STD 10Log K= 1.498). The conductivity of the encapsulation is 10 times the effective rock conductivity. The flow factor corresponds to average flow, average as regards the flow of different realisations. Total flow factor = Total flow_{Stochastic} / Total flow_{Uniform}

- Regional flow along the tunnel is denoted by squares.
- Regional flow at a right angles to the tunnel is denoted by triangles

Chapter 8.

Establishment of the model of repository SFL 3-5

8.1 Introduction

In the following chapter we will establish a model of the repository SFL 3-5. The purpose of the modelling is to study the performance of the tunnel system as regards the flow of groundwater in the tunnels. We will also study different alternatives of flow barriers and other measures to limit the flow in the tunnels. It will not be a site-specific model, hence, the flow in the tunnels will be given as a multiple of an unknown regional flow.

The basic concept is to make a detailed model of the repository, including different barriers etc, and also too include a part of the surrounding rock mass. Through the model, we will generate a regional flow of groundwater. This flow will be enhanced or reduced in the tunnel system, dependent on the design of the tunnels. This is what we call the performance of the tunnel layout.

8.2 Conceptual model

Introduction

The conceptual model includes information of the studied media (repository and rock mass) and the physical processes governing groundwater flow, but it includes only information relevant as regards the objectives of the study.

Studied scenario

During the construction of the repository and while the repository is loaded and kept open, the tunnels of the repository will be kept dry. It follows that the groundwater system of the surrounding rock mass will be drained by the repository tunnels. The repository will create a lowering of the groundwater heads in an area larger than the repository. Finally, when the repository is abandoned and no longer kept dry, it will become filled with groundwater, the groundwater head will raise in the repository and in the surrounding rock mass, and after some time reach a new equilibrium. The tunnels will mainly act as conductive features and cause a changed groundwater flow pattern, compared to the situation without the repository. The groundwater flow will converge towards the upstream part of a highly conductive tunnel and diverge from the downstream part. The size of the flow in the tunnels, will depend on the hydraulic properties of the rock mass and the materials inside the tunnels, but also on the size and the direction of the regional groundwater flow. The layout of the repository is given in Appendix E.

Time dependency

The studied situation is after the repository has been closed and the groundwater situation has reached an equilibrium. Thus, the situation is not time dependent.

Flow medium

The repository will be located in a fractured rock. As the site is not decided no site-specific data are available. The barriers inside the tunnels consist of sand and bentonite as well as a concrete encapsulation.

Regional groundwater flow

No detailed information of the regional groundwater flow is available, as the location of the site is not decided. Therefore, any direction of regional flow is possible.

Model size

The model should include the entire repository, as it is defined in Appendix E, and a part of the surrounding rock mass. The model should be large enough to minimize boundary constraints.

Physical processes

The model should be capable of simulating groundwater flow, in the rock mass as well as in the tunnels.

8.3 Mathematical-numerical model

Introduction

Based on the conceptual model, a formal model is established. The formal model is a mathematical description of the conceptual model, it is established by the use of a computer code. The formal model is used for simulations.

Mathematical approach

The formal model is a three-dimensional mathematical-numerical description of the studied hydraulic system. The analysis will be based on the continuum approach, as discussed in Chapter 2. We will use a finite difference model (GEOAN), see Appendix A, the model was first presented by Holmén (1992).

Finite difference mesh and layout of repository

Meshes of different size have been used to represent the studied system. The purpose of using different meshes was to estimate the boundary constraints affecting the models. Regardless of the size of the models studied, the layout of the repository was the same in all models. The layout of the tunnels in the model follows, as much as possible, the preliminary layout, as given by Forsgren *et al* (1996) and presented in Appendix E. We will slightly adjust and generalize the layout, to make it possible to represent the layout by the numerical method used. A general overview of the size of the different parts of the repository is given in Table 8.1, both for the preliminary design and for the generalized layout used in the models. The layout of the repository, as defined in all models (meshes), is given in Figures 8.1. and 8.2.

A comparison between the preliminary design and the generalized layout (Table 8.1) demonstrates that the differences are small. Thus, we believe that the repository layout, as included in the models, is a good representation of the actual layout, as given in the preliminary design.

Most of the blocks (cells) representing the rock mass were of the same size 10x10x10m in the models used for estimation of the boundary effects; in the final model, used for predictive simulations, the blocks representing the rock mass had a varying size - the size was invreased towards the boundary. The final model is given in Figure 8.4.

The regional flow and the boundary conditions

The model represents a limited part of the rock mass, the regional groundwater flow is created by the use of boundary conditions. This is done by assigning all blocks (cells) along the outer boundary of the model the prescribed head condition. The head of these cells is calculated in such a way that they will generate a flow through the model, according to a defined direction and gradient (see Appendix C.). All other blocks in the model are of the continuous type. The size of the regional flow is given by the gradient between the boundaries and the conductivity of the flow medium. These properties will be selected in such a way that the regional specific flow will be equal to 1 m/s. We want

this size of the regional flow, because if the regional flow is 1 m/s, the flow in the tunnels will be multiples of this flow, and consequently directly proportional to an unknown regional flow. The direction of the regional flow is defined in accordance with a system of horizontal and vertical angles, given in Figure 8.3.

Hydraulic Conductivity

The actual hydraulic conductivity of the rock mass is unknown, as no site-specific data are available, but the hydraulic conductivity of the materials inside the tunnels can be prescribed, based on available material and desired function of the barriers.

The purpose of the study is to predict the flow through the tunnels after closure. The flow in the tunnels will be calculated as multiples of an unknown regional flow. The lay-out of the repository is fixed (length of tunnels etc). It follows from this, that the absolute size of the hydraulic conductivity of a studied medium is of limited interest. *If the flow in the tunnels is expressed as a multiple of the regional flow, it is the contrast in hydraulic conductivity between the rock mass and the materials in the tunnels which determines the flow in the tunnels.*

To get the best numerical results, and for reasons of flexibility as well as for the purpose of getting a regional flow equal to 1 m/s, the rock mass of the model was assigned a hydraulic conductivity equal to 1 m/s. The conductivity values of all other media (the tunnels) were related to this value. We call the conductivity values used in the model "relative conductivity values". The relative values are equal to the conductivity contrasts between the rock mass and the studied media.

If we want absolute values instead of the relative values, it is not difficult to recalculate the conductivity values used (the relative conductivity) to absolute values. All we have to do is to select the conductivity of a specific medium, i.e. the rock mass, and use this value together with the relative conductivities to calculate the absolute conductivity of all other media. In other words, we relate the conductivity of the other media to the "known" conductivity of a specific medium (the rock mass). We call these conductivity values, that have been related to the conductivity values used in the model, the absolute conductivities.

For the case of simplicity, in the following discussions we will use the relative hydraulic conductivity of the discussed medium.

The rock mass was assigned a hydraulic conductivity by the use of an isotropic conductivity formulation; although in reality the conductivity of a fractured rock is anisotropic. The conductivity was set to 1 (relative value), see Table 8.2.

SFL 3 contains a flow barrier and an encapsulation. The encapsulation was defined as a homogeneous medium with a conductivity equal to 10 times that of the rock mass (relative value). The flow barrier was also defined as a homogeneous medium with a conductivity that was varied between different scenarios, between, 0.001 to 100000 times that of the rock mass (relative values). The conductivity values are given in Table 8.2.

SFL 4 contains no flow barriers and no encapsulation. The tunnel was modelled as empty, or filled with sand and gravel. It was defined as a homogeneous medium with a conductivity that was varied between different scenarios, between, 0.1 to 100000 times that of the rock mass (relative values), see Table 8.2.

SFL 5 contains a flow barrier and an encapsulation. The encapsulation was defined as a homogeneous medium with a conductivity equal to 10 times that of the rock mass

(relative value). The flow barrier was also defined as a homogeneous medium with a conductivity that was varied between different scenarios, it was varied between: 0.001 to 100000 times that of the rock mass (relative values). The conductivity values are given in Table 8.2.

The plug that seals a tunnel, was defined by the use of an anisotropic conductivity formulation. For a plug, the conductivity in the direction of the tunnel was set as representing: 1 m of bentonite and 5 m of concrete. The conductivity of the concrete was defined as equal to that of the rock mass. The conductivity of the bentonite was defined as 10 times smaller than that of the rock mass (relative value), see Table 8.2

Compared to the conductivity of the rock mass, a structure (a tunnel or a barrier) that is as much as 10000 or 100000 times more permeable, could be regarded as an empty structure, that is a structure with no filling, see the concept of threshold conductivity in Section 3.

Access tunnels

For the construction of the repository and for the transportation of the nuclear waste down to the repository, access tunnels need to be constructed. Different alternatives have been discussed, three major alternatives are possible: (i) vertical shafts, (ii) a ramp (a spiral ramp or an inclined, approximately straight ramp), or (iii) a combination of both alternatives. The different alternatives produce different arrangements of connecting the SFL 4 tunnel to the access tunnels. For the lay-out of the repository itself, the differences are minor. The alternatives of access tunnel arrangement are discussed in Forsgren *et al* (1996). Whatever the alternative to be used in the final design, it is important that the access tunnels are carefully separated from the repository when the repository is closed and abandoned. It is otherwise possible that the access tunnels may work as large antennas and lead groundwater through the access tunnels towards the repository and, as a consequence, increase the groundwater flow through the repository.

The purpose of our model is to study the situation after the repository has been closed and abandoned. Hence, in our model we presume that the access tunnels are separated from the repository in such a way that they do not influence the flow of the repository. Because of this assumption, we do not need to include the access tunnels in our model of the repository.

In reality a perfect separation is not possible, but if efficient plugs are installed in the access tunnels and/or the access tunnels are backfilled with a low-permeability filling, the effects that they may cause on the flow inside the repository is minor. We believe that the generalization of not including the access tunnels is an acceptable generalization.

8.4 System of angles defining the direction of the regional flow

The direction of the regional flow can be described by a horizontal angle and a vertical angle. The models are based on a cartesian coordinate system, the horizontal angles are given clockwise from the positive direction of the Y-axis, the vertical angles are given upwards or downwards from the plane defined by the X- and Y-axis i.e. the horizontal plane. For the models that include the repository, this system of angles is defined in Figure 8.3.

For the cardinal directions of the regional flow, the system gives the following angles:

<u>Code</u>	<u>Direction</u>	<u>Horizontal angle</u>	<u>Vertical angle</u>
U:	Vertical flow	Undefined	+90 or -90 deg.
A:	Horizontal, along SFL 3 and 5.	0 or 180 degrees	0 degrees
Q:	Horizontal, at right angle to SFL 3 & 5	90 or 270 degrees	0 degrees

8.5 Estimation of boundary effects

Method for estimation of boundary effects

We will study the flow in the tunnels of the repository for different directions of the regional flow. For the estimation of boundary effects we will use the numerical method of multiple meshes, method B1, as described in Section 4.

Studied part of the repository, direction of regional flow

The analysis of boundary effects will be carried out for the total flow of SFL 4; because this is the part of the repository that is most influenced by the specified head condition at the outer boundaries of the models. For SFL 4, the largest boundary effects will occur when the regional flow is in the horizontal plane, as the SFL 4 tunnel forms a large closed structure in the horizontal plane (see Figure 8.1). SFL 4 is a closed and approximately quadratic structure in the horizontal plane; it follows that the horizontal direction of the regional flow is not as important as the vertical direction. For the analysis of boundary effects we have set the direction of the regional flow in the horizontal plane and along the Y-axis of the model. The direction of the regional flow could also be defined in accordance with a system of horizontal and vertical angles, as given in Figure 8.3. For this system the angles become: horizontal= 0 degrees, vertical= 0 degrees.

Size and hydraulic conductivity of models

We will use three-dimensional models with a block size of 10x10x10m. We will use different models with successively larger meshes, the minimum distance between the repository and the outer boundary of the models will be increased from 20m (two blocks) to 80m (eight blocks). To get an efficient model for the predictive simulations, we will also use a model with a varying block size, in this model the block size is increased towards the boundaries. In the models of this section (Sec.8.5), the conductivity of SFL 4 tunnel was set to 10000 times that of the rock mass, the conductivity of the flow barriers of SFL 3 and SFL 5 were set to 0.1 times that of the rock mass.

Results

The different values of calculated flow in the tunnel of SFL 4, predicted by different models with regular meshes, could be used for estimation of boundary effects and for an estimation of the correct flow, see Section 4. The results of the analyses are given in Figures 8.5 and 8.6 (a Table is included in Fig.8.6). As demonstrated in the figures, the error in predicted flow decreases as the size of the model increases. The correct flow was estimated by the use of the method given in Section 4 (method of multiple meshes, B1).

Using a three-dimensional model with a rock block size of 10x10x10 m and a minimum number of 8 blocks between the studied tunnel and the boundary (model M8), we will overestimate the flow; for SFL 4, the overestimation in predicted total flow will be about 20 percent of the estimated correct total flow. Compared to the models of previous chapters (see Table.4.1 and Table 6.1) these errors are larger; that is because the repository is a larger structure than the structures previously studied.

One way of getting a smaller error is to increase the number of blocks between the repository and the outer boundary of the model, that is the same as increasing the size of the model. By the use of 17 blocks of size 10x10x10m (distance 165m) between the

repository and the outer boundary, the error will probably be less than 10 percent. But such a model would include more than 60000 blocks, which would make the model numerically heavy.

For a uniform continuum model, we could without conceptual problems, use a mesh in which the sizes of the blocks vary e.g. the block size is increased towards the outer boundary of the model. For a stochastic continuum model it is more complicated. If blocks of different size represent the same heterogeneous medium, we will get different conductivity distributions that represent the same type of rock mass in the same model. This will cause effects that need to be considered (see Section 5.10). However, no such problems occur for a uniform continuum model. By increasing the block size towards the boundaries, we will still have the same lay-out at the center of the mesh (the repository) but the distance from the repository to the outer boundary of the model will be increased, for the same number of blocks. So, by using this concept we can reduce the boundary effects as we increase the size of the model. We can establish a model in which the boundary effects are small and in which the number of block is small as well.

A model with increased block size towards the boundaries, but with the same lay-out of the repository as for the models with regular meshes, is given in Figure 8.4. For this model, the predicted total flow in SFL 4 is only 1 percent larger than the estimated correct flow. Such an error is acceptable, and the error for other parts of the repository, or for other directions of the regional flow, is about the same or smaller. Note that we need models with regular meshes to be able to estimate the correct flow (see Chapter 4).

8.6 The mesh selected for predictive simulations

For the uniform continuum simulations, presented in the next chapter, we will use a model with a mesh as given in Figure 8.4. The mesh contains a minimum number of 6 blocks between the tunnels and the outer boundaries of the model. The size of the blocks representing the rock mass will be increased towards the outer boundaries, but the lay-out of the repository will be the same as in the models with a regular mesh (see Figure 8.1 and 8.2). The minimum distance between the repository and the outer boundaries of the model is about 230m. The model will contain about 28000 blocks.

The boundary effects, caused by the specified head boundaries, will give an overestimation of the flow in the tunnels. For the model, given in Figure 8.4 and for the predicted total flow of the SFL 4 tunnel, the maximum error is an overestimation of about 1 percent. Such an error is acceptable, and the error for other parts of the repository (SFL 3 and SFL 5), is about the same or smaller.

8.7 Alternative lay-out of repository

The study will include the effects of different conductivity values of the flow barriers surrounding SFL 3-5. Additionally, we will study different lay-outs as regards plugs installed at different places in the tunnels of the repository. In the basic lay-out, given in Figures 8.1 and 8.2, plugs occur at both ends of the SFL 3 and SFL 5 tunnels. Two alternative lay-outs have been studied.

- (i) No plugs occur inside the repository, the only barriers will be the flow barriers that surround SFL 3 and SFL 5.
- (ii) Eight plugs occur inside the repository, four plugs inside SFL 4, distributed in a symmetric way, and plugs at the ends of the SFL 3 and SFL 5.

The meshes of the models representing the two alternative lay-outs are given in Figure 8.7

Table 8.1 SIZE OF REPOSITORY, PRELIMINARY LAYOUT, AND GENERALIZED LAYOUT OF THE MODEL.

Table (i) Size of tunnels and caverns in the preliminary layout (Forsgren et al, 1996).

TUNNEL	Length (m)	Width (m)	Height (m)	Volume (m ³)
SFL 3 (cavern)	133	14	about 19	about 34000
SFL 4 (tunnel)	about 900	8	6.5	40000
SFL 5 (cavern)	133	14	about 19	about 34000

Table (ii) Size of tunnels and caverns in the model.

TUNNEL	Length (m)	Width (m)	Height (m)	Volume (m ³)
SFL 3 (cavern)	140	14	19	37240
SFL 4 (tunnel)	892	8	8	51712
SFL 5 (cavern)	140	14	19	37240

Table (iii) Size of the encapsulation in the preliminary layout (Forsgren et al, 1996).

TUNNEL	Length (m)	Width (m)	Height (m)	Volume (m ³)
SFL 3 (encap.)	114.6	10.8	10.7	13300
SFL 5 (encap.)	114.6	10.8	10.7	13300

Table (iv) Size of the encapsulation in the model.

TUNNEL	Length (m)	Width (m)	Height (m)	Volume (m ³)
SFL 3 (encap.)	120	10	10	12000
SFL 5 (encap.)	120	10	10	12000

Table (v) Size of the flow barrier in the preliminary layout (Forsgren et al, 1996).

TUNNEL	Thickness at each side of the encapsulation (m)	Thickness above the encapsulation (m)	Thickness below the encapsulation (m)
SFL 3 (flow barr.)	about: 1 - 2	about: 7 - 8	about: 1
SFL 5 (flow barr.)	about: 1 - 2	about: 7 - 8	about: 1

Table (vi) Size of the flow barrier in the model.

TUNNEL	Thickness of flow barrier (m) The position is given in relation to the encapsulation			Transport and load areas at both ends of the encapsulation.		Tot. Volume (m ³) Including tsp. and load areas
	At sides	Above	Below	Length (m)	Volume (m ³)	
SFL 3 (flow barr.)	2	10	2	one end: 20	Total: 7120	31160
SFL 3 (flow barr.)	2	10	2	one end: 20	Total: 7120	31160

Table 8.2

REPOSITORY MODEL OF SFL 3-5. Hydraulic conductivity of different media, as they are defined in the model. In the model, the conductivity is defined as a relative conductivity. A relative conductivity is equal to the conductivity contrast, between the rock mass and the studied media. By using relative values, we can calculate absolute values for different assumptions of the rock mass conductivity.

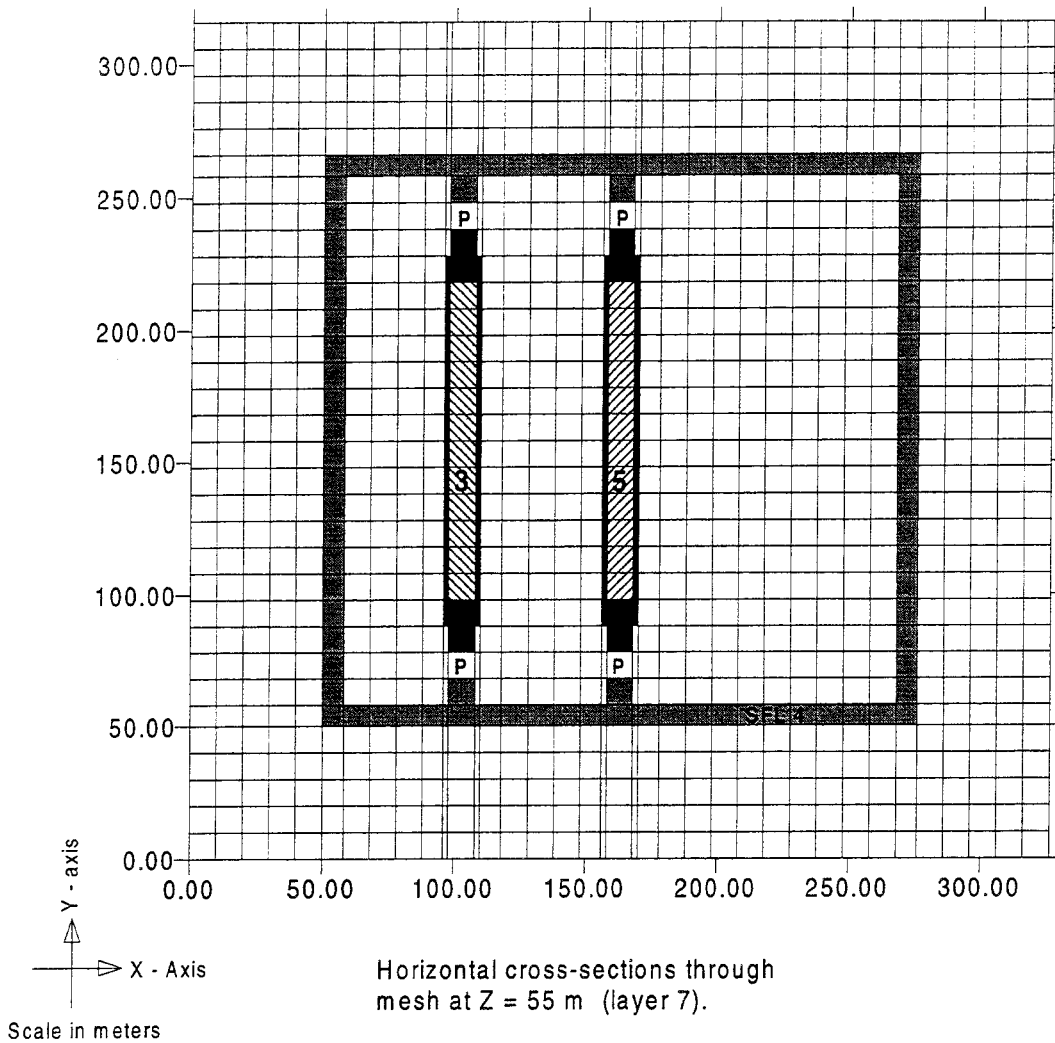
The table gives absolute conductivity values for two different assumptions of the rock mass conductivity.

ASSUMPTION 1: Rock mass conductivity is 1×10^{-9} m/s

ASSUMPTION 2: Rock mass conductivity is 1×10^{-8} m/s.

Two different cases will be discussed and compared in Chapter 9, these two cases are called: Case 1 and Case 2. The conductivities of different parts of the repository, as defined for these two cases, are given in the table below.

	MEDIUM	Hydraulic conductivity of the model (relative values) (conductivity contrasts)	ASSUMPTION 1. Hydraulic conductivity, Absolute values (m/s) (1)	ASSUMPTION 2. Hydraulic conductivity, Absolute values (m/s) (1)
Rock mass	Rock mass	1	10^{-9}	10^{-8}
SFL 3	Flow barrier (9 alternatives)	0.001, 0.01, 0.1 1, 10, 100 1000, 10000, 100000	$10^{-12}, 10^{-11}, 10^{-10}$ $10^{-9}, 10^{-8}, 10^{-7}$ $10^{-6}, 10^{-5}, 10^{-4}$	$10^{-11}, 10^{-10}, 10^{-9}$ $10^{-8}, 10^{-7}, 10^{-6}$ $10^{-5}, 10^{-4}, 10^{-3}$
	CASE 1	100000	10^{-4}	10^{-3}
	CASE 2	0.1	10^{-10}	10^{-9}
	Concrete encapsulation	10	10^{-8}	10^{-7}
SFL 4	Sand filling inside tunnel (7 alternatives)	0.1, 1, 10, 100 1000, 10000, 100000	$10^{-10}, 10^{-9}, 10^{-8}, 10^{-7}$ $10^{-6}, 10^{-5}, 10^{-4}$	$10^{-9}, 10^{-8}, 10^{-7}, 10^{-6}$ $10^{-5}, 10^{-4}, 10^{-3}$
	CASE 1	10000	10^{-5}	10^{-4}
	CASE 2	10000	10^{-5}	10^{-4}
SFL 5	Flow barrier (9 alternatives)	0.001, 0.01, 0.1, 1, 10, 100, 1000, 10000, 100000	$10^{-12}, 10^{-11}, 10^{-10},$ $10^{-9}, 10^{-8}, 10^{-7},$ $10^{-6}, 10^{-5}, 10^{-4}$	$10^{-11}, 10^{-10}, 10^{-9},$ $10^{-8}, 10^{-7}, 10^{-6},$ $10^{-5}, 10^{-4}, 10^{-3}$
	CASE 1	100000	10^{-4}	10^{-3}
	CASE 2	0.1	10^{-10}	10^{-9}
	Concrete encapsulation	10	10^{-8}	10^{-7}
Plug	Concrete plug (thickness 5 m)	1	10^{-9}	10^{-8}
	Bentonite barrier (thickness 1 m)	0.1	10^{-10}	10^{-9}
(1) $K_{abs.X} = K_{rel.X} / K_{rock}$ $K_{abs.x}$ = Absolute conductivity of medium X $K_{rel.X}$ = Relative conductivity of medium X K_{rock} = The assumed conductivity of the rock mass, this is the "known value" that all other values are related to.				







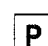
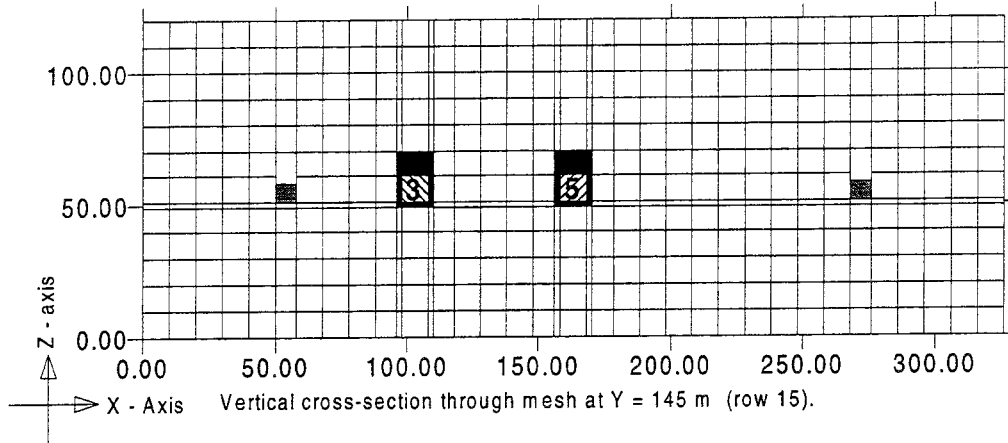
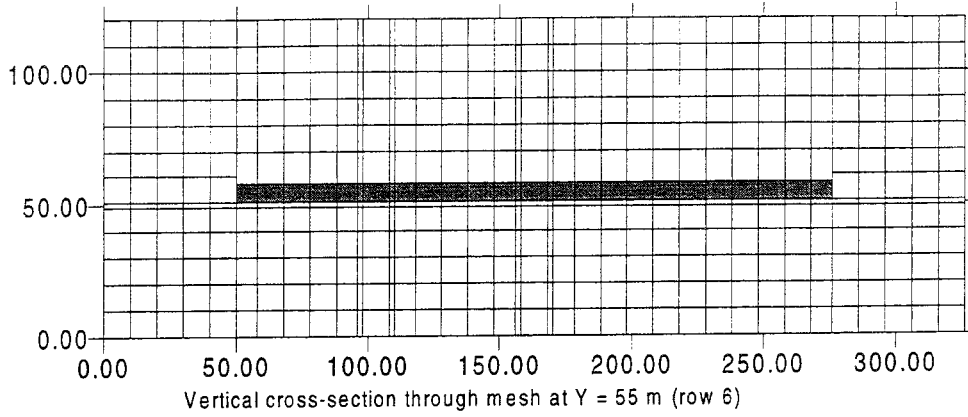
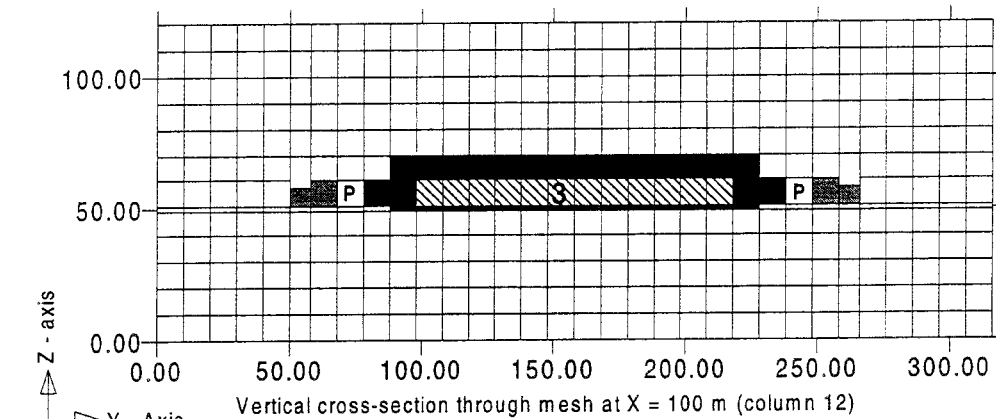
-  Cells representing the rock mass.
-  Cells representing SFL 3 encapsulation.
-  Cells representing SFL 5 encapsulation.
-  Cells representing flow barriers, surrounding SFL 3 and SFL 5 encapsulations.
-  Cells representing a sealing barrier - a plug.

FIGURE 8.1
REPOSITORY MODEL, RC5, HORIZONTAL CROSS-SECTION
 Example of regular mesh, horizontal cross-section.
 Outside of the repository, most cells have the same size: 10 x 10 x 10 m.
 Minimum distance from tunnels to mesh boundary is 50 m (5 blocks).



Scale in meters



Scale in meters







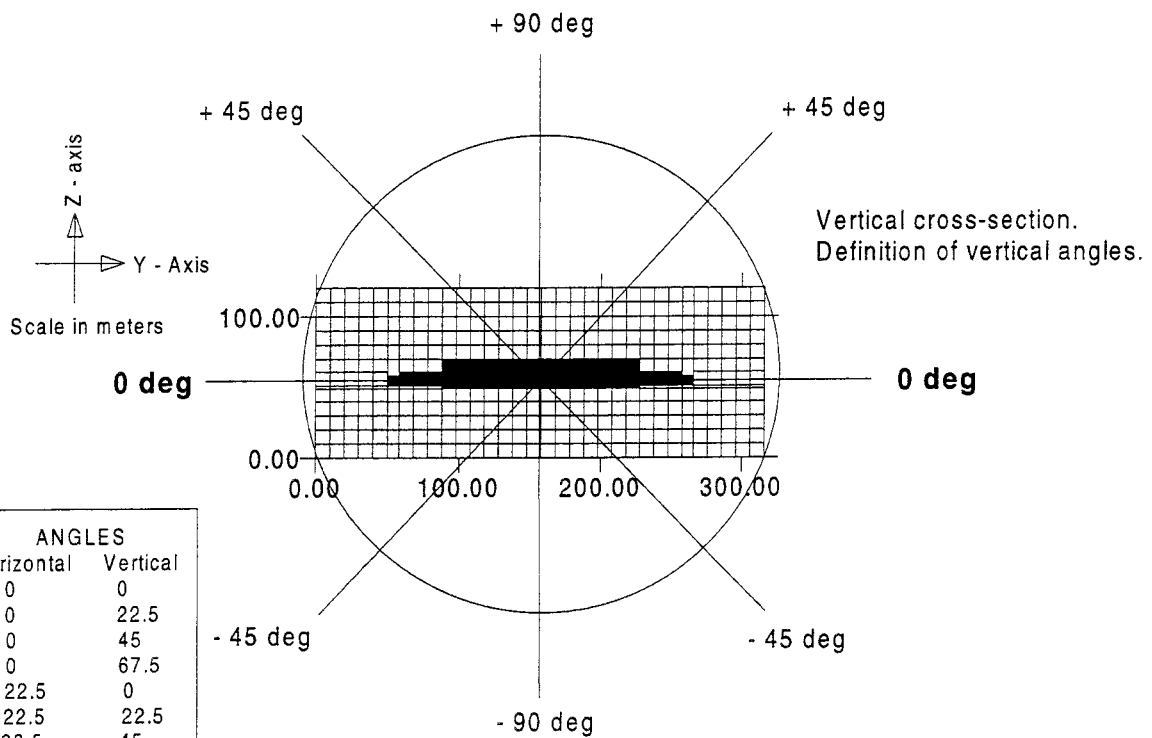
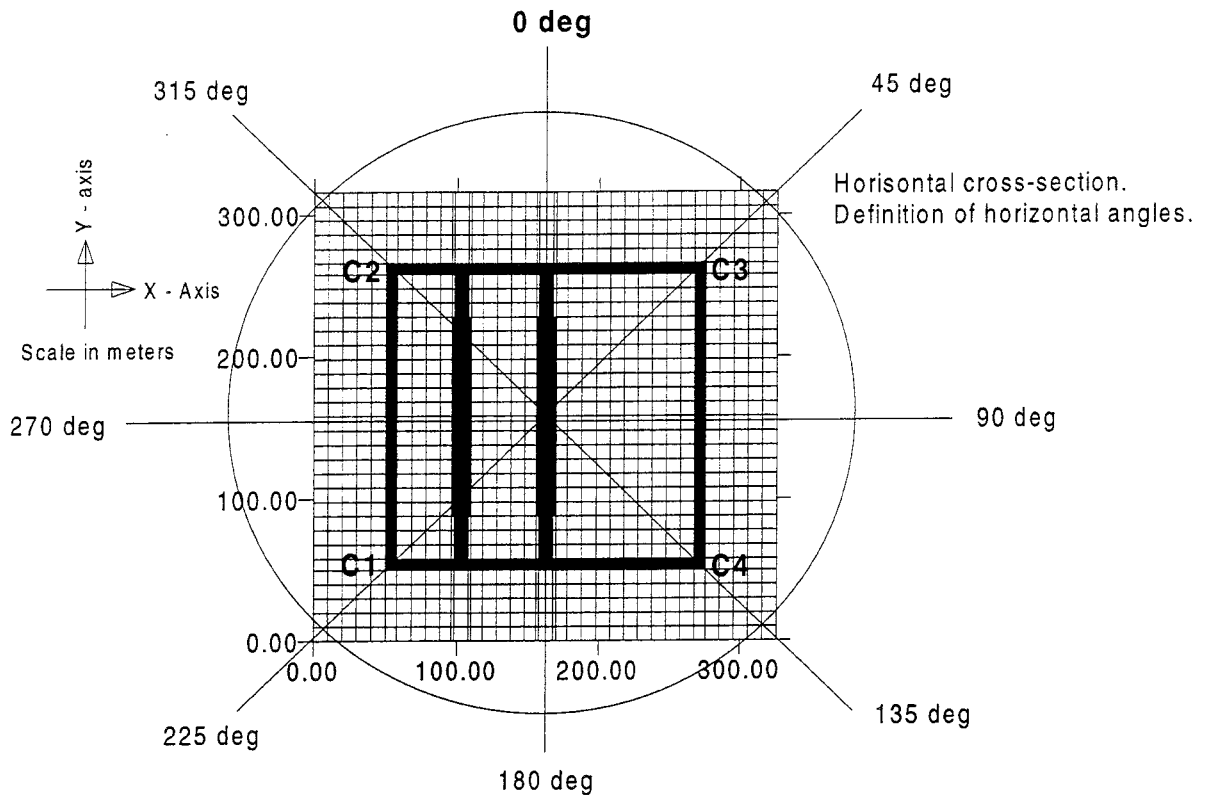
- | | | | |
|---|---|---|---|
|  | Cells representing the rock mass. |  | Cells representing flow barriers, surrounding SFL 3 and SFL 5 encapsulations. |
|  | Cells representing SFL 3 encapsulation. |  | Cells representing a sealing barrier - a plug. |
|  | Cells representing SFL 4. | | |
|  | Cells representing SFL 5 encapsulation. | | |

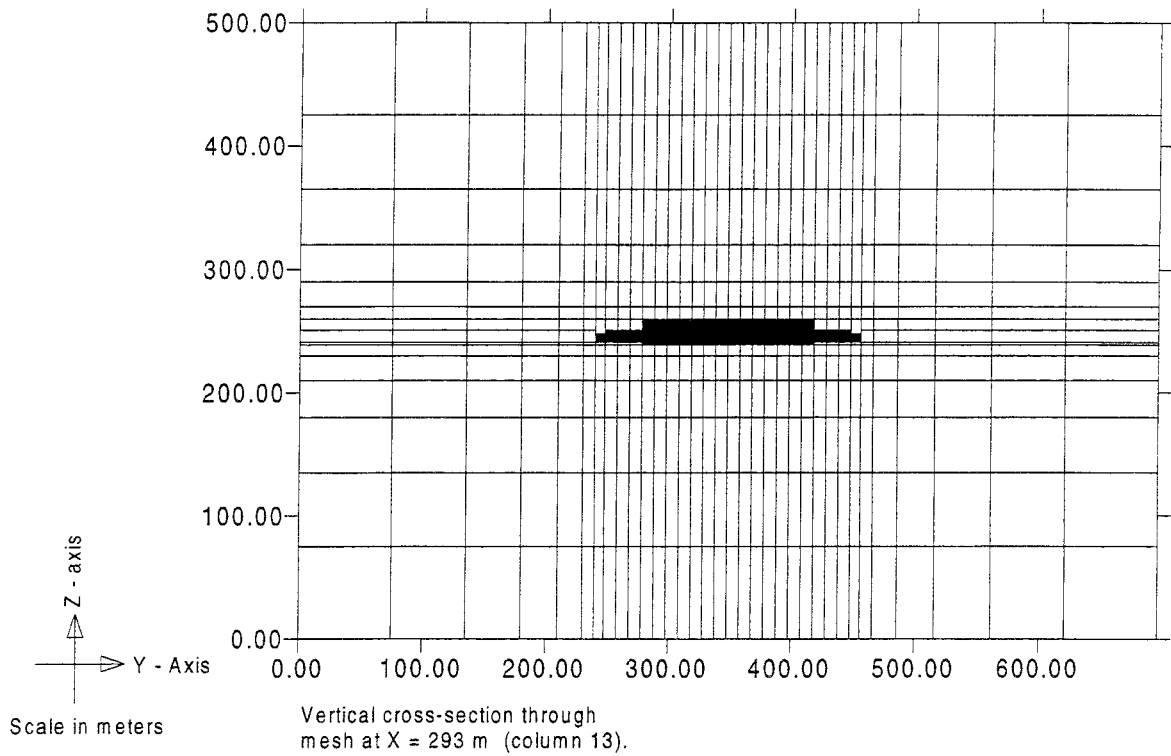
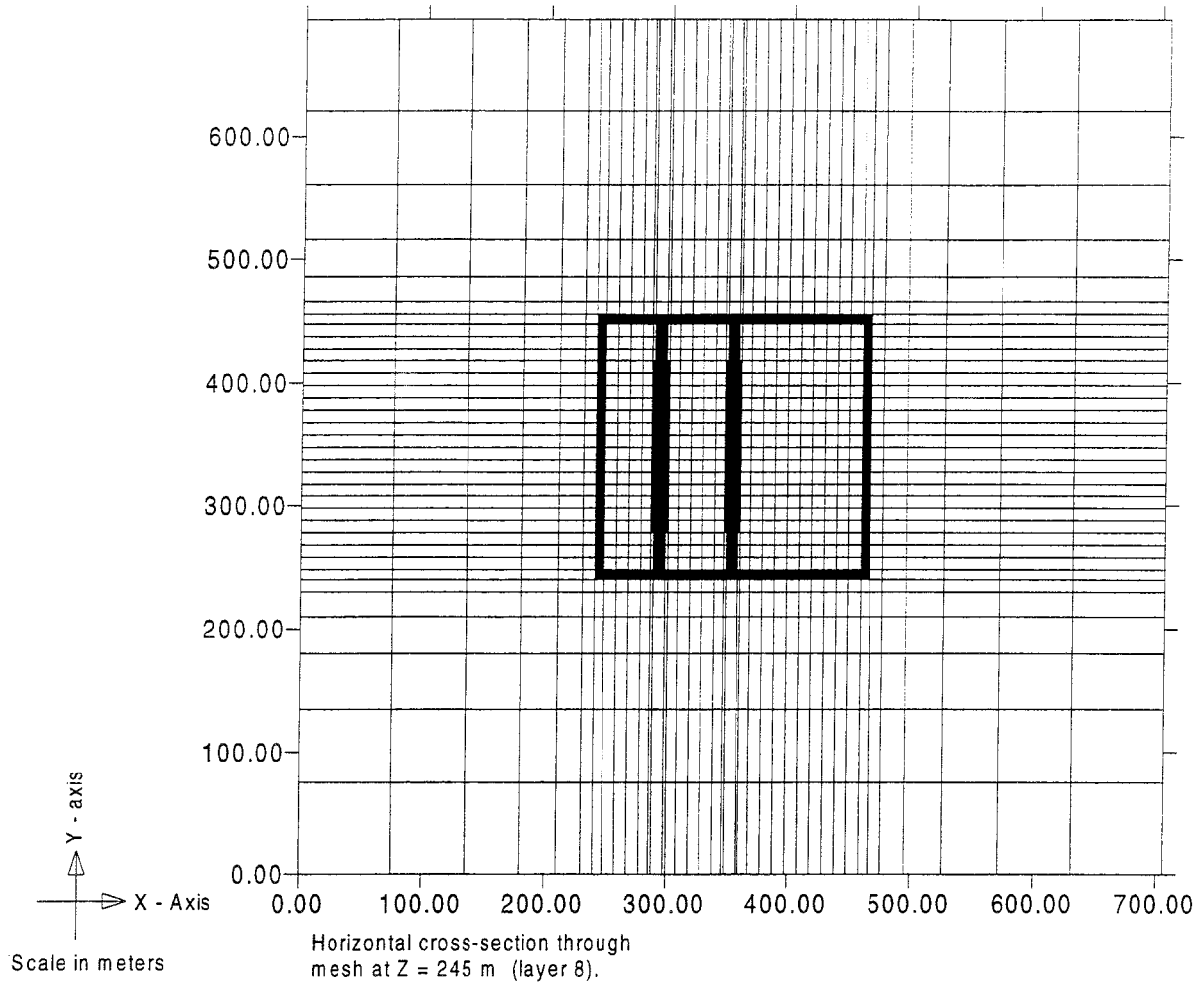
FIGURE 8.2
REPOSITORY MODEL, RC5, VERTICAL CROSS-SECTIONS
 Example of regular mesh, vertical cross-sections. Outside of the repository, most cells have the same size: 10 x 10 x 10 m. Minimum distance from tunnels to mesh boundary is 50 m (5 blocks)



CODE	ANGLES	
	Horizontal	Vertical
A	0	0
B	0	22.5
C	0	45
D	0	67.5
E	22.5	0
F	22.5	22.5
G	22.5	45
H	22.5	67.5
I	45	0
J	45	22.5
K	45	45
L	45	67.5
M	67.5	0
N	67.5	22.5
O	67.5	45
P	67.5	67.5
Q	90	0
R	90	22.5
S	90	45
T	90	67.5
U	-	90

- Cells representing the rock mass.
- Cells representing the repository.

FIGURE 8.3
REPOSITORY MODEL, SYSTEM OF ANGLES
Example of mesh, horizontal cross-section and vertical cross-section. System of horizontal and vertical angles, used for definition of the direction of the regional groundwater flow.





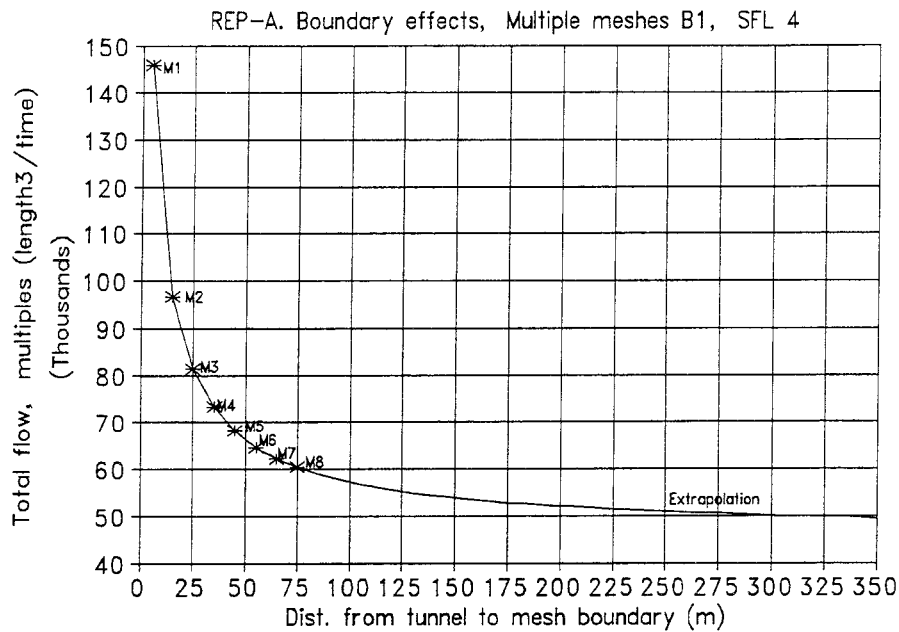
-  Cells representing the rock mass, uniform continuum.
-  Cells representing different parts of the repository: SFL 3, 4 and 5.

FIGURE 8.4 REPOSITORY MODEL, ME6.
The mesh of the model used for the predictive simulations. The cell size is increased towards the boundaries of the mesh. Horizontal and vertical cross-sections. Minimum distance from tunnels to mesh boundary is 240 m.

(i)
Size of total
flow in SFL 4
versus size of
mesh.



(ii)
Change in total
flow in SFL 4
versus size of
mesh.

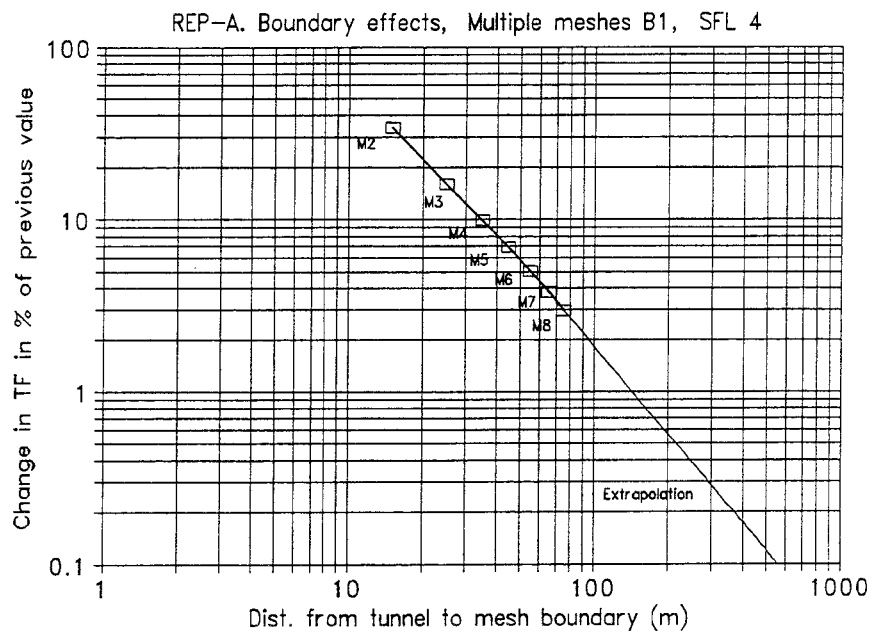
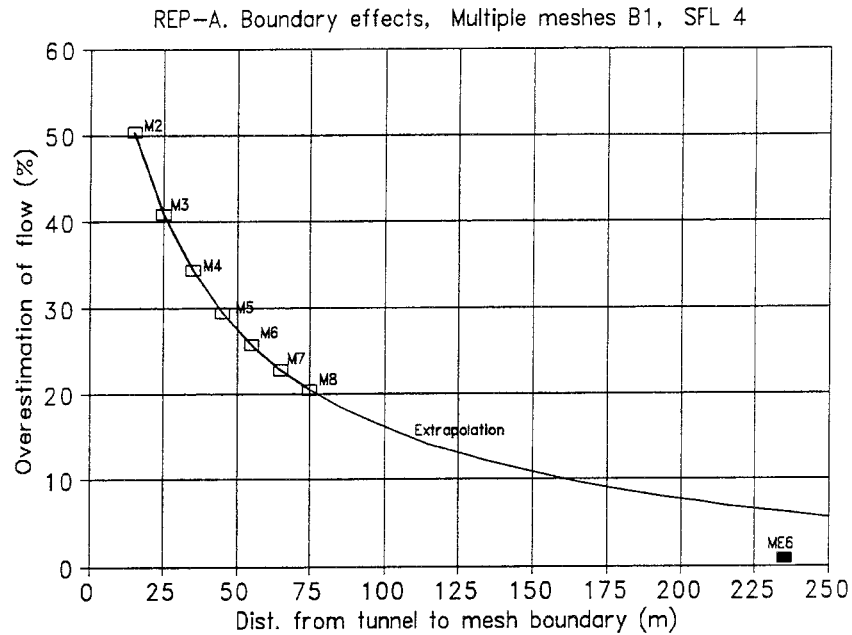


Figure 8.5 REPOSITORY MODEL,UC, BOUNDARY EFFECTS, MULTIPLE MESHES B1
Change in calculated total flow (TF) in the SFL 4 tunnel, versus size of finite difference mesh (model). The change in flow is expressed in percent of the flow predicted by the previous smaller mesh. M1 - M8 denote different meshes. The method of multiple meshes was used for estimation of boundary effects, method B1 as described in Chap.4. The conductivity of the SFL 4 tunnel is 10000 times that of the rock mass. The conductivity of the SFL 3 and 5 flow barriers are 0.1 times that of the rock mass. The rock mass is represented by cells (blocks) of size 10x10x10m. The regional flow is directed along Y-axis, size: 1 m/s (Hor.angle=0°, Vert.angle=0°).

(i)
Overestimation
of total flow in
SFL 4 versus
size of mesh.

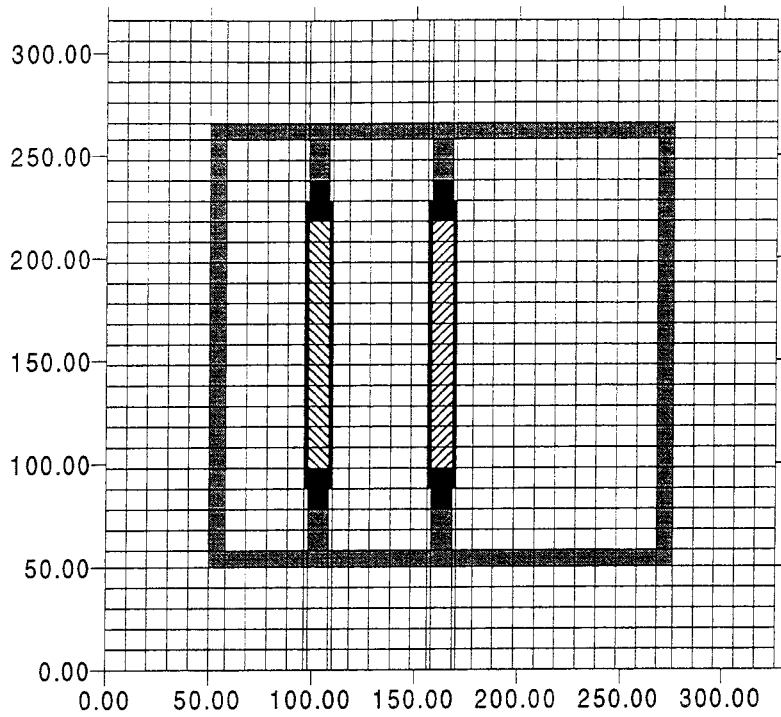


(ii) The values

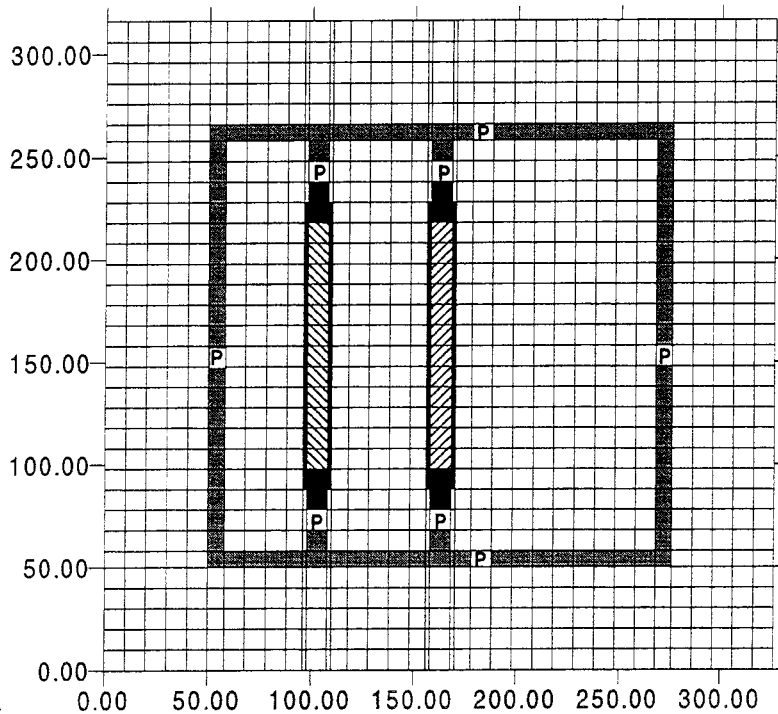
Numerical method		B1
Direction of regional flow		Horizontal along SFL 3 and 5
Conductivity of SFL 4		10000 x K rock
MESH	Distance to boundary (1)	Error in predicted total flow (SFL 4) (2)
M2 (regular)	15m (2 blocks)	50.3 %
M3 (regular)	25m (3 blocks)	40.9 %
M4 (regular)	35m (4 blocks)	34.3 %
M5 (regular)	45m (5 blocks)	29.5 %
M6 (regular)	55m (6 blocks)	25.7 %
M7 (regular)	65m (7 blocks)	22.8 %
M8 (regular)	75m (8 blocks)	20.4 %
ME6 (irregular) (3)	240m (6 blocks)	0.8 %
<p>(1) Minimum distance between tunnel and boundary of mesh.</p> <p>(2) The total flow is defined as all water that visits the structure studied, it is calculated on the base of a mass balance taken over the envelope of the structure studied. The error is based on the extrapolated total flow, set as the correct flow (see Sec.4.). The error is defined as: $\text{Error} = \text{ABS}(100 - [(\text{correct.total.flow}) / (\text{calc.total.flow} / 100)])$</p> <p>(3) For mesh ME6 the rock block size is increased towards the outer boundaries.</p>		

Figure 8.6

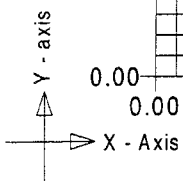
REPOSITORY MODEL, ESTIMATION OF ERROR IN PREDICTED FLOW
The error in the predicted flow in SFL 4 caused by boundary effects, versus meshes of different type and size. For other parts of the repository, the error is about the same or smaller. The errors were estimated by the use of the method of multiple meshes, as given in Chapter 4. The studied models are uniform continuum models.



Alternative (i):
No plugs inside the repository.



Alternative (ii):
Plugs in all tunnels:
at both ends of SFL 3 and SFL 5,
at four locations in SFL 4.



Horizontal cross-sections through the repository.

Scale in meters






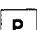
-  Cells representing the rock mass.
-  Cells representing SFL 3 encapsulation.
-  Cells representing SFL 4.
-  Cells representing SFL 5 encapsulation.
-  Cells representing flow barriers, surrounding SFL 3 and SFL 5 encapsulations.
-  Cells representing a section of the repository containing a plug.

FIGURE 8.7
ALTERNATIVE LAY-OUT OF REPOSITORY
Two studied alternatives:
(i) No plugs inside the repository
(ii) With plugs in all tunnels.
The plugs are assumed to consist of both concrete and bentonite and have a length of approximately 5 m.

Chapter 9.

Results of modelling of repository SFL 3-5

9.1 Introduction

In the following chapter we will present the results of the generic modelling of the groundwater flow through the repository SFL 3-5.

This is a generic modelling, it is not a site-specific modelling. The actual regional flow is unknown. In the models, the size of the regional specific flow is set to one.

In the models we have prescribed the size of the regional flow, it is the same in all studied models and scenarios. As the size is prescribed, it is possible to represent the rock mass by a homogeneous medium. The homogeneous rock mass could be looked upon as a heterogeneous rock mass with a zero amount of heterogeneity. Hence, the homogeneous rock mass is a base case, to which the effects of the heterogeneity could be added. In Section 9.7, we have included the effects of the heterogeneity of the rock mass, as regard the flow inside the repository. This was done based on the results given in Chapters 6 and 7, in those chapters the effects were studied for some general scenarios. The effects of a heterogeneous rock mass, as given in Chapters 6 and 7, were added to the results produced by models with a homogeneous rock mass. It should be pointed out that this is possible as our study is a generic study and the size of the regional flow is the same for all scenarios. For a few scenarios we have used the stochastic continuum approach and the regional model. But for most of the calculations we have used the uniform continuum approach.

The encapsulations of SFL 3 and SFL 5 will be surrounded by a flow barrier. The purpose of a flow barrier is to limit the flow that passes through the encapsulation. The barrier could be a structure less permeable than the rock mass, and divert the flow away from the encapsulation; such a barrier is called a negative barrier. The barrier could also function as a structure more permeable than the rock mass and the encapsulation, and lead the flow around the encapsulation; such a barrier is called a positive barrier.

As regards the flow of groundwater in the tunnels of the repository, we have studied the following.

- The effects of different directions of the regional flow.
- The effects of a positive or a negative flow barrier, surrounding the SFL 3 and SFL 5 encapsulations; i.e. different values of the conductivity of the flow barriers.
- The effects of different conductivity values of the back filling in SFL 4.
- The distribution of flow inside the SFL 4 tunnel.
- The effects of alternative lay-outs as regards plugs in the tunnels.
- The effects of the heterogeneity of the rock mass as regards the flow in the repository.

The flows of the different parts of the repository were calculated as (i) a specific flow, which is the same as a flow per unit area [$\text{length}^3/(\text{length}^2 \text{ time})$] = [$\text{Length}/\text{time}$] and as (ii) a total flow [$\text{length}^3/\text{time}$]. The size of the predicted flow should be regarded as a multiple of the size of an unknown regional flow. Hence, the flow will be given as X times an unknown flow. The unknown regional flow should be expressed as a specific flow.

9.2 Sensitivity to direction of regional flow

Introduction

The size and the distribution of the flow inside the repository, depends on the direction of the regional flow. We have studied the variation (sensitivity) of the flow in the tunnels, as regard the direction of the regional flow, by conducting a large number of simulations, representing different directions. The directions have been selected in such a way that they represent the whole sphere of possible directions. Due to the nature of groundwater flow and the symmetric shape of the repository, only one eighth of the sphere needs to be studied, the other directions will, as regards size of flow, produce the same results. We have studied 21 different directions, given in the table of Figure 8.3. These 21 directions were transformed to 114 values that represent the whole sphere. The directions of regional flow that have been studied are denoted by capital letters from A to U, see Figure 8.3. The models were based on the uniform continuum approach.

Scenarios

Sensitivity studies have been performed for two different scenarios, named: Case 1 and Case 2. The two scenarios constitute two possible alternatives of design of the flow barriers surrounding the encapsulations of SFL 3 and SFL 5. Case 1 represents a positive barrier, in which the barrier filling is sand or gravel; Case 2 represents a negative barrier, in which the barrier filling is bentonite. The only difference between the scenarios is the conductivity of the flow barriers. The conductivity of the different parts of the repository is given in Table 8.2.

- Case 1 the conductivity of the SFL 3,5 flow barrier is 100000 times that of the rock mass.
- Case 2 the conductivity of the SFL 3,5 flow barrier is 0.1 times that of the rock mass.

In both scenarios, the conductivity of SFL 4 is 10000 times that of the rock mass, this conductivity produces a flow in SFL 4 which is very close to maximum flow (Section 9.3).

General behavior of the flow inside the repository

The flow inside the repository will vary along the tunnels. The size of the flow in the tunnels depends on:

- (i) the lay-out of the tunnels, e.g. direction, length and size,
- (ii) the properties of the filling and the flow barriers inside the tunnels,
- (iii) the direction and size of the regional groundwater flow, as well as
- (iv) the heterogeneity of the surrounding rock mass.

As regards the different parts of the repository, due to flow barriers, concrete encapsulations and size of the studied portion of the repository, the smallest flow occurs in the encapsulations of SFL 3 and SFL 5. The tunnel of SFL 4 is the longest tunnel and no flow barriers exist inside it. Hence, the largest flow occurs in SFL 4.

From a general point of view, as regards direction of the regional flow, the flow in the repository will vary in the following way.

- *Specific flow.* As the tunnels are located in the horizontal plane, the largest average specific flow inside a tunnel will occur when the regional flow is in the horizontal plane and directed in an angle close to the direction of the longest part of the studied tunnel. The smallest average specific flow inside a tunnel will occur when the regional flow is directed at right angles to the length of the studied tunnel. As the repository layout forms a closed structure in the horizontal plane, minimum specific flow inside the repository will occur at vertical regional flow.
- *Total flow.* It is more difficult to predict the total flow than the specific flow, as the total flow depends on the area exposed in the direction of the regional flow, as well as

of the tunnel conductivity. If the conductivity of the tunnel is small, compared to the conductivity of the rock mass, or slightly larger than that of the rock mass, maximum total flow will occur for a direction of regional flow that gives a large area exposed to the regional flow, minimum total flow will occur for a direction that gives a small exposed area. The opposite will occur if the tunnel is much more permeable than the rock mass, if the conductivity of the tunnel is large, maximum total flow will occur when the regional flow is parallel to the tunnel and minimum when the regional flow is at right angles to the tunnel.

It should be noted that extreme values of average specific flow and total flow do not always occur for the same direction of the regional groundwater flow, even if the structure studied is homogeneous. Additionally, as the tunnels of the repository are in different directions and have different properties, maximum (or minimum) flow for different parts of the repository will not occur for the same direction of the regional flow. Study for example Case 1, the direction of regional flow that produces maximum flow in SFL 4, gives minimum flow in SFL 3 and SFL 5.

Inside the tunnels the flow will vary. The flow in a tunnel will vary, depending on the overall flow pattern of the groundwater, as caused by the tunnel lay-out and the direction of the regional flow, as well as on the discrete nature of the fractured rock, see Section 9.5.

Results

The results of the simulations, the flow in different parts of the repository, versus direction of the regional flow, are given in the following figures and table:

- SFL 4 in Figure 9.1
- SFL 3 in Figures 9.2 (barrier) and 9.3 (encapsulation)
- SFL 5 in Figures 9.4 (barrier) and 9.5 (encapsulation).

The figures might need an explanation. The X-axis and the Y-axis of the figures represent all possible directions of regional flow in the horizontal and vertical plane. The prescribed angles (horizontal and vertical) are defined in accordance with the system given in Figure 8.3. The figures are based on 114 calculated values representing the whole sphere of possible directions of regional flow. Interpolation between these values was done by the use of a kriging routine. The size of the flow should be regarded as a multiple of the size of an unknown regional groundwater flow.

The simulations demonstrate the following.

- *Total flow in the SFL 4 tunnel.* For both cases, maximum flow takes place when the regional flow is horizontal and at right angles to the SFL 3 and SFL 5 tunnels (Q). For Case 2, the variations in flow, for different angles in the horizontal plane, are smaller than for Case 1. For both scenarios, minimum flow takes place when the regional flow is vertical (U).

Case 1: minimum= 11280, maximum= 56740, mean= 34940, maximum/minimum= 5.0

Case 2: minimum= 11250, maximum= 53930, mean= 35620, maximum/minimum= 4.8

- *Total flow in the flow barriers of SFL 3 and 5.*
 - Case 1, positive barriers. Both SFL 3 and SFL 5 demonstrate very much the same behavior. However, SFL 5 forms an extra flow barrier when the regional flow is horizontal or close to horizontal, which gives a somewhat smaller flow in SFL 3 than in SFL 5. The largest flow takes place when the regional flow is (i) vertical (U) or (ii) horizontal and directed along the barriers (A). Minimum flow takes place when the

regional flow is horizontal and directed at right angles to the barriers (Q).

- Case 2, negative barriers. For SFL 3, the largest flow takes place when the regional flow is vertical (U). Minimum flow takes place when the regional flow is horizontal and directed along the barriers (A). For SFL 5, the pattern is a little more complicated. The largest flow takes place when the regional flow is inclined 45 degrees from the horizontal and at right angles to the barrier (S). But, as for SFL 3, minimum flow takes place when the regional flow is horizontal and directed along the barriers (A).

Case 1, SFL 3: *minimum*= 3050, *maximum*= 5970, *mean*= 4960, *maximum/minimum*= 2.0

Case 1, SFL 5: *minimum*= 3070, *maximum*= 6240, *mean*= 5270, *maximum/minimum*= 2.0

Case 2, SFL 3: *minimum*= 780, *maximum*= 1570, *mean*= 1230, *maximum/minimum*= 2.0

Case 2, SFL 5: *minimum*= 830, *maximum*= 1720, *mean*= 1380, *maximum/minimum*= 2.1

• *Total flow in the encapsulation of SFL 3 and 5.*

- Case 1, in which the encapsulation is protected by a positive barrier. Both SFL 3 and SFL 5 demonstrate very much the same behavior. But as for the barriers, the flow in the SFL 3 encapsulation is somewhat smaller than the flow in the SFL 5 encapsulation. The largest flow takes place when the regional flow is vertical (U). Minimum flow takes place when the regional flow is horizontal and directed at right angles to the barriers (Q).

- Case 2, in which the encapsulation is protected by a negative barrier. The behavior of the flow in the encapsulation will be similar to that of the Case 2 barriers. For SFL 3, the largest flow takes place when the regional flow is vertical (U). Minimum flow takes place when the regional flow is horizontal and directed along the barriers (A). For SFL 5 the largest flow takes place when the regional flow is inclined 45 degrees from the horizontal direction and at right angles to the barrier (S). Minimum flow takes place when the regional flow is horizontal and directed along the barriers (A).

Case 1, SFL 3: *minimum*= 0.6 , *maximum*= 1.8 , *mean*= 1.3 , *maximum/minimum*= 3.0

Case 1, SFL 5: *minimum*= 0.7 , *maximum*= 1.8 , *mean*= 1.5 , *maximum/minimum*= 2.6

Case 2, SFL 3: *minimum*= 345 , *maximum*= 621 , *mean*= 498 , *maximum/minimum*= 1.8

Case 2, SFL 5: *minimum*= 404 , *maximum*= 677 , *mean*= 558 , *maximum/minimum*= 1.7

The flow is much smaller in the encapsulation protected by the positive barrier (Case 1) than in the encapsulation protected by the negative barrier (Case 2). This is because the conductivity contrast between the barrier and the rock mass is larger in Case 1 than in Case 2. The efficiency of a flow barrier will be discussed in the next section.

9.3 Sensitivity to the conductivity of the flow barriers in SFL 3 and SFL 5

The flow in the flow barriers and in the encapsulations were calculated using different values of conductivity of the flow barriers. Three cardinal directions of the regional groundwater flow were studied, named A , Q , U (see Figure 8.3).

A: Regional flow along SFL 3 and 5: Hor.angle=0°, Vert.angle=0°
Q: Regional flow at right angle to SFL 3 and 5: Hor.angle=90°, Vert.angle=0°
U: Regional flow is vertical: Hor.angle=-, Vert.angle=90°

The conductivity of the different parts of the repository is given in Table 8.2. The conductivity of the flow barriers was varied and the conductivity of SFL 4 was set to 10000 times that of the rock mass. The models were based on the uniform continuum approach. The results of the simulations are given in the following figures:

- SFL 3 in: Figures 9.6 (barrier) and 9.7 (encapsulation).
- SFL 5 in: Figures 9.8 (barrier) and 9.9 (encapsulation).

The results for SFL 3 and SFL 5 are very similar, as they have an identical lay-out in the model. The simulations demonstrate the following.

- *SFL 3 and 5, Flow barrier (Figures 9.6 and 9.8).* The flow in the flow barrier will vary depending on the conductivity of the flow barrier. The flow in the barriers will be similar to the flow of a homogeneous tunnel, see Chapter 3, and to the flow of the previously discussed barriers, see Chapter 7. If the flow barrier has a small conductivity the flow will be small, if the conductivity is large the flow will be large. For a barrier, as for a homogeneous tunnel (see Chapter 3), an increase in the conductivity of the flow barrier will only have a large effect on the flow in the barrier, if the barrier conductivity is small. If the conductivity of a flow barrier is large a much more conductive barrier will not have a much larger flow, as the flow of such a barrier is mainly dependent on the conductivity of the surrounding rock mass. The threshold conductivity, defined in Chapter 3, is also applicable to the flow barrier. The maximum flow in a barrier with a large conductivity (a positive barrier) is 3050 to 6200, depending on the direction of the regional flow. The flow in a barrier with a small conductivity (a negative barrier) decreases with decreasing conductivity. However, from a practical point of view it is difficult to construct a very low-permeable barrier. A negative barrier, with a conductivity which is 0.1 times that of the rock mass, gives a flow of 780 to 1720, depending on the direction of the regional flow.

- *SFL 3 and 5, Encapsulation (Figures 9.7 and 9.9).* The flow in the encapsulation will also vary depending on the conductivity of the flow barrier, as demonstrated in Section 7. The flow barrier will reduce the flow in the encapsulation. The larger the contrast between the conductivity of the flow barrier and the conductivity of the rock mass, the smaller the flow in the encapsulation. The encapsulation is assumed to have a conductivity which is 10 times that of the rock mass. Therefore, the conductivity contrast of a positive barrier needs to be about half an order of magnitude larger than the conductivity contrast of a negative barrier, to be as effective as a negative barrier. By using a positive flow barrier, with a conductivity that is 100 000 times that of the rock mass, it is possible to reduce the flow in the encapsulation with about 3 orders of magnitude, compared to an unprotected encapsulation. A negative barrier needs to have a conductivity that is smaller than 0.1 times that of the rock mass, to significantly reduce the flow in the encapsulation, and for a large reduction of flow in the encapsulation, the conductivity of a negative barrier needs to be extremely small.

- *SFL 4, tunnel.* The flow in the SFL 4 tunnel is not much affected by the conductivity of the flow barriers surrounding the SFL 3 and 5 encapsulations.

Studying the results given in the figures, and remembering that the effective conductivity of the rock mass is very small, it is concluded that a large reduction in flow through the encapsulation is more easily obtained if the barrier is a positive barrier than if it is a negative barrier. This follows from the fact that it is difficult to make a barrier which is much less permeable than the effective conductivity of the rock mass (bentonite barrier), but it is very easy to make a barrier which is much more permeable than the effective conductivity of the rock mass (sand or gravel barrier, etc).

9.4 Sensitivity to conductivity of back filling in SFL 4

The flow in a tunnel depends on the conductivity of the tunnel filling. However, the conductivity of the tunnel will only have a large effect on the flow in the tunnel if the tunnel conductivity is small, compared to the conductivity of the rock mass. If the conductivity of a tunnel is large, compared to the conductivity of the rock mass, a tunnel

with an even larger conductivity, will not have a much larger flow, as the flow of such a scenario is mainly dependent on the conductivity of the surrounding rock mass. The concept of threshold conductivity is applicable to the SFL 4 tunnel (see Chapter 3).

The flow in the SFL 4 tunnel was calculated for different values of conductivity of the SFL 4 tunnel. Three directions of the regional groundwater flow were studied, named A, Q and U (see Figure 8.3). Q is the direction that gives the largest flow in SFL 4, presuming that the tunnel has a large conductivity.

A: Regional flow along SFL 3 and 5:	Hor.angle=0°, Vert.angle=0°
Q: Regional flow at right angle to SFL 3 and 5:	Hor.angle=90°, Vert.angle=0°
U: Regional flow is vertical:	Hor.angle=-, Vert.angle=90°

The conductivities of the different parts of the repository is given in Table 8.2. The conductivities of the flow barriers of SFL 3 and 5 were set to 100000 times that of the rock mass. The models were based on the uniform continuum approach.

The results as regards the flow in SFL 4 is given in Figure 9.10. The figure demonstrates that the SFL 4 tunnel reaches its largest flow when the conductivity of the tunnel is four orders of magnitude larger than that of the surrounding rock mass. A larger conductivity of the tunnel will only have a minimal effect on the flow in the tunnel. The maximum total flow is about 60 000 times the regional flow, considering all directions (Section 9.2).

If we use a tunnel filling that is one order of magnitude less conductive than that of the rock mass, the maximum total flow in the SFL 4 tunnel will be about 4000 times the regional flow. Vertical regional flow will produce maximum flow in SFL 4, if the conductivity is smaller than that of the rock mass. Hence, the effect of using a backfill in the SFL 4 tunnel, a backfill that is one order of magnitude less conductive than the rock mass (bentonite), is that we will get a total flow in SFL 4 that is between 0.02 and 0.07 times the total flow of an SFL 4 tunnel that is completely without filling, all directions of regional flow considered.

The conductivity of the SFL 4 tunnel may influence the flow of SFL 3 and SFL 5. This is demonstrated in Figure 9.11. The figure gives the flow of SFL 3, the flow of SFL 5 is very similar.

- The SFL 4 tunnel will **not** influence the flow in SFL 3 and SFL 5 if the regional flow is (i) vertical or close to vertical or (ii) if the conductivity of SFL 4 is less than 100 times that of the rock mass.
- For a conductivity of the SFL 4 tunnel which is larger than 100 times that of the rock mass, the SFL 4 tunnel will act as a positive flow barrier, that will limit the flow in SFL 3 and SFL 5. The SFL 4 tunnel will lead the water around the SFL 3 and SFL 5 tunnels, presuming that the SFL 4 tunnel is permeable enough. This effect is most pronounced for horizontal, or close to horizontal, regional flow, but the effect is significant even for a regional flow that is inclined 45 degrees from horizontal.

For the scenarios: Case 1 and Case 2 (see Section 9.2), the conductivity of the SFL 4 tunnel is 10000 times that of the rock mass. Hence, for these two cases the flow in SFL 3 and 5 is reduced, due to the large conductivity of the SFL 4 tunnel. We have estimated the reduction. For the barriers and the encapsulations of SFL 3 and SFL 5, the reduction is about 0.5 times for regional flow of directions A and Q; for more vertically inclined directions the reduction is lower, and it is zero for vertical flow. The reduction stated is in comparison to a situation without an SFL 4 tunnel.

It follows from the above, that if the conductivity of SFL 4 is smaller than 10000 times that of the rock mass, the flow in SFL 3 and SFL 5 will be larger than the results given in Section 9.2, about 1 to 2 times larger, depending on the direction of the regional flow.

For larger values of conductivity of the SFL 4 tunnel, larger than 10000 times that of the rock mass, the flow in SFL 3 and SFL 5 will be smaller than the results given in Section 9.2. Hence, for values of conductivity of the SFL 4 tunnel that are larger than 10000 times that of the rock mass, the flow in the SFL 4 tunnel will not be much increased, but the flows of SFL 3 and SFL 5 will be reduced, presuming that the regional flow is not vertical or close to vertical.

9.5 Variation of specific flow inside the SFL 4 tunnel

In the previous sections we have discussed the average specific flow of a tunnel and the expected total flow of a tunnel, these properties correspond to the whole of the tunnel. In this section we will study the variation (distribution) of the flow inside the SFL 4 tunnel. The variation of the specific flow inside two straight tunnels, of the lengths 100m and 200m respectively, is given in Section 6.8.

Inside a tunnel the flow will vary, depending on:

- The tunnel lay-out, e.g. length, size, filling etc.
- The direction of the regional flow.
- The heterogeneity of the surrounding rock mass.

For a large tunnel with a large conductivity, the variation of the flow inside the tunnel is mainly dependent on the direction of the regional flow in relation to the tunnel lay-out. In the upstream part of such a tunnel, groundwater will flow towards the tunnel from the surrounding rock mass, and into the tunnel. The flow inside the tunnel will increase, and reach its maximum somewhere in the middle of the tunnel. In the downstream part of the tunnel, the flow inside the tunnel will decrease and water will flow out from the tunnel. For all directions of regional flow, there will be an upstream and a downstream part. If the regional flow is directed at right angles to the tunnel, the upstream and downstream parts are opposite and parallel along the tunnel.

The variation of flow inside a tunnel in a homogeneous rock mass will be smooth and continuous. For a tunnel placed in a heterogeneous rock mass, the increase and decrease of flow will be given by the total effects of all fractures that are connected to the tunnel, as well as by the nature of the tunnel. A tunnel, with or without filling, can be looked upon as a continuous medium, and if the tunnel is large, many fractures are connected to the tunnel. Therefore, the flow inside a tunnel, placed in a heterogeneous rock mass, will not be as heterogeneous as the flow of the surrounding rock mass; compared to the heterogeneous flow of the rock mass, the variation of the flow inside a tunnel is smooth and continuous.

Close to large connecting fracture zones it is likely that the flow in a tunnel is large, but not necessarily larger than at other sections of the tunnel, where few or no fractures connect to the tunnel. This follows from the condition of continuity of flow and because the tunnel, with or without filling, is a large structure that connects many fractures.

This is illustrated in Figures 9.12 and 9.13, as well as in Appendix D, Figures D.1 through D.4. The figures give the variation of the specific flow inside the SFL 4 tunnels for six different directions of regional groundwater flow, and for a homogeneous rock mass as well as for a heterogeneous rock mass. In the models, the rock mass was defined as a

uniform continuum (homogeneous medium) or as a stochastic continuum (heterogeneous medium) with properties representing the Äspö rock mass. The variation of specific flow inside a tunnel is also given in Figure 6.20, this figure gives the flow for straight tunnels of the lengths 100m and 200m respectively, for two directions of the regional groundwater flow.

The maximum average specific flow in the SFL 4 tunnel takes place when the regional flow is in the horizontal plane; for other directions of regional flow, that are inclined from the horizontal plane, the flow will be less. The flow in the tunnel depends on the projected length of the tunnel in the direction of the regional flow. The SFL 4 tunnel is a homogeneous structure and the tunnel is in the horizontal plane. For a direction of regional flow that is along the tunnel but inclined 45 degrees from the horizontal plane, the projected length of the tunnel is $1/\sqrt{2}$ times the projected length at horizontal regional flow. Hence, the flow in the tunnel for a regional flow along the tunnel but inclined 45 degrees from the horizontal plane should be approximately $1/\sqrt{2}$ times the flow predicted for a horizontal regional flow, which it is (see Figure 9.12).

One interesting phenomenon is the drop in specific flow that takes place at the four corners of the tunnel (at C1, C2, C3 and C4, see Figure 8.3). This is because at the corners the flow changes its direction by 90 degrees. The average direction of flow, at the corners, is about 45 degrees from the direction of flow along the rest of the tunnel. The area of a cross section through the tunnel, taken at 45 degrees from the main axes (longitudinal axis) of the tunnel, is $\sqrt{2}$ times larger than the area of a cross section taken at right angles to the tunnel. The size of the volume flow [length³/time] will not change much, as the water flows along the corner, but the cross section area is larger at the corner, than at the rest of the tunnel. Hence, the specific flow will drop with a factor equal to $1/\sqrt{2}$ at the corners. This is a nice reminder that the concept of specific flow should be used with some care.

The variation of the flow inside a tunnel as large as the SFL 4 tunnel is mainly dependent on the direction of the regional flow, and not so much dependent on the heterogeneity of the surrounding rock mass. This is demonstrated in Figure 9.13 and in Figures D.3 and D.4 of Appendix D. In Figure 9.13 we compare the variation of flow in the SFL 4 tunnel, obtained for a homogeneous rock mass (uniform continuum), to the variation of flow obtained for a possible realization of the heterogeneous properties of the rock mass (stochastic continuum); a similar comparison is also given in Figure 6.20. The heterogeneity represents the properties at Äspö. The comparison of tunnels in a homogeneous and in a heterogeneous rock mass yields the following conclusions.

- The expected flow inside a tunnel is larger if the tunnel is in a heterogeneous rock mass than if the tunnel is in a homogeneous rock mass.
- Along a tunnel, the general trend of increase and decrease of flow inside the tunnel is the same for a tunnel in a homogeneous rock mass and for a tunnel in a heterogeneous rock mass. This is the variation produced by the direction of the regional flow.
- As regards SFL 4, if we scale the distribution presenting the variation of flow in the tunnel, obtained with a homogeneous and a heterogeneous rock mass, in such a way that both will produce the same average specific flow in the tunnel, and compare the shape of the distributions, we note that the distributions obtained with a heterogeneous rock mass deviates from the distribution obtained with a homogeneous rock mass. The deviation is random but it is not large compared to the average specific flow in the tunnel. A comparison of the scaled distributions, given in Fig.9.13, reveals deviations that are smaller than 40% of the average specific flow in the tunnel.

9.6 Sensitivity to plugs in tunnels

The repository will be separated from the access tunnels by plugs and barriers of different types. In the preliminary design, plugs will also be placed inside the repository, at the ends of the SFL 3 and SFL 5 tunnels, where these tunnels connect to the SFL 4 tunnel. In this section we will investigate the effects of these internal plugs, we will also investigate if extra plugs inside the SFL 4 tunnel will limit the flow in SFL 4 or in other ways affect the flow inside the repository.

Three different lay-outs have been studied, they are given in Figure 8.7.

- Scenario (1): preliminary design, plugs at the ends of the SFL 3 and 5 tunnels.
- Scenario (2): no plugs inside the repository.
- Scenario (3): plugs at the ends of the SFL 3 and 5 tunnels, as well as four plugs in the SFL 4 tunnel.

Three cardinal directions of the regional groundwater flow were studied, named A , Q and U (see Figure 8.3).

A: Regional flow along SFL 3 and 5: Hor.angle=0°, Vert.angle=0°
Q: Regional flow at right angle to SFL 3 and 5: Hor.angle=90°, Vert.angle=0°
U: Regional flow is vertical: Hor.angle= -, Vert.angle=90°

The conductivity of the different parts of the repository is given in Table 8.2. The conductivity of the SFL 3 and 5 flow barriers was set to 100000 times that of the rock mass, and the conductivity of SFL 4 was set to 10000 that of the rock mass, like in Case 1 of Section 9.2. The hydraulic properties of the plugs are also defined in Table 8.2. The models were based on the uniform continuum approach.

Minimum effects of the plugs will occur for vertical regional flow, the plugs will have the largest effect when the regional flow is horizontal or close to horizontal.

The results of the simulations will be given in comparison with the results of the preliminary design, as defined below.

$$\text{Flow change} = \frac{\text{Flow alternative design}}{\text{Flow preliminary design}} \quad (9.1)$$

The comparison is given in Table 9.1 and Table 9.2, a summary is presented below.

- *Scenario 2: no plugs.* The flow through the repository will be increased, if the plugs are taken away and the repository will contain no internal plugs.
 - For the encapsulations of SFL 3 and SFL 5, as regards total flow, the increase will be between 1.1 to 5.2 times, depending on the direction of the regional flow.
 - For the barriers of SFL 3 and SFL 5, as regards total flow, the increase will be between 1.2 to 3.3 times, depending on the direction of the regional flow.
 - For the SFL 4 tunnel, as regards total flow, the increase will be between 1.2 to 1.7 times, depending on the direction of the regional flow.
- *Scenario 3: plugs at the ends of SFL 3 and 5, four plugs in SFL 4.* The flow through the repository will be changed, both increased and decreased, depending on the direction of the regional flow, if extra plugs are placed in SFL 4. This is because SFL 4 functions as a positive flow barrier for SFL 3 and 5 when the regional flow is horizontal or close to horizontal. Plugs in SFL 4 will reduce this effect.

- For the encapsulations of SFL 3 and SFL 5, as regards total flow, a regional flow of direction A gives an increase of about 2 times and a regional flow of direction Q gives a decrease of about 0.7 times, for vertical regional flow (U) there is no change.
- For the barriers of SFL 3 and SFL 5, as regards total flow, a regional flow of direction A gives an increase of about 2 times and a regional flow of direction Q gives a decrease of about 0.5 times, for vertical regional flow (U) there is no change.
- For the SFL 4 tunnel, as regards total flow, the decrease will be between 1 to 0.7 times, depending on the direction of the regional flow.

9.7 Sensitivity to heterogeneity of the rock mass

Introduction

For a site-specific model it is necessary to include the heterogeneity of the rock mass in the model. Otherwise the model will not produce the correct regional flow, e.g. the size of the regional flow will be wrong. This modelling of the repository is a generic study, it is not a site-specific modelling. The actual regional flow is unknown. In the models, the size of the regional specific flow is set to one. The size of the predicted flows in different parts of the repository should be regarded as multiples of the size of an unknown regional flow.

Methodology

As we have prescribed the size of the regional flow, it is possible to represent the rock mass by a homogeneous medium. The homogeneous rock mass could be looked upon as a heterogeneous rock mass with a zero amount of heterogeneity. Hence, the homogeneous rock mass is a base case, to which the effects of the heterogeneity could be added. In this section we have included the effects of the heterogeneity of the rock mass, as regards the flow inside the repository. This was done based on the results given in Chapters 6 and 7; in those chapters the effects were studied for some general scenarios. The effects of a heterogeneous rock mass, given in Chapters 6 and 7, were added to the results produced by models with a homogeneous rock mass. It should be pointed out that this is possible, as our study is a generic study and the size of the regional flow is the same for all scenarios.

The effects of the heterogeneity of the rock mass were studied by using the stochastic continuum approach. The results of the stochastic continuum modelling are based on statistical analyses of many realizations of the conductivity field. In this section, when we refer to the flow of a tunnel placed in a heterogeneous rock mass, we mean the average flow of many different realizations - the most probable outcome, the expected flow. The possible variation of the flow of a tunnel, depending on the heterogeneous properties of the rock mass, is described by the standard deviation and is given in the figures of Chapters 6 and 7.

The general conclusions given in the following sections are valid for at least 70 percent of the realizations of a studied scenario - the expected value plus and minus one standard deviation ($m-\sigma$ and $m+\sigma$). Hence, they are valid with a probability of at least 70 percent.

As regards the expected flow of a tunnel, the effects of the heterogeneity of the rock mass will increase the flow of a tunnel, compared to a homogeneous rock mass. The size of the increase depends on: (i) the amount of heterogeneity, (ii) the lay-out of the tunnel, e.g. length (scale) and (iii) the conductivity of the tunnel. The increase in flow can be given as a flow factor, defined in equation 6.1. By using the flow factor and the results of the uniform continuum modelling of the repository, in which the repository was surrounded by a homogeneous rock mass, it is possible to calculate the flow of a repository

surrounded by a heterogeneous rock mass, in the way given below.

$$SQ_{\text{stochastic continuum}} = SQFAC * SQ_{\text{uniform continuum}} \tag{9.2}$$

$$TF_{\text{stochastic continuum}} = TFFAC * TF_{\text{uniform continuum}}$$

- $SQFAC$ = Specific flow factor.
- $SQ_{\text{stochastic continuum}}$ = Specific flow in a tunnel placed in a heterogeneous medium.
- $SQ_{\text{uniform continuum}}$ = Specific flow in a tunnel placed in a homogeneous medium.
- $TFFAC$ = Total flow factor.
- $TF_{\text{stochastic continuum}}$ = Total flow in a tunnel placed in a heterogeneous medium.
- $TF_{\text{uniform continuum}}$ = Total flow in a tunnel placed in a homogeneous medium.

The flow factors

Based on the results presented in Chapters 6 and 7 (see Fig.6.12, Fig.6.17, Fig.6.19, Fig.7.11 and Fig.7.14), we have estimated flow factors as regards total flow, flow factors that correspond to different parts of the repository and different directions of the regional flow. We will use flow factors that represent the expected flow, by expected flow we mean the most probable outcome. These flow factors will produce the expected flow of a repository in a heterogeneous rock mass. It is possible to estimate flow factors that correspond to another statistical condition, e.g. flow factors that represent the 90th percentile. The flow factors that we will use represent a heterogeneous rock mass of Äspö properties, as defined in Chapters 5, 6 and 7.

The flow factors as regards expected total flow, for different directions of the regional flow, and for different parts of the repository, are given in Figure 9.14. For SFL 4, the flow factors vary between 2.0 to 2.2, for SFL 3 and SFL 5 the flow factors vary between 2.0 and 2.8, depending on the direction of the regional flow.

Results as regards direction of regional flow

By using equation 9.2 , the flow factors given in Figure 9.14 and the total flow given in Figures 9.1 to 9.5, we have calculated the flows in different parts of the repository for different directions of the regional flow. The studied scenario is Case 1 (see Table 8.2.). The results of the simulations are given in the following figures and table:

- SFL 4 Case 1: in Figure 9.15.
- SFL 3 Case 1: in Figure 9.16 (barrier and encapsulation).
- SFL 5 Case 1: in Figure 9.17 (barrier and encapsulation).

Studying the figures and comparing them to the figures representing the flow of tunnels in a homogeneous rock mass, we note the following. For SFL 4, no large changes have occurred, except that the expected flow has been increased about two times. For SFL 3 and SFL 5, the expected flow has increased 2 to 2.8 times. The distinct change is that for a heterogeneous rock mass the size of the expected flow in the SFL 3 and SFL 5 is most increased for a regional flow that is vertical or close to vertical. The results for SFL 3 and SFL 5 are very similar, as they have an identical lay-out in the model.

- *Expected total flow in the SFL 4 tunnel.* Maximum flow occurs when the regional flow is horizontal and at right angles to the SFL 3 and SFL 5 tunnels (Q). Minimum flow occurs place when the regional flow is vertical (U).

Case 1: minimum= 24820, maximum= 115180, mean= 78042, maximum/minimum= 4.6

- *Expected total flow in a positive flow barrier of SFL 3 and 5.*

Both SFL 3 and SFL 5 demonstrate very much the same behavior. However, SFL 5 forms an extra flow barrier when the regional flow is horizontal, or close to horizontal, which gives a somewhat smaller flow in SFL 3 than in SFL 5. The largest flow occurs when the regional flow is vertical (U). Minimum flow occurs when the regional flow is horizontal and directed at right angles to the barriers (Q).

Case 1, SFL 3: minimum= 8390, maximum= 16180, mean= 12400, maximum/minimum= 1.9

Case 1, SFL 5: minimum= 8450, maximum= 16210, mean= 13130, maximum/minimum= 1.9

- *Expected total flow in the encapsulation of SFL 3 and 5.*

The encapsulations are protected by positive barriers. Both SFL 3 and SFL 5 demonstrate very much the same behavior. But as for the barriers, the flow in the SFL 3 encapsulation is somewhat smaller than the flow in the SFL 5 encapsulation. The largest occurs when the regional flow is vertical (U). Minimum flow occurs when the regional flow is horizontal and directed along the barriers (A).

Case 1, SFL 3: minimum= 1.5 , maximum= 5.0 , mean= 3.4 , maximum/minimum= 3.3

Case 1, SFL 5: minimum= 1.6 , maximum= 5.0 , mean= 3.8 , maximum/minimum= 3.1

9.8 Conclusions - Summary

Below will follow a short recapitulation of the results given in this chapter.

9.8.1 Sensitivity to the conductivity of the flow barriers in SFL 3-5

SFL 3 and 5, Flow barriers. The flow in the barriers will vary depending on the conductivity of the barriers. The maximum flow is about 6500 times the size of the regional flow.

SFL 3 and 5, Encapsulations. The flow barrier will reduce the flow in the encapsulation. The larger the contrast between the conductivity of the flow barrier and the conductivity of the rock mass, the smaller the flow in the encapsulation. By using a positive flow barrier, with a conductivity that is 100 000 times that of the rock mass, it is possible to reduce the flow in the encapsulation with about 3 orders of magnitude, compared to an unprotected encapsulation. A negative barrier needs to have a conductivity that is smaller than 0.1 times that of the rock mass, to significantly reduce the flow in the encapsulation, and for a large reduction of flow in the encapsulation, the conductivity of a negative barrier needs to be extremely small.

SFL 4. The flow in SFL 4 is not much affected by the conductivity of the flow barriers.

9.8.2 Sensitivity to direction of regional flow

SFL 4. Depending on the direction of the regional flow, the total flow of SFL 4 may vary within a range of 5 times, maximum total flow is about 60000 times the size of the regional flow.

SFL 3 and 5, Flow barriers. Depending on the direction of the regional flow, the total flow of SFL 3 and 5 flow barriers may vary within a range of 2 times. For a positive barrier, the maximum total flow is about 6500 times the size of the regional flow. For a negative barrier (bentonite), the maximum total flow is about 1750 times the size of the regional flow.

SFL 3 and 5, Encapsulations. Depending on the direction of the regional flow, the total flow of SFL 3 and 5 encapsulations may vary within a range of 3 times. For an encapsulation protected by a positive barrier, the maximum total flow is about 2 times the size of the regional flow. For an encapsulation protected by a negative barrier (bentonite), the maximum total flow is about 680 times the size of the regional flow.

9.8.3 Sensitivity to conductivity of back filling in SFL 4

SFL 4. For an SFL 4 tunnel with a conductivity that is four orders of magnitude larger than that of the rock mass, or for a tunnel with an even larger conductivity (e.g. an empty tunnel), the maximum total flow is about 60000 times the size of the regional flow. If the conductivity of the tunnel filling is one order of magnitude smaller than that of the rock mass, the maximum total flow is about 4000 times the size of the regional flow.

SFL 3 and 5 flow barriers and encapsulation. If the regional flow is in the horizontal plane, or close to the horizontal plane, the models predict the following. The conductivity of the SFL 4 tunnel will influence the flow in SFL 3 and 5. Hence, if the SFL 4 tunnel has a small conductivity, much smaller than 10000 times that of the rock mass, the flow in SFL 3 and 5 will be increased about 2 times, compared to the maximum flow given in Sec.9.8.2. If the SFL 4 tunnel has a large conductivity, much larger than 10000 times that of the rock mass, the flow in SFL 3 and 5 will be reduced, compared to the maximum flow given in Sec.9.8.2.

9.8.4 Sensitivity to plugs in tunnels

The following results are given in comparison with the preliminary design.

No plugs inside repository. The total flow in SFL 4 tunnel will be increased about 2 times, at the most. The flow in SFL 3 and 5 encapsulations will be increased about 6 times, at the most. The flow in SFL 3 and 5 barriers will be increased about 4 times, at the most.

Four extra plugs in SFL 4. The total flow in SFL 4 tunnel will be decreased between 1 and 0.7 times, depending on direction of regional flow. As regards the total flow of the SFL 3 and SFL 5 barriers and encapsulations, the effects of the extra plugs will vary depending on direction of regional flow, from a decrease of about 0.5 times to an increase of about 3 times.

9.8.5 Sensitivity to heterogeneity of rock mass

A heterogeneous rock mass will increase the flow in the repository, compared to a homogeneous rock mass having the same conductivity. A rock mass with a heterogeneity representing the Äspö properties will produce the following increase in total flow. The increase in flow corresponds to the expected flow (the most probable outcome).

SFL 4. The flow will be increased about 2 - 2.2 times depending on direction of regional flow. This gives a maximum flow of about 120000 times the size of the regional flow.

SFL 3 and SFL 5 flow barriers and encapsulation. The flow will be increased about 2 - 2.8 times depending on direction of regional flow. For a positive barrier, the maximum flow will be about 17000 times the size of the regional flow. For an encapsulation protected by a positive barrier, the maximum flow will be about 5.0 times the size of the regional flow.

Table 9.1 SENSITIVITY TO ALTERNATIVE LAY-OUTS, EFFECTS OF PLUGS, SCEN.2
 The table presents the effect of a change in tunnel lay-out, compared to the preliminary design. The table gives the change in flow that will occur if the plugs at the ends of the SFL 3 and SFL 5 tunnels are taken away (Scenario 2).

Scenario	Structure	Direction of regional flow. (see Figure 8.3)	Effect on flow	
			Specific flow	Total flow
<p><u>Scenario 2.</u> In comparison with the preliminary design, all the plugs inside the repository are taken away.</p> <ul style="list-style-type: none"> • No plugs in the repository 	SFL 3 Encapsulation (=SFL 5 encap.)	A: Ha=0, Va=0	Increases 5.2 times	Increases 5.2 times
		Q: Ha=90, Va=0	Increases 4.3 times	Increases 2.3 times
		U: Ha= -, Va=90	Increases 1.1 times	Increases 1.1 times
	SFL 3 Barrier (=SFL 5 barrier)	A: Ha=0, Va=0	Increases 5.5 times	Increases 3.3 times
		Q: Ha=90, Va=0	Increases 6.7 times	Increases 2.5 times
		U: Ha= -, Va=90	Increases 1.8 times	Increases 1.2 times
	SFL 4 tunnel	A: Ha=0, Va=0	<u>Decreases</u> 0.4 times	Increases 1.7 times
		Q: Ha=90, Va=0	Increases 1.1 times	Increases 1.2 times
		U: Ha= -, Va=90	Increases 4.1 times	Increases 1.3 times

Table 9.2 SENSITIVITY TO ALTERNATIVE LAY-OUTS, EFFECTS OF PLUGS, SCEN.3
 The table presents the effect of a change in tunnel lay-out, compared to the original design. The table gives the change in flow that will occur if four plugs are added in the SFL 4 tunnel (Scenario 3).

Scenario	Structure	Direction of regional flow. (see Figure 8.3)	Effect on flow	
			Specific flow	Total flow
<p><u>Scenario 3</u> In comparison with the original design, plugs are added at four locations in the SFL 4 tunnel</p> <ul style="list-style-type: none"> • Plugs at both ends of SFL 3 and SFL 5, four plugs in SFL 4. 	SFL 3 Encapsulation (=SFL 5 encap.)	A: Ha=0, Va=0	Increases 2.0 times	Increases 2.1 times
		Q: Ha=90, Va=0	Decreases 0.77 times	Decreases 0.77 times
		U: Ha= -, Va=90	No change	No change
	SFL 3 Barrier (=SFL 5 barrier)	A: Ha=0, Va=0	Increases 2.0 times	Increases 2.0 times
		Q: Ha=90, Va=0	Decreases 0.32 times	Decreases 0.56 times
		U: Ha= -, Va=90	No change	No change
	SFL 4 tunnel	A: Ha=0, Va=0	Decreases 0.28 times	Decreases 0.67 times
		Q: Ha=90, Va=0	Decreases 0.34 times	Decreases 0.67 times
		U: Ha= -, Va=90	Decreases 0.45 times	Decreases 0.96 times

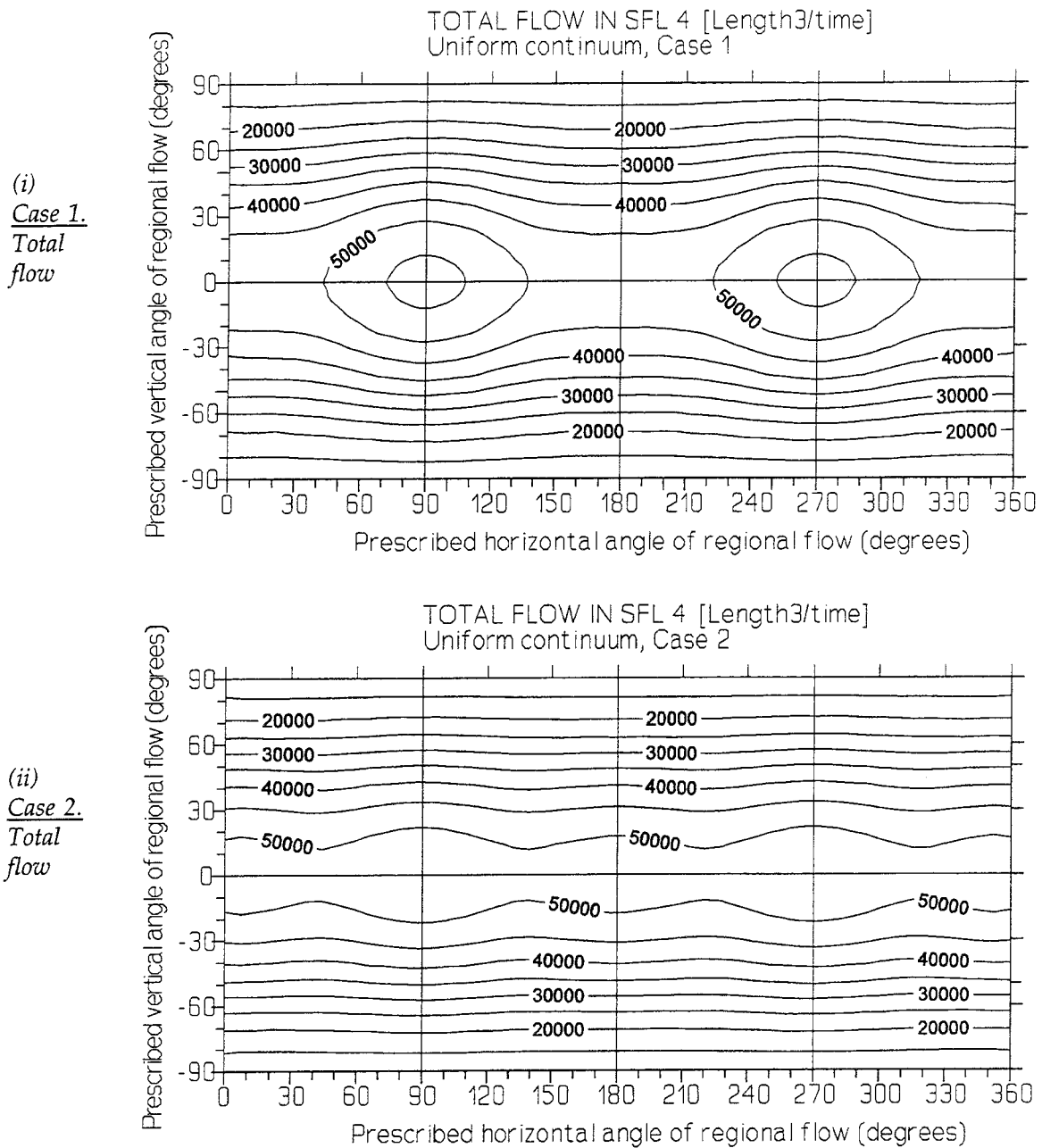


Figure 9.1

**FLOW IN THE SFL 4 TUNNEL, HOMOGENEOUS ROCK MASS.
SENSITIVITY TO DIRECTION OF THE REGIONAL FLOW.**

Total flow in the SFL 4 tunnel for two scenarios: (i) Case 1 and (ii) Case 2.

Sensitivity of flow, as regards the direction of the regional groundwater flow.

- Case 1: conductiv. of SFL 3,5 flow barriers is 100000 times that of the rock mass
- Case 2: conductiv. of SFL 3,5 flow barriers is 0.1 times that of the rock mass.

The rock mass is defined as homogeneous, - it is a uniform continuum model.

The X-axis and the Y-axis of the figure represent all possible directions of regional flow in the horizontal and vertical plane. The prescribed angles (horizontal and vertical) are defined in accordance with the system given in Figure 8.3. The figures are based on 114 calculated values, representing the whole sphere of possible directions of regional flow. Interpolation between these values was done by the use of a kriging routine. The size of the flow should be regarded as a multiple of the size of an unknown regional groundwater flow.

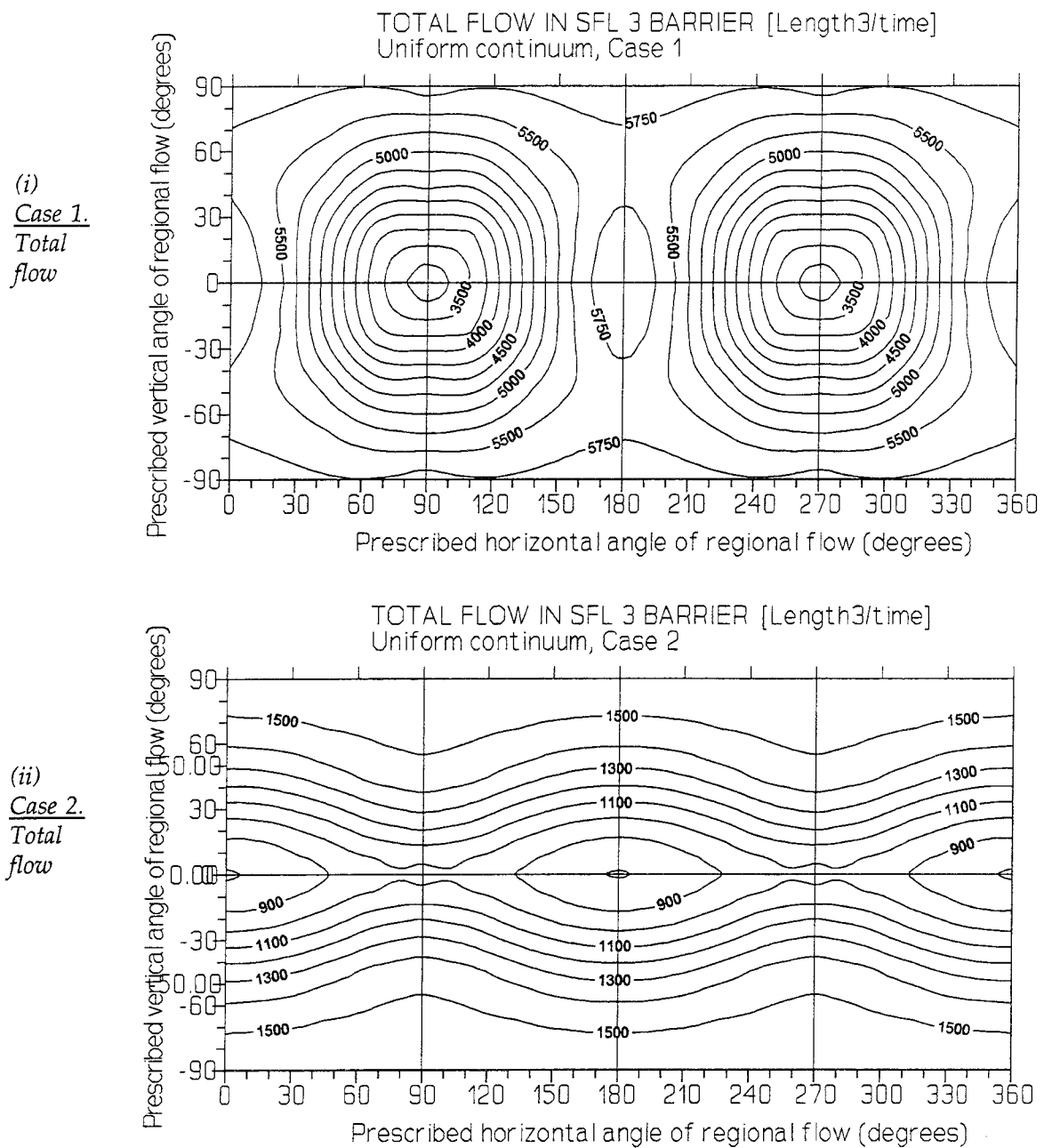


Figure 9.2

**FLOW IN THE SFL 3 BARRIER, HOMOGENEOUS ROCK MASS.
SENSITIVITY TO DIRECTION OF THE REGIONAL FLOW.**

Total flow in the SFL 3 flow barrier, for two scenarios: (i) Case 1 and (ii) Case 2.

Sensitivity of flow, as regards the direction of the regional groundwater flow.

- Case 1 the conductivity of the flow barriers is 100000 times that of the rock mass
- Case 2 the conductivity of the flow barriers is 0.1 times that of the rock mass.

The rock mass is defined as homogeneous, - it is a uniform continuum model.

The X-axis and the Y-axis of the figure represent all possible directions of regional flow in the horizontal and vertical plane. The prescribed angles (horizontal and vertical) are defined in accordance with the system given in Figure 8.3. The figures are based on 114 calculated values, representing the whole sphere of possible directions of regional flow. Interpolation between these values was done by the use of a kriging routine. The size of the flow should be regarded as a multiple of the size of an unknown regional groundwater flow.

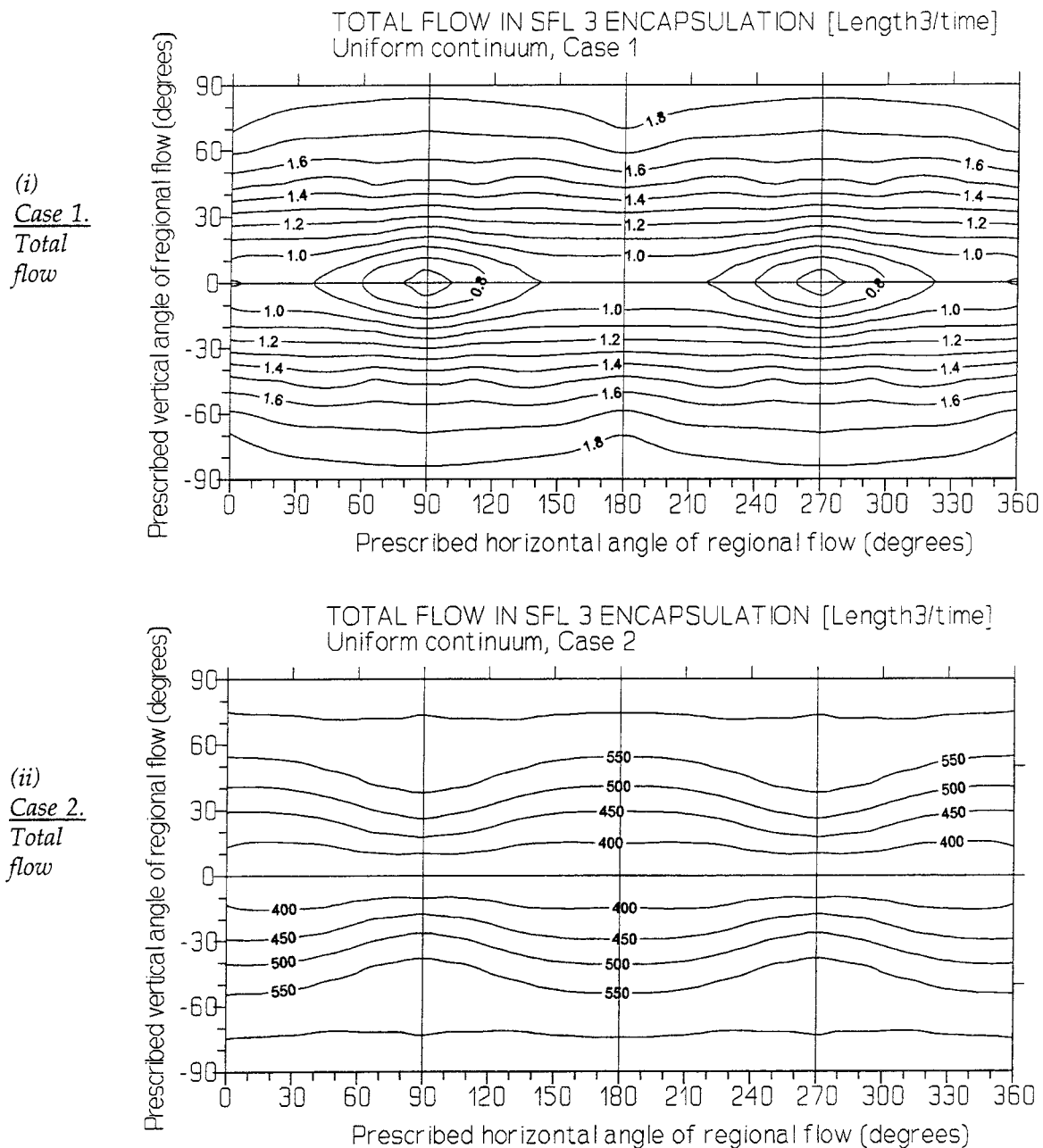


Figure 9.3 FLOW IN THE SFL 3 ENCAPSULATION, HOMOGENEOUS ROCK MASS. SENSITIVITY TO DIRECTION OF THE REGIONAL FLOW.
Total flow in the SFL 3 encapsulation for two scenarios: (i) Case 1 and (ii) Case 2. Sensitivity of flow, as regards the direction of the regional groundwater flow.

- Case 1 the conductivity of the flow barriers is 100000 times that of the rock mass
- Case 2 the conductivity of the flow barriers is 0.1 times that of the rock mass.

The rock mass is defined as homogeneous, - it is a uniform continuum model.

The X-axis and the Y-axis of the figure represent all possible directions of regional flow in the horizontal and vertical plane. The prescribed angles (horizontal and vertical) are defined in accordance with the system given in Figure 8.3. The figures are based on 114 calculated values representing the whole sphere of possible directions of regional flow. Interpolation between these values was done by the use of a kriging routine. The size of the flow should be regarded as a multiple of the size of an unknown regional groundwater flow.

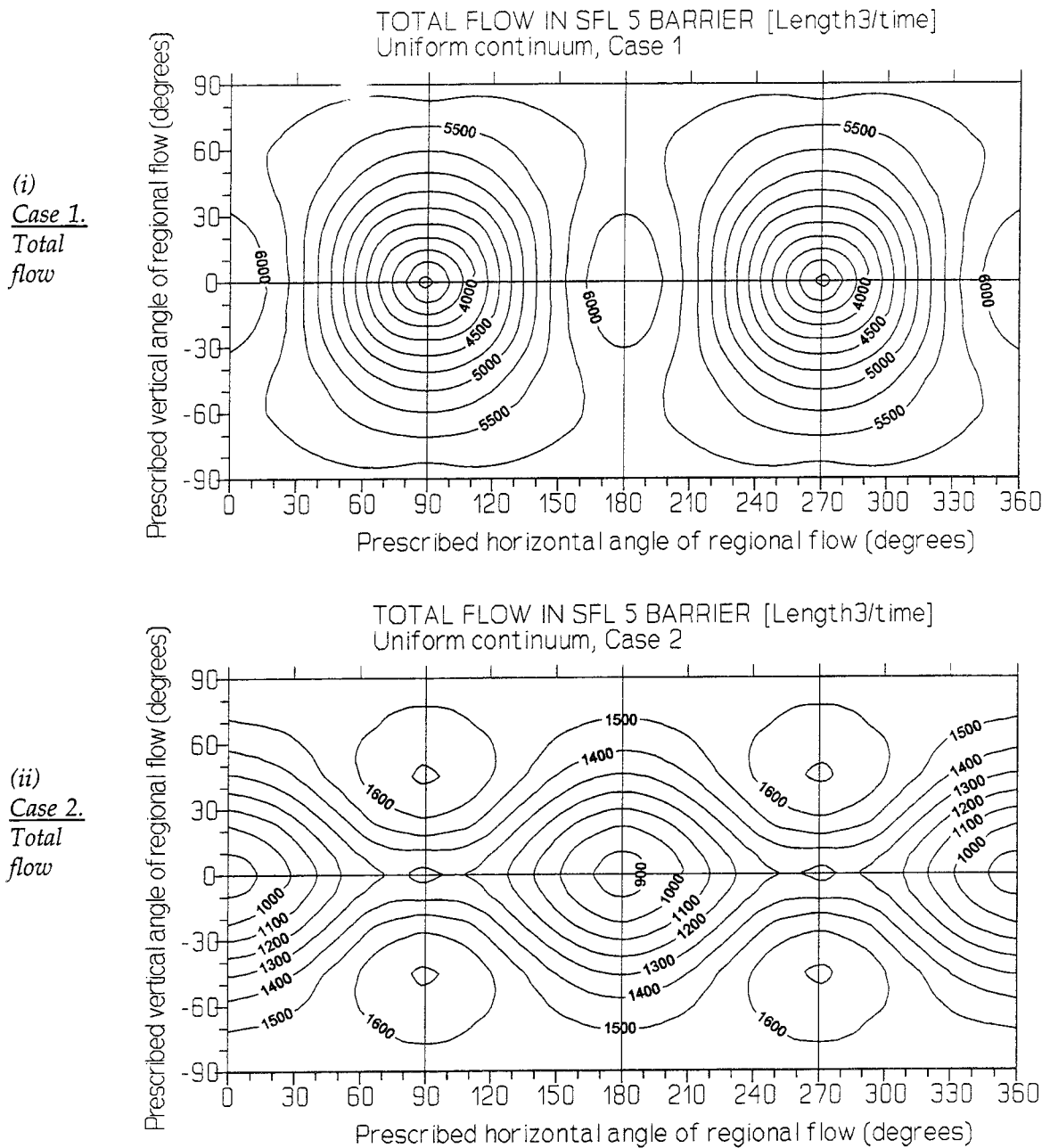


Figure 9.4

**FLOW IN THE SFL 5 BARRIER, HOMOGENEOUS ROCK MASS.
SENSITIVITY TO DIRECTION OF THE REGIONAL FLOW.**

Total flow in the SFL 5 flow barrier, for two scenarios: (i) Case 1 and (ii) Case 2. Sensitivity of flow, as regards the direction of the regional groundwater flow.

- Case 1 the conductivity of the flow barriers is 100000 times that of the rock mass
- Case 2 the conductivity of the flow barriers is 0.1 times that of the rock mass.

The rock mass is defined as homogeneous, - it is a uniform continuum model.

The X-axis and the Y-axis of the figure represent all possible directions of regional flow in the horizontal and vertical plane. The prescribed angles (horizontal and vertical) are defined in accordance with the system given in Figure 8.3. The figures are based on 114 calculated values, representing the whole sphere of possible directions of regional flow. Interpolation between these values was done by the use of a kriging routine. The size of the flow should be regarded as a multiple of the size of an unknown regional groundwater flow.

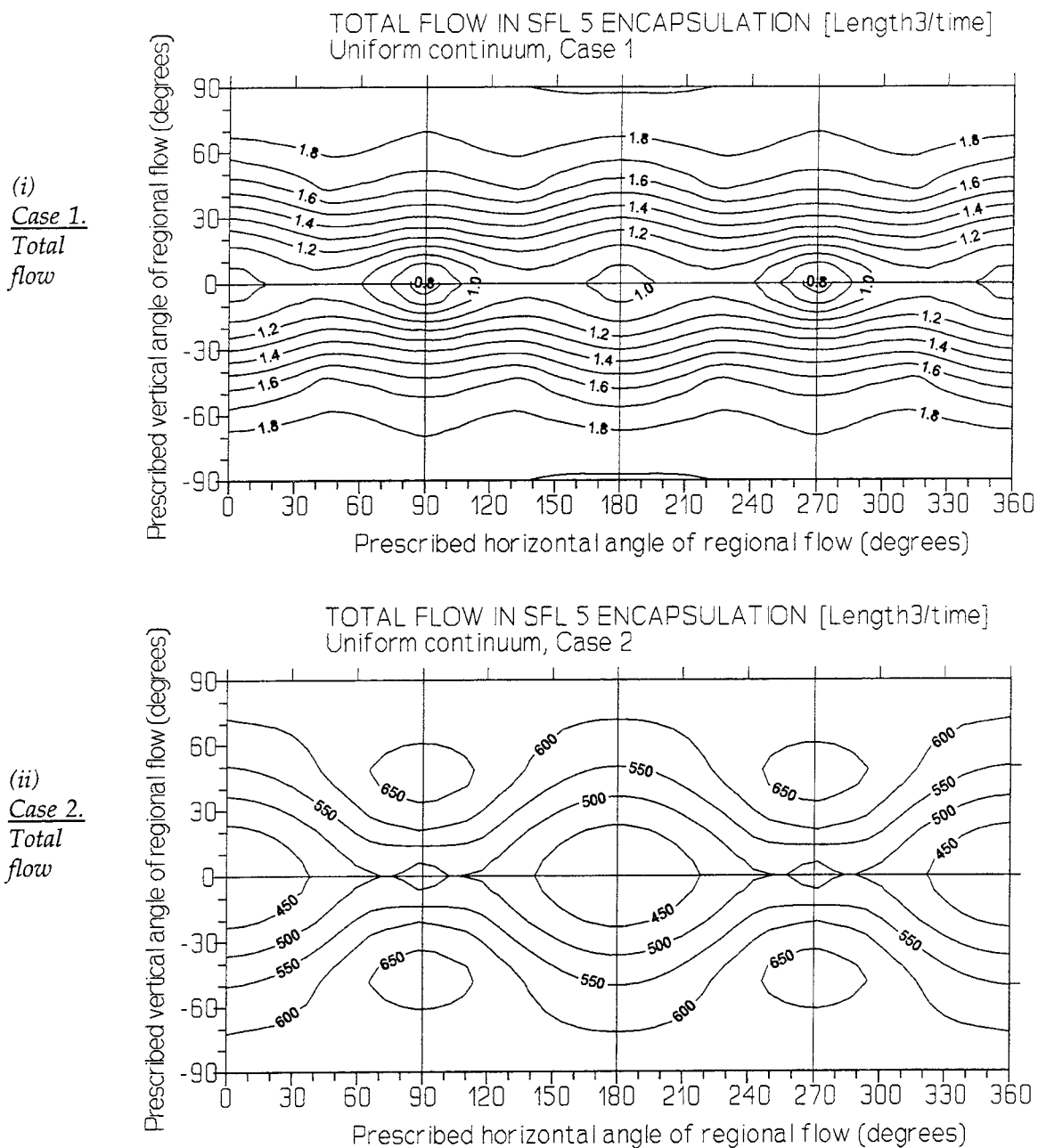


Figure 9.5

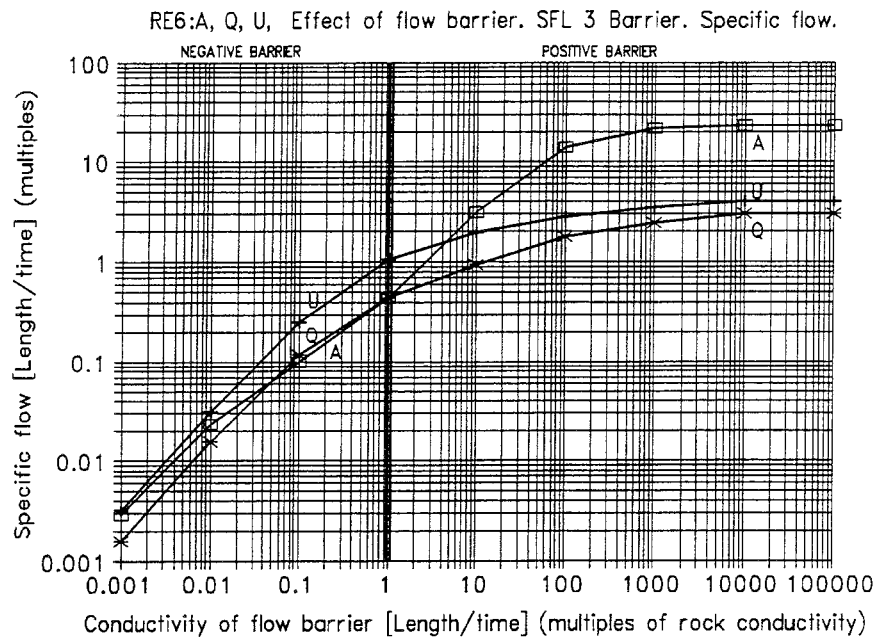
FLOW IN THE SFL 5 ENCAPSULATION, HOMOGENEOUS ROCK MASS. SENSITIVITY TO DIRECTION OF THE REGIONAL FLOW.

Total flow in the SFL 5 encapsulation for two scenarios: (i) Case 1 and (ii) Case 2. Sensitivity of flow, as regards the direction of the regional groundwater flow.

- Case 1 the conductivity of the flow barriers is 100000 times that of the rock mass
 - Case 2 the conductivity of the flow barriers is 0.1 times that of the rock mass.
- The rock mass is defined as homogeneous, - it is a uniform continuum model.

The X-axis and the Y-axis of the figure represent all possible directions of regional flow in the horizontal and vertical plane. The prescribed angles (horizontal and vertical) are defined in accordance with the system given in Figure 8.3. The figures are based on 114 calculated values, representing the whole sphere of possible directions of regional flow. Interpolation between these values was done by the use of a kriging routine. The size of the flow should be regarded as a multiple of the size of an unknown regional groundwater flow.

(i)
Specific flow
in the SFL 3
flow barrier



(ii)
Total flow
in the SFL 3
flow barrier

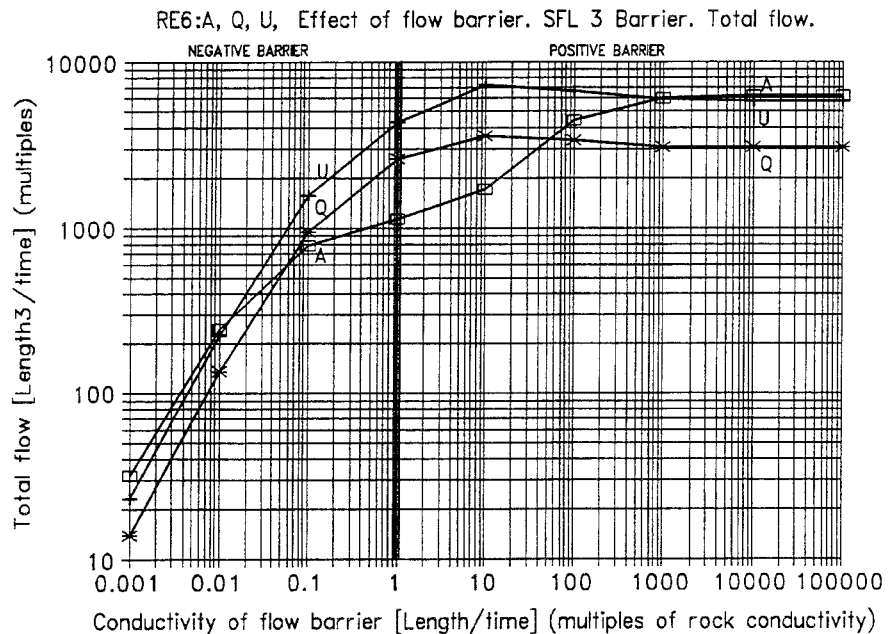
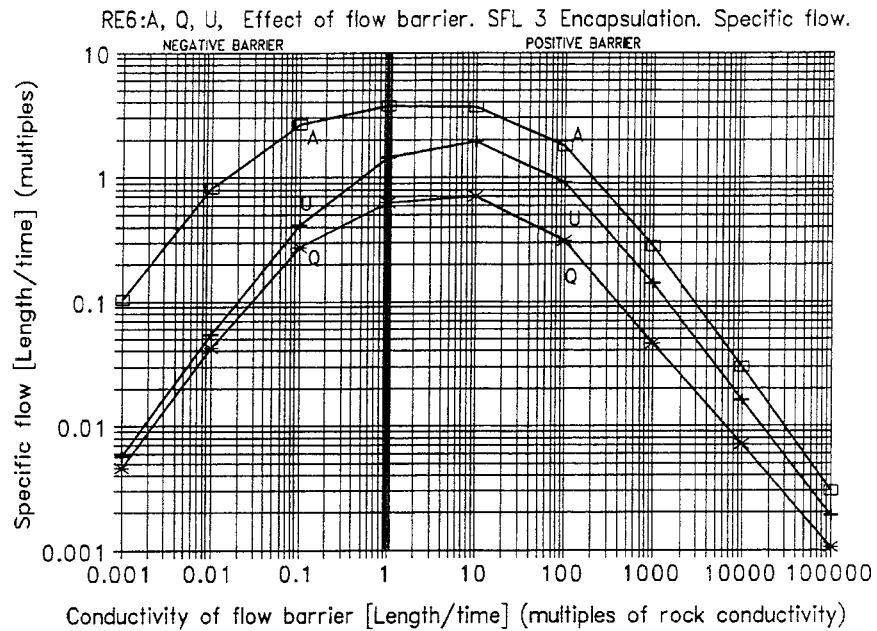


Figure 9.6 FLOW IN SFL 3 FLOW BARRIER, SENSITIVITY TO BARRIER CONDUCT. Specific flow (i) and Total flow (ii) in the flow barrier of SFL 3, versus the conductivity of the flow barrier. The encapsulation has a conductivity which is 10 times that of the rock mass. Plugs are at the ends of the SFL 3 and 5 tunnels. The SFL 4 tunnel has a conductivity which is 10000 times that of the rock mass. The rock mass is defined as homogeneous - uniform continuum model. The flow is given as multiples of an unknown regional flow.

The regional flow is directed as follows (see Figure 8.3):

A: Along SFL 3:	Hor.angle=0° Vert.angle=0°, denoted by: squares
Q: At right angle to SFL 3:	Hor.angle=90° Vert.angle=0°, denoted by: crosses
U: Vertical flow:	Hor.angle=- Vert.angle=90°, denoted by: pluses

(i)
Specific flow
in the SFL 3
encapsulation



(ii)
Total flow
in the SFL 3
encapsulation

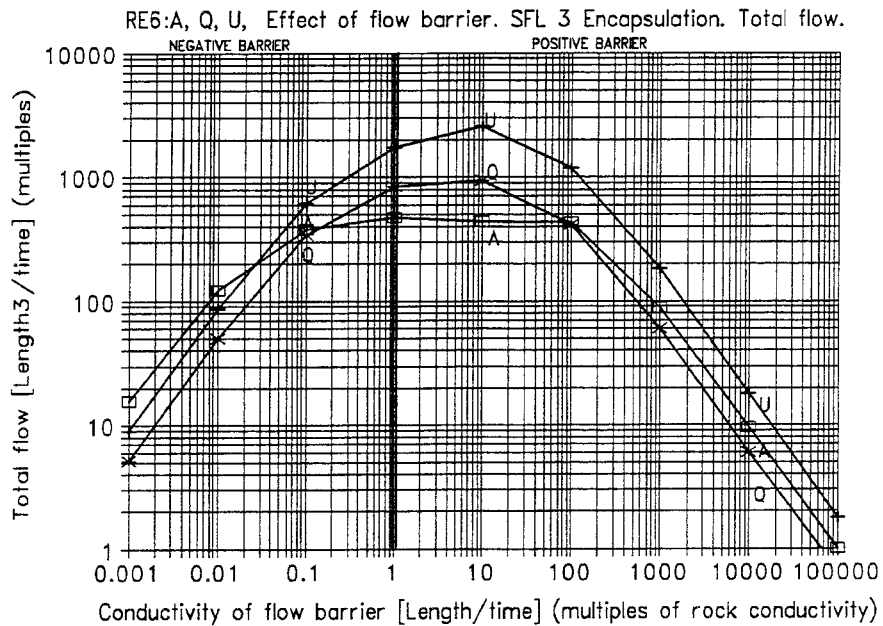
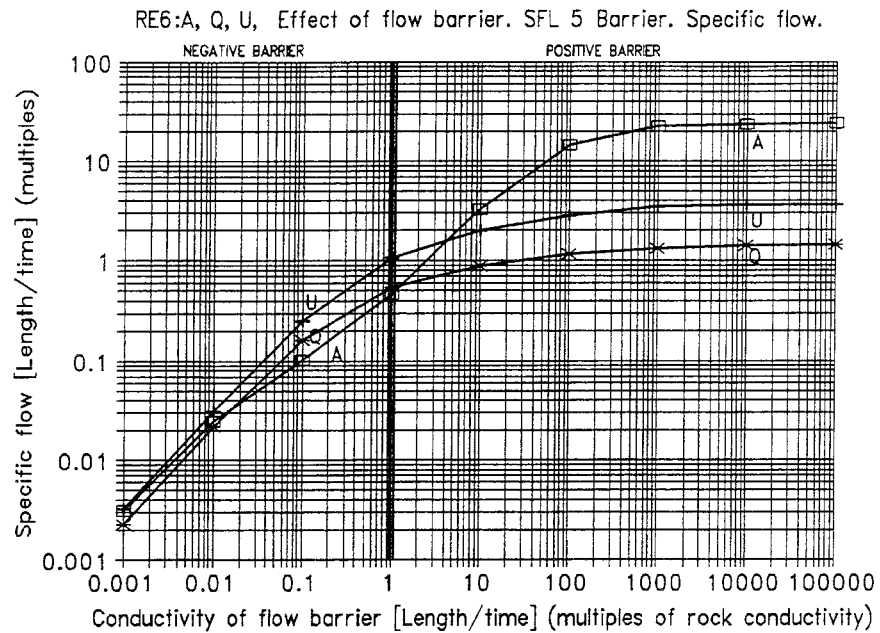


Figure 9.7 FLOW IN SFL 3 ENCAPSULATION, SENSITIVITY TO BARRIER CONDUCTIVITY
Specific flow (i) and Total flow (ii) in the encapsulation of SFL 3, versus the conductivity of the flow barrier. The encapsulation has a conductivity which is 10 times that of the rock mass. Plugs are at the ends of the SFL 3 and 5 tunnels. The SFL 4 tunnel has a conductivity which is 10000 times that of the rock mass. The rock mass is defined as homogeneous - uniform continuum model. The flow is given as multiples of an unknown regional flow.

The regional flow is directed as follows (see Figure 8.3):

A: Along SFL 3:	Hor.angle=0° Vert.angle=0°, denoted by: squares
Q: At right angle to SFL 3:	Hor.angle=90° Vert.angle=0°, denoted by: crosses
U: Vertical flow:	Hor.angle=- Vert.angle=90°, denoted by: pluses

(i)
Specific flow
in the SFL 5
flow barrier



(ii)
Total flow
in the SFL 5
flow barrier

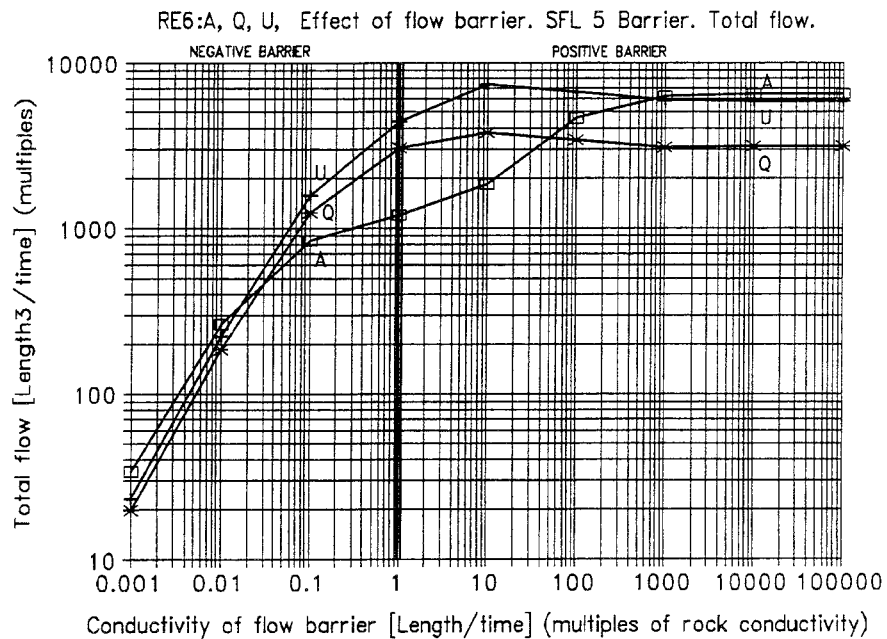
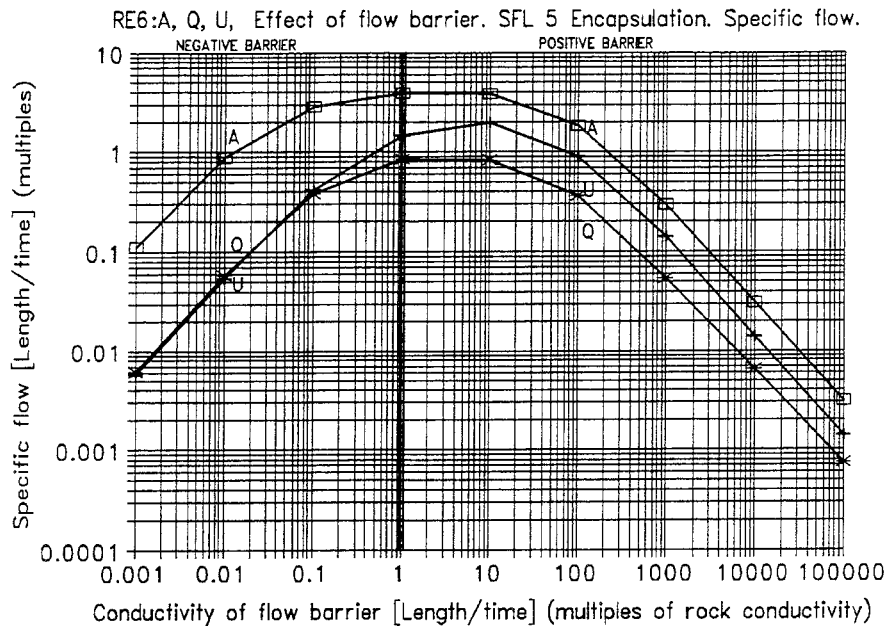


Figure 9.8 FLOW IN SFL 5 FLOW BARRIER, SENSITIVITY TO BARRIER CONDUCT. Specific flow (i) and Total flow (ii) in the flow barrier of SFL 5, versus the conductivity of the flow barrier. The encapsulation has a conductivity which is 10 times that of the rock mass. Plugs are at the ends of the SFL 3 and 5 tunnels. The SFL 4 tunnel has a conductivity which is 10000 times that of the rock mass. The rock mass is defined as homogeneous - uniform continuum model. The flow is given as multiples of an unknown regional flow.

The regional flow is directed as follows (see Figure 8.3):

A: Along SFL 5:	Hor.angle=0° Vert.angle=0°, denoted by: squares
Q: At right angle to SFL 5:	Hor.angle=90° Vert.angle=0°, denoted by: crosses
U: Vertical flow:	Hor.angle=- Vert.angle=90°, denoted by: pluses

(i)
Specific flow
in the SFL 5
encapsulation



(ii)
Total flow
in the SFL 5
encapsulation

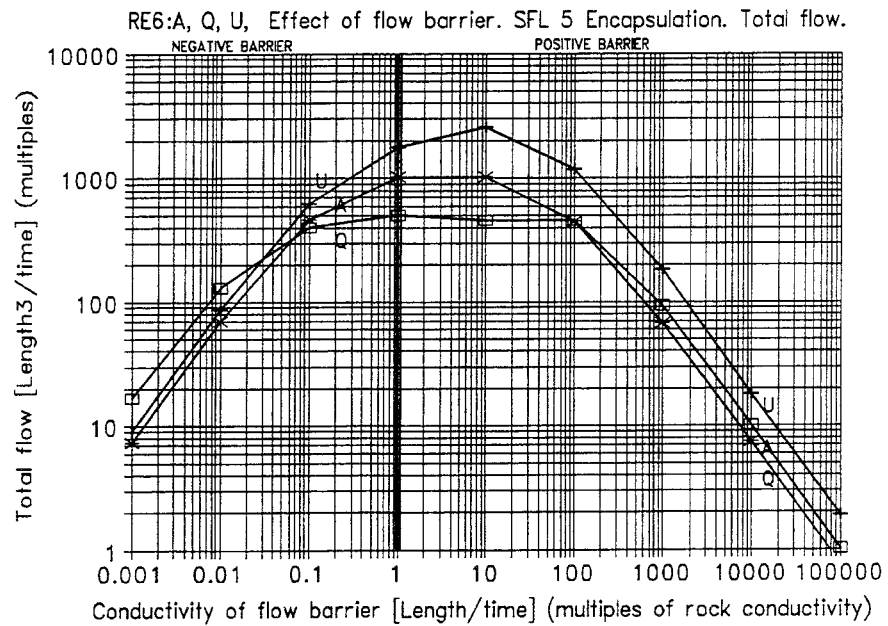


Figure 9.9 FLOW IN SFL 5 ENCAPSULATION, SENSITIVITY TO BARRIER CONDUCT Specific flow (i) and Total flow (ii) in the encapsulation of SFL 5, versus the conductivity of the flow barrier. The encapsulation has a conductivity which is 10 times that of the rock mass. Plugs are at the ends of the SFL 3 and 5 tunnels. The SFL 4 tunnel has a conductivity which is 10000 times that of the rock mass. The rock mass is defined as homogeneous - uniform continuum model. The flow is given as multiples of an unknown regional flow.

The regional flow is directed as follows (see Figure 8.3):

- | | |
|-----------------------------|--|
| A: Along SFL 5: | Hor.angle=0° Vert.angle=0°, denoted by: squares |
| Q: At right angle to SFL 5: | Hor.angle=90° Vert.angle=0°, denoted by: crosses |
| U: Vertical flow: | Hor.angle=- Vert.angle=90°, denoted by: pluses |

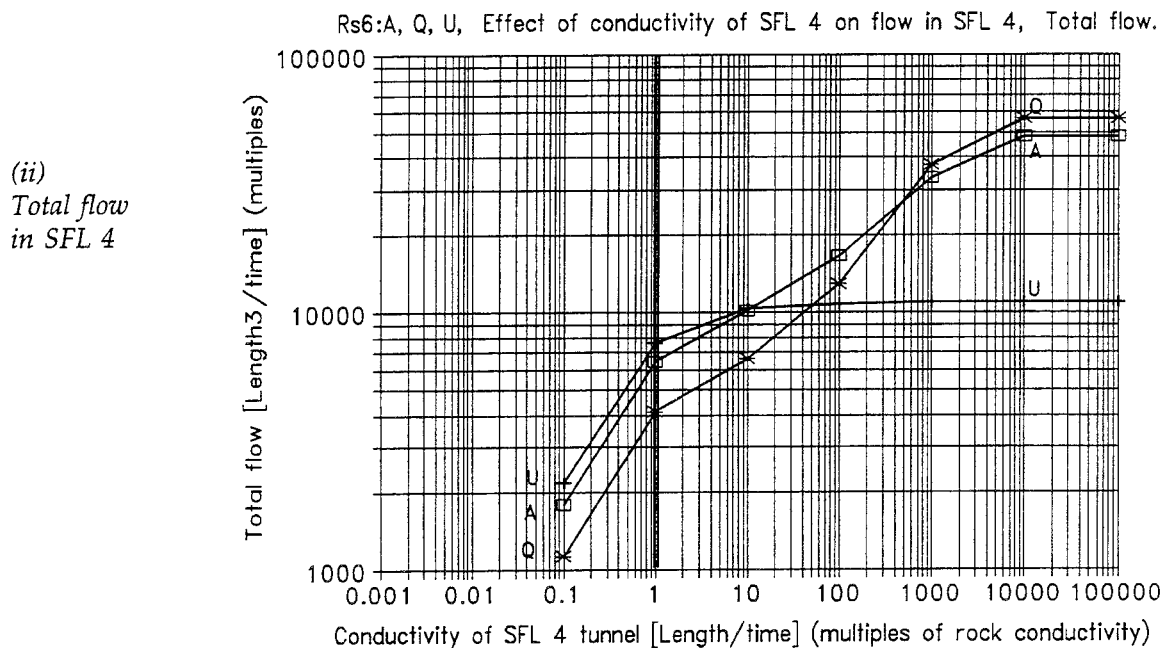
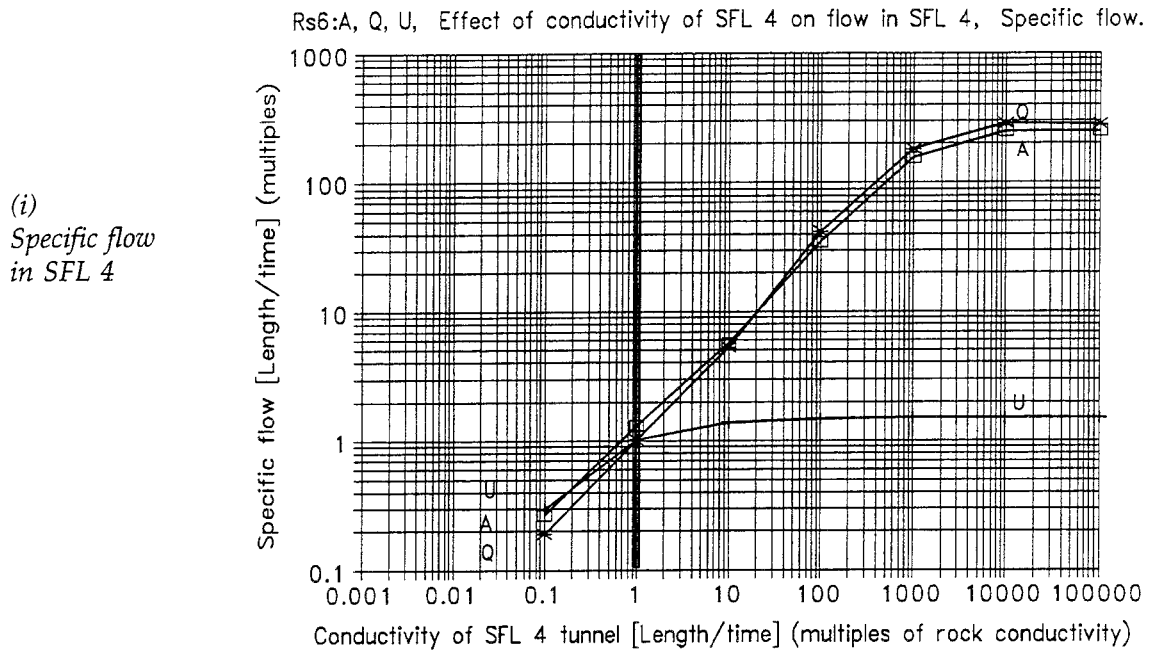


Figure 9.10 FLOW IN SFL 4, SENSITIVITY TO CONDUCTIVITY OF SFL 4.
Specific flow (i) and Total flow (ii) in the tunnel of SFL 4, versus the conductivity of the tunnel. The SFL 3 and 5 encapsulations have a conductivity which is 10 times that of the rock mass. The flow barriers of SFL 3 and 5 have a conductivity which is 100000 times that of the rock mass. Plugs are at the ends of SFL 3 and 5 tunnels. The rock mass is defined as homogeneous - uniform continuum model. The flow is given as multiples of an unknown regional flow.

The regional flow is directed as follows (see Figure 8.3):

A: Along SFL 3 and 5: Hor.angle=0° Vert.angle=0°, denoted by: squares
 Q: At right angle to SFL 3, 5: Hor.angle=90° Vert.angle=0°, denoted by: crosses
 U: Vertical flow: Hor.angle=- Vert.angle=90°, denoted by: pluses

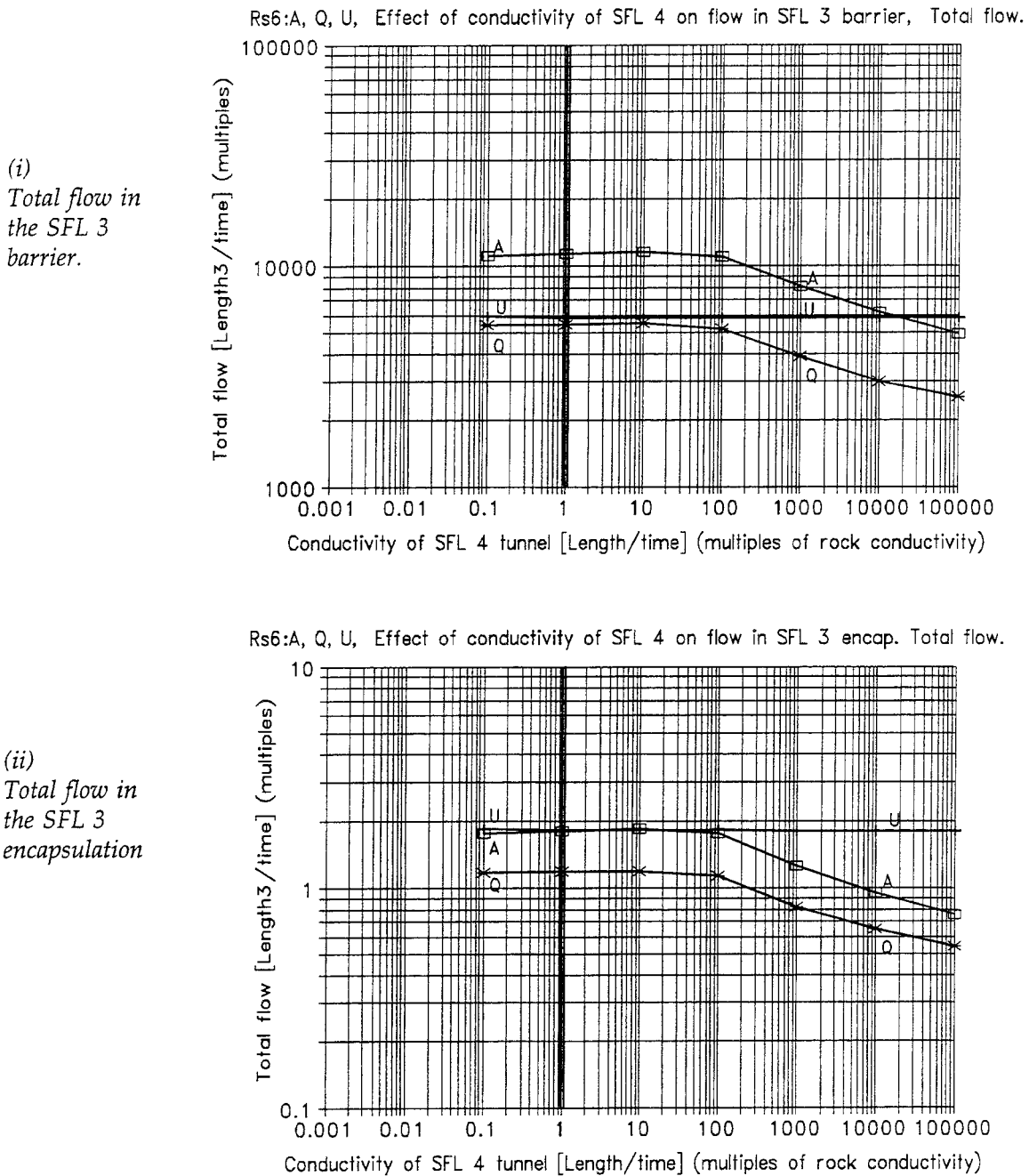
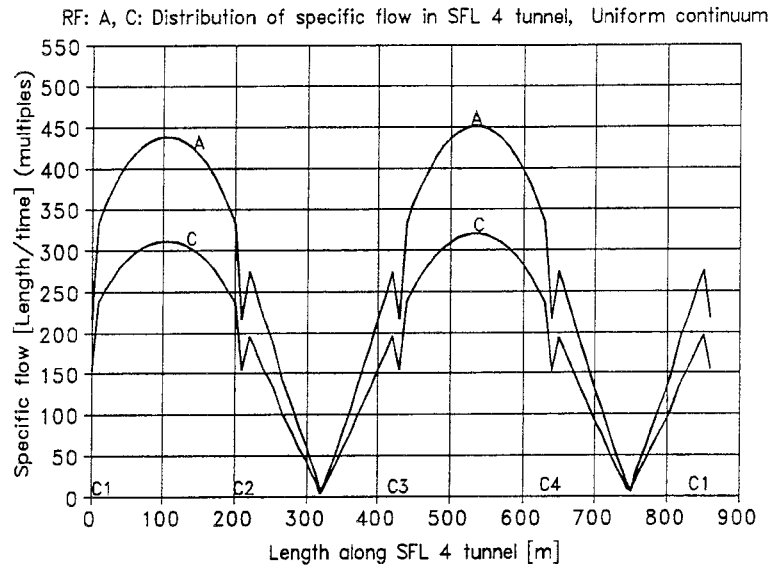


Figure 9.11 FLOW IN SFL 3, SENSITIVITY TO CONDUCTIVITY OF SFL 4. Total flow in (i) the SFL 3 barrier and in (ii) the SFL 3 encapsulation, versus the conductivity of the SFL 4 tunnel. The SFL 3 and 5 encapsulations have a conductivity which is 10 times that of the rock mass. The flow barriers of SFL 3, 5 have a conductivity which is 100000 times that of the rock mass. Plugs are at the ends of SFL 3 and 5 tunnels. The rock mass is defined as homogeneous -uniform continuum model. The flow is given as multiples of an unknown regional flow.

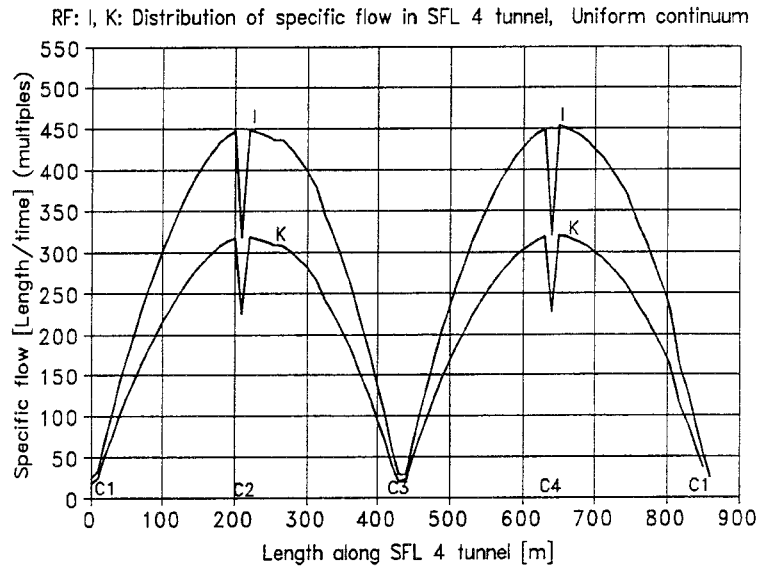
The regional flow is directed as follows (see Figure 8.3):

- | | |
|-------------------------------|--|
| A: Along SFL 3 and 5: | Hor.angle=0° Vert.angle=0°, denoted by: squares |
| Q: At right angle to SFL 3,5: | Hor.angle=90° Vert.angle=0°, denoted by: crosses |
| U: Vertical flow: | Hor.angle=- Vert.angle=90°, denoted by: pluses |

(i)
 Specific flow in the SFL 4 tunnel
 versus length of tunnel.
 Direction of regional flow:
 A: Hor.= 0 deg, Vert.=0 deg
 C: Hor.= 0 deg, Vert.=45 deg
 (see Figure 8.3)



(ii)
 Specific flow in the SFL 4 tunnel
 versus length of tunnel.
 Direction of regional flow:
 I: Hor.= 45 deg, Vert.=0 deg
 K: Hor.= 45 deg, Vert.=45 deg
 (see Figure 8.3)



(iii)
 Specific flow in the SFL 4 tunnel
 versus length of tunnel.
 Direction of regional flow:
 Q: Hor.= 90 deg, Vert.=0 deg
 S: Hor.= 90 deg, Vert.=45 deg
 (see Figure 8.3)

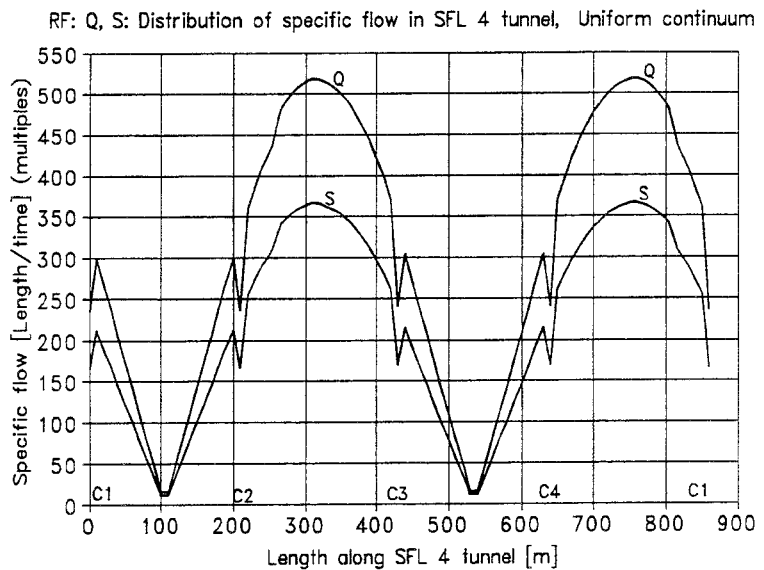
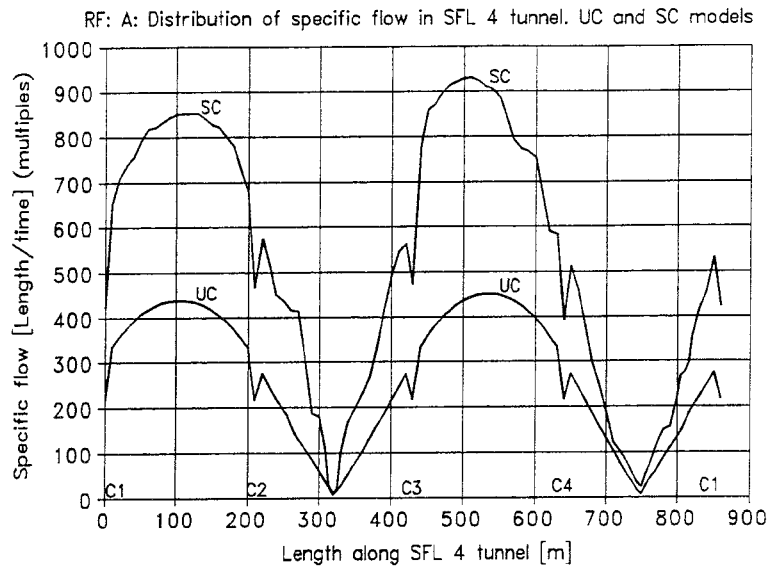
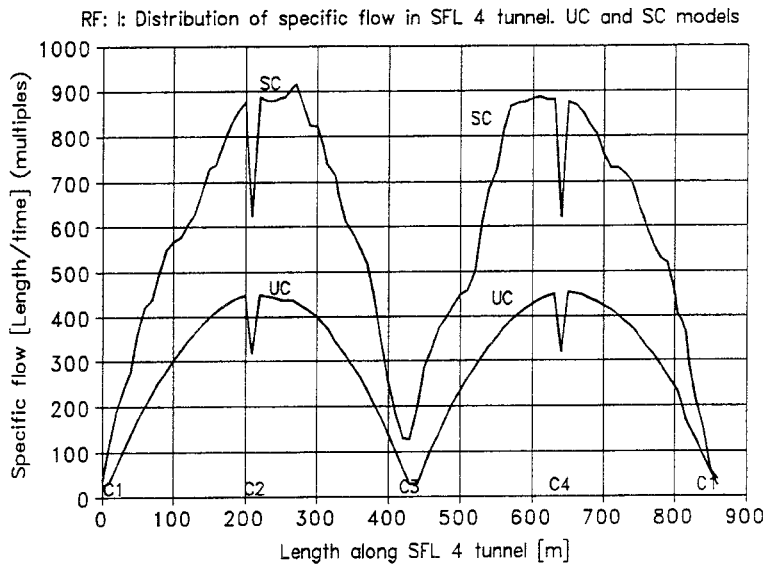


FIGURE 9.12
 DISTRIBUTION OF SPECIFIC
 FLOW IN THE SFL 4 TUNNEL.
 UNIFORM CONT. MODELS.
 The SFL 4 tunnel has a length of
 about 900 m, it is a closed structure
 and in the horizontal plane its lay-out
 forms a rectangle, C1, C2, C3 and C4
 denotes the four corners of this
 rectangle, see Figure 8.3.

(i) Specific flow in the SFL 4 tunnel versus length of tunnel.
 The rock mass is represented by.
 SC: Stochastic continuum,
 results of one realization.
 UC: Uniform continuum.
 Direction of regional flow:
 A: Hor.= 0 deg, Vert.=0 deg
 (see Figure 8.3)



(ii) Specific flow in the SFL 4 tunnel versus length of tunnel.
 The rock mass is represented by.
 SC: Stochastic continuum,
 results of one realization.
 UC: Uniform continuum.
 Direction of regional flow:
 I: Hor.= 45 deg, Vert.=0 deg
 (see Figure 8.3)



(iii) Specific flow in the SFL 4 tunnel versus length of tunnel.
 The rock mass is represented by.
 SC: Stochastic continuum,
 results of one realization.
 UC: Uniform continuum.
 Direction of regional flow:
 Q: Hor.= 90 deg, Vert.=0 deg
 (see Figure 8.3)

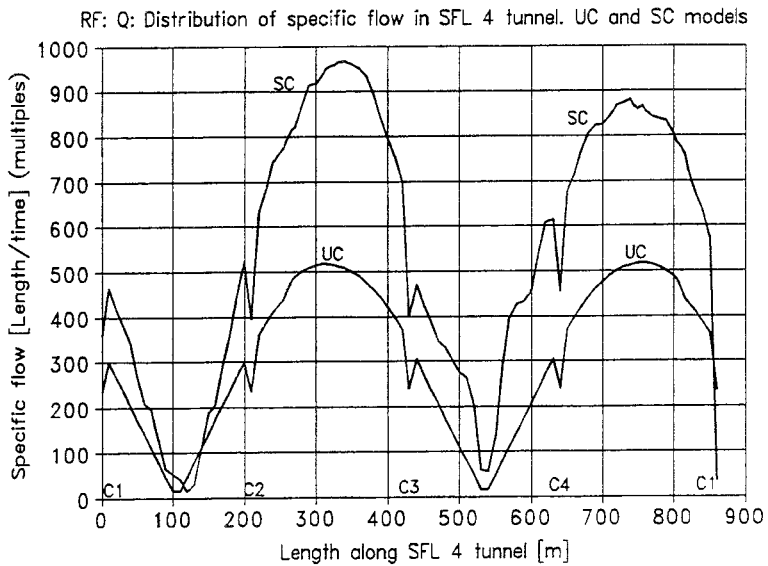


FIGURE 9.13
 DISTRIBUTION OF SPECIFIC FLOW IN THE SFL 4 TUNNEL. UNIFORM CONT. AND STOCHASTIC CONT. MODELS. The SFL 4 tunnel has a length of about 900 m, it is a closed structure and in the horizontal plane its lay-out forms a rectangle, C1, C2, C3 and C4 denotes the four corners of this rectangle, see Figure 8.3.

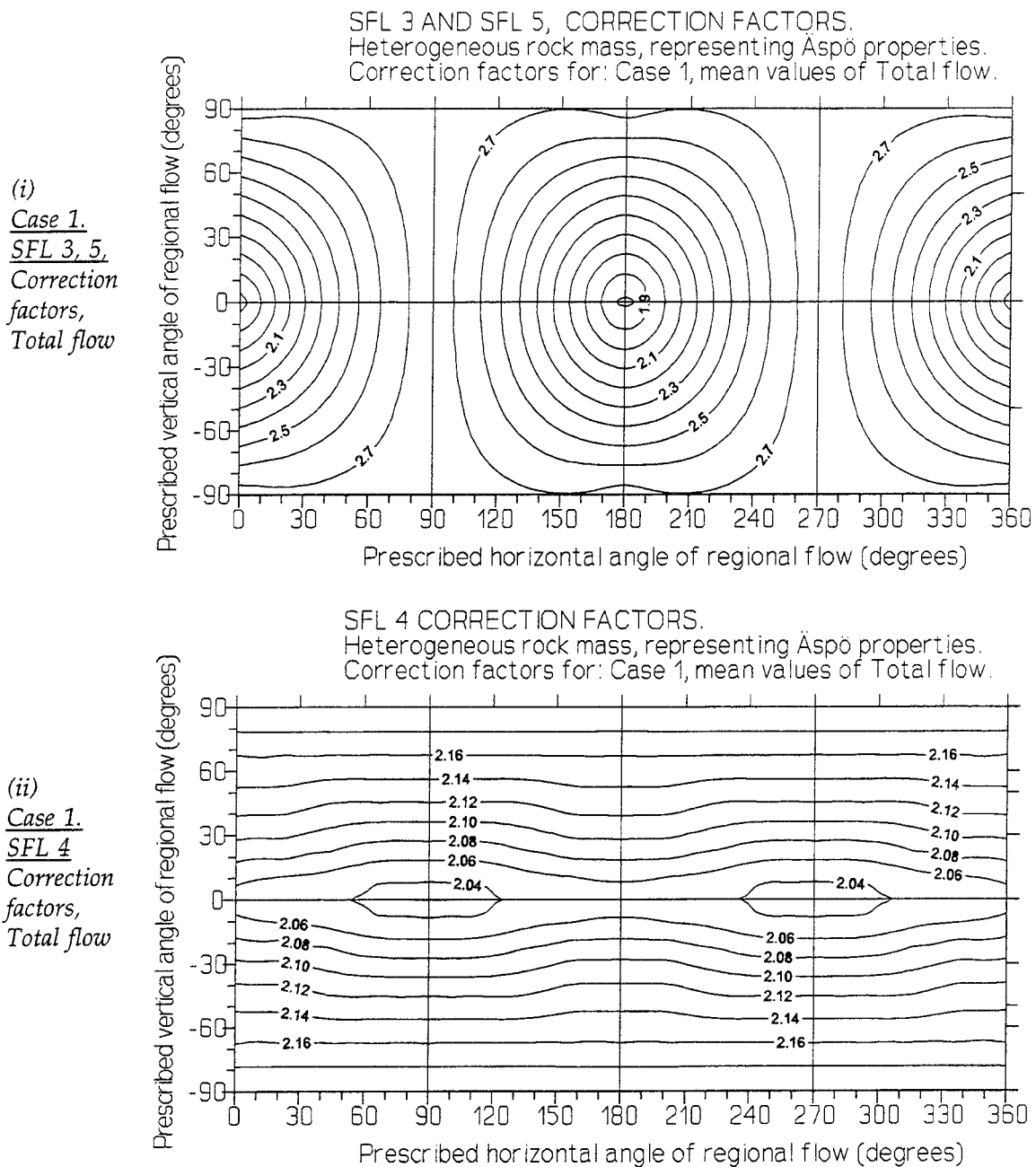


Figure 9.14

**CORRECTION FACTORS FOR HETEROGENEOUS ROCK MASS.
SENSITIVITY TO DIRECTION OF THE REGIONAL FLOW.**

Correction factors for Total flow, as regards a heterogeneous rock mass of Äspö properties. The figure gives the factors versus the direction of the regional groundwater flow. The factors correspond to the mean value of the range within which the total flow may vary, - they represent the most probable outcome. Regarding the conductivity of the repository, the factors represent Case 1.

The X-axis and the Y-axis of the figure represent all possible directions of regional flow in the horizontal and vertical plane. The prescribed angles (horizontal and vertical) are defined in accordance with the system given in Figure 8.3. The figures are based on 114 calculated values, representing the whole sphere of possible directions of regional flow. Interpolation between these values was done by the use of a kriging routine. The size of the flow should be regarded as a multiple of the size of an unknown regional groundwater flow.

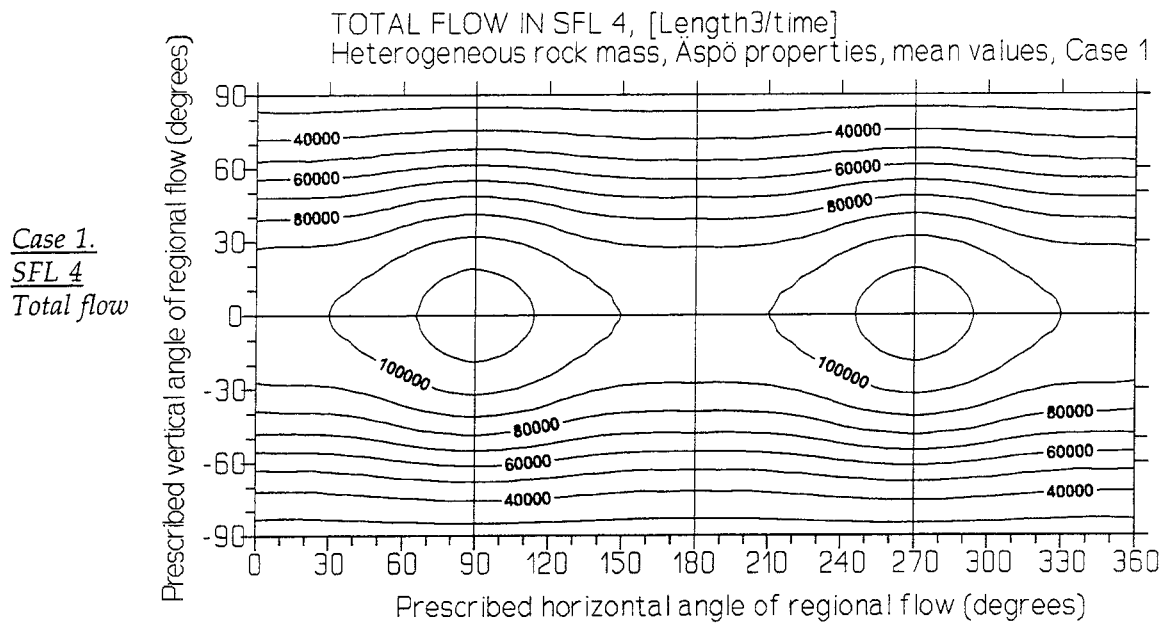


Figure 9.15 EXPECTED TOTAL FLOW IN SFL 4, HETEROGENEOUS ROCK MASS. SENSITIVITY TO DIRECTION OF THE REGIONAL FLOW.
Total flow in SFL 4, versus the direction of the regional groundwater flow. The values represent a system with a heterogeneous rock mass, with properties according to Äspö. The total flow given, corresponds to the mean value of the range within which the total flow may vary, it represents the most probable outcome. The conductivities of the repository represent Case 1.

The X-axis and the Y-axis of the figure represent all possible directions of regional flow in the horizontal and vertical plane. The prescribed angles (horizontal and vertical) are defined in accordance with the system given in Figure 8.3. The figures are based on 114 calculated values, representing the whole sphere of possible directions of regional flow. Interpolation between these values was done by the use of a kriging routine. The size of the flow should be regarded as a multiple of the size of an unknown regional groundwater flow.

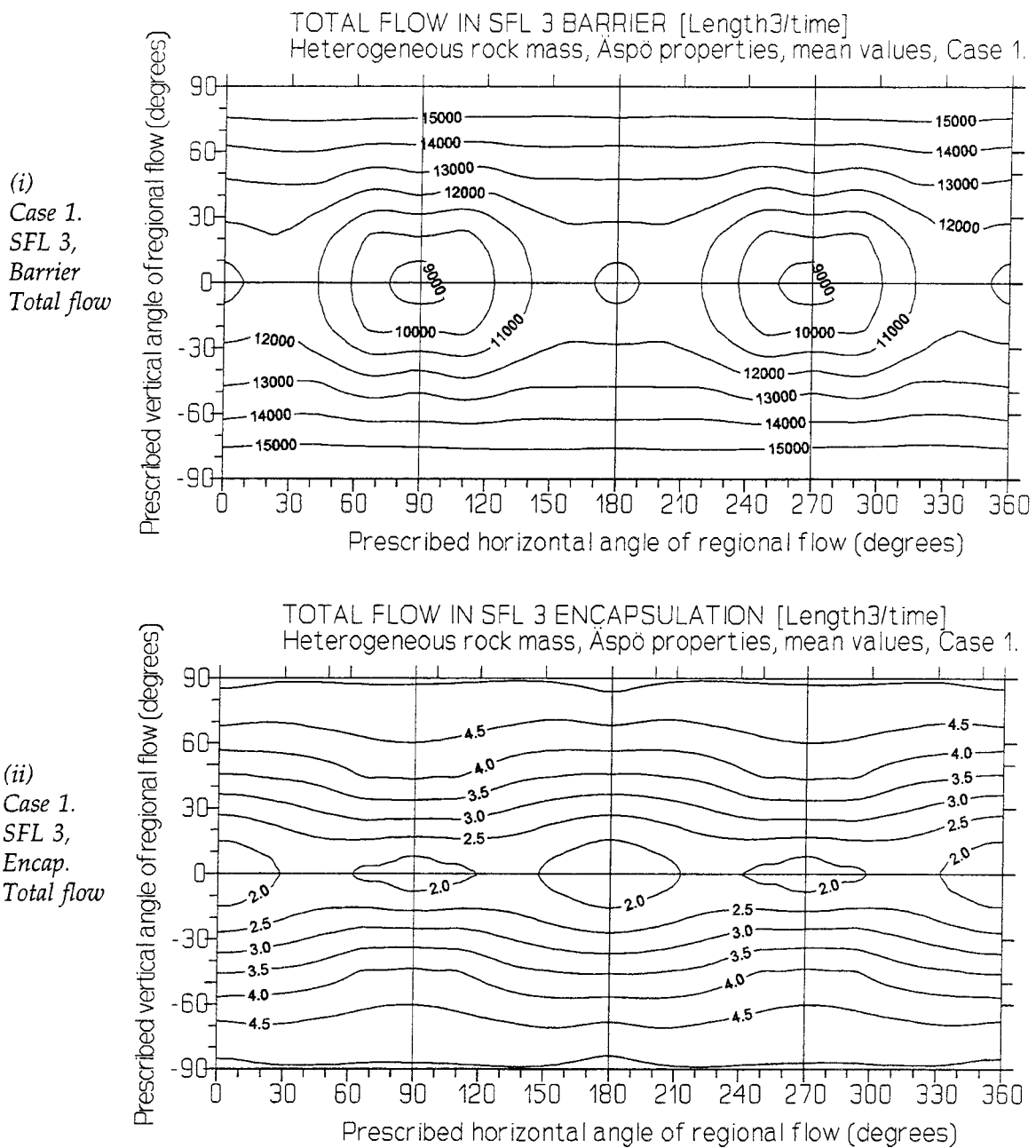


Figure 9.16

**EXPECTED FLOW IN SFL 3, HETEROGENEOUS ROCK MASS.
SENSITIVITY TO DIRECTION OF THE REGIONAL FLOW.**

Total flow in SFL 3: (i) barrier and (ii) encapsulation, versus the direction of the regional groundwater flow. The values represent a system having a heterogeneous rock mass with properties according to Äspö. The total flow given, corresponds to the mean value of the range within which the total flow may vary, it represents the most probable outcome. The conductivities of the repository represent Case 1.

The X-axis and the Y-axis of the figure represent all possible directions of regional flow in the horizontal and vertical plane. The prescribed angles (horizontal and vertical) are defined in accordance with the system given in Figure 8.3. The figures are based on 114 calculated values, representing the whole sphere of possible directions of regional flow. Interpolation between these values was done by the use of a kriging routine. The size of the flow should be regarded as a multiple of the size of an unknown regional groundwater flow.

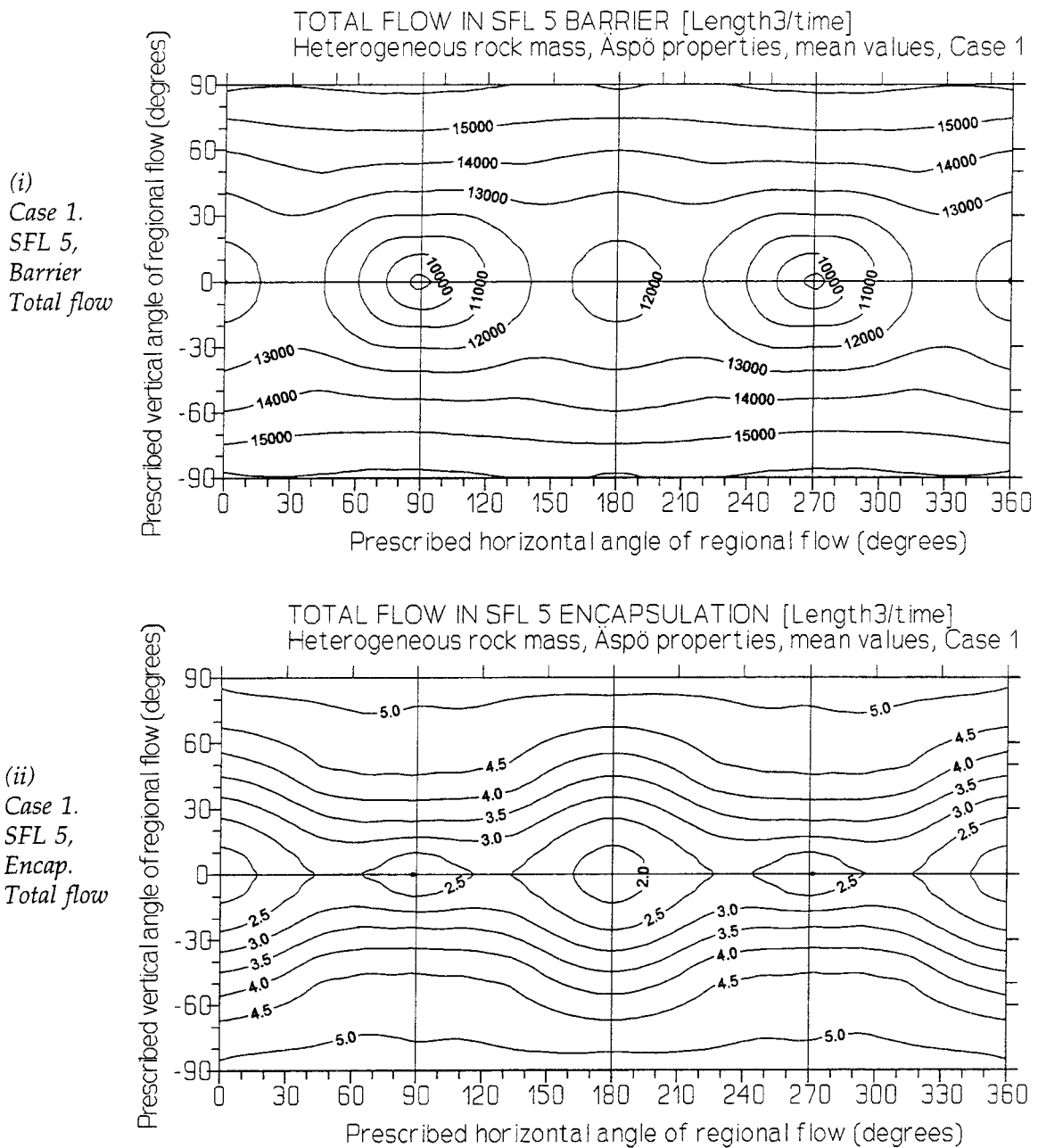


Figure 9.17

**EXPECTED FLOW IN SFL 5, HETEROGENEOUS ROCK MASS.
SENSITIVITY TO DIRECTION OF THE REGIONAL FLOW.**

Total flow in SFL 5: (i) barrier and (ii) encapsulation, versus the direction of the regional groundwater flow. The values represent a system having a heterogeneous rock mass with properties according to Äspö. The total flow given, corresponds to the mean value of the range within which the total flow may vary, it represents the most probable outcome. The conductivities of the repository represent Case 1.

The X-axis and the Y-axis of the figure represent all possible directions of regional flow in the horizontal and vertical plane. The prescribed angles (horizontal and vertical) are defined in accordance with the system given in Figure 8.3. The figures are based on 114 calculated values representing the whole sphere of possible directions of regional flow. Interpolation between these values was done by the use of a kriging routine. The size of the flow should be regarded as a multiple of the size of an unknown regional groundwater flow.

Chapter 10.

General conclusions

10.1 Introduction

This section will contain some general conclusions. It is not a summary or a recapitulation of results and conclusions previously given in this study. Detailed conclusions as regards the results of the different chapters are given at the end of each chapter.

10.2 Application of the results on a site specific scenario

The flow values presented in this study are given as multiples of a regional specific flow, with other words as multiples of the size of an unknown regional flow. Thus, to obtain a flow of a studied tunnel, for a certain site specific scenario, we multiply the results given in this study by the assumed size of the regional specific flow. As regards a solute in the groundwater with a known concentration, the flow values could be used to predict the advection. This study is a generic study of groundwater flow in tunnels, we have not studied diffusion of a solute in the groundwater (discussed in Sec.2.10).

10.3 Results of study

Below is a presentation of the objectives of the study and where to find the corresponding results and conclusions.

Objectives: To study the size of the flow in a tunnel as regards the direction of the regional flow of groundwater. The size of the flow in a tunnel as regards the conductivity, the length and the width of a tunnel. The size of the maximum theoretical flow in a tunnel.

Results: The results concerning the above discussed is given in Chapter 3, see Section 3.14.

Objectives: To study the effects of the heterogeneity of the surrounding rock mass, as regards the flow in a tunnel. Consideration of the amount of heterogeneity and the direction of the regional flow, as well as the size and the conductivity of the tunnel.

Results: The results concerning the above discussed is given in Chapter 6 and Chapter 7, see Sections 6.8 and 7.9.

Objectives: To study the effects of flow barriers in a tunnel, as regards the flow in a tunnel. Consideration of the size and the conductivity of the flow barriers, as well as the size and the conductivity of the tunnel; we will also consider a heterogeneous rock mass and different directions of the regional flow.

Results: The results concerning the above discussed is given in Chapter 7 and Chapter 9, see Sections 7.9 and 9.8.

Objectives: To study an example of a system of closed tunnels. We will study the flow through the tunnels of the planned repository for long-lived, low and middle active nuclear waste, called SFL 3-5. We will estimate the flow through this repository, considering different properties of the tunnel system.

Results: The results concerning the above discussed is given in Chapter 8 and Chapter 9, see Section 9.8.

Objectives: It is a purpose of this study to investigate the stochastic continuum approach, as regards the representation of a scale-dependent heterogeneous conductivity. It is a purpose of this study to propose a method for the scaling of measured conductivity values, a method that is consistent with the stochastic continuum approach. We will also propose a method for calculation of the node-to-node conductivity (homogenized conductivity) in finite difference models which use the stochastic continuum approach.

Results: The results concerning the above discussed is given in Chapter 5, see Section 5.10.

Objectives: To compare the effects of the different parameters controlling the flow through a closed tunnel or a system of closed tunnels (a repository). Establish an order of precedence, as regards the parameters of importance.

Results: The results concerning the above discussed is given in this chapter, see Section 10.4.

10.4 Order of precedence, as regards the parameters controlling the flow through a closed tunnel

Parameters that control the size of the regional groundwater flow are not included in this study. This is a generic study, therefore only parameters that influence the flow through tunnels at the scale of the tunnels are included in the study.

For a regional flow of a given size, which is the most important local parameter controlling the flow through a closed tunnel ? The answer is that the most important parameter depends on the studied scenario.

The flow in a tunnel depends on the conductivity of the tunnel. However, due to the nature of flow, there is a maximum flow in a tunnel that depends on the conductivity contrast between the tunnel and the surrounding rock mass as well as on the direction of the regional flow. If the tunnel has a small conductivity, the flow in the tunnel will be small, if the conductivity is large the flow in the tunnel will be large. But, an increase of the conductivity of the tunnel will only have a large effect on the flow in the tunnel, if the tunnel conductivity is small. If the conductivity of a tunnel is large a much more conductive tunnel will not have a much larger flow, as the flow in such a tunnel is mainly dependent on the conductivity of the surrounding rock mass. Thus, the conductivity will only be of importance if it is smaller than a certain threshold value. To reduce the flow in a tunnel of length 250 m, the back fill conductivity has to be smaller than about 70 times the rock mass conductivity for a regional flow at right angles to the tunnel and smaller than about 1500 times the rock mass conductivity for a regional flow along the tunnel.

For tunnels that have no back fill, or for tunnels that have a back fill with a large conductivity, important parameters are the length of the tunnel and the direction of the regional flow. As regards the direction of the regional flow, the maximum flow in a tunnel will occur for a regional flow directed along the tunnel. If the regional flow is directed along the tunnel, the total flow in the tunnel will increase in a non-linear way with increased tunnel length. If the regional flow is directed at right angles to the tunnel, the total flow in the tunnel will increase in a linear way with increased tunnel length. Thus, the direction of the regional flow becomes more and more important as the length of the tunnel becomes large. For a tunnel of length 250m the maximum theoretical flow may vary about 5 times depending on direction of regional flow, presuming that the rock mass is homogeneous. We presume that the length of a tunnel is much larger than the width of a tunnel; for such tunnels the width is of much less importance than the length.

The expected flow of a tunnel in a heterogeneous rock mass will be larger than that of a similar tunnel in a homogeneous rock mass, presuming that the regional flow is of the same size for both types of rock mass. The larger the amount of heterogeneity, the larger the increase in expected flow. The variation in expected tunnel flow, as regards the direction of the regional flow, will be smaller if the rock mass is heterogeneous than if it is homogeneous. The effects of the heterogeneity will decrease with increased tunnel length. Consider a heterogeneous rock mass like the rock at Äspö HRL, for an empty tunnel of length 250m the increase in expected total flow is about 1.3 to 2.7 times, depending on the direction of the regional flow. However, it is possible that the increase in flow might be larger or smaller than the above given values, as they are expected values. With a probability of about 70 percent, the increase will be within a range of 1 to 3 times. As previously stated, the effects of the heterogeneity will decrease with increased tunnel length; for Äspö properties the increase in flow, due to the rock mass heterogeneity, can be ignored for tunnel lengths of 1000m to 2000m, depending on the direction of the regional flow.

Thus, if the conductivity of the tunnel is much smaller than the threshold conductivity, the tunnel conductivity is the most important parameter. If the tunnel conductivity is larger than the threshold conductivity and the tunnel has a length of 250 m or more, the most important parameter is probably the direction of the regional flow, and it becomes more important as the length of the tunnel is increased. Consider a rock mass like the heterogeneous rock at Äspö HRL, if the tunnel length is shorter than about 500 m, the heterogeneity will be an important parameter, for tunnels shorter than about 250 m, the heterogeneity is probably the most important parameter; the heterogeneity could be the most important parameter for tunnels longer than 250 m, but that is not likely.

To limit the groundwater flow that passes through an encapsulation inside a tunnel, a flow barrier can be installed between the encapsulation and the tunnel walls. The barrier can be a structure less permeable than the rock mass, and divert the flow away from the encapsulation; such a barrier is called a negative barrier. The barrier can also function as a structure more permeable than the rock mass and the encapsulation, and lead the flow around the encapsulation; such a barrier is called a positive barrier. The effect of the barrier depends on the conductivity contrasts between the barrier and (i) the encapsulation and (ii) the surrounding rock mass. The larger the conductivity contrast between the barrier and the rock mass, the smaller the flow in the encapsulation. A flow barrier is a very efficient method of reducing the flow in an encapsulation/tunnel. Consider the encapsulations of the SFL 3 and SFL 5 tunnels. By using a positive flow barrier, with a conductivity that is 100 000 times that of the rock mass, it is possible to reduce the flow in the encapsulation with about 3 orders of magnitude, compared to an unprotected encapsulation. A negative barrier needs to have a conductivity that is smaller than 0.1 times that of the rock mass, to significantly reduce the flow in the encapsulation, and for a large reduction of flow in the encapsulation, the conductivity of a negative barrier needs to be extremely small. Remembering that the effective conductivity of the rock mass is very small, it is concluded that a large reduction in flow through the encapsulation is more easily obtained if the barrier is a positive barrier than if it is a negative barrier. This follows from the fact that it is difficult to make a barrier which is much less permeable than the effective conductivity of the rock mass (bentonite barrier), but it is very easy to make a barrier which is much more permeable than the effective conductivity of the rock mass (sand or gravel barrier, etc).

As regards an encapsulation, surrounded by a flow barrier, the most important parameter of the system is the conductivity of the flow barrier. The importance of tunnel length, direction of regional flow, rock mass heterogeneity etc. is small, compared to the reduction of flow, given by a properly functioning flow barrier.

Chapter 11.

References

- ABRAMOVICH, B., and INDELMAN, P., 1995: "Effective permeability of log-normal isotropic random media." *J. Phys. A: Math. gen.* 28 (1995), 693-700.
- AXELSSON, C-L., E-K. JONSSON, J. GEIER and W. DERSHOWITZ, 1990: "Discrete fracture modeling" *SKB Progress Report 25-89-21, October 1990. Swedish nuclear fuel and waste management Co. Box 5864 S-10248 Stockholm.*
- BAKR, A.A., GELHAR, L.W., GUTJAHR, A.L. and McMILLAN, J.R., 1978: "Stochastic analysis of spatial variability in subsurface flow. Part 1: comparison of one and three dimensional flows" *Water Resources Resources.* 14(2), 263-271.
- BEAR, J., and VERRUIJT, A., 1987: "Modeling groundwater flow and pollution". *D. Reidel publishing company, P.O. Box 17, 3300 AA Dordrecht, Holland. ISBN 1-55608-014-X*
- BEAR, J., and BACHMAT, Y., 1990: *Introduction to Modeling of Transport Phenomena in Porous Media. Kluwer Academic Publishers, Dordrecht, The Netherlands. ISBN 0-7923-0557-4*
- BEAR, L., 1993: "Flow and Contaminant Transport in Fractured Rocks"
Edited by: Bear, Tsang and de Marsily. Academic press, Inc. ISBN 0-12-083980-6.
- BESANT, and RAMSEY, 1920: *Hydrodynamics* (edn. 2, 1920) p 169
- BIRD, R.B, W.E. STEWART and LIGHTFOOT, 1960: "Transport Phenomena" *Wiley & Sons.*
- CARSLAW, H.S. and J.C. JAEGER, 1959: "Conduction of Heat in Solids (second edition)" *Oxford University Press, Walton Street, Oxford ox2 6dp, ISBN 0 19 853303 9.*
- DAGAN, G., 1979: "Models of groundwater flow in statistically homogeneous porous formations" *Water Resour. Res.*, 15(1), 47-63.
- DAGAN, G., 1982: "Stochastic modeling of groundwater flow by unconditional and conditional probabilities, 2. The solute transport" *Water Resour. Res.*, 18(4), 835-848.
- DAGAN, G., 1984: "Solute transport in heterogeneous porous formations"
J. Fluid Mech., 145, 151-177.
- DAGAN, G., 1986: "Statistical theory of groundwater flow and transport: Pore to laboratory, laboratory to formation, and formation to regional scale" *Water Resour. Res.*, 22(9), 1205-1345.
- DAGAN, G., 1987: "Theory of solute transport by groundwater" *Annual Reviews of Fluid Mechanics*, 19, 183-215.
- DAGAN, G., 1988: "Time dependent macrodispersion for solute transport in anisotropic heterogeneous aquifers" *Water Resour. Res.*, 24(9), 1491-1500.
- DAGAN, G., 1993: "High-order correction of effective permeability of heterogeneous isotropic formations of lognormal conductivity distribution." *Trans. Porous Media* 12 (1993), 279-290.
- DARCY, H., 1856: "Les Fontaines Publiques de la Ville de Dijon" *Dalmont, Paris, France.*

- DYKAR, B., and KITANIDIS, P., 1992: "Determination of the effective hydraulic conductivity for heterogeneous porous media using a numerical spectral approach 1. Method. *Water Resour. Res.*, 28(4), 1155-1166.
- DYKAR, B., and KITANIDIS, P., 1992: "Determination of the effective hydraulic conductivity for heterogeneous porous media using a numerical spectral approach 2. Results. *Water Resour. Res.*, 28(4), 1167-1178.
- FOLLIN, S., 1992a: "Numerical Calculations on Heterogeneity of Groundwater Flow" *Department of Land and Water Resources Royal Institute of Technology S-10044 Stockholm Sweden, (Dissertation), ISSN 0348-4955, ISBN 91-7170-077-3.*
- FOLLIN, S., 1992b: "On the interpolation of double-packer tests in heterogeneous porous media: numerical simulations of continuum analogue" *SKB Technical Report 92-36, December 1992. Swedish nuclear fuel and waste management Co. Box 5864 S-10248 Stockholm.*
- FORSGREN, E., LANGE, F., and LARSSON, H., 1996: "SFL 3-5 Layoutstudie" *SKB Arbets Rapport, AR D-96-016, December 1996. Swedish nuclear fuel and waste management Co. Box 5864 S-10248 Stockholm.*
- FREEZE, R.A., 1975: "A stochastic-conceptual analysis of one-dimensional groundwater flow in non uniform homogeneous media" *Water Resour. Res.*, 11(5), 725-741.
- FREEZE, R.A., CHERRY, J.A., 1979: "Groundwater" *Prentice-Hall, Inc., ISBN 0-13-365312-9.*
- GEIER, J.E. and C-L. AXELSSON, 1991: "Discrete fracture modelling of the Finnsjön rock mass Phase 1: Feasibility study" *SKB Technical Report 91-13, March 1991. Swedish nuclear fuel and waste management Co. Box 5864 S-10248 Stockholm.*
- GEIER, J.E., C-L. AXELSSON, L. HÄSSLER and A. BENABDERRAHMANE, 1992: "Discrete fracture modelling of the Finnsjön rock mass, Phase 2" *SKB Technical Report 92-07, April 1992. Swedish nuclear fuel and waste management Co. Box 5864 S-10248 Stockholm.*
- GEIER, J.E. and T.W. DOE, 1992: "Discrete fracture modelling of the Finnsjön rock mass, supplementary interpretations of actual and simulated well test data" *SKB Arbetsrapport 92-45, September 1992. Swedish nuclear fuel and waste management Co. Box 5864 S-10248 Stockholm.*
- GELHAR, L.W., 1976: "Effects of hydraulic conductivity variations on groundwater flows". *Proc. Int. Symp. Stochastic-Hydraulics (2nd. IAHR Congress, Lund, Sweden).*
- GELHAR, L.W. and AXNESS, C.L 1983: "Three-dimensional stochastic analysis of macrodispersion in aquifers" *Water Resour. Res.*, 19(1), 161-180.
- GUSTATAFSON, G., R. STANFORS, and P. WIKBERG, 1989: "Swedish hard rock laboratory evaluation of 1988 year preinvestigations and description of the target area, the island of Äspö". *SKB Technical Report 89-16, June 1989. Swedish nuclear fuel and waste management Co. Box 5864 S-10248 Stockholm.*
- GUTJAHN, A.L., GELHAR, L.W., BAKR, A.A. and McMILLAN, J.R., 1978: "Stochastic analysis of spatial variability in subsurface flow. Part 2: Evaluation and application" *Water Resoures Resources. 14(5), 953-960.*

- HASHIN, Z., and SHTRIKMAN, S., 1962: "A Variational Approach to the Theory of the Effective Magnetic Permeability of Multiphase Materials" *Journal of Applied Physics*, 33.
- HOLMÉN, J.G., 1992: "A three-dimensional finite difference model for calculation of flow in the saturated zone". *Department of quaternary geology, University of Uppsala, Uppsala, Sweden, ISBN 91-7376-119-2, ISSN 0348-2979.*
- HÄSSLER, L., 1991: "Grouting of Rock - Simulation and Classification" *Department of Rock Mechanics Royal Institute of Technology S-10044 Stockholm Sweden, (Dissertation), ISBN 91-7170-060-9.*
- JACOB, C.E., and LOHMAN, S. 1952: "Non steady flow to a well of constant drawdown in an extensive aquifer" *Trans. Am. Geophys. Union*, 33(4), 559-569.
- KRUMBEIN, W.C., 1936: "Application of the logarithmic moments to size frequency distributions of sediments". *J. Sed. Petrol.* 6(1), 35-47.
- LACHASSAGNE, P., LEDOUX, E., and de MARSILY, 1989: "Evaluation of hydrogeological parameters in heterogeneous porous media" *Groundwater Management: Quantity and Quality (Proceedings of the Benidorm Symposium, October 1989), IAHS Publ. no. 188. 1989.*
- LANDAU, L.D., and LIFSHITZ, E.M., 1960: "Electrodynamics of continuous media" *Pergamon, Oxford, 1969.*
- LAMÉ, 1837: *Liouville's J.* 2.
- LA POINTE, P., P. WALLMAN and S. FOLLIN, 1995: "Estimation of effective block conductivities based on discrete network analyses using data from the Äspö site". *SKB Technical Report 95-15, September 1995. Swedish nuclear fuel and waste management Co. Box 5864 S-10248 Stockholm.*
- LARSSON, E., 1997: "Groundwater flow through a natural fracture, flow experiments and numerical modelling" *Department of Geology, Chalmers University of Technology, S-41296, Göteborg, Sweden. ISSN 0348-2367, Publ. A 82, 1997, Thesis for the Licentiate degree.*
- LAW, J., 1944: "A statistical approach to the interstitial heterogeneity of sand reservoirs". *Trans. Am. Inst. Min. Metall. Pet. Engrs.* 155, 202-222.
- LIEDHOLM, M., 1991a: "Technical note no.8, In: Liedholm, M. (ed.)" *Conceptual Modeling of Äspö Technical Notes 1-17, SKB Progress Report 25-90-16a, Swedish nuclear fuel and waste management Co. Box 5864 S-10248 Stockholm.*
- LIEDHOLM, M., 1991b: "Technical note no.9, In: Liedholm, M. (ed.)" *Conceptual Modeling of Äspö Technical Notes 1-17, SKB Progress Report 25-90-16a, Swedish nuclear fuel and waste management Co. Box 5864 S-10248 Stockholm.*
- LINDGREN, M., K. BRODÉN, J. CARLSSON, M. JOHANSSON and K. PERS, 1994: "Low and intermediate level waste for SFL 3-5". *SKB AR 94-32, May 1994. Swedish nuclear fuel and waste management Co. Box 5864 S-10248 Stockholm.*
- MATHERON, G., 1967: "Eléments pour une théorie des milieux poreux." *Masson, Paris, France. 1967.*

- MOYE, D.G., 1967: "Diamond drilling for foundation exploration"
Civ. Eng. Trans. 7th, Inst. Eng. Australia, 95-100.
- NEUMAN, S., P., 1982: "Statistical characterization of aquifer heterogeneities; an overview", In: *Recent trends in hydrogeology (ed. by T.N. Narashiman), 81-102. Spec. Pap. Geol. Soc. Am. 189*
- NEUMAN, S., P., 1987: "Stochastic continuum representation of fractured rock permeability as an alternative REV and fracture network concepts", In: Farmer, I.W. et al (eds.) *Proc. 28th U.S. Symp. Rock. Mech., 533-561, Balkema, Rotterdam.*
- NEUMAN, S., P., C.L. WINTER, and C.M. NEWMAN 1987: "Stochastic theory of field-scale Fickian dispersion in anisotropic porous media" *Water Resour. Res., 23(3), 453-466.*
- NEUMAN, S., P., 1988: "A proposed conceptual framework and methodology for investigating flow and transport in Swedish crystalline rocks" *SKB AR 88-37. Swedish nuclear fuel and waste management Co. Box 5864 S-10248 Stockholm.*
- NEUMAN, S., P., and ORR, S., 1993: "Prediction of steady state flow in nonuniform geologic media by conditional moments: exact nonlocal formalism, effective conductivities and weak approximation." *Water Resour. Res., 29(2), 341-364.*
- POLLOCK, D., W., 1989: "Documentation of computer program to compute and display path lines using results from the U.S. Geological survey modular three-dimensional finite difference ground-water flow model". (MODPATH manual). *U.S. Geological survey 411 National Center Reston, VA 22092 USA.*
- SNOW, D., T., 1968: "Rock fracture spacings, openings, and porosities" *J. Soil Mech. Found. Div., Proc. Amer. Soc. Civil Engrs., 94, pp. 73-91.*
- STRACK, O., 1989: "Groundwater Mechanics" *Prentice-Hall Inc., Englewood Cliffs, New Jersey, 07632 USA.*
- STRANG, G., 1986: "Introduction to Applied Mathematics" *Wellesley-Cambridge Press, Wellesley, MA 02181 USA.*
- PRESS, W., TEUKOLSKY, S., VETTERLING, W., and FLANNERY, B., 1992: "Numerical Recipes in fortran. The art of scientific computing. Second edition" *Cambridge University Press, ISBN 0 521 43064 X.*
- WALTON, W. C., and NEIL, I. C., 1963: "Statistical analysis of specific capacity data for a dolomite aquifer". *J. Geophys. Res. 68(8), 2251-2262.*
- WEN, X-H., and GÓMES-HERNÁNDEZ, J.,J., 1996: "Upscaling hydraulic conductivities in heterogeneous media: An overview" *Journal of Hydrology 183 (1996) Elsevier Science B.V., Journals Department. P.O. Box 211, 1000 AE Amsterdam, Netherlands"*
- WIKBERG, P. (ed), G. GUSTAFSON, I. RHÉN, and R. STANFORS, 1991: "Äspö Hard Rock Laboratory. Evaluation and conceptual modelling based on the pre-investigations 1986-1990". *SKB Technical Report 91-22, June 1991. Swedish nuclear fuel and waste management Co. Box 5864 S-10248 Stockholm.*
- WITHERSPOON, P., WANG, J., IWAI, K., and GALE, J., 1980: "Validity of cubic law for fluid flow in a deformable rock fracture", *Water Resour. Res., 16(6): 1016-1024, 1980.*

APPENDIX A

The continuum approach, the finite difference method and the GEOAN model

TABLE OF CONTENTS

PAGE

A.1	THE CONTINUUM APPROACH	A.3
A.1.1	Introduction	A.3
A.1.2	The porous medium and the continuum approach	A.3
A.1.3	Types of flow	A.4
A.1.4	Piezometric head and specific discharge	A.4
A.1.5	Darcy's law	A.4
A.1.6	General motion equation	A.5
A.1.7	Continuity equation	A.6
A.1.8	Original differential equation	A.6
A.2	THE FINITE DIFFERENCE EQUATION FOR SATURATED FLOW	A.7
A.2.1	Introduction	A.7
A.2.2	Finite differences	A.7
A.2.3	Spatial discretization, cells and nodes	A.8
A.2.4	System of cell index	A.9
A.2.5	Basic flow equation	A.9
A.2.6	Simplifying finite differentials	A.11
A.2.7	Formulation of cell to cell flow equations	A.12
A.2.8	Formulation of a finite difference equation	A.14
A.3	ESTABLISHMENT OF A SYSTEM OF EQUATIONS	A.15
A.3.1	Introduction	A.15
A.3.2	Implicit method, one system of equations for all cells	A.15
A.3.3	Explicit method, one system of equations for each cell	A.17
A.4	PROCEDURE OF ITERATION	A.20
A.4.1	Introduction	A.20
A.4.2	Convergence	A.20
A.4.3	Accuracy	A.21
A.4.4	Steady state condition	A.21
A.4.5	Non steady state condition (transient condition)	A.21
A.4.6	Implicit method	A.22
A.4.7	Explicit method	A.22
A.5	THE GEOAN MODEL	A.24
A.6	REFERENCES	A.25
	FIGURES	A.27

A.1 THE CONTINUUM APPROACH

A.1.1 Introduction

The following appendix contains: (i) a short mathematical description of the flow of a fluid in a porous medium, based on the continuum approach, and a presentation of how to obtain the original differential equation, (ii) a presentation of a method of replacing the original differential equation by a system of equations, the method being a finite difference method which is used in the GEOAN model, and (iii) a short presentation of the GEOAN groundwater model.

For a more detailed description of the continuum approach we refer to: Bear and Verruit (1987), Bear and Bachmat (1990), and Strack (1989).

A.1.2 The porous medium and the continuum approach

A *porous medium* consists of a solid matrix and a void space. The void space is called pores. Some examples of porous media are sand, morain, sandstone and highly fissured rock. The pores are occupied by one or more fluid phases (e.g. water and air). The fluid flows through a complex network of pores/fractures.

The flow of a fluid in a porous medium may be described by mathematical equations at a small scale (microscopical level). However, this approach is impractical for a system in which the pores are small (e.g. a system of gravel and morain), as the actual complex distribution of the pore network is unknown. For a system in which the pores are represented by fractures, having a larger size (e.g. fractured rock), it might be possible.

A very small volume of the porous medium might contain void space only or solid matrix only. A slightly larger volume might contain both void space and solid matrix. As the studied volume of the porous medium is increased, the quota between the volume of void space and the volume of solid matrix will change, until a certain volume is reached where the quota will no longer change. At a certain volume, the value of an averaged characteristic of the structure of the porous medium (e.g. conductivity) is a function of the location of the volume and of time only; this volume is called a *representative elementary volume* (REV).

By the use of a REV we pass from the *small scale*, at which we consider small local variations of the studied property, to the *large scale*, at which we consider volume averaged quantities.

To obtain the flow of a fluid at the large scale, we use the *continuum approach*. The continuum approach replaces the actual porous medium by a representative continuum to which spatially defined values of the hydraulic properties can be assigned (e.g. conductivity). By assigning averaged values to the studied medium, we obtain fields of variables which are differentiable functions of the space coordinates.

If we want to study the flow at a scale smaller than the REV, we could do so by describing the variation in hydraulic properties of the porous medium, for volumes smaller than the REV, by the use of a stochastic description, a approach in which the hydraulic properties of volumes smaller than the REV are described by probability density distributions (e.g. a log-normal distribution). The probability distributions describe the variation of the studied properties, at the scale of the studied volumes. The approach is called the *stochastic continuum approach*.

A.1.3 Types of flow

Saturated flow occurs in a medium, the void space of which is filled with a single fluid. *Unsaturated flow* or *flow of multiple phases* occurs in a medium the void space of which is not completely filled with a single fluid. Saturated flow through a porous medium might be classified according to the pressure conditions under which it occurs. The flow is called *confined* if it occurs between two impermeable boundaries. For such flow conditions the medium is called a confined medium. Under confined conditions the pressure of the fluid is greater than the atmospheric pressure. *Unconfined* flow occurs in a medium, the upper boundary of which is a water table. Such a flow medium is called an unconfined medium. The *phreatic surface* is a surface within the zone of saturation of an unconfined flow medium, along which the pressure is atmospheric.

A.1.4 Piezometric head and specific discharge

The *piezometric head* (piez.head) at a certain point in a body of geological material (a flow medium) is defined as the level to which water rises in a open tube. The piez.head is measured with respect to a reference level. The piez.head can be expressed in terms of pressure and elevation as follows;

$$\phi_x = \frac{P_x}{\rho g} + Z \quad (1.1)$$

ϕ_x = Piezometric head at point x [dimension: Length]
 P_x = Pressure at point x [dimension: Force / Length²]
 ρ = Density of fluid (water) [dimension: Mass / Length³]
 g = Acceleration of gravity [dimension: Length / time²]
 Z = Elevation of point p above a reference level [dimension: Length]

The *specific discharge*, q , is defined as the volume of water flowing through a unit area of flow medium per unit time. The dimension of specific discharge is, $[L^3 / (L^2 * t)]$.

A.1.5 Darcy's law

In 1856, Henry Darcy (Darcy, 1856) presented an investigation about the flow of water in vertical homogeneous sand filters. Darcy found out that the amount of flow, $Q [L^3]$, is (i) proportional to the cross-sectional area, $A [L^2]$, (ii) proportional to the difference in water level elevations between inflow and outflow reservoirs $h_1 - h_2 [L]$, and (iii) inversely proportional to the filter length, $L [L]$. These conclusions give Darcy's law.

$$Q = K \frac{A (h_1 - h_2)}{L} \quad (1.2)$$

The proportionality constant, $K [L / s]$, is known as the *hydraulic conductivity*. The hydraulic conductivity is a combined property of a medium and the fluid moving through it. The hydraulic conductivity is therefore dependent on both the properties of the medium and the properties of the fluid. Using the concept of piez.head, Equ.1.2 becomes.

$$Q = K \frac{A (\phi_1 - \phi_2)}{L} \quad (1.3)$$

Using the concept of specific discharge with, $q = Q/A$, gives:

$$q = K \frac{\phi_1 - \phi_2}{L} \quad (1.4)$$

The piez.head inside a filter varies linearly over the length of the filter. If a coordinate system is chosen with the x axis directed along the axis of the filter and the origin located at the beginning of the filter, we may write the following expression for the piez.head.

$$\phi = \frac{\phi_2 - \phi_1}{L} x + \phi_1 \quad (1.5)$$

It follows from Eq.1.5 that,

$$\frac{d\phi}{dx} = \frac{\phi_2 - \phi_1}{L} \quad (1.6)$$

Based on Eq.1.6 it is possible to write Eq.1.4 in the following way:

$$q_x = -K \frac{d\phi}{dx} \quad (1.7)$$

The index x in q_x denotes that the specific discharge is in the x direction.

Darcy's law is an empirical relation for the specific discharge in terms of the piez.head. Expressed in terms of the piez.head Darcy's law is only valid for a fluid of constant density.

A.1.6 General motion equation

Darcy's law is an empirical relationship. Many attempts have been made to derive Darcy's law, or more generally, the motion equation for a fluid phase in a porous medium, from more fundamental physical laws. "Although a number of different approaches have been employed in these researches, most of them recognize that the motion equation for a fluid phase inside the void space of a porous medium, must be obtained by considering the *momentum balance equation* (often referred to as the *motion equation*) of that phase, regarded as a continuum." Bear and Verruit (1987).

By assuming that the porous medium is non-deformable, and that the inertial effects and the internal friction inside the fluid are negligible, the general motion equation, for a fluid of constant density in an anisotropic and inhomogeneous medium, can be written as:

$$\mathbf{q} = -\mathbf{K} \nabla \phi = \left\{ \begin{array}{l} q_x = -K_x \frac{\partial \phi}{\partial x} \\ q_y = -K_y \frac{\partial \phi}{\partial y} \\ q_z = -K_z \frac{\partial \phi}{\partial z} \end{array} \right\} \quad (1.8)$$

\mathbf{q} = specific discharge vector

\mathbf{K} = anisotropic conductivity (a second-rank tensor)

ϕ = piezometric head

q_x, q_y, q_z = components of \mathbf{q}

K_x, K_y, K_z = components of \mathbf{K}

A.1.7 Continuity equation

A complete description of flow requires knowledge of four unknowns: q_x , q_y , q_z and ϕ . Three equations are provided by the general motion equation; the fourth equation is provided by the continuity condition. Assuming constant density, the continuity condition can be stated as follows, *the sum of all flows into and out of an elementary volume must be equal to the rate of change in storage within the volume*. This condition can be mathematically stated as the continuity equation (S_s = Specific storage),

$$\frac{\partial q_x}{\partial x} + \frac{\partial q_y}{\partial y} + \frac{\partial q_z}{\partial z} = S_s \frac{\partial \phi}{\partial t} \quad (1.9)$$

A.1.8 Original differential equation

The general motion equation and the continuity equation together provide four equations for the four unknowns: q_x , q_y , q_z and ϕ . Substituting the specific discharge components of Eq.1.8 into Eq.1.9 gives a differential equation which is the governing equation for flow in a porous medium (constant fluid density, X direction and Y direction in the horizontal plane, Z direction in the vertical plane),

$$\frac{\partial}{\partial x} \left(K_x \frac{\partial \phi}{\partial x} \right) + \frac{\partial}{\partial y} \left(K_y \frac{\partial \phi}{\partial y} \right) + \frac{\partial}{\partial z} \left(K_z \frac{\partial \phi}{\partial z} \right) - VF = S_s \frac{\partial \phi}{\partial t} \quad (1.10)$$

- K_x, K_y, K_z = Hydraulic conductivity along coordinate axes [L / t]
 ϕ = Piezometric head [L]
 VF = Volumetric flux, represents inflow and outflow of water [t^{-1}]
 S_s = Specific storage of porous material [L^{-1}]
 t = Time [t]

The hydraulic conductivity and the specific storage are, in general, functions of space and the volumetric flux per unit volume, i.e. a function of space and time.

Equation 1.10, together with initial conditions and boundary conditions, constitutes a mathematical representation of a flow system. The initial conditions are initial values of the piezometric head. The boundary conditions define the piezometric head or the flow at the boundary of the studied system. Analytical solutions to Eq.1.10 normally exists only for generalized cases. Consequently, equation 1.10 is solved with numerical methods, the finite difference method is such a numerical method.

A.2 THE FINITE DIFFERENCE EQUATION FOR SATURATED FLOW

A.2.1 Introduction

The finite difference method was the first method used for the numerical solution of partial differential equations. The method replaces the partial derivatives in the differential equation by finite differences. The finite differences are formulated with respect to a depending variable at a discrete number of points in time and space. If the original partial differential equation is linear, a linear system of algebraic equations will be obtained. This system of equations must then be solved. Instead of a continuous function describing the value of a variable in time and space, the value of the variable will only be obtained at selected points in time and space.

Development of the flow equation in finite difference form follows from the application of the mass balance equation. Assuming constant density, the mass balance equation can be stated as the continuity equation: *the sum of all flows into and out of a volume must be equal to the rate of change in storage within the volume.* The finite differentials will be formulated based on equations describing the flow into and out from a volume.

A.2.2 Finite differences

The partial derivatives of equation 1.10 can be formulated as follows.

$$\frac{\partial}{\partial x} \left(K_x \frac{\partial \phi}{\partial x} \right) = K_x \frac{\partial^2 \phi}{\partial x^2} + \frac{\partial \phi}{\partial x} \frac{\partial K_x}{\partial x} \quad (2.1)$$

$$\frac{\partial}{\partial y} \left(K_y \frac{\partial \phi}{\partial y} \right) = K_y \frac{\partial^2 \phi}{\partial y^2} + \frac{\partial \phi}{\partial y} \frac{\partial K_y}{\partial y} \quad (2.2)$$

$$\frac{\partial}{\partial z} \left(K_z \frac{\partial \phi}{\partial z} \right) = K_z \frac{\partial^2 \phi}{\partial z^2} + \frac{\partial \phi}{\partial z} \frac{\partial K_z}{\partial z} \quad (2.3)$$

The finite difference method approximates the partial derivatives by finite differences. A finite difference can be formulated in several ways. Below follows three different ways of writing a finite difference approximation for the first and second derivative of the piezometric head $\phi(x,y)$ as regards x .

The forward finite difference approximation is based on values in the positive direction of the x axis, as regards the point $\phi_{(x,y)}$

$$\text{Derivative of the first order: } \frac{d\phi}{dx} \approx \frac{\Delta\phi}{\Delta x} = \frac{\phi_{(x+\Delta x, y)} - \phi_{(x, y)}}{\Delta x} \quad (2.4)$$

$$\text{Derivative of the second order: } \frac{d^2\phi}{dx^2} \approx \frac{\Delta^2\phi}{\Delta x^2} = \frac{\phi_{(x+2\Delta x, y)} - 2\phi_{(x+\Delta x, y)} + \phi_{(x, y)}}{(\Delta x)^2} \quad (2.5)$$

The backward finite difference approximation is based on values in the negative direction of the x axis, as regard the point $\phi_{(x, y)}$

$$\text{Derivative of the first order: } \frac{d\phi}{dx} \approx \frac{\Delta\phi}{\Delta x} = \frac{\phi_{(x, y)} - \phi_{(x-\Delta x, y)}}{\Delta x} \quad (2.6)$$

$$\text{Derivative of the second order: } \frac{d^2\phi}{dx^2} \approx \frac{\Delta^2\phi}{\Delta x^2} = \frac{\phi_{(x, y)} - 2\phi_{(x-\Delta x, y)} + \phi_{(x-2\Delta x, y)}}{(\Delta x)^2} \quad (2.7)$$

Central finite difference approximation is based on values both in the positive and negative direction of the x axis, as regards the point $\phi_{(x, y)}$

$$\text{Derivative of the first order: } \frac{d\phi}{dx} \approx \frac{\Delta\phi}{\Delta x} = \frac{\phi_{(x+\frac{1}{2}\Delta x, y)} - \phi_{(x-\frac{1}{2}\Delta x, y)}}{\Delta x} \quad (2.8)$$

$$\text{Derivative of the second order: } \frac{d^2\phi}{dx^2} \approx \frac{\Delta^2\phi}{\Delta x^2} = \frac{\phi_{(x+\Delta x, y)} - 2\phi_{(x, y)} + \phi_{(x-\Delta x, y)}}{(\Delta x)^2} \quad (2.9)$$

$$\Delta x = 1 \text{ gives: } \frac{\Delta^2\phi}{\Delta x^2} = \phi_{(x+1, y)} - 2\phi_{(x, y)} + \phi_{(x-1, y)} \quad (2.10)$$

In this study, and in the GEOAN model, the central finite difference formulation has been used to approximate the partial derivatives as regard the x , y and z directions. Backward finite difference formulation has been used to approximate the partial derivative as regards time (t).

A.2.3 Spatial discretization, cells and nodes

To solve the differential equation by the use of the finite difference method, it is necessary to make a spatial discretization. The studied system is divided into a number of volumes, called the cells. Every cell represents a volume of the studied flow medium (i.e. soil and rock) and can be assigned hydraulic properties reflecting the actual properties of the studied system. We will obtain a solution of the differential equation valid at the center of every cell. The points located at the center of the cells are called the nodes. With reference to a Cartesian coordinate system, the cells should form a system of columns, rows and layers. The rows are directed in the horizontal plane, along the x axis and the columns are directed in the horizontal plane along the y axis. The layers consist of both rows and columns, each layer representing a three-dimensional body in space (see Figure A.1). The cells can be of different size, but the following conditions must be fulfilled:

- The central point of all cells in a column (the nodes) must have the same x coordinate. All cells of a column must have the same dimension in the x direction.
- The central point of all cells in a row (the nodes) must have the same y coordinate. All cells of a row must have the same dimension in the y direction.

In the obtained system of cells all columns are parallel to the y axis and all rows are parallel to the x axis. It is not necessary that a layer is perpendicular to the z axis. The upper and lower boundaries of a layer can take the shape of inclined planes or even curved surfaces in space.

The system of cells, arranged in columns, rows and layers, is called the mesh.

A.2.4 System of cell index

Every cell in the mesh is addressed by its column, row and layer number. A Cartesian system of index will be used, as demonstrated in Figure A.1.

The cell_(i, j, k) is a cell with column number i, row number j, and layer number k.

Following the direction of the coordinate axis, cell_(i-1, j, k) is a cell in the same row and the same layer as cell_(i, j, k) but placed one step in the negative direction of the x axis with respect to cell_(i, j, k). Cell_(i+1, j, k) is placed one step in the positive direction of the x axis with respect to cell_(i, j, k).

Cell_(i, j-1, k) is a cell in the same column and the same layer as cell_(i, j, k) but placed one step in the negative direction of the y axis with respect to cell_(i, j, k). Cell_(i, j+1, k) is placed one step in the positive direction of the y axis with respect to cell_(i, j, k).

Cell_(i, j, k-1) is a cell in the same column and the same row as cell_(i, j, k) but placed one step in the negative direction of the z axis with respect to cell_(i, j, k) (cell_(i, j, k-1) is placed below cell_(i, j, k)). Cell_(i, j, k+1) is placed one step in the positive direction of the z axis with respect to cell_(i, j, k) (cell_(i, j, k+1) is placed above cell_(i, j, k)).

A.2.5 Basic flow equations

Sign convention

The flow into and out of a cell will have signs according to the following definition.

- Flow in the positive direction of the x, y and z axes will be defined as positive.
- Flow in the negative direction of the x, y and z axes will be defined as negative.

Flow equations

Application of Darcy's law gives the flow between two cells.

$$Q = K \frac{\phi_{diff}}{L} Aw \quad (2.11)$$

Q = Flow between two cells [L³ t⁻¹]

K = Hydraulic conductivity [L t⁻¹]

ϕ_{diff} = Difference in piezometric head between the central points of the two cells (the nodes) [L]

L = Distance between the central points of the two cells (the nodes) [L]

Aw = Wet area [L²]

The size of the wet area depends on the location of the phreatic surface. If both cells are fully saturated (both cells are beneath the phreatic surface) the wet area is given by the cell size.

$$Aw = W H \quad (2.12)$$

Aw = Wet area [L²]

W = Width of the two cells [L]

H = Height of the two cells [L]

If one or both of the two cells are not fully saturated, the phreatic surface occurs in one or both of the cells. Under these conditions the wet area has to be calculated on the base of both the elevation of the phreatic surface in the cells and the size of the cells. In this study, and in the GEOAN model, the calculation is carried out as an interpolation based on (i) the boundary condition of the cells, (ii) the head at the center of the cells (at the nodes) and (iii) the size of the cells.

$$Aw = f (L_1 , L_2 , \phi_1 , \phi_2 , W , B_1 , B_2) \quad (2.13)$$

- $Aw =$ Wet area [L^2]
- $L_1 =$ Horizontal length of cell₁ [L]
- $L_2 =$ Horizontal length of cell₂ [L]
- $\phi_1 =$ Elevation of the phreatic surface in cell₁ [L]
- $\phi_2 =$ Elevation of the phreatic surface in cell₂ [L]
- $W =$ Width of the two cells [L]
- $B_1 =$ Bottom elevation of cell₁ [L]
- $B_2 =$ Bottom elevation of cell₂ [L]

All cells will have individual conductivity values, these values might be the same or different. If the conductivity of two neighbouring cells are not the same, we will need to calculate an average conductivity, which represents the conductivity between the two neighboring nodes. This conductivity value, calculated on the base of an averaging method, is called the homogenized conductivity.

The homogenized conductivity could be calculated in different ways. For models that are based on a deterministic continuum approach, the homogenized conductivity should be calculated as the harmonic average. However, if we use the finite difference method as a part of a stochastic continuum approach, other ways of calculating the homogenized conductivity could be considered, such as the calibrated harmonic method, this is further discussed in Chapter 5.

The homogenized conductivity could also be expressed as a resistance, the concept of resistance is defined in analogy with the resistance to flow of electricity. For the homogenized conductivity, calculated as the harmonic average, and for the homogenized conductivity expressed as a resistance, the following formulas are used.

$$K_H = \frac{L_1 + L_2}{\frac{L_1}{K_1} + \frac{L_2}{K_2}} \quad R = \frac{L_1 + L_2}{K_H} \quad (2.14)$$

- $K_H =$ Homogenized conductivity [$L t^{-1}$]
- $R =$ Resistance [t]
- $L_1 =$ Distance between the central point of cell₁ and the cell boundary [L]
- $L_2 =$ Distance between the central point of cell₂ and the cell boundary [L]
- $K_1 =$ Hydraulic conductivity of cell₁ [$L t^{-1}$]
- $K_2 =$ Hydraulic conductivity of cell₂ [$L t^{-1}$]

Using the concept of homogenized conductivity in equation 2.11 gives:

$$Q = K_H \phi_{diff} L^{-1} Aw \quad (2.15)$$

Using the concept of resistance in equation 2.11 gives:

$$Q = \phi_{diff} R^{-1} Aw \quad (2.16)$$

A.2.6 Simplifying finite differentials

Different cells may have different conductivity values. But, in the basic flow equation (Equ.3.15 or Equ.3.16) one value of homogenized conductivity or resistance is used instead of two conductivity values. By using the concept of a homogenized conductivity or a resistance, when formulating the basic flow equation between two cells, different conductivity values will be homogenized into one value between the two studied cells. This makes it possible to simplify the partial derivatives.

The partial derivative for flow in the x direction:

$$\frac{\partial}{\partial x} \left(K_x \frac{\partial \phi}{\partial x} \right) = K_x \frac{\partial^2 \phi}{\partial x^2} + \frac{\partial \phi}{\partial x} \frac{\partial K_x}{\partial x} \quad (2.17)$$

It is possible to simplify this equation as follows:

$$\frac{\partial K_{xH}}{\partial x} = 0 \Rightarrow \frac{\partial}{\partial x} \left(K_{xH} \frac{\partial \phi}{\partial x} \right) = K_{xH} \frac{\partial^2 \phi}{\partial x^2} \quad (2.18)$$

K_x = Hydraulic conductivity in the x direction [L / t]

ϕ = Piezometric head [L]

K_{xH} = Homogenized conductivity in the x direction [L / t]

On the analogy of simplifying the partial derivative for flow in the x direction, the partial derivative for flow in the y and z directions are simplified as follows:

$$\frac{\partial K_{yH}}{\partial y} = 0 \Rightarrow \frac{\partial}{\partial y} \left(K_{yH} \frac{\partial \phi}{\partial y} \right) = K_{yH} \frac{\partial^2 \phi}{\partial y^2} \quad (2.19)$$

K_y = Hydraulic conductivity in the y direction [L / t]

ϕ = Piezometric head [L]

K_{yH} = Homogenized conductivity in the y direction [L / t]

$$\frac{\partial K_{zH}}{\partial z} = 0 \Rightarrow \frac{\partial}{\partial z} \left(K_{zH} \frac{\partial \phi}{\partial z} \right) = K_{zH} \frac{\partial^2 \phi}{\partial z^2} \quad (2.20)$$

K_z = Hydraulic conductivity in the z direction [L / t]

ϕ = Piezometric head [L]

K_{zH} = Homogenized conductivity in the z direction [L / t]

A.2.7 Formulation of cell to cell flow equations

The development of the flow equation in the finite difference form - the finite difference equation, follows from the application of the mass balance equation. In other words, the finite difference equation is based on a set of equations describing the flow into and out of a cell.

The flow, into and out of a cell, in the x direction

The flow through cell_(i, j, k) in the x direction, can be written as:

- The flow from cell_(i-1, j, k) to cell_(i, j, k) (2.21)

$$Q_{(i-1, j, k) \rightarrow (i, j, k)} = \left(\phi_{(i-1, j, k)} - \phi_{(i, j, k)} \right) R_{(i-1, j, k) \rightarrow (i, j, k)}^{-1} Aw_{(i-1, j, k) \rightarrow (i, j, k)}$$

$$\begin{aligned} Q_{(i-1, j, k) \rightarrow (i, j, k)} &= \text{Flow from cell}_{(i-1, j, k)} \text{ to cell}_{(i, j, k)} [L^3 t] \\ \phi_{(i-1, j, k)} &= \text{Piezometric head at the central point of cell}_{(i-1, j, k)} [L] \\ \phi_{(i, j, k)} &= \text{Piezometric head at the central point of cell}_{(i, j, k)} [L] \\ R_{(i-1, j, k) \rightarrow (i, j, k)} &= \text{Resistance between the central points of cell}_{(i-1, j, k)} \text{ and cell}_{(i, j, k)} [t] \\ Aw_{(i-1, j, k) \rightarrow (i, j, k)} &= \text{Wet area between cell}_{(i-1, j, k)} \text{ and cell}_{(i, j, k)} [L^2] \end{aligned}$$

- The flow from cell_(i, j, k) to cell_(i+1, j, k) (2.22)

$$Q_{(i, j, k) \rightarrow (i+1, j, k)} = \left(\phi_{(i, j, k)} - \phi_{(i+1, j, k)} \right) R_{(i, j, k) \rightarrow (i+1, j, k)}^{-1} Aw_{(i, j, k) \rightarrow (i+1, j, k)}$$

$$\begin{aligned} Q_{(i, j, k) \rightarrow (i+1, j, k)} &= \text{Flow from cell}_{(i, j, k)} \text{ to cell}_{(i+1, j, k)} [L^3 t] \\ \phi_{(i, j, k)} &= \text{Piezometric head at the central point of cell}_{(i, j, k)} [L] \\ \phi_{(i+1, j, k)} &= \text{Piezometric head at the central point of cell}_{(i+1, j, k)} [L] \\ R_{(i, j, k) \rightarrow (i+1, j, k)} &= \text{Resistance between the central points of cell}_{(i, j, k)} \text{ and cell}_{(i+1, j, k)} [t] \\ Aw_{(i, j, k) \rightarrow (i+1, j, k)} &= \text{Wet area between cell}_{(i, j, k)} \text{ and cell}_{(i+1, j, k)} [L^2] \end{aligned}$$

We can now replace the partial derivative for the flow in the x direction with a finite difference.

$$K_x \frac{\partial^2 \phi}{\partial x^2} \approx K_x \frac{\Delta^2 \phi}{\Delta x^2} \quad (2.23)$$

$$\begin{aligned} K_x \frac{\Delta^2 \phi}{\Delta x^2} &= \left(\phi_{(i-1, j, k)} - \phi_{(i, j, k)} \right) R_{(i-1, j, k) \rightarrow (i, j, k)}^{-1} Aw_{(i-1, j, k) \rightarrow (i, j, k)} \\ &\quad - \left(\phi_{(i, j, k)} - \phi_{(i+1, j, k)} \right) R_{(i, j, k) \rightarrow (i+1, j, k)}^{-1} Aw_{(i, j, k) \rightarrow (i+1, j, k)} \end{aligned} \quad (2.24)$$

The right-hand side of equation 2.24 is a finite difference formulation of the partial derivative. This is evident if all dimensions, and the conductivity, are set to one; equation 2.24 becomes:

$$\frac{\Delta^2 \phi}{\Delta x^2} = \phi_{(x-1, j, k)} - 2\phi_{(i, j, k)} + \phi_{(i+1, j, k)} \quad (2.25)$$

This equation is similar to equation 2.10, which presents the central finite difference in its simplest form.

The flow, into and out of a cell, in y direction

The flow through cell_(i, j, k) in the y direction, can be written as:

- The flow from cell_(i, j-1, k) to cell_(i, j, k) (2.26)

$$Q_{(i, j-1, k) \rightarrow (i, j, k)} = \left(\phi_{(i, j-1, k)} - \phi_{(i, j, k)} \right) R_{(i, j-1, k) \rightarrow (i, j, k)}^{-1} Aw_{(i, j-1, k) \rightarrow (i, j, k)}$$

- The flow from cell_(i, j, k) to cell_(i, j+1, k) (2.27)

$$Q_{(i, j, k) \rightarrow (i, j+1, k)} = \left(\phi_{(i, j, k)} - \phi_{(i, j+1, k)} \right) R_{(i, j, k) \rightarrow (i, j+1, k)}^{-1} Aw_{(i, j, k) \rightarrow (i, j+1, k)}$$

Replacing the partial derivative for flow in the y direction with a finite difference gives:

$$K_y \frac{\partial^2 \phi}{\partial y^2} \approx K_y \frac{\Delta^2 \phi}{\Delta y^2} \quad (2.28)$$

$$K_y \frac{\Delta^2 \phi}{\Delta y^2} = \left(\phi_{(i, j-1, k)} - \phi_{(i, j, k)} \right) R_{(i, j-1, k) \rightarrow (i, j, k)}^{-1} Aw_{(i, j-1, k) \rightarrow (i, j, k)} \quad (2.29)$$

$$- \left(\phi_{(i, j, k)} - \phi_{(i, j+1, k)} \right) R_{(i, j, k) \rightarrow (i, j+1, k)}^{-1} Aw_{(i, j, k) \rightarrow (i, j+1, k)}$$

The flow, into and out of a cell, in z direction

The flow through cell_(i, j, k) in the z direction, can be written as:

- The flow from cell_(i, j, k-1) to cell_(i, j, k) (2.30)

$$Q_{(i, j, k-1) \rightarrow (i, j, k)} = \left(\phi_{(i, j, k-1)} - \phi_{(i, j, k)} \right) R_{(i, j, k-1) \rightarrow (i, j, k)}^{-1} Aw_{(i, j, k-1) \rightarrow (i, j, k)}$$

- The flow from cell_(i, j, k) to cell_(i, j, k+1) (2.31)

$$Q_{(i, j, k) \rightarrow (i, j, k+1)} = \left(\phi_{(i, j, k)} - \phi_{(i, j, k+1)} \right) R_{(i, j, k) \rightarrow (i, j, k+1)}^{-1} Aw_{(i, j, k) \rightarrow (i, j, k+1)}$$

Replacing the partial derivative for flow in the y direction with a finite difference gives

$$K_z \frac{\partial^2 \phi}{\partial z^2} \approx K_z \frac{\Delta^2 \phi}{\Delta z^2} \quad (2.32)$$

$$K_z \frac{\Delta^2 \phi}{\Delta z^2} = \left(\phi_{(i, j, k-1)} - \phi_{(i, j, k)} \right) R_{(i, j, k-1) \rightarrow (i, j, k)}^{-1} Aw_{(i, j, k-1) \rightarrow (i, j, k)} \quad (2.33)$$

$$- \left(\phi_{(i, j, k)} - \phi_{(i, j, k+1)} \right) R_{(i, j, k) \rightarrow (i, j, k+1)}^{-1} Aw_{(i, j, k) \rightarrow (i, j, k+1)}$$

The change in piezometric head in a cell, with respect to time

The partial derivative of the *piezometric head with respect to time* in equation 1.10, will be replaced by a backward finite difference.

$$\frac{\partial \phi}{\partial t} \approx \frac{\Delta \phi_{(i, j, k, t)}}{\Delta t} = \frac{\phi_{(i, j, k, t)} - \phi_{(i, j, k, t-\Delta t)}}{\Delta t} \quad (2.34)$$

$$\begin{aligned} \phi_{(i, j, k, t)} &= \text{Piezometric head at the central point of cell}_{(i, j, k)} \text{ at time } = t \text{ [L]} \\ \phi_{(i, j, k, t-\Delta t)} &= \text{Piezometric head at the central point of cell}_{(i, j, k)} \text{ at time } = t-\Delta \text{ [L]} \\ \Delta t &= \text{Time step [t]} \end{aligned}$$

A.2.8 Formulation of a finite difference equation

Application of the continuity condition on the cell-to-cell flow equations yields a finite difference equation valid for the cell_(i, j, k).

$$\begin{aligned} &+ \left(\phi_{(i-1, j, k)} - \phi_{(i, j, k)} \right) R_{(i-1, j, k) \rightarrow (i, j, k)}^{-1} Aw_{(i-1, j, k) \rightarrow (i, j, k)} \\ &- \left(\phi_{(i, j, k)} - \phi_{(i+1, j, k)} \right) R_{(i, j, k) \rightarrow (i+1, j, k)}^{-1} Aw_{(i, j, k) \rightarrow (i+1, j, k)} \\ &+ \left(\phi_{(i, j-1, k)} - \phi_{(i, j, k)} \right) R_{(i, j-1, k) \rightarrow (i, j, k)}^{-1} Aw_{(i, j-1, k) \rightarrow (i, j, k)} \\ &- \left(\phi_{(i, j, k)} - \phi_{(i, j+1, k)} \right) R_{(i, j, k) \rightarrow (i, j+1, k)}^{-1} Aw_{(i, j, k) \rightarrow (i, j+1, k)} \\ &+ \left(\phi_{(i, j, k-1)} - \phi_{(i, j, k)} \right) R_{(i, j, k-1) \rightarrow (i, j, k)}^{-1} Aw_{(i, j, k-1) \rightarrow (i, j, k)} \\ &- \left(\phi_{(i, j, k)} - \phi_{(i, j, k+1)} \right) R_{(i, j, k) \rightarrow (i, j, k+1)}^{-1} Aw_{(i, j, k) \rightarrow (i, j, k+1)} \\ &= Ss_{(i, j, k)} Vol_{(i, j, k)} \left(\phi_{(i, j, k, t)} - \phi_{(i, j, k, t-\Delta t)} \right) \Delta t^{-1} + Q_{spec(i, j, k, t)} \end{aligned} \quad (2.35)$$

Where the right-hand side of equation 2.35 is:

$$\begin{aligned} Ss_{(i, j, k)} &= \text{Specific storage [L}^{-1}\text{]} \\ Vol_{(i, j, k)} &= \text{Volume of cell}_{(i, j, k)} \text{ [L}^3\text{]} \\ \phi_{(i, j, k, t)} &= \text{Piezometric head in cell}_{(i, j, k)} \text{ at time } = t \text{ [L]} \\ \phi_{(i, j, k, t-\Delta t)} &= \text{Piezometric head in cell}_{(i, j, k)} \text{ at time } = t-\Delta t \text{ [L]} \\ \Delta t &= \text{Time step [t]} \\ Q_{spec(i, j, k)} &= \text{Specified flow into or out from cell}_{(i, j, k)} \text{ [L}^3 \text{ t}^{-1}\text{]} \end{aligned}$$

Under steady state conditions, the flow is time-independent. When the flow is time-independent no storage effects occur. Hence, at steady state conditions, the right-hand side of equation 2.35 will be simplified to include just the specified flow term.

A.3 ESTABLISHMENT OF A SYSTEM OF EQUATIONS

A.3.1 Introduction

Applying the finite difference equation (equation 2.35) to a system of cells produces a linear system of equations. There are two different ways of establishing the system of equations: (i) the implicit method and (ii) the explicit method. When we have established the system of equations, it has to be solved with respect to the unknown parameters (piezometric head and/or flow).

A.3.2 Implicit method, one system of equations for all cells

The implicit method expresses the unknown value at cell_(i, j, k) in terms of the initial value at that cell and the unknown values at the six cells surrounding that cell. Because the values at the surrounding cells are also unknown, all values must be determined simultaneously. This leads to one system of equations for all cells.

To apply the finite difference equation (equation 2.35) on the system of cells, it needs to be slightly rewritten. To make the equation more clear, the resistance (R) and the wet area (Aw) will be multiplied with each other and form six constants.

$$C_1 = R_{(i-1, j, k) \rightarrow (i, j, k)} Aw_{(i-1, j, k) \rightarrow (i, j, k)} \quad (3.1)$$

$$C_2 = R_{(i, j, k) \rightarrow (i+1, j, k)} Aw_{(i, j, k) \rightarrow (i+1, j, k)} \quad (3.2)$$

$$C_3 = R_{(i, j-1, k) \rightarrow (i, j, k)} Aw_{(i, j-1, k) \rightarrow (i, j, k)} \quad (3.3)$$

$$C_4 = R_{(i, j, k) \rightarrow (i, j+1, k)} Aw_{(i, j, k) \rightarrow (i, j+1, k)} \quad (3.4)$$

$$C_5 = R_{(i, j, k-1) \rightarrow (i, j, k)} Aw_{(i, j, k-1) \rightarrow (i, j, k)} \quad (3.5)$$

$$C_6 = R_{(i, j, k) \rightarrow (i, j, k+1)} Aw_{(i, j, k) \rightarrow (i, j, k+1)} \quad (3.6)$$

Using the previously defined constants and gathering all independent terms on the right-hand side, equation 2.35 will be written as:

$$\begin{aligned} & -Ss_{(i, j, k)} Vol_{(i, j, k)} \Delta t^{-1} \phi_{(i, j, k)} \\ & + \left(\phi_{(i-1, j, k)} - \phi_{(i, j, k)} \right) C_1 \\ & - \left(\phi_{(i, j, k)} - \phi_{(i+1, j, k)} \right) C_2 \\ & + \left(\phi_{(i, j-1, k)} - \phi_{(i, j, k)} \right) C_3 \\ & - \left(\phi_{(i, j, k)} - \phi_{(i, j+1, k)} \right) C_4 \\ & + \left(\phi_{(i, j, k-1)} - \phi_{(i, j, k)} \right) C_5 \\ & - \left(\phi_{(i, j, k)} - \phi_{(i, j, k+1)} \right) C_6 \\ & = \\ & -Ss_{(i, j, k)} Vol_{(i, j, k)} \phi_{(i, j, k, t-\Delta t)} \Delta t^{-1} + Q_{spec(i, j, k)} \end{aligned} \quad (3.7)$$

All the piezometric head values on the left-hand side are to be calculated. If non steady state conditions prevail, these values refer to time = t. The piez.head value on the right hand side is the initial piez.head. If non steady-state conditions prevail, this value refers to the time = t-Δt, where Δt is the time step.

The equation 3.7 will be written in such a way that the piez.head values, to be calculated are preceded by coefficients. These coefficients can be calculated on the base of the initial conditions.

$$\begin{aligned}
& -\left(Ss_{(i,j,k)} Vol_{(i,j,k)} \Delta t^{-1} - C_1 - C_2 - C_3 - C_4 - C_5 - C_6\right) \phi_{(i,j,k)} \\
& + C_1 \phi_{(i-1,j,k)} \\
& + C_2 \phi_{(i+1,j,k)} \\
& + C_3 \phi_{(i,j-1,k)} \\
& + C_4 \phi_{(i,j+1,k)} \\
& + C_5 \phi_{(i,j,k-1)} \\
& + C_6 \phi_{(i,j,k+1)} \\
& = \\
& -Ss_{(i,j,k)} Vol_{(i,j,k)} \phi_{(i,j,k,t-\Delta t)} \Delta t^{-1} + Q_{spec(i,j,k)}
\end{aligned} \tag{3.8}$$

An equation of this type will be formulated for each cell, with varying piez.heads. Before the equations can be put together into a system of equations, additional terms have to be added to all equations in such a way that all unknown values of all cells are included in all equations. However, the finite difference equation for a single cell is formulated only for the closest adjacent cells, so all the additional variables are preceded by coefficients with the value zero. The final equation, formulated for each cell, will have the same number of terms as the number of cells in the studied system. For a continuous cell, a cell for which the piez.head may vary, all but seven terms will be preceded by coefficients having a value of zero. For a no-continuous cell, i.e. a cell with a specified piez.head, all but one term will be preceded by coefficients having a value of zero.

For a continuous cell, the seven divergent coefficients can be written as:

$$\begin{aligned}
K1 &= -Ss_{(i,j,k)} Vol_{(i,j,k)} \Delta t^{-1} - C_1 - C_2 - C_3 - C_4 - C_5 - C_6 \\
K2 &= C_1 \\
K3 &= C_2 \\
K4 &= C_3 \\
K5 &= C_4 \\
K6 &= C_5 \\
K7 &= C_6
\end{aligned} \tag{3.9}$$

The value of the right-hand side is:

$$RHS = -Ss_{(i,j,k)} Vol_{(i,j,k)} \phi_{(i,j,k,t-\Delta t)} \Delta t^{-1} + Q_{spec(i,j,k)} \tag{3.10}$$

These coefficients can be calculated on the basis of the initial conditions.

Gathering all the equations into a consistent system of equations will produce a system with primarily zero entries, occurring in regular patterns. When the system of equations has been solved, the piez.head is known in all cells. The flow between the cells has to be calculated on the base of these obtained piez.head values.

A.3.3 Explicit method, one system of equations for each cell

The explicit method expresses the unknown value at cell_(i,j,k) in terms of the initial value at that cell and the initial values at the six cells surrounding cell_(i,j,k). As all the values at the surrounding cells are known, it is possible to formulate a separate system of equations for the studied cell. This leads to one system of equations for each cell.

To establish the system of equations, the finite difference equation (equation 2.35) has to be rewritten. It will be separated into six flow equations and one continuity equation, as follows:

The flow from cell_(i-1,j,k) to cell_(i,j,k) (3.11)

$$Q_{(i-1,j,k) \rightarrow (i,j,k)} = \left(\phi_{(i-1,j,k)} - \phi_{(i,j,k)} \right) R_{(i-1,j,k) \rightarrow (i,j,k)}^{-1} Aw_{(i-1,j,k) \rightarrow (i,j,k)}$$

The flow from cell_(i,j,k) to cell_(i+1,j,k) (3.12)

$$Q_{(i,j,k) \rightarrow (i+1,j,k)} = \left(\phi_{(i,j,k)} - \phi_{(i+1,j,k)} \right) R_{(i,j,k) \rightarrow (i+1,j,k)}^{-1} Aw_{(i,j,k) \rightarrow (i+1,j,k)}$$

The flow from cell_(i,j-1,k) to cell_(i,j,k) (3.13)

$$Q_{(i,j-1,k) \rightarrow (i,j,k)} = \left(\phi_{(i,j-1,k)} - \phi_{(i,j,k)} \right) R_{(i,j-1,k) \rightarrow (i,j,k)}^{-1} Aw_{(i,j-1,k) \rightarrow (i,j,k)}$$

The flow from cell_(i,j,k) to cell_(i,j+1,k) (3.14)

$$Q_{(i,j,k) \rightarrow (i,j+1,k)} = \left(\phi_{(i,j,k)} - \phi_{(i,j+1,k)} \right) R_{(i,j,k) \rightarrow (i,j+1,k)}^{-1} Aw_{(i,j,k) \rightarrow (i,j+1,k)}$$

The flow from cell_(i,j,k-1) to cell_(i,j,k) (3.15)

$$Q_{(i,j,k-1) \rightarrow (i,j,k)} = \left(\phi_{(i,j,k-1)} - \phi_{(i,j,k)} \right) R_{(i,j,k-1) \rightarrow (i,j,k)}^{-1} Aw_{(i,j,k-1) \rightarrow (i,j,k)}$$

The flow from cell_(i,j,k) to cell_(i,j,k+1) (3.16)

$$Q_{(i,j,k) \rightarrow (i,j,k+1)} = \left(\phi_{(i,j,k)} - \phi_{(i,j,k+1)} \right) R_{(i,j,k) \rightarrow (i,j,k+1)}^{-1} Aw_{(i,j,k) \rightarrow (i,j,k+1)}$$

Gathering the known piez.head values on the right-hand side and the unknown piez.head values on the left-hand side, the six flow equations will be written as:

$$\phi_{(i, j, k)} + R_{(i-1, j, k) \rightarrow (i, j, k)} Aw_{(i-1, j, k) \rightarrow (i, j, k)}^{-1} Q_{(i-1, j, k) \rightarrow (i, j, k)} = \phi_{(i-1, j, k)} \quad (3.17)$$

$$-\phi_{(i, j, k)} + R_{(i, j, k) \rightarrow (i+1, j, k)} Aw_{(i, j, k) \rightarrow (i+1, j, k)}^{-1} Q_{(i, j, k) \rightarrow (i+1, j, k)} = -\phi_{(i+1, j, k)} \quad (3.18)$$

$$\phi_{(i, j, k)} + R_{(i, j-1, k) \rightarrow (i, j, k)} Aw_{(i, j-1, k) \rightarrow (i, j, k)}^{-1} Q_{(i, j-1, k) \rightarrow (i, j, k)} = \phi_{(i, j-1, k)} \quad (3.19)$$

$$-\phi_{(i, j, k)} + R_{(i, j, k) \rightarrow (i, j+1, k)} Aw_{(i, j, k) \rightarrow (i, j+1, k)}^{-1} Q_{(i, j, k) \rightarrow (i, j+1, k)} = -\phi_{(i, j+1, k)} \quad (3.20)$$

$$\phi_{(i, j, k)} + R_{(i, j, k-1) \rightarrow (i, j, k)} Aw_{(i, j, k-1) \rightarrow (i, j, k)}^{-1} Q_{(i, j, k-1) \rightarrow (i, j, k)} = \phi_{(i, j, k-1)} \quad (3.21)$$

$$-\phi_{(i, j, k)} + R_{(i, j, k) \rightarrow (i, j, k+1)} Aw_{(i, j, k) \rightarrow (i, j, k+1)}^{-1} Q_{(i, j, k) \rightarrow (i, j, k+1)} = -\phi_{(i, j, k+1)} \quad (3.22)$$

The continuity condition yields the seventh equation:

$$\begin{aligned} & + Q_{(i-1, j, k) \rightarrow (i, j, k)} - Q_{(i, j, k) \rightarrow (i+1, j, k)} \\ & + Q_{(i, j-1, k) \rightarrow (i, j, k)} - Q_{(i, j, k) \rightarrow (i, j+1, k)} \\ & + Q_{(i, j, k-1) \rightarrow (i, j, k)} - Q_{(i, j, k) \rightarrow (i, j, k+1)} \\ & = \\ & Ss_{(i, j, k)} Vol_{(i, j, k)} \left(\phi_{(i, j, k, t)} - \phi_{(i, j, k, t-\Delta t)} \right) \Delta t^{-1} + Q_{spec(i, j, k)} \end{aligned} \quad (3.23)$$

Gathering all independent terms on the right hand side, equation 3.23 will be written as:

$$\begin{aligned} & - Ss_{(i, j, k)} Vol_{(i, j, k)} \Delta t^{-1} \phi_{(i, j, k, t)} \\ & + Q_{(i-1, j, k) \rightarrow (i, j, k)} - Q_{(i, j, k) \rightarrow (i+1, j, k)} \\ & + Q_{(i, j-1, k) \rightarrow (i, j, k)} - Q_{(i, j, k) \rightarrow (i, j+1, k)} \\ & + Q_{(i, j, k-1) \rightarrow (i, j, k)} - Q_{(i, j, k) \rightarrow (i, j, k+1)} \\ & = \\ & - Ss_{(i, j, k)} Vol_{(i, j, k)} \phi_{(i, j, k, t-\Delta t)} \Delta t^{-1} + Q_{spec(i, j, k)} \end{aligned} \quad (3.24)$$

The continuity equation 3.24, together with the six flow equations 3.17 - 3.22, gives a quadratic system of equations, which has the form:

$$\left\{ \begin{array}{l}
(1) \quad +\phi_{(i,j,k)} + R_{(i-1,j,k) \rightarrow (i,j,k)} Aw_{(i-1,j,k) \rightarrow (i,j,k)}^{-1} Q_{(i-1,j,k) \rightarrow (i,j,k)} = +\phi_{(i-1,j,k,t-\Delta t)} \\
(2) \quad -\phi_{(i,j,k)} + R_{(i,j,k) \rightarrow (i+1,j,k)} Aw_{(i,j,k) \rightarrow (i+1,j,k)}^{-1} Q_{(i,j,k) \rightarrow (i+1,j,k)} = -\phi_{(i+1,j,k,t-\Delta t)} \\
(3) \quad +\phi_{(i,j,k)} + R_{(i,j-1,k) \rightarrow (i,j,k)} Aw_{(i,j-1,k) \rightarrow (i,j,k)}^{-1} Q_{(i,j-1,k) \rightarrow (i,j,k)} = +\phi_{(i,j-1,k,t-\Delta t)} \\
(4) \quad -\phi_{(i,j,k)} + R_{(i,j,k) \rightarrow (i,j+1,k)} Aw_{(i,j,k) \rightarrow (i,j+1,k)}^{-1} Q_{(i,j,k) \rightarrow (i,j+1,k)} = -\phi_{(i,j+1,k,t-\Delta t)} \\
(5) \quad +\phi_{(i,j,k)} + R_{(i,j,k-1) \rightarrow (i,j,k)} Aw_{(i,j,k-1) \rightarrow (i,j,k)}^{-1} Q_{(i,j,k-1) \rightarrow (i,j,k)} = +\phi_{(i,j,k-1,t-\Delta t)} \\
(6) \quad -\phi_{(i,j,k)} + R_{(i,j,k) \rightarrow (i,j,k+1)} Aw_{(i,j,k) \rightarrow (i,j,k+1)}^{-1} Q_{(i,j,k) \rightarrow (i,j,k+1)} = -\phi_{(i,j,k+1,t-\Delta t)} \\
(7) \quad -Ss_{(i,j,k)} Vol_{(i,j,k)} \Delta t^{-1} \phi_{(i,j,k)} \\
\quad + Q_{(i-1,j,k) \rightarrow (i,j,k)} - Q_{(i,j,k) \rightarrow (i+1,j,k)} \\
\quad + Q_{(i,j-1,k) \rightarrow (i,j,k)} - Q_{(i,j,k) \rightarrow (i,j+1,k)} \\
\quad + Q_{(i,j,k-1) \rightarrow (i,j,k)} - Q_{(i,j,k) \rightarrow (i,j,k+1)} \\
= -Ss_{(i,j,k)} Vol_{(i,j,k)} \phi_{(i,j,k,t-\Delta t)} \Delta t^{-1} + Q_{spec(i,j,k)} \quad (3.25)
\end{array} \right.$$

The system of equations consists of seven equations and seven unknown variables. The unknown variables are the piez.head in the cell and the flow into and out of the cell.

The piez.head value on the left-hand side is the unknown piez.head. If non steady state conditions prevail, this value refers to time = t. The piez.head values on the right hand side are the initial piez.heads. If non steady state conditions prevail, these values refer to the time = t-Δt, where Δt is the time step. The resistances and the wet areas are calculated on the base of the initial piez.head values.

A system of equations of this type will be formulated for each cell with varying piez.head (continuous cells). The system of equations will be formulated and solved cell by cell. When the system of equations is solved, the piez.head in the studied cell is obtained, as well as the flow in and out of the cell.

A.4 PROCEDURE OF ITERATION

A.4.1 Introduction

When using the finite difference method to solve flow problems, the first step is to formulate the finite difference equation and the system of equations. The next step is to find a set of values which satisfies the finite difference equation. These values are obtained by solving the system of equations in an iterative procedure.

The finite difference method is an iterative method; the result of the calculations will improve if the calculations are repeated. The start values of the first iteration are the initial conditions. The initial conditions describe the known state of the considered system at some initial time. The resulting values of the first iteration are the start values of the second iteration, and so on. The procedure is iterative, because all coefficients of the system of equations are calculated on the basis of the start values. Hence, the coefficients are not representative of the system at the end of the iteration (at the end of the time step).

A.4.2 Convergence

A numerical procedure must converge to be reliable. There are two requirements for convergence: *stability* and *consistency* (Strang, 1987).

- The first requirement is stability, if the calculated solutions (set of values) obtained from the iteration are approaching some unknown solution, the numerical procedure is stable. If they grow away from each other, the numerical procedure is unstable. If the system is unstable it will not converge.
- The second requirement is consistency, the numerical equation should reduce to the exact continuum equation, when all finite intervals approach zero. The studied numerical procedure is consistent, see Sec. A.2.

The stability requirement imposes restrictions on the size of the time step in an explicit formulation of a non steady flow problem (see Sec.A.3). It provides an upper limit for the magnitude of the time step in relation to the spatial size and the hydraulic conductivity of the cells in the mesh, see Bear and Verruit (1987).

The implicit method (see Sec.A.3) is unconditionally stable, which means that for all (positive) values of the time step, errors will dissipate in time, see Bear and Verruit (1987).

The differences between the start values and the resulting values of an iteration occur because the start values do not satisfy the finite difference equation. In a converging procedure, the difference between the start values and the resulting values will become smaller for each iteration. When the differences are smaller than a defined number, the iterative procedure has converged. The resulting values are an acceptable estimation of the unknown set of values which satisfies the finite difference equation. The defined number which determines if the procedure has converged or not, is called the convergence criteria. The convergence criteria is a number selected on the basis of the purpose and nature of the studied flow problem.

A.4.3 Accuracy

If the numerical procedure converges, the difference between the unknown true exact solution and the obtained solution decreases as the number of iterations increases. The accuracy of the numerical procedure will increase when the number of iterations increase. However, the numerical procedure may converge towards a solution which is not the true, exact solution. This can be expected if the mesh is too coarse to correctly represent the studied domain, or if the size of two neighboring cells are very different. "The gain in flexibility when using a variable mesh size is partly balanced by a loss of accuracy." Bear and Verruit (1987).

A.4.4 Steady state condition

Steady-state conditions occur when the flow at each point has time-independent characteristics, although spatial variability may occur. Under steady state conditions the flow rates into and out from the studied system are equal. The time-independent characteristics of the steady state condition leads to a time-independent initial condition; any reasonable set of values are acceptable as initial condition.

A.4.5 Non steady state condition (transient condition)

Non steady state conditions occur when the flow (velocity) changes in magnitude or direction with time. Under non steady state conditions, it is possible that the flow rates into and out from the studied system are not equal.

If a system under steady state conditions is disturbed by a change in the flow conditions, it will take time for the system to adjust to the new flow conditions. During this time period the system is under non steady state conditions. The non steady state flow is, among other parameters, dependent on storage or release of water in the flow medium. The release or storage of water in the flow medium will delay the transition to a new steady state condition. The storage terms in the finite difference equation control the amount of water released from (or added to) a unit flow medium per unit decline (or rise) of piez.head.

The starting values of a non steady state simulation are the known values of the considered system at some initial time. The results of a non steady state simulation are the flow and the piez.head distribution at a later point in time. The iterative procedure of a non steady state simulation differs slightly from the iterative procedure of a steady state simulation. Under steady state conditions, every iteration is a step towards the steady state solution. Under non steady state conditions, every iteration is a step in time and the resulting values represent the condition of the studied system at a later point in time. The resulting values are influenced by the approximation of the time derivative. All coefficients of the system of equations are calculated on the basis of the start values. Hence, the coefficients are not representative of the system at the end of the time step. To minimize the effect of this error, the number of time steps (iterations) has to be large.

To determine the necessary number of time steps (iterations), the non steady state simulation has to be repeated with an increased number of time steps (iterations). Each simulation will produce a set of resulting values at the studied point in time. Each simulation is compared to the previous one; when the differences between the resulting values are less than the specified acceptable error (the convergence criteria), the non steady-state simulation has converged.

A.4.6 Implicit method

The implicit method leads to one large system of equations representing all cells in the mesh. Only the piez.head values of the cells are expressed in the system of equations; in an iteration of the mesh only the piez.head values are calculated. If the studied mesh contains 100 cells, one iteration of the mesh will lead to the solution of a system of equations containing 100 unknown variables.

For the implicit method, the iterative procedure is dependent on the coefficients of the system of equations. The coefficients are determined by the homogenized conductivity, possibly expressed as a resistance, and the wet area. If confined conditions occur, the resistance and the wet area will not change. Hence, if confined conditions occur, only one iteration is necessary for obtaining the solution to the differential equation. If unconfined conditions occur, an iterative procedure is necessary to obtain an estimate of the solution to the differential equation.

Only the piez.head values are obtained when the system of equations is solved, the flow between the cells is calculated on the basis of the obtained piez.head values.

Under non steady-state conditions, the large system of equations will be solved once, for each time step. Because the mesh of cells is represented by one system of equations, solving the system of equations will yield the piez.head simultaneously in all cells.

The advantage of the implicit method is that the time step may be chosen much larger than for the explicit method. Disadvantages are a more complex system of equations.

A.4.7 Explicit method

The explicit method leads to one system of equations for each cell in the studied system. One iteration of the mesh, means the calculation of both the piez.head values of all cells and the flow into and out from all cells. If the studied mesh contains 100 cells, one iteration of the mesh will lead to the solution of 100 systems of equations, each containing 7 unknown variables (3-dimensions).

For the explicit method, the iterative procedure is dependent on both the homogenized conductivity, possibly expressed as a resistance, and the wet area, as well as the piez.head in the surrounding cells. Because the piez.head values of the surrounding cells are included in the system of equations, an iterative procedure is always necessary. Both the piez.head values and the flow into and out from the cells are obtained when the system of equations is solved.

Since the calculations of the piez.head values are carried out cell by cell and the calculations are dependent of the piez.head values at the surrounding cells, it is of interest when the piez.head values of the cells are updated. Two different methods are identified.

- Explicit method 1. The piez.head value of the studied cell is updated immediately after the system of equations representing the cell is solved. The calculated piez.head in the next cell will be dependent on the new piez.head value of the last studied cell. The initial set of piez.head values will be changed along the iteration of the mesh.
- Explicit method 2. The piez.head value of the studied cell is not updated until all systems of equations are solved. The same set of initial piez.head values will be used.

Before a time step (iteration), all cells are at the same point in time. During the iteration of the mesh, solved cells will turn to the new point in time while unsolved cells are at the old point in time. If 'explicit method 1' is used, a cell inside the mesh might be surrounded by cells being at both the new and the old point in time. If 'explicit method 2' is used a cell inside the mesh will always be surrounded by cells at the old point in time.

When using the explicit method, it is important to use a large number of time steps (iterations), as the method will underestimate the change in piez.head during a time step (iteration). As previously discussed, the stability requirement imposes restrictions on the size of the time step in an explicit formulation of a non steady flow problem.

Another disadvantage which may occur when the cells are solved cell by cell, is that the order of the sequence will influence the cells in a regular pattern. If the number of iterations are few, this may lead to a regular distortion of the calculated values. However, this distortion is limited and it is easy to minimize it by starting the sequence at different cells and by alternating the sequence direction (alternating number order).

The cell-by-cell solving procedure also involves advantages. It is possible to let the results of a previously processed cell influence the processing of another cell. For example: if 'explicit method 1' is used a cell could, during the iteration of the mesh, change boundary conditions, from confined conditions to unconfined conditions. The following cells, in the cell-by-cell sequence, will treat this cell with the new boundary condition. Very complicated interactions between cells could be implemented.

The explicit method has the advantage of flexibility and simplicity, but demands small time steps. The explicit method is particularly attractive for complicated flow analyses, such as analyses involving flow of multiple phases (unsaturated - saturated flow).

A.5 THE GEOAN MODEL

Introduction

The GEOAN model is a numerical model for calculation of groundwater head and flow in three dimensions. The model is developed by the author of this study and was first presented in Holmén (1992). Below follows a short description of the model.

Original differential equation

The GEOAN model is based on the continuum approach. The partial differential equation describing groundwater flow is established as described in Section A.1. The presumptions and generalizations for establishing the equation are also discussed in this section, see Sec.A.1.2 and Sec.A.1.6.

Numerical method for solving the differential equation

The GEOAN model uses the finite difference method for solving the original partial differential equation. The finite difference method is a numerical method, described in previous sections (Sec.A.1 - A.4). The finite difference method replaces the differential equation with a system of equations. The model can establish the system of equations both by the use of the implicit method and the explicit method (see Section A.3).

Solving the system of equations

The solver is an algorithm which solves the established system of equations. The GEOAN model provides the user with several different solvers, both direct solvers (e.g. Gaussian elimination) and iterative solvers (e.g. the method of successive relaxation). To save computer memory, the model stores only the non-zero coefficients and the right-hand side values of the system of equations. This is done by the use of a pointer matrix.

Boundary conditions

The GEOAN model provides the user with a large number of different boundary conditions. The model is capable of changing the boundary conditions of a cell during the course of iterations. The model can handle unsaturated cells in a generalized way. The model can combine cells of the following types in the same mesh: confined, unconfined, unsaturated, saturated, specified head and specified flow, etc., and is also capable of changing these conditions during the course of iterations. This makes the model capable of simulating a phreatic surface that moves and passes from one layer to another. The model can also simulate the interaction between the phreatic surface and the ground surface. This is done as the model changes the boundary conditions of the cells, with respect to the elevation of the phreatic surface and the elevation of the ground surface. The model will transport the water that flows out at discharge areas to the next cell in the direction of the topographic gradient, in this way the model simulates surface water flows. Hence, based on the topography (the ground elevation) the model can simulate recharge areas and discharge areas and how they change in size with time, and also rivers, lakes and creeks.

Convergence criterion

The GEOAN model calculates the flow into and out of the model, and optionally the flow into and out of a structure inside the model (e.g. a tunnel), at the end of every iteration (time step). The convergence criterion could be formulated both for (i) the maximum acceptable change in head during an iteration and (ii) the maximum acceptable error in flow, as calculated after every iteration. The GEOAN model could supervise one or both of the criteria given above, not combined or combined in a logical expression (AND, OR). The possibility of having a convergence criterion related to both head and flow is important when comparing the results of different models with large differences in conductivity.

Programming language

The GEOAN model is a numerical model. The computer code is developed in the FORTRAN programming language.

Random number generation

The stochastic continuum method involves the generation of random numbers, based on a given probability distributions. The GEOAN model uses an advanced, long period, random number generator, given by Press *et al* (1992), (the *ran2* generator, p.272-273). This generator produces random numbers, uniformly distributed. Transformation of the uniform distribution to a normal distribution (transformation of a uniform-distributed deviate to a normal-distributed deviate) is done by an algorithm given in Press *et al* (1992), (the *gasdev* algorithm, p.280)

Flowpaths

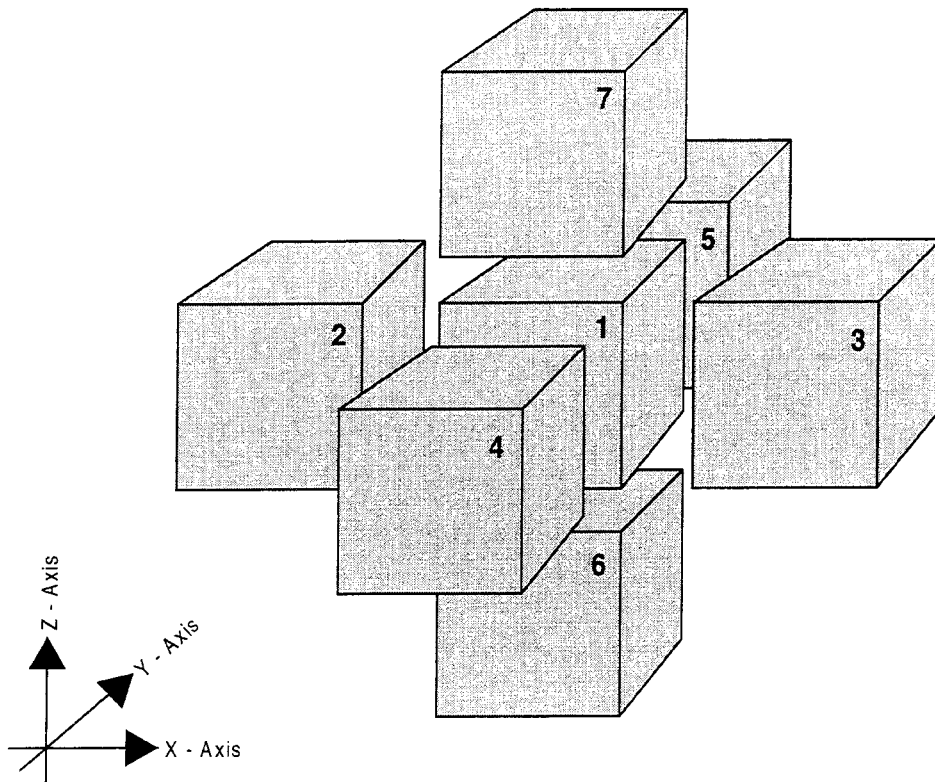
The flow pattern of the groundwater can be illustrated by the use of flowpaths. The GEOAN model creates flowpaths by the use of simulated particles, particles that follow the flow of groundwater through the model. The particle tracking algorithm could also be used for estimation of transportation times, transport processes, etc. For calculation of flowpaths, both an semi-analytical method (Pollock, 1989) and a numerical method is available.

Verification

The GEOAN model has been verified. The verification was carried out as a comparison between results produced by the GEOAN model and results produced by analytical solutions, the studied problems were generalized problems for which analytical solutions are available. More complicated problems have also been studied, by comparing the results produced by the GEOAN model to results produced by other numerical models, models that uses the finite element method. The verifications have been carried out for both steady state conditions and non steady state conditions. The verification demonstrates that the GEOAN model correctly solves all the studied problems. The verification is presented in Holmén, (1992).

A.6 REFERENCES

- BEAR, J., and BACHMAT, Y., 1990: Introduction to Modeling of Transport Phenomena in Porous Media. *Kluwer Academic Publishers, Dordrecht, The Netherlands.*
- BEAR, J., and VERRUIT, A., 1987: Modeling Groundwater Flow and Pollution. *D. Reidel Publishing Company, Dordrecht, The Netherlands.*
- DARCY, H., 1856: Les Fontaines Publiques de la Ville de Dijon. *Dalmont, Paris, France.*
- HOLMÉN, J.G., 1992: "A three-dimensional finite difference model for calculation of flow in the saturated zone". *Department of quaternary geology, University of Uppsala, Uppsala, Sweden. ISBN 91-7376-119-2, ISSN 0348-2979.*
- POLLOCK, D., W., 1989: "Documentation of computer program to compute and display path lines using results from the U.S. Geological survey modular three-dimensional finite difference ground-water flow model". (MODPATH manual). *U.S. Geological survey 411 National Center Reston, VA 22092 USA.*
- PRESS, W., TEUKOLSKY, S., VETTERLING, W., and FLANNERY, B., 1992: "Numerical Recipes in fortran. The art of scientific computing. Second edition" *Cambridge University Press, ISBN 0 521 43064 X.*
- STRACK, O., 1989: Groundwater Mechanics. *Prentice-Hall Inc., Englewood Cliffs, New Jersey, 07632 USA.*
- STRANG, G., 1986: Introduction to Applied Mathematics. *Wellesley-Cambridge Press, Wellesley, MA 02181 USA.*



Number	Index
1.	Cell (i , j , k)
2.	Cell (i-1 , j , k)
3.	Cell (i+1 , j , k)
4.	Cell (i , j-1 , k)
5.	Cell (i , j+1 , k)
6.	Cell (i , j , k-1)
7.	Cell (i , j , k+1)

FIGURE A.1

DISCRETIZATION OF THE FLOW MEDIUM.

To solve the original differential equation, by use of the finite difference method, it is necessary to make a spatial discretization. The studied medium is divided into a number of cells. With reference to a Cartesian coordinate system, the cells should form a system of columns, rows and layers.

The rows are directed in the horizontal plane along the x-axis and the columns are directed in the horizontal plane along the y-axis.

The layers consist of both rows and columns. Every layer represents a three-dimensional body in space. The system of cells is called a mesh.

The figure presents CELL(i , j , k) and the six adjacent cells.

For increased clarity , the seven cells are separated from each other, in a finite difference mesh the cells are connected.

APPENDIX B

Analytical method for calculation of steady flow in closed tunnels

TABLE OF CONTENTS

PAGE

B.1 ANALYTICAL METHOD B.3
B.1.1 Introduction B.3
B.1.2 Definition of terms B.3
B.1.3 Flow in a sphere B.4
B.1.4 Flow in an infinitely long cylinder. B.5
B.1.5 Flow in an ellipsoid B.6
B.2 GEOMETRIC PROPERTIES OF AN ELLIPSOID B.10
B.3 COMPARISON BETWEEN ANALYTICAL AND NUMERICAL METHOD . B.10
B.4 REFERENCES B.11

TABLES B.12 - B.13
FIGURES B.14 - B.16

B.1 ANALYTICAL METHOD

B.1.1 Introduction

Mathematical methods derived for calculation of conduction of heat or electric current are applicable for calculation of groundwater flow, if confined conditions could be assumed for the flow medium, or the position of the phreatic surface is known. Before efficient computers became available, analytical methods were derived for a large number of problems. The problem of steady flow of heat or fluid in a medium containing an object having a different conductivity than the surrounding medium, is of technical importance and analytical methods have been derived. "Mathematically, it is precisely the same (problem) as that of induced magnetization in a body of the same shape placed in a uniform external field, and solutions will be found in text books on electricity and magnetism" (Carslaw and Jaeger, 1959).

In this appendix analytical formulas are given, formulas that defines the head inside a sphere, a cylinder and a spheroid (an ellipsoid). The formulas are taken from Carslaw and Jaeger (1959). They were originally derived for calculations of heat in solids and have been rewritten and developed to be applicable for flow of groundwater.

The formulas presume steady state conditions. The rock mass is represented by an infinitely large homogeneous isotropic medium. The basic formulas give the head inside a sphere and an ellipsoid, for any direction of the regional flow; and the head inside a cylinder, if the regional flow is directed at right angles to the main axis of the cylinder. For these scenarios, the head inside the studied structure will vary in a linear way, and consequently, the gradient and the specific flow will be a constant inside the structure.

The specific flow of groundwater is:

$$q = K I \quad (\text{B:1})$$

$q = \text{Specific flow [m/s]}$
 $K = \text{Conductivity [m/s]}$
 $I = \text{Gradient [-]}$

The head inside the studied structure is ϕ_t and the head outside is ϕ_r . The head gradient outside the studied structure tends to I_r at great distance (gradient of regional groundwater flow).

B.1.2 Definition of terms

In the following sections we will use terms that correspond to the geometry of an ellipsoid, terms like: main axis, short axis, cross-section at right angles to the main axis, cross-section at right angles to the short axis, etc. These terms are defined in Figure 3.1 and Figure B.1. When we discuss the direction of the regional flow, the direction will be given in relation to the shape of an ellipsoid, e.g. flow along main axes, flow along short axis, such directions are demonstrated in Figure 3.1.

B.1.3 Flow in a sphere

The head in the sphere is (Carslaw and Jaeger, 1959):

$$\phi_t = \frac{3 K_r I_r}{2 K_r + K_t} x \quad (\text{B:2})$$

K_r = Conductivity of the rock mass [m/s]

K_t = Conductivity of the studied body [m/s]

I_r = Head gradient of regional flow at great distance [m]

ϕ_t = Head in the studied body [m]

x = Coordinate (origo at center of sphere) [m]

The head gradient in the sphere is the derivative of the head:

$$I_t = \frac{d\phi_t}{dx} = \frac{3 K_r I_r}{2 K_r + K_t} \quad (\text{B:3})$$

I_t = Head gradient in the studied body [-]

Flow in a sphere compared to the regional flow in the rock:

$$\frac{q_t}{q_r} = \frac{K_t \frac{3 K_r I_r}{2 K_r + K_t}}{K_r I_r} \quad (\text{B:4})$$

q_t = Specific flow in the studied body (tunnel) [m/s]

q_r = Specific flow in the rock [m/s]

We reduce the equation above, the following equation will be obtained:

$$\frac{q_t}{q_r} = \frac{3 K_t}{2 K_r + K_t} \quad (\text{B:5})$$

An infinitely permeable sphere gives the following relationship.

$$\frac{q_t}{q_r} = \frac{3 K_t}{2 K_r + K_t} \quad K_t \rightarrow \infty \quad \text{gives:} \quad \frac{q_t}{q_r} \rightarrow 3 \quad (\text{B:6})$$

B.1.4 Flow in an infinitely long cylinder.

Regional flow is directed at right angles to the length of the cylinder (regional flow along the short axis of the cylinder)

The head in the cylinder is (Carslaw and Jaeger, 1959):

$$\phi_t = \frac{2 K_r I_r}{K_r + K_t} x \quad (\text{B:7})$$

The head gradient in the cylinder is:

$$I_t = \frac{d\phi_t}{dx} = \frac{2 K_r I_r}{K_r + K_t} \quad (\text{B:8})$$

Flow in a cylinder compared to the regional flow in the rock:

$$\frac{q_t}{q_r} = \frac{K_t \frac{2 K_r I_r}{K_r + K_t}}{K_r I_r} \quad (\text{B:9})$$

We reduce the equation above, the following equation will be obtained:

$$\frac{q_t}{q_r} = \frac{2 K_t}{K_r + K_t} \quad (\text{B:10})$$

An infinitely permeable cylinder gives the following relationship.

$$\frac{q_t}{q_r} = \frac{2 K_t}{K_r + K_t} \quad K_t \rightarrow \infty \text{ gives: } \frac{q_t}{q_r} \rightarrow 2 \quad (\text{B:11})$$

B.1.5 Flow in an ellipsoid.

A spheroid can be described by the use of three axes: a , b and c , at right angles. If two axes are equal, the spheroid is called an ellipsoid. The axes of the ellipsoid are related as, $a > b = c$. Hence, the long axis is a and the two short axes are b and c . Geometrical data, as well as the shape of different ellipsoids, are given in Figure B.1.

Presuming a Cartesian coordinate system, the main axis is along the x axis of the system, the short axes are along the y and z axes; the ellipsoid is:

$$\frac{x^2}{a^2} + \frac{y^2}{b^2} + \frac{z^2}{c^2} = 1 \quad (\text{B:12})$$

The head gradient of the regional flow of groundwater is defined by a vector:

$$\bar{v} = (I_1, I_2, I_3) \quad (\text{B:13})$$

I_1 = Component of head gradient of regional flow, component along x axis

I_2 = Component of head gradient of regional flow, component along y axis

I_3 = Component of head gradient of regional flow, component along z axis

For any point (x,y,z) , let λ be the positive root of:

$$\frac{x^2}{a^2+\lambda} + \frac{y^2}{b^2+\lambda} + \frac{z^2}{c^2+\lambda} = 1 \quad (\text{B:14})$$

Based on the integrals below, it is possible to calculate the head inside and outside of the studied ellipsoid (Carslaw and Jaeger, 1959).

$$A_\lambda = \frac{1}{2}abc \int_\lambda^\infty \frac{du}{(a^2+u)\Delta(u)}$$

$$B_\lambda = \frac{1}{2}abc \int_\lambda^\infty \frac{du}{(b^2+u)\Delta(u)} \quad (\text{B:15})$$

$$C_\lambda = \frac{1}{2}abc \int_\lambda^\infty \frac{du}{(c^2+u)\Delta(u)}$$

$$\Delta(u) = \sqrt{(a^2+u)(b^2+u)(c^2+u)}$$

The integrals all satisfy Laplaces equation. The head inside the ellipsoid is ϕ_i (Carslaw and Jaeger, 1959):

$$\phi_i = \frac{1}{1 + A_0 \left(\frac{K_i - K_r}{K_r} \right)} I_1 x + \frac{1}{1 + B_0 \left(\frac{K_i - K_r}{K_r} \right)} I_2 y + \frac{1}{1 + C_0 \left(\frac{K_i - K_r}{K_r} \right)} I_3 z \quad (\text{B:16})$$

$$\phi_i = C_1 I_1 x + C_2 I_2 y + C_3 I_3 z$$

The constants C_1 , C_2 and C_3 are given by the ellipsoid shape and the conductivity contrast.

The head outside the ellipsoid is ϕ_r (Carslaw and Jaeger, 1959):

$$\phi_r = I_1 x + I_2 y + I_3 z - \frac{\left(\frac{K_t - K_r}{K_r}\right) I_1 A_\lambda x}{1 + A_0 \left(\frac{K_t - K_r}{K_r}\right)} - \frac{\left(\frac{K_t - K_r}{K_r}\right) I_2 B_\lambda y}{1 + B_0 \left(\frac{K_t - K_r}{K_r}\right)} - \frac{\left(\frac{K_t - K_r}{K_r}\right) I_3 C_\lambda z}{1 + C_0 \left(\frac{K_t - K_r}{K_r}\right)} \quad (\text{B:17})$$

According to Carslaw and Jaeger (1959), the integral analysis above goes back at least to Lamé (1837).

$A_\lambda, B_\lambda, C_\lambda$ are integrals, A_0, B_0, C_0 are the integrals $A_\lambda, B_\lambda, C_\lambda$ with $\lambda = 0$. If the axes of the ellipsoid are $a > b = c$, then these integrals are calculated as presented below (Equations B.18 through B.23). The evaluation of the integrals are taken from Carslaw and Jaeger (1959), they refer to Besant and Ramsey (1920).

$$A_\lambda = \frac{(1 - e_0^2)}{e_0^3} \left(\frac{1}{2} \ln \frac{1+e_\lambda}{1-e_\lambda} - e_\lambda \right) \quad (\text{B:18})$$

$$B_\lambda = C_\lambda = \frac{(1 - e_0^2)}{2e_0^3} \left(\frac{e_\lambda}{1-e_\lambda^2} - \frac{1}{2} \ln \frac{1+e_\lambda}{1-e_\lambda} \right) \quad (\text{B:19})$$

$$A_0 = \frac{(1 - e_0^2)}{e_0^3} \left(\frac{1}{2} \ln \frac{1+e_0}{1-e_0} - e_0 \right) \quad (\text{B:20})$$

$$B_0 = C_0 = \frac{(1 - e_0^2)}{2e_0^3} \left(\frac{e_0}{1-e_0^2} - \frac{1}{2} \ln \frac{1+e_0}{1-e_0} \right) \quad (\text{B:21})$$

$$e_\lambda = \sqrt{\frac{(a^2 - b^2)}{(a^2 + \lambda)}} \quad ; \quad e_0 = \sqrt{\frac{(a^2 - b^2)}{a^2}} \quad (\text{B:22})$$

If b/a is small we have approximately:

$$A_0 = \frac{b^2}{a^2} \left(\ln \left(\frac{2a}{b} \right) - 1 \right) \quad (\text{B:23})$$

Flow in an ellipsoid, the regional flow is directed along the main axis of the ellipsoid.

If the regional flow is directed along the main axes of an ellipsoid, equation B.16 will be reduced to:

$$\phi_t = \frac{I_1}{1 + A_0 \left(\frac{K_t - K_r}{K_r} \right)} x \quad (\text{B:24})$$

The head gradient, I_t , inside the ellipsoid is the derivative of the head.

$$I_t = \frac{d \phi_t}{d x} = \frac{I_1}{1 + A_0 \left(\frac{K_t - K_r}{K_r} \right)} \quad (\text{B:25})$$

Specific flow in an ellipsoid, compared to the regional flow in the rock:

$$\frac{q_t}{q_r} = \frac{K_t \left(\frac{I_1}{1 + A_0 \left(\frac{K_t - K_r}{K_r} \right)} \right)}{K_r I_1} = \frac{\frac{K_t}{K_r}}{1 + A_0 \left(\frac{K_t}{K_r} - 1 \right)} \quad (\text{B:26})$$

An infinitely permeable ellipsoid gives the following relationship, presuming that the regional flow is directed along the main axis of the ellipsoid.

$$\frac{q_t}{q_r} = \frac{\frac{K_t}{K_r}}{1 + A_0 \left(\frac{K_t}{K_r} - 1 \right)} \quad K_t \rightarrow \infty \text{ gives: } \frac{q_t}{q_r} \rightarrow \frac{1}{A_0} \quad (\text{B:27})$$

Flow in an ellipsoid, the regional flow is directed along the short axis of the ellipsoid.

In analogy with the above demonstrated for regional flow along the main axis, we will have the following expression for the specific flow in the ellipsoid when the regional flow is directed along the short axis.

$$\frac{q_t}{q_r} = \frac{\frac{K_t}{K_r}}{1 + B_0 \left(\frac{K_t}{K_r} - 1 \right)} \quad K_t \rightarrow \infty \text{ gives: } \frac{q_t}{q_r} \rightarrow \frac{1}{B_0} \quad (\text{B:28})$$

Flow in an ellipsoid for any direction of regional flow.

Equation B.16 is a function giving the variation of head inside an ellipsoid. The equation reveals that the head inside an ellipsoid varies in a linear way and depends on (i) the size and direction of the regional flow and (ii) the properties of the studied system (shape and conductivity) as well as on (iii) the studied position (coordinates). It is possible to write the equation by the use of three constants representing the properties of the studied system. The constants C_1 , C_2 and C_3 are given by the ellipsoid shape and the conductivity contrast between the ellipsoid and the surroundings (rock mass). The constants are not dependent on direction or size of the regional flow or coordinates; the equation becomes.

$$\phi_t = C_1 I_1 x + C_2 I_2 y + C_3 I_3 z \quad (\text{B:29})$$

The flow in the ellipsoid depends on the regional flow. The direction of the regional flow is defined by a direction vector, with components: J_1 , J_2 and J_3 along the x , y and z axes.

$$\bar{v} = (J_1, J_2, J_3) \quad |\bar{v}| = \sqrt{J_1^2 + J_2^2 + J_3^2} = 1 \quad (\text{B:30})$$

Presuming that the size of the regional flow is one, the components of the regional flow: I_1 , I_2 , I_3 , are equal to the direction vector: $I_1=J_1$, $I_2=J_2$, $I_3=J_3$. The gradient of the flow inside the ellipsoid (I_t) is given by the direction vector of the regional flow and the partial derivatives of equation B.29.

$$I_t = J_1 \frac{\partial \phi_t}{\partial x} + J_2 \frac{\partial \phi_t}{\partial y} + J_3 \frac{\partial \phi_t}{\partial z} \quad (\text{B:31})$$

$$I_t = J_1 C_1 J_1 + J_2 C_2 J_2 + J_3 C_3 J_3$$

If the regional flow is one, the flow in the ellipsoid is a multiple of the regional flow. The specific flow inside an ellipsoid is given by (i) the conductivity of the ellipsoid, times (ii) the head gradient inside the ellipsoid. Hence, for any size and direction of regional flow, the following equation is applicable:

$$\frac{q_t}{q_r} = K_t C_1 J_1^2 + K_t C_2 J_2^2 + K_t C_3 J_3^2 \quad (\text{B:32})$$

The three constants C_1 , C_2 and C_3 are defined by equation B.16. Replacing the three constants in equation B.32 by the full expressions, gives the following equation: (B:33)

$$\frac{q_t}{q_r} = K_t \left(\frac{1}{1 + A_0 \left(\frac{K_t - K_r}{K_r} \right)} \right) J_1^2 + K_t \left(\frac{1}{1 + B_0 \left(\frac{K_t - K_r}{K_r} \right)} \right) J_2^2 + K_t \left(\frac{1}{1 + C_0 \left(\frac{K_t - K_r}{K_r} \right)} \right) J_3^2$$

An infinitely permeable ellipsoid gives the following relationship.

$$K_t \rightarrow \infty \quad \text{gives:} \quad \frac{q_t}{q_r} \rightarrow \frac{J_1^2}{A_0} + \frac{J_2^2}{B_0} + \frac{J_3^2}{C_0} \quad (\text{B:34})$$

Flow in an ellipsoid, balance as regards direction of regional flow

It is possible to estimate at what ellipsoid conductivity, the total flow in the ellipsoid is the same for: (i) regional flow along the main axes of the ellipsoid and (ii) regional flow along the short axes of the ellipsoid. The conductivity value is calculated by combining equation B.27 and B.28, and include terms for the areas in direction of the regional flow.

$$\left(\frac{\frac{K_t}{\overline{K_r}}}{1 + B_0 \left(\frac{K_t}{\overline{K_r}} - 1 \right)} \right) P_2 = \left(\frac{\frac{K_t}{\overline{K_r}}}{1 + A_0 \left(\frac{K_t}{\overline{K_r}} - 1 \right)} \right) P_1 \quad (\text{B:35})$$

B.2 GEOMETRIC PROPERTIES OF AN ELLIPSOID

An ellipsoid is a three dimensional body, it is a sphere that has been 'extended' along one or two axes. The ellipsoid is defined by three axes: A , B and C . The main axes is the longest axes it is A , the two shorter axes are B and C . Each of these axes are split into semi axes (compare with the radius of a sphere), the semi axis are denoted as a , b , and c . The length of the ellipsoid along an axes is two times the length of the semi axes: $A=2a$, $B=2b$, $C=2c$. The volume of and ellipsoid is.

$$\text{Volume} = \frac{4}{3} \pi a b c \quad (\text{B:36})$$

An ellipsoid with center at (x_0, y_0, z_0) and semi axes a, b, c , has the following equation.

$$\frac{(x-x_0)^2}{a^2} + \frac{(y-y_0)^2}{b^2} + \frac{(z-z_0)^2}{c^2} = 1 \quad (\text{B:37})$$

We are interested in ellipsoids with: $a > b = c$, the following areas and formulas are used.

P_1 = Maximum area of cross section at right angles to main axes (maximum width).

P_2 = Maximum area of cross section at right angles to short axes.

P_3 = Average area of cross section at right angles to main axes (average width).

$$\begin{aligned} P_1 &= \pi b^2 \\ P_2 &= \pi a b \\ P_3 &= \frac{2}{3} P_1 \end{aligned} \quad (\text{B:38})$$

B.3 COMPARISON BETWEEN ANALYTICAL AND NUMERICAL METHODS

A comparison between numerical and analytical models are given in Chapter 3. That comparison is based on Tables B.1 and B.2 as well as on Figures B.2 and Figure B.3. These tables and figures are given at the end of this appendix.

B.4 REFERENCES

BESANT, and RAMSEY, 1920: Hydrodynamics (edn. 2, 1920) p 169

CARSLAW, H.S. and J.C. JAEGER, 1959: "Conduction of Heat in Solids (second edition)" *Oxford University Press, Walton Street, Oxford ox2 6dp, ISBN 0 19 853303 9.*

LAMÉ, 1837: *Liouville's J.* 2.

Table B.1 COMPARISON BETWEEN ANALYTICAL AND NUMERICAL METHOD.

The regional flow was directed along the short axes of the structures.

A comparison of an analytical model predicting the flow in an ellipsoid and a numerical model predicting the flow in a rectangular parallel-epiped; for different values of conductivity and length of the studied structures. For each studied scenario the structures have the same length in both methods. The two cases corresponds to different shapes of the circular cross-sections of the ellipsoids.

- Case A has a maximum area of cross-section perpendicular to main axes: 100 m^2
 - Case B has an average area of cross-section perpendicular to main axes: 100 m^2 .
- The parallel-epiped has a rectangular cross-section perpendicular to the short axes with an area of 100 m^2 .

Table (i) Specific flow

Case	Length of Structure [m]	DIFFERENCE IN PREDICTED SPECIFIC FLOW [m/s]. In percent of specific flow predicted by numerical model. (1)							
		K 0.001	K 0.01	K 0.1	K 1	K 10	K 100	K 1000	K(2) 10000
A	50	-35.5	-34.9	-29.4	0	32.7	39.6	40.4	40.8
	100	-35.2	-34.6	-28.9	0	30.0	36.1	36.8	36.8
	200	-35.4	-34.7	-29.0	0	29.4	35.2	35.8	35.9
B	50	-36.7	-36.1	-30.5	0	35.1	42.6	43.5	43.9
	100	-35.7	-35.1	-29.4	0	31.0	37.3	38.0	38.0
	200	-35.5	-34.9	-29.2	0	29.7	35.6	36.3	36.3

Table (ii) Total flow

Case	Length of Structure [m]	DIFFERENCE IN PREDICTED TOTAL FLOW. [m ³ /s] In percent of total flow predicted by numerical model. (1)							
		K 0.001	K 0.01	K 0.1	K 1	K 10	K 100	K 1000	K(2) 10000
A	50	-42.9	-42.3	-37.5	-11.4	17.6	23.7	24.3	24.5
	100	-42.6	-42.0	-37.0	-11.4	15.2	20.6	21.2	21.3
	200	-42.7	-42.2	-37.1	-11.4	14.6	19.8	20.4	20.4
B	50	-31.3	-30.7	-24.6	8.5	46.6	54.8	55.6	55.8
	100	-30.2	-29.6	-23.4	8.5	42.2	49.0	49.8	49.9
	200	-30.1	-29.4	-23.1	8.5	40.7	47.2	47.9	48.0

Table (iii) Notes

<p>(1) The difference is calculated as: $(\text{Flow analytical} - \text{Flow numerical}) / (\text{Flow numerical} / 100)$ Hence, a negative difference means that the flow predicted by the analytical method is less than the flow predicted by the numerical method.</p> <p>(2) The values in this column (K) refers to the conductivity of the structures, they could be looked upon as multiples of the conductivity of the surrounding rock mass.</p>
--

Table B.2 COMPARISON BETWEEN ANALYTICAL AND NUMERICAL METHOD.
The regional flow was directed along the main axes of the structures.
A comparison of an analytical model predicting the flow in an ellipsoid and a numerical model predicting the flow in a rectangular parallel-epiped; for different values of conductivity and length of the studied structures. For each studied scenario the structures have the same length in both methods. The two cases corresponds to different shapes of the circular cross-sections of the ellipsoids.

- Case A has a maximum area of cross-section perpendicular to main axes: 100 m²
- Case B has an average area of cross-section perpendicular to main axes: 100 m².

The parallel-epiped has a rectangular cross-section perpendicular to the main axes with an area of 100 m².

Table (i) Specific flow

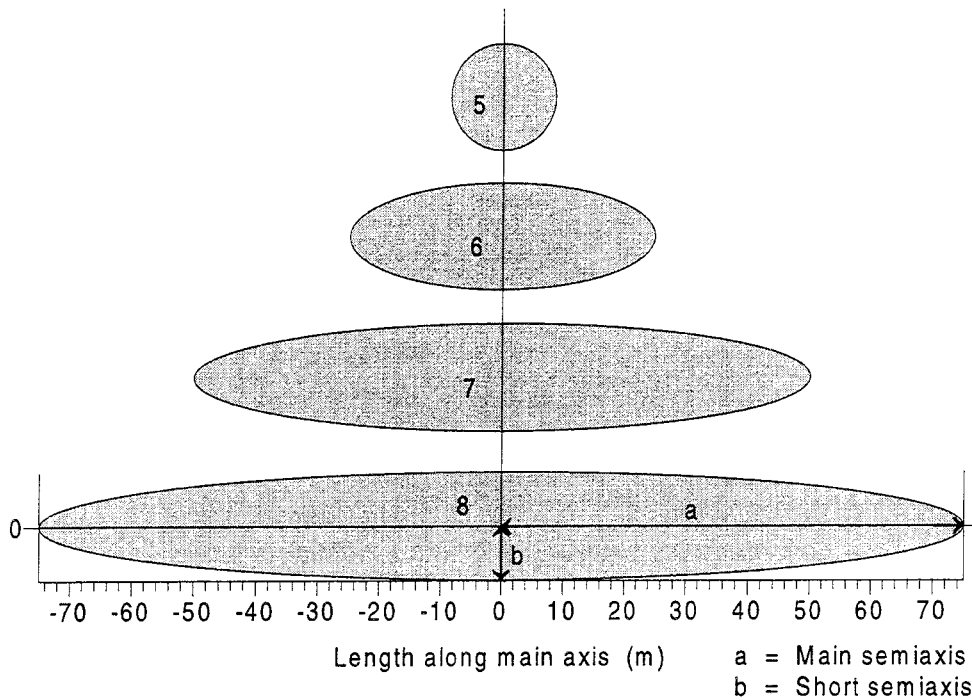
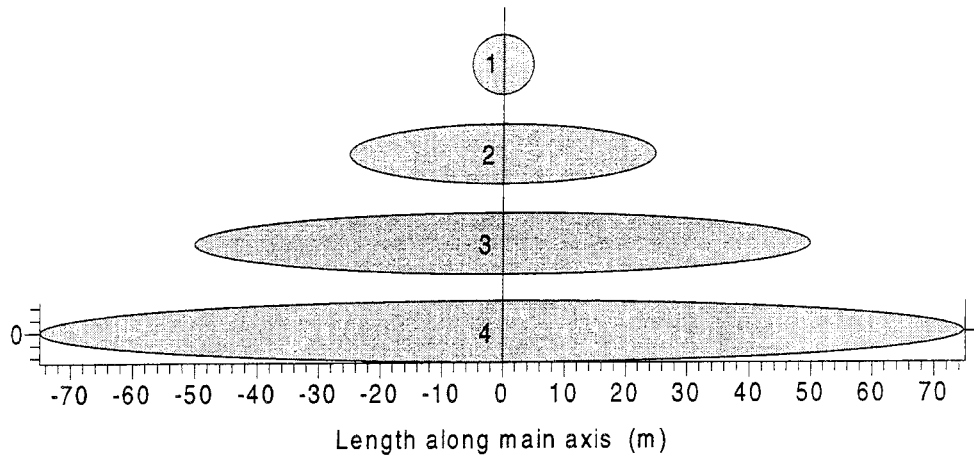
Case	Length of Structure [m]	DIFFERENCE IN PREDICTED SPECIFIC FLOW [m/s]. In percent of specific flow predicted by numerical model. (1)							
		K 0.001	K 0.01	K 0.1	K 1	K 10	K 100	K 1000	K(2) 10000
A	50	-18.4	-18.1	-15.2	0	18.1	25.0	26.9	28.5
	100	-11.4	-11.2	-9.3	0	12.4	20.5	23.1	23.6
	200	-6.5	-6.4	-5.3	0	8.3	17.0	21.4	20.4
B	50	-16.6	-16.3	-13.5	0	6.0	-1.2	-2.5	-1.5
	100	-10.6	-10.4	-8.6	0	5.7	-3.5	-8.0	-8.5
	200	-6.3	-6.1	-5.0	0	5.5	-0.3	-9.6	-12.8

Table (ii) Total flow

Case	Length of Structure [m]	DIFFERENCE IN PREDICTED TOTAL FLOW. [m ³ /s] In percent of total flow predicted by numerical model. (1)							
		K 0.001	K 0.01	K 0.1	K 1	K 10	K 100	K 1000	K(2) 10000
A	50	-68.7	-68.2	-63.3	0	-5.0	-4.9	-4.7	-6.2
	100	-70.2	-69.7	-64.9	0	-7.3	-10.5	-10.1	-10.0
	200	-70.6	-70.2	-65.5	0	-4.7	-11.9	-12.2	-12.1
B	50	-52.0	-51.3	-43.9	50	27.9	12.7	9.8	7.8
	100	-54.8	-54.1	-47.0	50	30.7	7.5	0.7	0.1
	200	-55.8	-55.1	-48.0	50	39.3	12.7	-2.0	-4.5

Table (iii) Notes

<p>(1) The difference is calculates as: (Flow analytical - Flow numerical) / (Flow numerical / 100) Hence, a negative difference means that the flow predicted by the analytical method is less than the flow predicted by the numerical method.</p> <p>(2) The values in this column (K) refers to the conductivity of the structures, they could be looked upon as multiples of the conductivity of the surrounding rock mass.</p>



DATA FOR DIFFERENT ELLIPSOIDS (3-D)

Num.	Length [2a] (m)	Main semiaxis [a] Length (m)	Short semiaxis [b] Length (m)	Volume (m ³)	Cross-section at right angles to main axis	
					Maximum (m ²)	Average (m ²)
1	9.772072	4.886025	4.886025	488.6	75.0	50.0
2	50.0	25.0	4.886025	2500.0	75.0	50.0
3	100.0	50.0	4.886025	5000.0	75.0	50.0
4	150.0	75.0	4.886025	7500.0	75.0	50.0
5	17.480881	8.740387	8.740387	2796.9	240.0	160.0
6	50.0	25.0	8.740387	8000.0	240.0	160.0
7	100.0	50.0	8,740387	16000.0	240.0	160.0
8	150.0	75.0	8.740387	24000.0	240.0	160.0

FIGURE B.1
GEOMETRIC DATA AND SHAPE OF DIFFERENT ELLIPSOIDS.

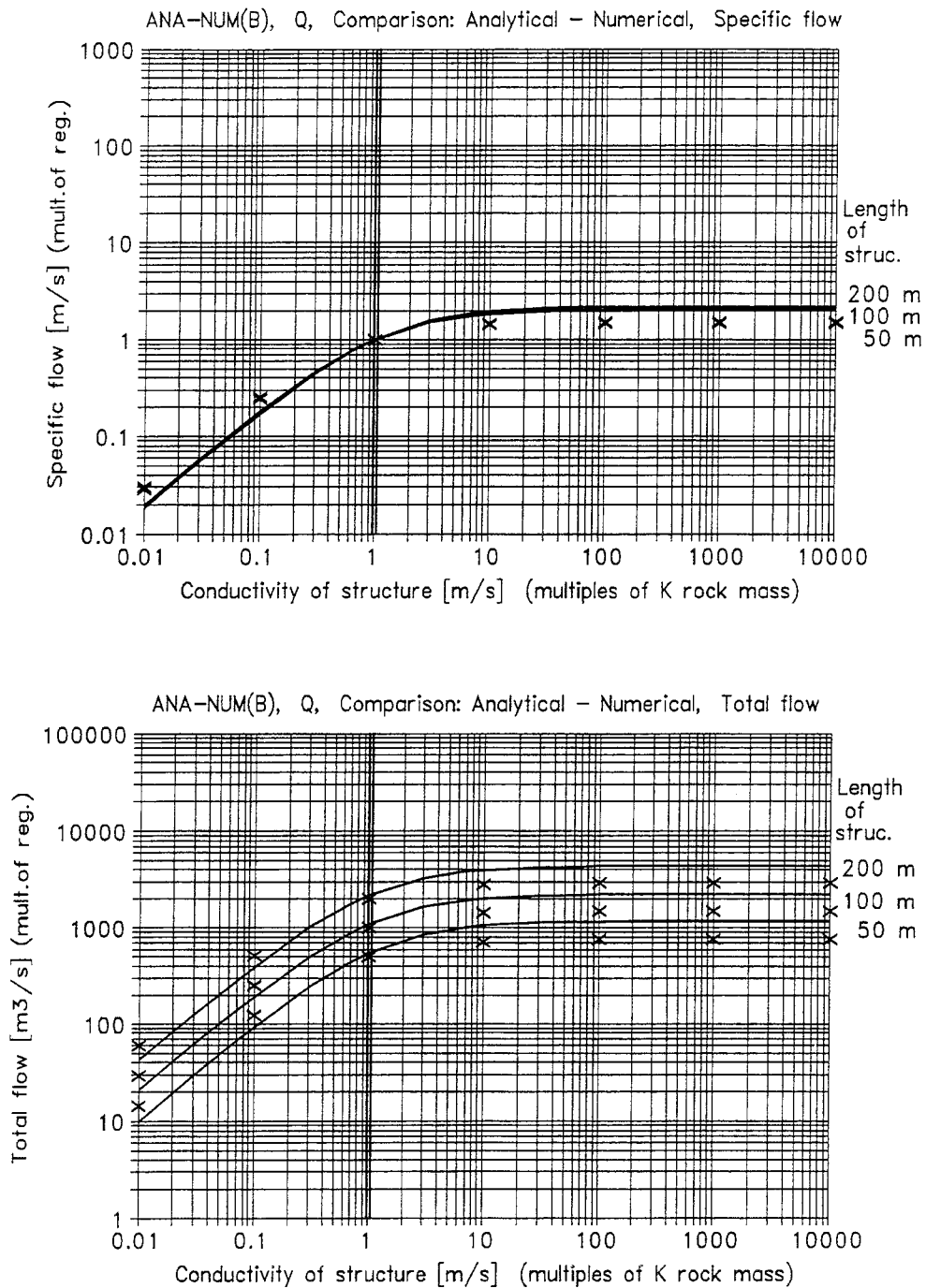


Figure B.2

COMPARISON: ANALYTICAL SOLUTION - NUMERICAL SOLUTION.

The regional flow is directed along the short axes of the structure studied.

The numerical model represents a rectangular parallel-epiped, which has a cross section of 100m^2 (the smallest cross section). The analytical model represents an ellipsoid, defined according to Case B, which has an average cross section of 100m^2 (at right angles to the main axes). The conductivity of the studied structure is given as a multiple of the conductivity of the surrounding rock. Both models uses the uniform continuum approach

- The lines are given by the analytical model (the ellipsoid)
- The crosses are given by the numerical model (the parallel-epiped).

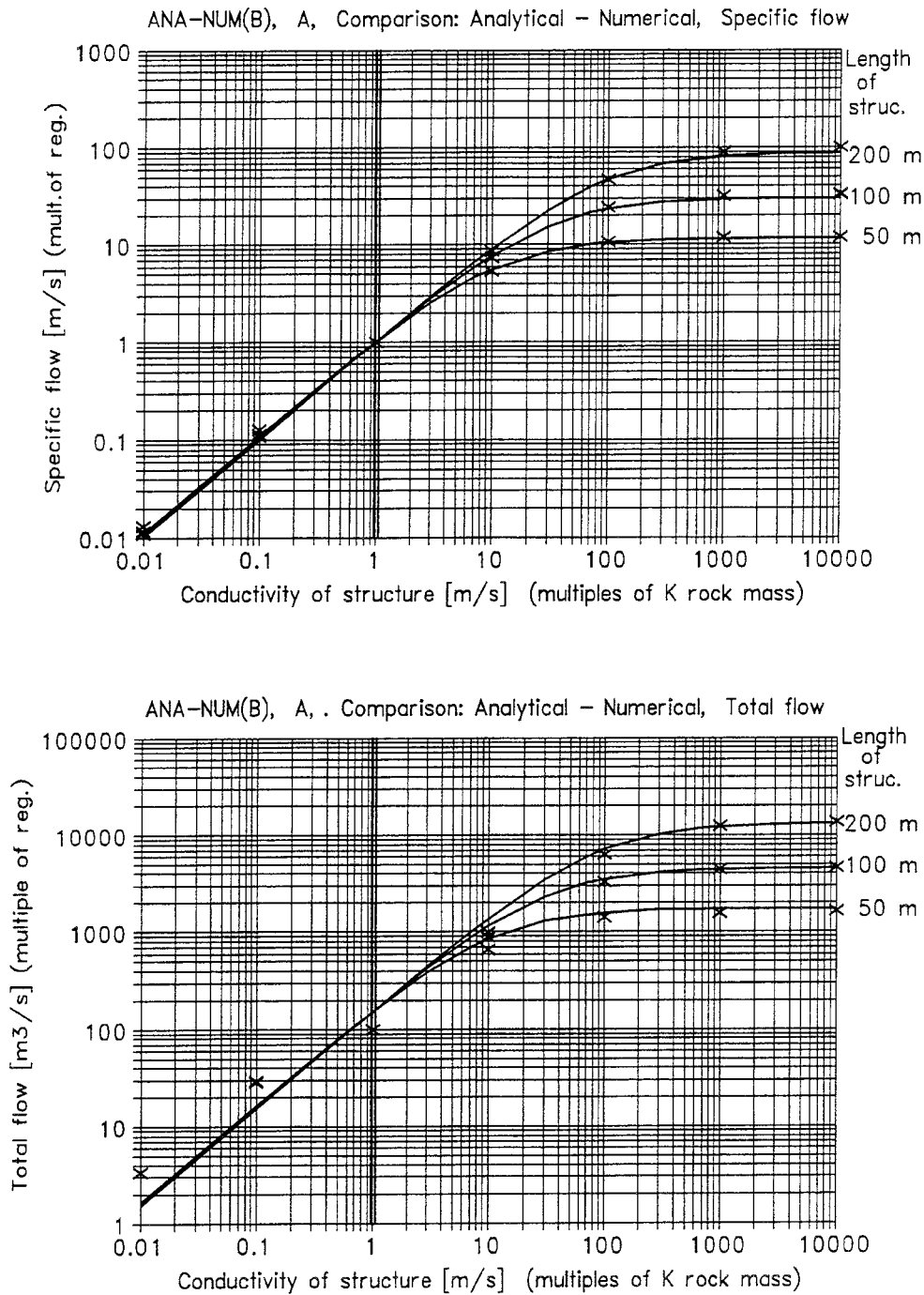


Figure B.3

COMPARISON: ANALYTICAL SOLUTION - NUMERICAL SOLUTION.

The regional flow is directed along the main axes of the structure studied.

The numerical model represents a rectangular parallel-epiped, which has a cross section of 100m^2 (the smallest cross section). The analytical model represents an ellipsoid, defined according to Case B, which has an average cross section of 100m^2 (at right angles to the main axes). The conductivity of the studied structure is given as a multiple of the conductivity of the surrounding rock. Both models uses the uniform continuum approach

- *The lines are given by the analytical model (the ellipsoid)*
- *The crosses are given by the numerical model (the parallel-epiped).*

APPENDIX C

Method for generation of regional flow in a numerical model

<u>TABLE OF CONTENTS</u>	<u>PAGE</u>
C.1 METHOD FOR GENERATION OF REGIONAL FLOW	C.3
FIGURES	C.5

C.1 METHOD FOR GENERATION OF REGIONAL FLOW

In the numerical models, the regional flows are created as all cells along the boundaries of the models meshes are assigned prescribed head conditions. The head values of these cells will be varied in such a way that the head gradient, between the boundaries of the model, will cause a flow through the model. Below, a method is presented for calculation of the head values, from a given direction and gradient of the specified regional flow.

The regional flow is assumed to be a uniform flow in the domain studied. A pressure surface representing a certain pressure in a uniform flow field can be represented by a plane in space - a pressure plane. The normal to the pressure plane gives the direction of the flow (see Figure C.1). The user specifies the **direction of the regional flow** by giving two angles: (i) an angle in the horizontal plane and (ii) an angle in the vertical plane. The angles are defined in relation to a cartesian coordinate system (X axis and Y axis in the horizontal plane, Z axis in the vertical plane). For example, the angle in the horizontal plane could be given clockwise from the positive direction of the Y axis, and the angles in the vertical plane could be given as a positive or a negative inclination from the horizontal plane.

Direction of regional flow: $\alpha = \text{angle in the horizontal plane}$
 $\beta = \text{angle in the vertical plane}$

A plane **Q** can be defined on the basis of the angles defining the direction of regional flow. This is done in two steps: (i) a plane is taken from the horizontal plane and inclined from the horizontal plane with the same angle as the given vertical angle β , and (ii) the plane studied is moved in the horizontal plane as defined by the angle α . When this is done, the plane studied (**Q**) will be parallel to the normal of the pressure planes (at right angles to the pressure planes), see Figure C.1. The plane **Q** is defined by three coordinates, origo is one of the coordinates, the other two coordinates are given below.

Coordinates of plane Q:

$$\begin{array}{lll} X_{P1}= 0 & Y_{P1}= 0 & Z_{P1}= 0 \\ X_{P2}= \cos(\alpha) & Y_{P2}= \sin(\alpha) & Z_{P2}= \tan(\beta) \\ X_{P3}= \cos(\alpha+90) & Y_{P3}= \sin(\alpha+90) & Z_{P3}= 0 \end{array}$$

The equation of the plane **Q** can be calculated on the basis of the three coordinates, as follows.

$$\begin{array}{l} \text{Plane Q has the Equation: } A X + B Y + C Z + D = 0 \\ A = ((Y_{P2}-Y_{P1})(Z_{P3}-Z_{P1})) - ((Y_{P3}-Y_{P1})(Z_{P2}-Z_{P1})) \\ B = ((Z_{P2}-Z_{P1})(X_{P3}-X_{P1})) - ((Z_{P3}-Z_{P1})(X_{P2}-X_{P1})) \\ C = ((X_{P2}-X_{P1})(Y_{P3}-Y_{P1})) - ((X_{P3}-X_{P1})(Y_{P2}-Y_{P1})) \\ D = (-A X_{P1}) - (B Y_{P1}) - (C Z_{P1}) \end{array} \quad (C:1)$$

The plane **Q** represents the uniform flow field as regards the coordinate system, assuming that the pressure at origo is zero and that the gradient along the direction of flow is equal to one. The equation of the plane **Q** (C:1) makes it possible to calculate the pressure at any given point in space, based on the following conclusion: **The pressure at a studied point in space is equal to the elevation (Z coord.) of the nearest point in the plane Q.**

To be able to calculate what point in the plane **Q** is located closest to the studied point, it is necessary to give an expression for the line between the two points (the point in space and the point in the plane **Q**).

The plane Q has the normal vector:

$$\vec{n} = \begin{pmatrix} A \\ B \\ C \end{pmatrix} \quad (C:2)$$

The studied point in space has the coordinates:

$$X_{stud}, Y_{stud}, Z_{stud}$$

The line between the studied point in space and the point in the plane is given as an equation in parameter form:

$$\begin{aligned} X &= X_{stud} + A t \\ Y &= Y_{stud} + B t \\ Z &= Z_{stud} + C t \end{aligned} \quad (C:3)$$

Three steps are necessary to get the coordinates of the unknown point in the plane Q.

(i) The equation above (C:3) is substituted into the equation of the plane Q (C:1), which gives the equation below.

$$A (X_{stud} + A t) + B (Y_{stud} + B t) + C (Z_{stud} + C t) + D = 0 \quad (C:4)$$

(ii) The equation above (C:4) is solved for the parameter t , which gives:

$$t = \frac{-A X_{stud} - B Y_{stud} - C Z_{stud} - D}{A^2 + B^2 + C^2} \quad (C:5)$$

(iii) An expression for the coordinates of the unknown point in the plane Q is produced as the expression for parameter t (C:5) is substituted into the equation of the line (C:3). The elevation of the point on the plane is given by the Z coordinate.

$$Z = Z_{stud} + C \left(\frac{-A X_{stud} - B Y_{stud} - C Z_{stud} - D}{A^2 + B^2 + C^2} \right) \quad (C:6)$$

The value Z represents the head at the studied point in space at: $X_{stud}, Y_{stud}, Z_{stud}$
 We remember that the plane Q represents a uniform flow field as regards the coordinate system, assuming that the pressure at origo is zero and that the gradient along the direction of flow is equal to one. Hence, unless these conditions are correct we need to scale the values calculated above. This is done in two steps, the adjustments are simple as the flow field is uniform. The head at a known point is given by the user, the head at the same point is calculated by the method given above. The difference between the two values is the adjustment constant which should be added to all calculated head values. The gradient in the direction of the uniform flow is given by the user. Based on this gradient a scale factor is calculated and all head values calculated with the method given above are multiplied with the scale factor. By using the method presented above, it is possible to calculate head values and assign these values to all cells in the mesh. These head values will be the correct head values for a uniform three-dimensional flow field.

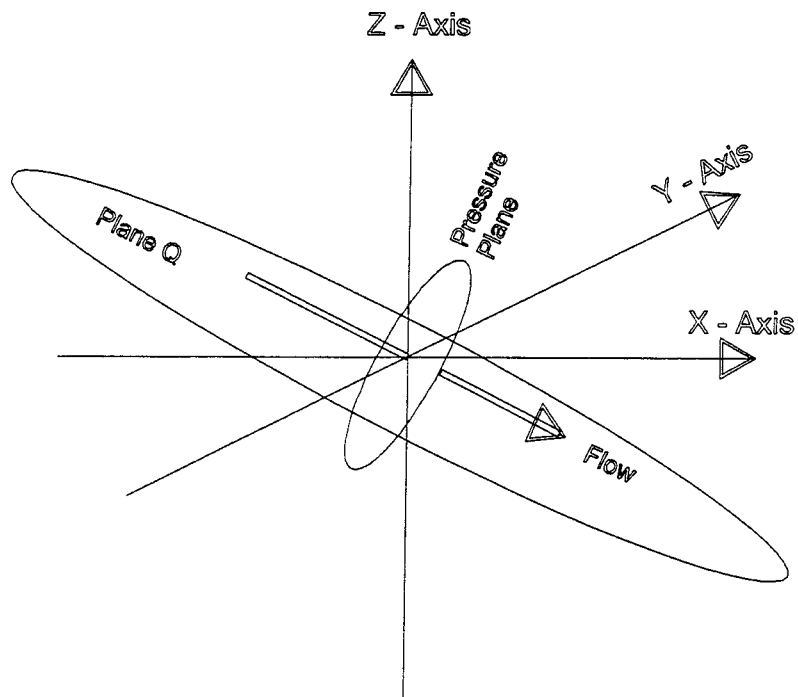


Figure C.1 GENERATION OF REGIONAL FLOW.
 The coordinate system, the plane Q, a pressure plane and the vector representing the uniform flow. The X axis and the Y axis are in the horizontal plane, the Z axis is in the vertical plane.

APPENDIX D

Distribution of specific flow in the repository SFL 3-5

TABLE OF CONTENTS

PAGE

D.1 DISTRIBUTION OF SPECIFIC FLOW IN REPOSITORY SFL 3-5 D.3
D.1.1 Introduction D.3

TABLES D.3
FIGURES D.4 - D.7

D.1 DISTRIBUTION OF SPECIFIC FLOW IN REPOSITORY SFL 3-5

D.1.1 Introduction

The figures given in this Appendix demonstrate results obtained from simulations with the repository model. This model is the same as the model discussed in Chapter 8 and Chapter 9. The hydraulic conductivity of the model is given in the Table D.1 (below).

*Table D.1 REPOSITORY MODEL OF SFL 3-5.
Hydraulic conductivity of different media, as they are defined in the model. In the model the conductivity is defined as a relative conductivity. A relative conductivity is equal to the conductivity contrast between the rock mass and the studied media. By the using relative values we can calculate absolute values for different assumptions of the rock mass conductivity.*

The table gives absolute conductivity values for two different assumptions of the rock mass conductivity.

ASSUMPTION 1: Rock mass conductivity is 1×10^{-9} m/s

ASSUMPTION 2: Rock mass conductivity is 1×10^{-8} m/s.

	MEDIUM	Hydraulic conductivity in model (relative values) (conductivity contrasts)	ASSUMPTION 1. Hydraulic conductivity, Absolute values (m/s) (1)	ASSUMPTION 2. Hydraulic conductivity, Absolute values (m/s) (1)
Rock mass	Rock mass	1	10^{-9}	10^{-8}
SFL 3	Flow barrier (9 alternatives)	100000	10^{-4}	10^{-3}
	Concrete encapsulation	10	10^{-8}	10^{-7}
SFL 4	Sand filling inside tunnel (2 alternatives)	10000	10^{-5}	10^{-4}
SFL 5	Flow barrier (9 alternatives)	100000	10^{-4}	10^{-3}
	Concrete encapsulation	10	10^{-8}	10^{-7}
Plug	Concrete plug (thickness 5 m)	1	10^{-9}	10^{-8}
	Bentonite barrier (thickness 1 m)	0.1	10^{-10}	10^{-9}

(1) $K_{abs.X} = K_{rel.X} / K_{rock}$

$K_{abs.x}$ = Absolute conductivity of medium X

$K_{rel.X}$ = Relative conductivity of medium X

K_{rock} = The assumed conductivity of the rock mass, this is the "known value" that all other values are related to

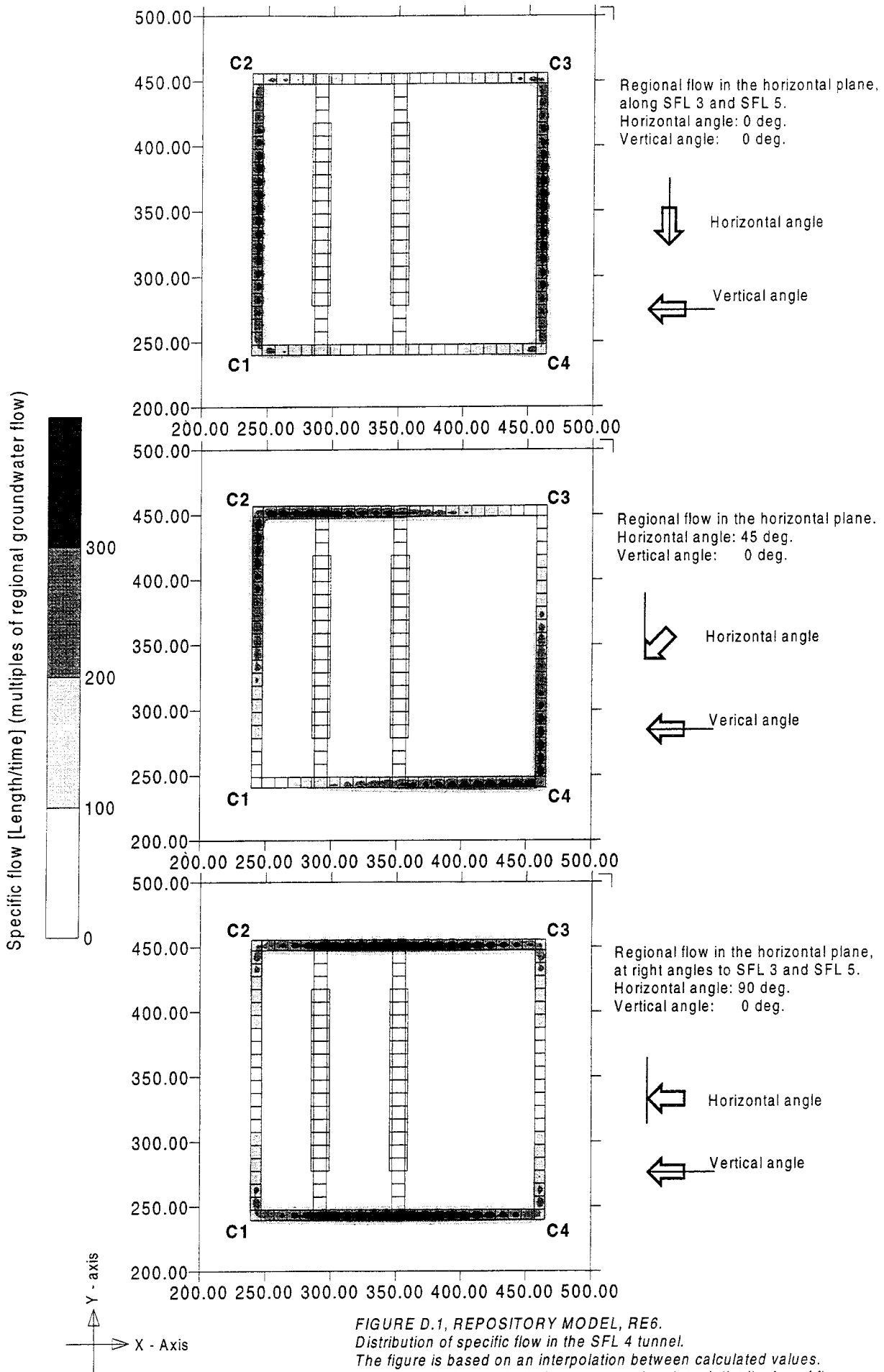


FIGURE D.1, REPOSITORY MODEL, RE6.

Distribution of specific flow in the SFL 4 tunnel.

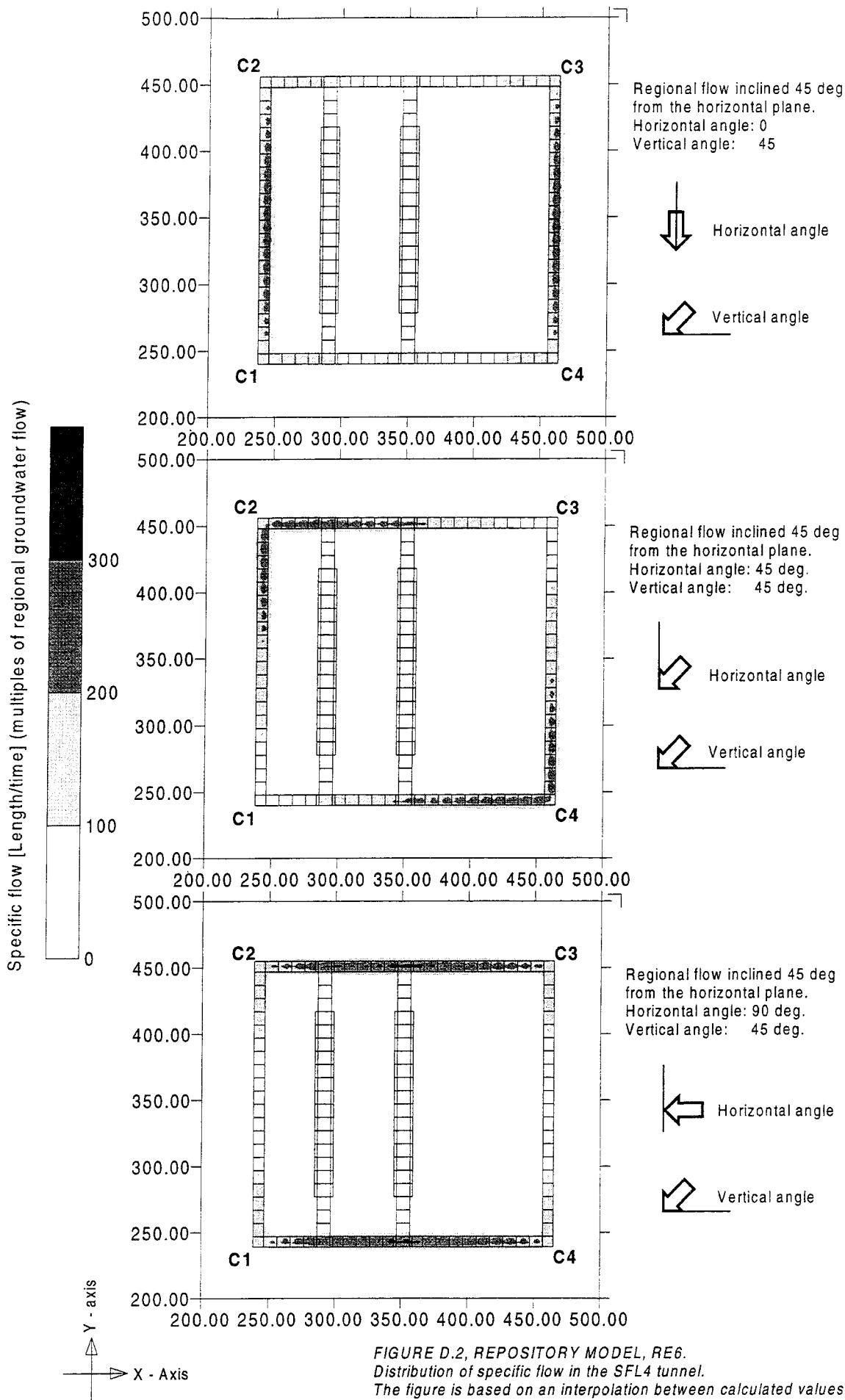
The figure is based on an interpolation between calculated values.

The interpolation method gives a somewhat dotted distribution of flow.

The actual distribution of flow is continuous. The flow is given as a

multiple of an unknown regional flow. Regional flow is horizontal.

The model is three dimensional and uses the uniform continuum approach.



Scale in meters

Horizontal cross-sections through the SFL 4 tunnel.

FIGURE D.2, REPOSITORY MODEL, RE6.

Distribution of specific flow in the SFL4 tunnel.

The figure is based on an interpolation between calculated values.

The interpolation method gives a somewhat dotted distribution of flow.

The actual distribution of flow is continuous. The flow is given as a multiple

of an unknown regional flow. Regional flow is inclined 45 deg. from horizontal.

The model is three dimensional and uses the uniform continuum approach.

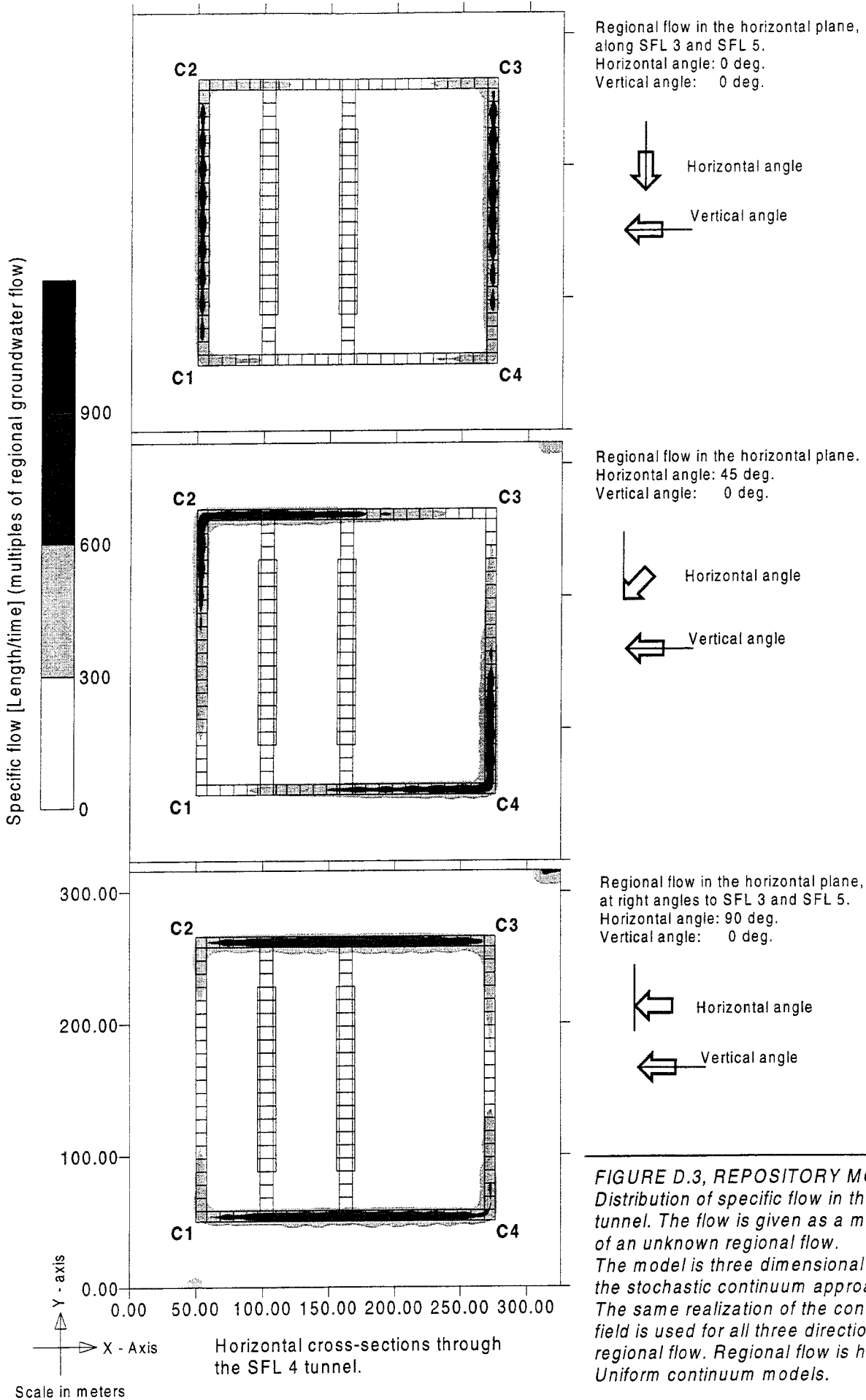
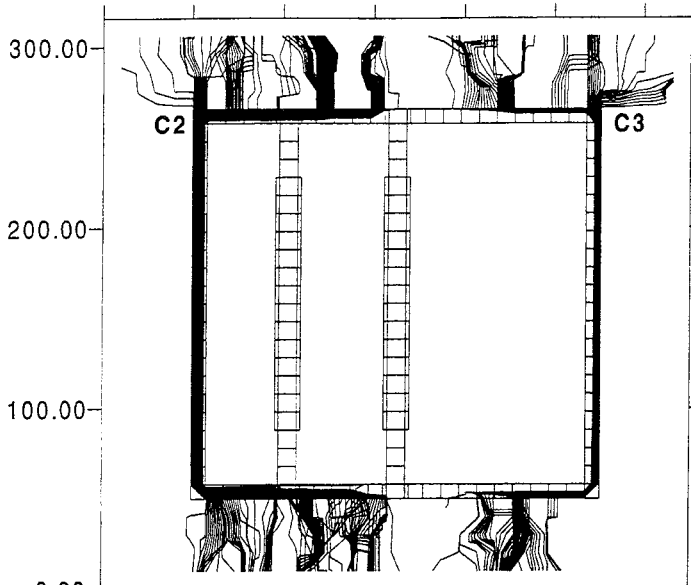
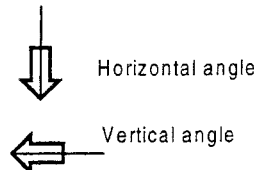


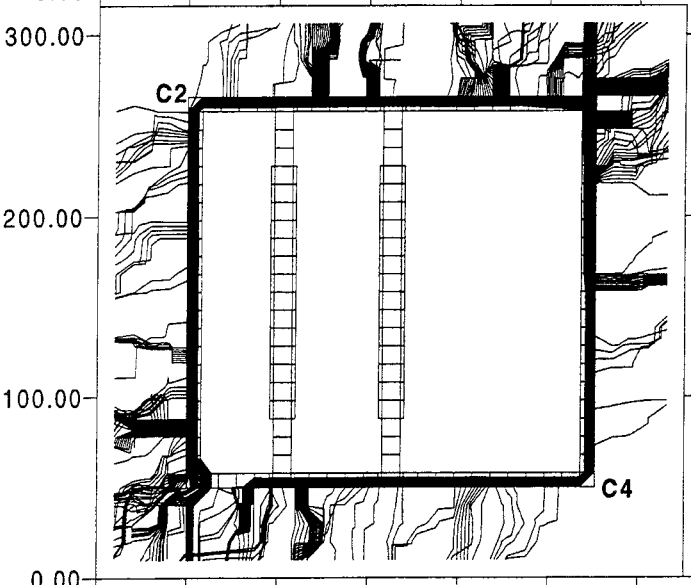
FIGURE D.3, REPOSITORY MODEL,RS5.
Distribution of specific flow in the SFL 4 tunnel. The flow is given as a multiple of an unknown regional flow. The model is three dimensional and uses the stochastic continuum approach. The same realization of the conductivity field is used for all three directions of regional flow. Regional flow is horizontal. Uniform continuum models.



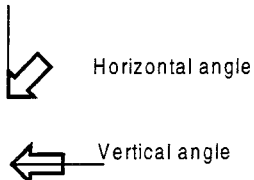
Regional flow in the horizontal plane,
along SFL 3 and SFL 5.
Horizontal angle: 0 deg.
Vertical angle: 0 deg.



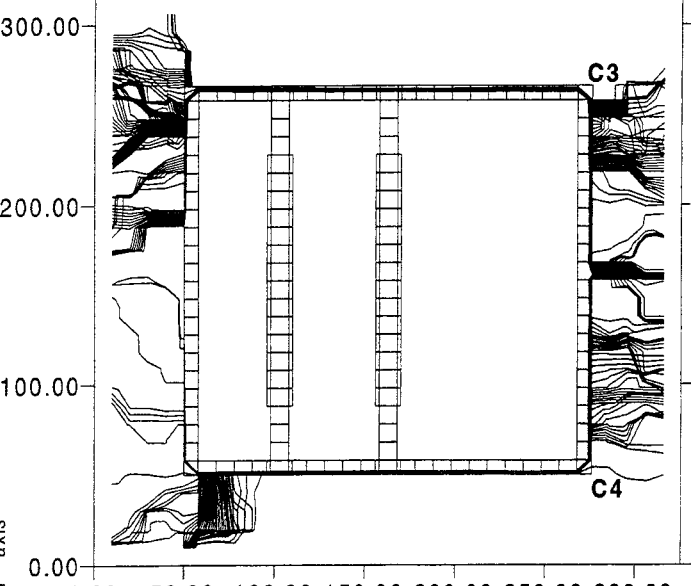
Starting points of flowpaths
between C2 and C3,
at the upstream vertical
face of the tunnel.



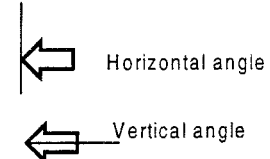
Regional flow in the horizontal plane.
Horizontal angle: 45 deg.
Vertical angle: 0 deg.



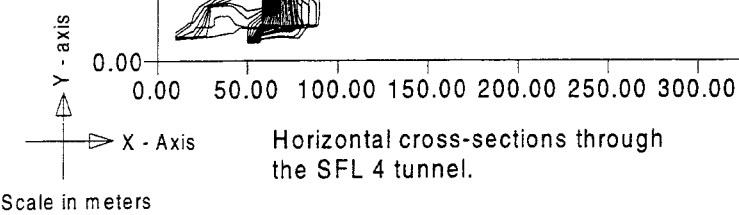
Starting points of flowpaths
between C2 and C4,
at the upstream vertical
face of the tunnel.



Regional flow in the horizontal plane,
at right angles to SFL 3 and SFL 5.
Horizontal angle: 90 deg.
Vertical angle: 0 deg.



Starting points of flowpaths between C3 and C4,
at the upstream vertical face of the tunnel.



Horizontal cross-sections through
the SFL 4 tunnel.

FIGURE D.4, REPOSITORY MODEL, RS5.
Flowpaths demonstrating an example of the
flowpattern in tunnels and rock mass. The
flowpaths are generated from starting points
between the upstream corners of the
SFL 4 tunnel (C2, C3, C4). The larger the
number of flowpaths, the larger the flow.
Only the path of the water entering SFL 4
at the starting points is demonstrated.
The model is three-dimensional and uses
the stochastic continuum approach.
The same realization of the conductivity field
is used for all three directions of regional flow.

APPENDIX E

Preliminary lay-out of repository SFL 3-5

TABLE OF CONTENTS

PAGE

E.1	PRELIMINARY LAY-OUT OF REPOSITORY SFL 3-5	E.2
E.1.1	Introduction	E.2
E.2	REFERENCES	E.2
	FIGURES E.1 and E.2	E.3 - E.4

E.1 PRELIMINARY LAY-OUT OF REPOSITORY SFL 3-5

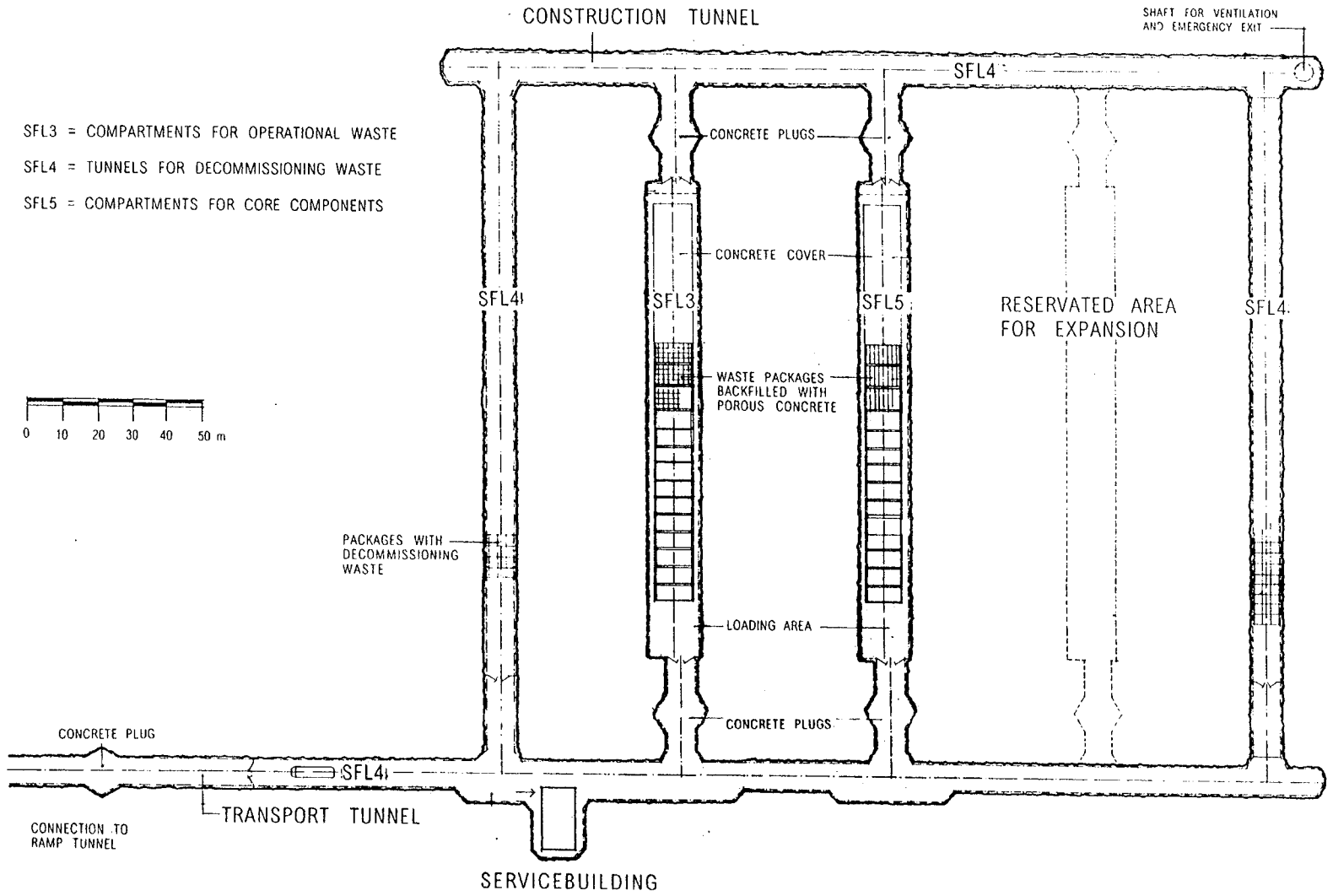
E.1.1 Introduction

The following figures give a brief presentation of the preliminary lay-out of the repository SFL 3-5. The preliminary lay-out of the repository is taken from, Forsgren *et al*, (1996).

E.2 REFERENCES

FORSGREN, E., LANGE, F., and LARSSON, H., 1996: "SFL 3-5 Layoutstudie"
SKB Arbets Rapport, AR D-96-016, December 1996. Swedish nuclear fuel and waste management Co. Box 5864 S-10248 Stockholm.

Figure E.1 Horizontal cross-section through repository SFL 3-5 (preliminary lay-out).



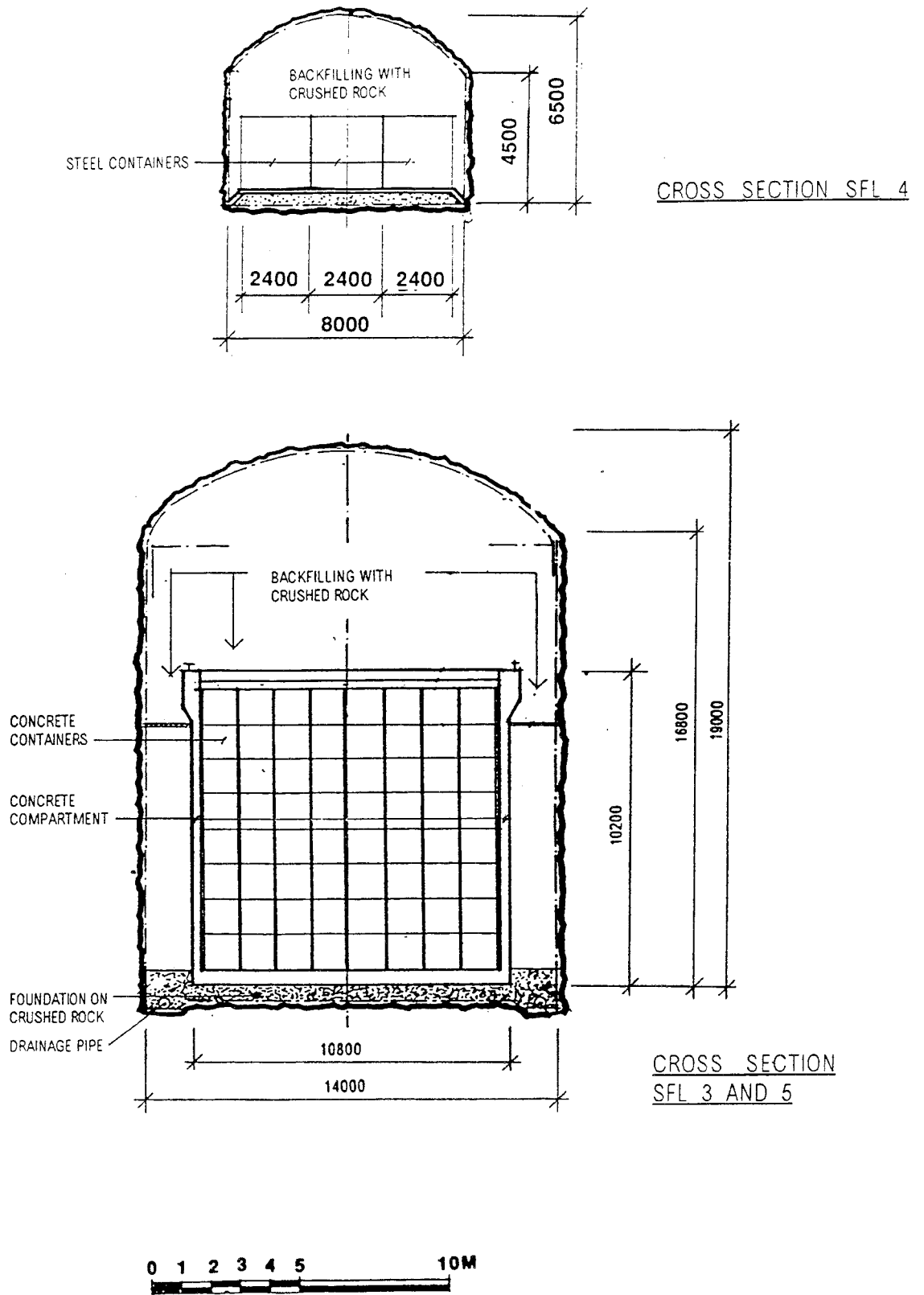


Figure E.2 Vertical cross-sections through parts of repository SFL 3-5 (preliminary lay-out).

List of SKB reports

Annual Reports

1977-78

TR 121

KBS Technical Reports 1 – 120

Summaries

Stockholm, May 1979

1979

TR 79-28

The KBS Annual Report 1979

KBS Technical Reports 79-01 – 79-27

Summaries

Stockholm, March 1980

1980

TR 80-26

The KBS Annual Report 1980

KBS Technical Reports 80-01 – 80-25

Summaries

Stockholm, March 1981

1981

TR 81-17

The KBS Annual Report 1981

KBS Technical Reports 81-01 – 81-16

Summaries

Stockholm, April 1982

1982

TR 82-28

The KBS Annual Report 1982

KBS Technical Reports 82-01 – 82-27

Summaries

Stockholm, July 1983

1983

TR 83-77

The KBS Annual Report 1983

KBS Technical Reports 83-01 – 83-76

Summaries

Stockholm, June 1984

1984

TR 85-01

Annual Research and Development Report 1984

Including Summaries of Technical Reports Issued during 1984. (Technical Reports 84-01 – 84-19)

Stockholm, June 1985

1985

TR 85-20

Annual Research and Development Report 1985

Including Summaries of Technical Reports Issued during 1985. (Technical Reports 85-01 – 85-19)

Stockholm, May 1986

1986

TR 86-31

SKB Annual Report 1986

Including Summaries of Technical Reports Issued during 1986

Stockholm, May 1987

1987

TR 87-33

SKB Annual Report 1987

Including Summaries of Technical Reports Issued during 1987

Stockholm, May 1988

1988

TR 88-32

SKB Annual Report 1988

Including Summaries of Technical Reports Issued during 1988

Stockholm, May 1989

1989

TR 89-40

SKB Annual Report 1989

Including Summaries of Technical Reports Issued during 1989

Stockholm, May 1990

1990

TR 90-46

SKB Annual Report 1990

Including Summaries of Technical Reports Issued during 1990

Stockholm, May 1991

1991

TR 91-64

SKB Annual Report 1991

Including Summaries of Technical Reports Issued during 1991

Stockholm, April 1992

1992

TR 92-46

SKB Annual Report 1992

Including Summaries of Technical Reports Issued during 1992

Stockholm, May 1993

1993

TR 93-34

SKB Annual Report 1993

Including Summaries of Technical Reports Issued during 1993

Stockholm, May 1994

1994

TR 94-33

SKB Annual Report 1994

Including Summaries of Technical Reports Issued during 1994

Stockholm, May 1995

1995

TR 95-37

SKB Annual Report 1995

Including Summaries of Technical Reports Issued during 1995

Stockholm, May 1996

1996

TR 96-25

SKB Annual Report 1996

Including Summaries of Technical Reports Issued during 1996

Stockholm, May 1997

List of SKB Technical Reports 1997

TR 97-01

Retention mechanisms and the flow wetted surface – implications for safety analysis

Mark Elert

Kemakta Konsult AB

February 1997

TR 97-02

Äspö HRL – Geoscientific evaluation 1997/1. Overview of site characterization 1986–1995

Roy Stanfors¹, Mikael Erlström²,

Ingemar Markström³

¹ RS Consulting, Lund

² SGU, Lund

³ Sydkraft Konsult, Malmö

March 1997

TR 97-03

Äspö HRL – Geoscientific evaluation 1997/2. Results from pre-investigations and detailed site characterization. Summary report

Ingvar Rhén (ed.)¹, Göran Bäckblom (ed.)², Gunnar Gustafson³, Roy Stanfors⁴, Peter Wikberg²

¹ VBB Viak, Göteborg

² SKB, Stockholm

³ VBB Viak/CTH, Göteborg

⁴ RS Consulting, Lund

May 1997

TR 97-04

Äspö HRL – Geoscientific evaluation 1997/3. Results from pre-investigations and detailed site characterization. Comparison of predictions and observations. Geology and mechanical stability

Roy Stanfors¹, Pär Olsson², Håkan Stille³

¹ RS Consulting, Lund

² Skanska, Stockholm

³ KTH, Stockholm

May 1997

TR 97-05

Äspö HRL – Geoscientific evaluation 1997/4. Results from pre-investigations and detailed site characterization. Comparison of predictions and observations. Hydrogeology, groundwater chemistry and transport of solutes

Ingvar Rhén¹, Gunnar Gustafson², Peter Wikberg³

¹ VBB Viak, Göteborg

² VBB Viak/CTH, Göteborg

³ SKB, Stockholm

June 1997

TR 97-06

Äspö HRL – Geoscientific evaluation 1997/5. Models based on site characterization 1986–1995

Ingvar Rhén (ed.)¹, Gunnar Gustafson²,

Roy Stanfors⁴, Peter Wikberg⁴

¹ VBB Viak, Göteborg

² VBB Viak/CTH, Göteborg

³ RS Consulting, Lund

⁴ SKB, Stockholm

May 1997

TR 97-07

A methodology to estimate earthquake effects on fractures intersecting canister holes

Paul La Pointe, Peter Wallmann, Andrew Thomas,

Sven Follin

Golder Associates Inc.

March 1997

TR 97-08

Äspö Hard Rock Laboratory Annual Report 1996

SKB

April 1997

TR 97-09

A regional analysis of groundwater flow and salinity distribution in the Äspö area

Urban Svensson

Computer-aided Fluid Engineering AB

May 1997